APPLICATION OF ORGANOCATALYSIS TO THE SYNTHESIS OF

CHIRAL MORPHOLINES, PIPERAZINES, AZIRIDINES, AZETIDINES,

β-FLUOROAMINES, AND γ-FLUOROAMINES; DISCOVERY OF SELECTIVE

PHOSPHOLIPASE D INHIBITORS WITH OPTIMIZED IN VIVO PROPERTIES

By

Matthew C. O'Reilly

Dissertation

Submitted to the Faculty of the

Graduate School of Vanderbilt University

in partial fulfillment of the requirements

for the degree of

DOCTOR OF PHILOSOPHY

in

Chemistry

August, 2014

Nashville, Tennessee

Approved:

Professor Craig W. Lindsley

Professor Brian O. Bachmann

Professor H. Alex Brown

Professor Gary A. Sulikowski

For Erica,

My Parents, and

My Brother

Strange is our situation here upon Earth. Each of us comes for a short visit, not knowing why,

yet sometimes seeming to a divine purpose. From the standpoint of daily life, however, there

is one thing we do know: that man is here for the sake of other men…for the countless

unknown souls with whose fate we are connected by a bond of sympathy. Many times a day I

realize how much my own outer and inner life is built upon the labors of my fellowmen, both

living and dead, and how earnestly I must exert myself in order to

give in return as much as I have received.

-Albert Einstein

ACKNOWLEDGEMENTS

exemplary job of teaching all of my graduate courses relevant to modern organic synthesis. Professors Brian Bachmann and Larry Marnett fostered my interest in chemical biology throughout formal coursework and beyond. I thoroughly enjoyed being a teaching assistant for the graduate course "Fundamentals of Chemical Biology," where Prof. Marnett illuminated the intricacies of graduate level course design. Alex Brown has been an ideal collaborator, and his laboratory—especially Dr. Sarah Scott—have helped me understand the principles of pharmacology and biology involved in our collaboration. Sarah performed almost all of the screening—and all of the cancer assays—involved in my collaboration with the Brown Lab.

Senior graduate students and postdocs had a large impact on my initial laboratory and academic efforts. Dr. Chris Tarr, now a staff scientist in the VCNDD, sat next to me and helped me through the process of designing experiments and directing my research efforts. While Chris had the most impact on me during my seminal efforts in the Lindsley Lab, Drs. Stephen Chau and Steven Townsend—who were graduate students in the Sulikowski lab at the time—fostered my interest in organic chemistry and were supportive voices when things were tough during my early studies. All of these mentors are now friends, and I am excited to see what the future holds for all of us.

The Lindsley Lab, as a whole, has been a place of support throughout graduate school. On a personal level, I have had a wonderful time with the Lindsley Lab graduate students and postdocs throughout the last 5 years. We have had great times at Christmas parties, scientific meetings, New Year's Eve celebrations, paintball games, bars, concerts, and sporting events. The camaraderie gained outside of lab has carried over into the lab space

and has generated more creativity and support between students. We have had many fun times, we miss those that have already left, and I will miss those that I leave behind.

One integral part of my graduate studies has been the support staff. Nathan Kett and Matt Mulder have always been available when instruments need to be fixed or different analytical equipment is necessary for our projects. If the support staff was not always there to help when problems arise, I am convinced that all Lindsley Lab students would have to add time to their degrees.

I have earned nothing exclusively through my own efforts, and I am so thankful for all of the undeserved blessings I have received. I did not choose where I was born or who I was born from, but these facts of my life have given me all that I could desire. I was blessed to have a mother and father who gave me everything that was necessary for my success while also refraining from giving me that which was superfluous. They gave me the tools for life allowing me to thrive while also teaching me the joy of moderation. The greatest gift I have ever received is the love of my family. My family, and my life, would be horribly changed without my brother, Mike. I would be worse at every aspect of life without Mike's unwavering love and support. When I reflect, I realize he has challenged—and still challenges—me to be more compassionate, more competitive, and all around a better person.

More than anyone else, I am so thankful to have my wife, Erica, in my life. I have been blessed to find the person who knows and accepts me for exactly who I am. In the times when life in the lab was tough, you were always able to make me forget the pains of the moment and just enjoy life. To sum it up, you are the best part of my life. I also cannot thank your parents enough. When I first arrived in Nashville, they made me feel so welcome,

giving me their love and support. They truly are my second set of parents, and I am so blessed to have them in my life.

TABLE OF CONTENTS

LIST OF TABLES

LIST OF FIGURES

LIST OF SCHEMES

LIST OF ABBREVIATIONS

Å	Angstrom(s)
Ac	acetyl
AD	Alzheimer's disease
ADME	absorption, distribution, metabolism, and excretion
α	specific rotation
aq	aqueous
APP	amyloid precursor protein
Ar	aryl
Bn	benzyl
Boc	*tert*-butoxycarbonyl
br	Broad
Bu	butyl
c	concentration (in g/100 mL)
cat	catalytic
Cbz	carboxybenzyl
$CDCl_3$	deuterated chloroform
CH_2Cl_2	dichloromethane
$CHCl_3$	chloroform
CNS	central nervous system
CRC	concentration-response curve
Cy	cyclohexyl

d	doublet
DAG	diacylglycerol
DAST	(diethylamido)sulfur trifluoride
DCE	1,2-dichloroethane
DCM	dichloromethane
dd	doublet of doublets
ddd	doublet of doublet of doublets
DEAD	diethylazodicarboxylate
DIAD	diisopropylazodicarboxylate
DIBAL	diisobutylaluminum hydride
DIEA	*N*,*N*-diisopropylethylamine
dm	doublet of multiplets
DMAP	4-dimethylaminopyridine
DMF	*N*,*N*-dimethylformamide
DMS	dimethyl sulfide
DMSO	dimethyl sulfoxide
dq	doublet of quartets
dr	diastereomeric ratio
dt	doublet of triplets
ee	enantiomeric excess
ELSD	evaporative light scattering detector
eq	equivalent(s)
ES	Electrospray

Et	ethyl
Et$_2$O	diethyl ether
Et$_3$N	triethylamine
EtOAc	ethyl acetate
EtOH	ethanol
FDA	food and drug administration
g	gram
GFP	green fluorescence protein
hr	hour(s)
H$_2$O	water
HATU	1-[Bis(dimethylamino)methylene]-1H-1,2,3-triazolo[4,5-b]pyridinium 3-oxid hexafluorophosphate
hERG	human ether a-go-go-related gene
Hex	hexanes
HPLC	high performance liquid chromatography
HRMS	high resolution mass spectrometry
Hz	hertz
i	iso
IC$_{50}$	half maximal inhibitory concentration
Im	imidazole
IP	intraperitoneally
IPA	isopropyl alcohol
i-Pr	isopropyl

J	coupling constant (in Hz)
kcal	kilocalorie(s)
kg	kilogram(s)
KHMDS	potassium *bis*(trimethylsilyl)amide
K_i	binding constant
KO^{t}Bu	potassium *tert*-butoxide
LAH	lithium aluminum hydride
LCMS	liquid chromatography-mass spectrometry
LDA	lithium diisopropylamide
LHMDS	lithium *bis*(trimethylsilyl)amide
LPA	lysophosphatidic acid
LTP	long term potentiation
M	molar (moles per liter)
m	multiplet
MDO	multidimensional optimization approach
Me	methyl
MeCN	acetonitrile
MeOH	methanol
mg	milligram(s)
MHz	megahertz
min	minute(s)
mL	milliliter(s)
MLPCN	Molecular Libraries Probe Center Network

mol	mole(s)
Ms	mesyl or methanesulfonate
MS	molecular sieves
MsCl	mesyl chloride or methanesulfonyl chloride
NaBH(OAc)$_3$	sodium triacetoxyborohydride
nBuLi	*n*-butyllithium
nBuOH	*n*-butanol
NCS	*N*-chlorosuccinimide
ND	not determined
NFSI	*N*-fluorobenzenesulfonimide
nM	nanomolar
NMR	nuclear magnetic resonance spectroscopy
n-PrOH	*n*-propanol
ºC	degrees Celsius
p	para
p	pentet
PA	phosphatidic acid
PC	phosphatidyl choline
Pd/C	palladium on carbon
Ph	phenyl
Ph$_3$P	triphenylphosphine
PhMe	toluene
Phth	phthalimide

PIP$_2$	phosphatidylinositol(4,5)biphosphate
pK_a	logarithmic measure of the acid dissociation constant
PKC	protein kinase C
PLD	phospholipase D
pM	picomolar
PMB	para methoxybenzyl
PS	polymer-supported
PtdBuOH	phosphatidylbutanol
q	quartet
R	any organic substituent
R$_f$	retention factor
rt	room temperature
rxn	reaction
s	singlet
SAR	structure activity relationships
sec	second(s)
sept	septet
sext	sextet
SFC	supercritical fluid chromatography
t	tert
t	triplet
TBAF	tetra-*n*-butylammonium fluoride
TBDPS	*tert*-butyldiphenylsilyl

TBS	*tert*-butyldimethylsilyl
t-Bu	*tert*-butyl
*t*BuLi	*tert*-butyl lithium
temp	temperature(s)
Tf	triflate
Tf$_2$O	triflic anhydride or trifluoromethanesulfonic anhydride
TFA	trifluoroacetic acid
THF	tetrahydrofuran
TLC	thin-layer chromatography
TMS	trimethylsilyl
Ts	tosyl or 4-toluenesulonyl
TsCl	tosyl chloride or 4-toluenesulfonyl chloride
UV	ultraviolet
VU	Vanderbilt University
δ	chemical shifts (in ppm)
Δ	heat
μg	microgram
μM	micromolar
μW	microwave heating

STATEMENT OF DISSERTATION

My doctoral research has focused on (i) using organocatalysis to prepare enantioenriched pharmaceutically relevant scaffolds and (ii) preparing isoenzyme selective inhibitors of phospholipase D. My training has mainly focused on the synthetic aspects of the projects that are presented. While I had a part in analysis of the assays performed with the different compounds, I did not perform the assays myself.

(i) Methodologies for asymmetric chlorination and fluorination of aldehydes have recently been reported; the potential of such building blocks in organic synthesis, however, were yet be exploited.[1–4] A main project of mine was to fully unveil the synthetic potential of enantioenriched chlorinated and fluorinated aldehydes or alcohols as chiral building blocks toward the synthesis of various pharmaceutically relevant scaffolds. Morpholines, piperazines, azetidines, and aziridines are biologically relevant scaffolds and are often used as important synthetic intermediates. These scaffolds, however, are often difficult to prepare in enantioenriched form. By utilizing organocatalysis to arrive at chiral β-chloro alcohols, I was able to generate all of these scaffolds through a novel and facile manifold of reactions in good overall yields and excellent

Fig. I. Organocatalytic access to enantioenriched pharmaceutically relevant scaffolds
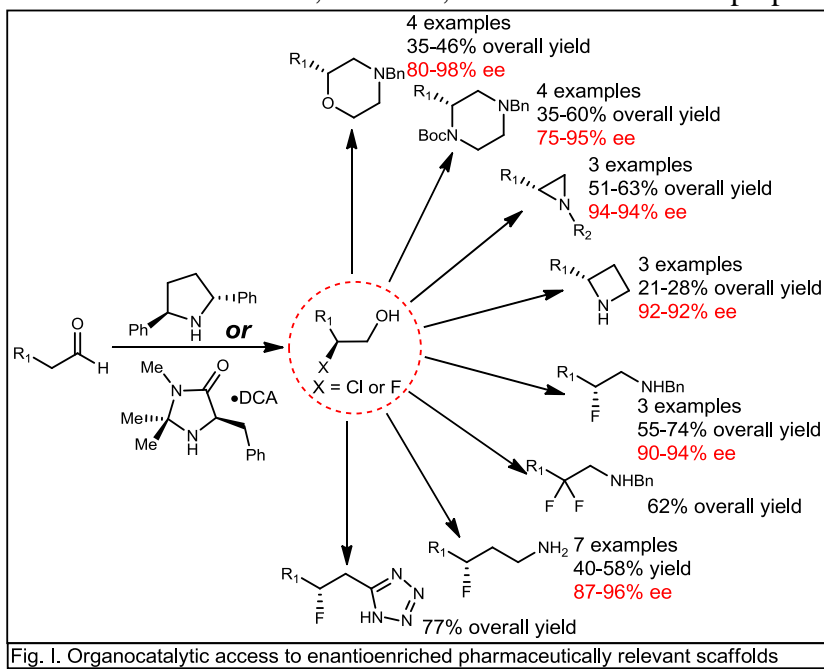
enantiomeric excess (**Fig. I**).[5–7] Importantly, these synthetic methods provide access to these enantioenriched scaffolds from achiral aldehydes, of which hundreds are commercially available. In a similar vein, I found that organocatalytic asymmetric fluorination methods provide access to fluoro-aldehydes from achiral aldehydes. Fluorination is a common method used to improve a compounds metabolic stability, bioavailability, ancillary pharmacology profile, protein-ligand interactions, and CNS exposure.[8–10] Using organocatalysis to generate enantioenriched β-fluoro alcohols, I was able to utilize a general reaction pathway towards chiral fluorinated scaffolds of pharmaceutical relevance (**Fig. I**).[11] Of note, the chiral fluorinated scaffolds would have previously been accessed through alternate chemistry that is frequently plagued with low yields, rearrangements, and dehydration products. Our method offers a considerable advantage compared to past literature precedent.

(ii) Phospholipase D (PLD)—an enzyme that catalyzes the hydrolysis of phosphatidyl choline to phosphatidic acid (PA)—has two mammalian isoforms that share 53% sequence homology. PA is a lipid second messenger involved in various signaling cascades. Aberrant PLD activity—and atypical PA concentrations—have been implicated in a number of human diseases.[12] Until recently, there were no ways to chemically modulate either PLD isoenzyme selectively; therefore, it was difficult to distinguish between phenotypes driven by aberrant PLD1 or PLD2 activity. Prior to my work, a highly potent and selective PLD1 inhibitor was discovered in the Lindsley lab,[13,14] but PLD2 inhibitors with enhanced selectivity profiles remained highly desirable.[15,16] Therefore, I spearheaded a medicinal chemistry campaign to discover selective PLD2 inhibitors with improved physiochemical and DMPK properties. This effort produced compounds with enhanced potency and selectivity.[17] Moreover, a key

stereocenter was identified during the process that immensely increases PLD1 potency with

IC_{50} amplifications of 200 to 590-fold (**Fig. II**). Modifications to incorporate a pyridyl group

delivered the most selective PLD2 inhibitor, and the

scaffold was found to have significantly improved *in*

vivo properties compared to previous compounds (**Fig.**

II).[18] These lead compounds were screened in a wide

range of *in vitro* anticancer and antiviral assays and

were found to significantly affect pathogenic

phenotypes. My compounds are now being applied to

delineate the role of PLD2 function in various disease

states.

X = H, PLD1 IC_{50} > 20,000 nM
PLD2 IC_{50} = 355 nM
53-fold selective
X = CH_3 (*S*), PLD1 IC_{50} = 86 nM
PLD2 IC_{50} = 120 nM
X = CH_3 (*R*), PLD1 IC_{50} = 1,400 nM
PLD2 IC_{50} = 3,450 nM

PLD1 IC_{50} = 6 nM
PLD2 IC_{50} = 20 nM

PLD1 IC_{50} = 30,000 nM
PLD2 IC_{50} = 360 nM
80 fold selective
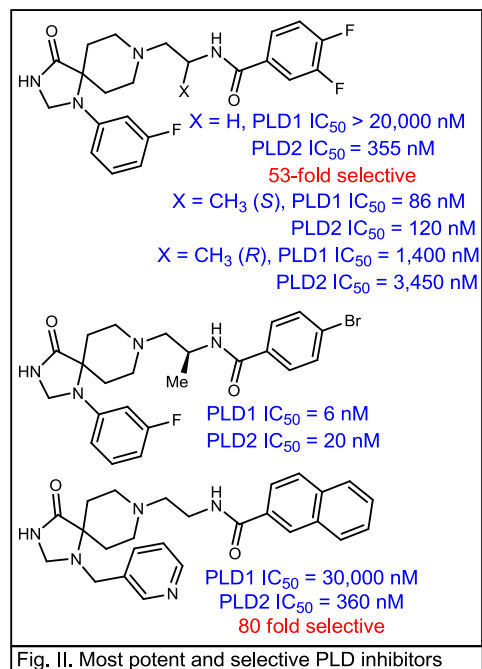
Fig. II. Most potent and selective PLD inhibitors

CHAPTER I

APPLICATION OF ORGANOCATALYSIS TO THE SYNTHESIS OF CHIRAL

MORPHOLINES, PIPERAZINES, AZIRIDINES, AZETIDINES,

β-FLUOROAMINES, AND γ-FLUOROAMINES

1.1 Access to chiral, C2-functionalized morpholines and piperazines from prochiral aldehydes using organocatalysis

1.1.1 Privileged structures in drug discovery

Throughout the process of modern drug discovery, a key observation was made involving different chemical scaffolds. While some small molecule chemotypes were found to be highly selective for a single target of interest, other scaffold types were promiscuous. In essence, compounds derived from promiscuous scaffolds were not always active on a single biological target; instead, compound libraries derived from promiscuous scaffolds were capable of acting as ligands for a diverse array of biological targets. These promiscuous scaffolds were termed "privileged structures" by Evans in the late 1980s,[1] and while the initial work dealt solely with the benzodiazepine scaffold, that work has expanded to a large assortment of small organic molecules that have been validated as privileged structures.[2,3] Privileged structures are widely utilized in the drug discovery process because while the core of the privileged structure provides activity at a range of biological targets, substitution to the scaffold can enable selective activity at targets of therapeutic relevance.[2,3] For instance, piperazine **1.1**—a frequently utilized privileged structure—can be elaborated to Dropropizine

1.2, Fleroxacin **1.3**, or Mepiprazole **1.4**, showing the piperazine privileged structure to induce antitussive, antibacterial, and tranquilizer effects respectively (**Figure 1.1.1.1**).
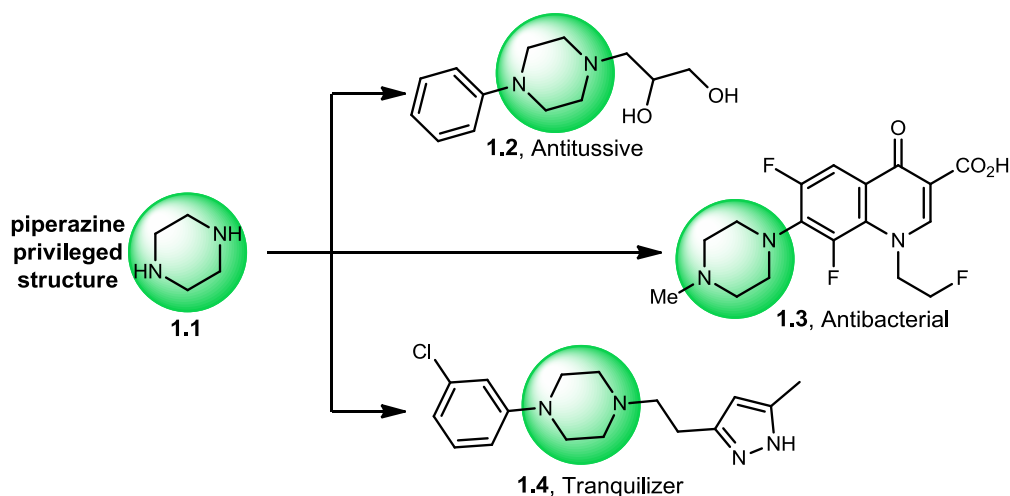
Figure 1.1.1.1 Piperazines illustrating the diverse bioactivity of priviliged structures

If the Molecular Design Limited Drug Data Report (MDDR), a database containing biologically active compounds from the journal and patent literature, is consulted, it provides additional evidence for the idea of privileged structures. For piperazines specifically, the database found 2,271 *N*-aryl piperazine scaffolds with broad bioactive properties. This expansive set of piperazine molecules includes 16 FDA approved pharmaceuticals and 23 piperazines in phase II or III clinical trials.[4] Compounds derived from this privileged structure cover 18 therapeutic indications, showing the piperazine moiety to be active at a wide range of therapeutic targets. One additional advantage of utilizing privileged structures in the search for novel drugs and probe compounds involves their validated *in vivo* properties. Essentially, since privileged structures are a key moiety in a large number of approved drugs, that illustrates their chemotypes have the inherent physical properties biasing them towards optimal compound absorption, distribution, and circulation, which will likely provide these molecules access to the desired biological target of interest.

Since compounds based on privileged structures can be biologically active at more than one target, it is important that chemists have the synthetic means of providing these molecules with any desired molecular framework. Indeed, synthetic means of selectively accessing different enantiomers, diastereomers, or regioisomers of the desired compounds are necessary to make the promiscuous privileged structure selective for the target of interest. Morpholines and piperazines are two privileged structures that, despite their presence in a large assortment of approved pharmaceuticals, lack a general asymmetric approach for synthesis. A considerable portion of my dissertation involved developing a common approach to synthesize chiral, C2-functionalized morpholines and piperazines from prochiral aldehydes.

1.1.2 Biological significance of morpholines and piperazines

Morpholines and piperazines are 6-membered heterocycles with either an oxygen or nitrogen in the 1 and 4 positions of the ring (**Figure 1.1.2.1**). The biological activity of morpholine and piperazine based scaffolds is extremely diverse;[4,5] an incomplete sampling of their pharmaceutical applications show morpholines and piperazines to be a key chemical moiety in antidepressants **1.5**,[6] antibiotics **1.6**,[7] antipsychotics **1.7**,[8] anticancer agents **1.8**,[9] and antihypertensive agents **1.9** (**Figure 1.1.2.1**)[10].
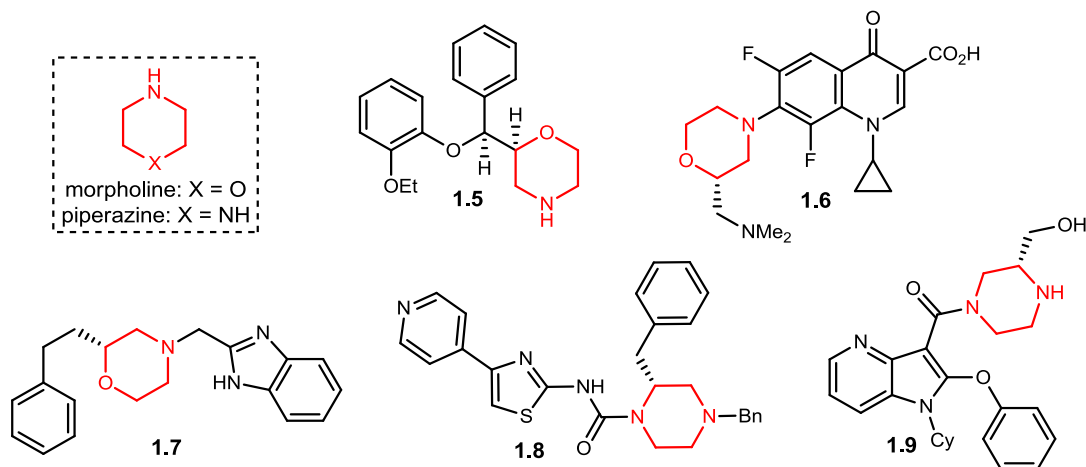
Figure 1.1.2.1 Examples of biologically active C-2 substituted morpholines and piperazines

While **Figure 1.1.2.1** shows examples of biologically active chiral, carbon substituted morpholines and piperazines, this class of privileged structures is underrepresented in approved drugs. In fact, FDA approved morpholine and piperazine containing compounds are almost entirely restricted to those substituted only at the heteroatoms. These FDA approved drugs are mainly achiral, therefore, and this stems partially from the difficulty related to preparing these carbon substituted morpholines and piperazines as single enantiomers. Indeed, the patent literature is rife with carbon substituted morpholine and piperazine scaffolds synthesized, biologically tested, and patented as racemic mixtures.[11–13] This deficiency illustrates the need for novel synthetic methods of preparing morpholine and piperazine scaffolds as single enantiomers.

1.1.3 Synthetic precedent for carbon substituted morpholines

This section details the most successful synthetic methods to access chiral morpholines. When considering morpholines retrosynthetically, disconnections result between the heteroatoms and the neighboring carbons of the ring. Three possibilities result from these disconnections providing (**i**) an aminoalcohol and a bifunctional electrophile, (**ii**)

amine and alcohol functional groups each containing embedded electrophiles, or (**iii**) a

monosubstituted amine and a bifunctional electrophile containing an ether (**Figure 1.1.3.1**).
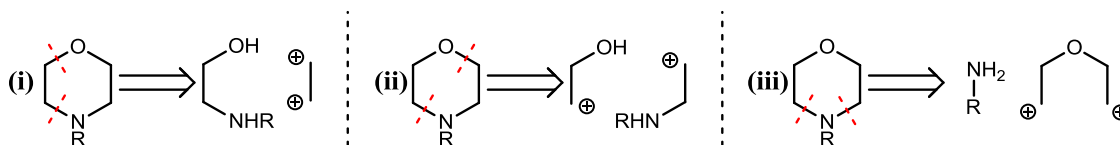
Figure 1.1.3.1 Retrosynthetic disconnections of morpholines

To synthesize morpholines as a single enantiomer, retrosynthetic disconnection (**i**) is the

most common. Indeed, chiral aminoalcohols are frequently commercially available since they

can be easily derived from chiral pool reagents. All amino acids are aminoalcohol precursors

after simple synthetic manipulations, so the field has taken advantage of the chiral pool when

in need of chiral morpholines. This approach, however, limits the supply of chiral

morpholines since they must be derived from available chiral aminoalcohols. An approach

not reliant on the chiral pool, therefore, would be advantageous.

The most useful method based on retrosynthetic disconnection (**i**) was developed in

2008 by Aggarwal and coworkers.[14] They developed a vinyl diphenyl sulfonium triflate salt

that reacts with aminoalcohols to generate morpholines in excellent yields. To generate the

salt, they performed a substitution reaction with diphenyl sulfide and the bromo

trifluoromethanesulfonate **1.10**. With bromide salt **1.11** in hand, an elimination reaction

afforded the vinyl diphenyl sulfonium triflate salt **1.12**, which is the reactive species driving

their morpholine forming method (**Scheme 1.1.3.1A**). With that reactive specie in hand,

chiral aminoalcohols **1.13** were added to the vinyl diphenyl sulfonium triflate salt **1.12** to

form morpholines **1.14** through an annulation reaction (**Scheme 1.1.3.1B**).
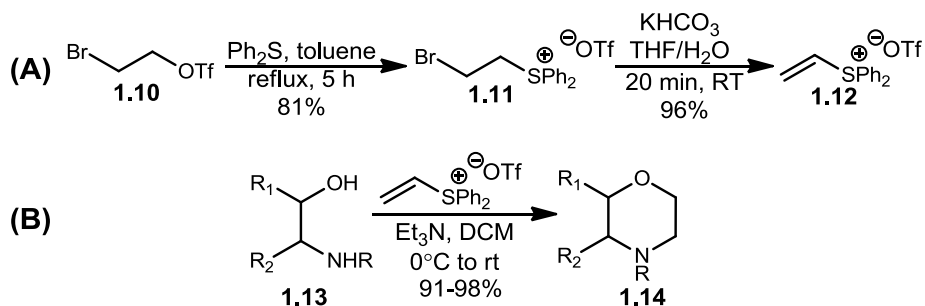
Scheme 1.1.3.1 (a) Synthesis of vinyl diphenyl sulfonium triflate salt (b) Use of salt to synthesize carbon substituted morpholines. Scheme adapted from ref 14.

Mechanistically, the diphenyl sulfonium triflate salt is proposed to act as a Michael acceptor while the disubstituted amine adds as a nucleophile to the β-position. This forms an ylide which takes part in a proton transfer with the hydroxyl group. That hydroxyl anion can then nucleophilically displace diphenyl sulfide by way of an intramolecular backside attack, forming the morpholine product as a result (**Scheme 1.1.3.2**).

pseudo conjugate addition   ylide proton transfer   intramolecular backside attack   morpholine product
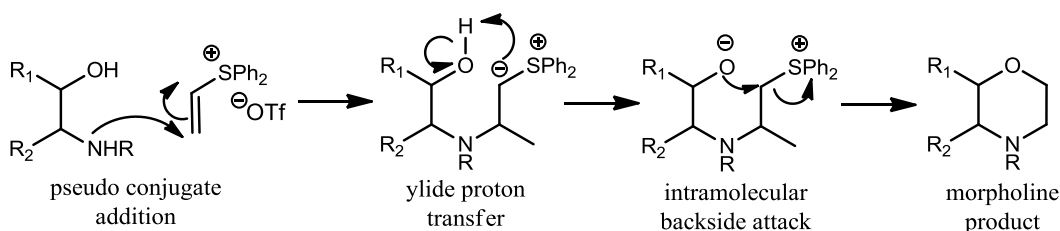
Scheme 1.1.3.2 Proposed mechanistic pathway to morpholines. Scheme adapted from ref 14.

One of the subtle drawbacks of this method was the instability of the vinyl diphenyl sulfonium triflate salt **1.12**. It is sensitive to decomposition, especially on large scale. To remove this liability, Aggarwal and coworkers improved their method to utilize the bromide salt **1.11**—a stable crystalline compound—in the morpholine forming reaction. They substitute sodium hydride for triethylamine in the last step of their sequence, which facilitates elimination to the vinyl diphenyl sulfonium triflate salt **1.12** *in situ* prior to the aminoalcohol annulation.[15]

While this method employing the vinyl diphenyl sulfonium triflate salt has been widely utilized to efficiently prepare morpholines, it lacks any asymmetric steps. Preparation of an enantioenriched morpholine, therefore, relies on the ability to obtain it from the chiral pool. This limits the broad accessibility of morpholine substrates to what one can find commercially, which is the major liability of this successful method.

Myers and coworkers utilized retrosynthetic disconnection (**ii**) while accessing morpholines.[16] Following those disconnection, they envisioned access to chiral morpholines using a chiral epoxide and aminoalcohol after various synthetic manipulations (**Figure 1.1.3.2**).
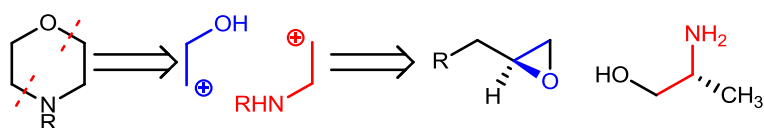
Figure 1.1.3.2 Morpholine retrosynthetic disconnections

To bring this envisioned route to fruition, chiral epoxide **1.15** was nucleophilically opened by alanine derived chiral aminoalcohol **1.16** to furnish diol **1.17** in 99% yield. The amine had to be protected with a tosyl group to eliminate unwanted reactions in future steps, and this synthetic manipulation afforded the tosyl trisubstituted amine **1.18** in 77% yield. Sodium hydride and tosyl imidazole was then utilized to promote sulfonylation of the primary alcohol and displacement of that tosyl leaving group with the chiral secondary alcohol to provide morpholine **1.19** in near quantitative yield. Removal of the tosyl group was then enacted with sodium in liquid ammonia to provide the desired, unprotected, chiral morpholine **1.20** in quantitative yield (**Scheme 1.1.3.3**).[16]
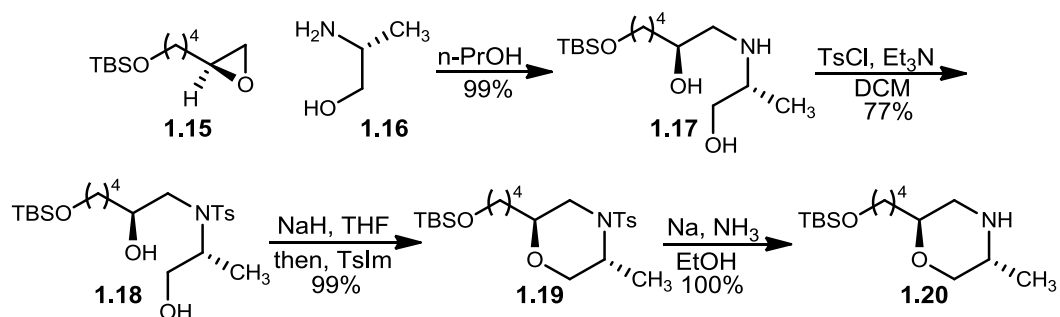
Scheme 1.1.3.3 Synthetic route to carbon substituted morpholines. Scheme adapted from ref. 16

While this method provided chiral morpholine **1.20** in an excellent 75% overall yield, there were some deficiencies when the reactions were utilized with different substrates. Specifically, when the reaction sequence was attempted with phenyl or benzyl substituted aminoalcohols, it was ineffective and modifications to the route were necessary to provide the corresponding morpholines. Even with the route modifications, the morpholine substrates were still prepared in high overall yield; however, the method cannot be considered general if it needs to be modified for substrates with slight modifications and only three morpholine substrates were synthesized in the letter. Additionally, this method does not generate asymmetry since all the chirality in the product morpholine is derived from the chiral epoxide and chiral aminoalcohol. Akin to the method using the vinyl diphenyl sulfonium triflate salt, this method is dependent on the chiral pool of reagents and/or methods to obtain chiral epoxides. With the limitations noted, this powerful method generates morpholines in high yields with preservation of chirality, enabling access to optically active morpholines.[16]

Retrosynthetic disconnection (**iii**) is least common among methods to generate morpholines, but it is possible to use sugar derivatives and primary amines to generate chiral morpholines. Overhand and coworkers utilized D-ribose to arrive at the elaborated azido acetal starting material **1.21** in 57% overall yield. At that stage, they cleaved the acetal with

hydrochloric acid in 82% yield, and cleaved diol **1.22** to dial **1.23** in 95% yield, which was in equilibrium with the hemiacetal **1.24**. This species underwent a double reductive amination with an assortment of primary amines to fashion morpholine type **1.25** in poor to moderate yields.[17] This reaction manifold can tolerate various sugar starting materials and amines, providing access to various morpholines through this reaction pathway (**Scheme 1.1.3.4**).
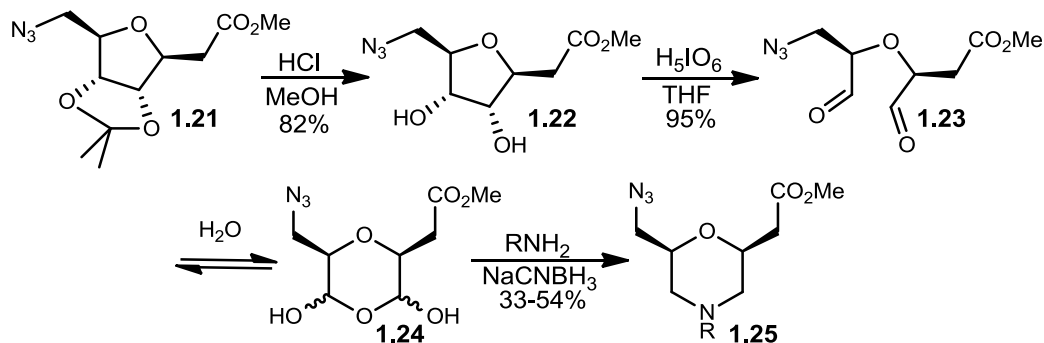
Scheme 1.1.3.4 Synthetic route to sugar derived chiral morpholines. Scheme adapted from ref 17.

This method suffers from a number of shortcomings. Low yields in the final step make this approach difficult to generate large quantities of the morpholines, and the approach requires more steps when compared to other existing methods. This reaction pathway—and all methods reviewed—rely heavily on the chiral pool. Therefore, the substitution pattern and absolute configuration is determined at the outset by the commercially available chiral sugars.

It is clear that a common method of accessing carbon substituted optically active morpholines would be advantageous for synthetic chemists. The methods highlighted are state of the art, but it is obvious that they share a common deficiency. Namely, they all rely on optically active precursors to provide the chiral building blocks that will lead to chiral morpholines. Additionally, most of these methods are solely for morpholines (Aggarwal and coworkers showed their method can be applied to piperazines[14]), and it would be

advantageous to have a common method to apply for both morpholines and piperazines, since these types of scaffold are privileged structures known to have diverse biological activities. Before detailing our progress making common methods to synthesize morpholines and piperazines, a short discussion of known methods of chiral piperazine synthesis will be discussed.

1.1.4   Synthetic precedent for carbon substituted piperazines

Just as the methods for chiral morpholine synthesis largely rely on the chiral pool, the same pattern holds true for chiral piperazine synthesis. Essentially every method that makes carbon functionalized piperazines use precursors from the chiral pool. Additionally, piperazine synthesis frequently uses amino acids and results in diketopiperazines. If the piperazine is desired, therefore, the diketopiperazines must undergo additional functional group interconversions that can complicate synthesis. The most common, state of the art, and relevant methods of piperazine synthesis will be explored.

The Ugi reaction is a one pot, four component reaction utilizing an acid, aldehyde, amine, and isonitrile. This method has been employed to make diverse libraries of diketopiperazines since any of the four components can be altered to yield a different reaction product. Campbell and coworkers used a resin to make this reaction sequence extraordinarily facile.[18] The amine **1.26** was coupled to an insoluble resin, and through sequential addition of the aldehyde **1.27**, isonitrile **1.28**, and acid **1.29**, Boc protected amine **1.30** is produced. This acyclic substrate was treated with acid to cleave the Boc group, and refluxing in toluene allowed for cyclization with concomitant cleavage from the resin to form diketopiperazines **1.31** (**Scheme 1.1.4.1**).
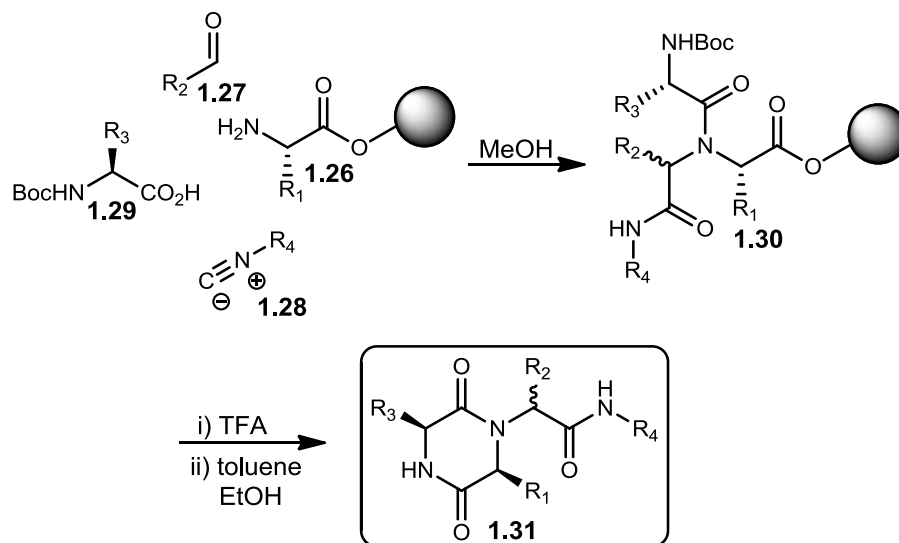
Scheme 1.1.4.1 Resin bound Ugi reaction to prepare piperazine libraries. Scheme adapted from ref 18.

This procedure allows access to chiral diketopiperazines that could be further reduced to form piperazines. Unfortunately, this—and essentially all Ugi processes—result in mixtures of stereoisomers. Different Ugi reaction protocols have been created to access many types of diketopiperazines, [19–21] but any enantioenrichment is a result of using chiral pool reagents, which limits the scope of these methods.

An additional method by Husson and coworkers makes use of a chiral auxiliary to ultimately obtain an enantioenriched piperazine. The ketopiperazine, with the chiral auxiliary on the amide nitrogen, is deprotonated to form an enolate, which can alkylate in high diastereomeric excess.[22] To synthesize the ketopiperazines to be used in asymmetric *C*-alkylation, chiral aminoalcohol **1.32** and Boc-glycine **1.33** were coupled using standard amide coupling conditions in 95% yield to obtain amide **1.34**. The amide was reduced to a disubstituted amine and the alcohol was protected as silyl ether **1.35** in 70% yield. Bromoacetic acid was coupled to disubstituted amine **1.35** to obtain trisubstituted amine **1.36** in 80% yield, and the material was subjected to a base induced cyclization and silyl ether

cleavage to afford ketopiperazines **1.37** in 64% yield, which is the substrate for the asymmetric *C*-alkylation. The enolate was formed with ^{t}BuLi, and it was reacted with methyl iodide, benzyl bromide, and allyl bromide forming those chiral ketopiperazines **1.38** in yields from 60-80% and all greater than 95:5 dr (**Scheme 1.1.4.2**).
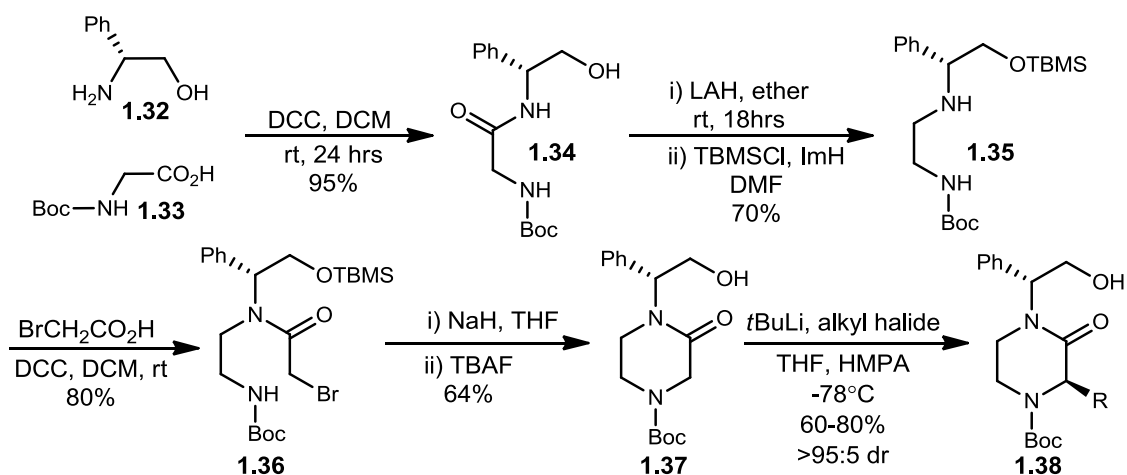
Scheme 1.1.4.2 Approach to chiral piperazines using a chiral auxiliary. Scheme adapted from ref 22.

Chiral ketopiperazines **1.38** are essentially differentially protected since the chiral auxiliary can be removed under reductive conditions and the Boc group can be removed with acid. Reduction of the amide would provide the chiral piperazine, an elusive chiral privileged structure. Unfortunately, this method is not without its deficiencies. It cannot be considered general since only three substrates were made, and the product must be modified reductively to arrive at the chiral piperazine. Additionally, a method would be desirable that required far less forcing conditions in the last step. With all of those considerations stated, this is a viable route to a number of enantioenriched piperazines following chiral auxiliary cleavage.

While the previous method allows for enantioenriched material to be prepared, a number of groups have applied a palladium catalyzed carboamination reaction to rapidly prepare piperazines in high dr.[23,24] Wolfe and coworkers begin with chiral Boc-amino acids

1.39 and couple disubstituted allyl amines, reducing the resultant amide to the diamine **1.40** in moderate yields. The Boc group is cleaved with acid and the amine is coupled to an aryl group under Buchwald-Hartwig conditions to furnish the aniline **1.41** in moderate yields. A final diastereoselective carboamination reaction with migratory insertion into the alkene provided *cis*-piperazine **1.42** in excellent dr (**Scheme 1.1.4.3**).
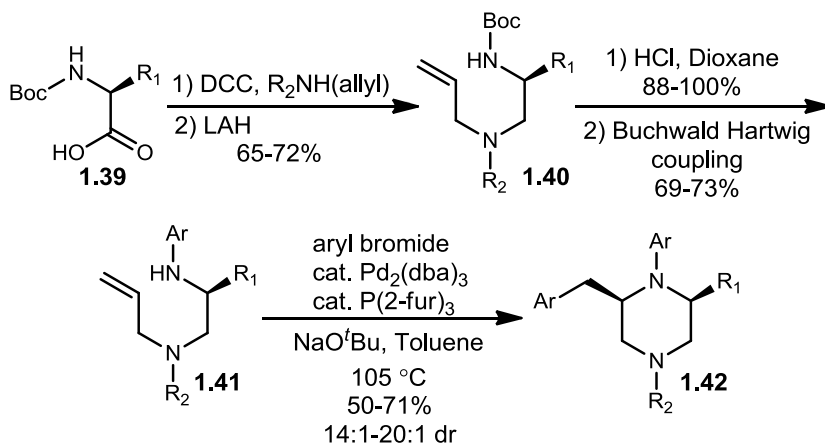
Scheme 1.1.4.3 Approach to *cis* chiral piperazines via carboamination. Scheme adapted from ref 23.

This approach is limited by the substituents that are necessary in each position, and it can only make *cis*-disubstituted *N*-aryl piperazines. The final configuration, once again, is set by the stereocenter present in the chiral starting materials. We can consider this approach, therefore, reliant on the chiral pool to induce its desired stereochemistry.

An additional carboamination approach was discovered by Michael and coworkers. Unlike the chemistry above resulting in favored diequatorial stereochemistry, this carboamination chemistry results in axial and equatorial substituents.[24] Opening of sulfamidate **1.43** with allylamine and cleavage of the sulfamic acid provided diamine **1.44** in good yields. Similar to the previous method, palladium mediated hydroamination—using these specific protecting groups—provides the *trans* disubstituted piperazine **1.45** in excellent yield and good to excellent diastereoselectivity (**Scheme 1.1.4.4**).

13
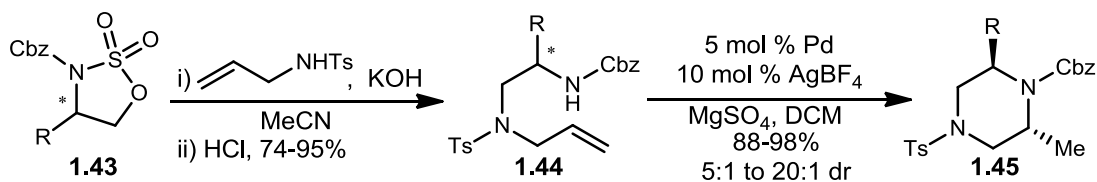
Scheme 1.1.4.4 Approach to *trans* chiral piperazines via carboamination. Scheme adapted from ref 24.

A crystal structure was procured of the *trans*-dimethyl piperazine, and it had adopted the twist-boat conformation. While this conformation is usually disfavored in a cyclohexane by 5.3 kcal/mol,[25] that value would be slightly less for a piperazine with partially sp^2 hybridized heteroatoms as part of the ring system. Additionally, the Cbz protecting group experiences allylic strain with the methyl groups in the chair conformation, shifting the equilibrium toward the more favorable twist-boat (**Figure 1.1.4.1**).
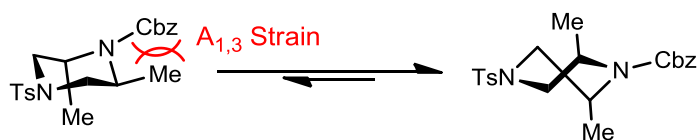
Figure 1.1.4.1 Chair to twist-boat ring flip

While this additional method of synthesizing piperazines increases the substrate scope available using current methods, it also relies on the chiral pool to generate its diastereoselectivity, and its substrate scope is limited.[24]

All things considered, there are available methods to obtain piperazines, but they all rely on either the chiral pool or chiral auxiliaries to drive their stereoselectivity.[26–30] We can clearly state, therefore, that various methods exist to access both morpholines and piperazines in the literature. The precedent for forming these privileged structures, however, is limited to specific substitution patterns and is fragmented into discrete methodologies to access either morpholines or piperazines using the chiral pool. Thus, we determined this area was ripe for

the development of a general new methodology with a unified approach toward chiral morpholines and piperazines starting from achiral materials.

1.1.5 Envisioned rationale to access chiral morpholines and piperazines

The Jørgensen and MacMillan groups concurrently discovered an organocatalytic method to asymmetrically chlorinate aldehydes.[31,32] The research groups used different small molecule amine containing organic catalysts that could be used substoichiometrically. These amines work by condensing on the aldehyde to form an enamine, which enantioselectively chlorinates by way of electrophilic chloride sources, and hydrolysis of the organocatalyst imine provides the free catalyst and the α-chloro aldehyde (**Figure 1.1.5.1A**). This reaction system is clean and efficient yielding the chloroaldehyde product in high yield and excellent enantiomeric excess (ee). Lindsley and coworkers applied the α-chlorination technology while developing a one-pot synthesis of aziridines (**Figure 1.1.5.1B**).[33] Their method utilizes
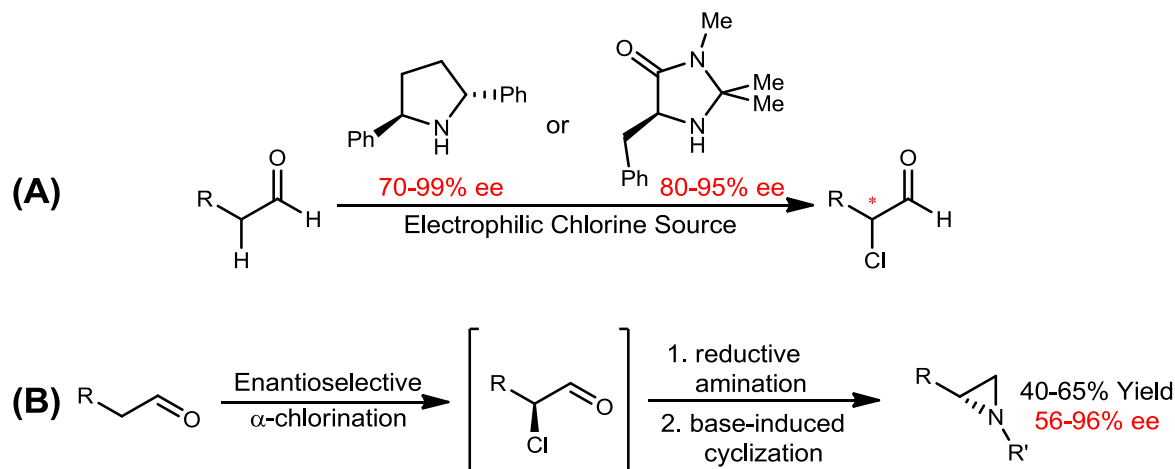
Figure 1.1.5.1 (a) Jørgensen and MacMillan's methods to enantioselectively chlorinate aldehydes (b) Lindsley methodology to form chiral aziridines from aldehydes. Figure adapted from ref 23 and 24.

the α-chloroaldehyde as a bifunctional electrophile. In the method, a monosubstituted amine undergoes a reductive amination with the aldehyde functionality followed by a stereospecific

backside intramolecular displacement inverting the stereocenter. This reaction cascade delivered aziridines in good overall yields and moderate to excellent enantioselectivity.[33]

While considering the asymmetric synthesis of morpholines and piperazines from achiral precursors, we reasoned the α-chloroaldehyde could be used as a chiral bifunctional electrophile that could be reacted with aminoalcohols or diamines to fashion C-functionalized morpholines and piperazines (**Scheme 1.1.5.1A**). Indeed, we envisioned enantioselectively chlorinating achiral aldehydes **1.46** using diphenylpyrrolidine catalyst **1.47** to arrive at α-chloroaldehydes **1.48**. An aminoalcohol or diamine would be used to perform a chemoselective reductive amination fashioning β-chloro aminoalcohols or β-chloro diamines **1.49**. Next, we would develop conditions to facilitate the 6-*exo-tet* cyclization providing the desired chiral morpholines or piperazines **1.50** (**Scheme 1.1.5.1B**).
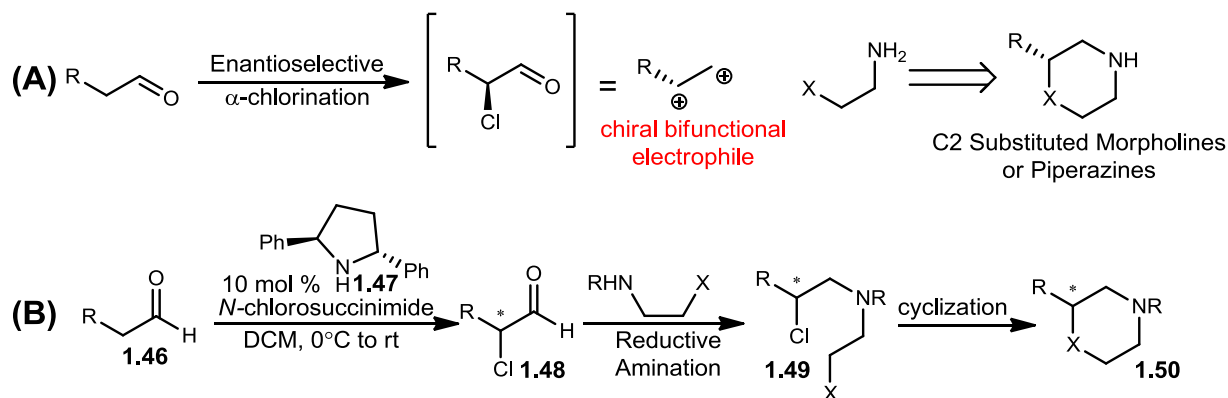
Scheme 1.1.5.1 (a) Envisioned use of the a chloroaldehyde as a bifunctional electrophile (b) Proposed synthetic route to chiral morpholines and piperazines

We determined this route to be desirable and advantageous compared to state of the art methods because (i) morpholines and piperazines could be synthesized following a common method, (ii) chiral precursors are not necessary to fashion enantioenriched morpholines and piperazines since any achiral aldehyde can be used, and (iii) an organocatalytic approach is favorable compared to approaches utilizing chiral auxiliaries or the chiral pool.

1.1.6 General access to chiral C2 substituted morpholines and piperazines—1st generation method

To follow our envisioned method for access to chiral C2 substituted morpholines and piperazines, we began the reaction sequence using a racemic proline catalyst. Racemic proline facilitated the aldehyde chlorination giving a racemic mixture of the α-chloroaldehyde, which was used in subsequent reactions to validate the reaction pathway. Additionally, the racemic compound allowed chiral separatory conditions to be discovered using chiral supercritical fluid chromatography (SFC), which were necessary for later determinations of % ee. Since our lab was able to utilize a similar reaction pathway to synthesize chiral aziridines in a one pot protocol only requiring purification at the last step,[33] we began these studies attempting to generate conditions where only a single purification step was necessary. We began our studies with dodecanal **1.51**, which was chlorinated with DL-proline and *N*-chlorosuccinimide in DCM (**Scheme 1.1.6.1**). Addition of pentanes and cold filtration provided the racemic α-chloroaldehyde **1.52** in relatively high purity, which was subjected to reductive amination conditions developed for the aziridine chemistry.[33] After workup, the reductive amination product was subjected to basic cyclization conditions in polar aprotic solvents to furnish morpholine **1.53**.
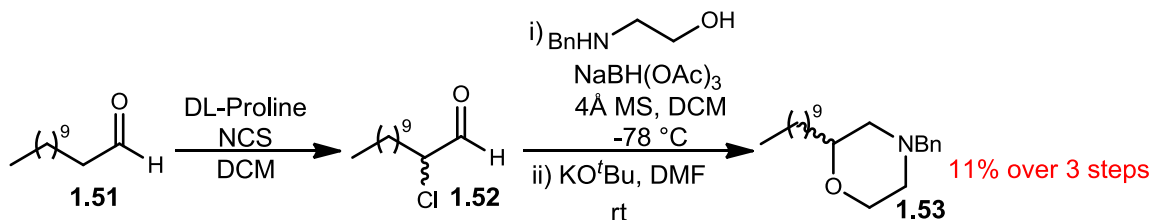
Scheme 1.1.6.1 Preliminary one pot approach to morpholine synthesis. Scheme adapted from ref 34.

While isolation of product morpholine **1.53** from the reaction sequence was encouraging, significant optimization was necessary to improve the 11% overall yield. At this point, effort

transitioned to analysis of each step in the reaction sequence to potentially improve the overall yield.

Regarding the asymmetric chlorination step of the reaction sequence, our research group spent great effort extensively screening organocatalysts to ensure that the diphenyl pyrrolidine catalyst was ideal.[33] To ensure that the use of racemic proline was not responsible for the low overall yield, 5-phenyl pentanal **1.54** was chlorinated under standard reaction conditions using DL-proline. Following the aforementioned cold pentanes wash and filtration, which removed insoluble succinimide and proline, we found that the α-chloroaldehyde **1.55** was produced in 90% yield and was effectively pure for successive reactions (**Scheme 1.1.6.2**).
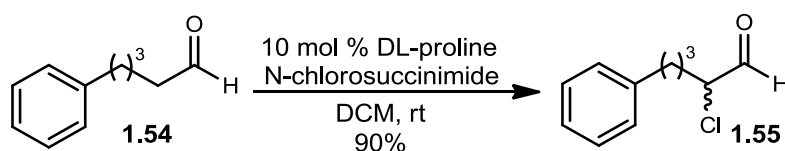
Scheme 1.1.6.2 Optimization of the racemic α-chlorination

Moving our efforts to examine the reductive amination of the chloroaldehyde, we found that analysis of the reaction by TLC and ^{1}H NMR showed complete consumption of the starting material. Upon aqueous workup and column chromatography, however, an excess of 30% of the starting material aldehyde was isolated. Since consumption of the chloroaldehyde was observed using ^{1}H NMR, through disappearance of the characteristic aldehyde peak, we reasoned that it must be temporarily transformed into a chemical species distinct by TLC and ^{1}H NMR analysis. The aldehyde, therefore, could be reformed from this distinct species during the process of aqueous workup and flash column chromatography. We proposed that the presumed iminium ion **1.56** that forms in the first step of the reaction could have two simultaneous mechanistic pathways, one of which would act to mask the aldehyde

as a different functionality. Essentially, the expected pathway consists of a hydride from sodium triacetoxyborohydride adding to the iminium ion to provide the desired β-chloro aminoalcohol **1.57**. The undesirable pathway, we proposed, involved the tethered ethanol moiety acting as a latent nucleophile, which could add to the iminium ion to form oxazolidine **1.58**. This reaction pathway was confirmed by ^{1}H NMR of the crude material. The oxazolidine proton, indicated in **Scheme 1.1.6.3**, was observed as doublets, consistent with the described theory.
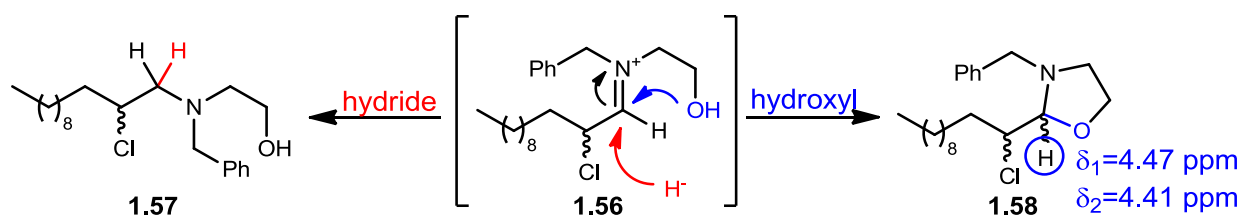
Scheme 1.1.6.3 Competing pathways intercept reactive iminium ion. Scheme adapted from ref 34.

Since greater than 30% of our material was being shuttled to the oxazolidine during this reaction, alternative strategies or conditions were necessary to circumvent this problem. Two approaches were pursued to prevent formation of the oxazolidine. Silyl ether protection of ethanolamine's alcohol functionality would render the alcohol unreactive towards nucleophilic addition; therefore, the reductive amination was performed with TBS protected ethanolamine. Treatment of the silyl ether **1.59** with TBAF facilitated cleavage of the TBS group, affording the β-chloro aminoalcohol **1.60** in 45-65% yield over three steps from the aldehyde **1.46** (**Scheme 1.1.6.4**). While we were satisfied with the improved yield using the silyl protecting group, we also decided to seek alternative reductive amination conditions to obtain protecting group free conditions. In essence, we reasoned that oxazolidine byproduct **1.61** is in equilibrium with the iminium ion precursor **1.62**. If we could find conditions to catalyze the interconversion between these species, therefore, the iminium ion form should

19

be trapped by hydride addition. If this was the case, the reaction should be driven to completion as hydride addition reduces the iminium ion/oxazolidine species to the β-chloro aminoalcohol **1.60**.   After exhaustively screening conditions, sodium cyanoborohydride and acetic acid in THF was found to facilitate this transformation protecting group free in comparable yields, and the two step protocol was advantageous because it removed the previously necessary silyl cleavage step (**Scheme 1.1.6.4**). With the ideal reductive amination conditions in hand, efforts turned toward optimization of the cyclization transformation.
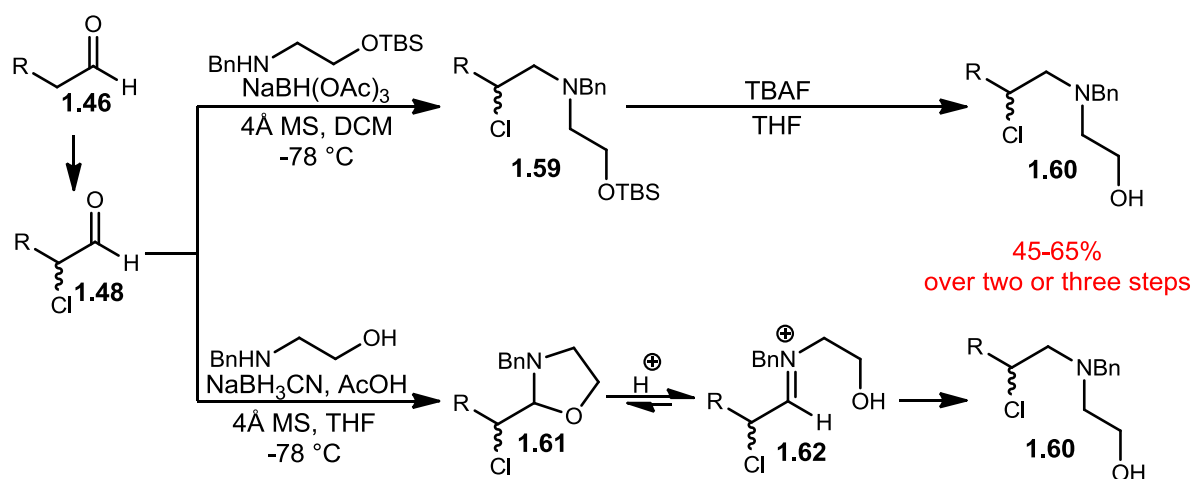
Scheme 1.1.6.4 Alternative routes to β-chloro aminoalcohols

Considering the final cyclization step toward morpholines, the original conditions (KO^{t}Bu, DMF, rt) led to full consumption of the starting material, but appreciable decomposition was noted. Before screening other conditions, we thought it prudent to examine those original conditions to determine what side products were forming. After examining the ^{1}H NMR of the crude material following aqueous workup, we observed a considerable amount of aldehyde. Because no aldehyde is present throughout the desired reaction, we considered side reactions that could produce aldehydes given the known reaction conditions (**Scheme 1.1.6.5**). We rationalized that a common reaction competing

20

with substitution is elimination, and deprotonating the hydrogen vicinal to the trisubstituted amine **1.60** to eliminate chloride forms an enamine **1.63**. Consequently, enamine **1.63** can protonate upon aqueous workup to form iminium ion **1.64**, which can hydrolyze to form aldehyde **1.46** and *N*-benzyl ethanolamine. This undesired reaction pathway explains the observed aldehyde, and by measuring the molar quantity of aldehyde formed we determined that greater than 30% of the starting material was shunted into this undesired reaction pathway.
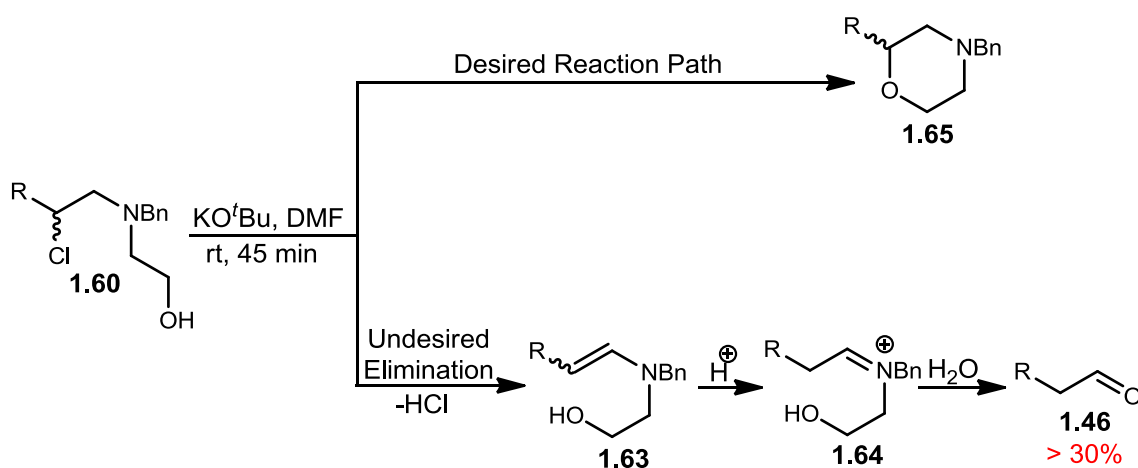
Scheme 1.1.6.5 Undesired aldehyde formation during basic cyclization

After extensively screening bases, solvents, and temperatures, we determined the optimal cyclization conditions to be five molar equivalents of KO^{t}Bu in acetonitrile at -20 ^{o}C.

We applied the optimized set of conditions to a limited substrate scope. The conditions successful converted achiral aldehydes into C2 substituted morpholines in moderate to excellent enantioselectivity (**Scheme 1.1.6.6**). Oddly, the racemic analogs had uniformly higher yields than their asymmetric cohorts. This may have been due to the initial chlorination being lower yielding. Moreover, the pentane wash was not as effective at removing the chiral catalyst compared to proline from the reaction. The diphenylpyrrolidine catalyst, therefore, could have competed in the reductive amination or caused other unwanted

side reactions. These issues aside, we were able to successfully convert achiral starting materials into chiral morpholines using this easy three step method.[34]
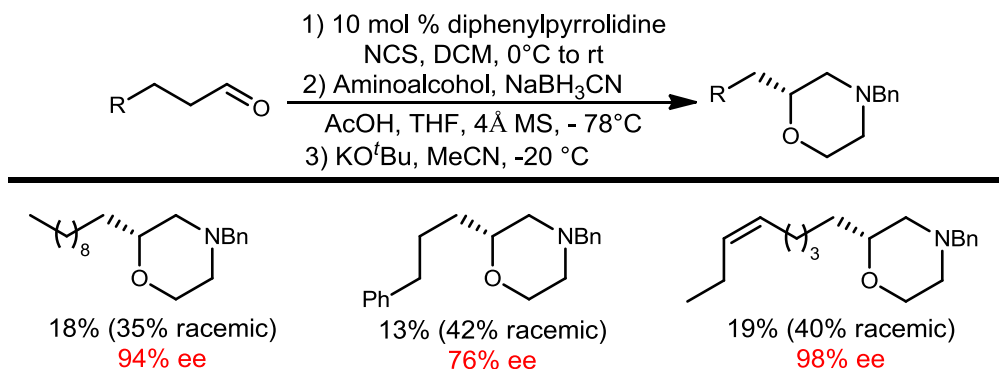
Scheme 1.1.6.6 Conditions for the synthesis of chiral C2 substituted morpholines. Scheme adapted from ref 34.

With this reaction sequence in hand, efforts now focused on applying it to the synthesis of chiral piperazines.

To apply the conditions developed for morpholines to piperazine synthesis, the ideal diamine source had to be chosen for the reductive amination, cyclization sequence. Related to that diamine choice, the final piperazine product, if synthesized for a medicinal chemistry project, may need to be derivatized on the differential amine components. To form a piperazine where further chemistry can be performed on the nitrogen atom of choice, the final piperazine—arising from the diamine—needs to be differentially protected, such that each protecting group can be removed selectively. To that end, ethylene diamine with Boc and benzyl protecting groups would allow for selective protecting group cleavage with acidic or reductive conditions respectively. This allows the piperazine products to take part in library synthesis with controlled access to either amine (**Figure 1.1.6.1**)
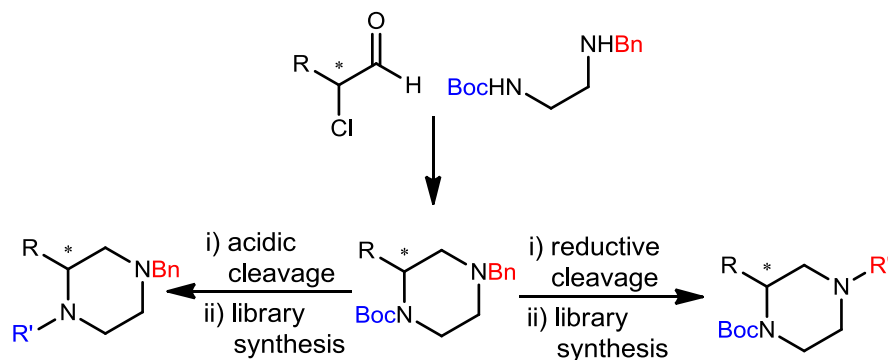
Figure 1.1.6.1 Diamine choice provides differential protection and cleavage potential

.

This diamine protecting group strategy distinguishes the amines by varying their nucleophilicity. Since the Boc protected amine has sp^2 character, it is less nucleophilic than the benzyl amine. This discrepancy in nucleophilicity allows the benzyl amine to participate chemoselectively in the reductive amination step without side reactions caused by the Boc amine. This permits the original reductive amination conditions to be utilized instead of the modified conditions used during morpholine synthesis. Using dodecanal **1.51** in the reaction protocol without column chromatography until piperazine **1.66**, we observed formation of the β-chloro diamine **1.67** by LC-MS, but the basic cyclization conditions optimized for morpholine synthesis were ineffective for piperazine synthesis (**Scheme 1.1.6.7**).
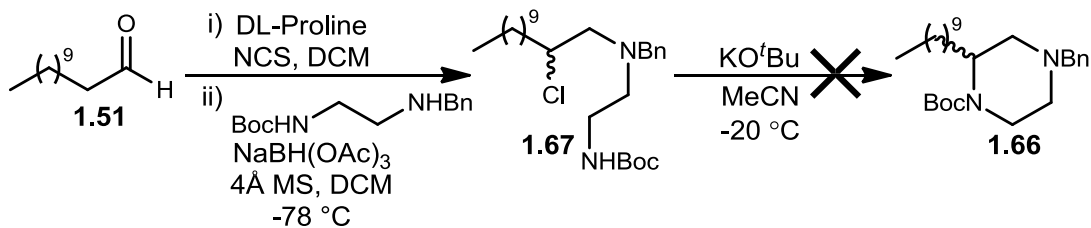
Scheme 1.1.6.7 Preliminary one pot approach to piperazine synthesis

While it would have been advantageous to have a single set of conditions for both morpholine and piperazine synthesis, it is not surprising that the cyclization of the Boc amine required different conditions compared to a hydroxyl group.

23

While we considered cleaving the Boc group prior to cyclization, which we reasoned would increase the nucleophilicity of the amine, potentially facilitating an *in situ* cyclization, we first screened cyclization conditions with the intact Boc amine. By simply varying the base and solvent, we found that changing from acetonitrile to DMF facilitated full conversion of the starting material (**Table 1.1.6.1**).
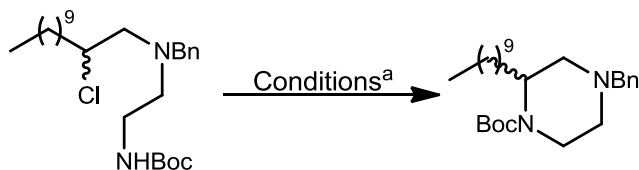
base	equivalents	solvent	conversion[b](%)
KO^{t}Bu	1.7	DMF	>99
KO^{t}Bu	1.7	MeCN	<50
KO^{t}Bu	1.7	THF	NDP
NaH	1.2	DMF	>70
NaH	1.2	MeCN	NDP
NaH	1.2	THF	NDP
KHMDS	1.2	MeCN	NDP
KHMDS	1.2	THF	NDP

[a]All reactions were run at room temperature for 16 hours at a concentration of 0.02 M. NDP = no desired product. [b]Conversion determined by LC/MS and ^{1}H NMR.

Table 1.1.6.1 Conditions screened for base induced cyclization

Through further optimization efforts, the best conditions were determined to be 5 equivalents of KO^{t}Bu in DMF at -20 ⁰C.

24

With ideal conditions in hand, the method was applied to several piperazine analogs (**Scheme 1.1.6.8**). The yields for the three step method of forming piperazines were uniformly better than for their analogous morpholines.
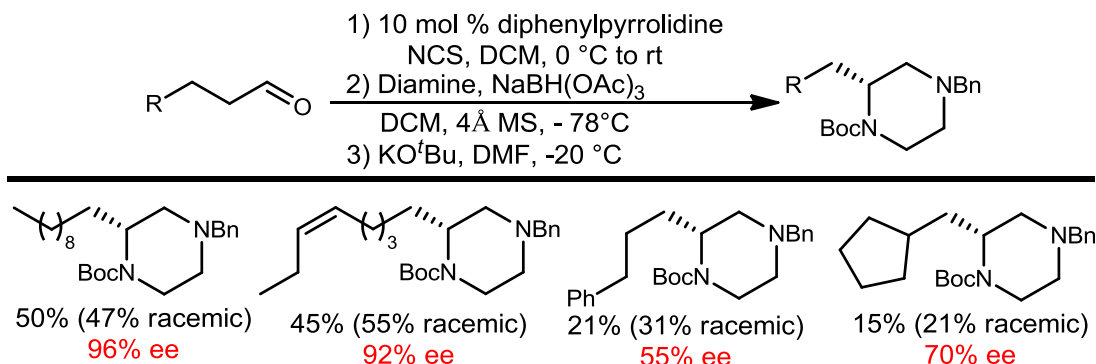
Scheme 1.1.6.8 Conditions for the synthesis of chiral C2 substituted differentially protected piperazines. Scheme adapted from ref 34.

This new methodology presents a unified approach toward both morpholines and piperazines and generates these scaffolds in moderate to excellent % ee. While the conditions to synthesize morpholines and piperazines are not exact, the method only varies (i) the hydride source and solvent in the reductive amination step and (ii) the solvent during the cyclization step. Importantly, the method allows highly enantioenriched chiral morpholines and piperazines to be synthesized from achiral aldehydes.

1.1.7   1st generation method review

After considering the state of the art methods to access morpholines and piperazines, we knew improvements could be made by developing a method that (i) did not rely on the chiral pool, (ii) did not utilize chiral auxiliaries, and (iii) was broadly applicable to morpholines and piperazines. Fortunately, since the method allowed chiral morpholines and piperazines to be synthesized from readily available achiral aldehydes, all of these conditions were met.[34] Additionally, the new method provided morpholines and piperazines with

handles that gave easy access to further derivatization. Cleavage of the benzyl or Boc protecting groups on either morpholines or piperazines could be performed in near quantitative yields, which provides easy access to library synthesis. With those clearly advantageous attributes of the new method noted, there were also numerous weaknesses. While the reaction cascade could be scaled up to generate gram quantities of the morpholines or piperazines, the 26% average overall yield was suboptimal. Moreover, variable enantioselectivity was a formidable problem. We attributed the variability to the acidity of the α-chloroaldehyde's α-proton, which is deprotonated during the keto/enol tautomerization, destroying the newly formed stereocenter. And finally, synthetic methods are best—and most often employed—when they lack extreme temperatures and long reaction times. Running the reductive amination at -78 °C overnight made this reaction sequence less desirable. Therefore, while we saw this method as a success that could be directly implemented in industry to generate molecular diversity in a hit-to-lead campaign, we knew that there were improvements that could be realized.

1.1.8 General access to chiral C2 substituted morpholines and piperazines—2nd generation method

To address the variable enantioselectivity of our previous method, we had to determine what was causing the problem. Based on literature precedent,[32] we knew that the chlorination was occurring in excellent enantioselectivity, but working with the chloroaldehyde resulted in decreased selectivity. We observed this while performing trials of our morpholine synthesis on the same substrate. Essentially, if the chloroaldehyde is not used immediately in the reductive amination, the % ee erodes. Experimentally, we have used dodecanal and made the resultant morpholine in 95% ee, but if α-chloro dodecanal is left at

room temperature for several hours we have observed the enantiomeric excess to decrease to 55% (**Figure 1.1.8.1**). We believed that excellent enantiomeric excess could be retained, therefore, that if the α-chloroaldehyde is simply used immediately after synthesis and kept at low temperatures. After performing the reaction sequence an additional four times with this experimental understanding, however, we observed the % ee to vary from 78-94% ee (**Figure 1.1.8.1**).
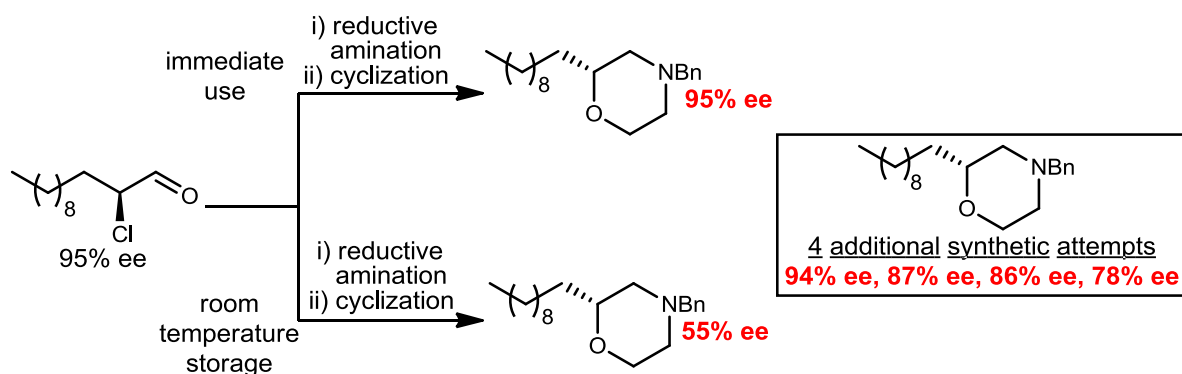
Figure 1.1.8.1 Variability in % ee derived from chloroaldehyde epimerization

To improve the method and remove the possibility for variable % ee, a modification to the reaction protocol was necessary. To address this issue while keeping the envisioned method in mind, we imagined modifying the α-chloro aldehyde to a different configurationally stable bifunctional electrophile (**Figure 1.1.8.2**). With this modification to the method, we could continue to use aminoalcohols or diamines to consecutively react with a single electrophilic unit.
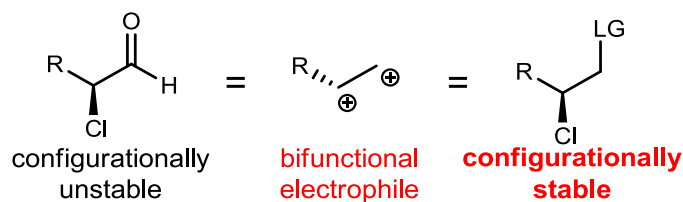
Figure 1.1.8.2 Envisioned plan to modify configurationally unstable α-chloro aldehyde to a β-chloro leaving group

27

Following this synthetic plan, we reasoned that reduction of α-chloro aldehydes to alcohols would provide (i) a new molecular species that was configurationally stable and (ii) a functional group allowing for facile modification to a wide variety of leaving groups. Since methanesulfonyl chloride is widely used to convert hydroxyl groups into leaving groups,[35] we reasoned that modification of β-chloro alcohols to β-chloro mesylates would provide a reactive intermediate capable of facilitating substitution reactions with aminoalcohols and/or diamines. To this end, dodecanal **1.51** was chlorinated, reduced to chloroalcohol **1.68**, and reacted with MsCl to provide β-chloromesylate **1.69**, which was stable to aqueous workup and column chromatography, in 80% overall yield (**Scheme 1.1.8.1**).
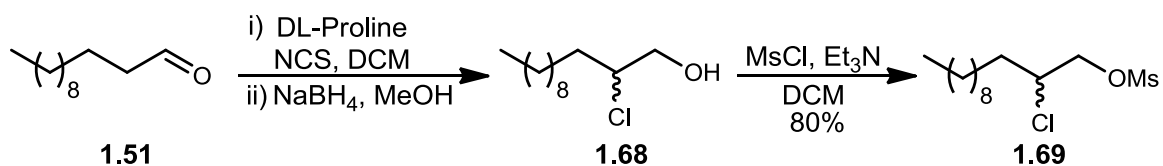
Scheme 1.1.8.1 Synthesis of chloromesylate

We reasoned this species could be the bifunctional electrophile necessary to facilitate alkylation with either aminoalcohols or diamines, and various solvent systems and temperatures were screened to facilitate this transformation (**Table 1.1.8.1**). Unfortunately, the β-chloromesylate—under all conditions screened —did not deliver the desired product. It was either unreactive showing no reaction progress at room temperature or the material decomposed to a complex mixture of products when enough energy was applied. All things considered, since the β-chloro mesylate gave way to no desired products under classical alkylation conditions, we turned our efforts to the synthesis of other bifunctional electrophiles to slightly perturb the reactivity of the system.

$\text{(CH}_2)_8$ ...OMs →(conditions[a])→ $\text{(CH}_2)_8$ ...NBn, Cl, NHBoc
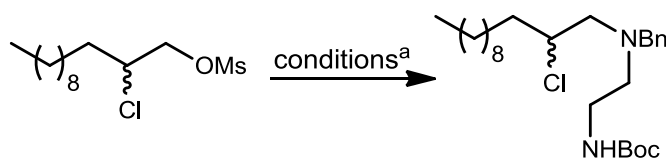
Solvent	Temperature	Conversion[b]
DMF	24	none
MeCN	24	none
THF	24	none
THF/DMF	24	none
DMF	100	decomposition
MeCN	100	decomposition
THF	100	none
THF/DMF	100	decomposition

[a]All reactions were run with 1.5 eq. diamine, 5 eq. K_2CO_3 at 0.1 M for 16 hours.
[b]Conversion determined by LC-MS, TLC and ^{1}H NMR

Table 1.1.8.1 Conditions screened to displace mesylate with diamine

Transforming the β-chloroalcohol to β-chlorohalides retained the same reactivity patterns as the aforementioned β-chloromesylate. Therefore, we rationalized that a leaving group more reactive than the mesylate may be necessary to facilitate the desired reaction. By consulting the literature,[36] we saw that while mesylate and tosylate leaving groups have similar reactivity rates in substitution reactions, a chloride is far slower and a trifluoromethanesulfonate (triflate) leaving group is far more reactive (**Table 1.1.8.2**). Since halides and mesylates were not reactive enough for the desired substitution reaction with diamines, therefore, we reasoned that triflates may be suitable leaving groups to permit the desired reaction.

Leaving Group	k_{rel}
$CF_3SO_3^-$	1.4×10^8
p-toluenesolfonate	3.7×10^4
$CH_3SO_3^-$	3.0×10^4
Cl^-	1.0

Table 1.1.8.2 Relative reactivity rates in substitution reactions. Data from ref 36.

Gratifyingly, we were able to develop a one-pot reaction to form the triflate from β-chloroalcohols and displace the triflate *in situ* with either a differentially protected diamine or *N*-benzyl ethanolamine. At this point, the β-chloro aminoalcohols or β-chloro diamines were identical to those developed using the 1st generation method, so base mediated cyclization was possible using the same conditions. To show the new methods utility—and superiority compared to the last method—we prepared several chiral β-chloroalcohols (**Scheme 1.1.8.2**).[32,37] Importantly, these chiral alcohols could be prepared from an enormous number of achiral readily available aldehydes. Treatment of these aldehydes **1.46** with the chiral organocatalyst **1.47** and electrophilic chlorine facilitated the transformation to the chiral α-chloro aldehyde **1.48**, and reduction of that aldehyde with NaBH$_4$ provided the configurationally stable β-chloro alcohols **1.70** in good yields (72-83%) with excellent asymmetric induction.
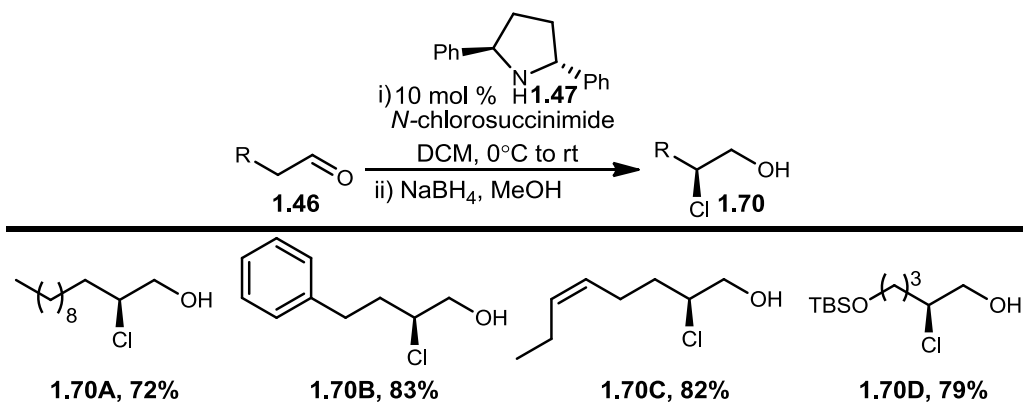
Scheme 1.1.8.2 Synthesis of chiral β-chloro alcohols. Scheme adapted from ref 37.

With the chloroalcohols in hand, we applied the newly developed displacement conditions. Triflic anhydride was added to the chloroalcohols **1.70** with 2,6-lutidine in DCM at -78 °C followed by the addition of either *N*-benzyl ethanolamine **1.71** or *N*-benzyl-*N'*-boc-ethylenediamine **1.72**, which were allowed to react overnight. These conditions facilitated β-chloro triflate formation followed by chemoselective alkylation in a one pot protocol giving

30

way to β-chloro aminoalcohols **1.73** or β-chloro diamines **1.74** in moderate to good yield (63-87%), delivering the intermediates one step away from chiral morpholines and piperazines (**Scheme 1.1.8.3**).
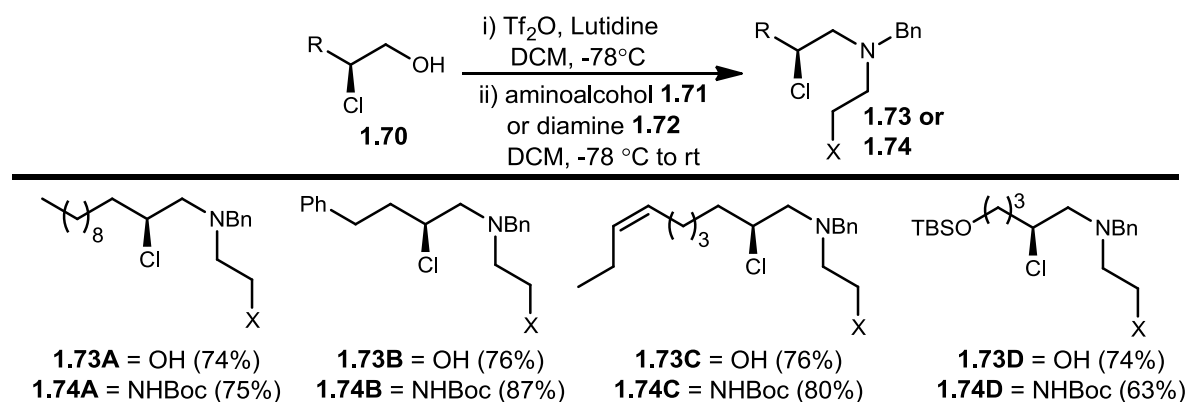
Scheme 1.1.8.3 Synthesis of chiral β- chloro aminoalcohols and β-chloro diamines. Scheme adapted from ref 37.

With substrates **1.73A-D** and **1.74A-D** in hand, we utilized our optimized cyclization conditions for morpholines (KO^{t}Bu, MeCN, -20 °C) and piperazines (KO^{t}Bu, DMF, -20 °C) generating C2-functionalized, chiral morpholines **1.75A-D** and piperazines **1.76A-D** in uniformly greater overall yield and enantioselectivity compared to the 1st generation method (**Scheme 1.1.8.4**).[34,37]
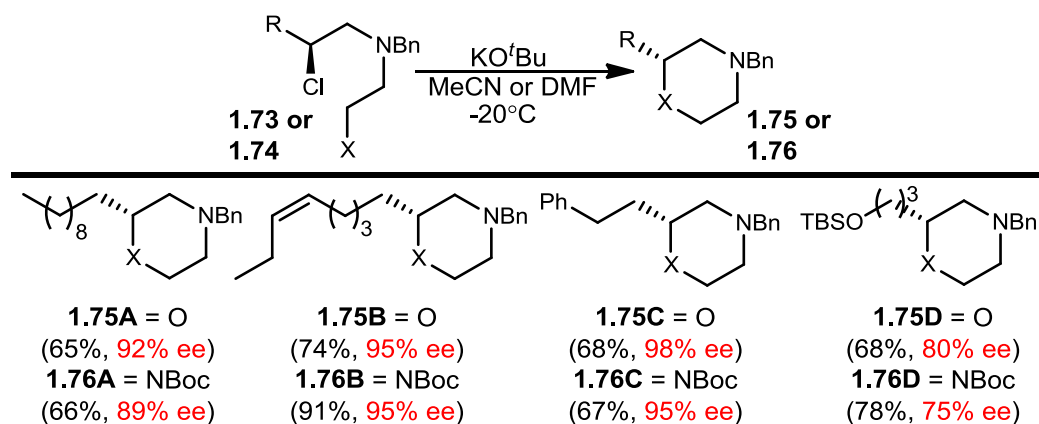
Scheme 1.1.8.4 Synthesis of chiral morpholines and piperazines. Scheme adapted from ref 37.

Importantly, no % ee variability (less than experimental error) existed for individual substrates, illustrating the α-chloro aldehyde to be responsible for the % ee inconsistency during the 1st generation method. The only substrate where moderate enantioselectivity was problematic was the silyl ether morpholine and piperazine, and the lower % ee was due to the initial α-chlorination step, which was expected based on literature precedent.[32,38] Regarding the overall yields, this new method generates morpholines in 35-46% overall yield, a considerable improvement compared to the 13-19% overall yield of the 1st generation approach. The improvement for piperazines was also noteworthy with overall yields of 36-60% compared to the 15-50% yields of the 1st generation method.

To illustrate the synthetic relevance of our newly developed method, we looked into the patent literature for biologically active compounds that could be accessed through our synthetic manifold. A chiral C2-substituted morpholine **1.77**—directly related to one of the compounds in our substrate scope—was reported to be a specific dopamine subtype 4 ($D_{4)}$ antagonist, which is a target of relevance for antipsychotic therapeutics. While the patent claimed a single enantiomer of **1.77** to be more active at D_4, it did not disclose the absolute stereochemistry at C2. Ambiguous stereochemistry in the patent is likely the result of their racemic synthesis (**Scheme 1.1.8.5**). They began with racemic epoxide **1.78**, which they opened with aminosulfate **1.79** to generate racemic morpholine **1.80** in 38% yield. Alkylation of the morpholine nitrogen with 2-chloromethyl benzimidazole **1.81** provided them racemic **1.77**, which was resolved into its two enantiomers using HPLC with a chiral column. This synthesis resulted in a less than 10% yield of their final enantioenriched material, and the final stereochemical information was unknown.
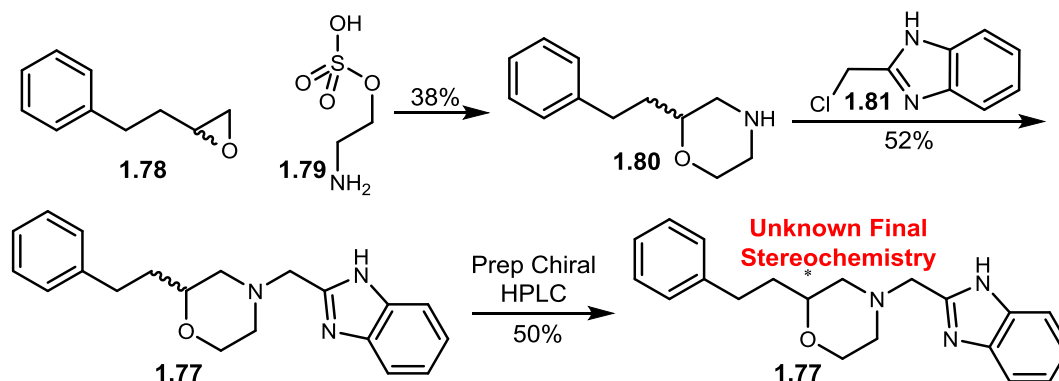
Scheme 1.1.8.5 Patent synthesis of D$_4$ antagonist

We saw the unknown absolute configuration and low overall yield surrounding this D$_4$ antagonist as an opportunity to showcase our new morpholine/piperazine method while also investigating these compounds for enantiospecific activity at D$_4$. To do this, we utilized previously synthesized morpholine **1.75C**, which contained the exact phenylethyl R-group that is a substituent of the D$_4$ antagonist. By starting with this material, which was synthesized in 43% overall yield, we cleaved the benzyl group with hydrogenolysis and followed that with 2-chloromethyl benzimidazole alkylation of the morpholine to arrive at D$_4$ antagonist **1.77** in 35% overall yield and 98% ee—a significant improvement compared to the literature precedent (**Scheme 1.1.8.6**).
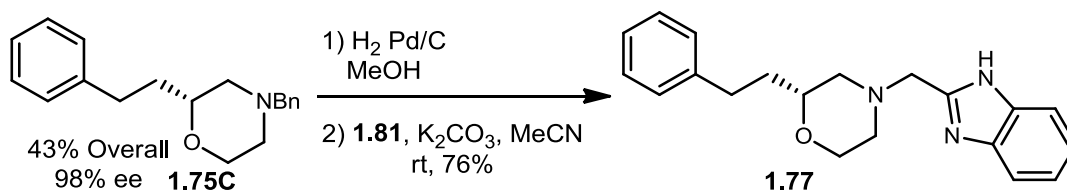
Scheme 1.1.8.6 Enantioselective synthesis of D$_4$ antagonist. Scheme adapted from ref 37.

Fortunately, our method allowed us to prepare D$_4$ antagonist **1.77** as the racemate and as each enantiomer so that they could each be tested for their activity at the different dopamine receptor subtypes. They were tested in a radio ligand binding assay where **1.77**—if

33

it binds the receptor—will displace radioactive dopamine from the receptor. Displaced dopamine can be detected and quantified to calculate a binding constant (K_i) for the compound of interest. This assay showed the two enantiomers of **1.77** to be devoid of activity at D_1 and D_2 while being highly selective for D_4 compared to D_3. There is clear enantiospecific activity since S-**1.77** is inactive at D_4 and has extremely modest activity at D_3, compared to R-**1.77**, which is twice as potent compared to the racemate at D_4, indicating all of the racemate's activity at D_4 is coming solely from the R enantiomer. This data further underscores the power of our method to synthesize chiral, C2-functionalized morpholines and piperazines.
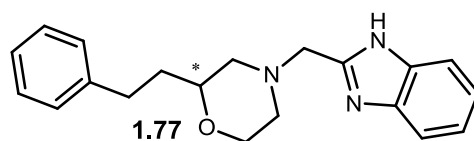
Cmpd	D_1		D_2		D_3		D_4	
	K_i	IC_{50}	K_i	IC_{50}	K_i	IC_{50}	K_i	IC_{50}
(±)-**1.77**	>100	>100	>100	>100	10.8	31.8	0.14	0.36
(R)-**1.77**	>100	>100	>100	>100	15.7	46.2	0.07	0.18
(S)-**1.77**	>100	>100	>100	>100	25.9	76.4	>100	>100

Table 1.1.8.3 Enantiospecific activity of **1.77** on dopamine receptors. Table adapted from ref 37.

In summary, our 2nd generation method to access chiral morpholines and piperazines circumvents many of the limitations of our initial approach. This novel route fills a void in the synthetic chemistry literature, giving us access to chiral morpholines and piperazines from achiral starting materials, while literature precedent always involves either the chiral pool or stoichiometric chiral auxiliaries. In essence, our 2nd generation method is a three pot protocol allowing access to enantioenriched C2 substituted morpholines and piperazines, and it avoids the weaknesses of the 1st generation approach. Namely, by modifying the reaction

protocol to reduce the α-chloro aldehyde to a β-chloroalcohol, the critical chloro stereocenter was rendered configurationally stable, which allowed us to avoid large deviations in % ee. Additionally, this reaction protocol increases the average overall yields from 26% to 45% and avoids long term extreme reaction conditions, since the previous reductive amination step was run at -78 °C for greater than 16 hours. The notable advantage of our novel approach to morpholines and piperazines is illustrated in our synthesis of morpholine D_4 antagonist, and optimization of this scaffold for activity at D_4 is currently underway in our laboratory

1.2 General access to chiral β-fluoroamines and γ-fluoroamines from prochiral aldehydes using organocatalysis

1.2.1 Fluorine in the pharmaceutical industry

While 5-fluorouracil, the first fluorine containing drug, was discovered in 1957, fluorinating biologically active compounds did not become commonplace until the 1970s.[39] Since that time, the unique qualities of organofluorine compounds have intrigued chemists,[40,41] and fluorinating biologically active compounds to augment their biological and physical properties is now commonplace. In fact, 20-25% of compounds in the pharmaceutical pipeline,[42] 20% of approved drugs, and 30% of agrochemicals contain at least one fluorine atom.[43,44] These fluorinated compounds are not isolated to treating specific disease states; instead, fluorine is an essential component of leading drugs targeting heart disease (atorvastatin, *Lipitor*),[44] depression (fluoxetine, *Prozac*),[45] cancer (fulvestrant, *Faslodex*),[46] bacterial infection (ciprofloxacin, *Ciprobay*),[47] and viral infection (efavirenz),[48] to name a few (**Figure 1.2.1.1**).

35
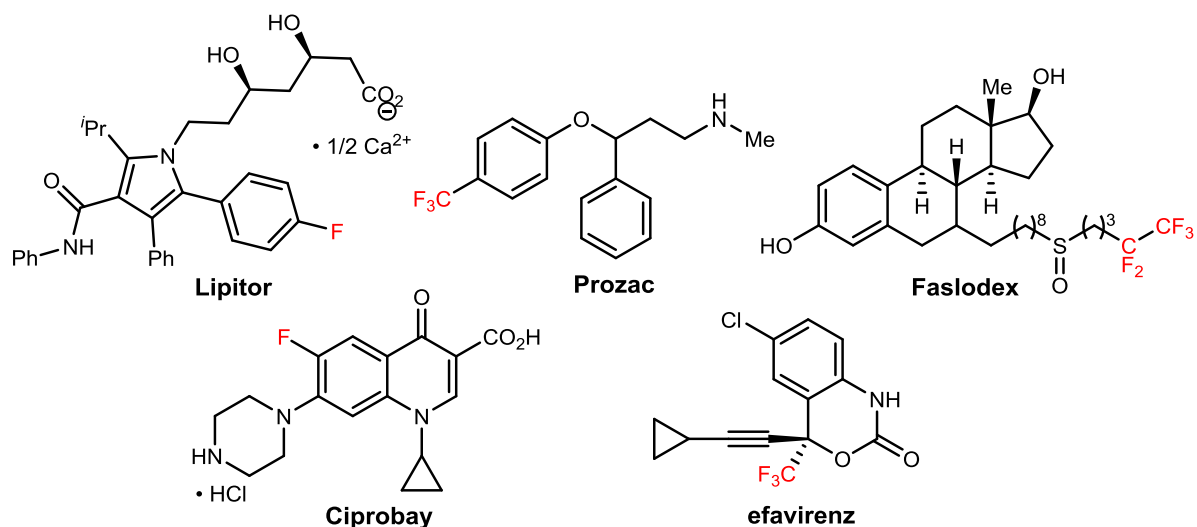
Figure 1.2.1.1 Successful fluorinated pharmaceuticals

Fluorine is often added to biologically active compounds to decrease ancillary pharmacology, block metabolic liabilities, increase bioavailability, and modulate protein:ligand interactions.[42,49] It is possible to alternate fluorine for different atoms because the C-F bond is inert, and fluorine has a relatively small size. Fluorine is most commonly used to replace hydrogen atoms, hydroxyl groups, or the oxygen of carbonyls since fluorine's atomic radius, the C-F bond length, and the bond polarity is comparable to a C-H or C-O.[50] Fluorine's incorporation into molecules generally increases hydrophobicity, but fluorine is polar possessing the highest electronegativity value of all elements. The C-F bond is the strongest of all carbon single bonds; formation of the bond, therefore, is thermodynamically favorable.[43] **Table 1.2.1.1** displays atomic radii, electronegativity, bond length, and bond strength data for fluorine and atoms fluorine commonly replaces.[41]

Atom	Electronegativity (Pauling Scale)	Atomic Radius (Å)	Bond Length (C-X, Å)	Bond Energy *k*cal/mol
H	2.1	1.2	1.09	98.8
C	2.5	1.7	1.54	83.1
N	3.0	1.55	1.47	69.7
O	3.5	1.52	1.43	84.0
F	4.0	1.47	1.35	105.4
Cl	3.0	1.74	1.77	78.5

Table 1.2.1.1 Properties of fluorine and comparison atoms

1.2.2 Biological effects of organic fluorination

When a drug is introduced orally into the body, it must (i) be stable enough to survive the acidic environment in the stomach, (ii) have the necessary physical properties to be absorbed into the blood stream, (iii) have chemical characteristics providing for a reasonable half-life, (iv) have a limited number of off target effects rendering it safe, and (v) be potent and efficacious at its anticipated biological target to provoke the desired biological effect. Since the human body is xenophobic, attempting to rid itself of foreign substances for its own safety, designing a compound that meets all of these criteria is difficult. The drug discovery process, therefore, is based on a multidimensional optimization (MDO) approach.[40] This means that potency, selectivity, and efficacy cannot be the only compound characteristics studied during the lead optimization process. Instead, physiochemical properties such as absorption, distribution, metabolism, excretion (ADME), and safety of the lead compounds must be considered equally compared to potency and efficacy while designing the molecule. Fortunately, fluorine chemistry has been a central instrument in the medicinal chemist's toolbox to balance all of these properties in MDO.[42,44,49,51]

While practicing MDO for a cholesterol uptake inhibitor, scientists at Schering-Plough had to consider how their lead compounds were metabolized.[52,53] Generally, prior to compound elimination from the body, a class of enzymes called Cytochrome P450s oxidize the compound making it more water soluble and therefore easier to remove from the body. If oxidation by these enzymes can be prevented, it results in a longer half-life giving the compounds more time to affect their molecular targets. In this case, the scientists realized that their lead compound **SCH 48461** was being metabolized too rapidly. By isolating the metabolites, they realized phenyl oxidation and methoxy demethylation were decreasing the half-life to unacceptable levels while other metabolites actually resulted in a more potent compound. To address the metabolites resulting in a low half-life, they substituted fluorine atoms in those positions—effectively blocking metabolism—while they pre-activated the metabolism resulting in benzylic oxidation and demethylation, which resulted in a more potent compound (**Figure 1.2.2.1**).
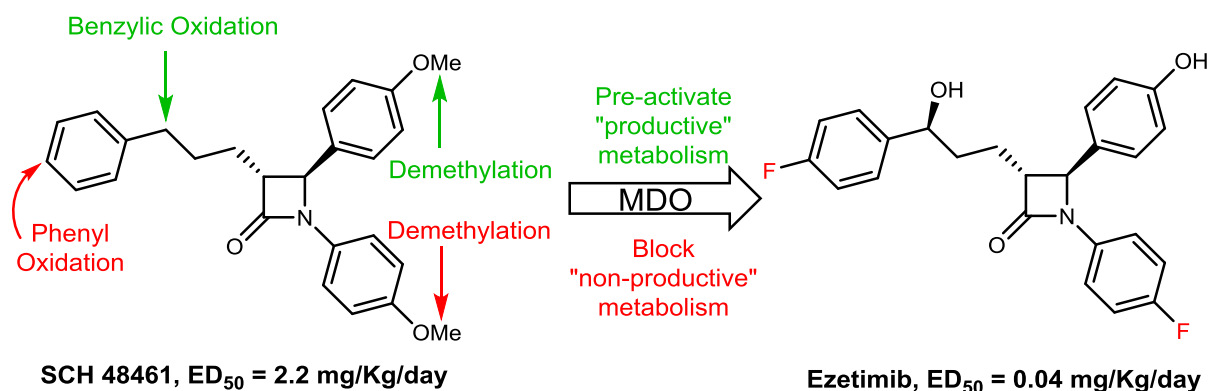
Figure 1.2.2.1 Fluorine addition blocks compound metabolism

This MDO process resulted in **Ezetimib**, which is an FDA approved drug that can be dosed at a fifty-five-fold lower dose than the previous lead compound.

Many factors contribute to C-F bonds having low metabolic liabilities, and it has become common practice to substitute a fluorine atom onto a molecule to prevent metabolism. In the case of anti-inflammatory celecoxib (*Celebrex*), a lead compound contained both a trifluoromethyl group and a 4-fluorophenyl ring (**Figure 1.2.2.2**). While this compound was potent and efficacious, it suffered from an unusual problem. Most biologically active compounds to be used *in vivo* require intense effort to obtain a suitable half-life. Celecoxib's precursor, however, had a half-life of 9 days, much longer than what is safe and desirable. To increase metabolism, therefore, they substituted a metabolically labile methyl group in the position of a fluorine atom (**Figure 1.2.2.2**), which decreased the half-life of the FDA approved drug to a desirable 3.5 hours.[49,54] This example illustrates the stability of the C-F bond to metabolism *in vivo*.
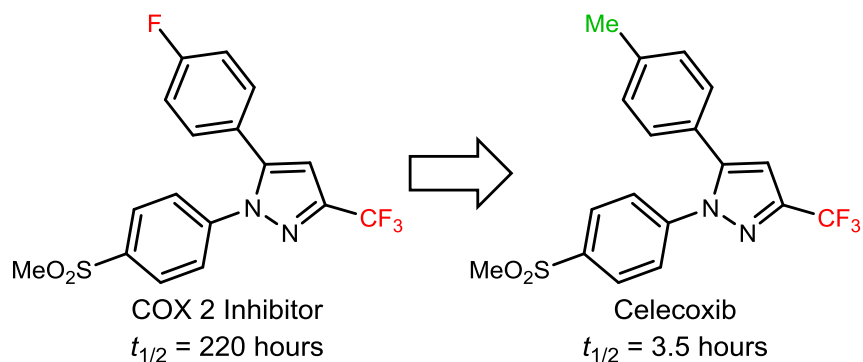
Figure 1.2.2.2 Fluorine-methyl replacement sensitizes metabolism

Besides having an impact on metabolism, fluorine can have a significant impact on the binding interactions between the ligand and protein.[42,49] The extra lipophilicity gained by replacing a hydrogen with a fluorine usually results in slightly increased binding affinity by way of nonspecific nonpolar interactions.[55] Additionally, fluorine can take part in polar interactions with the amino acid backbone or negatively charged side chains of its binding partner. These interactions commonly result from C-F---C=O or C-F---H-N of the amino acid

backbone,[56] and while they are not usually termed hydrogen bonds, they are strong interactions that can result in conformational changes within the binding pocket. In an attempt to discover novel serine protease inhibitors, Böhm and coworkers solved crystal structures of two compounds only differing in an aryl H or F (**Figure 1.2.2.3**).[49] They found the two compounds to have different conformations, and they hypothesize this to be the result of the fluorine atom having a polar interaction with an N-H side chain. Importantly, the fluorinated congener was six times more potent than the des-fluoro compound.
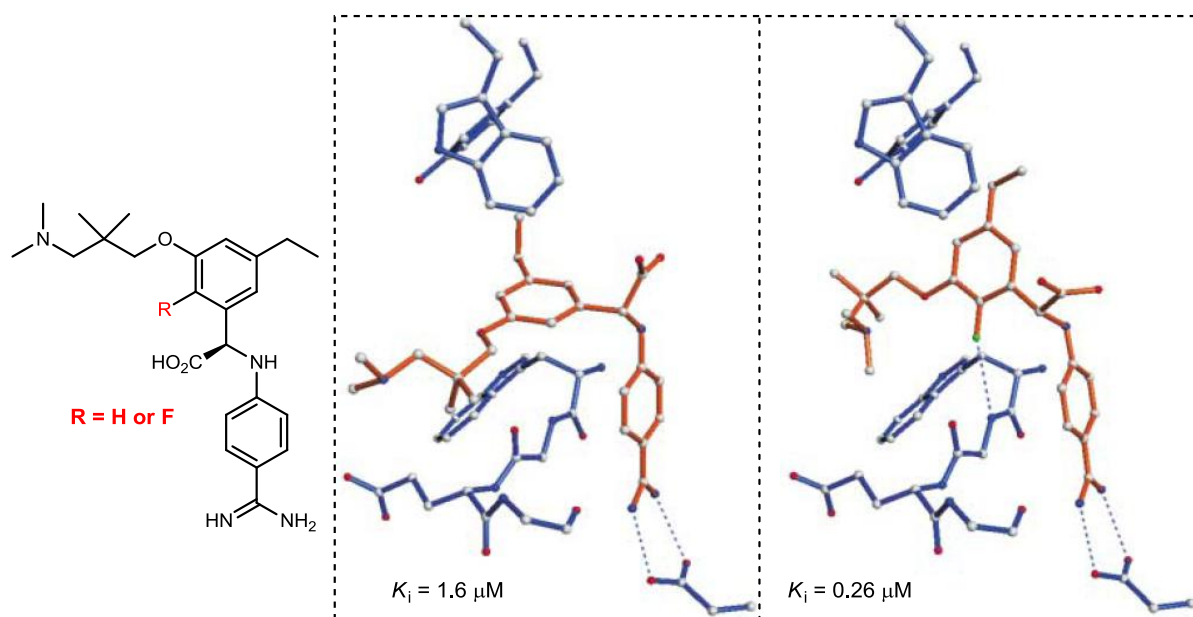
Figure 1.2.2.3 Fluorine causes conformational shift based on binding interactions. Figure adapted from ref 49.

The majority of FDA approved drugs contain basic amine functionalities, and this functional group contributes in a major way to all aspects of the MDO process.[40] Amine protonation state can have major impacts on protein binding, bioavailability,[57,58] off target effects,[59,60] and generally all physiochemical properties of small molecules. Fluorine, through induction, has a major impact on the pK_a of adjacent functional groups.[40] To modulate the basicity of amine containing small molecules, therefore, fluorine is often added to the

40

molecule in close proximity to the amine, modulating its pK_a and impacting those physiochemical properties. Since fluorine is the most electronegative element, its effect on nearby amines is substantial, changing their pK_a on a logarithmic scale. To fully optimize amine containing small molecules for ideal physiochemical properties and potency, rational and structure based modulation of amine basicity gives the medicinal chemist fine-tuned control during MDO.

While the pK_a of an aliphatic protonated amine is 10.7, addition of fluorine in the γ-position decreases that value to 9.7. Moving the fluorine into the β-position shifts the pK_a to 9.0, addition of γ-geminal difluoro atoms decreases it further to 8.7, and β-geminal difluorination decreases the pK_a to 7.3 (**Figure 1.2.2.4**).
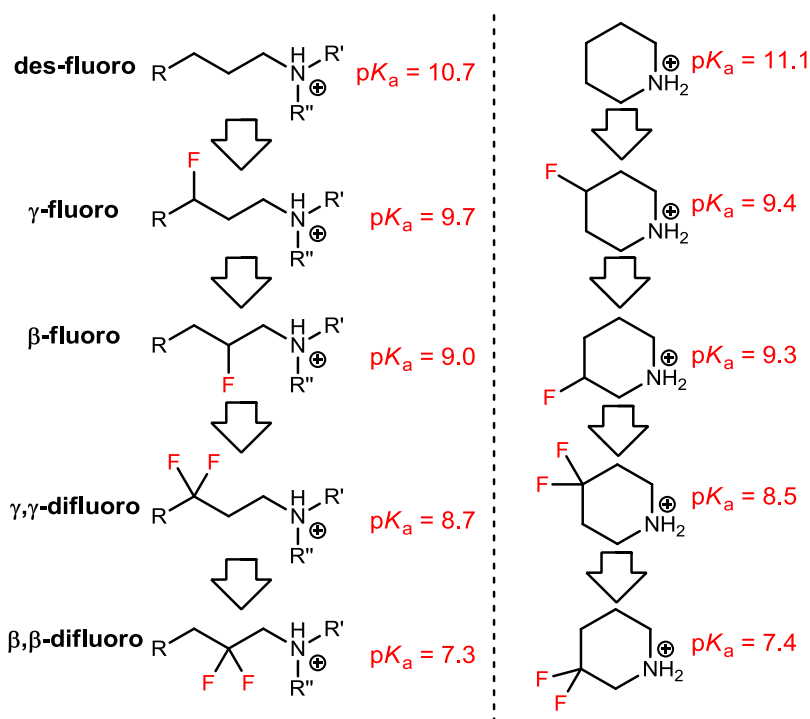
Figure 1.2.2.4 Fluorine modulates amine basicity. Figure adapted from ref 40.

Fluorine substitution allows the medicinal chemist to access a wide range of pK_a values, allowing powerful control over protonation state, which is essential when simultaneously

optimizing a compound for potency, bioavailability, metabolism, and safety—the standard process of MDO.[40,42,49]

Chemists at Merck utilized this strategy while optimizing a compound to treat migraines.[61] They prepared a series of piperidinyl indoles to be selective for the 5-HT$_{1D}$ receptor, but bioavailability and CNS penetrance were issues with lead compound **1.82**. To modify the protonation state of the piperidine, they added a β-fluorine, which decreased the pK_a of the conjugate acid more than 1 unit. This had little effect on binding or selectivity, but it dramatically increased bioavailability to acceptable levels (**Figure 1.2.2.5**).[42,61]

Piperidine pK_a = 9.7
5-HT$_{1D}$ IC$_{50}$ = 0.3 nM
poor bioavailability

Piperidine pK_a = 8.7
5-HT$_{1D}$ IC$_{50}$ = 0.9 nM
good bioavailability
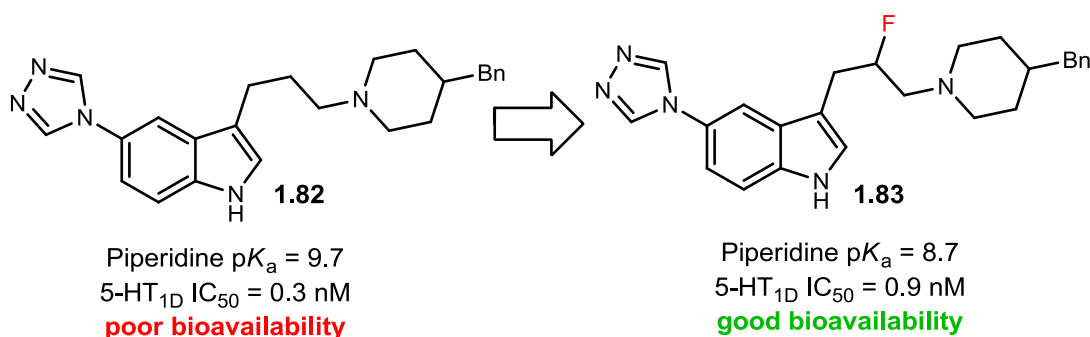
Figure 1.2.2.5 β-fluorination increases bioavailability. Figure adapted from ref 61.

In another case, γ-fluorination of another piperidinyl indole increased oral bioavailability. This effort was to discover a selective 5-HT$_2$ antagonist for the treatment of schizophrenia.[62] While the lead compound **1.84** was a potent and efficacious antagonist, oral dosing of **1.84** showed only trace amounts to be absorbed and circulated through the body. To decrease the basicity of the piperidine, a γ-fluorine was introduced to the piperidine to make compound **1.85**. That scaffold modification resulted in a modest potency increase and allowed 18% of the dosed compound to reach circulation. Following that modification, they found the major metabolite to be indole oxidation, which again was limiting compound bioavailability. To address that, they added another fluorine atom to the site of oxidation to

make antagonist **1.86**, and that modification resulted in a seven-fold increase in potency and made the compound 80% bioavailable (**Figure 1.2.2.6**).

1.84
5-HT$_{2A}$ K$_i$ = 0.99 nM
% bioavailability = trace

1.85
5-HT$_{2A}$ K$_i$ = 0.43 nM
% bioavailability = 18%

1.86
5-HT$_{2A}$ K$_i$ = 0.06 nM
% bioavailability = 80%
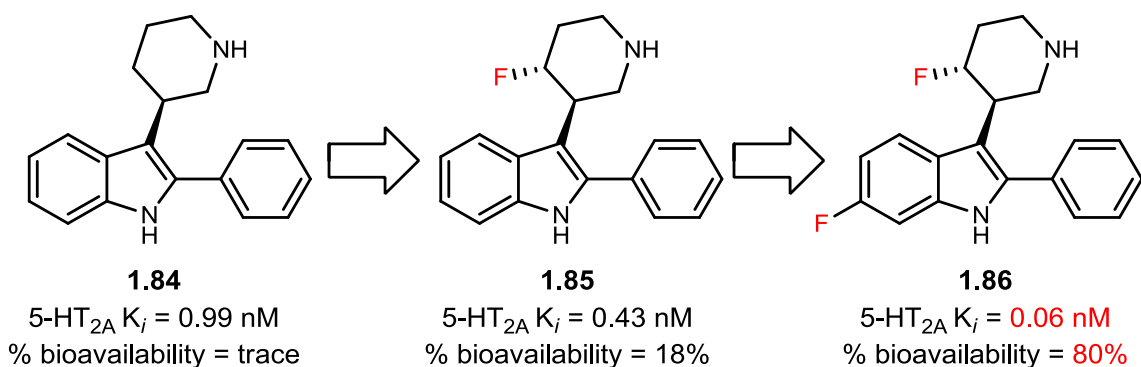
Figure 1.2.2.6 γ-fluorination increases bioavailability and blocks metabolic liability. Figure adapted from ref 62.

1.2.3 Synthetic methods for compound fluorination

While fluorinating biologically relevant compounds can benefit the physical and biological properties of the molecules, medicinal chemists—and nature—have not mastered the synthesis of organofluorine chemistry. Fluorine is the thirteenth most abundant element on Earth, yet only 21 fluorine containing natural products have been isolated compared to thousands of natural products containing the heavier halogens.[63,64] While there are many known haloperoxidases that catalyze the addition of chlorine and bromine, there are no fluoroperoxidases known. Additionally, natural fluoride is a hard anion, which causes it to form a very tight hydration shell decreasing its nucleophilicity and general reactivity. Natural fluoride, with its hydration shell, is so unreactive that the first known fluorinating enzyme— reported in 2002—must dehydrate fluoride in the active site prior to the subsequent substitution reaction. [65,66] These qualities, along with those already stated, make selective fluorination of organic compounds exceedingly difficult.

Since fluorine carbon bonds are difficult to form, conditions for C-F bond construction are extremely valuable. Medicinal chemists, therefore, appreciate commercially

available reagents that facilitate formation of this bond. That being said, there are several types of commercial reagents available for this purpose, and they can be largely divided into nucleophilic and electrophilic fluorine sources (**Figure 1.2.3.1**).[44,51]
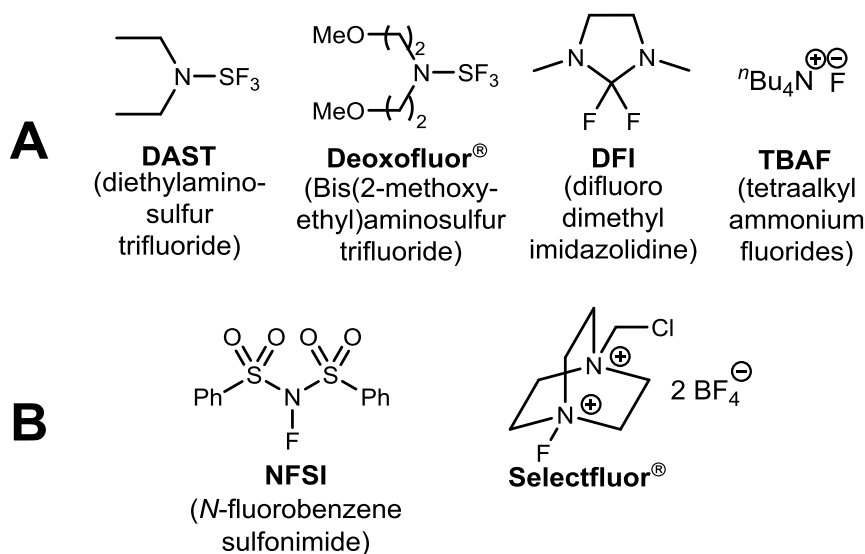
Figure 1.2.3.1 (a) Common nucleophilic fluorination reagents
(b) Common electrophilic fluorination reagents

Nucleophilic fluorination sources generally react with alcohols, carbonyls, good leaving groups, epoxides, and sometimes activated olefins. DAST, Deoxofluor®, and DFI react with carbonyls and alcohols to form difluoro and monofluoro alkyl compounds. DAST and Deoxofluor® are commercially available and DFI is readily available from other commercial materials.[67] While these reagents form achiral difluoro alkyl compounds from achiral ketones or aldehydes, they form chiral monofluoro alkyl compounds with inversion of stereochemistry when reacted with chiral secondary alcohols (**Scheme 1.2.3.1**).[51,68] Tetraalkylammonium fluorides are more often used to displace reactive leaving groups,[61] open halonium ions or epoxides,[69] or they can be used to trifluoromethylate in a process termed oxidative desulfurization—fluorination (**Scheme 1.2.3.1**).[70] These nucleophilic

reagents provide access to a wide assortment of fluorination patterns, and in some cases they can deliver chiral organofluorine compounds.
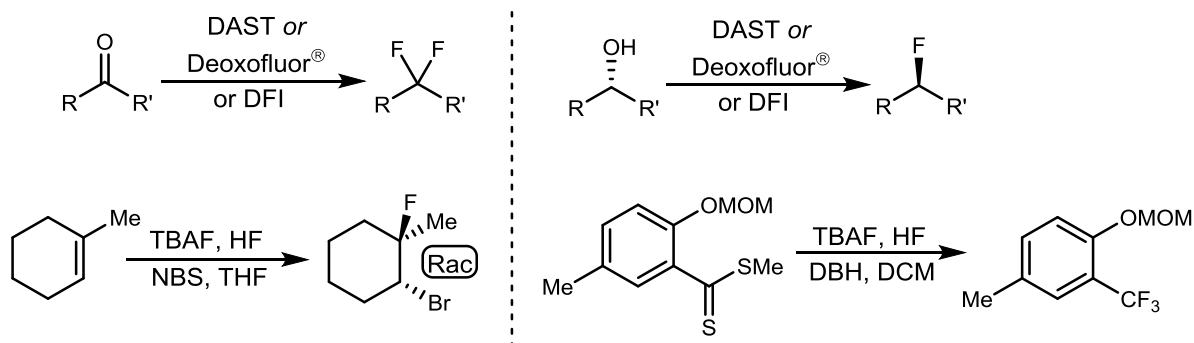
Scheme 1.2.3.1 Uses of the common nucleophilic fluorination reagents

The electrophilic fluorine sources generally deliver "F[+]" from an N-F bond,[71] and they are most frequently employed to add fluorine to a carbanion generated from a carbonyl species, a lithiated aryl ring, or to nucleophilic heterocycles (**Scheme 1.2.3.2**).[44,51]
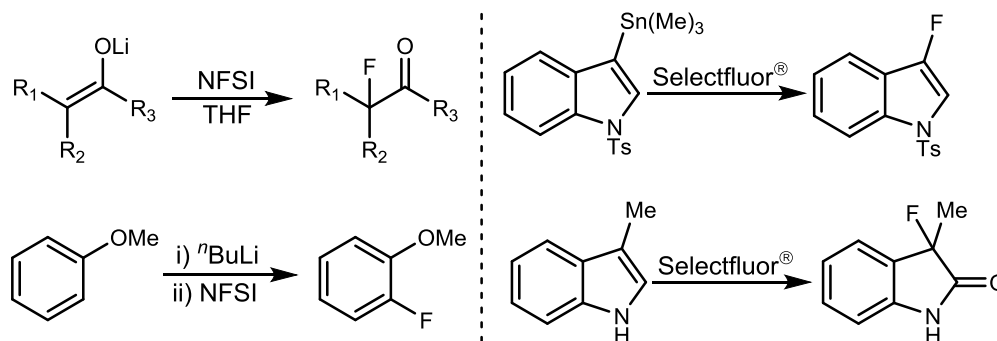
Scheme 1.2.3.2 Uses of the common electrophilic fluorination reagents

While all of these sources of fluorine are achiral, whether they are nucleophilic or electrophilic, they can be utilized simultaneously with a chiral additive to prepare enantioenriched fluorinated materials. The ability to synthesize C—F bonds asymmetrically is valuable since (i) differential biological activity is frequently observed for different enantiomers, (ii) chiral syntheses avoid otherwise necessary and tedious chiral

chromatography, and (iii) asymmetric synthesis provides knowledge of the absolute stereochemistry, which is desirable and useful while developing intellectual property.

To prepare chemical scaffolds containing chiral fluorine, DAST is most frequently utilized with a chiral secondary alcohol, which is thought to undergo an enantiospecific S_N2 mechanism resulting in an organofluorine compound with inversion of configuration. For example, treatment of the α-hydroxy amide **1.87** with DAST follows that pattern of reactivity resulting in inversion of configuration to fluoride **1.88** (**Scheme 1.2.3.3A**).[72] Unfortunately, the reagent sometimes proves to be unreliable, and reaction of hydroxyl-sterol derivative **1.89** with DAST resulted in conversion to the fluoride **1.90** in high yield with retention of configuration, likely through an S_N1 reaction mechanism (**Scheme 1.2.3.3B**).[73] Additionally, reaction of alcohol **1.91** with DAST went through an S_N1 pathway, which resulted in an undesired rearrangement to the tertiary carbocation that was trapped by the nucleophilic fluoride to generate tertiary achiral fluoride **1.92** (**Scheme 1.2.3.3C**).[74]
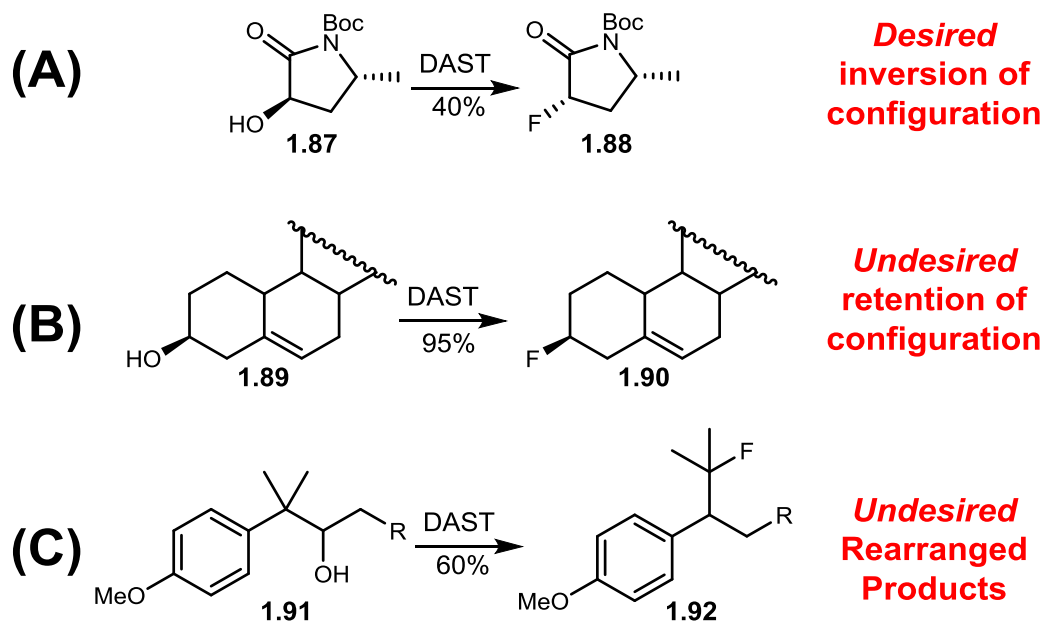
Scheme 1.2.3.3 DAST fluorination can be unpredictable

Further complicating matters, one must generate a chiral alcohol, which is not a trivial endeavor, prior to reaction with DAST to produce the chiral fluorine. A single enantioselective reaction installing the chiral fluorine would be advantageous to this reaction protocol.

While a variety of other asymmetric fluorination reactions exist, after considering the importance of β and γ-fluoroamines as discussed above, we saw a need for methods to effectively and consistently synthesize these amines from readily available and achiral starting materials. Prior to efforts in the Lindsley Lab, the only methods facilitating access to β or γ-fluoroamines relied predominantly on the classical DAST technology.[68] From 2005 to 2006, organocatalytic asymmetric fluorination of aldehydes emerged as a powerful method to prepare chiral fluoro aldehydes directly from achiral aldehydes.[75] In fact, four separate research groups reported enantioselective organocatalytic fluorination of aldehydes during this time period. The Enders group was first to report the fluorination reaction, but their catalyst and conditions only gave modest yield and enantioselectivity (**Figure 1.2.3.2**).[76] Shortly thereafter, the Barbas,[77] Jørgensen,[78–81] and MacMillan[82,83] groups simultaneously disclosed catalyst systems that enabled enantioselective fluorination of achiral aldehydes. Each of their methods drastically improved upon the % ee from Ender's method, and each set of reaction conditions had a very similar substrate scope (**Figure 1.2.3.2**).
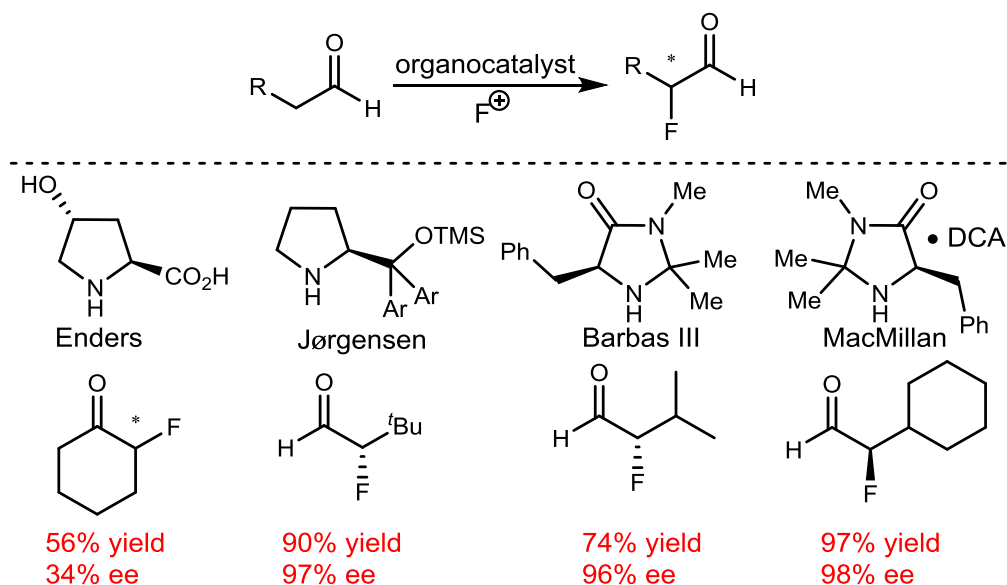
Figure 1.2.3.2 Organocatalytic enantioselective fluorination of aldehydes

Since these methods facilitated rapid access to chiral fluoro aldehydes, the Lindsley lab envisioned these α-fluoro aldehydes could be useful intermediates in a reaction pathway leading to chiral β-fluoroamines. Essentially, this was done through a two-step protocol consisting of α-fluorination of an achiral aldehyde following MacMillan's protocol,[82] then standard reductive amination conditions to arrive at β-fluoroamines in high yields and enantioselectivity (**Scheme 1.2.3.4**).[84]
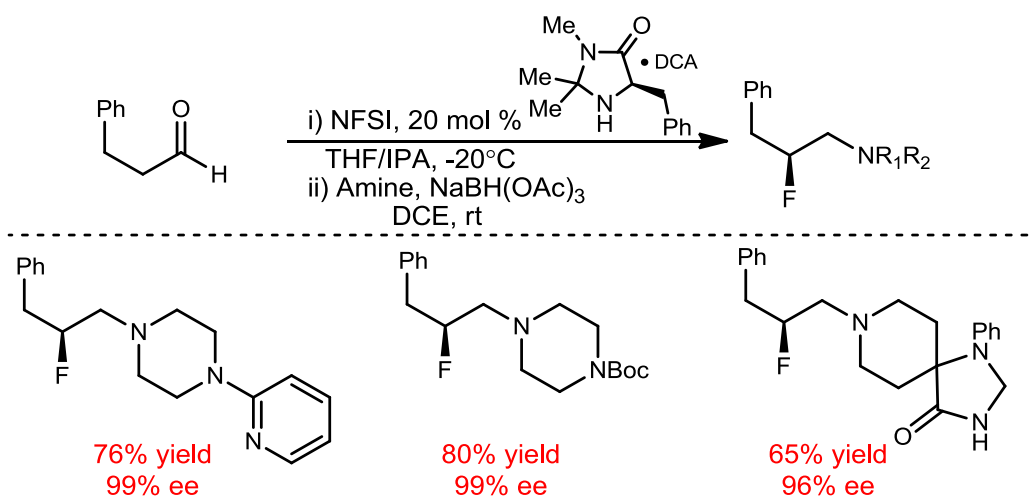
Scheme 1.2.3.4 General route to β−fluoroamines. Scheme adapted from ref 84.

This route also facilitated access to β,β-difluoroamines; therefore, this chemistry can be used to modulate the pK_a of basic amines in biologically active compounds from 10.7 (des-fluoro) to 9.0 (β-fluoroamine) to 7.3 (β,β-difluoroamine). This chemistry represented a considerable improvement in the art of preparing diverse chiral β-fluoroamines from readily available precursors. Since the α-fluoro aldehyde was used in this reaction pathway, however, storage of that intermediate would lead to immediate deterioration of % ee. Additionally, access to γ-fluoroamines was not possible through this reaction manifold. With those aspects of this method in mind, a route capable of accessing both β and γ-fluoroamines would be advantageous.

1.2.4   Envisioned access to β and γ-fluoroamines

Our labs previous work preparing chiral β-fluoroamines,[84] aziridines,[33] morpholines,[34] and piperazines were all based on utilizing an epimerizable α-halo aldehyde. In all cases, if the chiral halogenated aldehyde was left at room temperature, the % ee would deteriorate. To circumvent this problem while accessing morpholines and piperazines, we modified our procedure to reduce the epimerizable α-chloro aldehyde to the configurationally stable β-chloro alcohol.[37] That adjustment resulted in further modification of the reaction procedure; namely, the hydroxyl group was transformed to a reactive leaving group, which was displaced by aminoalcohols or diamines instead of the reductive amination from the former reaction sequence. This result led our lab to reflect on our β-fluoroamine reaction protocol. Specifically, we imagined a modification to the reaction sequence providing more reliable access to enantioenriched β-fluoroamines and β,β-difluoroamines while also giving a reaction path to γ-fluoroamines and a variety of other fluorinated scaffolds.

Analogous to our modification to the morpholine/piperazine synthesis, we envisioned an enantioselective organocatalytic fluorination of achiral aldehydes **1.93** followed by reduction of the aldehyde to provide configurationally stable β-fluoroalcohol **1.94**. At this point, the hydroxyl could be converted into a leaving group and substitution with amines would generate β-fluoroamines **1.95**. In a similar vein, if the leaving group was instead displaced by cyanide, that would generate β-fluoronitrile **1.96**. This intermediate is useful because of its high oxidation state, a molecular species poised to access a variety of fluorinated scaffolds. Importantly, full reduction of the nitrile would give access to the desired γ-fluoroamine **1.97**, but nitrile **1.96** could also be (i) hydrolyzed to the carboxylic acid, (ii) hydrolyzed to the carboxylic amide, (iii) partially reduced to the aldehyde, (iv) hydrolyzed to amide oxime **1.98**, or (v) reacted with sodium azide, facilitating a formal 3 + 2 addition to form the tetrazole **1.99** (**Scheme 1.2.4.1**)
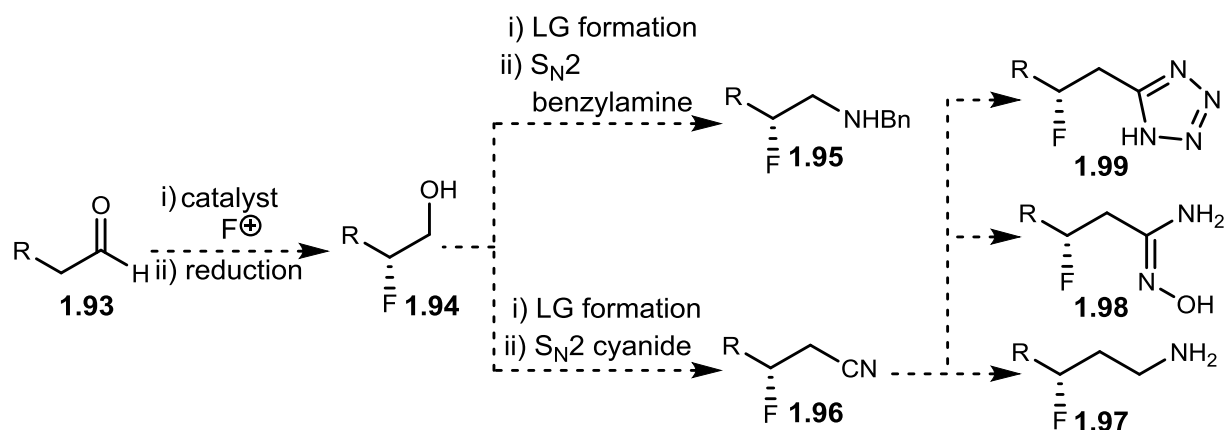
Scheme 1.2.4.1 Envisioned route to numerous fluorinated scaffolds
.

1.2.5   General access to β and γ-fluoroamines

To validate our envisioned approach, we prepared a number of β-fluoroalcohol substrates using MacMillan's organocatalytic approach.[82] Treatment of aldehyde **1.93** with 20 mol % organocatalyst **1.100** and NFSI facilitated the transformation to α-fluoroaldehydes.

At this point, workup and a solvent change allowed the aldehydes to be treated with sodium borohydride to reduce them to chiral β-fluoroalcohols **1.94**. As expected, these conditions allowed for the preparation of β-fluoroalcohols **1.94A-G** in good yields and excellent enantioselectivity (**Scheme 1.2.5.1**).
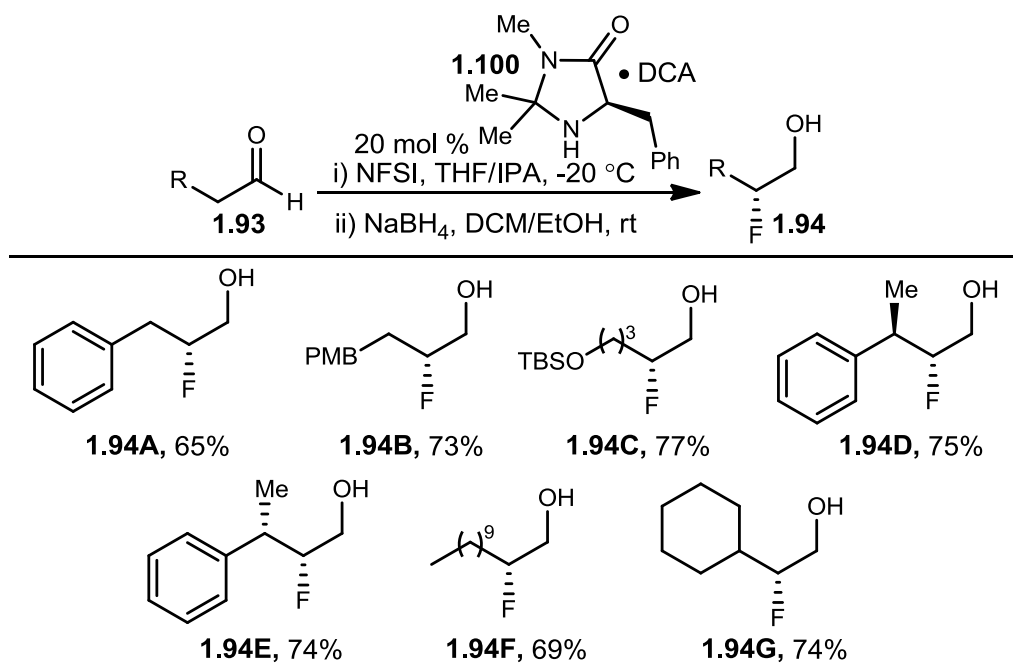
Scheme 1.2.5.1 Synthesis of β-fluoroalcohols. Scheme adapted from ref 85.

At this point, application of the previously developed aminoalcohol/diamine alkylation conditions to β-fluoroalcohols (triflic anhydride, DCM, then nucleophilic amine) allowed for clean conversion to the β-fluoroamines. This reaction pathway provided β-fluoroalcohols **1.101A-C** in high yield and excellent enantioselectivity (**Scheme 1.2.5.2**).
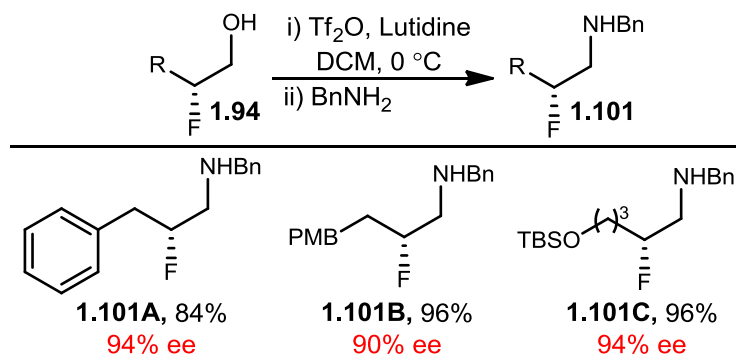
Scheme 1.2.5.2 Synthesis of β-fluoroamines. Scheme adapted from ref 85.

While overall yield and enantioselectivity is only slightly better than the previous Lindsley Lab method,[84] this new strategy sets the key stereocenter in a configurationally stable way, preventing any loss of % ee, leading to reproducibly high enantioselectivity.[85] This method allows pK_a perturbation of the amine's conjugate acid from 10.7 to 9.0.

To further decrease the basicity of amines, sometimes β,β-difluoro substitution results in optimized physiochemical properties. To illuminate whether this approach would allow access to the difluoroamine variant, organocatalytic difluorination of aldehyde **1.102** with excess NFSI and proline organocatalyst followed by sodium borohydride reduction led to β,β-difluoroalcohol **1.103** in 77% yield. Treatment of this compound with triflic anhydride and benzylamine facilitated substitution to the β,β-difluoroamine **1.104** (**Scheme 1.2.5.3**), which would result in a pK_a shift from 10.7 to 7.3.[85]
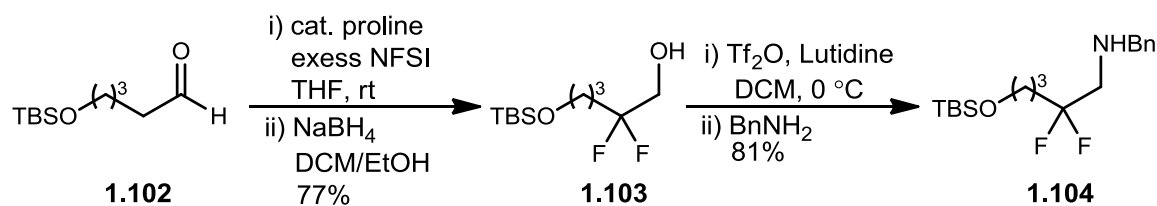
Scheme 1.2.5.3 Synthesis of silyl ether β,β-difluoroamine. Scheme adapted from ref 85.

While the ability to access β-fluoroamines and β,β-difluoroamines from this reaction manifold was gratifying, with noted benefits compared to former methods, we now focused

52

our attention on γ-fluoroamines, a very difficult chemotype to access. We initially examined the possibility of alkylating cyanide using fluoro-tosylates. β-fluoroalcohol congener **1.105** was treated with tosyl chloride to generate β-fluoro tosylate **1.106** in good yield. An assortment of solvents and temperatures were then screened for their ability to facilitate the S_N2 transformation generating β-fluoronitrile **1.107** (**Table 1.2.5.1**).

Solvent	Cyanide Source	Temperature[b]	Conversion[c]
DMSO	NaCN, 5 eq.	mw 150°C	complex mixture
MeCN	NaCN, 5 eq.	mw 120°C	none
DMF	NaCN, 5 eq.	mw 140°C	none
THF	NaCN, 5 eq..	mw 150°C	none
DMSO	NaCN, 3 eq.	room temp	none
DMSO	NaCN, 3 eq.	60°C	< 50%
DMSO	NaCN, 3 eq.	mw 100°C	full conversion
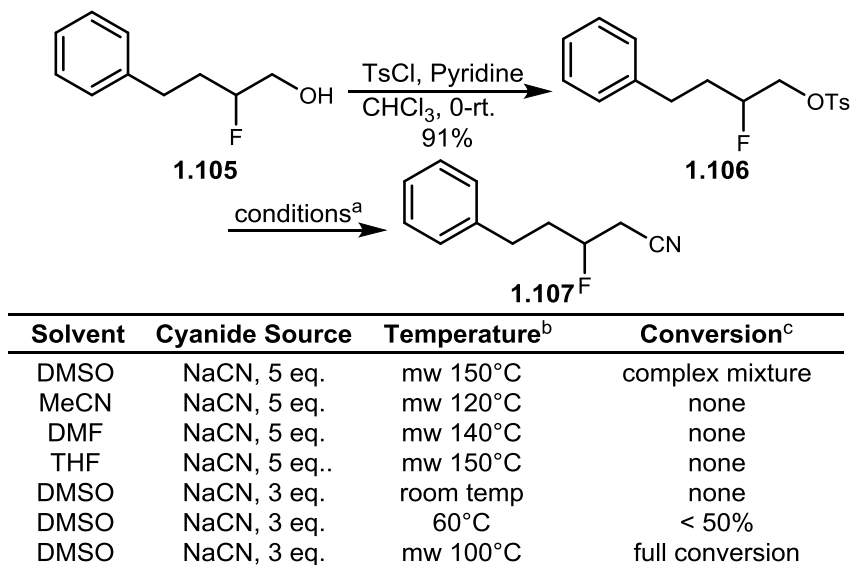
[a]All reactions were run with 0.2 M [b]mw denotes reaction was run in a microwave reactor
[c]Conversion determined by LC-MS, TLC and ^{1}H NMR

Table 1.2.5.1 Conditions screened to displace tosylate with cyanide

While sodium cyanide in DMSO was found to fully consume β-fluoro tosylate **1.106**, the product formed was not β-fluoronitrile **1.107**. Instead, a double displacement occurred with cyanide leading to bis-cyano adduct **1.108** and none of the desired β-fluoronitrile **1.107** (**Scheme 1.2.5.4**).
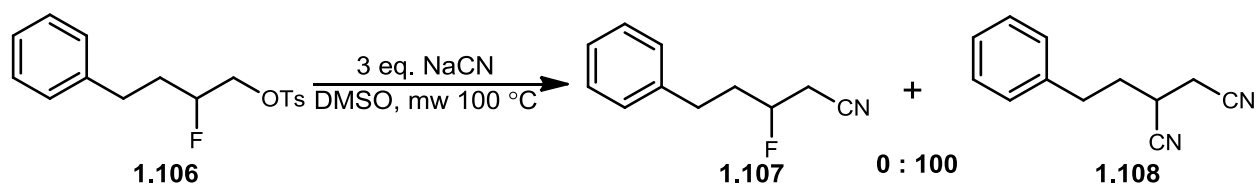
Scheme 1.2.5.4 Reaction produces bis-cyano adduct. Scheme adapted from ref 85.

In hopes of only undergoing a single S_N2 reaction with cyanide, the reaction conditions were modified to only use a single equivalent of sodium cyanide. Essentially, if only one equivalent was available, we postulated that it would be fully consumed by the first substitution reaction of the tosylate, and there would be no cyanide remaining for the second displacement of the fluoride. Unfortunately, we observed 50% conversion of the starting material to the bis-cyano adduct **1.108** under these conditions, leaving 50% of the starting material unreacted.[85] At this point, we reasoned that the β-fluorine was inductively withdrawing from the tosylate, decreasing its reactivity as a leaving group by way of δ^+ delocalization across vicinal carbon atoms. This made an S_N2 reaction of the tosylate kinetically more unfavorable than the second displacement of the fluoride. Essentially, when the activation energy barrier of one displacement was breached, the second displacement was less energetically demanding leading to the *bis*-cyano product. This led us to consider different leaving groups to modulate the energetics of this single displacement.

We next assessed the β-fluoro triflate for the desired single displacement, since triflate leaving groups are orders of magnitude more reactive than tosylates.[36] We treated β-fluoroalcohols with triflic anhydride to form β-fluoro triflate **1.109**, which was remarkably stable when compared to known triflates from literature precedent. In fact, β-fluoro triflate **1.109** could be chromatographed with conventional normal phase silica gel chromatography, a technique that usually results in triflate hydrolysis. Solvents, temperatures, cyanide equivalents, and additives were screened to assess the reactivity of the β-fluoro triflate (**Table 1.2.5.2**). Optimal conditions were found that resulted in single displacement of β-fluoro triflate **1.109** and formation of β-fluoronitrile **1.96**. Catalytic 18-crown-6 with 10 equivalents of potassium cyanide in acetonitrile were the optimal conditions to facilitate the

transformation.[85] This protocol resulted in full conversion without any formation of bis-cyano adduct.
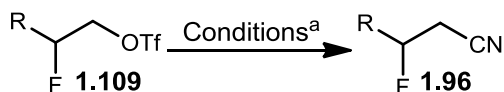
Solvent	Cyanide Source	Temperature	Consumption[b]	Additive
DCM	KCN, 15 eq.	room temp, 24hrs	23%	18-C-6
DCM	KCN, 5 eq.	50°C, 18hrs	50%	18-C-6
DCM	KCN, 20 eq.	55°C	none	none
THF	KCN, 10 eq..	room temp	none	18-C-6
THF	KCN, 10 eq.	55°C	<10%	18-C-6
MeCN	KCN, 10 eq.	room temp	100% conversion	18-C-6
MeCN	KCN, 10 eq.	room temp	none	none

[a]All reactions were run with 0.2 M for > 16 hours [b]Consumption determined by LC-MS, TLC and ^{1}H NMR

Table 1.2.5.2 Conditions screened to displace triflate with cyanide. Scheme adapted from ref 85.

Following these conditions, we applied the reaction to the set of β-fluoro alcohols (**1.94A-G**) we had synthesized. The cyanide substitution conditions were general for all the substrates, yielding β-fluoronitriles **1.96A-G** with an average yield of 82% (**Scheme 1.2.5.5**).
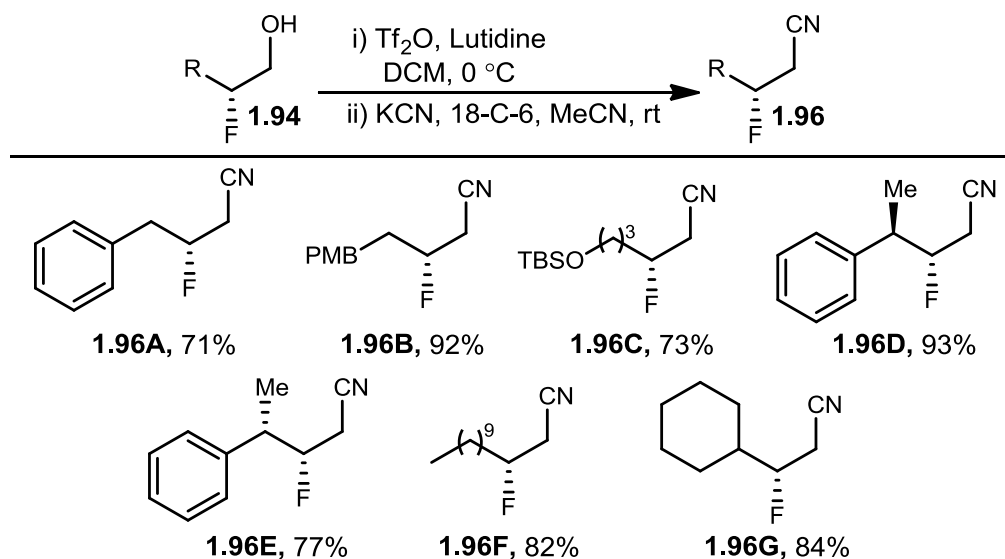
Scheme 1.2.5.5 Synthesis of β-fluoronitriles. Scheme adapted from ref 85.

With these β-fluoronitriles in hand, effort turned toward ascertaining optimal reduction conditions to generate the desired γ-fluoroamines.

55

Normally, reduction of nitriles can be accomplished using lithium aluminum hydride or Pd/C with hydrogenation conditions. Unfortunately, these conditions resulted in low yields of the desired amine and were accompanied by decomposition and/or defluorination. Ultimately, we found milder conditions using $InCl_3/NaBH_4$ in THF, which forms $InCl_2H$ *in situ*. These conditions facilitated clean reduction of the β-fluoronitriles **1.96A-G** to the γ-fluoroamines **1.97A-G** with an 85% average yield (**Scheme 1.2.5.6**).[85]
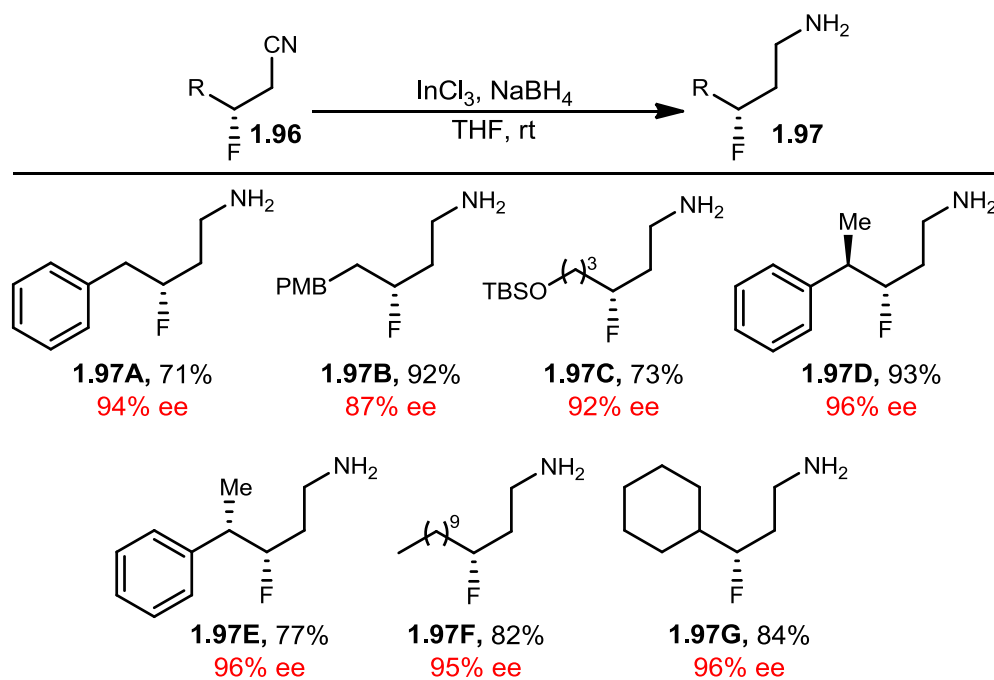
Scheme 1.2.5.6 Synthesis of γ-fluoroamines. Scheme adapted from ref 85.

This three-pot process (aldehyde fluorination/reduction, cyanide substitution, and nitrile reduction) smoothly provided chiral γ-fluoroamines in excellent enantioselectivity (87-96% ee) and good overall yields (40-58%). Importantly, this process utilizes a commercial organocatalyst that is available as both enantiomers, which provides access to γ-fluoroamines as a single desired enantiomer from achiral aldehydes in a quick reaction protocol.

Importantly, this reaction manifold provides a method to modulate the pK_a of biologically active amine containing ligands. It offers the ability to fine tune pK_a from 10.7 of

the parent amine, to 9.7 (γ-fluorine), to 9.0 (β-fluorine), to 7.3 (β,β-difluoro), giving control

over 3.5 logarithmic pK_a units. We also desired to access γ,γ-difluoroamines, to add an

additional level of control; however, we were unable to facilitate S_N2 reaction of the β,β-

difluorotriflate with cyanide despite surveying a broad array of reaction conditions (**Table**

1.2.5.3).[85]

| Solvent	Cyanide	Additive	Temperature	Result[b]
MeCN	KCN	18-C-6	room temp (24 hrs)	decomposition
MeCN	KCN	water cosolvent	MW 90 (30min)	decomposition
MeCN	KCN	18-C-6	MW 120 (10min)	decomposition
THF	KCN	water cosolvent	room temp (16 hrs)	no conversion
THF	KCN	water cosolvent	50°C (16 hrs)	slow decomposition
THF	KCN	water cosolvent	MW 150 (45 min)	10% isolated yield[c]
THF	KCN	water cosolvent	room temp (16 hrs)	no conversion
THF	KCN	MeOH cosolvent	MW 130 (30min)	slow decomposition
THF	KCN	18-C-6	MW 160 (45min)	decomposition
^{t}BuOH	KCN	none	MW 120 (10min)	little/no conversion
^{t}BuOH	KCN	none	MW 150 (45min)	moderate decomp.
DMSO	KCN	none	70°C (10min)	decomposition
DMSO	KCN	none	room temp (14 hrs)	decomposition
DCM	TBA • CN	none	room temp (2 hrs)	decomposition[d]
MeCN	TBA • CN	none	room temp (15min)	decomposition[d]

[a]All reactions were run with 0.2 M [b]Consumption determined by TLC and ^{1}H NMR [c]Reaction could not be reproduced on a larger scale [d]no fluorine was observed in the decomposed material

Table 1.2.5.3 Conditions screened to displace β,β-difluoro triflate with cyanide. Table adapted from ref 85.

1.2.6 β-fluoronitriles: access to diverse fluorinated scaffolds

While planning this method to access β and γ-fluoroamines, we envisioned the β-

fluoronitrile as an intermediate poised to access a variety of fluorinated scaffolds using the

nitrile as a handle. We reasoned that any reaction conditions we found to perform functional

group conversions on the nitrile would be directly applicable to our β-fluoronitriles.

Unfortunately, we observed the fluorine atom to be more reactive than expected. Standard hydrolysis conditions leading to fluoro carboxylic acids or fluoro carboxylic amides also facilitated elimination of fluoride as a leaving group. Additionally, we followed literature precedent to facilitate (i) 3 + 2 addition of azide to the nitrile forming the tetrazole **1.99** and (ii) hydroxylamine hydrolysis of the nitrile to the amide oxime **1.98**, which is a precursor for oxadiazole synthesis.[86–88] Unfortunately, these conditions predominantly led to defluorination presumably through elimination. By decreasing the temperatures of both reactions, however, we facilitated both reactions without accompanied elimination, albeit over extended reaction times (**Scheme 1.2.6.1**).[85]
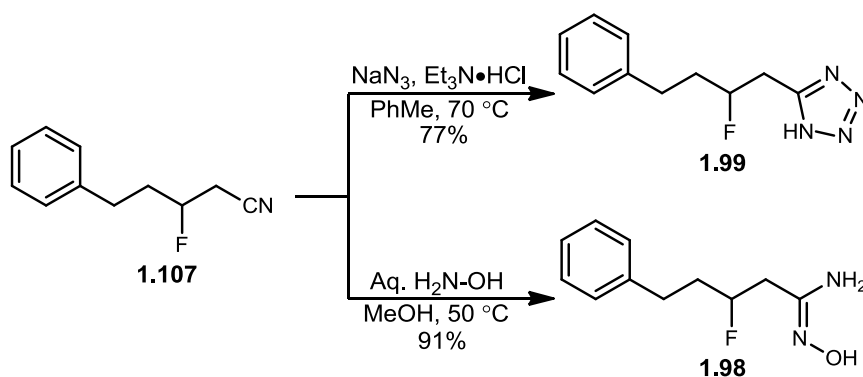
Scheme 1.2.6.1 Synthesis of β-fluoro tetrazole and β-fluoro amide oxime. Scheme adapted from ref 85.

We determined, therefore, that β-fluoronitriles are multifunctional intermediates poised to access a large number of fluorinated scaffolds, but reaction conditions must be optimized for each β-fluoronitrile modification, since literature precedent frequently results in C-F bond cleavage.

In summary, this fluorination method was a powerful extension of the previous β-fluoroamine method,[84] providing access to the same chiral β-fluoroamines and β,β-difluoroamines through a reaction manifold eliminating the possibility for racemization of the key stereocenter. Additionally, this work generates a pathway to chiral γ-fluoroamines, a

chemotype difficult to prepare and something our previous method lacked entirely. These chiral γ-fluoroamines can be accessed in good overall yields (40-58%) and excellent enantioselectivity (87-96% ee) from achiral commercial aldehydes. Importantly, outside of classical DAST chemistry, this work provides the only pathway to chiral γ-fluoroamines, to the best of our knowledge. Moreover, the chiral β-fluoronitrile lynchpin can provide access to numerous fluorinated functional groups and heterocyclic ring systems with slight perturbations of pK_a and electronic properties, which can have substantial impact on the compound's physiochemical properties.

1.3 Preliminary access to chiral *N*-alkyl aziridines and chiral C2-functionalized azetidines from prochiral aldehydes using organocatalysis

1.3.1 Importance of aziridine and azetidine heterocycles

Aziridines represent an important class of nitrogen containing heterocycles since (i) they are part of numerous natural products and (ii) they are powerful chiral intermediates that can impart their chirality on more advanced intermediates through ring opening reactions.[89] Aziridines **1.108** are 3-membered nitrogen containing rings, which results in considerable ring strain (27 kcal/mol) that can be relieved through nucleophilic ring opening. The synthetic utility of these heterocycles is derived from the ability to open chiral aziridines regioselectively.[89,90] While numerous methods exist for the synthesis of chiral aziridines including chiral pool approaches,[90] asymmetric catalysis,[91,92] and chiral auxiliaries,[93] the generality of these methods is limited while considering the carbon and nitrogen substituents tolerated by each approach. After considering the available methods, it becomes clear that general routes to access chiral 1,2-disubstituted terminal aziridines **1.109** remain rare, and asymmetric access to this aziridine subtype, as a result, is limited (**Figure 1.3.1.1**).[33,94]
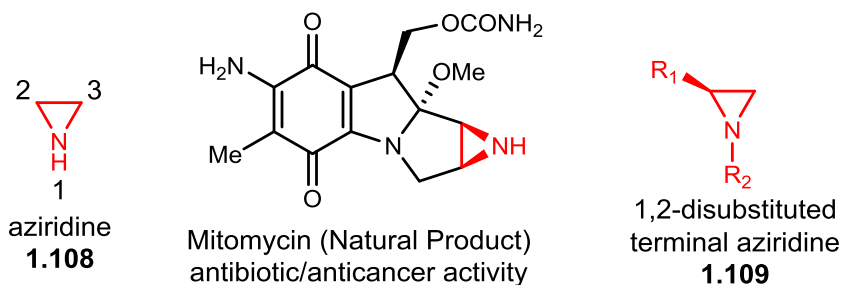
Figure 1.3.1.1 Aziridine heterocycles

Azetidines **1.110** are 4-membered nitrogen containing heterocycles that have received little attention from the synthetic community despite their presence in biologically active compounds.[95–97] One possible explanation for this fact is azetidines are much less frequently found in natural products compared with larger aza-heterocycles, and it is kinetically and thermodynamically unfavorable to form the 4-membered ring system. Compared to the smaller 3-membered or larger 5 and 6-membered aza-heterocycles, there are far fewer synthetic methods for their enantiopure preparation, especially when considering general methods.[98] Among the different methods to synthesize azetidines, access to chiral C2 substituted azetidines **1.111** are rare (**Figure 1.3.1.2**).
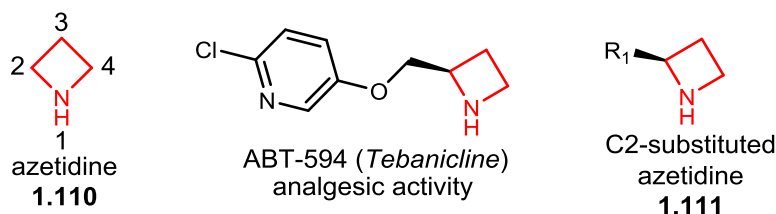

Figure 1.3.1.2 Azetidine heterocycles

After using organocatalysis to make chiral morpholines, piperazines, and fluorinated scaffolds, we saw the potential of using similar chemistry to extend the reaction pathway to aziridines and azetidines. Prior research in our lab had focused on using organocatalysis to access chiral aziridines.[33] By coupling that chemistry to the reactions described earlier in this chapter,[34,85] we reasoned that access to chiral aziridines and azetidines was possible.

60

1.3.2 Envisioned access to aziridines and azetidines

In 2010, Fadeyi, Schulte, and Lindsley developed access to chiral *N*-alkyl terminal aziridines.[33] They utilized a short reaction cascade involving asymmetric chlorination, reductive amination, and base-induced cyclization to generate aziridines in good overall yields and moderate to excellent enantioselectivity (**scheme 1.3.2.1**).
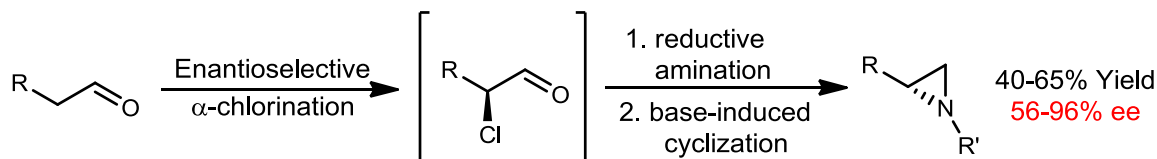

Scheme 1.3.2.1 Synthesis of chiral aziridines. Scheme adapted from ref 33.

This chemistry was a major improvement compared to the literature precedent for synthesizing chiral 1,2-disubstituted terminal aziridines. The method, however, suffered from variable enantioselectivity, since the α-chloroaldehyde taking part in the reductive amination was not configurationally stable. Since this methods deficiency was shared by our first generation chiral morpholine and piperazine method,[34] we reasoned that the same approach leading to consistent enantioinduction for morpholines and piperazines could be utilized to improve the aziridine methodology. Namely, if we could remove the reductive amination from the reaction sequence and instead make the bifunctional electrophile configurationally stable, there would no longer be deterioration of enantiomeric excess.

To improve the method, we reasoned that the same asymmetric chlorination and reduction of aldehyde **1.112** would deliver enantioenriched β-chloroalcohols **1.113** that were configurationally stable. At that point, we could utilize the conditions that were developed to make β-chloro aminoalcohols, β-chloro diamines, and β-fluoroamines by forming the β-chloro triflate and facilitating substitution reaction with primary amines. At that point, we would have a β-chloroamine, which could be cyclized to form aziridines **1.114** in the same

61

way as was previously reported (**Scheme 1.3.2.2**).[33] Additionally, the β-chloro triflate could be displaced by cyanide, just as in the γ-fluoroamine reaction pathway, to form β-chloronitrile **1.115,** which could be used to access chiral C2-substituted azetidines **1.116** after reduction of the nitrile and cyclization of the resultant amine.[85]
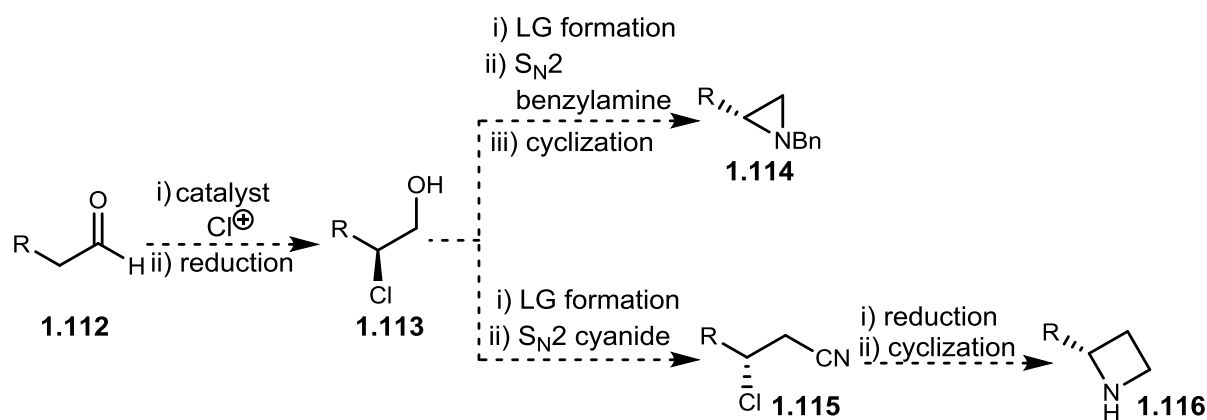
Scheme 1.3.2.2 Envisioned route to chiral aziridines and azetidines

### 1.3.3   Preliminary access to chiral *N*-alkyl aziridines

To validate the approach toward chiral *N*-alkyl terminal aziridines, we began work with three standard achiral aldehydes.   Treatment of aldehydes **1.112** with diphenylpyrrolidine catalyst and *N*-chlorosuccinimide in DCM followed by sodium borohydride reduction facilitated conversion to the chiral β-chloroalcohols **1.113** in moderate to excellent yields. We then performed a one-pot triflate formation, benzylamine alkylation, and base induced cyclization to form aziridines **1.114A-C** in a 3-step yield ranging from 69-82% overall. The overall yields for this sequence were at the high end compared to substrates from the previous aziridine methodology,[33] and the enantioselectivity was consistently over 90% ee (**Scheme 1.3.3.1**).[99]
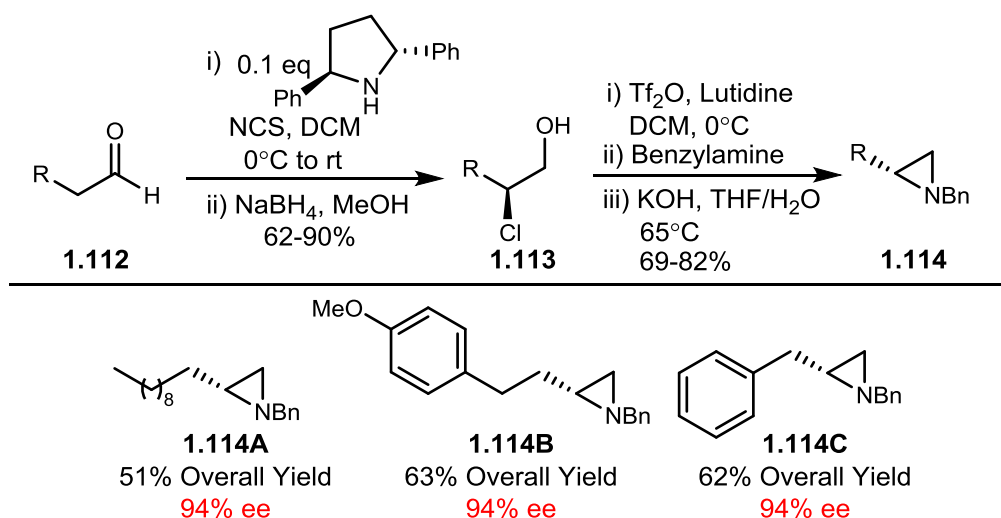
Scheme 1.3.3.1 Synthesis of chiral aziridines

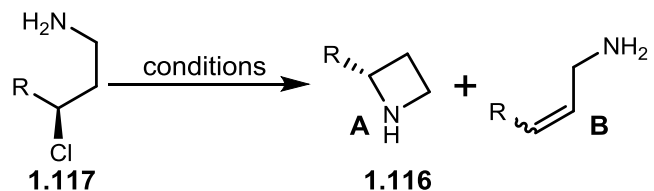### 1.3.4 Preliminary access to chiral C2-functionalized azetidines

To access azetidines, we had to access the γ-chloroamines prior to optimizing the cyclization reaction. As these steps had been optimized during our work with fluoroamine chemistry,[85] all of the reactions progressed as expected, giving us rapid access to a small assortment of chiral γ-chloroamines (**Scheme 1.3.4.1**).
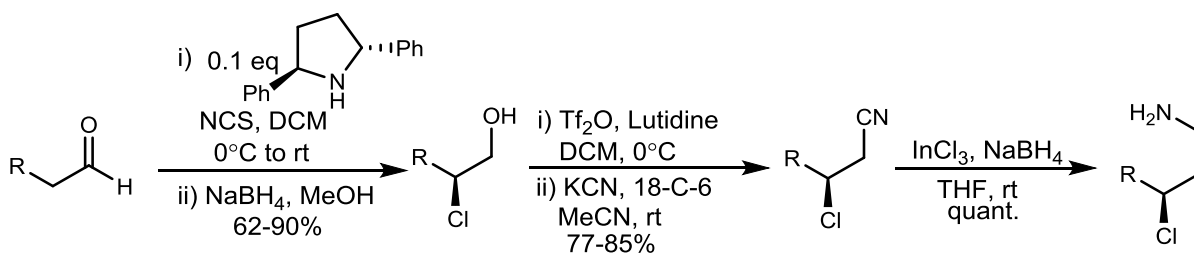
Scheme 1.3.4.1 Synthesis of chiral γ-chloroamines

While we initially tried the conditions successfully facilitating 3-*exo*-tet cyclization of β-chloroamines to aziridines (KOH, THF/H$_2$O, 65 °C), these conditions led to minimal consumption of the γ-chloroamine starting material. Additionally, when other conditions were tried, we observed substantial elimination of the chloride to the olefin. To find optimal conditions, we performed a broad screening of different bases, solvents, temperatures, and

additives to determine what would best facilitate this cyclization transformation and minimize the undesired elimination (**Table 1.3.4.1**).


Base	Solvent	Temperature	Additive	Conversion (A:B)
K$_2$CO$_3$	NMP	25 °C	--	0%
K$_2$CO$_3$	NMP	120 °C	--	40% (2:1)
K$_2$CO$_3$	NMP	180 °C	--	80% (2:1)
--	THF/H$_2$O^a	150 °C^b	--	75% (1.5:1)
KOH	THF/H$_2$O^a	65°C	--	<5% (3:1)
KOH	THF/H$_2$O^a	120 °C^b	--	<5% (3:1)
KOH	THF/H$_2$O^a	170 °C^b	--	100% (3:1)
K$_2$CO$_3$	DMF	25 °C	AgNO$_3$	0%
K$_2$CO$_3$	DMF	65 °C	AgNO$_3$	40% (2:1)
NaH	DMF	25 °C	--	0%
NaH	DMF	65 °C	--	0%
NaH	DMF	65 °C	15-C-5	<5% (0:1)
KHMDS	DMF	25 °C	--	100% (0:1)

^{a}The ration between solvents was 1:1 ^{b}reactions were run in the microwave reactor for 45 minutes at the temperature indicated

**Table 1.3.4.1** Conditions screened to facilitate azetidine ring closure

Fortunately, we found conditions that were able to promote ring closure in a 3:1 ratio with the elimination pathway. KOH in THF/H$_2$O (1:1) with forcing thermal conditions promoted γ-chloroamine **1.117** cyclization to azetidine **1.116**, and we were able to apply these conditions to a preliminary set of aldehydes. While we were able to isolate product azetidine from the mixture, the yields were rather low, ranging from 30-38% (**Scheme 1.3.4.2**).
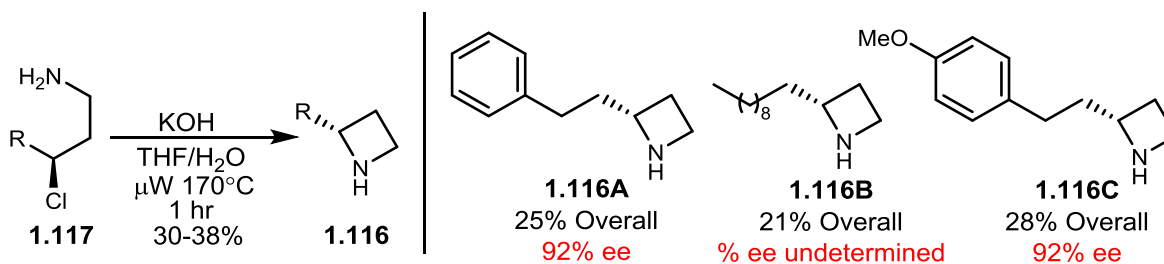
Scheme 1.3.4.2 Synthesis of chiral C2-substituted azetidines

64

While the single step yield was low, the overall yields were—in many cases—higher than literature precedent (21-28% overall); and, despite forcing thermal conditions the reaction proceeded stereospecifically, maintaining high levels of enantioinduction (>90% ee).

To highlight the practicality of the azetidine reaction pathway, we looked to the patent literature for C2-substituted azetidines with interesting biological activity. We found that azetidine **1.118** is a subunit of a calcium sensing receptor antagonist, and literature precedent prepared **1.118** in 7 steps and 8.7% overall yield.[100] We decided to make this compound using our method, to emphasize its advantages. Beginning with commercially available aldehyde **1.119**, we performed our chlorination and reduction in 84% yield to generate β-chloroalcohol **1.120**. Triflate formation and cyanide alkylation went smoothly in 74% yield, and β-chloronitrile **1.121** was reduced to the amine and cyclized to the azetidine **1.118** in 28% yield (**Scheme 1.3.4.3**). Our route, therefore, resulted in an asymmetric synthesis of **1.118** in 18% overall yield—double the literature method—and 91% ee in fewer steps than the known method.[99]
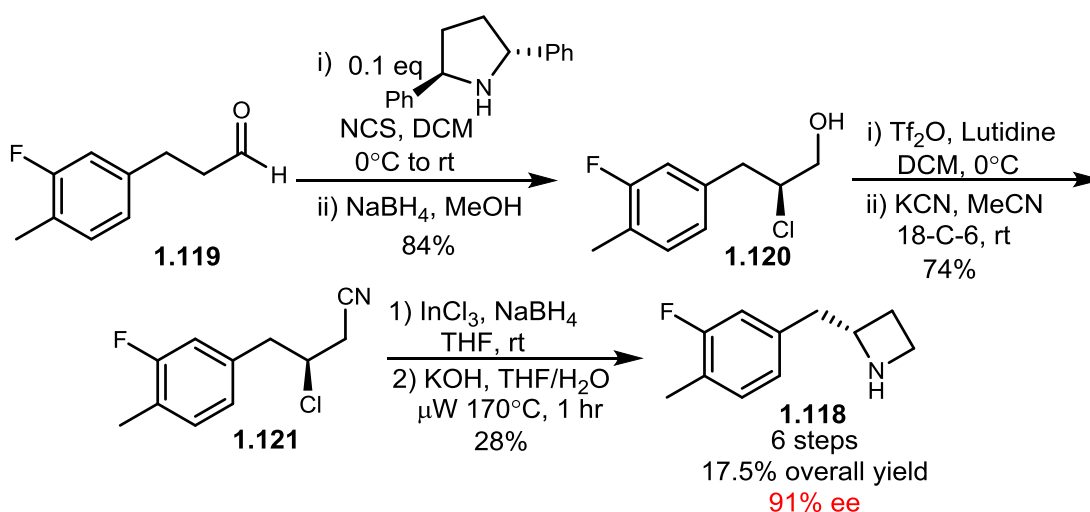
Scheme 1.3.4.3 Synthesis of calcium sensing receptor antagonist **1.118**

In summary, this reaction pathway represents a major advantage over the previous aziridine method since there is no possibility for erosion of enantioselectivity. While we are in the process of generating more examples for the substrate scope, the aziridines that have been made are in good overall yields (51-63%) and excellent enantioselectivity (94-94% ee). Additionally, this reaction manifold gives access to chiral C2-substituted azetidines, a heterocycle that is historically difficult to prepare. This method prepares azetidines in yields from 18-28% overall and in excellent enantioselectivity (>90% ee). Investigation of the reaction scope is underway, and refinements may result in increased yields.

References

(1)   B. E. Evans , K. E. Rittle , M. G. Bock , R. M. DiPardo , R. M. Freidinger , W. L.
        Whitter , G. F. Lundell , D. F. Veber , P. S. AndersonR. S. L. Chang, V. J. Lotti, D. J.
        Cerino, T. B. Chen, P. J. Kling, K. A. Kunkel, J. P. Springer, J. H. Methods for Drug
        Discovery: Development of Potent, Selective, Orally Effective Cholecystokinin
        Antagonists. *J. Med. Chem.* **1988**, *31*, 2235–2246.

(2)   DeSimone, R. W.; Currie, K. S.; Mitchell, S. A.; Darrow, J. W.; Pippin, D. A.
        Privileged Structures: Applications in Drug Discovery. *Comb. Chem. High
        Throughput Screen.* **2004**, *7*, 473–493.

(3)   Welsch, M. E.; Snyder, S. a; Stockwell, B. R. Privileged Scaffolds for Library Design
        and Drug Discovery. *Curr. Opin. Chem. Biol.* **2010**, *14*, 347–361.

(4)   Nilsson, J. W.; Thorstensson, F.; Kvarnström, I.; Oprea, T.; Samuelsson, B.; Nilsson,
        I. Solid-Phase Synthesis of Libraries Generated from a 4-Phenyl-2-Carboxy-
        Piperazine Scaffold. *J. Comb. Chem.* **2001**, *3*, 546–553.

(5)   Wijtmans, R.; Vink, M. K.; Schoemaker, H. E.; van Delft, F. L.; Blaauw, R. H.;
        Rutjes, F. P. Biological Relevance and Synthesis of C-Substituted Morpholine
        Derivatives. *Synthesis (Stuttg).* **2004**, *2004*, 641–662.

(6)   Hajós, M.; Fleishaker, J. C.; Filipiak-Reisner, J. K.; Brown, M. T.; Wong, E. H. F. The
        Selective Norepinephrine Reuptake Inhibitor Antidepressant Reboxetine:
        Pharmacological and Clinical Profile. *CNS Drug Rev.* **2004**, *10*, 23–44.

(7)   Sakurai, N.; Sano, M.; Hirayama, F.; Kuroda, T.; Uemori, S.; Moriguchi, A.;
        Yamamoto, K.; Ikeda, Y.; Kawakita, T.; Industries, Y. P. Synthesis and Structure-
        Activity Relationships of 7-(2-Aminoalkyl)morpholinoquinolones as Anti-
        Helicobacter Pylori Agents. *Bioorg. Med. Chem. Lett.* **1998**, *8*, 2185–2190.

(8)   Kulagowski, J. J.; Broughton, H. B.; Curtis, N. R.; Mawer, I. M.; Ridgill, M. P.;
        Baker, R.; Emms, F.; Freedman, S. B.; Marwood, R.; Patel, S.; et al. 3-[[4-(4-
        Chlorophenyl)piperazin-1-Yl]- Methyl]-1H-pyrrolo[2,3-B]pyridine: An Antagonist
        with High Affinity and Selectivity for the Human Dopamine D4 Receptor. *J. Med.
        Chem.* **1996**, *39*, 1941–1942.

(9)   Lawrence, N.J.; Pireddu, R.S.; Sebti, S. M. Pyridyl thiazole-based ureas as inhibitors
        of RHO associated protein kinase (ROCK) and methods of use, 2011.

(10)   Scheiper, B.; Matter, H.; Steinhagen, H.; Böcskei, Z.; Fleury, V.; McCort, G.
        Structure-Based Optimization of Potent 4- and 6-Azaindole-3-Carboxamides as Renin
        Inhibitors. *Bioorg. Med. Chem. Lett.* **2011**, *21*, 5480–5486.

(11) Ancliff, R. A.; Cook, C. M.; Eldred, C. D.; Gore, P. M.; Harrison, L. A.; Hayes, M. A.; Cook, C. M.; Eldred, C. D.; Gore, P. M.; Harrison, L. A.; Hayes, M. a.; Hodgeson, S. t.; Judd, D. B.; Keeling, S. E.; Lewell, X. Q.; Mills, G.; Robertson, G. M.; Swans, M. Preparation of Morpholineylmethylureas as CCR-3 Antagonists: WO 03082861, 2003.

(12) Leeson, P. D.; Showell, G. A.; Ramsner, R. Morpholine Derivatives as Dopamine Receptor Subtype Ligands: PCT/GB1994/002557, 1994.

(13) Stokbroekx, R. A.; Van der Aa, M. J. M. Preparation of Antirhinoviral (thio)morpholinyl and Piparazinyl Alkylphenol Ethers: EP 398426 A1 19901122, 1990.

(14) Yar, M.; McGarrigle, E. M.; Aggarwal, V. K. An Annulation Reaction for the Synthesis of Morpholines, Thiomorpholines, and Piperazines from Beta-Heteroatom Amino Compounds and Vinyl Sulfonium Salts. *Angew. Chem. Int. Ed. Engl.* **2008**, *47*, 3784–3786.

(15) Yar, M.; McGarrigle, E. M.; Aggarwal, V. K. Bromoethylsulfonium Salt--a More Effective Annulation Agent for the Synthesis of 6- and 7-Membered 1,4-Heterocyclic Compounds. *Org. Lett.* **2009**, *11*, 257–260.

(16) Lanman, B. a; Myers, A. G. Efficient, Stereoselective Synthesis of Trans-2,5-Disubstituted Morpholines. *Org. Lett.* **2004**, *6*, 1045–1047.

(17) Grotenbreg, G. M.; Christina, A. E.; Buizert, A. E. M.; van der Marel, G. a; Overkleeft, H. S.; Overhand, M. Synthesis and Application of Carbohydrate-Derived Morpholine Amino Acids. *J. Org. Chem.* **2004**, *69*, 8331–8339.

(18) Szardenings, A. K.; Burkoth, T. S.; Lu, H. H.; Tien, D. W.; Campbell, D. a. A Simple Procedure for the Solid Phase Synthesis of Diketopiperazine and Diketomorpholine Derivatives. *Tetrahedron* **1997**, *53*, 6573–6593.

(19) Hulme, C.; Cherrier, M.-P. Novel Applications of Ethyl Glyoxalate with the Ugi MCR. *Tetrahedron Lett.* **1999**, *40*, 5295–5299.

(20) Marcaccini, Stefano; Pipino, Roberto; Pozo, M. C. A Facile Synthesis of 2,5-Diketopiperazines Based on Isocyanide Chemistry. *Tetrahedron Lett.* **2001**, *42*, 2727–2728.

(21) Kennedy, A. L.; Fryer, A. M.; Josey, J. A. A New Resin-Bound Universal Isonitrile for the Ugi 4CC Reaction: Preparation 2 , 5-Diketopiperazines and 1,4-Benzodiazepine-2,5-Diones. *Org. Lett.* **2002**, *4*, 1167–1170.

(22)   Schanen, Vincent; Riche, Claude; Chiaroni, Angele; Quirion, Jean-Charles; Husson,
        H.-P. Asymmetric Synthesis . XXX1. Synthesis of 2-Substituted Piperazines from
        Chiral Non-Racemic Lactams. *Tetrahedron Lett.* **1994**, *35*, 2533–2536.

(23)   Piperazines, N.; Nakhla, J. S.; Wolfe, J. P. A Concise Asymmetric Synthesis of Cis-
        2,6-Disubstituted N-Aryl Piperazines via Pd-Catalyzed Carboamination Reactions.
        Org. Lett. **2007**, *9*, 3279–3282.

(24)   Cochran, B. M.; Michael, F. E. Synthesis of 2,6-Disubstituted Piperazines by a
        Diastereoselective Palladium-Catalyzed Hydroamination Reaction. *Org. Lett.* **2008**,
        10, 329–332.

(25)   Eliel, E. L.; Wilen, S. H. *Stereochemistry of Organic Compounds*; John Wiley and
        Sons: New York City, 1994; p. 689.

(26)   Li, H.-Y.; Jin, Y.; Morisseau, C.; Hammock, B. D.; Long, Y.-Q. The 5-Substituted
        Piperazine as a Novel Secondary Pharmacophore Greatly Improving the Physical
        Properties of Urea-Based Inhibitors of Soluble Epoxide Hydrolase. *Bioorg. Med.
        Chem.* **2006**, *14*, 6586–6592.

(27)   Viso, A.; Fernández de la Pradilla, R.; Flores, A.; García, A.; Tortosa, M.; López-
        Rodríguez, M. L. Synthesis of Highly Substituted Enantiopure Piperazines and
        Ketopiperazines from Vicinal N-Sulfinyl Diamines. *J. Org. Chem.* **2006**, *71*, 1442–
        1448.

(28)   Crestey, F.; Witt, M.; Jaroszewski, J. W.; Franzyk, H. Expedite Protocol for
        Construction of Chiral Regioselectively N-Protected Monosubstituted Piperazine, 1,4-
        Diazepane, and 1,4-Diazocane Building Blocks. *J. Org. Chem.* **2009**, *74*, 5652–5655.

(29)   Maity, Prantik; Konig, B. Synthesis and Structure of 1,4-Dipiperazino Benzenes:
        Chiral Terphenyl-Type Peptide Helix Mimetics. *Org. Lett.* **2008**, *10*, 1473–1476.

(30)   Pohlmann, A.; Schanen, V.; Guillaume, D.; Quirion, J. Efficient Synthesis of
        Conformationally Constrained Peptidomimetics Containing 2-Oxopiperazines 1. *J.
        Org. Chem.* **1997**, *62*, 1016–1022.

(31)   Brochu, M. P.; Brown, S. P.; MacMillan, D. W. C. Direct and Enantioselective
        Organocatalytic Alpha-Chlorination of Aldehydes. *J. Am. Chem. Soc.* **2004**, *126*,
        4108–4109.

(32)   Halland, N.; Braunton, A.; Bachmann, S.; Marigo, M.; Jørgensen, K. A. Direct
        Organocatalytic Asymmetric Alpha-Chlorination of Aldehydes. *J. Am. Chem. Soc.*
        2004, *126*, 4790–4791.

(33)   Fadeyi, O. O.; Schulte, M. L.; Lindsley, C. W. General Access to Chiral N-Alkyl
        Terminal Aziridines via Organocatalysis. *Org. Lett.* **2010**, *12*, 3276–3278.

(34) O'Reilly, M. C.; Lindsley, C. W. Enantioselective Synthesis of C2-Functionalized, N-Protected Morpholines and Orthogonally N,N'-Protected Piperazines via Organocatalysis. *Tetrahedron Lett.* **2012**, *53*, 1539–1542.

(35) Vaillancourt, V.; Cudahy, M. M. Methanesulfonyl Chloride. *Encycl. reagents Org. Synth.* **2007**, 1–23.

(36) Noyce, Donald S; Virgilio, J. A. The Synthesis and Solvolysis of 1-Phenylethyl Disubstituted Phosphines. *J. Org. Chem.* **1972**, *37*, 2643–2647.

(37) O'Reilly, M. C.; Lindsley, C. W. A General, Enantioselective Synthesis of Protected Morpholines and Piperazines. *Org. Lett.* **2012**, *14*, 2910–2913.

(38) Marigo, M.; Bachmann, S.; Halland, N.; Braunton, A.; Jørgensen, K. A. Highly Enantioselective Direct Organocatalytic Alpha-Chlorination of Ketones. *Angew. Chem. Int. Ed. Engl.* **2004**, *43*, 5507–5510.

(39) Clark, F. H. *How Modern Medicines Are Discovered*; Clark, F. H., Ed.; Futura Publishing: Mount Kisko, NY, 1973.

(40) Morgenthaler, M.; Schweizer, E.; Hoffmann-Röder, A.; Benini, F.; Martin, R. E.; Jaeschke, G.; Wagner, B.; Fischer, H.; Bendels, S.; Zimmerli, D.; et al. Predicting and Tuning Physicochemical Properties in Lead Optimization: Amine Basicities. *ChemMedChem* **2007**, *2*, 1100–1115.

(41) O'Hagan, D. Understanding Organofluorine Chemistry. An Introduction to the C-F Bond. *Chem. Soc. Rev.* **2008**, *37*, 308–319.

(42) Purser, S.; Moore, P. R.; Swallow, S.; Gouverneur, V. Fluorine in Medicinal Chemistry. *Chem. Soc. Rev.* **2008**, *37*, 320–330.

(43) Furuya, T.; Kamlet, A. S.; Ritter, T. Catalysis for Fluorination and Trifluoromethylation. *Nature* **2011**, *473*, 470–477.

(44) Müller, K.; Faeh, C.; Diederich, F. Fluorine in Pharmaceuticals: Looking beyond Intuition. *Science (80-.).* **2007**, *317*, 1881–1886.

(45) Wong, D. T.; Bymaster, F. P.; Engleman, E. A. Prozac (Fluoxetine, Lilly 110140), The First Selective Serotonin Uptake Inhibitor and an Antidepressant Drug: Twenty Years Since Its First Publication. *Life Sci.* **1995**, *57*, 411–441.

(46) Robertson, J. F. R.; Come, S. E.; Jones, S. E.; Beex, L.; Kaufmann, M.; Makris, a; Nortier, J. W. R.; Possinger, K.; Rutqvist, L.-E. Endocrine Treatment Options for Advanced Breast Cancer--the Role of Fulvestrant. *Eur. J. Cancer* **2005**, *41*, 346–356.

(47) Drlica, K.; Malik, M. Fluoroquinolones: Action and Resistance. *Curr. Top. Med. Chem.* **2003**, *3*, 249–282.

(48) Adkins, J. C.; Noble, S. Efavirenz. *Drugs* **1998**, *56*, 1055–1066.

(49) Böhm, H.-J.; Banner, D.; Bendels, S.; Kansy, M.; Kuhn, B.; Müller, K.; Obst-Sander, U.; Stahl, M. Fluorine in Medicinal Chemistry. *ChemBioChem* **2004**, *5*, 637–643.

(50) Biffinger, J. C.; Kim, H. W.; DiMagno, S. G. The Polar Hydrophobicity of Fluorinated Compounds. *ChemBioChem* **2004**, *5*, 622–627.

(51) Hagmann, W. K. The Many Roles for Fluorine in Medicinal Chemistry. *J. Med. Chem.* **2008**, *51*, 4359–4369.

(52) Clader, J. W. The Discovery of Ezetimibe: A View from Outside the Receptor. *J. Med. Chem.* **2004**, *47*, 1–9.

(53) Rosenblum, S. B.; Huynh, T.; Afonso, A.; Davis, H. R.; Yumibe, N.; Clader, J. W.; Burnett, D. A. A Designed , Potent , Orally Active Inhibitor of Cholesterol Absorption. *J. Med. Chem.* **1998**, *41*, 973–980.

(54) Penning, T. D.; Talley, J. J.; Bertenshaw, S. R.; Carter, J. S.; Collins, P. W.; Docter, S.; Graneto, M. J.; Lee, L. F.; Malecha, J. W.; Miyashiro, J. M.; et al. Synthesis and Biological Evaluation of the 1,5-Diarylpyrazole Class of Cyclooxygenase-2 Inhibitors: Identification of 4-[5-(4-Methylphenyl)-3-(trifluoromethyl)-1H-Pyrazol-1-Yl]benze Nesulfonamide (SC-58635, Celecoxib). *J. Med. Chem.* **1997**, *40*, 1347–1365.

(55) Chou, Y.-L.; Davey, D. D.; Eagen, K. a; Griedel, B. D.; Karanjawala, R.; Phillips, G. B.; Sacchi, K. L.; Shaw, K. J.; Wu, S. C.; Lentz, D.; et al. Structure-Activity Relationships of Substituted Benzothiophene-Anthranilamide Factor Xa Inhibitors. *Bioorg. Med. Chem. Lett.* **2003**, *13*, 507–511.

(56) Boehm, J. C.; Smietana, J. M.; Sorenson, M. E.; Garigipati, R. S.; Gallagher, T. F.; Sheldrake, P. L.; Bradbeer, J.; Badger, a M.; Laydon, J. T.; Lee, J. C.; et al. 1-Substituted 4-Aryl-5-Pyridinylimidazoles: A New Class of Cytokine Suppressive Drugs With Low 5-Lipoxygenase and Cyclooxygenase Inhibitory Potency. *J. Med. Chem.* **1996**, *39*, 3929–3937.

(57) Avdeef, A. *Absorption and Drug Development: Solubility, Permeability, and Charge State*; Wiley: Hoboken, 2003.

(58) Avdeef, A. Physicochemical Profiling (solubility, Permeability and Charge State). *Curr. Top. Med. Chem.* **2001**, *1*, 277–351.

(59) Alberati, D.; Hainzl, D.; Jolidon, S.; Krafft, E. a; Kurt, A.; Maier, A.; Pinard, E.; Thomas, A. W.; Zimmerli, D. Discovery of 4-Substituted-8-(2-Hydroxy-2-Phenyl-

Cyclohexyl)-2,8-Diaza-spiro[4.5]decan-1-One as a Novel Class of Highly Selective GlyT1 Inhibitors with Improved Metabolic Stability. *Bioorg. Med. Chem. Lett.* **2006**, *16*, 4311–4315.

(60)   Jamieson, C.; Moir, E. M.; Rankovic, Z.; Wishart, G. Medicinal Chemistry of hERG Optimizations: Highlights and Hang-Ups. *J. Med. Chem.* **2006**, *49*, 5029–5046.

(61)   Niel, M. B. Van; Collins, I.; Beer, M. S.; Broughton, H. B.; Cheng, S. K. F.; Goodacre, S. C.; Heald, A.; Locker, K. L.; Macleod, A. M.; Morrison, D.; et al. Fluorination of 3-(3-(Piperidin-1-Yl)propyl) Indoles and 3-(3-(Piperazin-1-Yl)propyl) Indoles Gives Selective Human 5-HT 1D Receptor Ligands with Improved Pharmacokinetic Profiles. *J. Med. Chem.* **1999**, *42*, 2087–2104.

(62)   Rowley, M.; Hallett, D. J.; Goodacre, S.; Moyes, C.; Crawforth, J.; Sparey, T. J.; Patel, S.; Marwood, R.; Thomas, S.; Hitzel, L.; et al. 3-(4-Fluoropiperidin-3-Yl)-2-Phenylindoles as High Affinity, Selective, and Orally Bioavailable h5-HT(2A) Receptor Antagonists. *J. Med. Chem.* **2001**, *44*, 1603–1614.

(63)   Gribble, G. W. *Progress in the Chemistry of Organic Natural Products*; Herz, W.; Kirby, G. W.; Moore, R. E.; Steglich, W.; Tamm, C., Ed.; 68th ed.; Springer, 1996; pp. 1–148.

(64)   Gribble, G. W. *Progress in the Chemistry of Organic Natural Products*; Kinghord, A. D.; Falk, H.; Kobayashi, J., Ed.; 91st ed.; Springer, 2009; pp. 1–613.

(65)   Hagan, D. O.; Schaffrath, C.; Cobb, S. L.; Hamilton, J. T. G. Biosynthesis of an Organofluorine Molecule. *Nature* **2002**, *461*, 279.

(66)   Dong, C.; Huang, F.; Deng, H.; Schaffrath, C. Crystal Structure and Mechanism of a Bacterial Fluorinating Enzyme. *Nature* **2004**, *427*, 561–565.

(67)   Hayashi, H.; Sonoda, H.; Fukumura, K.; Nagata, T. 2,2-Difluoro-1,3-Dimethylimidazolidine (DFI). A New Fluorinating Agent. *Chem. Commun. (Camb).* **2002**, 1618–1619.

(68)   Shimizu, M.; Hiyama, T. Modern Synthetic Methods for Fluorine-Substituted Target Molecules. *Angew. Chemie Int. Ed.* **2005**, *44*, 214–231.

(69)   Camps, F.; Chamorro, E.; Gasol, V.; Guerrero, A. Efficient Utilization of Tetrabutylammonium Bifluoride in Halofluorination Reactions. *J. Org. Chem.* **1989**, *54*, 4294–4298.

(70)   Furuta, Satoru; Kuoboshi, Manabu; Hiyama, T. A Facile Synthesis of Trifluoromethyl-and 3,3,3-Trifluoropropenyl Substituted Aromatic Compounds by the Oxidative Desulfurization-Fluorination of the Corresponding Carbodithioates. *Bull. Chem. Soc. Jpn.* **1999**, *72*, 805–819.

(71)   Lal, G. S.; Pez, G. P.; Syvret, R. G. Electrophilic NF Fluorinating Agents. *Chem. Rev.*
        1996, *96*, 1737–1756.

(72)   Avent, Anthony G.; Bowler, Andrew N.; Doyle, Paul M.; Marchand, Christina M.;
        Young, D. W. Stereospecific Synthesis of 4-Fluoroglutamic Acids. *Tetrahedron Lett.*
        1992, *33*, 1509–1512.

(73)   Rozen, S.; Faust, Y.; Ben-yakov, H. A New Method for Fluorination of Sterols.
        1Tetrahedron Lett. **1979**, *20*, 1823–1826.

(74)   Uneme, Hideki; Okada, Y. Synthesis of Non-Ester Pyrethroids Having a 1-Fluoro-1-
        Methylethyl Group Using 1,2-Migration of an Aryl Group. *Bull. Chem. Soc. Jpn.*
        1992, *65*, 2401–2410.

(75)   Shibata, N.; Ishimaru, T.; Nakamura, S.; Toru, T. New Approaches to Enantioselective
        Fluorination: Cinchona Alkaloids Combinations and Chiral Ligands/metal Complexes.
        J. Fluor. Chem. **2007**, *128*, 469–483.

(76)   Enders, D.; Hüttl, M. R. Direct Organocatalytic A-Fluorination of Aldehydes and
        Ketones. *Synlett* **2005**, 0991–0993.

(77)   Steiner, D. D.; Mase, N.; Barbas, C. F. Direct Asymmetric Alpha-Fluorination of
        Aldehydes. *Angew. Chem. Int. Ed. Engl.* **2005**, *44*, 3706–3710.

(78)   Brandes, S.; Niess, B.; Bella, M.; Prieto, A.; Overgaard, J.; Jørgensen, K. A. Non-
        Biaryl Atropisomers in Organocatalysis. *Chem. Eur. J.* **2006**, *12*, 6039–6052.

(79)   Marigo, M.; Fielenbach, D.; Braunton, A.; Kjaersgaard, A.; Jørgensen, K. A.
        Enantioselective Formation of Stereogenic Carbon-Fluorine Centers by a Simple
        Catalytic Method. *Angew. Chem. Int. Ed. Engl.* **2005**, *44*, 3703–3706.

(80)   Marigo, M.; Jørgensen, K. A. Organocatalytic Direct Asymmetric Alpha-Heteroatom
        Functionalization of Aldehydes and Ketones. *Chem. Commun. (Camb).* **2006**, 2001–
        2011.

(81)   Franze, J.; Marigo, M.; Fielenbach, D.; Wabnitz, T. C.; Kjærsgaard, A.; Jørgensen, K.
        A. A General Organocatalyst for Direct a-Functionalization of Aldehydes:
        Stereoselective C - C , C - N , C - F , C - Br , and C - S Bond-Forming Reactions .
        Scope and Mechanistic Insights. *J. Am. Chem. Soc.* **2005**, *127*, 18296–18304.

(82)   Beeson, T. D.; Macmillan, D. W. C. Enantioselective Organocatalytic Alpha-
        Fluorination of Aldehydes. *J. Am. Chem. Soc.* **2005**, *127*, 8826–8828.

(83)   Huang, Y.; Walji, A. M.; Larsen, C. H.; MacMillan, D. W. C. Enantioselective
        Organo-Cascade Catalysis. *J. Am. Chem. Soc.* **2005**, *127*, 15051–15053.

(84)   Fadeyi, O. O.; Lindsley, C. W. Rapid , General Access to Chiral B-Fluoroamines and B,B-Difluoroamines via Organocatalysis. *Org. Lett.* **2009**, *11*, 943–946.

(85)   O'Reilly, M. C.; Lindsley, C. W. A General, Enantioselective Synthesis of B- and Γ-Fluoroamines. *Tetrahedron Lett.* **2013**, *54*, 3627–3629.

(86)   Vorona, S.; Artamonova, T.; Zevatskii, Y.; Myznikov, L. An Improved Protocol for the Preparation of 5-Substituted Tetrazoles from Organic Thiocyanates and Nitriles. *Synthesis (Stuttg).* **2014**, *46*, 781–786.

(87)   Koguro, K.; Oga, T.; Mitsui, S.; Orita, R. Novel Synthesis of 5-Substituted Tetrazoles from Nitriles. *Synthesis (Stuttg).* **1998**, 910–914.

(88)   Copp, R. R.; Abraham, B. D.; Farnham, J. G.; Twose, T. M. Process Research Towards a Scalable Synthesis of the Muscarinic M1 Receptor Subtype Selective Agonist MCD-386. *Org. Process Res. Dev.* **2011**, *15*, 1344–1347.

(89)   Pellissier, H. Recent Developments in Asymmetric Aziridination. *Tetrahedron* **2010**, *66*, 1509–1555.

(90)   Tanner, D. Chiral Aziridines—Their Synthesis and Use in Stereoselective Transformations. *Angew. Chemie Int. Ed. English* **1994**, *33*, 599–619.

(91)   Muller, P.; Fruit, C. Enantioselective Catalytic Aziridinations and Asymmetric Nitrene Insertions into CH Bonds. *Chem. Rev.* **2003**, *103*, 2905–2919.

(92)   Mossner, C.; Bolm, C. *Transition Metals for Organic Synthesis*; Beller, M.; Bolm, C., Ed.; 2nd ed.; Wiley-WCH Verlag: Weinheim, 2004; pp. 389–402.

(93)   Osborn, H. M. I.; Sweeney, J. B. The Asymmetric Synthesis of Aziridines. *Tetrahedron: Asymmetry* **1997**, *8*, 1693–1715.

(94)   Malkov, A. V; Stoncius, S.; Kocovský, P. Enantioselective Synthesis of 1,2-Diarylaziridines by the Organocatalytic Reductive Amination of Alpha-Chloroketones. *Angew. Chem. Int. Ed. Engl.* **2007**, *46*, 3722–3724.

(95)   Kapoor, R.; Chawla, R.; Singh, S.; Yadav, L. Organocatalytic Asymmetric Synthesis of 1,2,4-Trisubstituted Azetidines by Reductive Cyclization of Aza-Michael Adducts of Enones. *Synlett* **2012**, *23*, 1321–1326.

(96)   Enders, D.; Gries, J.; Kim, Z.-S. Asymmetric Synthesis of 2-Mono- and 2,3-Trans-Disubstituted Azetidines. *European J. Org. Chem.* **2004**, *2004*, 4471–4482.

(97)   Brandi, A.; Cicchi, S.; Cordero, F. M. Novel Syntheses of Azetidines and Azetidinones. *Chem. Rev.* **2008**, *108*, 3988–4035.

(98)   Couty, F.; Evano, G.; Prim, D. Synthesis of Chiral Non Racemic Azetidines. *Minireviews Org. Chem.* **2004**, *1*, 133–148.

(99)   O'Reilly, Matthew C; Senter, Timothy J; Lindsley, C. W. A Lynchpin Approach for the Enantioselective Synthesis of Aziridines and Azetidines. *Unpubl. Results*.

(100)   Nakao, Akira; Gotanda, Kentoku; Aoki, Kzumasa; Kaneko, Satoru; Arita, Tsuyoshi; Fujimhiiki, T. Biphenyl-Cyclic Amine Compound. WO/2010/113860, PCT/JP2010/055546, 2010.

Experimental for chiral C2-subsituted morpholines and piperazines

All reagents were purchased from Sigma-Aldrich Corp., TCI America, Rieke Metals, Inc. and were used without purification. Analytical thin-layer chromatography (TLC) was performed on 250 μm silica plates from Sorbent Technologies. Visualization was accomplished via UV light, and/or the use of ninhydrin, iodine, and potassium permanganate solutions followed by application of heat. Chromatography was performed using Silica Gel 60 (230-400 mesh) from Sorbent Technologies or Silica RediSep Rf flash columns on a CombiFlash Rf automated flash chromatography system. All ^{1}H and ^{13}C NMR spectra were recorded on a Bruker AV-400 (400 MHz) instrument. Chemical shifts are reported in ppm relative to residual solvent peaks as an internal standard set to δ 7.26 and δ 77.16 (CDCl$_3$). Data are reported as follows: chemical shift, multiplicity (s = singlet, d = doublet, t = triplet, q = quartet, p = pentet, br = broad, dd = doublet of doublets, dq = doublet of quartets, td = triplet of doublets, pd = pentet of doublets, m = multiplet), coupling constat (Hz), integration. Low resolution mass spectra (LCMS) were recorded on an Agilent 1200 LCMS with electrospray ionization. High resolution mass spectra (HRMS) were recorded on a Waters Qtof-API-US plus Acuity system with ES as the ion source. Analytical high performance liquid chromatography (HPLC) was performed on an Agilent 1200 analytical LCMS with UV detection at 214 nm and 254 nm along with ELSD detection. Chiral separations were performed on a Thar Investigator II supercritical fluid chromatograph (SFC) utilizing Chiralcel® OD, OD-Cl, OJ, and Chiralpak® IA columns. Optical rotations were acquired on a Jasco P-2000 polarimeter at 23 ^{0}C and 589 nm. The specific rotations were calculated according to the equation $[\alpha]23/D = 100\alpha/l \times c$ where l is the path length in decimeters and c is the concentration in g/100 mL.

Procedure for Chiral Chloro-alcohol Synthesis
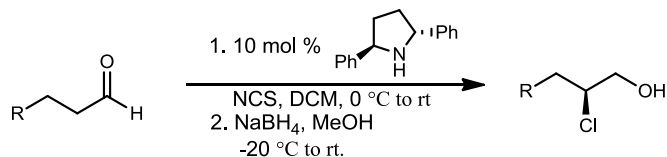
To a solution of aldehyde (1 mmol) and (2R, 5R)-2,5-diphenylpyrrolidine (0.1 eq., 0.1 mmol) in DCM (2.0 mL) was added *N*-chlorosuccinimide (173 mg, 1.3 mmol, 1.3 eq.) at 0 ^{0}C. The reaction was kept at 0 ^{0}C for 1 hour at which point it was allowed to warm to ambient temperature. It was then stirred until the aldehyde was completely consumed as determined by ^{1}H NMR spectroscopy of the reaction mixture. The reaction was then cooled to 0 ^{0}C and diluted with methanol (10 mL). NaBH$_4$ (189 mg, 5 mmol, 5 eq) was added in several portions and the mixture was stirred for 30 minutes and quenched via the addition of water. The reaction was extracted 3X with EtOAc, dried with MgSO$_4$, and concentrated.
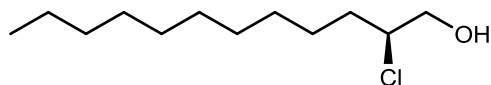
(*S*)-2-chlorododecan-1-ol **(1.70A)**

The product was prepared according to the chiral chloro-alcohol synthesis procedure and purified by silica chromatography (6:1 Hexanes/EtOAc) to afford the product as a clear oil (159.5 mg, 72.2%). ^{1}H NMR (400.1 MHz, CDCl$_3$) δ (ppm): 3.99 (s, br, 1H); 3.78-3.75 (m, 1H); 3.67-3.62 (m, 1H); 2.37-2.27 (m, 1H); 1.80-1.64 (m, 2H); 1.55-1.46 (m, 1H); 1.42-1.36 (m, 1H); 1.25 (s, br, 14H); 0.87 (t, *J* = 6.5 Hz, 3H). ^{13}C NMR (100.6 MHz, CDCl$_3$) δ (ppm): 66.92, 65.22, 34.18, 31.81, 29.49, 29.46, 29.34, 29.23, 29.03, 26.24, 22.59, 14.01. Specific rotation [—= -41.0^0 (*c* = 100, MeOH).
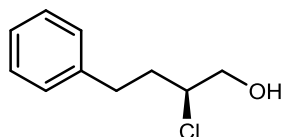
(*S*)-2-chloro-4-phenylbutan-1-ol **(1.70B)**

The product was prepared according to the chiral chloro-alcohol synthesis procedure and purified by silica chromatography (6:1 Hexanes/EtOAc) to afford the product as a clear oil (154 mg, 83%). ^{1}H NMR (400.1 MHz, CDCl$_3$) δ (ppm): 7.33-7.20 (m, 5H); 4.02-3.96 (m, 1H); 3.82-3.67 (m, 2H); 2.94-2.87 (m, 1H); 2.80-2.73 (m, 1H); 2.09-1.99 (m, 3H). ^{13}C NMR (100.6 MHz, CDCl$_3$) δ (ppm): 140.61, 128.49, 128.47, 126.17, 66.92, 64.02, 35.75, 32.30. Specific rotation [─= -43.1° (*c* = 100, MeOH).
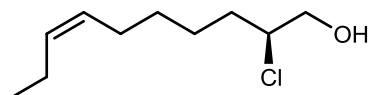
(*S,Z*)-2-chlorodec-7-en-1-ol **(1.70C)**

The product was prepared according to the chiral chloro-alcohol synthesis procedure and purified by silica chromatography (6:1 Hexanes/EtOAc) to afford the product as a clear oil (157 mg, 82%). ^{1}H NMR (400.1 MHz, CDCl$_3$) δ (ppm): 5.36-5.23 (m, 2H); 3.97-3.91 (m, 1H); 3.74-3.68 (m, 1H); 3.65-3.59 (m, 1H); 2.87 (s, br, 1H); 2.03-1.95 (m, 4H); 1.79-1.60 (m, 2H); 1.56-1.47 (m, 1H); 1.43-1.28 (m, 3H); 0.91 (td, J_1 = 1.97 Hz, J_2 = 7.50 Hz, 3H). ^{13}C NMR (100.6 MHz, CDCl$_3$) δ (ppm): 131.86, 128.52, 68.81, 64.80, 34.07, 29.10, 26.73, 25.83, 20.41, 14.23. Specific rotation [─= -31.3° (*c* = 100, MeOH).
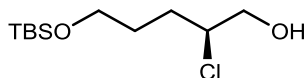
(*S*)-5-((*tert*-butyldimethylsilyl)oxy)-2-chloropentan-1-ol **(1.70D)**

The product was prepared according to the chiral chloro-alcohol synthesis procedure and purified by silica chromatography (9:1 Hexanes/EtOAc) to afford the product as a clear oil (199 mg, 79%). ^{1}H NMR (400.1 MHz, CDCl$_3$) δ (ppm): 4.10-4.04 (m, 1H); 3.83-3.77 (m, 1H); 3.71-3.63 (m, 3H); 2.11-2.06 (m, 1H); 1.94-1.85 (m, 1H); 1.81-1.71 (m, 2H); 1.68-1.53 (m, 1H); 0.89 (S, 9H); 0.047 (S, 6H). ^{13}C NMR (100.6 MHz, CDCl$_3$) δ (ppm): 66.85, 64.86, 62.30, 30.70, 29.25, 25.83, 18.21, -5.43. HRMS (TOF, ES+) C$_{11}$H$_{25}$ClO$_2$Si [M+H]$^+$ calc. mass 253.1391, found 253.1393. Specific rotation [— = -13.8 (*c* = 100, MeOH).

General Procedure for Chiral Chloro-Aminoalcohol Synthesis
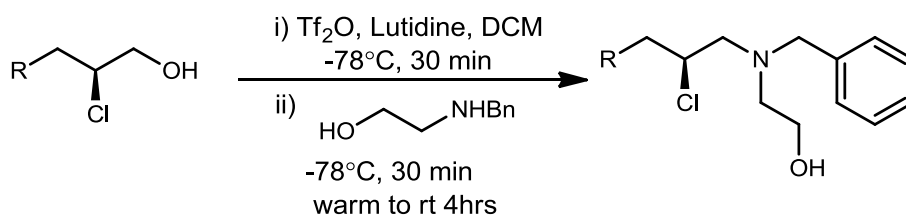
Lutidine (10 eq.) was added to a solution of chloro alcohol (1 eq.) in DCM (0.1 M) in a flame dried flask under an argon atmosphere and the reaction was cooled to -78 ^{0}C. Triflic Anhydride (1.3 eq.) was added dropwise to the reaction and it was allowed to stir for 30 minutes. To this reaction, still at -78 ^{0}C, was added the aminoalcohol (2 eq.) dropwise, dissolved in 1 mL of DCM. This reaction was allowed to warm to room temperature over the next 4 hours and was quenched with water and brine. It was extracted 3X with EtOAc, dried with MgSO$_4$, and concentrated before purification.
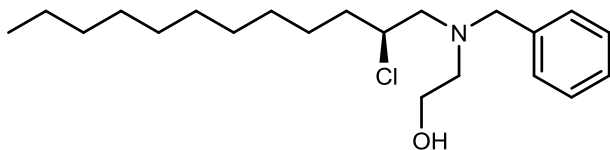
(*S*)-2-(benzyl(2-chlorododecyl)amino)ethanol **(1.73A)**
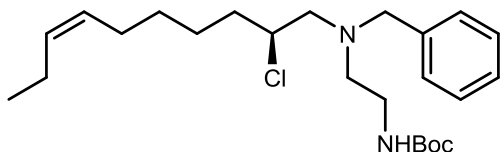
The product was prepared according to the chloro amino alcohol procedure on a 0.36 mmol

scale and purified by silica chromatography (9:1 Hexanes/EtOAc) to afford the product as a

clear oil (94 mg, 0.27 mmol, 74%). ^{1}H NMR (400.1 MHz, CDCl$_3$) δ (ppm): 7.39-7.32 (m,

4H); 7.31-7.26 (m, 1H); 4.0-3.9 (m, 1H); 3.79-3.65 (m, 2H); 3.65-3.53 (m, 2H), 2.90-2.62

(m, 5H); 1.81-1.70 (m, 1H); 1.66-1.45 (m, 2H); 1.29 (s, br, 15H); 0.92 (t, *J* = 6.81). ^{13}C

NMR (100.6 MHz, CDCl$_3$) δ (ppm): 138.29, 128.97, 128.38, 127.34, 61.44, 61.21, 59.43,

58.75, 56.27, 35.98, 31.84, 29.53, 29.49, 29.39, 29.26, 29.06, 26.14, 22.63, 14.07. HRMS

(TOF, ES+) C$_{21}$H$_{37}$NOCl [M+H]$^{+}$ calc. mass 354.2564, found 354.2563. Specific rotation

[—= -8.8° (*c* = 100, MeOH).
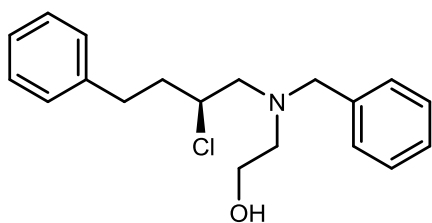
(*S*)-2-(benzyl(2-chloro-4-phenylbutyl)amino)ethanol **(1.73B)**

The product was prepared according to the chloro amino alcohol procedure on a 0.38 mmol

scale and purified by silica chromatography (9:1 Hexanes/EtOAc) to afford the product as a

clear oil (91 mg, 0.29 mmol, 76%). ^{1}H NMR (400.1 MHz, CDCl$_3$) δ (ppm): 7.40-7.20 (m,

10H); 3.99-3.90 (m, 1H); 3.76-3.53 (m, 4H); 2.96-2.63 (m, 7H); 2.18-2.07 (m, 1H); 1.99-

1.88 (m, 1H). ^{13}C NMR (100.6 MHz, CDCl$_3$) δ (ppm): 140.85, 138.20, 128.97, 128.49,

128.46, 128.42, 127.38, 126.11, 61.14, 60.30, 59.34, 58.82, 56.28, 37.60, 32.30. HRMS

(TOF, ES+) $C_{19}H_{25}ClNO$ $[M+H]^+$ calc. mass 318.1625, found 318.1624. Specific rotation [—= -15.1° (c = 100, MeOH).
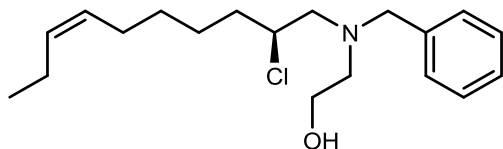
(*S*,*Z*)-2-(benzyl(2-chlorodec-7-en-1-yl)amino)ethanol **(1.73C)**

The product was prepared according to the chloro amino alcohol procedure on a 0.29 mmol scale and purified by silica chromatography (9:1 Hexanes/EtOAc) to afford the product as a clear oil (71 mg, 0.22 mmol, 76%). ^{1}H NMR (400.1 MHz, CDCl$_3$) δ (ppm): 7.39-7.30 (m, 4H); 7.30-7.24 (m, 1H); 5.43-5.26 (m, 2H); 3.98-3.88 (m, 1H); 3.78-3.63 (m, 2H); 3.63-3.50 (m, 2H); 2.87-2.61 (m, 5H); 2.09-1.97 (m, 4H); 1.80-1.69 (m, 1H); 1.64-1.45 (m, 2H); 1.43-1.22 (m, 4H); 0.96 (s, *J* = 7.53, 3H). ^{13}C NMR (100.6 MHz, CDCl$_3$) δ (ppm): 138.24, 131.87, 128.96, 128.63, 128.39, 128.35, 61.33, 61.15, 59.39, 58.73, 56.24, 35.87, 29.14, 26.14, 25.76, 20.45, 14.30. HRMS (TOF, ES+) $C_{19}H_{31}ClNO$ $[M+H]^+$ calc. mass 324.2094, found 324.2094. Specific rotation [—= -9.5° (c = 100, MeOH).
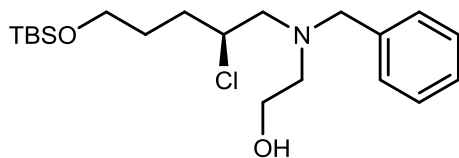

(*S*)-2-(benzyl(5-((*tert*-butyldimethylsilyl)oxy)-2-chloropentyl)amino)ethanol **(1.73D)**
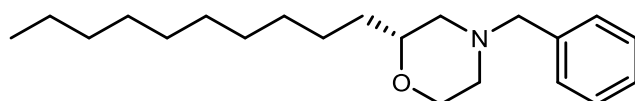
The product was prepared according to the chloro amino alcohol procedure on a 0.37 mmol scale and purified by silica chromatography (9:1 Hexanes/EtOAc) to afford the product as a clear oil (106 mg, 0.27 mmol, 74%). ^{1}H NMR (400.1 MHz, CDCl$_3$) δ (ppm): 7.36-7.23 (m,

5H); 4.03-3.93 (m, 1H); 3.78-3.49 (m, 6H); 2.83-2.69 (m, 4H); 2.68-2.59 (m, 1H); 1.95-1.83

(m, 1H); 1.79-1.67 (m, 1H); 1.66-1.51 (m, 2H); 0.89 (s, 9H); 0.04 (s, 6H). ^{13}C NMR (100.6

MHz, CDCl$_3$) δ (ppm): 138.24, 128.95, 128.38, 127.33, 62.30, 61.24, 61.20, 59.40, 58.77,

56.20, 32.45, 29.33, 25.88, 18.24, -5.38. HRMS (TOF, ES+) C$_{20}$H$_{37}$NO$_2$ClSi [M+H]$^+$ calc.

mass 386.2282, found 386.2282. Specific rotation [—= -5.7° (c = 100, MeOH).

General Procedure for Chiral Chloro-Diamine Synthesis
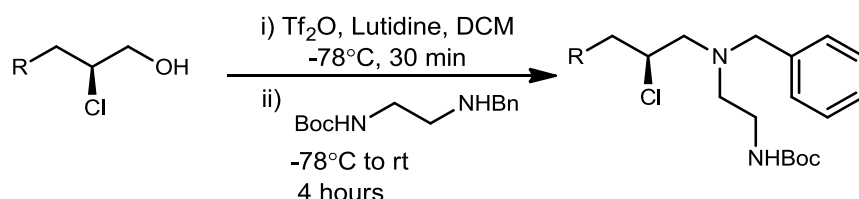
Lutidine (10 eq.) was added to a solution of chloro alcohol (1 eq.) in DCM (0.1 M) in a flame

dried flask and the reaction was cooled to -78 ^{0}C. Triflic Anhydride (1.3 eq.) was added

dropwise to the reaction and it was allowed to stir for 30 minutes. To this reaction, still at -

78 ^{0}C, was added the diamine (2 eq.) dropwise, dissolved in 1 mL of DCM. This reaction

was allowed to warm to room temperature over the next 4 hours and was quenched with

water and brine. It was extracted 3X with EtOAc, dried with MgSO$_4$, and concentrated

before purification.
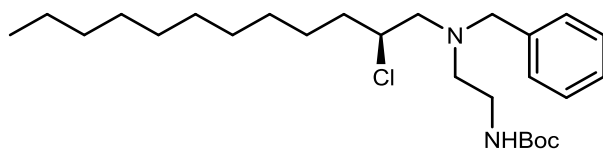
(S)-*tert*-butyl (2-(benzyl(2-chlorododecyl)amino)ethyl)carbamate **(1.74A)**

The product was prepared according to the chloro diamine procedure on a 0.23 mmol scale

and purified by silica chromatography (9:1 Hexanes/EtOAc) to afford the product as a clear

oil (78 mg, 0.17 mmol, 75%). ^{1}H NMR (400.1 MHz, CDCl$_3$) δ (ppm): 7.34-7.30 (m, 4H);

7.29-7.24 (m, 1H); 5.04 (s, br, 1H); 3.94-3.86 (m, 1H); 3.71-3.61 (m, 2H); 3.27-3.10 (m, 2H);

2.81-2.69 (m, 2H); 2.67-2.55 (m, 2H); 1.85-1.74 (m, 1H); 1.61-1.55 (m, 1H); 1.44 (s, 9H);

1.28 (s, 16H); 0.90 (t, $J = 7.01$, 3H). ^{13}C NMR (100.6 MHz, CDCl$_3$) δ (ppm): 156.07, 138.59,

128.87, 128.28, 127.18, 78.84, 61.32, 59.42, 54.01, 38.13, 35.94, 31.82, 29.51, 29.48, 29.39,

29.24, 29.06 (one set of coincident signals), 28.33, 26.11, 22.60, 14.04. HRMS (TOF, ES+)

C$_{26}$H$_{46}$N$_2$O$_2$Cl [M+H]$^{+}$ calc. mass 453.3248, found 453.3245. Specific rotation [— = -7.0^{o}

(c = 100, MeOH).
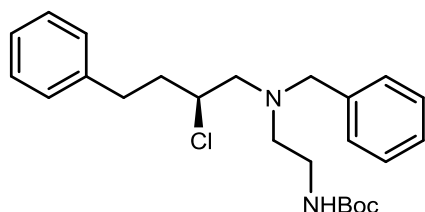
(S)-*tert*-butyl (2-(benzyl(2-chloro-4-phenylbutyl)amino)ethyl)carbamate **(1.74B)**

The product was prepared according to the chloro diamine procedure on a 0.27 mmol scale

and purified by silica chromatography (9:1 Hexanes/EtOAc) to afford the product as a clear

oil (97 mg, 0.23 mmol, 87%). ^{1}H NMR (400.1 MHz, CDCl$_3$) δ (ppm): 7.37-7.19 (m, 10H);

5.00 (s, br, 1H); 3.91-3.83 (m, 1H); 3.60 (s, 2H); 3.25-3.08 (m, 2H); 2.92-2.83 (m, 1H); 2.81-

2.68 (m, 3H); 2.64-2.51 (m, 2H); 2.23-2.12 (m, 1H); 1.93-1.82 (m, 1H); 1.47 (s, 9H). ^{13}C

NMR (100.6 MHz, CDCl$_3$) δ (ppm): 155.94, 140.97, 138.62, 128.88, 128.47, 128.33, 127.21,

126.06, 78.84, 61.28, 60.18, 54.00, 39.20, 37.53, 32.29, 28.42. HRMS (TOF, ES+) C$_{24}$H-

$_{34}$N$_2$O$_2$Cl [M+H]$^{+}$ calc. mass 417.2309, found 417.2308. Specific rotation [— = -5.5^{o} (c =

100, MeOH).

(*S*,*Z*)-*tert*-butyl (2-(benzyl(2-chlorodec-7-en-1-yl)amino)ethyl)carbamate **(1.74C)**

The product was prepared according to the chloro diamine procedure on a 0.41 mmol scale and purified by silica chromatography (9:1 Hexanes/EtOAc) to afford the product as a clear oil (138 mg, 0.33 mmol, 80%). ^{1}H NMR (400.1 MHz, CDCl$_3$) δ (ppm): 7.35-7.28 (m, 4H); 7.28-7.23 (m, 1H); 5.41-5.26 (m, 2H); 4.97 (s, br, 1H); 3.92-3.84 (m, 1H); 3.69-3.60 (m, 2H); 3.26-3.09 (m, 2H); 2.79-2.66 (m, 2H); 2.66-2.52 (m, 2H); 2.08-1.98 (m, 4H); 1.84-1.74 (m, 1H); 1.63-1.46 (m, 2H); 1.43 (s, 9H); 1.41-1.22 (m, 3H); 0.96 (t, *J* = 7.5, 3H). ^{13}C NMR (100.6 MHz, CDCl$_3$) δ (ppm): 155.93, 138.69, 131.80, 128.85, 128.68, 128.28, 127.16, 78.79, 61.32 (one set of coincident signals), 59.43, 54.05, 38.19, 35.81, 29.18, 28.36, 26.83, 25.75, 20.46, 14.32. HRMS (TOF, ES+) C$_{24}$H$_{40}$N$_2$O$_2$Cl [M+H]$^+$ calc. mass 423.2778, found 423.2779. Specific rotation [⎯]= -7.0^o (*c* = 100, MeOH).
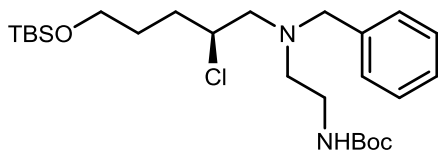
(*S*)-*tert*-butyl (2-(benzyl(5-((*tert*-butyldimethylsilyl)oxy)-2-chloropentyl)amino)ethyl)carbamate **(1.74D)**
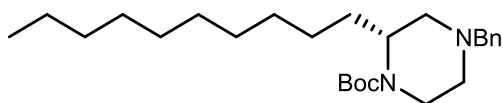
The product was prepared according to the chloro diamine procedure on a 0.37 mmol scale and purified by silica chromatography (9:1 Hexanes/EtOAc) to afford the product as a clear oil (113 mg, 0.23 mmol, 63%). ^{1}H NMR (400.1 MHz, CDCl$_3$) δ (ppm): 7.35-7.22 (m, 5H); 5.00 (s, br, 1H); 3.99-3.90 (m, 1H); 7.73-3.55 (m, 4H); 3.26-3.09 (m, 2H); 2.83-2.68 (m, 2H); 2.67-2.53 (m, 2H); 1.96- 1.88 (m, 1H); 1.79-1.68 (m, 1H); 1.66-1.54 (m, 2H); 1.43 (s, 9H);

0.90 (s, 9H); 0.05 (s, 6H). ^{13}C NMR (100.6 MHz, CDCl$_3$) δ (ppm): 155.97, 138.66, 128.84, 128.30, 127.15, 78.87, 62.43, 61.40, 61.31, 59.41, 53.95, 38.21, 32.51, 29.41, 28.35, 25.87, 18.24, -5.37. HRMS (TOF, ES+) C$_{25}$H$_{46}$N$_2$O$_3$ClSi [M+H]$^+$ calc. mass 485.2966, found 485.2970. Specific rotation [──= -2.7° (c = 100, MeOH).

## General Procedure for Chiral Morpholine Synthesis
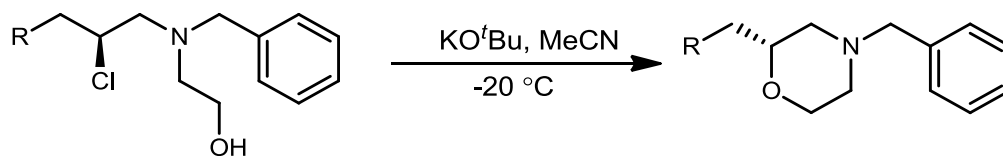
Potassium *tert*-butoxide (5 eq) was added to a solution of chloro-diamine (1 eq) in MeCN (0.02 M) at -20 °C. This reaction was followed via TLC, and upon consumption of starting material, diethyl ether followed by water was added to the reaction. It was extracted 3X with diethyl ether, dried with MgSO$_4$, and concentrated before purification.
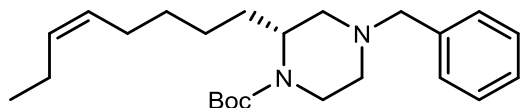

(*R*)-4-benzyl-2-decylmorpholine **(1.75A)**

The product was prepared according to the cyclization to morpholines procedure on a 0.19 mmol scale and was purified by silica chromatography (9:1 Hexanes/EtOAc) to afford the product as a clear oil (39 mg, 0.12 mmol, 65%), which was determined to have an ee of 92% by chiral SFC analysis (Chiralpak IA, t$_R$ (major) = 2.76 min, t$_R$ (minor) = 2.12 min, traces shown below). ^{1}H NMR (400.1 MHz, CDCl$_3$) δ (ppm): 7.32-7.24 (m, 5H); 3.84 (dq, J_1 = 11.5 Hz, J_2 = 1.8, 1H); 3.65 (td, J_1 = 11.5, J_2 = 2.5, 1H); 3.52-3.45 (m, 3H); 2.74-2.71, (m, 1H); 2.65 (dq, J_1 = 11.4, J_2 = 1.8, 1H); 2.14 (td, J_1 = 11.4, J_2 = 3.3, 1H); 1.87-1.82 (m, 1H); 1.5-

1.25 (m, 18H); 0.87 (t, J = 7.1, 3H). ^{13}C NMR (100.6 MHz, CDCl$_3$) δ (ppm): 137.76, 129.11, 128.17, 127.03, 75.76, 66.73, 63.29, 58.80, 53.12, 33.67, 31.83, 29.60, 29.52, 29.51, 29.45, 29.24, 25.33, 22.60, 14.04. HRMS (TOF, ES+) C$_{21}$H$_{36}$NO [M+H]$^+$ calc. mass 318.2797, found 318.2795. Specific rotation [—= +13.04$^{\mathbf{o}}$ (c = 100, MeOH).
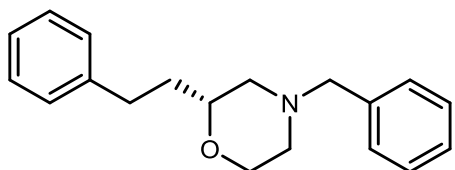
(*R*)-4-benzyl-2-phenethylmorpholine **(1.75C)**

The product was prepared according to the cyclization to morpholines procedure on a 0.15 mmol scale and was purified by silica chromatography (9:1 Hexanes/EtOAc) to afford the product as a clear oil (31 mg, 0.11 mmol, 74%), which was determined to have an ee of 95% by chiral SFC analysis (Chiralpak IB, t_R (major) = 3.36 min, t_R (minor) = 2.57 min, traces shown below). ^{1}H NMR (400.1 MHz, CDCl$_3$) δ (ppm): 7.39-7.25 (m, 7H); 7.24-7.18 (m, 3H); 3.92 (d, J = 11.12, 1H); 3.70 (td, J_1 = 2.38, J_2 = 11.12, 1H); 3.58-3.50 (m, 3H); 2.86-2.63 (m, 4H); 2.21 (td, J_1 = 3.18, J_2 = 11.12, 1H); 1.92 (t, J = 10.73, 1H); 1.89-1.78 (m, 1H); 1.74-1.63 (m, 1H). ^{13}C NMR (100.6 MHz, CDCl$_3$) δ (ppm): 141.97, 137.72, 129.12, 128.40, 128.27, 128.20, 127.07, 125.70, 74.82, 66.70, 63.27, 58.62, 53.16, 35.30, 31.54. HRMS (TOF, ES+) C$_{19}$H$_{24}$NO [M+H]$^+$ calc. mass 282.1858, found 282.1857. Specific rotation [—= +25.2$^{\mathbf{o}}$ (c = 100, MeOH).
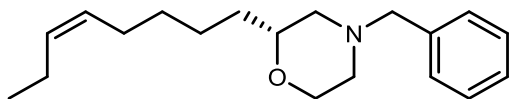
(*R*,*Z*)-4-benzyl-2-(oct-5-en-1-yl)morpholine **(1.75B)**

The product was prepared according to the cyclization to morpholines procedure on a 0.13 mmol scale and was purified by silica chromatography (9:1 Hexanes/EtOAc) to afford the product as a clear oil (26 mg, 0.09 mmol, 68%), which was determined to have an ee of 98% by chiral SFC analysis (Chiralpak IA, t_R (major) = 2.68 min, t_R (minor) = 1.79 min, traces shown below). ^{1}H NMR (400.1 MHz, CDCl$_3$) δ (ppm): 7.38-7.25 (m, 5H); 5.43-5.28 (m, 2H); 3.89-3.83 (m, 1H); 3.67 (td, J_1 = 11.34, J_2 = 2.39, 1H); 3.56-3.46 (m, 3H); 2.75 (d, J = 11.72, 1H); 2.67 (d, J = 11.73, 1H); 2.16 (td, J_1 = 11.62, J_2 = 3.66, 1H); 2.09-1.98 (m, 4H); 1.87 (t, J = 10.39, 1H); 1.56-1.21 (m, 7H); 0.97 (t, J = 7.95, 1H). ^{13}C NMR (100.6 MHz, CDCl$_3$) δ (ppm): 137.76, 131.62, 129.10, 128.95, 128.17, 127.03, 75.69, 66.74, 63.28, 58.77, 53.12, 33.56, 29.73, 26.90, 24.99, 20.42, 14.29.   HRMS (TOF, ES+) C$_{19}$H$_{30}$NO [M+H]$^+$ calc. mass 288.2327, found 288.2328.   Specific rotation [─ = +10.8^o (*c* = 100, MeOH).
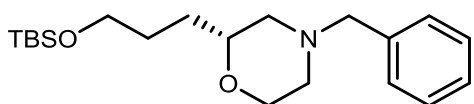
(*R*)-4-benzyl-2-(3-((*tert*-butyldimethylsilyl)oxy)propyl)morpholine **(1.75D)**

The product was prepared according to the cyclization to morpholines procedure on a 0.13 mmol scale and was purified by silica chromatography (9:1 Hexanes/EtOAc) to afford the product as a clear oil (26 mg, 0.09 mmol, 68%), which was determined to have an ee of 80% by chiral SFC analysis (Chiralpak IA, t_R (major) = 3.08 min, t_R (minor) = 2.66 min, traces shown below). ^{1}H NMR (400.1 MHz, CDCl$_3$) δ (ppm): 7.35-7.23 (m, 5H); 3.84 (dd, J_1 = 1.69, J_2 = 11.33, 1H); 3.69-3.55 (m, 3H); 3.54-3.44 (m, 3H); 2.74 (d, J = 10.79, 1H); 2.65 (d,

J = 11.26, 1H); 2.15 (td, J_1 = 3.13, J_2 = 11.21, 1H); 1.86 (t, J = 10.69, 1H); 1.70-1.58 (m,

1H); 1.58-1.40 (m, 3H); 0.89 (s, 9H); 0.039 (s, 6H). ^{13}C NMR (100.6 MHz, CDCl$_3$) δ (ppm):

137.76, 129.08, 128.18, 127.03, 75.56, 66.71, 63.27, 63.01, 58.75, 53.10, 29.97, 28.64, 25.91,

18.27, -5.36. HRMS (TOF, ES+) C$_{20}$H$_{36}$NO$_2$Si [M+H]$^+$ calc. mass 350.2515, found

350.2514. Specific rotation [‒= +11.1^0 (c = 100, MeOH).

General Procedure for Cyclization to Piperazines
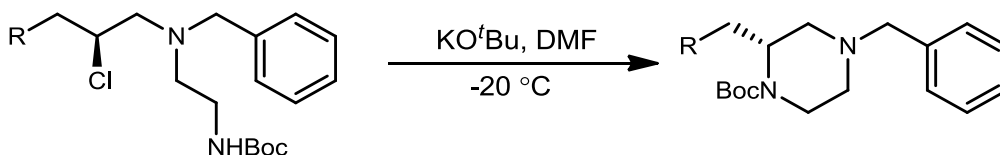
Potassium *tert*-butoxide (5 eq) was added to a solution of chloro-diamine (1 eq) in DMF

(0.02 M) at -20 ^{0}C. This reaction was followed via TLC and was typically done within 2

hours. Upon consumption of starting material, diethyl ether followed by water was added to

the reaction. It was extracted 3X with diethyl ether, dried with MgSO$_4$, and concentrated

before purification.

(*R*)-*tert*-butyl 4-benzyl-2-decylpiperazine-1-carboxylate **(1.76A)**

The product was prepared according to the cyclization to piperazines on a 0.12 mmol scale

and was purified by silica chromatography (9:1 Hexanes/EtOAc) to afford the product as a

clear oil (33mg, 0.08 mmol, 66%), which was determined to have an ee of 89% by chiral

SFC analysis (Lux Cellulose-4, t$_R$ (major) = 4.49 min, t$_R$ (minor) = 3.78 min, traces shown

below). ^{1}H NMR (400.1 MHz, CDCl$_3$) δ (ppm): 7.32-7.21 (m, 5H); 3.99 (s, br, 1H); 3.90-

3.82 (m, 1H); 3.53 (d, *J* = 13.2, 1H); 3.37 (d, *J* = 13.3, 1H); 3.05 (t, *J* = 12.5, 1H); 2.75-2.65

(m, 2H); 2.06-2.00 (m, 2H); 1.78-1.73 (m, 1H); 1.66-1.61 (m, 1H); 1.45 (s, 9H); 1.30-1.15

(m, 16H); 0.88 (t, *J* = 7.5, 3H). ^{13}C NMR (100.6 MHz, CDCl$_3$) δ (ppm): 154.81, 138.39,

128.68, 128.12, 126.93, 79.18, 62.80, 55.39, 53.29, 51.37, 39.24, 31.84, 29.74, 29.59, 29.56,

29.53, 29.50, 29.27, 28.38, 26.20, 22.52, 14.04. HRMS (TOF, ES+) C$_{26}$H$_{45}$N$_2$O$_2$ [M+H]$^+$

calc. mass 417.3481, found 417.3480. Specific rotation [—= -34.68^o (*c* = 100, MeOH).
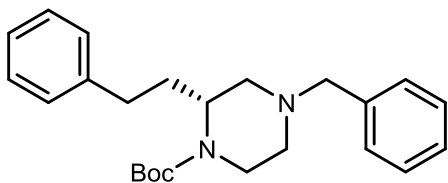
(*R*)-*tert*-butyl 4-benzyl-2-phenethylpiperazine-1-carboxylate **(1.76C)**

The product was prepared according to the cyclization to piperazines on a 0.165 mmol scale

and was purified by silica chromatography (9:1 Hexanes/EtOAc) to afford the product as a

clear oil (42mg, 0.11 mmol, 67%), which was determined to have an ee of 95% by chiral

SFC analysis (Chiralpak IA, t$_R$ (major) = 4.77 min, t$_R$ (minor) = 4.29 min, traces shown

below) . ^{1}H NMR (400.1 MHz, CDCl$_3$) δ (ppm): 7.40-7.26 (m, 7H); 7.25-7.17 (m, 3H); 4.14

(s, br, 1H); 3.96 (s, br, 1H); 3.60 (d, *J* = 13.4, 1H); 3.40 (d, *J* = 13.4, 1H); 3.15 (t, *J* = 12.8,

1H); 2.86-2.73 (m, 2H); 2.62-2.45 (m, 2H); 2.20-1.99 (m, 4H); 1.50 (s, 9H). ^{13}C NMR (100.6

MHz, CDCl$_3$) δ (ppm): 154.81, 142.11, 138.37, 128.78, 128.39 (set of two coincident

signals), 128.21, 127.05, 125.70, 79.41, 62.84, 55.10, 53.39, 51.35, 39.45, 32.65, 31.68,

28.40. HRMS (TOF, ES+) C$_{24}$H$_{33}$N$_2$O$_2$ [M+H]$^+$ calc. mass 381.2542, found 381.2545.

Specific rotation [—= -41.0^o (*c* = 100, MeOH).

(*R,Z*)-*tert*-butyl 4-benzyl-2-(oct-5-en-1-yl)piperazine-1-carboxylate (**1.76B**)

The product was prepared according to the cyclization to piperazines on a 0.15 mmol scale and was purified by silica chromatography (9:1 Hexanes/EtOAc) to afford the product as a clear oil (53mg, 0.137 mmol, 91%), which was determined to have an ee of 95% by chiral SFC analysis (Chiralpak IC, t_R (major) = 4.62 min, t_R (minor) = 4.10 min, traces shown below). ^{1}H NMR (400.1 MHz, CDCl$_3$) δ (ppm): 7.37-7.23 (m, 5H); 5.42-5.27 (m, 2H); 4.03 (s, br, 1H); 3.89 (d, *J* = 11.03, 1H); 3.56 (d, *J* = 13.42, 1H); 3.40 (d, *J* = 13.42, 1H); 3.08 (t, *J* = 10.90, 1H); 2.77 (d, *J* = 10.9, 1H); 2.68 (d, *J* = 11.32, 1H); 2.11-1.98 (m, 6H); 1.86-1.74 (m, 1H); 1.72-1.60 (m, 1H); 1.47 (s, 9H); 1.43-1.31 (m, 2H); 1.26-1.16 (m, 2H); 0.97 (t, *J* = 7.53, 3H). ^{13}C NMR (100.6 MHz, CDCl$_3$) δ (ppm): 154.79, 138.38, 131.57, 129.00, 128.69, 128.13, 126.94, 79.23, 62.79, 60.31, 55.41, 53.28, 51.31, 39.07, 29.61, 28.38 (one set of coincident signals), 27.01, 25.82, 20.44, 14.31. HRMS (TOF, ES+) C$_{24}$H$_{39}$N$_2$O$_2$ [M+H]$^+$ calc. mass 387.3012, found 387.3009. Specific rotation [— = -45.4° (*c* = 100, MeOH).
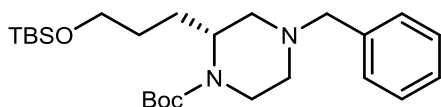
(*R*)-*tert*-butyl 4-benzyl-2-(3-((*tert*-butyldimethylsilyl)oxy)propyl)piperazine-1-carboxylate (**1.76D**)

The product was prepared according to the cyclization to piperazines on a 0.19 mmol scale and was purified by silica chromatography (9:1 Hexanes/EtOAc) to afford the product as a clear oil (68.5mg, 0.15 mmol, 78%), which was determined to have an ee of 75% by chiral SFC analysis (Lux Cellulose-2 (OZ), t_R (major) = 6.54 min, t_R (minor) = 5.73 min, traces shown below). ^{1}H NMR (400.1 MHz, CDCl$_3$) δ (ppm): 7.34-7.20 (m, 5H); 4.02 (s, br, 1H);

3.93-3.81 (m, 1H); 3.61 (t, J = 6.14, 2H); 3.52 (d, J = 13.09, 1H); 3.38 (d, J = 13.59, 1H); 3.05 (t, J = 11.58, 1H); 2.73 (d, J = 10.32, 1H); 2.66 (d, J = 11.27, 1H); 2.11-1.96 (m, 2H); 1.94-1.82 (m, 1H); 1.71-1.59 (m, 1H); 1.50-1.35 (m, 11H); 0.89 (s, 9H); 0.04 (s, 6H). ^{13}C NMR (100.6 MHz, CDCl$_3$) δ (ppm): 154.78, 138.41, 129.31, 128.65, 126.94, 79.28, 62.99, 62.76, 55.68, 53.22, 51.24, 38.91, 29.53, 28.37, 26.20, 25.89, 18.25, -5.32. HRMS (TOF, ES+) C$_{25}$H$_{45}$N$_2$O$_3$Si [M+H]$^+$ calc. mass 449.3199, found 449.3198. Specific rotation [─ = -29.9^o (c = 100, MeOH).

Procedure for Debenzylation and Formation of Dopamine Antagonist

1.75C → i. H$_2$, Pd/C, MeOH, rt; ii. 2-(chloromethyl) benzimidazole K$_2$CO$_3$, MeCN, rt → **1.77**
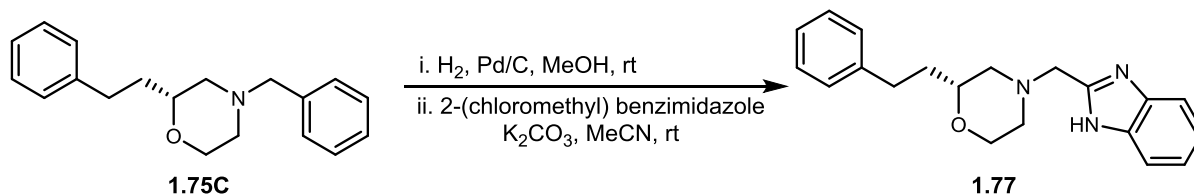
To a solution of benzyl protected morpholine (435 mg, 1.54 mmol) in methanol (31 mL, 0.05 M) under an argon atmosphere was added 0.2 eq of 10% Pd/C. The flask was then purged with H$_2$ and was left to react under a hydrogen atmosphere and followed via TLC and LC-MS until consumption of the starting material was determined. Upon consumption of the starting material, the reaction was filtered through celite, concentrated, and resuspended in MeCN (7.7 mL, 0.2 M). To this solution was added potassium carbonate (1,064 mg, 7.7 mmol) and 2-(chloromethyl) benzimidazole (256.6 mg, 1.54 mmol) and the reaction was left to stir overnight. The reaction was then quenched with water and was extracted 3X with ethyl acetate. The organic layer was dried with magnesium sulfate, filtered, and was concentrated. It was purified using flash column chromatography (5% methanol in dichloromethane) to afford the product as a waxy solid (376 mg, 1.17 mmol, 76%). ^{1}H NMR (400.1 MHz, CDCl$_3$) δ (ppm): 7.62 (s, br, 2H); 7.31-7.23 (m, 4H); 7.21-7.12 (m, 3H); 3.90-3.77 (m, 3H); 3.57 (td, J_1 = 11.63, J_2 = 2.10, 1H); 3.42-3.44 (m, 1H); 2.78-2.56 (m, 4H); 2.34 (td, J_1 = 11.65, J_2 = 3.43, 1H); 2.04 (t, J = 10.28, 1H); 1.84-1.73 (m, 1H); 1.63-1.53 (m, 1H). ^{13}C NMR (100.6 MHz, CDCl$_3$) δ (ppm): 151.82, 141.73, 138.69, 128.43, 128.35, 125.82, 122.45, 114.94, 74.68, 66.50, 58.69, 56.60, 53.35, 35.04, 31.36. HRMS (TOF, ES+) C$_{20}$H$_{24}$N$_3$O [M+H]$^+$ calc. mass 322.1919, found 322.1917. Specific rotation [—= +38.3^o (c = 100, MeOH).

Experimental for chiral β and γ-fluoroamines

All reagents were purchased from commercial suppliers and were purified as needed according to the procedures of Armarego and Chai.[1] Analytical thin-layer chromatography (TLC) was performed on 250 μm silica plates from Sorbent Technologies. Visualization was accomplished via UV light, and/or the use of ninhydrin, iodine, and potassium permanganate solutions followed by application of heat. Chromatography was performed using Silica Gel 60 (230-400 mesh) from Sorbent Technologies or Silica RediSep Rf flash columns on a CombiFlash Rf automated flash chromatography system. All ^{1}H and ^{13}C NMR spectra were recorded on a Bruker AV-400 (400 MHz) instrument. Chemical shifts are reported in ppm relative to residual solvent peaks as an internal standard set to δ 7.26 and δ 77.16 (CDCl$_3$) or δ 3.31 and δ 49.00 (MeOD). Data are reported as follows: chemical shift, multiplicity (s = singlet, d = doublet, t = triplet, q = quartet, p = pentet, sx = sextet, sp = septet, br = broad, dd = doublet of doublets, dq = doublet of quartets, td = triplet of doublets, pd = pentet of doublets, m = multiplet), coupling constant (Hz), integration. Low resolution mass spectra (LCMS) were recorded on an Agilent 1200 LCMS with electrospray ionization. High resolution mass spectra (HRMS) were recorded on a Waters QToF-API-US plus Acuity system with ES as the ion source. Analytical high performance liquid chromatography (HPLC) was performed on an Agilent 1200 analytical LCMS with UV detection at 214 nm and 254 nm along with ELSD detection. Chiral separations were performed on a Thar Investigator II supercritical fluid chromatograph (SFC) utilizing Chiralcel® OD, OD-Cl, OJ, and Chiralpak® IA columns. Optical rotations were acquired on a Jasco P-2000 polarimeter at 23 ^{0}C and 589 nm. The specific rotations were calculated according to the equation [α]23/D = 100α/*l* x *c* where *l* is the path length in decimeters and *c* is the concentration in g/100 mL.

General Procedure A—for fluorination and reduction of aldehydes.
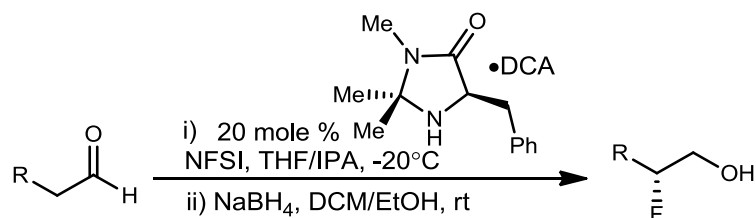
To a round-bottom flask equipped with a magnetic stir bar and charged with (*R*)-5-benzyl-2,2,3-trimethylimidazolidin-4-one dichloro acid salt (139 mg, 0.400 mmol) and *N*-fluorobenzenesulfonimide (3.15 g, 10.0 mmol) was added THF (8.0 mL) and iPrOH (1.0 mL). The mixture was stirred at room temperature until all solids were dissolved and was then cooled to -20^0 C. The aldehyde substrate (2 mmol) was then slowly added to the reaction mixture dissolved in THF (1.0 mL) and the mixture was left to stirred for 16 hours. The reaction was then diluted with Et$_2$O (20 mL), cooled to -78^{0}C, and filtered through a pad of silica gel, eluting with cold Et$_2$O (~50 mL). The resultant organic layer was washed with saturated NaHCO$_3$ (3 x 75 mL), saturated brine (75 mL), dried over MgSO$_4$, filtered, and concentrated. The resultant oil was the dissolved in DCM (12 mL) and EtOH (8 mL) and NaBH$_4$ (189 mg, 5.0 mmol) was added at room temperature, all at once. After 30 minutes, the reaction was cooled to 0^0 C and was quenched with saturated NH$_4$Cl (~100 mL). The mixture was stirred vigorously and allowed to warm to room temperature and stirred for an additional 30 minutes. 75 mL DCM was added to the suspension when it was extracted with DCM (3 x 75 mL). The combined organic extracts were then washed with NaHCO$_3$ (3 x 75 mL) and brine (75 mL), dried with MgSO$_4$, filtered and concentrated. Purification of the resultant oil was performed by flash column chromatography.
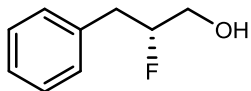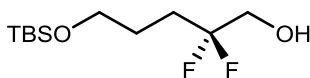
(R)-2-fluoro-3-phenylpropan-1-ol (**1.94A**)

The product was prepared according general procedure A, purified via flash column chromatography (15% ethyl acetate in hexanes) to afford the product was a clear oil (200 mg, 65% yield). ^{1}H NMR (400.1 MHz, CDCl$_3$) δ (ppm): 7.36-7.20 (m, 5H); 4.78 (dm, J = 49.0 Hz); 3.84-3.63 (m, 2H); 3.10-2.89 (m, 2H); 1.92 (s, br, 1H). ^{13}C NMR (100.6 MHz, CDCl$_3$) δ (ppm): 136.52 (d, J = 5.5 Hz), 129.33, 128.58, 126.75, 95.70 (d, J = 171.9 Hz), 64.01 (d, J = 21.7 Hz), 37.45 (d, J = 21.2 Hz). Specific rotation [―= +14.9^0 (c = 100, CHCl$_3$). HRMS (TOF, ES+) C$_9$H$_{11}$OFNa [M+Na]$^+$ calc. mass 177.0692, found 177.0692.
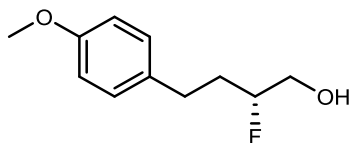
(R)-2-fluoro-4-(4-methoxyphenyl)butan-1-ol (**1.94B**)

The product was prepared according general procedure A, purified via flash column chromatography (25% ethyl acetate in hexanes) to afford the product was a waxy solid (291 mg, 73% yield). ^{1}H NMR (400.1 MHz, CDCl$_3$) δ (ppm): 7.13 (d, J = 8.6 Hz, 2H); 6.86 (d, J = 8.6 Hz, 2H); 4.56 (dm, J = 49.9 Hz, 1H); 3.79 (s, 3H); 3.74-3.59 (m, 2H); 2.92 (s, br, 1H); 2.82-2.56 (m, 2H); 2.07-1.92 (m, 1H); 1.89-1.71 (m, 1H). ^{13}C NMR (100.6 MHz, CDCl$_3$) δ (ppm): 157.89, 133.12, 129.33, 113.89, 93.72 (d, J = 168.7 Hz), 64.75 (d, J = 21.9), 55.20, 32.84 (d, J = 20.7), 30.11 (d, J = 4.7). Specific rotation [―= +24.2^0 (c = 100, CHCl$_3$). HRMS (TOF, ES+) C$_{11}$H$_{15}$O$_2$FNa [M+Na]$^+$ calc. mass 221.0956, found 221.0954.
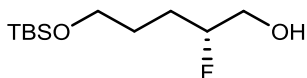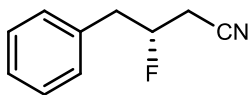
(*R*)-5-((*tert*-butyldimethylsilyl)oxy)-2-fluoropentan-1-ol (**1.94C**)

The product was prepared according general procedure A, purified via flash column chromatography (10% ethyl acetate in hexanes) to afford the product as a clear oil (365 mg, 77% yield). ^{1}H NMR (400.1 MHz, CDCl$_3$) δ (ppm): 4.52 (dm, J = 49.4 Hz, 1H); 3.70-3.53 (m, 4H); 3.31 (s, br, 1H); 1.69-1.48 (m, 4H); 0.84 (s, 9H); 0.00 (s, 6H). ^{13}C NMR (100.6 MHz, CDCl$_3$) δ (ppm): 94.12 (d, J = 169.2 Hz), 64.28 (d, J = 22.2 Hz), 62.47, 27.97 (d, J = 4.2 Hz), 27.37 (d, J = 20.8 Hz), 25.72, 18.04, -5.60. Specific rotation [ ]= 5.9^0 (c = 100, CHCl$_3$). HRMS (TOF, ES+) C$_{11}$H$_{26}$O$_2$FSi [M+H]$^+$ calc. mass 237.1686, found 237.1688.
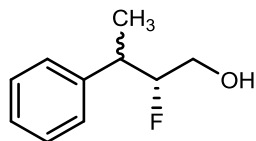
(2*R*)-2-fluoro-3-phenylbutan-1-ol (**1.94D**) (**1.94E**)

The product was prepared according general procedure A, purified via flash column chromatography (10% ethyl acetate in hexanes) to afford the product as a clear oil (249 mg, 74% yield, 1:1 dr). ^{1}H NMR—**Diastereomer A (less polar)** (400.1 MHz, CDCl$_3$) δ (ppm): 7.39-7.23 (m, 5H); 4.62 (dm, J = 49.1 Hz, 1H); 3.66-3.47 (m, 2H); 3.16-2.97 (m, 2H); 1.43 (d, J = 7.1 Hz, 3H). ^{1}H NMR—**Diastereomer B (more polar)** (400.1 MHz, CDCl$_3$) δ (ppm): 7.36-7.20 (m, 5H); 4.69 (dm, J = 48.5 Hz, 1H); 3.81-3.51 (m, 2H); 3.16-3.02 (m, 2H); 1.83 (s, br, 1H); 1.35 (d, J = 7.2 Hz, 3H). ^{13}C NMR—**Diastereomer A (less polar)** (100.6 MHz, CDCl$_3$) δ (ppm): 142.32 (d, J = 7.7 Hz), 128.66, 127.59, 126.89, 98.02 (d, J = 175.5 Hz), 63.02 (d, J = 21.6 Hz), 40.93 (d, J = 20.5 Hz), 17.19 (d, J = 4.9 Hz). ^{13}C NMR—

Diastereomer B (more polar) (125 MHz, CDCl$_3$) δ (ppm): 141.94, 128.63, 128.08, 127.02, 97.57 (d, J = 174.1 Hz), 63.60 (d, J = 22.6 Hz), 41.13 (d, J = 20.1 Hz), 17.54 (d, J = 6.1 Hz).

Specific rotation—**Diastereomer A (less polar)** [—= +12.3^0 (c = 100, CHCl$_3$). Specific

rotation—**Diastereomer B (more polar)** [—= +6.1^0 (c = 100, CHCl$_3$). HRMS (TOF,

ES+)–**Diastereomer A (less polar):** C$_{10}$H$_{13}$OFNa [M+Na]$^+$ calc. mass 191.0848, found

191.0848. HRMS (TOF, ES+)–**Diastereomer B (more polar):** C$_{10}$H$_{13}$OFNa [M+Na]$^+$ calc.
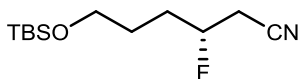
mass 191.0848, found 191.0847.
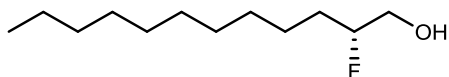
(*R*)-2-fluorododecan-1-ol (**1.94F**)

The product was prepared according general procedure A, purified via flash column chromatography (10% ethyl acetate in hexanes) to afford the product was a waxy solid (282 mg, 69% yield). ^{1}H NMR (400.1 MHz, CDCl$_3$) δ (ppm): 4.524 (dm, J = 51.3 Hz, 1H); 3.77-3.50 (m, 3H); 1.71-1.16 (m, 18H); 0.85 (t, J = 6.6 Hz, 3H).^{13}C NMR (100.6 MHz, CDCl$_3$) δ (ppm): 94.83 (d, J = 168.1 Hz), 64.96 (d, J = 22.1 Hz), 31.99, 31.08 (d, J = 20.6 Hz), 29.69, 29.65, 29.57, 29.54, 29.42, 25.02 (d, J = 4.8 Hz), 22.76, 14.14. Specific rotation [—= +9.6^0 (c = 100, CHCl$_3$). HRMS (TOF, ES+) C$_{12}$H$_{25}$OFNa [M+Na]$^+$ calc. mass 227.1787, found 227.1787.
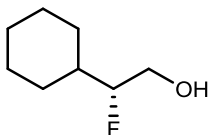
(*R*)-2-cyclohexyl-2-fluoroethanol (**1.94G**)
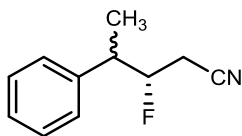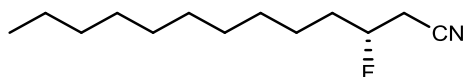
The product was prepared according general procedure A, purified via flash column chromatography (15% ethyl acetate in hexanes) to afford the product was a clear oil (236 mg, 81% yield). ^{1}H NMR (400.1 MHz, CDCl$_3$) δ (ppm): 4.20 (dm, J = 49.2 Hz, 1H); 3.70-3.57 (m, 2H); 3.21 (s, br, 1H); 1.79 (dm, br, J = 12.7, 1H); 1.73-1.49 (m, 5H); 1.26-0.93 (m, 5H). ^{13}C NMR (100.6 MHz, CDCl$_3$) δ (ppm): 98.38 (d, J = 169.6 Hz), 62.84 (d, J = 22.2 Hz), 38.79 (d, J = 18.8 Hz), 28.11 (dd, J_1 = 51.2 Hz, J_2 = 5.6 Hz), 26.14, 25.67 (d, J = 17.4 Hz). Specific rotation [—= 2.4^0 (c = 100, CHCl$_3$). HRMS (TOF, ES+) C$_8$H$_{15}$O$_2$FNa [M+Na]$^+$ calc. mass 169.1005, found 169.005.

General procedure B—procedure for preparation of difluoro-alcohols
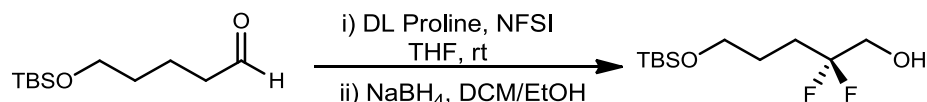
To a round-bottom flask equipped with a magnetic stir bar and charged with DL proline (103.5 mg, 0.9 mmol) and *N*-fluorobenzenesulfonimide (7.568 g, 24.0 mmol) was added THF (27 mL). The mixture was stirred at room temperature until all solids were dissolved and the aldehyde substrate (649.2 mg, 3 mmol) was then slowly added to the reaction mixture dissolved in THF (3.0 mL) and the mixture was stirred for 16 hours. The reaction was then diluted with Et$_2$O (20 mL), cooled to -78^{0}C, and filtered through a pad of silica gel, eluting with cold Et$_2$O (~75 mL). The resultant organic layer was washed with saturated NaHCO$_3$ (3x), saturated brine (1x), dried over MgSO$_4$, filtered, and concentrated. The

resultant oil was the dissolved in DCM (18 mL) and EtOH (12 mL) and NaBH$_4$ (283.7 mg, 7.5 mmol) was added at room temperature, all at once. After 30 minutes, the reaction was cooled to 0^{0}C and was quenched with saturated NH$_4$Cl (~100 mL). The mixture was stirred vigorously and allowed to warm to room temperature and stir for an additional 30 minutes. About 75 mL of DCM was added to the suspension and it was extracted with DCM (3x). The combined organic extracts were then washed with NaHCO$_3$ (3x) and brine (1x), dried with MgSO$_4$, filtered and concentrated. Purification of the resultant oil was performed by flash column chromatography.

5-((*tert*-butyldimethylsilyl)oxy)-2,2-difluoropentan-1-ol (**1.104**)

The product was prepared according general procedure B, purified via flash column chromatography (10% ethyl acetate in hexanes) to afford the product as a clear oil (586 mg, 77% yield). ^{1}H NMR (400.1 MHz, CDCl$_3$) δ (ppm): 3.73-3.60 (m, 4H); 3.49 (s, br, 1H); 2.03-1.85 (m, 2H); 1.75-1.63 (m, 2H); 0.87 (s, 9H); 0.03 (s, 6H). ^{13}C NMR (100.6 MHz, CDCl$_3$) δ (ppm): 123.52 (t, J = 241.5 Hz), 63.85 (t, J = 31.8 Hz), 62.59, 29.89 (t, J = 24.2 Hz), 25.97, 25.14 (t, J = 4.3 Hz), 18.39, -5.34. HRMS (TOF, ES+) C$_{11}$H$_{25}$O$_2$F$_2$Si [M+H]$^+$ calc. mass 255.1592, found 255.1592.

General Procedure C—procedure for preparation of fluoro-nitriles
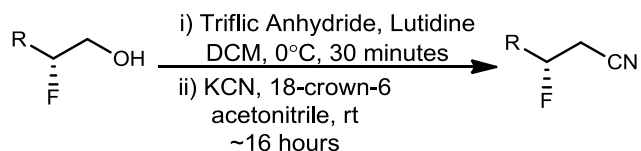
To a flame dried round-bottom flask equipped with a magnetic stir bar and charged with the chiral fluoro-alcohol (1 mmol) and lutidine (535 mg, 5.0 mmol) was added DCM (5 mL), and the mixture was cooled to 0^0C with stirring. Trifluoromethanesulfonic anhydride (339 mg, 1.2 mmol) was added to the reaction dropwise, and the mixture was left to stir for 30 minutes. The reaction was then diluted with Et_2O and water was added to quench the reaction. The mixture was extracted with Et_2O (3x), dried with $MgSO_4$, filtered, and concentrated. The resultant oil was transferred to a round-bottom flask equipped with a magnetic stir bar where it was dissolved in acetonitrile (4 mL), and 18-crown-6 (53 mg, 0.2 mmol) was added and allowed to dissolve with stirring. Potassium cyanide (651 mg, 10 mmol) was added to the reaction at room temperature and the reaction was left with vigorous stirring for the following 16 hours. The reaction was then quenched via the addition of saturated $NaHCO_3$ and it was extracted with DCM (3x). The organic extract was dried with $MgSO_4$, filtered, and concentrated and the resultant crude oil was purified via flash column chromatography.
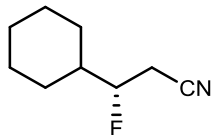
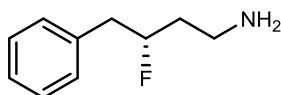(R)-3-fluoro-4-phenylbutanenitrile (**1.96A**)

The product was prepared according general procedure C, purified via flash column chromatography (15% ethyl acetate in hexanes, visualized TLC with KMnO$_4$) to afford the product was a clear oil (126 mg, 77% yield). ^{1}H NMR (400.1 MHz, CDCl$_3$) δ (ppm): 7.41-7.23 (m, 5H); 4.93 (dp, J_1 = 46.7 Hz, J_2 = 5.6 Hz, 1H); 3.21-2.97 (m, 2H); 2.75-2.52 (m, 2H). ^{13}C NMR (100.6 MHz, CDCl$_3$) δ (ppm): 134.77 (d, J = 5.6 Hz), 129.39, 128.86, 127.37, 116.07 (d, J = 5.4 Hz), 88.70 (d, J = 180.9 Hz), 40.17 (d, J = 20.8), 23.11 (d, J = 24.7 Hz). Specific rotation [—= -12.3^0 (c = 100, CHCl$_3$). HRMS (TOF, ES+) C$_{10}$H$_{10}$NFNa [M+Na]$^+$ calc. mass 186.0695, found 186.0692.
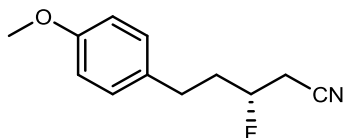
(R)-3-fluoro-5-(4-methoxyphenyl)pentanenitrile (**1.96B**)

The product was prepared according general procedure C, purified via flash column chromatography (20% ethyl acetate in hexanes, visualized TLC with KMnO$_4$) to afford the product was a clear oil (190 mg, 92% yield). ^{1}H NMR (400.1 MHz, CDCl$_3$) δ (ppm): 7.12 (d, J = 8.6 Hz, 2H); 6.86 (d, J = 8.6 Hz, 2H); 4.69 (dsx, J_1 = 47.5 Hz, J_2 = 5.3 Hz, 1H); 3.8 (s, 3H); 2.86-2.57 (m, 4H); 2.21-2.06 (m, 1H); 2.02-1.83 (m, 1H). ^{13}C NMR (100.6 MHz, CDCl$_3$) δ (ppm): 158.25, 132.05, 129.44, 114.97 (d, J = 6.1 Hz), 114.13, 87.49 (d, J = 177.9 Hz), 55.33, 36.16 (d, J = 20.3 Hz), 29.90 (d, J = 4.2 Hz), 24.10 (d, J = 25.5 Hz). Specific

rotation [── = +22.8⁰ (*c* = 100, CHCl₃). HRMS (TOF, ES+) $C_{12}H_{14}NFNa$ [M+Na]⁺ calc.

mass 230.0957, found 230.0955.

(*R*)-6-((*tert*-butyldimethylsilyl)oxy)-3-fluorohexanenitrile (**1.96C**)

The product was prepared according general procedure C, purified via flash column

chromatography (15% ethyl acetate in hexanes, visualized TLC with KMnO₄) to afford the

product was a clear oil (175 mg, 71% yield). ¹H NMR (400.1 MHz, CDCl₃) δ (ppm): 4.76

(dm, *J* = 47.5 Hz, 1H); 3.69-3.59 (m, 2H); 2.78-2.59 (m, 2H); 1.90-1.53 (m, 4H); 0.87 (s,

9H); 0.03 (s, 6H). ¹³C NMR (100.6 MHz, CDCl₃) δ (ppm): 116.03 (d, *J* = 5.8 Hz), 88.51 (d, *J*

= 177.4 Hz), 62.24, 31.11 (d, *J* = 20.4 Hz), 27.85 (d, *J* = 4.2 Hz), 25.94, 24.09 (d, *J* = 25.3

Hz), 18.30, -5.35. Specific rotation [── = +4.0⁰ (*c* = 100, CHCl₃). HRMS (TOF, ES+)

$C_{12}H_{25}NOFSi$ [M+H]⁺ calc. mass 246.1689, found 246.1690.

(3*S*)-3-fluoro-4-phenylpentanenitrile (**1.96D**) (**1.96E**)

The product (**diastereomer A**) was prepared according to general procedure C, purified via

flash column chromatography (10% ethyl acetate in hexanes, visualized TLC with KMnO₄)

to afford the product was a clear oil (164 mg, 93% yield). The product (**diastereomer B**) was

prepared according to general procedure C, purified via flash column chromatography (10%

ethyl acetate in hexanes, visualized TLC with KMnO₄) to afford the product was a clear oil

(137 mg, 77% yield). ^{1}H NMR—**Diastereomer A (less polar)** (400.1 MHz, CDCl$_3$) δ (ppm): 7.39-7.20 (m, 5H); 4.72 (dm, $J = 46.9$ Hz, 1H); 3.17-3.05 (m, 1H); 2.65-2.33 (m, 2H); 1.45 (dd, $J_1 = 6.9$ Hz, $J_2 = 1.3$ Hz, 3H). ^{1}H NMR—**Diastereomer B (more polar)** (400.1 MHz, CDCl$_3$) δ (ppm): 7.40-7.26 (m, 5H); 4.89 (dm, $J = 46.9$ Hz, 1H); 3.18-3.03 (m, 1H); 2.65-2.44 (m, 2H); 1.44 (d, $J = 7.3$ Hz, 3H). ^{13}C NMR—**Diastereomer A (less polar)** (100.6 MHz, CDCl$_3$) δ (ppm): 140.72 (d, $J = 8.3$ Hz), 129.23, 127.76, 127.59, 116.15 (d, $J = 3.3$ Hz), 92.21 (d, $J = 184.5$ Hz), 44.07 (d, $J = 20.0$ Hz), 22.56 (d, $J = 23.7$ Hz), 17.32 (d, $J = 4.1$ Hz). ^{13}C NMR—**Diastereomer B (more polar)** (100.6 MHz, CDCl$_3$) δ (ppm): 139.65 (d, $J = 1.2$ Hz), 128.78, 128.30, 127.53, 116.23 (d, $J = 7.7$ Hz), 91.58 (d, $J = 183.6$ Hz), 43.26 (d, $J = 19.1$ Hz), 22.04 (d, $J = 26.9$ Hz), 17.07 (d, $J = 5.5$ Hz). Specific rotation—**Diastereomer A (less polar)** [―= -41.8^0 ($c = 100$, CHCl$_3$). Specific rotation—**Diastereomer B (more polar)** [―= +41.0^0 ($c = 100$, CHCl$_3$). HRMS—**Diastereomer A (less polar)** (TOF, ES+) C$_{11}$H$_{13}$NF [M+H]$^+$ calc. mass 178.1032, found 178.1033. HRMS—**Diastereomer B (more polar)** (TOF, ES+) C$_{11}$H$_{13}$NF [M+H]$^+$ calc. mass 178.1032, found 178.1033.

(R)-3-fluorotridecanenitrile (**1.96F**)

The product was prepared according to general procedure C, purified via flash column chromatography (10% ethyl acetate in hexanes, visualized TLC with KMnO$_4$) to afford the product was a waxy solid (175 mg, 82% yield). ^{1}H NMR (400.1 MHz, CDCl$_3$) δ (ppm): 4.69 (dm, $J = 47.7$ Hz, 1H); 2.76-2.56 (m, 2H); 1.87-1.55 (m, 2H); 1.51-1.17 (m, 16H), 0.86 (t, $J = 7.0$ Hz, 3H). ^{13}C NMR (100.6 MHz, CDCl$_3$) δ (ppm): 116.11 (d, $J = 6.1$ Hz), 88.54 (d, $J = 177.4$ Hz), 34.27 (d, $J = 20.1$ Hz), 31.92, 29.58, 29.51, 29.41, 29.33, 29.17, 24.66 (d, $J = 4.4$

Hz), 24.02 (d, J = 25.6 Hz), 22.70, 14.11. Specific rotation [$-$ = +8.5^0 (c = 100, CHCl$_3$).

HRMS (TOF, ES+) C$_{13}$H$_{24}$NFNa [M+Na]$^+$ calc. mass 236.1790, found 236.1790.

(S)-3-cyclohexyl-3-fluoropropanenitrile (**1.96G**)

The product was prepared according to general procedure C, purified via flash column chromatography (10% ethyl acetate in hexanes, visualized TLC with KMnO$_4$) to afford the product was a clear oil (131 mg, 84% yield). ^{1}H NMR (400.1 MHz, CDCl$_3$) δ (ppm): 4.44 (dq, J_1 = 47.0 Hz, J_2 = 6.2 Hz, 1H); 2.78-2.60 (m,, 2H); 1.95-1.88 (m, 1H); 1.84-1.56 (m, 5H); 1.36-0.99 (m, 5H). ^{13}C NMR (100.6 MHz, CDCl$_3$) δ (ppm): 116.45 (d, J = 5.4 Hz), 92.18 (d, J = 179.6 Hz), 41.31 (d, J = 18.7 Hz), 27.84 (dd, J_1 = 78.4 Hz, J_2 = 4.8 Hz), 26.05, 25.55 (d, J = 26.3 Hz), 21.79 (d, J = 25.9 Hz). Specific rotation [$-$ = -4.2^0 (c = 100, CHCl$_3$). HRMS (TOF, ES+) C$_9$H$_{14}$NFNa [M+Na]$^+$ calc. mass 178.1008, found 178.1007.

General procedure D—preparation of γ-Fluoroamines
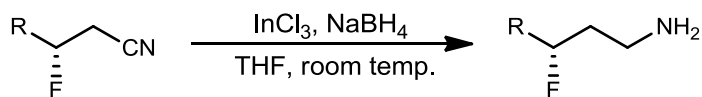
To a flame dried round-bottom flask equipped with a magnetic stir bar and charged with anhydrous InCl$_3$ (111 mg, 0.50 mmol) and NaBH$_4$ (56.7 mg, 1.50 mmol) was added anhydrous THF (1.2 mL) and the heterogeneous mixture was allowed to stir under argon for 1 hour. The nitrile substrate (0.5 mmol) was then slowly added to the reaction mixture in dissolved in THF (0.5 mL). The reaction was then allowed to stir and was monitored by TLC until completion (approx. 4 hrs). The solution was quenched by the dropwise addition of water (2 mL). This solution was then heated to 75 °C for 30 minutes, then MeOH (2 mL) was added to the mixture and it was again heated to 75 °C for an additional 30 minutes. The solution was then filtered, eluting with MeOH to remove any solid reaction components and the filtrate was concentrated under reduced pressure. The resultant crude material was purified via flash column chromatography (DCM/MeOH).

(R)-3-fluoro-4-phenylbutan-1-amine (**1.97A**)

The product was prepared according to general procedure D, purified via flash column chromatography (10% MeOH in DCM, visualize TLC with ninhydrin) to afford the product was a clear oil (73 mg, 87% yield), which was determined to have an ee of 94% by ^{19}F NMR of the (R) mosher amide of the final amine (^{19}F NMR (300 MHz, CDCl$_3$) δ (ppm): δ (minor) -180.70, δ (major) -180.94, fluorine NMR of racemic and enantioenriched mosher amides

shown below. ^{1}H NMR (400.1 MHz, CDCl$_3$) δ (ppm): 7.33-7.18 (m, 5H); 4.81 (dm, J = 49.0 Hz, 1H); 3.05-2.78 (m, 4H); 1.88-1.60 (m, 2H); 1.49 (s, br, 2H). ^{13}C NMR (100.6 MHz, CDCl$_3$) δ (ppm): 137.10 (d, J = 5.0 Hz), 129.42, 128.49, 126.65, 92.97 (d, J = 170.6 Hz), 41.86 (d, J = 21.1 Hz), 38.40, 38.29 (d, J = 14.5 Hz). Specific rotation [⎯= -2.1^0 (c = 100, CHCl$_3$).HRMS (TOF, ES+) C$_{10}$H$_{15}$NF [M+H]$^+$ calc. mass 168.1189, found 168.1190.
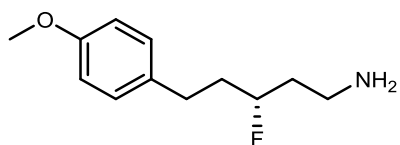
(R)-3-fluoro-5-(4-methoxyphenyl)pentan-1-amine (**1.97B**)

The product was prepared according to general procedure D, purified via flash column chromatography (10% MeOH in DCM, visualize TLC with ninhydrin) to afford the product was a clear oil (89 mg, 84% yield) which was determined to have an ee of 87% by ^{19}F NMR of the (R) mosher amide of the final amine (^{19}F NMR (300 MHz, CDCl$_3$) δ (ppm): δ (minor) -184.15, δ (major) -184.32, fluorine NMR of racemic and enantioenriched mosher amides shown below. ^{1}H NMR (400.1 MHz, MeOD) δ (ppm): 7.10 (d, J = 8.5 Hz, 2H); 6.82 (d, J = 8.7 Hz, 2H); 4.55 (dsp, J_1 = 49.8 Hz, J_2 = 4.0 Hz, 1H); 3.75 (s, 3H); 2.83-2.56 (m, 4H); 1.98-1.60 (m, 4H). ^{13}C NMR (100.6 MHz, MeOD) δ (ppm): 159.42, 134.76, 130.33, 114.87, 93.01 (d, J = 166.7 Hz), 55.63, 39.12 (d, J = 20.4 Hz), 38.81 (d, J = 4.1 Hz), 38.61 (d, J = 20.6 Hz), 31.40 (d, J = 4.6 Hz). Specific rotation [⎯= +11.6^0 (c = 100, CHCl$_3$).HRMS (TOF, ES+) C$_{12}$H$_{19}$NOF [M+H]$^+$ calc. mass 212.1451, found 212.1447.
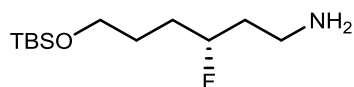
(*R*)-6-((*tert*-butyldimethylsilyl)oxy)-3-fluorohexan-1-amine (**1.97C**)

The product was prepared according general procedure D, purified via flash column chromatography (10% MeOH in DCM, visualize TLC with ninhydrin) to afford the product was a clear oil (107 mg, 86% yield) which was determined to have an ee of 92% by ^{19}F NMR of the (*R*) mosher amide of the final amine (^{19}F NMR (300 MHz, CDCl$_3$) δ (ppm): δ (minor) -184.15, δ (major) -184.32, fluorine NMR of racemic and enantioenriched mosher amides shown below. ^{1}H NMR (400.1 MHz, MeOD) δ (ppm): 4.60 (dm, J = 50.2 Hz, 1H); 3.71-3.55 (m, 2H); 2.84-2.70 (m, 2H); 1.87-1.53 (m, 6H); 0.91 (s, 9H); 0.07 (s, 6H). ^{13}C NMR (100.6 MHz, MeOD) δ (ppm): 93.73 (d, J = 166.4 Hz), 63.88, 39.27 (d, J = 20.5 Hz), 38.95 (d, J = 4.4 Hz), 32.97 (d, J = 21.1 Hz), 29.49 (d, J = 4.1 Hz), 26.41, 19.13, -5.18. Specific rotation [ ]= -4.2^{0} (*c* = 100, CHCl$_3$). HRMS (TOF, ES+) C$_{12}$H$_{29}$NOFSi [M+H]$^+$ calc. mass 250.2002, found 250.2001.
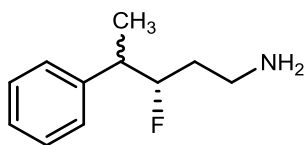
(3*S*)-3-fluoro-4-phenylpentan-1-amine (**1.97D**) (**1.97E**)

The product (**diastereomer A**) was prepared according to general procedure D, purified via flash column chromatography (10% MeOH in DCM, visualize TLC with ninhydrin) to afford the product was a clear oil (75 mg, 83% yield) which was determined to have an ee of 96% by ^{19}F NMR of the (*R*) mosher amide of the final amine (^{19}F NMR (300 MHz, CDCl$_3$) δ (ppm): δ (major) -186.34, δ (minor) -186.39, fluorine NMR of racemic and enantioenriched

mosher amides shown below. The product **(diastereomer B)** was prepared according to general procedure D, purified via flash column chromatography (10% MeOH in DCM, stain visualize with ninhydrin) to afford the product was a clear oil (82 mg, 90% yield) which was determined to have an ee of 96% by ^{19}F NMR of the (*R*) mosher amide of the final amine (^{19}F NMR (300 MHz, CDCl$_3$) δ (ppm): δ (minor) -187.23, δ (major) -187.43, fluorine NMR of racemic and enantioenriched mosher amides shown below. ^{1}H NMR—**Diastereomer A (less polar)** (400.1 MHz, MeOD) δ (ppm): 7.33-7.26 (m, 2H); 7.25-7.18 (m, 3H); 4.65 (dm, *J* = 49.0 Hz); 2.97-2.83 (m, 1H); 2.79-2.61 (m, 2H); 1.81-1.44 (m, 2H); 1.35 (d, *J* = 7.0 Hz). ^{1}H NMR—**Diastereomer B (more polar)** (400.1 MHz, MeOD) δ (ppm): 7.32-7.17 (m, 5H); 4.71 (dm, *J* = 48.9 Hz, 1H); 2.99-2.85 (m, 1H); 2.83-2.69 (m, 2H); 1.78-1.58 (m, 2H); 1.33 (d, *J* = 7.2 Hz, 3H). ^{13}C NMR—**Diastereomer A (less polar)** (100.6 MHz, MeOD) δ (ppm): 144.49 (d, *J* =6.8 Hz), 129.63, 128.89, 127.80, 97.34 (d, *J* = 173.3 Hz), 46.19 (d, *J* = 20.5 Hz), 39.10 (d, *J* = 3.5 Hz), 37.32 (d, *J* = 20.7 Hz), 17.67 (d, *J* = 5.4 Hz). ^{13}C NMR—**Diastereomer B (more polar)** (100.6 MHz, MeOD) δ (ppm): 143.62 (d, 2.3 Hz), 129.37, 129.28, 127.62, 96.81 (d, *J* = 172.8 Hz), 45.61 (d, *J* = 19.8 Hz), 38.98 (d, *J* = 4.0 Hz), 36.46 (d, *J* = 20.8 Hz), 17.96 (d, *J* = 5.9 Hz).Specific rotation—**Diastereomer A (less polar)** [―= -9.1^0 (*c* = 100, CHCl$_3$). Specific rotation— **Diastereomer B (more polar)** [―= -14.0^0 (*c* = 100, CHCl$_3$). HRMS—**Diastereomer A (less polar)** (TOF, ES+) C$_{11}$H$_{17}$NF [M+H]$^+$ calc. mass 182.1345, found 182.1343. HRMS—**Diastereomer B (more polar)** (TOF, ES+) C$_{11}$H$_{17}$NF [M+H]$^+$ calc. mass 182.1345, found 182.1346.
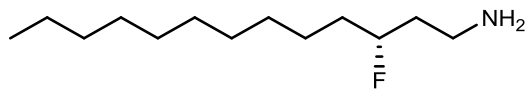
(*R*)-3-fluorotridecan-1-amine (**1.97F**)

The product was prepared according to general procedure D, purified via flash column chromatography (10% MeOH in DCM, visualize TLC with ninhydrin) to afford the product was a waxy solid (97 mg, 89% yield) which was determined to have an ee of 95% by ^{19}F NMR of the (*R*) mosher amide of the final amine (^{19}F NMR (300 MHz, CDCl$_3$) δ (ppm): δ (minor) -181.97, δ (major) -182.19, fluorine NMR of racemic and enantioenriched mosher amides shown below. ^{1}H NMR (400.1 MHz, MeOD) δ (ppm): 4.56 (dm, *J* = 49.7 Hz, 1H); 2.83-2.70 (m, 2H); 1.81-1.42 (m, 5H); 1.41-1.24 (m, 15H); 0.90 (t, *J* = 7.1 Hz, 3H). ^{13}C NMR (100.6 MHz, MeOD) δ (ppm): 93.81 (d, *J* = 166.3 Hz), 39.15 (d, *J* = 20.7 Hz), 38.95 (d, *J* = 4.4 Hz), 36.53 (d, *J* = 20.7 Hz), 33.08, 30.75, 30.73, 30.70, 30.62, 30.49, 26.22 (d, *J* = 4.6 Hz), 23.75, 14.47. Specific rotation [— = -4.6^0 (*c* = 100, CHCl$_3$).HRMS (TOF, ES+) C$_{13}$H$_{29}$NF [M+H]$^+$ calc. mass 218.2284, found 218.2283.
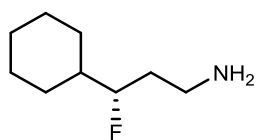
(*S*)-3-cyclohexyl-3-fluoropropan-1-amine (**1.97G**)
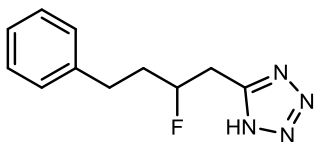
The product was prepared according to general procedure D, purified via flash column chromatography (10% MeOH in DCM, visualize TLC with ninhydrin) to afford the product was a clear oil (58 mg, 73% yield), which was determined to have an ee of 96% by ^{19}F NMR of the (*R*) mosher amide of the final amine (^{19}F NMR (300 MHz, CDCl$_3$) δ (ppm): δ (minor) -187.84, δ (major) -187.94, fluorine NMR of racemic and enantioenriched mosher amides

shown below. ^{1}H NMR (400.1 MHz, MeOD) δ (ppm): 4.30 (dm, J = 49.2 Hz, 1H); 2.89-2.72 (m, 2H); 1.92-1.84 (m, 1H); 1.83-1.62 (m, 5H); 1.57-1.42 (m, 1H); 1.36-1.00 (m, 5H). ^{13}C NMR (100.6 MHz, MeOD) δ (ppm): 97.39 (d, J = 168.6 Hz), 43.61 (d, J = 19.3 Hz), 39.1 (d, J = 3.8 Hz), 35.74 (d, J = 21.3 Hz), 29.20 (dd, J_1 = 97 Hz, J_2 = 5.7 Hz), 27.30 (d, J = 35.7 Hz), 29.94. Specific rotation [―= -19.0^0 (c = 100, CHCl$_3$).HRMS (TOF, ES+) C$_9$H$_{19}$NF [M+H]$^+$ calc. mass 160.1502, found 160.1502.

General Procedure E—preparation of β-fluoroamines or β,β-difluoroamines

Triflic anhydride (339 mg, 1.2 mmol) was added dropwise to a flame dried round bottom flask equipped with a magnetic stir bar and charged with the chiral fluoro alcohol or difluoro alcohol (1 mmol) and lutidine (535 mg, 5 mmol) in DCM (5 mL) under argon at 0°C. The reaction mixture was allowed to stir for 30 minutes before it was removed from the stir plate while still being kept at 0°C. A separate round bottom flask equipped with a magnetic stir bar and charged with benzylamine (1.07 g, 10.0mmol) in 2 mL of DCM was stirred at 0°C. The solution of the triflate was then added slowly to this new flask taking care to keep everything at 0°C, and after addition was complete, the flask was washed with an additional 2 mL of DCM and that was then added to the reaction to bring the total volume of DCM to 9 mL. The reaction was then allowed to warm to room temperature over the next hour and left to stir overnight (14-16 hours). The β,β-difluoroamines were allowed to react for 24 hours. A solution of saturated NaHCO$_3$ was added to quench the reaction and it was transferred to a

110

separatory funnel. There it was extracted 3X with DCM and the combined organic extracts were dried with MgSO$_4$, filtered, and concentrated under reduced pressure. The crude oil was then purified via flash column chromatography (hexanes/ethyl acetate).
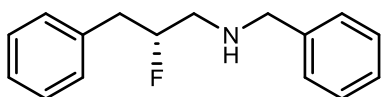
(*R*)-*N*-benzyl-2-fluoro-3-phenylpropan-1-amine (**1.101A**)

The product was prepared according to general procedure E, purified via flash column chromatography (20-50% ethyl acetate in hexanes, visualize TLC with ninhydrin) to afford the product was a clear oil (204 mg, 84% yield), which was determined to have an ee of 94% by chiral HPLC analysis (Chiralpak IA, t$_R$ (major) = 4.87 minutes, t$_R$ (minor) = 5.74 minutes, traces shown below). ^{1}H NMR (400.1 MHz, CDCl$_3$) δ (ppm): 7.42-7.23 (m, 10H); 4.91 (dm, *J* = 48.9 Hz, 1H); 3.91-3.81 (m, 2H); 3.13-2.78 (m, 4H); 1.86 (s, br, 1H). ^{13}C NMR (100.6 MHz, CDCl$_3$) δ (ppm): 140.09, 136.96 (d, *J* = 5.5 Hz), 129.40, 128.55, 128.50, 128.18, 127.10, 126.70, 94.07 (d, *J* = 171.2 Hz), 53.83, 52.38 (d, *J* = 21.0 Hz), 39.45 (d, *J* = 21.2 Hz). Specific rotation [― = -2.3^0 (*c* = 100, CHCl$_3$). HRMS (TOF, ES+) C$_{16}$H$_{19}$NF [M+H]$^+$ calc. mass 244.1502, found 244.1503.
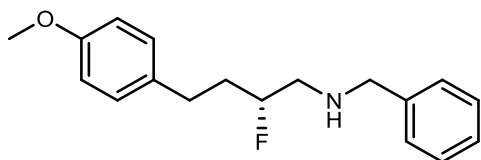
(*R*)-*N*-benzyl-2-fluoro-4-(4-methoxyphenyl)butan-1-amine (**1.101B**)

The product was prepared according to general procedure E, purified via flash column chromatography (20-50% ethyl acetate in hexanes, visualize TLC with ninhydrin) to afford

the product was a clear oil (277 mg, 96% yield), which was determined to have an ee of 90% by chiral HPLC analysis (Chiralpak IB, t_R (major) = 6.56 minutes, t_R (minor) = 5.93 minutes, traces shown below). ^{1}H NMR (400.1 MHz, CDCl$_3$) δ (ppm): 7.41-7.25 (m, 5H); 7.14 (d, J = 8.6 Hz, 2H); 6.87 (d, J = 8.6 Hz, 2H); 4.68 (dm, J = 50.0 Hz, 1H); 3.85 (s, 2H); 3.81 (s, 3H); 2.94-2.63 (m, 4H); 2.10-1.95 (m, 1H); 1.93-1.80 (m, 1H); 1.78 (s, br, 1H). ^{13}C NMR (100.6 MHz, CDCl$_3$) δ (ppm): 157.97, 140.10, 133.30, 129.40, 128.47, 128.13, 127.07, 113.92, 93.05 (d, J = 167.8 Hz), 55.26, 53.83, 53.07 (d, J = 20.9 Hz), 35.00 (d, J = 20.6 Hz), 30.36 (d, J = 4.6 Hz). Specific rotation [＝ +11.8^0 (c = 100, CHCl$_3$). HRMS (TOF, ES+) C$_{18}$H$_{23}$NOF [M+H]$^+$ calc. mass 288.1764, found 288.1762.
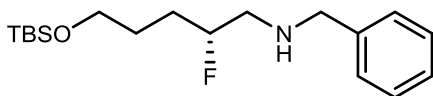
(*R*)-*N*-benzyl-5-((*tert*-butyldimethylsilyl)oxy)-2-fluoropentan-1-amine (**1.101C**)

The product was prepared according to general procedure E, purified via flash column chromatography (20-50% ethyl acetate in hexanes, visualize TLC with ninhydrin) to afford the product was a clear oil (314 mg, 96% yield), which was determined to have an ee of 94% by chiral HPLC analysis (Chiralpak ID, t_R (major) = 9.74 minutes, t_R (minor) = 10.65 minutes, traces shown below). ^{1}H NMR (400.1 MHz, CDCl$_3$) δ (ppm): 7.39-7.22 (m, 5H); 4.68 (dm, J = 50.0 Hz, 1H); 3.87-3.79 (m, 2H); 3.69-3.58 (m, 2H); 2.90-2.68 (m, 2H); 1.81-1.54 (m, 5H); 0.90 (s, 9H); 0.06 (s, 6H). ^{13}C NMR (100.6 MHz, CDCl$_3$) δ (ppm): 140.18, 128.54, 128.19, 127.12, 93.89 (d, J = 167.8 Hz), 62.76, 53.90, 53.24 (d, J = 20.9 Hz), 29.62 (d, J = 20.7 Hz), 28.43 (d, J = 4.3 Hz), 26.06, 18.43, -5.20. Specific rotation [＝ +0.6^0 (c

= 100, CHCl$_3$). HRMS (TOF, ES+) C$_{18}$H$_{33}$NOFSi [M+H]$^+$ calc. mass 326.2315, found 326.2318.
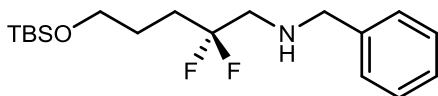
N-benzyl-5-((*tert*-butyldimethylsilyl)oxy)-2,2-difluoropentan-1-amine (**1.104**)

The product was prepared according to general procedure E, purified via flash column chromatography (20-50% ethyl acetate in hexanes, visualize TLC with ninhydrin) to afford the product was a clear oil (277 mg, 81% yield). ^{1}H NMR (400.1 MHz, CDCl$_3$) δ (ppm): 7.39-7.24 (m, 5H); 3.88 (s, 2H); 3.67 (t, *J* = 6.3 Hz, 2H); 2.95 (t, *J* = 14.1 Hz, 2H); 2.10-1.95 (m, 2H); 1.75-1.66 (m, 2H); 1.62 (s, 1H); 0.93 (s, 9H); 0.09 (s, 6H). ^{13}C NMR (100.6 MHz, CDCl$_3$) δ (ppm): 139.96, 128.55, 128.17, 127.23, 127.87 (t, *J* = 240.9 Hz), 62.52, 53.78, 52.70 (t, *J* = 28.4), 31.27 (t, *J* = 24.6 Hz), 26.04, 25.57 (t, *J* = 4.3 Hz) , 18.41, -5.23. HRMS (TOF, ES+) C$_{18}$H$_{32}$NOF$_2$Si [M+H]$^+$ calc. mass 344.2221, found 344.2219.

Procedure F—preparation of β-fluoro tetrazoles
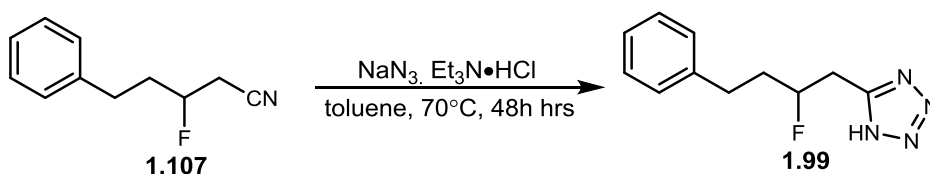
The mixture of fluoro-nitrile **1.107** (354 mg, 2 mmol), sodium azide (244 mg, 6 mmol), and triethylamine hydrochloride (517 mg, 6 mmol) in toluene (6 mL), in a round-bottomed flask equipped with a magnetic stir bar, was stirred and heated to 70 ^{0}C for 48 hours. After cooling to room temperature, the product was extracted with water (2 X 6 mL), and the aqueous layer was acidified with 1 mL of concentrated hydrochloric acid (38%). If a white solid did not immediately crash out of solution upon acidification, air was blown on the water for to

partially concentrate the water, and the β-fluoro-tetrazole then crashed out of solution as a white solid, which was collected using a Buchner funnel and was dried under reduced pressure. The solid was purified via reverse phase chromatography.

5-(2-fluoro-4-phenylbutyl)-1H-tetrazole (**1.99**)

The product was prepared according to general procedure F, and was purified via reverse phase chromatography (10-90% MeCN in water (0.1% TFA), to afford the product as a white solid (339 mg, 77% yield). ^{1}H NMR (400.1 MHz, MeOD) δ (ppm): 7.28-7.22 (m, 2H); 7.21-7.12 (m, 3H); 4.84 (dm, J = 48.8 Hz, 1H); 3.40-3.21 (m, 2H); 2.86-2.66 (m, 2H); 2.04-1.86 (m, 2H). ^{13}C NMR (100.6 MHz, MeOD) δ (ppm):154.38, 142.11, 129.50, 129.41, 127.11, 91.62 (d, J = 172.0 Hz), 37.43 (d, J = 20.5 Hz), 31.92 (d, J = 4.3 Hz), 30.2 (d, J = 22.3 Hz). HRMS (TOF, ES+) $C_{11}H_{14}N_4F$ [M+H]$^+$ calc. mass 221.1202, found 221.1201.

Procedure G—preparation of β-fluoro amide oxime
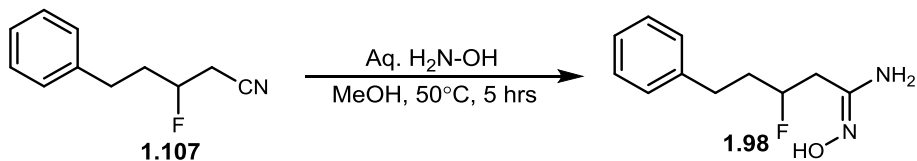
A mixture of fluoro-nitrile **1.107** (177 mg, 1 mmol) and aqueous hydroxylamine (66 mg, 2 mmol, from 50% aqueous solution) in methanol (1 mL) was added to a round-bottomed flask equipped with a magnetic stir bar and was heated to 50°C for 5 hours with stirring. The reaction was then concentrated under reduced pressure to evaporate all solvents and reagents.

Crude product was pure enough for use in future reactions, but was purified via reverse phase chromatography to obtain spectroscopically pure material.
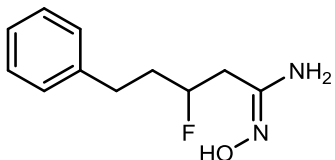
(*E*)-3-fluoro-*N'*-hydroxy-5-phenylpentanimidamide (**1.98**)

The product was prepared according to general procedure G, and was purified via reverse phase chromatography (10-90% MeCN in water (0.1% TFA), to afford the product as a white solid (191 mg, 91% yield). ^{1}H NMR (400.1 MHz, MeOD) δ (ppm): 7.31-7.24 (m, 2H); 7.23-7.15 (m, 3H); 4.79 (dm, J = 49.0 Hz, 1H); 2.89-2.63 (m, 4H); 2.09-1.85 (m, 2H). ^{13}C NMR (100.6 MHz, MeOD) δ (ppm): 161.66, 141.94, 129.57, 129.46, 127.23, 90.89 (d, J = 174.6), 37.66 (d, J = 20.1 Hz), 35.9 (d, J = 22.3 Hz), = 22.3 Hz), 31.82 (d, J = 3.9 Hz). HRMS (TOF, ES+) $C_{11}H_{16}N_2OF$ [M+H]$^+$ calc. mass 211.1247, found 211.1245.

Experimental for chiral aziridines and azetidines

All reagents were purchased from Sigma-Aldrich Corp., TCI America, Rieke Metals, Inc. and were used without purification. Analytical thin-layer chromatography (TLC) was performed on 250 μm silica plates from Sorbent Technologies. Visualization was accomplished via UV light, and/or the use of ninhydrin, iodine, and potassium permanganate solutions followed by application of heat. Chromatography was performed using Silica Gel 60 (230-400 mesh) from Sorbent Technologies or Silica RediSep Rf flash columns on a CombiFlash Rf automated flash chromatography system. All ^{1}H and ^{13}C NMR spectra were recorded on a Bruker AV-400 (400 MHz) instrument. Chemical shifts are reported in ppm relative to residual solvent peaks as an internal standard set to δ 7.26 and δ 77.16 ($CDCl_3$). Data are reported as follows: chemical shift, multiplicity (s = singlet, d = doublet, t = triplet, q = quartet, p = pentet, br = broad, dd = doublet of doublets, dq = doublet of quartets, td = triplet of doublets, pd = pentet of doublets, m = multiplet), coupling constat (Hz), integration. Low resolution mass spectra (LCMS) were recorded on an Agilent 1200 LCMS with electrospray ionization. High resolution mass spectra (HRMS) were recorded on a Waters Qtof-API-US plus Acuity system with ES as the ion source. Analytical high performance liquid chromatography (HPLC) was performed on an Agilent 1200 analytical LCMS with UV detection at 214 nm and 254 nm along with ELSD detection. Chiral separations were performed on a Thar Investigator II supercritical fluid chromatograph (SFC) utilizing Chiralcel® OD, OD-Cl, OJ, and Chiralpak® IA columns. Optical rotations were acquired on a Jasco P-2000 polarimeter at 23 °C and 589 nm. The specific rotations were calculated according to the equation $[\alpha]23/D = 100\alpha/l \; x \; c$ where l is the path length in decimeters and c is the concentration in g/100 mL.
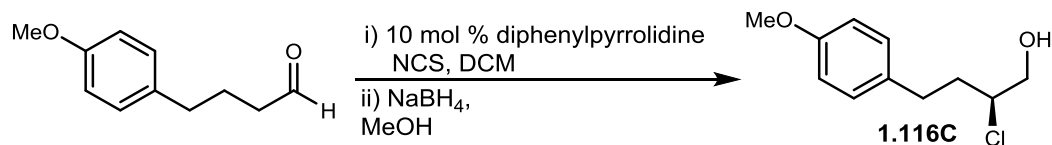
((S)-2-chloro-4-(4-methoxyphenyl)butan-1-ol) To a flame dried round-bottomed flask equipped with a magnetic stir bar, aldehyde (0.25 g, 1.40 mmol) was dissolved in DCM (2.81 mL) at 0 °C. To the stirred solution was added diphenylpyrrolidine catalyst (31 mg, 0.14 mmol) followed by *N*-chlorosuccinimide (0.24 g, 1.82 mmol). The solution was allowed to warm to rt over the next hour, and it was checked by ^{1}H NMR for consumption of the starting material (8 hrs). The reaction was then diluted with methanol (7.0 mL), cooled to 0 °C, and sodium borohydride (0.26 g, 7.02 mmol) was slowly added with stirring. The reaction was stirred for an additional 30 minutes, and was then quenched with water (30 mL). It was extracted into EtOAc (3 X 50 mL), the combined organic layer was dried with magnesium sulfate, filtered, and concentrated under reduced pressure. The crude material was then purified by flash column chromatography (4:1 Hex/EtOAc) to yield the desired product as a clear oil. (0.21 g, 77%). ^{1}H NMR (400.1 MHz, CDCl$_3$) δ (ppm): 7.12 (d, J = 8 Hz, 2H); 6.84 (d, J = 8 Hz, 2H); 3.97 (m, 1H); 3.79 (s, 3H); 3.68 (dd, J_1 = 11.5 Hz, J_2 = 6.5 Hz, 1H); 2.84 (dt, J_1 = 14 Hz, J_2 = 6.5 Hz, 1H); 2.71 (dt, J_1 = 14 Hz, J_2 = 8 Hz, 1H); 2.01 (m, 2H); 1.9 (br s, 1H).
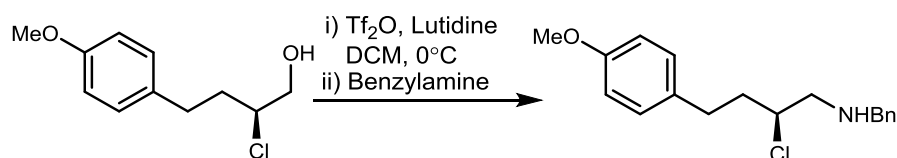
((S)-N-benzyl-2-chloro-4-(4-methoxyphenyl)butan-1-amine) To a flame dried round-bottomed flask equipped with a magnetic stir bar, starting material alcohol (0.18 g, 0.82

117

mmol) and lutidine (0.44 g, 4.09 mmol) were dissolved in DCM (4.1 mL) and the reaction was cooled to 0 °C. Triflic anhydride was added (0.28 g, 0.98 mmol) dropwise, and the solution was left to stir at 0 °C for 30 minutes. At that time, the triflate solution was taken up in a syringe and added dropwise to a stirring solution of benzylamine (0.88 g, 8.17 mmol) in DCM (1.5 mL) at 0 °C. The flask containing the triflate solution was washed 2 times with DCM (1 mL total) and added to the reaction. The solution was then allowed to warm to room temperature over an hour before leaving it to stir overnight. The reaction was quenched with saturated sodium bicarbonate (30 mL), diluted with DCM (25 mL), and extracted with DCM (3 X 30 mL). The organic layers were combined and washed with brine (1 X 100 mL), and the combined organic was dried with magnesium sulfate, filtered, and concentrated under reduced pressure to provide a crude yellow oil. The product was purified by flash column chromatography (9:0.9:0.1 DCM/MeOH/NH$_4$OH) to provide the product as a pale yellow oil (0.22 g, 88%). ^{1}H NMR (400.1 MHz, CDCl$_3$) δ (ppm): 7.33 (m, 4H); 7.26 (m, 1H); 7.10 (d, J = 9 Hz, 2H); 6.83 (d, J = 9 Hz, 2H); 4.03 (m, 1H); 3.80 (dd, J_1 = 14 Hz, J_2 = 13 Hz, 2H); 3.79 (s, 3H); 2.86 (dd, J_1 = 6 Hz, J_2 = 3 Hz, 2H); 2.80 (m, 1H); 2.01 (m, 2H). ^{13}C NMR (100.6 MHz, CDCl$_3$) δ (ppm): 157.94, 132.82, 129.39, 129.22, 128.42, 128.15, 128.07, 127.06, 120.12, 113.86, 113.80, 62.48, 55.34, 55.21, 53.25, 37.97, 31.52, 24.41.
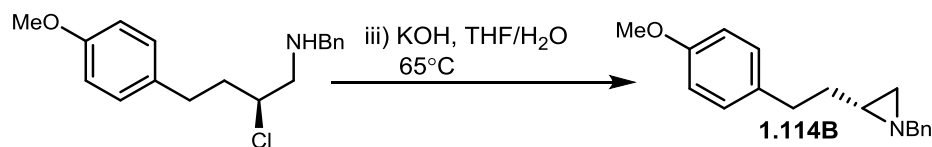
((R)-1-benzyl-2-(4-methoxyphenethyl)aziridine) In an open assimilation vial equipped with a magnetic stir bar, starting material amine (0.18 g, 0.82 mmol) was dissolved in 1:1 THF/water (4.1 mL), followed by the addition of KOH (0.25 g, 4.40 mmol). The vial was

sealed and stirred overnight at 65 °C. The reaction mixture was allowed to cool to ambient temperature prior to diluting with ethyl acetate (25 mL) and water (25 mL). The mixture was extracted with ethyl acetate (3 X 25 mL), and the combined organic was dried with magnesium sulfate, filtered, and concentrated under reduced pressure to provide a crude oil. The crude material was purified by flash column chromatography (1:1 H/E) to deliver the product as a pale yellow oil (0.18 g, 99%).
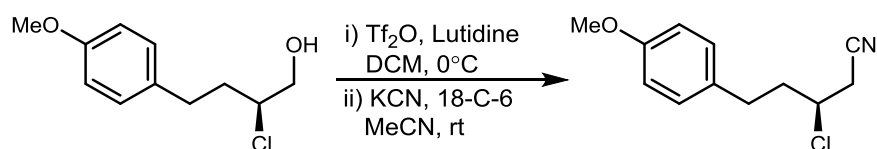
((S)-3-chloro-5-(4-methoxyphenyl)pentanenitrile) To a flame dried round-bottomed flask equipped with a magnetic stir bar, starting material alcohol (0.19 g, 0.89 mmol), and 2,6-lutidine (0.48 g, 4.44 mmol) was added DCM (4.4 mL) and the solution was cooled to 0 °C. Triflic anhydride (0.30 g, 1.07 mmol) was added to the mixture dropwise, and the solution was left to stir for 30 minutes. The reaction was then diluted with DCM (20 mL) and was washed with water (25 mL). the organic fraction was washed with brine (25 mL), dried with magnesium sulfate, filtered, and concentrated under reduced pressure. The crude oil was then dissolved in acetonitrile (4.4 mL) and 18-crown-6 (0.05 g, 0.18 mmol) followed by KCN (0.578 g, 8.88 mmol) was added to the mixture and it was allowed to stir at rt for 12 hours. The reaction was then quenched with saturated sodium bicarbonate (60 mL) and was extracted with DCM (3 X 50 mL). the combined organic fractions were dried with magnesium sulfate, filtered, and concentrated under reduced pressure. The crude oil was then purified by flash column chromatography (4:1 Hex/EtOAc) affording the desired product as a rose colored oil (0.15 g, 75%). ^{1}H NMR (400.1 MHz, CDCl$_3$) δ (ppm): 7.11 (d, J = 8.5 Hz,

2H); 6.85 (d, $J = 8.5$ Hz, 2H); 3.97 (q, $J = 6.5$ Hz, 1H); 3.79 (s, 3H); 2.84 (m, 1H); 2.80 (dd,

$J_1 = 5.6$ Hz, $J_2 = 5.6$ Hz, 2H); 2.72 (m, 1H); 2.12 (dd, $J_1 = 14$ Hz, $J_2 = 7$ Hz, 2H).
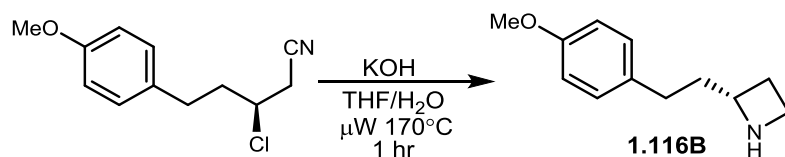
((R)-2-(4-methoxyphenethyl)azetidine) To a flame dried microwave vial with magnetic stir

bar was added InCl$_3$ (0.12 g, 0.54 mmol) and NaBH$_4$ (0.06 g, 1.63 mmol). Anhydrous THF

(1.2 mL) was added and the heterogeneous mixture was stirred under argon for 1 hour. The

starting material nitrile was added to that reaction mixture, and it was allowed to stir at room

temperature for 4 hours. The reaction was then quenched by dropwise addition of water (1.5

mL), and the reaction was stirred vigorously and heated to 75 °C for 30 minutes. KOH (0.16

g, 2.86 mmol) was then added and the vial was sealed and submitted to microwave

irradiation at 170 °C for 1 hour. The biphasic solution was extracted with EtOAc (3 X 10

mL), and the combined organic was washed with brine (1 X 30 mL). The combined organic

was dried with magnesium sulfate, filtered, and concentrated under reduced pressure. The

crude material was purified by flash column chromatography (9.0:0.9:0.1

DCM/MeOH/NH$_4$OH) to afford the desired product as a light yellow oil (40 mg, 48%).

Specific rotation [─ = -5.6^0 ($c = 1.0$, CHCl$_3$).

DISCOVERY OF NOVEL PHOSPHOLIPASE D INHIBITORS

2.1 Phospholipase D: a brief overview of its clinical relevance and chemical inhibition

2.1.1   Introduction to phospholipase D and phosphatidic acid signaling

Phosphatidic acid (PA) is an essential phospholipid component of cell membranes and accounts for 1-5% of the total lipid content in mammalian cells.[1] PA can be generated *de novo* from glycerol-3-phosphate through sequential enzyme catalyzed acylations of the hydroxyl groups, or it can also be formed through hydrolysis of phosphatidyl choline (PC). PA is involved in the cell structurally as a component of different membrane lipid bilayers, and it is a critical lipid species involved in metabolic pathways to different signaling chemicals including diacylglycerol (DAG) and lysophosphatidic acid (LPA). While only a minor constituent of lipid bilayers, PA has a major impact on the curvature of membranes and is involved in important membrane fusion events facilitating endo and exocytosis.[2,3] Additionally, PA is an important second messenger involved in the recruitment and regulation of different proteins. Specifically, PA can act as a node in membranes to interact with proteins facilitating translocation of these species across the bilayer (eg. Raf-1),[4,5] or binding of PA can directly regulate signaling proteins (eg. mTOR).[6] Aberrant PA signaling, which would result in abnormal regulation of its protein binding partners, is proposed to have major roles in many types of cancer,[7] neurodegenerative disorders,[8] and clotting disorders.[9] Since dysregulated PA signaling is considered to have a role in these various debilitating diseases, controlling PA biosynthesis could have an effect on these disease states. Proteins

that modulate PA concentrations, therefore, are being studied to determine whether they have a role in aberrant PA signaling.

Phospholipase D (PLD) is an enzyme that catalyzes the hydrolysis of PC, which accounts for 40-55% of phospholipid cellular mass, to PA. Thus, PLD could be responsible for abnormal levels of PA that could cause irregularities in cellular signaling, which warrants further investigation of PLD. PC is a glycerol with two esters and a phosphate containing a choline (**Figure 2.1.1.1**). The prevailing theory for an enzymatic mechanism of PC hydrolysis involves PLD facilitating choline cleavage from PC with concomitant formation of a histidine—phosphate bond. At this point, the substrate is activated for nucleophilic addition of water or a primary alcohol. This addition will occur with simultaneous cleavage of the newly formed histidine—phosphate bond to generate PA or a phosphatidyl alcohol (depending on the nucleophile).[10] The catalytic pocket is involved in a proton shuttle, and the side chains involved in these actions are depicted in **Figure 2.1.1.1**.
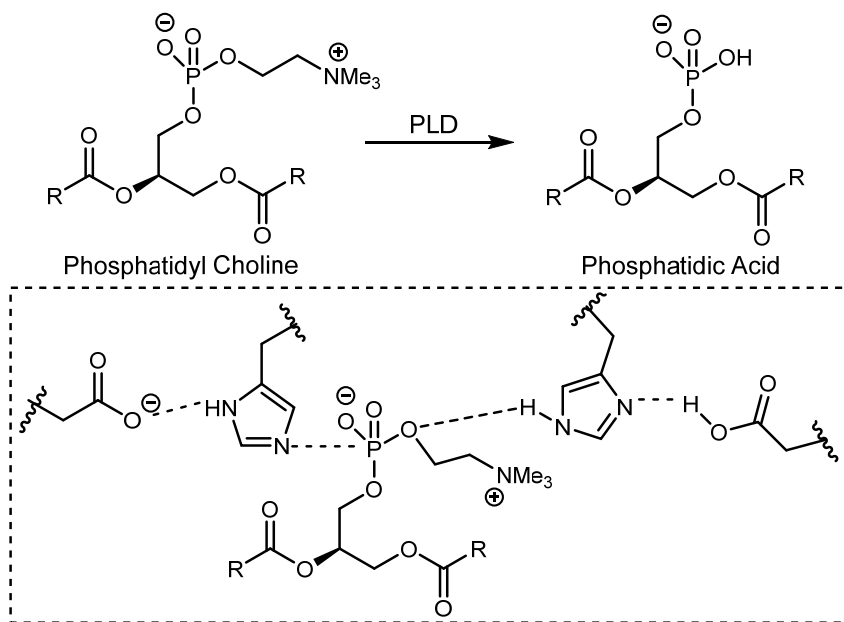
Figure 2.1.1.1 PLD catalysis

While over 4,000 PLD enzymes have been reported, the homology between most of these PLDs is minimal. To be considered a PLD, an enzyme only needs to catalyze the hydrolysis of PC to PA, but a more specific PLD superfamily of enzymes share a similar set of residues.[3] Namely, they share a conserved $HxKxxxxDx_6GSxN$ motif (commonly called HKD), which is consistently found within the catalytic domain. Based on that similarity, PLDs in this superfamily are proposed to catalyze PC hydrolysis following a similar reaction mechanism.[11] Mammals have two prominent isoforms of PLD (PLD1 and PLD2), and they share close to 50% sequence homology, mainly from semi conserved HKD, PX and PH regions (**Figure 2.1.1.2**). The enzymes are around 1,000 amino acids in length, and contain regions of phox homology (PX) and pleckstrin homology (PH), which are hypothesized to be essential for trafficking PLDs to lipid bilayers. The PX domains bind polyphosphoinositides with high specificity and both PX and PH domains bind anionic lipids with low specificity. Additionally, the PH regions contain two cysteine residues and the sulfide R-group can be palmitoylated resulting in additional favorable interactions with the plasma membrane.
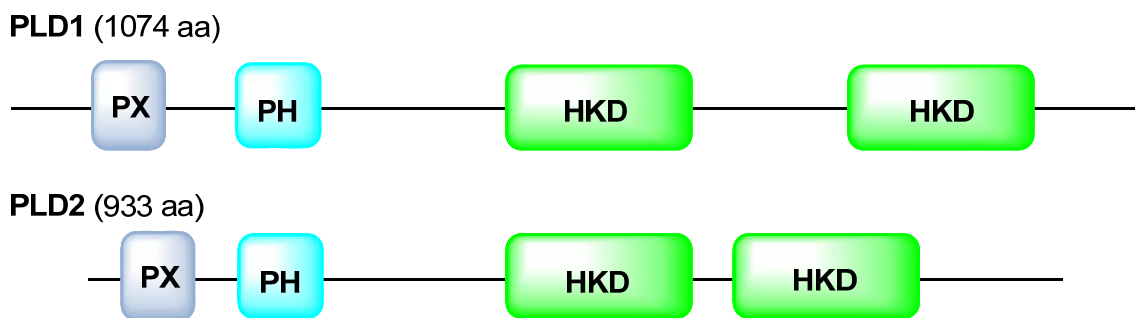
Figure 2.1.1.2 Mammalian PLD isoforms. Figure adapted from ref 3.

Since PLDs are major contributors to the overall PA content of the cell, their activity is tightly controlled by a number of molecular regulators.[3] Despite the relative similarity between the primary sequence of PLD1 and PLD2, they have different localization patterns, expression levels, and regulatory mechanisms depending on the cell type. Standard

regulation of PLD enzymes is important because their regulation and activity is directly related to PA concentrations and overall signaling levels. Regarding cellular localization, PLD1 is concentrated at the Golgi complex, secretory granules, and endosomes while PLD2 is largely present at the plasma membrane with smaller concentrations of PLD2 at the Golgi apparatus, caveolae, and endosomes.[12–15] A single consistency between PLD1 and PLD2 regulation is the need for phosphatidylinositol(4,5)biphosphate (PIP$_2$), which is an essential cofactor for the catalytic activity of both enzymes.[3,16] There is a large amount of evidence implicating phosphorylation as a means of activating and inhibiting PLD function, but data regarding the actual sites of phosphorylation and the kinases involved are conflicted.[3,7,8] Protein—protein interactions also play a large role in PLD activation, and while enormous amounts of data surround distinct proteins and their impact on the PLDs, the general accepted principles are that PLD1 activation requires protein kinase C (PKC) or small GTP binding proteins as allosteric activators while PLD2 may require small GTP binding proteins but is more often thought to be constitutively active.[3,16] While tight regulatory mechanisms exist for mammalian PLDs, it is recognized that dysregulated PLD could result in abnormal concentrations of PA. PLD activation and atypical PA signaling have been linked to short term responses such as secretion and cytoskeletal rearrangement and long term cellular responses including proliferation, differentiation, apoptosis, and cell survival.[3,16,17] These cellular phenotypes, and various *in vivo* studies have implicated aberrant PLD as a probable cause of many diseases. Recently, small molecule inhibitors of both PLD isoforms have emerged, and those tool compounds should allow PLD to be fully evaluated as a therapeutic target.

2.1.2 PLD as a therapeutic target

Subsection A—PLD signaling and Alzheimer's disease (AD)

PLD is proposed to have a major role in neurophysiology based on its high expression levels in the brain and its role in cytoskeletal rearrangement, membrane trafficking, and signal transduction.[18–20] The first reported evidence linking PLD to AD was discovered when investigating PLD activity in brain homogenates of AD patients. These studies found increased PLD activity compared to that of control subjects, showing the first correlation between PLD activity and AD.[21] More recently, vast amounts of data have highlighted the fact that PLD activity increases when cells are in contact with Aβ, the pathogenic protein constituent of the amyloid β plaques that form in patients with AD.[8] More evidence has implicated PLD as having an essential role during the trafficking of amyloid precursor protein (APP) throughout the cell, especially a role in budding the vesicles used to move APP from the Golgi to the plasma membrane. These studies, however, have been inconclusive, but it is clear that PLD is involved in significant crosstalk with other regulatory factors important in amyloidogenesis and the progression of AD.[8]

While the biochemical signaling pathways implicating PLD1 and PLD2 in AD are not fully understood, it is clear that the different PLD isoforms have distinct roles during the pathogenesis of AD. Recent *in vitro* and *in vivo* studies have validated PLD2's impact on AD progression.[22] The study suggests that PLD2 is involved in signal transduction downstream of Aβ. For *in vitro* analysis of PLD2, Oliveira and coworkers created a PLD2—green fluorescent protein (GFP) fusion protein, which allowed for PLD2 cell localization to be monitored by fluorescence. Since PLD2 is typically localized at the plasma membrane, cells treated with vehicle retained basal activity and their plasma membrane cellular localization

was confirmed by fluorescence microscopy. Conversely, when cells were stimulated with Aβ oligomers, PLD2 was observed throughout the cell, showing a regulatory role of Aβ on PLD2 activity. This suggests that PLD2 is active in the signal transduction pathway resulting in AD pathogenesis. Furthermore, they ensured that this effect was solely related to PLD2 by running the same study with a PLD1—GFP fusion protein resulting in no difference in cellular localization between vehicle and Aβ oligomer stimulation.[22]

Synaptic dysfunction is an additional symptom of AD, and neurons with significant Aβ load show reduced synaptic plasticity compared to healthy neurons when comparing long term potentiation (LTP). To test PLD2's effect on LTP, hippocampal slices were harvested from PLD2^{+/+} and PLD2^{-/-} mice. The study showed no difference in LTP comparing slices from wild type mice and PLD2 knockout mice treated with vehicle, demonstrating that a lack of PLD2 alone should have no impact on LTP. Wild type slices, when treated with Aβ oligomers, resulted in LTP impairment, which is consistent with the synaptotoxic impact of Aβ oligomers.[23–25] Conversely, LTP in PLD2 knockout slices was unaffected by Aβ oligomer treatment, giving LTP statistically identical to the samples that were treated with vehicle. This evidence validates PLD2's impact in Aβ mediated synaptotoxicity, implying a role for PLD2 downstream in the signal transduction pathway from Aβ.[22]

To further validate PLD2's role in AD progression, Oliveira and coworkers performed *in vivo* studies with an AD mouse model. PLD2^{+/+}, PLD2^{+/-}, and PLD2^{-/-} Tg2576 transgenic mice, which contain the Swedish APP (SwAPP) mutation, were tested alongside PLD2^{+/+}, PLD2^{+/-}, and PLD2^{-/-} wild type mice to look for impairments in memory. They utilized a contextual fear conditioning paradigm where mice are alerted to an aversive stimulus by an innocuous tone. Mice with unimpaired memory then react to the tone with a

126

freezing behavior that can be quantified. While all mice from the six separate genotypes showed no significant difference in the baseline testing, only one genotype (SwAPP, PLD2$^{+/+}$) displayed little contextual fear response when tested 24 hours later, showing the Alzheimer's mouse model with a full complement of *Pld2* to lack the contextual learning ability. Conversely, the AD mouse model, when lacking *Pld2*, exhibited contextual learning statistically identical to wild type mice, suggesting PLD2 is necessary for Aβ signal transduction leading to learning and memory deficits.[22]

These researchers performed one additional memory test with the six genotypes of mice to again investigate learning and memory as they relate to PLD2 and AD.[22] They used the radial arm water maze (RAWM) paradigm, which forces the mice to find a hidden platform while annotating mistakes by the mice to test spatial working memory. Again, SwAPP/PLD2$^{+/+}$ mice performed statistically worse than all other mouse genotypes, and the five other genotypes were statistically non-distinguishable (**Figure 2.1.2.4**). It must be noted, once more, that the AD mouse model when lacking copies of *Pld2* performed equally well compared to wild type mice, which indicates PLD2 must have a joint role with Aβ in AD progression.[8,22]

Subsection B—PLD signaling and cancer

While the myriad cancer signaling processes are quite complex, PLD overexpression and increased enzymatic activity have been observed in a large number of cancer types.[16,26] On a molecular signaling level, PLD has been implicated in a number of oncogenic pathways that promote cell growth, proliferation, and invasiveness, and these pathways involve the epidermal growth factor receptor,[27] matrix metalloproteinase expression,[28,29] p53,[30,31] mTOR,[32] and Ras.[33] Essentially, PLD has been implicated in oncogenic signaling through its

known protein—protein interactions and additionally through PAs ligand—protein interactions. The signaling networks involving PLD's contribution to tumorigenesis, invasion, and metastasis are expansive, but a recent provocative *in vivo* study involving Ras demonstrates PLD1 and PA's role in cancer.[34]

To give a brief overview of Ras, it is the given name of a superfamily of proteins that are present in many cell types. Since Ras is a small GTPase enzyme, it canonically facilitates signal transduction pathways started by G-proteins. It switches between binding GDP in a non-productive state, and binding GTP which promotes the active form of Ras.[35] While activated, Ras stimulates its downstream partners resulting in mitogenic signaling, provoking cell survival mechanisms. In healthy cells, active GTP-Ras quickly hydrolyzes to inactive GDP-Ras, ending the signal transduction pathways coding for proliferation and survival. Frequently, mutations in the *ras* gene cause the Ras protein to permanently adopt the "switched on" conformation without needing to bind GTP. This mutation can result in unchecked cell division leading to tumorigenesis and cancer.[35] The *ras* oncogene is the most prevalent cause of all known cancers, and the mutations that permanently activate Ras cause 20-25% of all human tumors, and this mutation is much more prevalent in other cancer subtypes (90% in pancreatic cancer).[36] While Ras itself has proven to be a difficult drug target, other members of the signal transduction pathway could be targeted to potentially generate the same chemotherapeutic effect. For instance, Raf-1 kinase is trafficked to the plasma membrane during the Ras induced signal cascade, the ability of Raf-1 kinase to translocate to the membrane is dependent on a direct interaction between the kinase and PA.[5,37] Therefore, one can reason that chemical inhibition of Raf-1 kinase or PLD may prevent that translocation event, ending the oncogenic signaling cascade.

This theory was tested *in vivo* by Exton and coworkers in a nude mice xenograft model.[34] In their study, they transformed Rat-2 fibroblasts with a catalytically inactive variant of PLD1 that was constitutively expressed (PLD1⁻). This gave them a line of Rat-2 fibroblasts that they could compare in studies against cells that were wild type (PLD1⁺). In essence, PLD1⁺ cells would have a normal complement of the enzymes generating normal volumes of PA, while the modified PLD1⁻ strain was inactive and would therefore have less PA. They transfected those cell lines with a mutant form of Ras ($HRas^{V12}$), which was mutated to be permanently active leading to tumor formation. These cells were injected into nude mice to observe potential tumorigenesis. When cells with catalytically active PLD1 and mutant HRas were injected, a large tumor formed after 10 days. Essentially, the HRas oncogenic signaling cascade was uninterrupted in these cells, which led to proliferation and tumor formation. When cells with catalytically inactive PLD1 and mutant HRas were injected, no tumor formed in mice during the same period of time. This illustrates that either PLD1 or PA are involved in the HRas induced oncogenic signaling which led to tumorigenesis, but the two variables are indistinguishable with these experiments alone. An additional experiment injected cells with catalytically inactive PLD1 and mutant HRas into cells, which is identical to the former example that produced no tumor. However, PA was injected into the mouse with the cells, and that mixture restored tumorigenesis.[34] These data demonstrate that PA formed by PLD1 was necessary for the HRas oncogenic signaling pathway.

While this striking example illustrates the importance of PLD in cellular signaling and cancer, the role of the two PLD isoforms is still under investigation as a therapeutic target. Since PLD activity and expression levels are heightened in clinical tissue samples of

tumors, that data further validates the need for additional research investigating the role of PLD activity in cancer progression.

2.1.3 Assaying for PLD Activity

The most direct measurement of PLD activity would be to monitor the direct conversion of PC to PA by PLD. Since (i) there are multiple pathways for biosynthesis of PA and (ii) PA is a metabolic intermediate that can be readily converted to DAG or LPA, however, a direct measurement of the amount of PA cannot correlate to PLD activity (**Figure 2.1.3.1**).
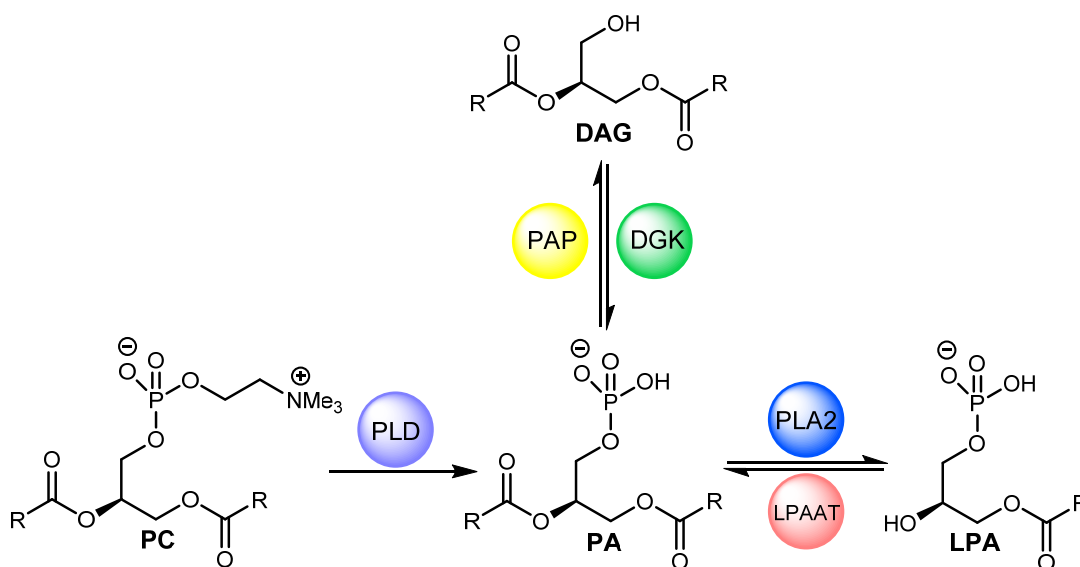
Figure 2.1.3.1 PA is a metabolic intermediate to DAG and LPA

If PLD catalyzed a reaction forming a product that was stable *in vivo*, that product could be quantified and directly related to PLD activity. Fortunately, PLD not only catalyzes the hydrolysis of PC to PA. Instead, it also catalyzes the transphosphatidylation reaction of PC with primary alcohols to generate phosphatidyl alcohols, which are stable molecular entities that can be quantified to determine PLD activity (**Figure 2.1.3.2**).
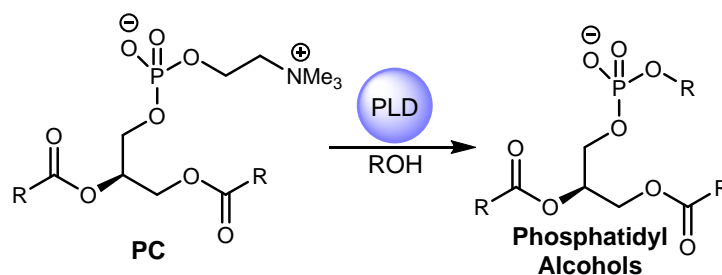
Figure 2.1.3.2 PLD catalyzes transphosphatidylation

Additionally, most PLD enzymes in the superfamily catalyze the transphosphatidylation reaction 1,000-fold faster than the hydrolysis reaction, which allows the reaction to occur at very low, non-toxic concentrations of primary alcohol.[38] This cellular PLD assay system, therefore, allows *n*-butanol to be added to the cellular mixture to participate in the transphosphatidylation reaction, and the product—phosphatidylbutanol (PtdBuOH)—can be detected by quantitative mass spectrometry. Since various alkyl side chains of PC exist, that gives way to a variety of PtdBuOH species that require measurement. Additionally, many of these PtdBuOH species are isobaric with different PAs; therefore, an additional experiment must be performed to accurately quantify PtdBuOH and correlate it to PLD activity. To shift the mass of the PtdBuOH species to an open region of the mass spectrum, deuterated *n*-butanol is added to a different cellular mixture making PtdBuOH-d_9, which results in a 9 dalton shift in mass to a non-isobaric region of the mass spectrum.

A typical experiment to quantify PLD activity consists of four experiments and is depicted below (**Figure 2.1.3.3**).[39] Experiment 1 (spectra A) contains no primary alcohol, so this is the control experiment resulting in no PtdBuOH. Experiment 2 (spectra B) corresponds to a sample where *tert*-butanol was added. Since PLD only catalyzes the transphosphatidylation reaction with primary alcohols, this experiment serves to prove that an alcohol is not causing a side reaction altering the mass spectral data. The spectrum for

experiment 2, therefore, should look very similar to experiment 1. In experiment 3 (spectra C), *n*-butanol was added to the reaction resulting in formation of PtdBuOH. The new peaks in the mass spectrum, therefore, should correspond to PtdBuOH species that were not present in experiments 1 or 2. The PtdBuOHs will overlap with some PA species, however, so this spectrum alone cannot be used to quantify total PtdBuOH formed. Experiment 4 (spectra D) will contain deuterated *n*-butanol, which will result in formation of PtdBuOH-d_9. All PtdBuOH-d_9 species will be shifted 9 Daltons in the mass spectrum, and can be measured against PtdBuOH-d_9 standards to quantify the amount of PtdBuOH-d_9, which can then be directly related to quantify PLD activity (**Figure 2.1.3.3**).[39]
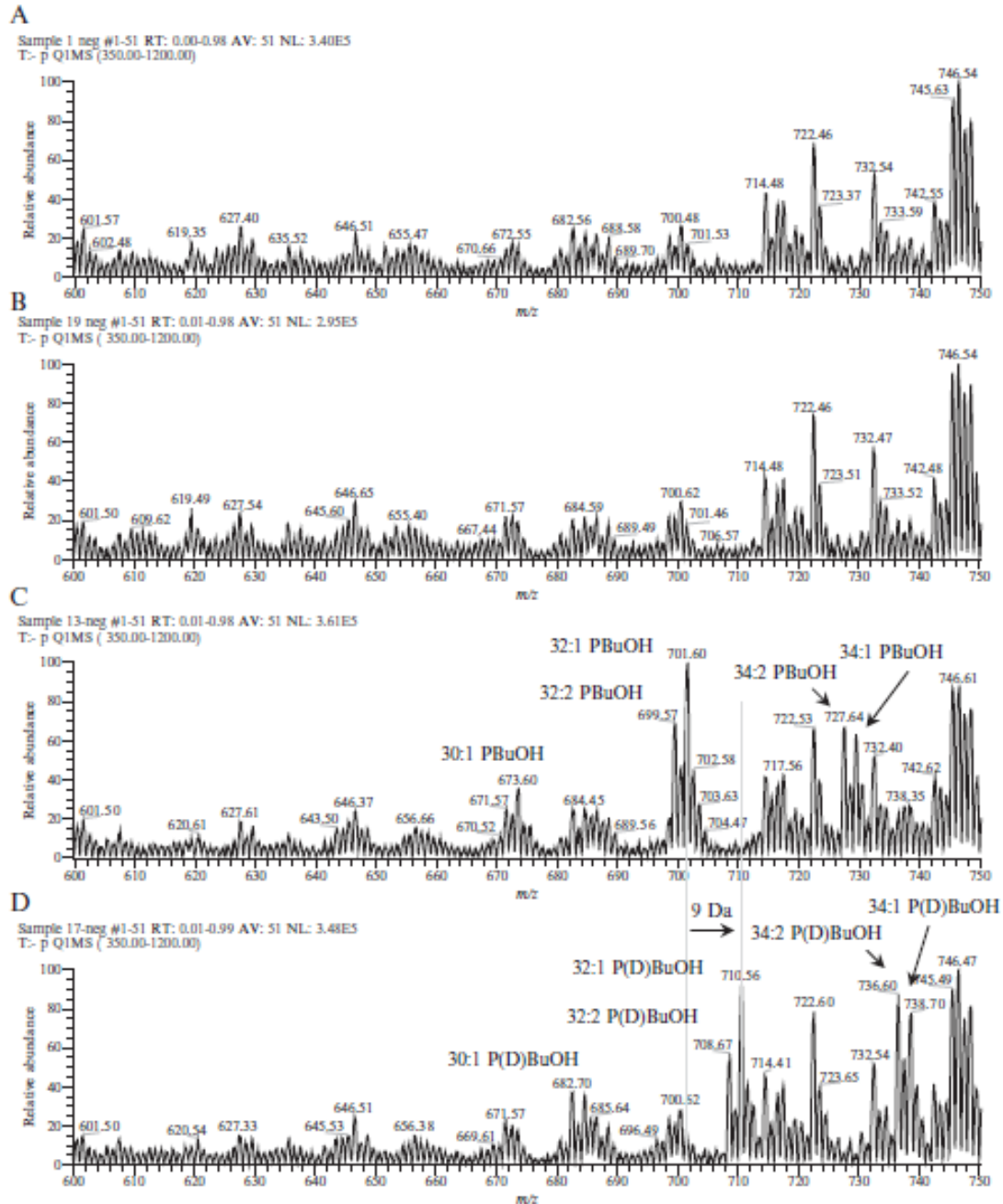
Figure 2.1.3.3 Measuring PLD activity by quantifying PtdBuOH. Figure adapted from ref 39.

2.1.4 Known Chemical Modulators of PLD

While genetic knockout studies have provided strong proof of concept that PLD inhibition is a therapeutically relevant strategy, these methods do not give temporal control of

PLD activity, nor are genetic methods therapeutically viable options for treating disease.[3,17] Small molecule chemical inhibitors, on the other hand, provide the ability to modulate a biological system in a time-based manner and are readily applied to biological systems compared to the tedious process of generating genetically modified organisms. Prior to recent discoveries of influential PLD inhibitors, n-butanol was often used in studies to "inhibit" PLD (**Figure 2.1.4.1**). It is known, however, that n-butanol is not a PLD inhibitor; instead, n-butanol is a competitive substrate taking part in the transphosphatidylation reaction forming PtdBuOH. While treating a system with n-butanol will serve to prevent formation of PA, PtdBuOH serves some of the same structural roles as PA, and directly inhibiting PLD catalysis is advantageous compared to this n-butanol paradigm. Prior to 2007, however, small molecule inhibitors of PLD were mainly indirect, very large concentrations were required to affect PLD, and the many of the known inhibitors lacked drug-like properties. These inhibitors include diethylstilbestrol, resveratrol, honokiol, presqualene diphosphate, raloxifene, tamoxifen, and SCH420789 (**Figure 2.1.4.1**).[40–46]
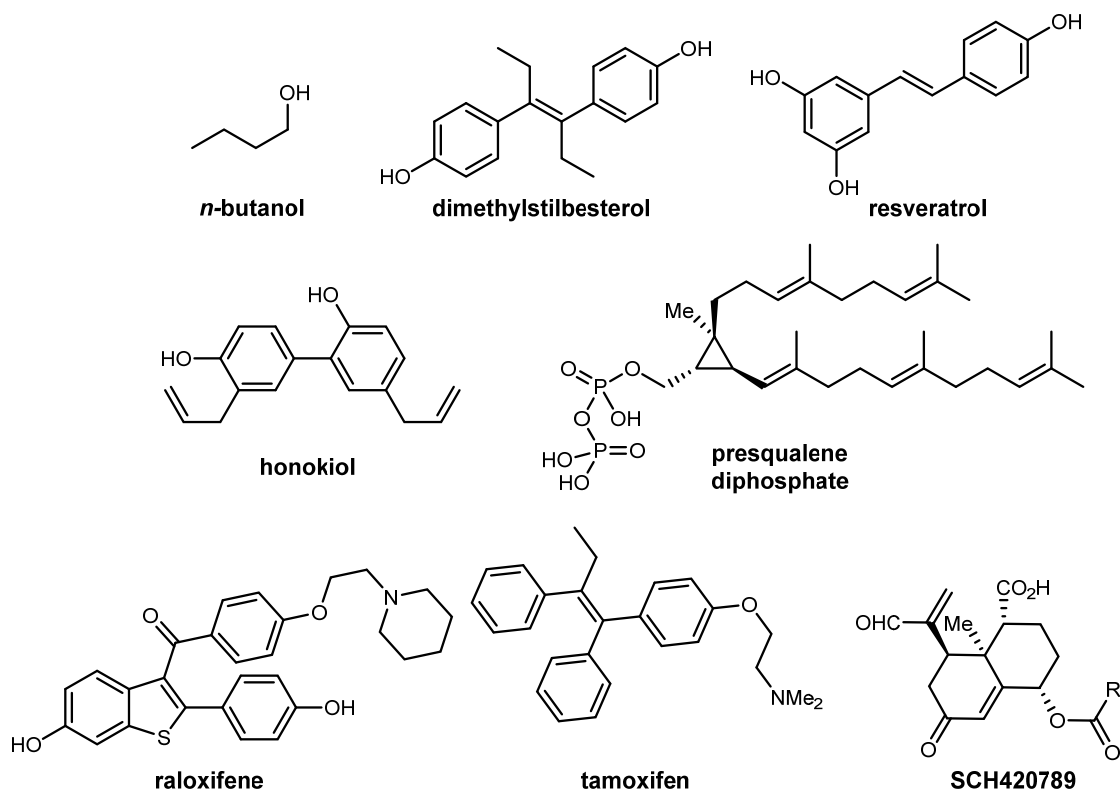
Figure 2.1.4.1 Structures of previously reported PLD inhibitors

One common characteristic shared by all of these inhibitors is their inability to inhibit PLD isoforms selectively. Since PLD1 and PLD2 have differential cell localizations, regulatory mechanisms, and roles in diseases, selective inhibition of a single PLD isoform would allow for modulation of the specific isoenzyme involved in each disease state, which would likely result in a more direct treatment of a disease with fewer side effects.

In 2007, scientists from Novartis published halopemide **2.1**, a compound previously dosed in clinical trials for neuroscience indications, to be a potent PLD inhibitor.[47] Through standard medicinal chemistry, the group reported an additional 14 structures that had enhanced inhibitory activity. FIPI **2.2**, their best compound with a reported PLD2 IC$_{50}$ of 200 nM, was a significant improvement compared to known PLD inhibitors, and **2.2** had good physiochemical properties in rats. These compounds represented the first potent PLD

inhibitors that could be used as *in vivo* tool compounds, but minimal SAR was reported in the initial letter (**Figure 2.1.4.2**).
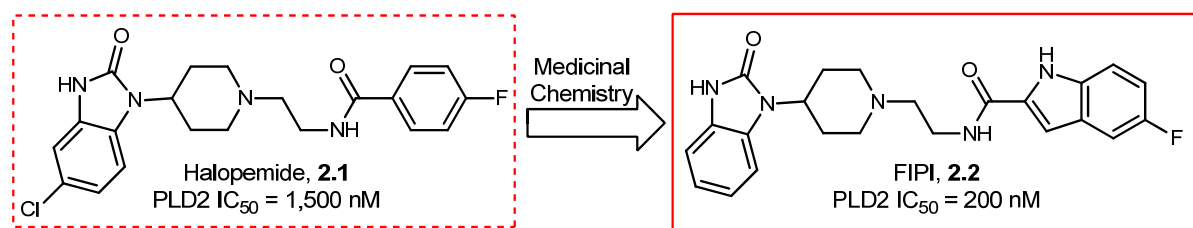
Figure 2.1.4.2 First potent PLD inhibitors. Figure adapted from ref 47.

The brief letter that reported the activity of these benzimidazolone scaffolds did not describe the assay methods, but they reported the compounds as PLD2 selective inhibitors. This caught the attention of the Brown and Lindsley groups as they knew potent and selective small molecule ligands would be invaluable tools to further probe PLD function. They were additionally encouraged by this new finding because halopemide was known to be involved in five separate clinical trials with over 100 patients in the 1970s and 1980s. This was encouraging because data from those trials showed halopemide reaching plasma concentrations between 100-360 ng/mL in these patients, and no adverse side effects or toxicities were noted.[48] Since PLD was likely inhibited at these concentrations of halopemide, therefore, it stands to reason that PLD inhibition is a therapeutically viable and safe mechanism. With these data noted, the Brown and Lindsley groups launched a medicinal chemistry campaign to probe the structure activity relationships (SAR) of this scaffold, and that effort—using the cell based assay described above—led them to reclassify halopemide and FIPI as PLD1 and PLD2 dual inhibitors that are slightly selective for PLD1 (halopemide PLD1 IC_{50} = 21 nM, PLD2 IC_{50} = 300 nM; FIPI PLD1 IC_{50} = 1 nM, PLD2 IC_{50} = 44 nM).[17]

In the medicinal chemistry effort to flesh out the SAR of the benzimidazolone scaffold, the Brown and Lindsley labs prepared a 3 X 3 X 30 matrix library of close to 270

analogs. To do this, they modified the headgroup with the *des*-chloro benzimidazolone and a triazaspirone, which is isosteric to the benzimidazole. They tested diversity in the linker region by adding groups containing chiral methyl substituents or a spiro cyclopentyl. Lastly, they used a large variety of acid chlorides to add in the aryl amide region to generate maximal diversity (**Figure 2.1.4.3**).
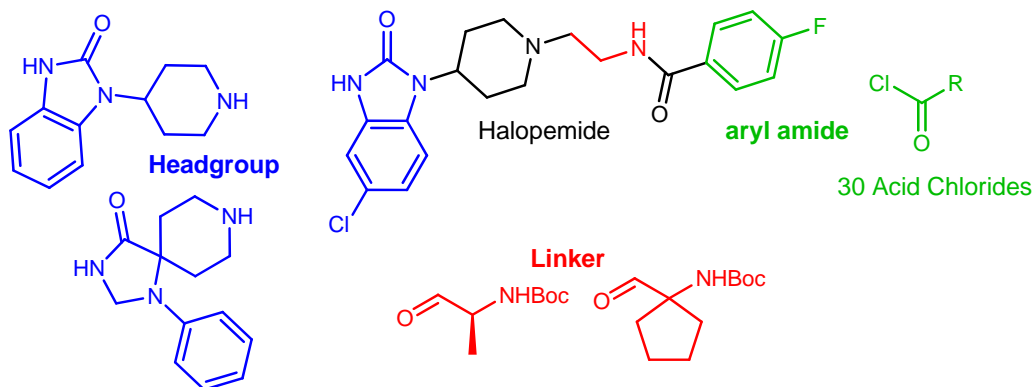
Figure 2.1.4.3 Library design to generate maximal SAR. Figure adapted from ref 17.

By preparing these analogs, they hoped to generate (i) more potent PLD inhibitors, (ii) selective PLD1 inhibitors, and (iii) selective PLD2 inhibitors. This large library was intended to sample vast quantities of chemical space by modifying the steric and electronic components of each region.

This process produced potent dual inhibitors, highly selective PLD1 inhibitors, and slightly selective PLD2 inhibitors.[17] Specifically, benzimidazolone **2.3** is a slightly PLD1 preferring dual inhibitor (PLD1 IC_{50} = 21 nM; PLD2 IC_{50} = 380 nM), chloro-benzimidazolone **2.4** is a selective PLD1 inhibitor (PLD1 IC_{50} = 11 nM; PLD2 IC_{50} = 1800 nM), and triazaspirone **2.5** is a marginally PLD2 preferring inhibitor (PLD1 IC_{50} = 1000 nM; PLD2 IC_{50} = 110 nM) (**Figure 2.1.4.4**).
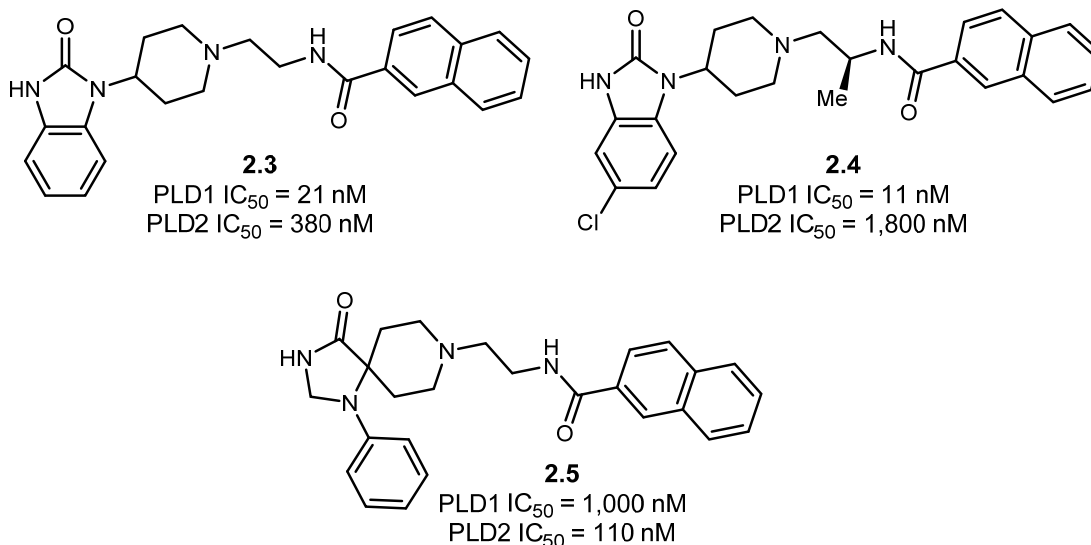
Figure 2.1.4.4 Notable PLD inhibitors from broad library

The SAR from those compound libraries was informative when developing new molecules. For instance, the methyl group on the linker region always conferred enhanced PLD1 activity compared to the *des*-methyl compound. Additionally, the triazaspirone headgroup consistently provided compounds with a moderate PLD2 preference.[17]

In order to increase PLD1 selectivity, additional work was done with the benzimidazolone scaffold. By maintaining the benzimidazolone headgroup, alternating halogens in place of the chlorine of **2.4**, changing between the ethyl linker and the chiral methyl linker, and modifying those scaffolds with the most potent aryl amides, compounds with unprecedented PLD1 selectivity and potency were generated (**Figure 2.1.4.5**). **2.6** was discovered during those efforts and is the most selective PLD1 inhibitor known.[49]
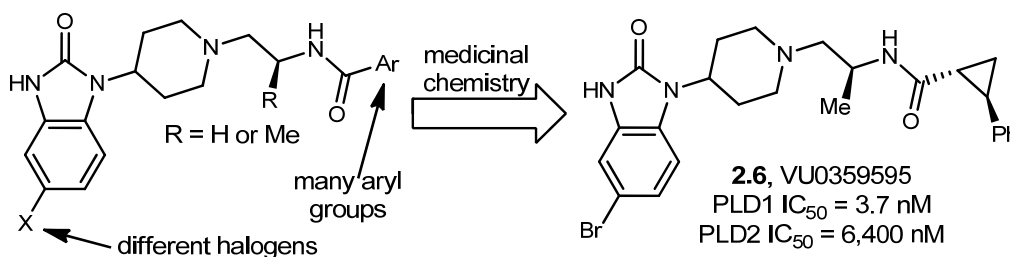
Figure 2.1.4.5 1,700-fold selective, potent PLD1 inhbitor. Figure adapted from ref 49.

2.6 combines aspects of the SAR greatly biasing compounds toward PLD1 selectivity including (i) the bromo-benzimidazolone, (ii) the (*S*)-methyl group in the linker region, and (iii) the *trans*-cyclopropyl phenyl amide. Since a highly selective (1,700-fold) and potent (PLD1 IC_{50} = 3.7 nM) PLD1 inhibitor was now available, work in the Brown and Lindsley labs now turned to development of a selective PLD2 inhibitor.

Efforts focused on the triazaspirone scaffold since previous work resulted in 10-fold selective PLD2 inhibitor **2.5**. Initially, they focused on varying the aryl amide while keeping the aniline moiety constant (**Figure 2.1.4.6**). This resulted in **2.7**, which was only slightly more PLD2 selective than **2.5** from the initial medicinal chemistry efforts.[17,50] However, **2.7** only had a modest improvement in selectivity (21-fold compared to 10-fold), and the quinolone ring favorably increased compound solubility compared to **2.5**. Instead of aryl amide modifications, Brown, Lindsley, and coworkers added halogens to the aniline ring in a similar fashion to the work that generated 1,700-fold PLD1 selective compound **2.6**. This effort resulted in 3-fluoroaniline triazaspirone VU0364739 **2.8**, which was 75-fold selective for PLD2 with a PLD2 IC_{50} of 20 nM. This quite selective PLD2 inhibitor, however, is still relatively potent at PLD1 (IC_{50} = 1,500 nM). Nevertheless, it was a large improvement compared to previous compounds since it increased both potency and selectivity (**Figure 2.1.4.6**).[51]
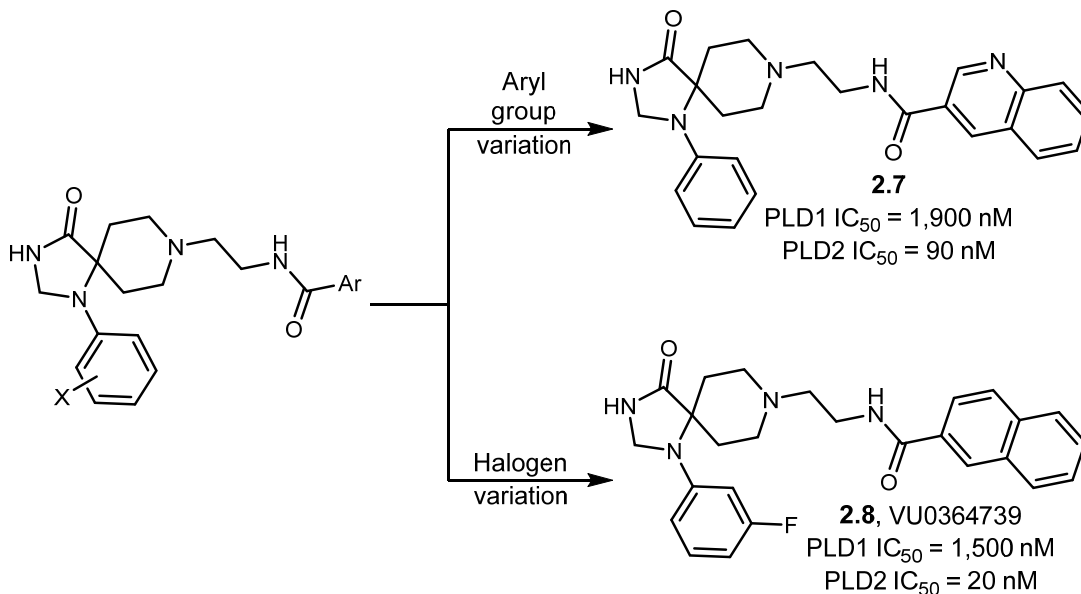
Figure 2.1.4.6 Chemical modifications resulting in selective PLD2 inhibitors

The newly developed inhibitors were invaluable for those who studied PLD. Previously, chemical inhibition of a single isoenzyme was impossible, but these new compounds made cellular assays examining PLD's role in various phenomena easy. In fact, in many of the communications regarding these newly developed inhibitors, the compounds were shown to be active against many cancer cell types.[17,51] While the new inhibitors represent a large step forward for those studying PLD, substantial improvements are still possible regarding PLD1 selective, PLD2 selective, and dual PLD inhibitors.

2.2 Discovery of phospholipase D inhibitors ML298 and ML299

2.2.1 Envisioned improvements to known PLD inhibitors

Considering the attributes of the known PLD inhibitors, we attempted to discover novel tool compounds with (i) enhanced PLD2 selectivity, (ii) DMPK profiles to complement the existing inhibitors, and (iii) reduced ancillary pharmacology compared to the known molecules. Examining the most useful tool compounds from previous efforts, our lab had discovered the 1,700-fold selective PLD1 inhibitor **2.6**, a potent dual inhibitor **2.3**, and

75-fold selective PLD2 inhibitor **2.8** (**Figure 2.2.1.1**). Looking at additional properties of PLD1 selective compound **2.6**, it was not CNS penetrant and had some off target effects, exerting binding affinities for 7 targets in a screen of 68 common molecular targets that include GPCRs, ion channels, and transporters. To improve our ability to target PLD1 selectively, compounds are needed that maintain this level of selectivity while addressing CNS penetrance and limit the off target liabilities of **2.6**. For dual inhibition of PLD1 and PLD2, **2.3** is potent, peripherally restricted, and has substantial off target binding. Lastly, for selective PLD2 inhibition, **2.8** is potent, quite selective, and CNS penetrant. It, like the other two compounds, also has off target liabilities affecting 11 of the common molecular targets (**Figure 2.2.1.1**).
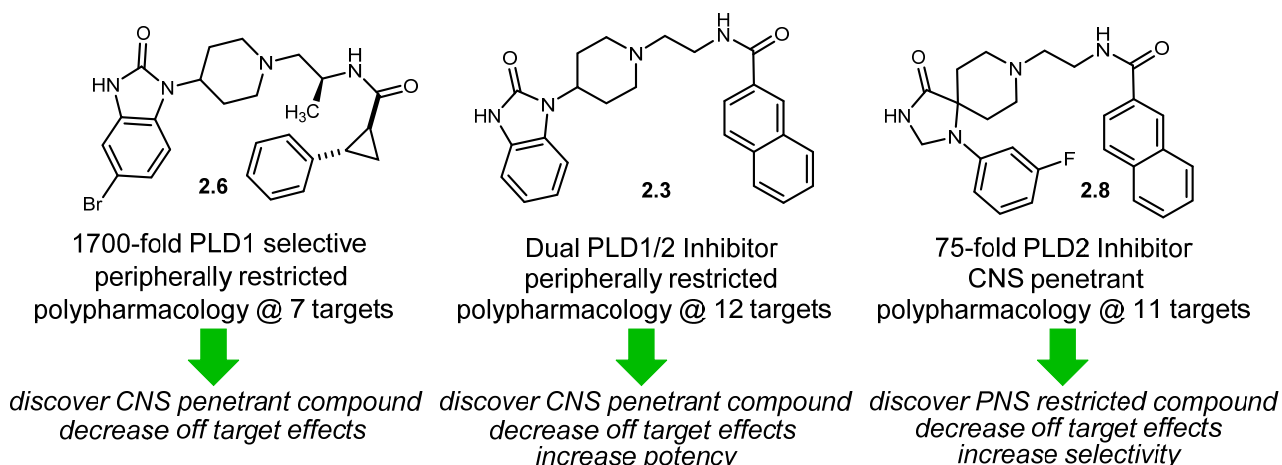
Figure 2.2.1.1 Hopeful improvements to historically useful PLD tool compounds

While PLD1 selective **2.6** can still be improved upon, there are more substantial improvements necessary when PLD2 selective compound **2.8** is considered. While this molecular probe is potent (PLD2 IC_{50} = 20 nM) and 75-fold selective, many of the assays this compound has been used in require concentrations above 1,500 nM (the PLD1 IC_{50}) to achieve a statistically significant effect. At those high concentrations, PLD1 may also be inhibited, and if this is the case the assay result cannot be linked to PLD2 alone based on

chemical inhibition. For instance, breast cancer cell proliferation was analyzed compared to vehicle, and when 75-fold selective PLD2 inhibitor **2.8** was used in the assay, a significant effect was seen only at 10 μM.[51] Since 10 μM is almost 7-times the PLD1 IC_{50} of **2.8**, it is unknown whether that significant decrease in cell growth is exclusively related to PLD2 or PLD1. Additionally, when an assay examining Caspase activity was performed to look at PLD2's contribution to apoptosis, 10 μM concentrations of **2.8** were again necessary to elicit a significant effect (**Figure 2.2.1.2**).[51]
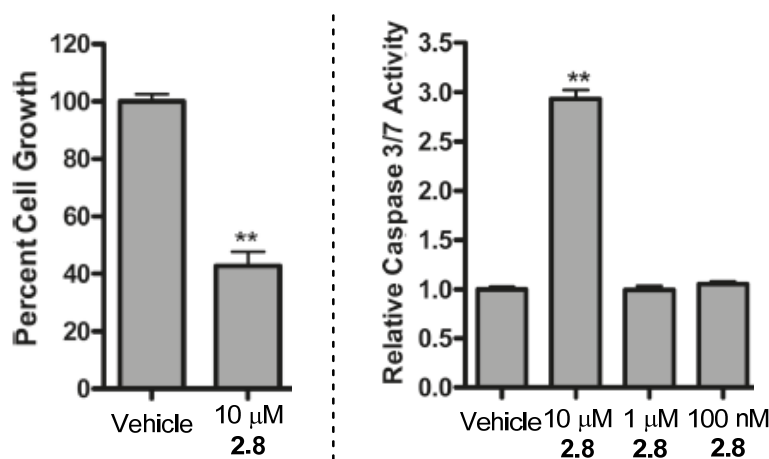
Figure 2.2.1.2 Assays where **2.8**'s effect could not be considered entirely PLD2 related. Figure adapted from ref 51.

2.2.2 Synthesis of 3-fluoro aniline triazaspirone scaffold

With the limitations of **2.8** noted, it was clear that selective PLD2 inhibitors that elicited significant cellular effects at concentrations less than the PLD1 IC_{50} would greatly impact the field. Work began, therefore, using the triazaspirone scaffold as a starting point, since its chemical properties had always promoted modest PLD2 selectivity. Additionally, only four compounds had been synthesized and tested with the 3-fluoroaniline ring, and since that halogenated aniline conferred PLD2 selectivity, we thought it prudent to maintain that core scaffold and alternate the aryl amide to generate maximal molecular diversity. To that end, synthesis of the triazaspirone core began with Strecker reaction of *N*-benzyl

piperidinone **2.9** and 3-fluoroaniline to afford crude nitrile **2.10**, which was hydrolyzed to the

carboxylic amide **2.11** with concentrated sulfuric acid in a 68-74% two-step yield. Forcing

microwave assisted conditions were required to close the spirocyclic five-membered ring

using trimethyl orthoformate followed by sodium borohydride reduction to provide benzyl

triazaspirone **2.12** in 12-20% yield. Hydrogenolysis allowed for benzyl cleavage furnishing

free piperidine **2.13** in 89-96% yield. To install the ethyl linker, reductive amination with

tert-butyl 2-oxoethylcarbamate was performed providing Boc-amine **2.14**, and the Boc-group

was successively cleaved with acid to generate free amine **2.15** in 58% yield over two-steps

(**Scheme 2.2.2.1**).
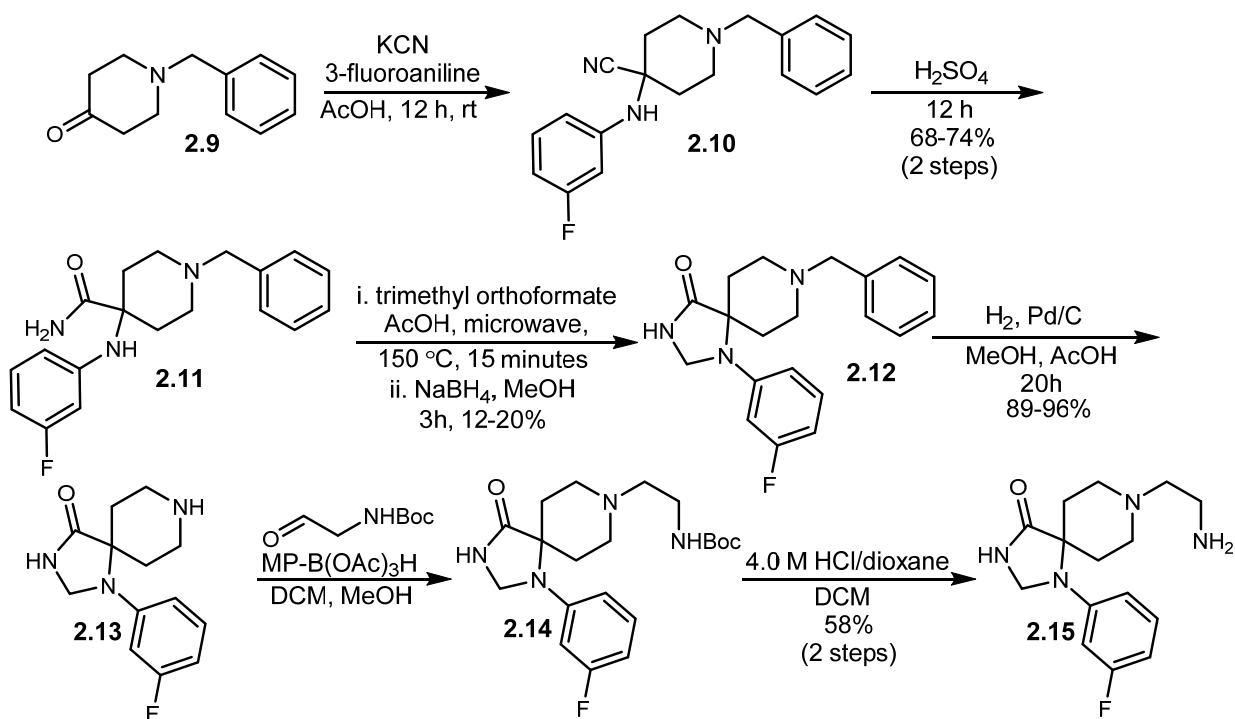
Scheme 2.2.2.1 Synthesis of 3-fluoro triazaspirone scaffold

This synthetic route allowed for the preparation of monosubstituted amine **2.15** on a gram

scale, which provided ample material to be used in acylations or amide couplings to generate

large numbers of amide analogs.[52]

2.2.3   Library synthesis with 3-fluoroaniline triazaspirone

Using monosubstituted amine **2.15** with various acid chlorides in DMF, acylation to amide triazaspirone resulted in various amide subtypes including alkyl amides, aryl amides, and methylene linked aryl amides. Generally, aryl amides were active inhibitors of PLD while the alkyl amides were inactive. **Table 2.2.3.1** highlights the compounds that were involved in this screen.

	R₁	R₂		R₁	R₂

The table displays chemical structures for compounds 2.16A through 2.16BB.

Compound	R₁	R₂
2.16A	3,4-dimethoxybenzyl	H
2.16B	benzyloxyethyl	H
2.16C	2,4-dichlorobenzyl	H
2.16D	4-butoxybenzyl	H
2.16E	cyclohexyl	H
2.16F	adamantyl	H
2.16G	3,4-difluorobenzyl	H
2.16H	3-fluorobenzyl	H
2.16I	2,6-difluorobenzyl	H
2.16J	3-chloropropyl	H
2.16K	tert-butyl	H
2.16L	thiophen-2-ylmethyl	H
2.16M	hexyl	H
2.16N	2-methylbenzyl	H
2.16O	phenylthiomethyl	H
2.16P	2,5-bis(trifluoromethyl)benzyl	H
2.16Q	3,5-dimethoxybenzyl	H
2.16R	3,4,5-trimethoxybenzyl	H
2.16S	diphenylmethyl	H
2.16T	4-(trifluoromethoxy)benzyl	H
2.16U	2-bromobenzyl	H
2.16V	isobenzofuran-1,3-dione	H
2.16W	biphenyl	H
2.16X	2-methylbenzyl	2-methylbenzoyl
2.16Y	3,4-difluorobenzyl	3,4-difluorobenzoyl
2.16Z	3-fluorobenzyl	3-fluorobenzoyl
2.16AA	2,6-difluorobenzyl	2,6-difluorobenzoyl
2.16BB	hexyl	hexanoyl

Table 2.2.3.1 Library altering the amide region of the PLD inhibitors.
Table adapted from ref 52.

The compounds were screened at a single-point concentration of 200 nM in cell lines

specifically characterized for PLD1 or PLD2 expression.[17] In this single-point assay, DMSO

145

is added as a negative control and a known PLD1/2 dual inhibitor is used as a positive control. Single-point at 200 nM is a low enough concentration to highlight any interesting compounds without directing us towards compounds that would ultimately be far less interesting than known inhibitors (**Figure 2.2.3.1**). From the single-point data, compounds **2.16G**, **2.16H**, and **2.16V** were considered interesting enough to warrant further characterization.
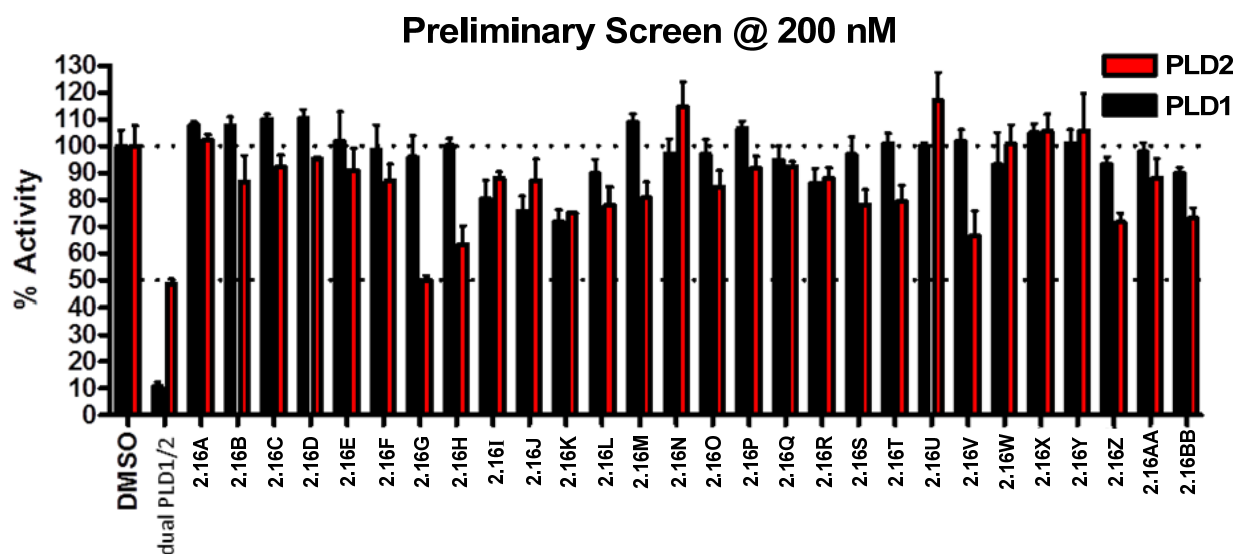
Figure 2.2.3.1 Preliminary screen of compounds for PLD inhbition. Figure adapted from Ref 52.

Therefore, concentration response curves (CRCs) were generated from these three compounds, and difluoro amide **2.16G** was found to be a potent and selective PLD2 inhibitor (PLD2 IC_{50} = 355 nM, >53-fold selective) with no measurable PLD1 inhibition at the upper end of the assay (PLD1 IC_{50} > 20,000 nM). This PLD2 inhibitor was later declared a molecular libraries probe center network (MLPCN) probe and assigned **ML298**. From this first scan, a 3-fluoro amide **2.16H** and aryl anhydride **2.16V** were also PLD2 selective compounds but were less selective than **ML298** (**Figure 2.2.3.2**).[52]
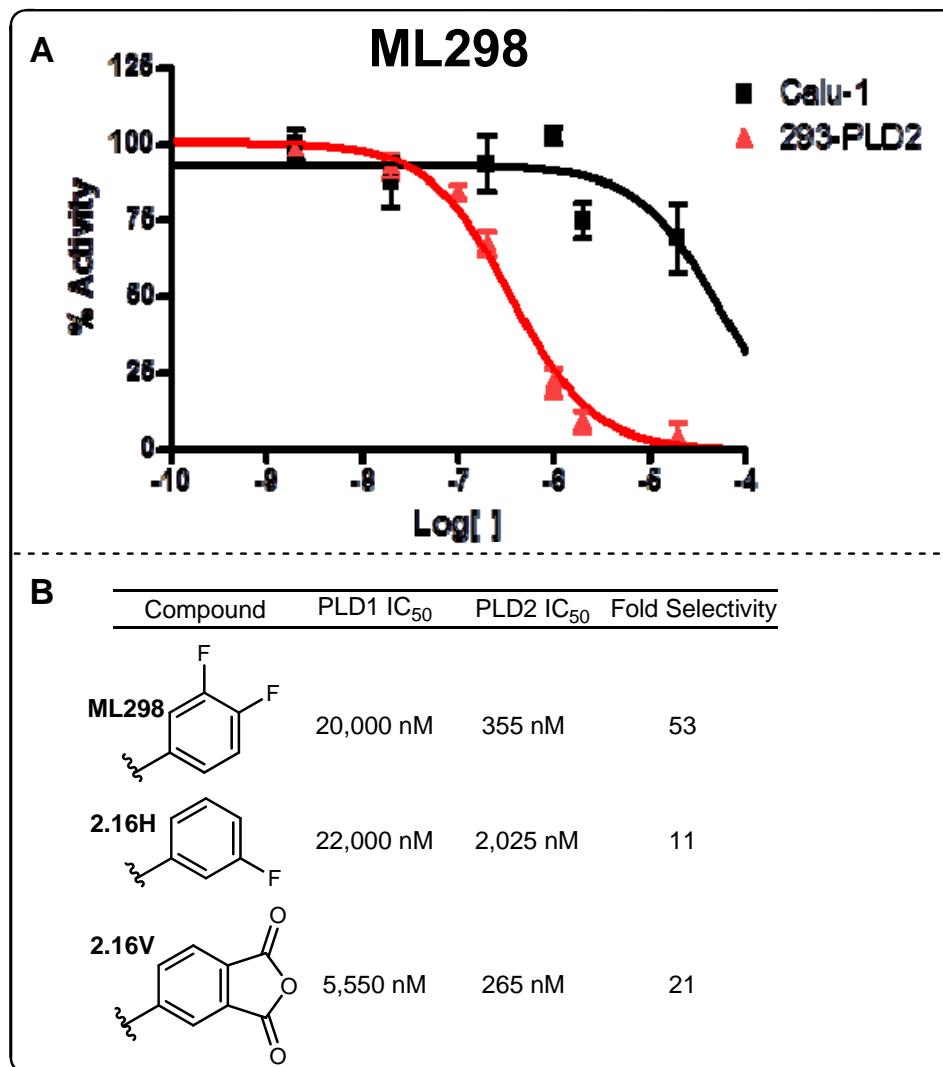
Figure 2.2.3.2 (a) CRC of **ML298**. (b) PLD selectivity data from first amide scan. Figure adapted from ref 52.

We were pleased to have found 3,4-difluoro compound **ML298** from this first amide scan, which remained potent at PLD2 while almost ablating PLD1 activity. While **ML298** was not as selective as naphthyl amide **2.8** (75-fold selectivity, PLD1 IC_{50} = 1.5 μM), we reasoned the decreased PLD1 potency could give rise to a more useful PLD2 selective compound since **ML298** does not impact PLD1 activity until concentrations over 20 μM. To test this hypothesis, **ML298** was taken into some cancer invasive migration assays while medicinal chemistry efforts continued on this scaffold.

Since we had success discovering a PLD2 selective probe from the triazaspirone scaffold, we reasoned that some additional modifications that were previously done to the benzimidazolone scaffold may facilitate similar bioactive properties on the triazaspirone scaffold. Specifically, when a methyl group was added to the linker region on the benzimidazolone, it consistently made the compounds more potent and/or selective for PLD1 compared to the *des*-methyl compound.[17,50] Therefore, we envisioned adding a methyl group to the linker region to potentially discover PLD1/2 dual inhibitors with properties to complement the known dual inhibitors based on the benzimidazolone scaffold.

Synthetically, we were able to add the chiral methyl group through the same chemistry that facilitated preparation of the *des*-methyl compound.[52] We then prepared a variety of aryl amides containing the methyl group, ensuring that compounds prepared with the chiral methyl group had a *des*-methyl congener with which the activity could be compared (**Figure 2.2.3.3**).
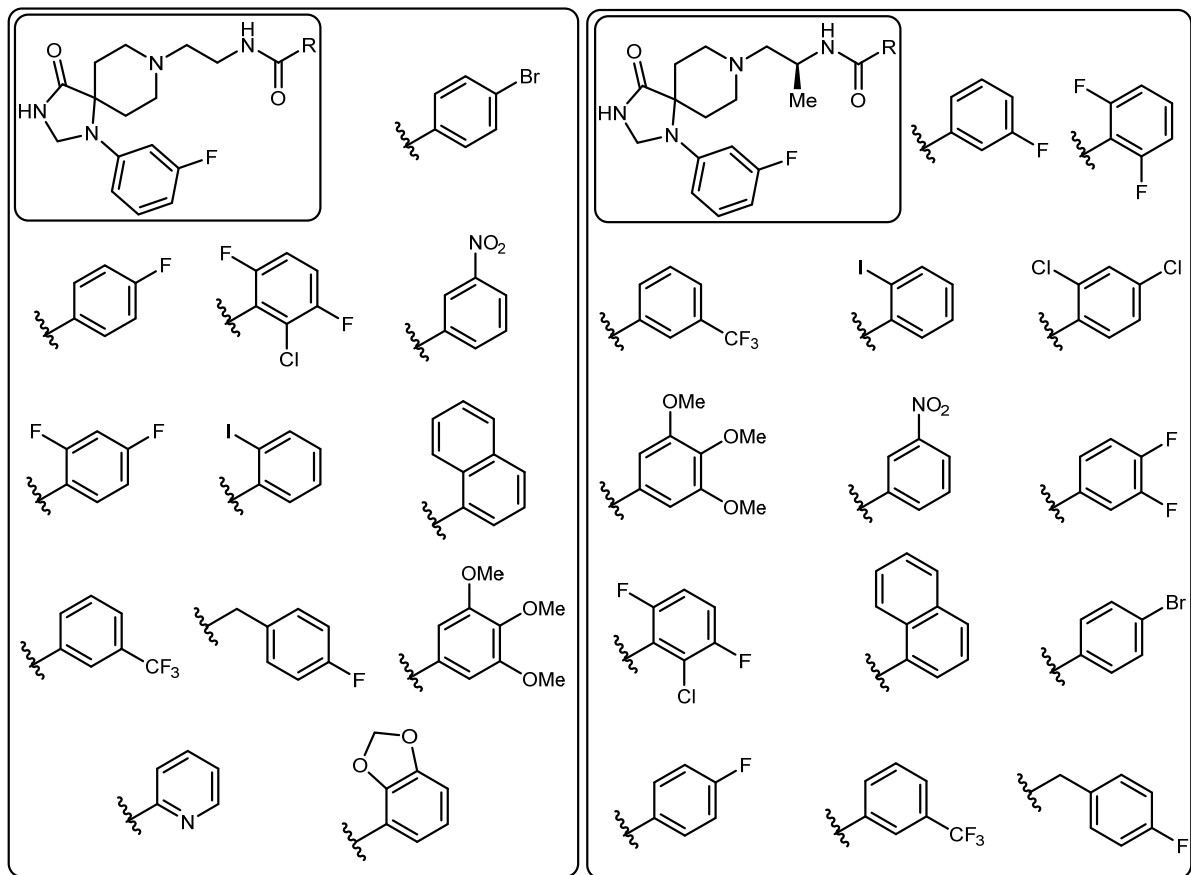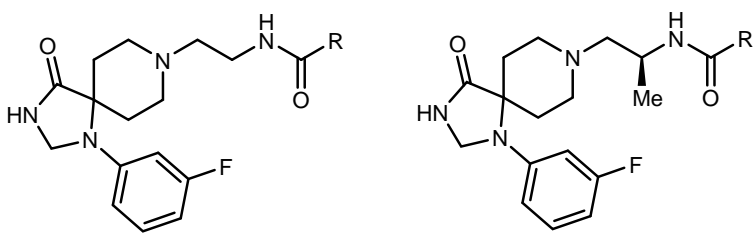
Figure 2.2.3.3 Compounds prepared in amide library 2

Single-point data was generated for this set of compounds, and the methyl group—as predicted—had a large effect on compound activity. The effect on PLD2 potency was modest, generally slightly increasing potency. The effect on PLD1 potency, however, was enormous (**Figure 2.2.3.4**).[52] When considering the 3,4-difluoro, 4-bromo, and 4-fluoro amides, addition of the (*S*)-methyl group increased PLD1 potency 233-fold, 257-fold, and 590-fold respectively. Addition of methyl substitution to biologically active scaffolds is commonly accompanied by enormous gains in potency, and the field has termed this phenomenon "the magic methyl effect."[53] Essentially, the methyl group on the benzimidazolone and triazaspirone is leading to conformational effects that are greatly increasing the binding affinity of the compounds. **2.17**, the 4-bromo compound containing

the (*S*)-methyl, was declared an MLPCN probe (**ML299**) since it is the most potent PLD1/2 dual inhibitor. It also has other benefits compared to the previous dual inhibitor, and those advantages will be discussed later.
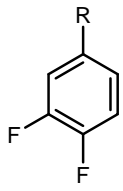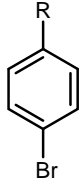
Figure 2.2.3.4 The magic methyl effect

This methyl effect prompted us to question whether the enhanced bioactivity would be enantiospecific in nature. Specifically, if it were an (*R*)-methyl instead of the opposite configuration, would the effect be as pronounced? This led us to synthesize an additional library of compounds with the opposite configuration at the methyl stereocenter, followed by single point screening and generation of CRCs.[52] Interestingly, enantiospecific activity existed that did not track between isoenzymes. To summarize the data, any configuration methyl group on the linker resulted in enhanced potency at PLD1. At PLD1, the (*R*)-methyl increased potency 14 to 20-fold whereas the (*S*)-methyl increased potency 232 to 590-fold. For PLD2, however, an (*R*)-methyl always resulted in decreased potency while an (*S*)-methyl

led to enhanced potency. Three congeners with this bioactivity pattern are illustrated in

Table 2.2.3.2.[52]
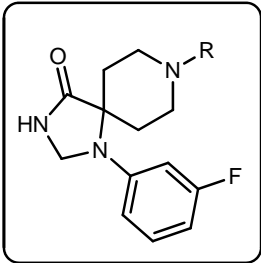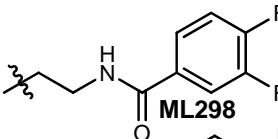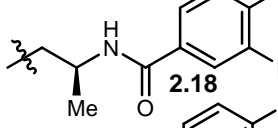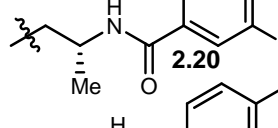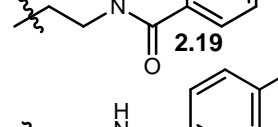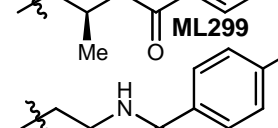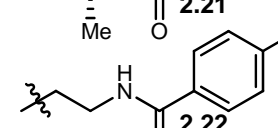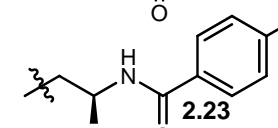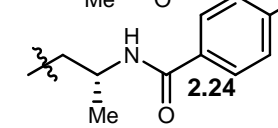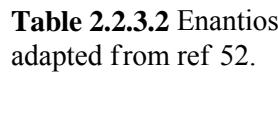
R	PLD1 IC$_{50}$	PLD2 IC$_{50}$
ML298	>20,000 nM	355 nM
2.18	86 nM	120 nM
2.20	1,400 nM	3,450 nM
2.19	1,540 nM	200 nM
ML299	6 nM	20 nM
2.21	75 nM	800 nM
2.22	11,800 nM	350 nM
2.23	20 nM	35 nM
2.24	760 nM	1,060 nM

Table 2.2.3.2 Enantiospecific bioactivity. Table
adapted from ref 52.

2.2.4   Anticancer activity of ML298 and ML299

With that SAR trend outlined, we next looked at the biological activity of these inhibitors. Previous work in the Brown and Lindsley labs had shown PLD1 and dual PLD1/2 inhibitors can block invasive migration of a triple negative breast cancer cell line (MDA-MB-231) and a U87-MG glioblastoma cell line, but siRNA studies showed PLD2 to likely be playing the dominant role in this phenomenon.[17] Therefore, the Transwell assay was performed to investigate invasive migration in the presence of the two new probe compounds (**Figure 2.2.4.1**). Dual inhibitor **ML299** showed a dose dependent decreasing invasion phenotype with statistical significance at 1 and 10 µM doses. This experiment does not distinguish which PLD isoform is responsible for the invasion phenotype, since the IC_{50} for both PLD1 and PLD2 inhibition is 6 and 20 nM respectively. When the assay was performed with PLD2 selective inhibitor **ML298**, however, a similar dose dependent decrease in invasion was observed gaining statistical significance at a 10 µM concentration.
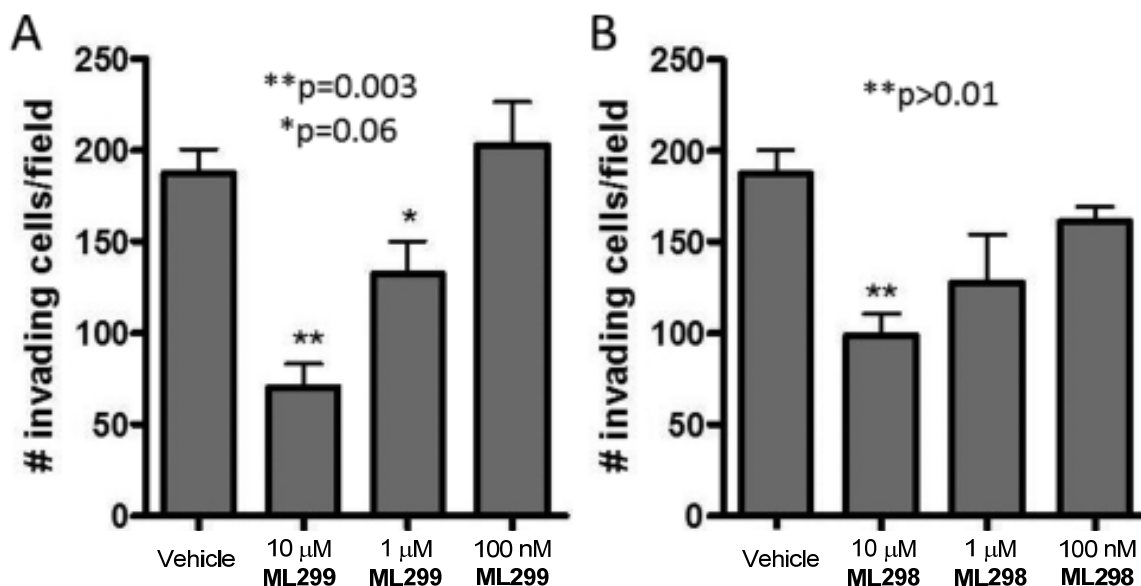
Figure 2.2.4.1 Invasive migration assay performed with (a) **ML299** and (b) **ML298.** Figure adapted from ref 52.

Since 10 µM is close to half of the necessary 20 µM concentration **ML298** needs to inhibit PLD1, this result suggests invasive migration to be a PLD2 controlled phenomenon.[52] Understandably, **ML299** shows a larger decrease in invasion compared to **ML298**, but that could be PLD2 related since **ML299**'s PLD2 IC_{50} is roughly 17-fold lower than **ML298**.

2.2.5 Physiochemical and DMPK properties

Now that our dual PLD1/2 inhibitor **ML299** and selective PLD2 inhibitor **ML298** were validated using cellular cancer models, we intended to compare them to previous inhibitors regarding their DMPK. One thing all PLD probes have in common is a high clearance rate, and these new compounds were not an exception to that trend.[49–51] While **ML299** and **ML298** possessed low but acceptable free fraction in rat and human plasma and acceptable CYP profiles, both compounds had rates of clearance in line with hepatic blood flow, rendering them impractical for oral administration.[52]   To circumvent first pass metabolism, therefore, the compounds were dosed intraperitoneally (IP). This route of administration provided excellent plasma levels for both **ML299** and **ML298** (**Figure 2.2.5.1**). Additionally, IP dosing gave the compounds access to the lung, and **ML299** seemed to deposit in that tissue. Moreover, this dosing paradigm allowed us to calculate CNS penetrance of our two probes, and while **ML299** was observed to enter the nervous system and reach concentrations 24 to 80-fold higher than the compound's IC_{50}'s, only trace amounts of **ML298** were detected in the CNS. Peripherally restricted probe **ML298**, therefore, is a good addition to the other PLD2 selective inhibitor **2.8**, since that compound has good CNS penetrance.
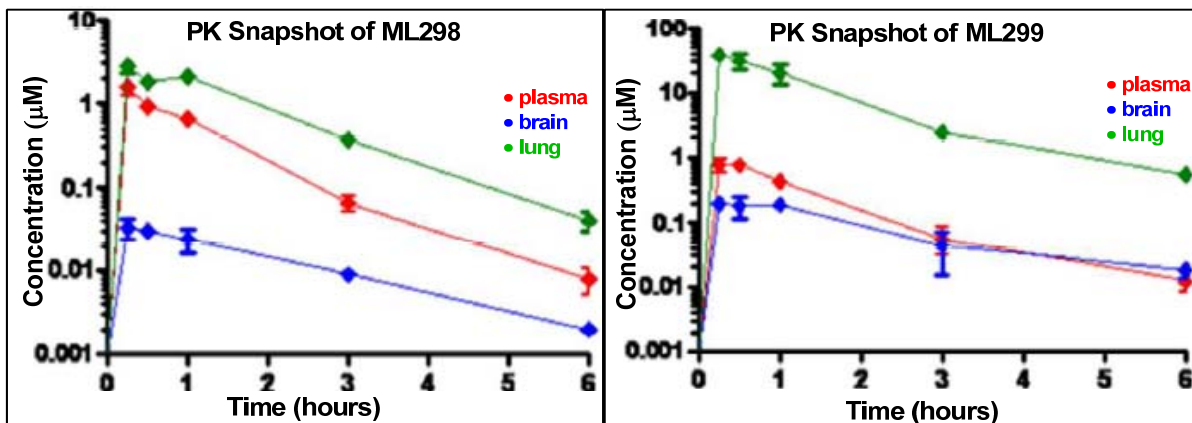
Figure 2.2.5.1 IP dosing of **ML298** and **ML299** leads to good distribution of PLD inhibitors. Figure adapted from ref 52.

The final comparison between **ML299**, **ML298**, and the previous probes involves the off target liabilities that each compound possesses. When **ML299** and **ML298** were screened against a panel of 68 common molecular targets including GPCRs, ion channels, and transporters, both were only active at 3 targets (compared to 12 and 11 targets from the previous dual and PLD2 selective inhibitors). To summarize, therefore, this medicinal chemistry campaign was focused on generating a selective PLD2 inhibitor with decreased off target effects and increased selectivity. By discovering **ML298**, we developed a compound that (i) had reduced ancillary pharmacology, (ii) had excellent PLD2 selectivity (no PLD1 inhibition @ >20 μM), and (iii) was restricted to the peripheral nervous system, an attribute complementing the previously existing isoform selective PLD2 inhibitor (**Figure 2.2.5.2**). Additionally, we desired a dual PLD1/2 inhibitor with decreased off target effects, increased potency, and CNS penetration. **ML299** provided us with a compound that met all of those criteria.[52]
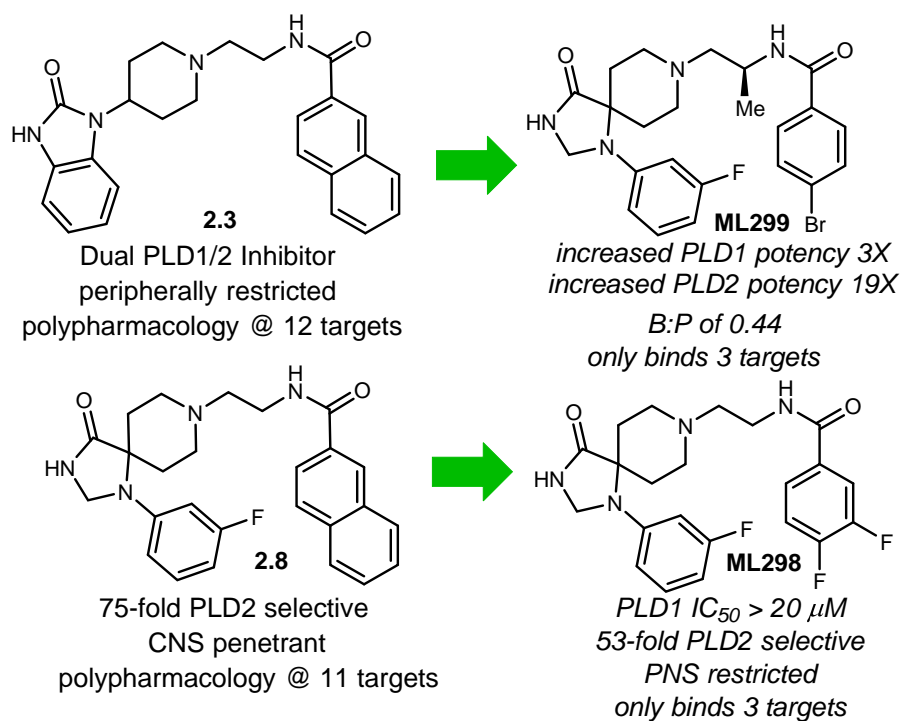
Figure 2.2.5.2 Comparison of new PLD inhibitors to known compounds

2.3 Discovery of 80-fold phospholipase D inhibitor with enhanced physiochemical properties

2.3.1   Plans to establish novel SAR for the triazaspirone scaffold

The addition of **ML298** and **ML299** to the existing complement of PLD inhibitors provided compounds with valuable attributes compared to what was available; however, there were still notable improvements that could be made. Namely, compounds with improved DMPK and physiochemical properties are desirable, and we are still in search for a greater than 1000-fold selective PLD2 inhibitor. As many SAR of the benzimidazolone and triazaspirone scaffolds have already been noted throughout previous studies, there was one segment of the compounds that was relatively unexplored. Throughout all previous studies, the *N*-aryl portion of the triazaspirone (previously called the aniline region *vide supra*) was underexplored with only a phenyl ring substituent (sometimes containing halogens) tested for biological activity. Therefore, we began a medicinal chemistry campaign surrounding that *N*-

aryl substitution planning to test a range of R-groups to evaluate SAR and potentially develop compounds with enhanced selectivity, DMPK, and physiochemical properties (**Figure 2.3.1.1**).
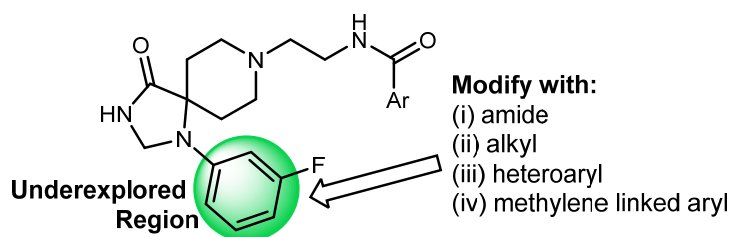
Figure 2.3.1.1 Plans to explore an underdeveloped region of the triazaspirone scaffold

2.3.2 Synthesis of triazaspirone advanced intermediate

To develop SAR for the amine of the imidazolone, a novel synthetic route for preparation of the fully elaborated structure without amine substitution would be ideal. If possible, that would allow for one step library synthesis from the penultimate intermediate. Therefore, we considered that a minor modification to the previous route, involving a Strecker reaction with ammonia, would allow for preparation of this penultimate intermediate after some minor protecting group modifications (**Scheme 2.3.2.1**). Beginning with *N*-benzyl piperidinone **2.9**, Strecker reaction followed by sulfuric acid hydrolysis delivered monosubstituted amine **2.25**. Treatment of **2.25** with formamide under thermal conditions promoted condensation, then sodium borohydride treatment facilitated reduction to imidazolone **2.26** in 20-25% yield. Subsequent Boc protection of the disubstituted amine and benzyl cleavage under reductive conditions delivered free piperidine, which was used in a reductive amination with (2-oxoethyl)carbamate **2.27** to deliver *bis*-Boc **2.28** in 55% yield over three steps. Acid mediated cleavage of the Boc protecting groups and selective acylation of the monosubstituted amine provided penultimate intermediate **2.29** in 51% over two steps, which we could then use in acylations, alkylations, reductive aminations, nucleophilic

aromatic substitution, and Pd catalyzed *N*-arylation chemistry. We chose the naphthyl aryl amide derivative since that substituent had historically promoted the highest degree of potency and selectivity.[51,52]
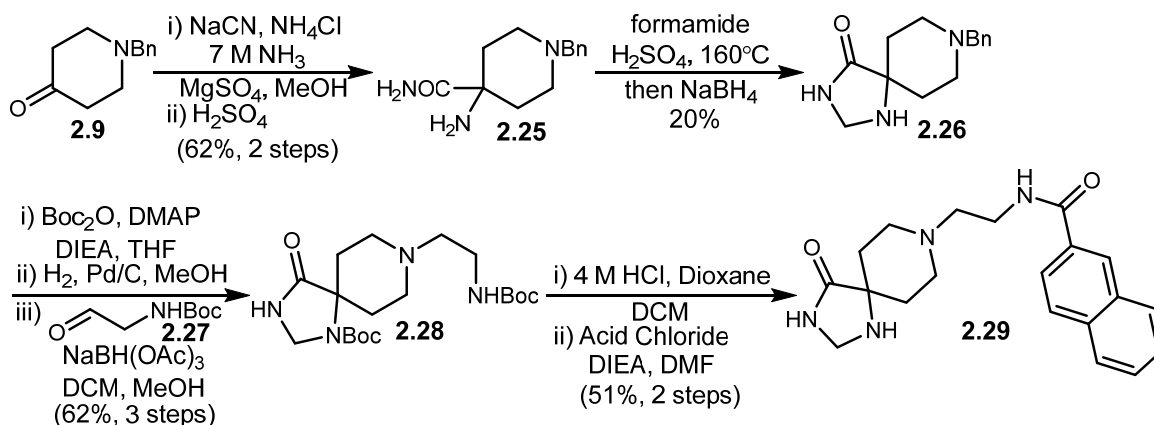
Scheme 2.3.2.1 Synthesis of penultimate intermediate for library synthesis

2.3.3 Synthesis of non *N*-aryl triazaspirone analogs

With penultimate intermediate **2.29** in hand, we wanted to immediately develop SAR trends from this region of the molecule. Therefore, we began acylations and alkylations of the disubstituted amine in an attempt to understand whether amides or methylene linked groups would confer potency and/or selectivity. It should be noted that the amine was quite unreactive. We reasoned this to be an effect of its sterically hindered space. Specifically, it is vicinal to a spiro center, which is similar to a *tert*-butyl group. Additionally, it is flanked on the other side by a methylene. Electronically, it is in a 5-membered ring system containing an amide, which inductively withdrawals from the amine, lowering its HOMO and decreasing its nucleophilicity. Essentially, acylations and alkylations of the amine were sluggish and gave low yields compared to primary amines, but we were able to prepare enough of the desired compounds to assay them for activity. Therefore, we made a library of ten compounds for a single point screen prior to designing future libraries (**Table 2.3.3.1**).
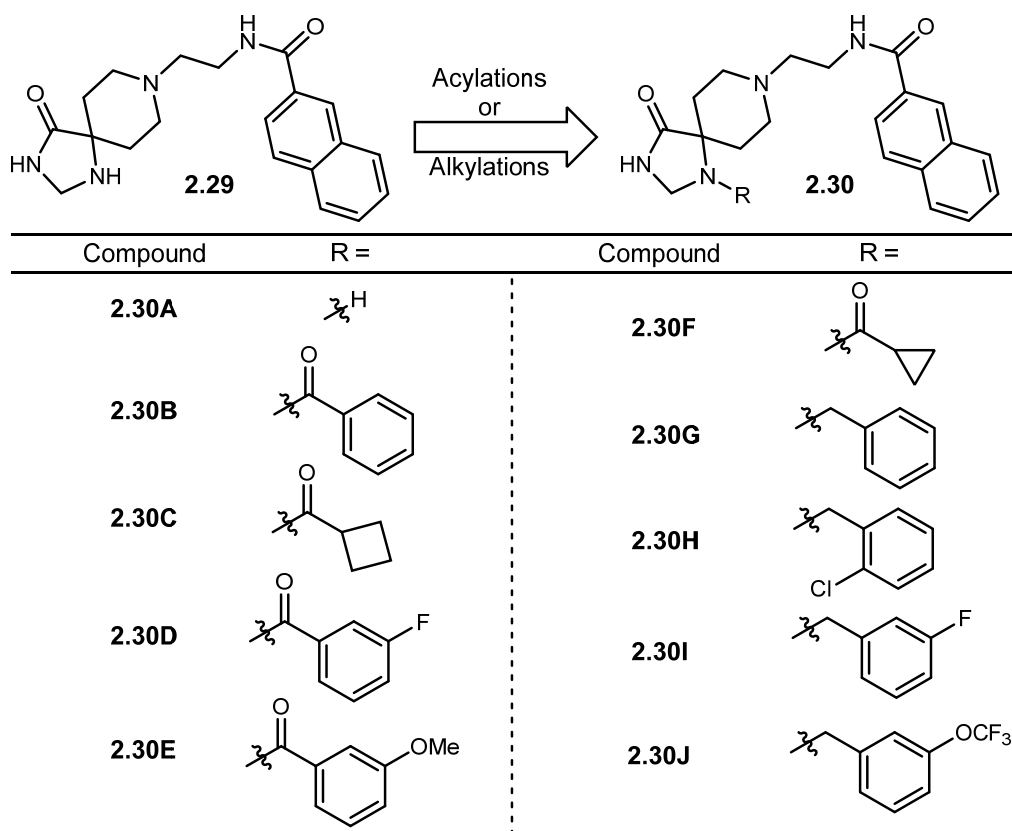
Table 2.3.3.1 Focused library of non *N*-aryl PLD inhibitors

When a major modification to the scaffold is accomplished, the single point screening is done at a larger concentration of compound, compared to the 200 nM concentrations used in the single-point shown *vide supra*. Since no non *N*-aryl species had been screened for PLD activity before, this was considered a major scaffold change. We performed the single-point screen, therefore, at 20 μM to ensure that no subtle activity of these compounds was missed. Gratifyingly, at this concentration, we were able to see major trends from the data (**Figure 2.3.3.1**). Methylene linked aryl groups appeared to be more potent than the amide variants, and amide linked small saturated rings appeared to be more potent compared to aryl amides. Additionally, the changes appeared to confer a preference for PLD2 inhibition for all but **2.30I**.
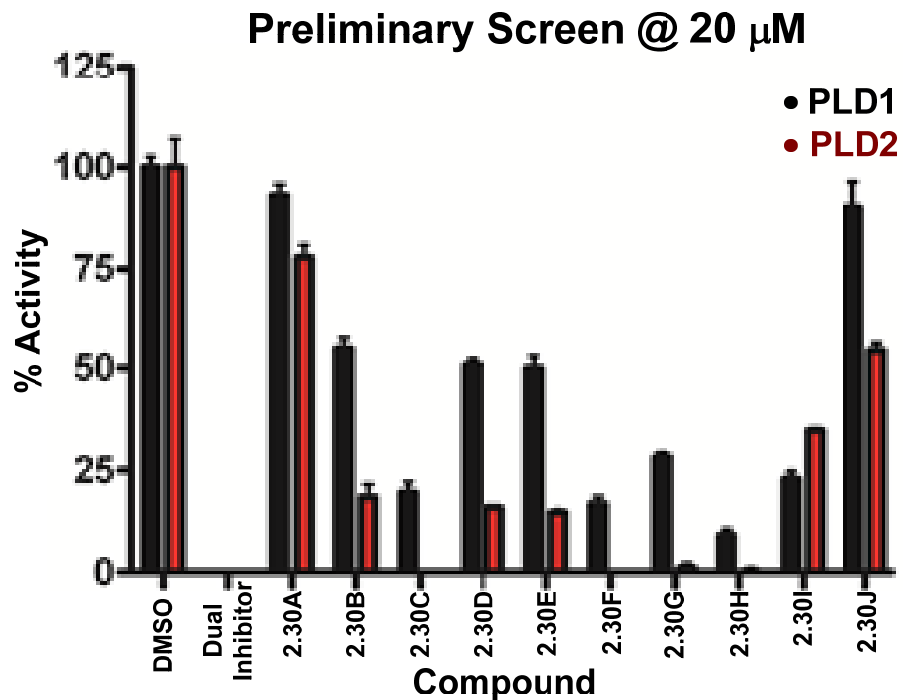
Figure 2.3.3.1 Single-point screen of focused library

This data encouraged us to design and synthesize an additional focused library of ten compounds focusing on methylene linked aryl groups. We wanted to flesh out additional SAR involving halogenation of the rings, and we hoped to add polar surface area by incorporating methylene linked pyridyl rings. Additionally, since the cyclopropyl amide looked promising from the single point data, we synthesized a methylene linked cyclopropane to further flesh out the SAR involving the amide (**Table 2.3.3.2**).
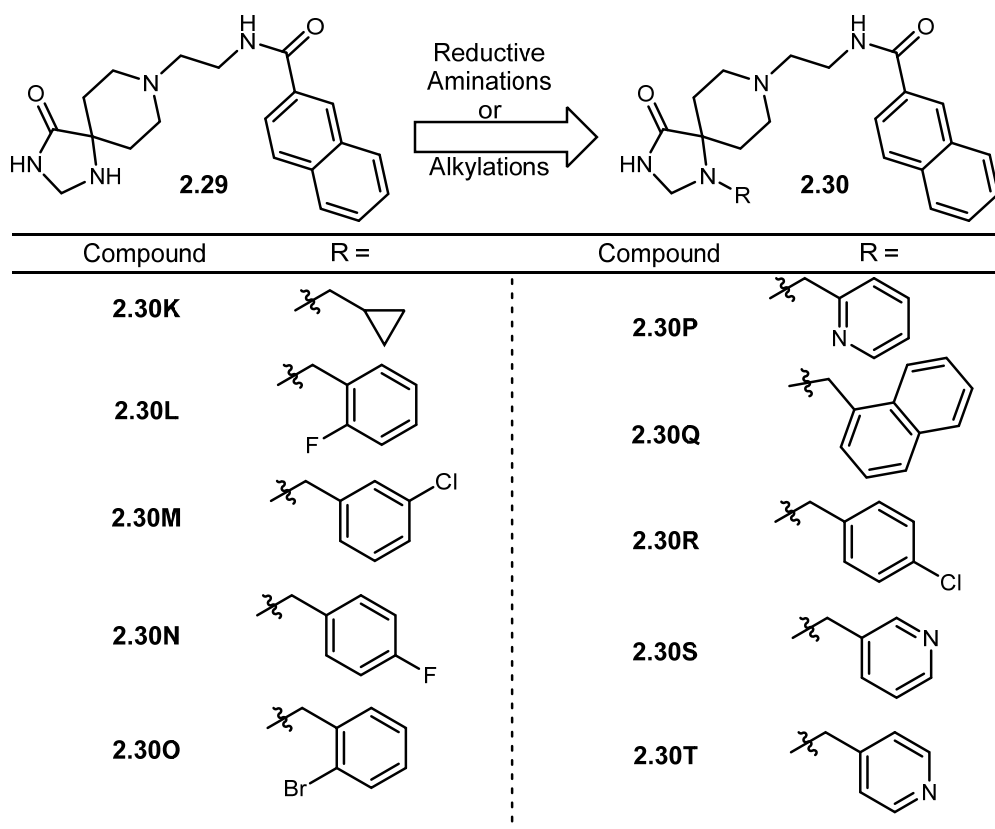
Table 2.3.3.2 Focused library of methylene linked aryl groups

These compounds were single-point screened at 20 µM. Delightfully, the SAR trend of PLD2 preference continued, and all but one of the compounds screened at this concentrations fully ablated PLD2 activity (**Figure 2.3.3.2**).
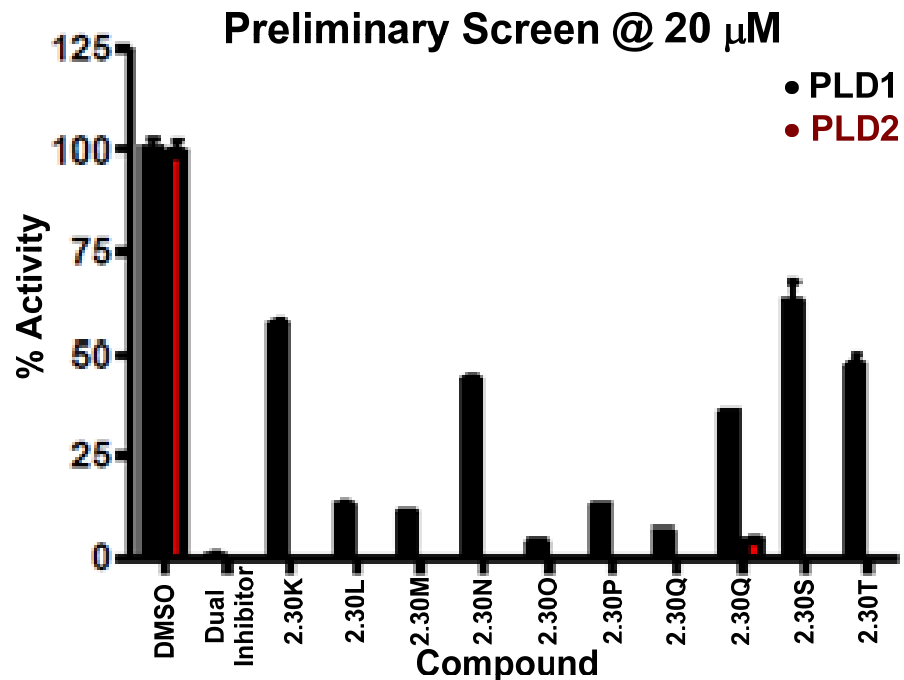
Figure 2.3.3.2 Single-point screen of methylene linked aryl groups

These data confirmed our suspicions that methylene linked aryl rings could confer PLD2 selective inhibition. Since the single-point data was generated at 20 μM, however, the relative potencies of these compounds were unknown. Therefore, CRCs of many of them were generated to develop a more thorough understanding of the SAR (**Table 2.3.3.3**).

161
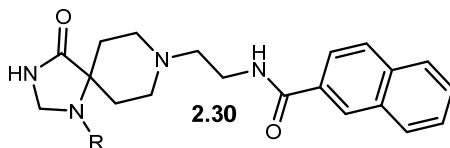
Compound	R =	PLD1 IC$_{50}$	PLD2 IC$_{50}$	Selectivity
2.30F		3,100 nM	290 nM	11-fold
2.30K		25,000 nM	2,050 nM	12-fold
2.30C		4,000 nM	320 nM	13-fold
2.30B		>30,000 nM	>10,000 nM	---
2.30G		8,260 nM	890 nM	9-fold
2.30I		>20,000 nM	>10,000 nM	---
2.30L		4,590 nM	205 nM	22-fold
2.30H		2,300 nM	110 nM	21-fold
2.30O		1,680 nM	160 nM	10-fold
2.30M		2,800 nM	250 nM	11-fold
2.30R		6,780 nM	1,540 nM	5-fold
2.30N		8,100 nM	1,780 nM	5-fold
2.30P		2,650 nM	145 nM	18-fold
2.30S		>30,000 nM	360 nM	>80-fold
2.30T		24,000 nM	850 nM	28-fold
2.30Q		1,500 nM	160 nM	9-fold

Table 2.3.3.3 IC$_{50}$ values for relevant PLD inhibiting analogs

From the CRCs, we found that a number of trends could describe the SAR. Specifically, halogenation of the ring, unless in the para-position, increased potency and/or selectivity for PLD2 compared to the naked phenyl ring. Additionally, the methylene linked aryl rings had enhanced potency compared to their amide congeners. The cyclopropane and cyclobutane rings, whether amide or methylene linked, were potent but only ~10-fold selective. The most interesting SAR was seen with regioisomeric methylene linked pyridyl rings. Namely, the 2-pyridyl analog **2.30P** was 18-fold selective for PLD2 inhibition (PLD2 IC_{50} = 145 nM), 3-pyridyl analog **2.30S** was >80-fold selective for PLD2 (PLD2 IC_{50} = 360 nM), and 4-pyridyl analog **2.30T** was 28-fold selective (PLD2 IC_{50} = 850 nM). We had, therefore, uncovered the most selective PLD2 isoform selective inhibitor known, to the best of our knowledge, with this 3-pyridyl benzyl amine **2.30S** replacing the *N*-aryl substitution. Compared to our recently developed PLD2 selective inhibitor **ML298** (PLD1 IC_{50} = 20,000 nM, PLD2 IC_{50} = 355 nM, 53-fold selective), by changing the 3-fluoroaniline substitution to a 3-pyridyl benzyl amine, we retained close to identical potency at PLD2 while decreasing PLD1 potency 10 μM—a significant decrease.

2.3.4 Focused library of *N*-pyridyl triazaspirone analogs

Since the new pyridyl group conferred such an exciting increase in selectivity, we contemplated whether the methylene linker was necessary. Essentially, we wondered if switching back to the *N*-aryl substitution with a pyridyl instead of a halogenated phenyl ring would confer enhanced potency or selectivity. We could synthesize those analogs through nucleophilic aromatic substitution or Pd-catalyzed coupling chemistry following our previous route; therefore, we prepared a small sampling of pyridyl rings with various substituents. We made two core structures with a 3-pyridyl fluoro aryl group **2.31** and a 3-pyridyl group **2.32**

and added six of the historically most potent aryl amides to determine whether directly linked

N-pyridyl group would confer potency and/or selectivity (**Figure 2.3.4.1**).
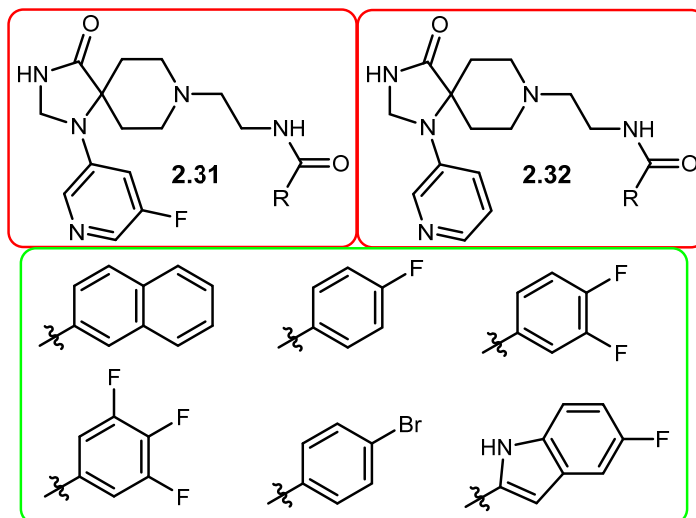
Figure 2.3.4.1 Analogs testing directly linked *N*-pyridyl groups with various aryl amides

Additionally, five analogs were made where the aryl amide was held constant as a naphthyl

group while the *N*-aryl group was modified with different pyridyl substitutions (**Figure 2.3.4.2**).
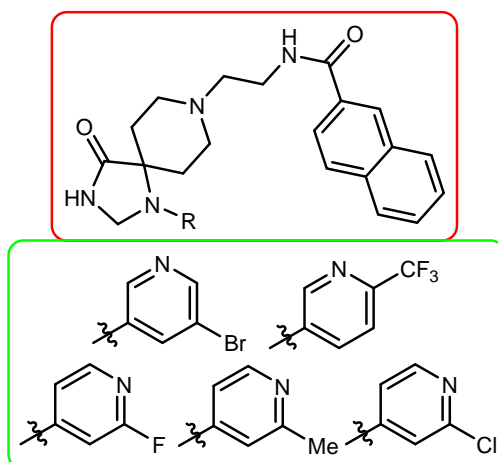
Figure 2.3.4.2 Analogs testing pyridyl *N*-aryl derivatives

These compounds were screened in a single-point assay at 2 μM. Since we expected them to

be somewhat active, we assumed that 20 μM concentrations would be too high to produce

interpretable SAR. Unfortunately, however, none of the compounds with the direct *N*-pyridyl substitution gave rise to inhibitors showing >75% inhibition at 2 μM. Therefore, we decided to move forward with the methylene linked 3-pyridyl ring system that conferred 80-fold selectivity.

2.3.5   Aryl amide libraries containing the 3-pyridyl benzylamine triazaspirone

Next, we wanted to understand whether retention of the 3-pyridyl group and analog synthesis of the aryl amide could result in a more potent and selective compound. Modification to the synthetic procedure, again, was necessary for facile library synthesis with formation of the aryl amide in the last step. While we initially worked on routes that would have provided our necessary penultimate intermediate **2.33** more directly (but ultimately were unsuccessful for a variety of reasons), we ultimately returned to our previous route using some slight procedural modifications and protecting group manipulations to obtain **2.33** (**Scheme 2.3.5.1**). We began with previously disclosed intermediate **2.26**, and again formed *bis*-Boc intermediate **2.28** through a Boc protection, hydrogenolysis, and reductive amination sequence. At this point, we needed to remove the Boc protecting groups and functionalize the more hindered and generally less nucleophilic amine chemoselectively over the primary amine to allow for easy synthesis of aryl amide analogs. While this was not possible directly, we decided to take advantage of the primary amine's comparatively high nucleophilicity by addition of an electrophilic protecting group that the more nucleophilic amine would react with preferentially. Therefore, *bis*-Boc **2.28** was treated with acid to cleave the Boc groups, and the triamine was then treated with phthalic anhydride, which reacted with the primary amine to form phthalamide **2.34**. After extensively screening reductive amination conditions, the reaction of **2.34** with 3-pyridine carboxaldehyde was

found to proceed only when neat acetic acid was used as the solvent. The product of that reaction was then treated with hydrazine to cleave the phthalamide and form free amine **2.33**, our penultimate intermediate for aryl amide library synthesis.
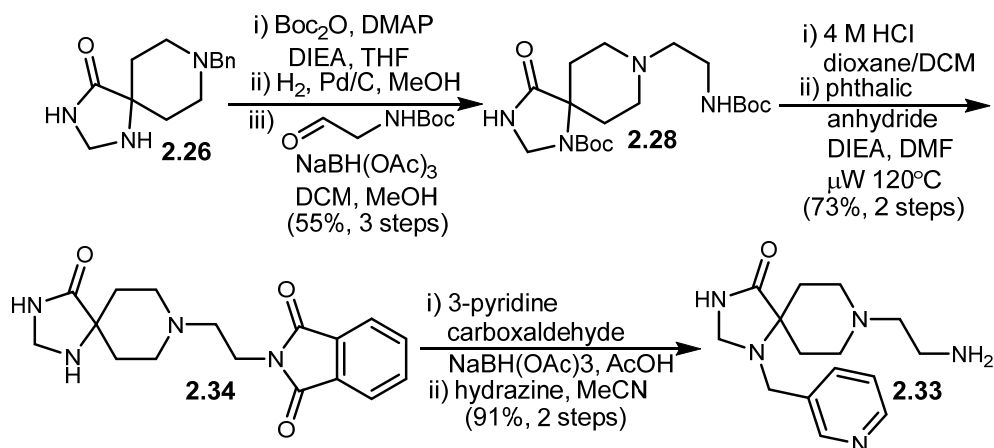
Scheme 2.3.5.1 Modified synthetic route for aryl amide analog synthesis

With **2.33** in hand, we performed acylation and amide coupling chemistry on the monosubstituted amine to generate maximal diversity in the aryl amide region. Our first expansive library included mainly substituted phenyl rings to furnish a library of compounds with similar amides compared to what was prepared while discovering **ML298** and **ML299**. Specifically, different regioisomers of fluorinated and/or chlorinated phenyl rings had significant impacts on the biological activity of previous PLD inhibitors; therefore, we synthesized many of the possible fluorinated and chlorinated ring permutations. Additionally, we added other substituents including a few heterocycles and a bicyclic ring that was previously of interest (**Figure 2.3.5.1**).
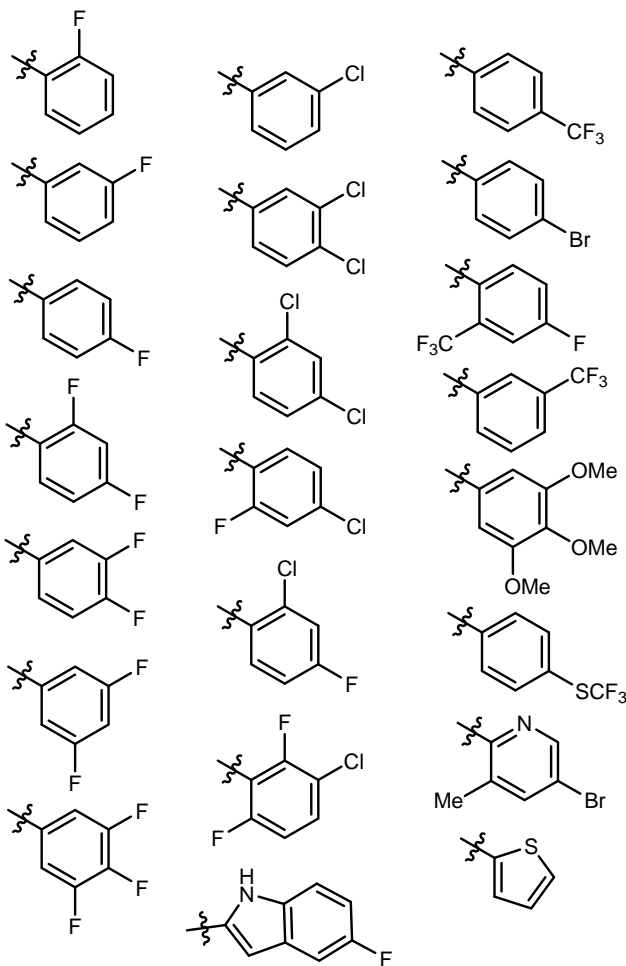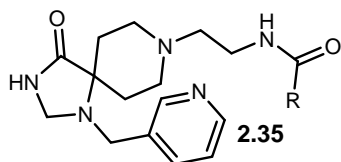
Figure 2.3.5.1 Analogs alternating aryl amides with pyridyl benzyl amine

These analogs were screened at 2 µM for inhibition of PLD1 and PLD2. Unfortunately, only two novel compounds from this library showed >50% inhibition of PLD2 at this concentration. Concentration response curves were generated for these compounds to obtain IC_{50} values, but the data was not superior to any of the known compounds. Fluoro-indole **2.35A** was potent (PLD2 IC_{50} = 120 nM), but was less selective than other equipotent compounds (26-fold PLD2 selective, PLD1 IC_{50} = 3,100 nM). Additionally, 3,4-dichloro

amide **2.35B** was found to be 16-fold selective for PLD2 inhibition, but it lacked potency (PLD2 IC$_{50}$ = 1,250 nM) (**Figure 2.3.5.2**).
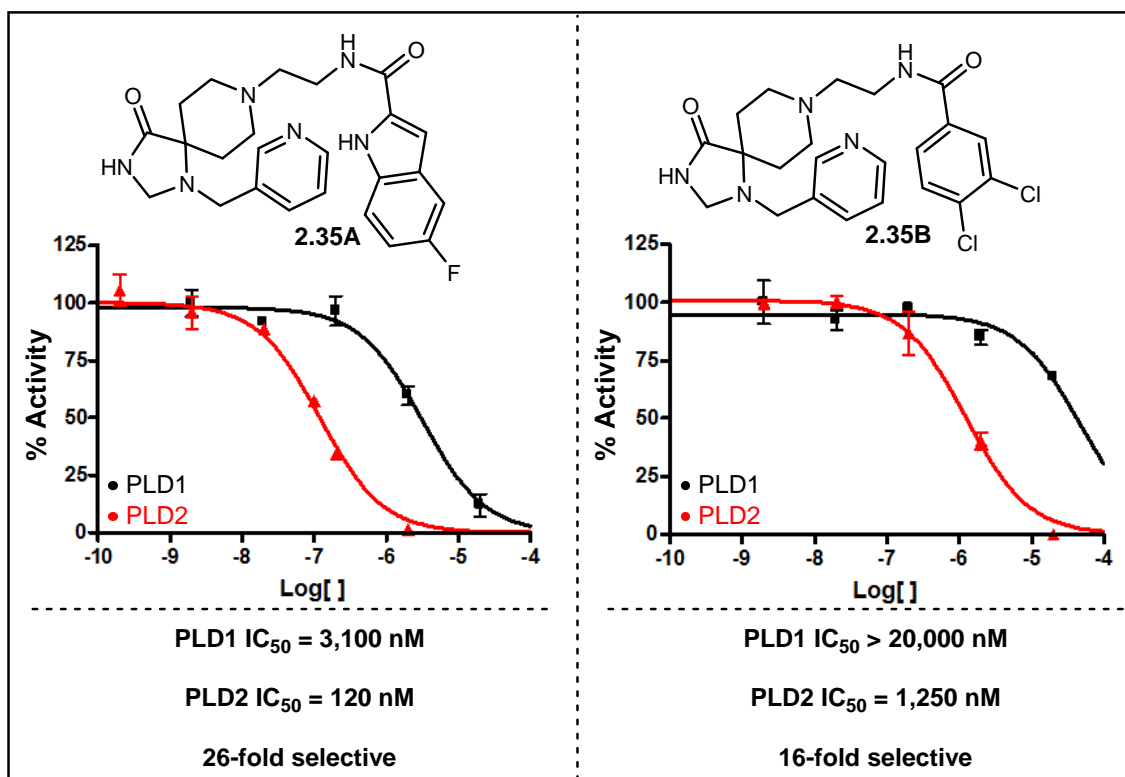
Figure 2.3.5.2 CRCs of fluoro-indole and dichloro inhibitors

This substituted phenyl ring library of compounds illustrated shallow SAR involving the aryl amide region. This group of compounds, however, propelled us to ask whether larger aromatic rings would provide robust SAR that could lead to more selective and potent PLD inhibitors. Essentially, we noted that fluoro-indole **2.35A** and naphthyl derivative **2.30S** provided potency at PLD2, and those were the only larger ring systems tested with this alternative non *N*-aryl pyridyl group. Additionally, the chlorine atoms of the 3,4-dichloro compound **2.35B** could be filling the spatial region of PLD enzymes that the larger ring systems occupy while binding PLD2, which would explain why that chlorinated variant showed modest PLD2 potency while other halogenated phenyl rings were largely inactive. To test the hypothesis that larger ring sizes of aryl amides could lead to enhanced PLD2

potency and/or selectivity, we generated an additional library of twenty bicyclic aryl amide

ring systems (**Table 2.3.5.1**).

2.35
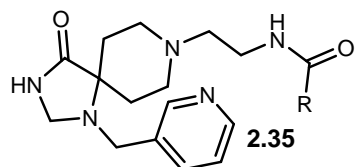
Compound	R =	Compound	R =
2.35C		**2.35M**	
2.35D		**2.35N**	
2.35E		**2.35O**	
2.35F		**2.35P**	
2.35G		**2.35Q**	
2.35H		**2.35R**	
2.35I		**2.35S**	
2.35J		**2.35T**	
2.35K		**2.35U**	
2.35L		**2.35V**	

Table 2.3.5.1 Library of biaryl amides

We used a single-point screen at 2 μM to evaluate these compounds' ability to inhibit PLD1 and/or PLD2. While we thought the size of a ring system would impact its ability to bind PLD, we observed that the electronics of the ring, heteroatom positioning, and halogenation also had large effects on biological activity. For instance, while previously discussed 80-fold selective naphthyl ring containing compound **2.30S** was potent and selective for PLD2, bromination or fluorination drastically decreased PLD potency (**2.35H** and **2.35I**), nitrogen incorporation (making it a quinolone, **2.35D**) almost ablated PLD potency, and regioisomeric quinolone rings also lacked potency (**2.35S**, **2.35T**, and **2.35U**). Indole containing compounds also showed this large variability in bioactivity. While regioisomer **2.35L** appeared potent and selective based on the single-point data, regioisomer **2.35M** and indoles with additional substituents (**2.35O**, **2.35R**, and **2.35V**) lacked potency at PLD1 and PLD2 (**Figure 2.3.5.3**).
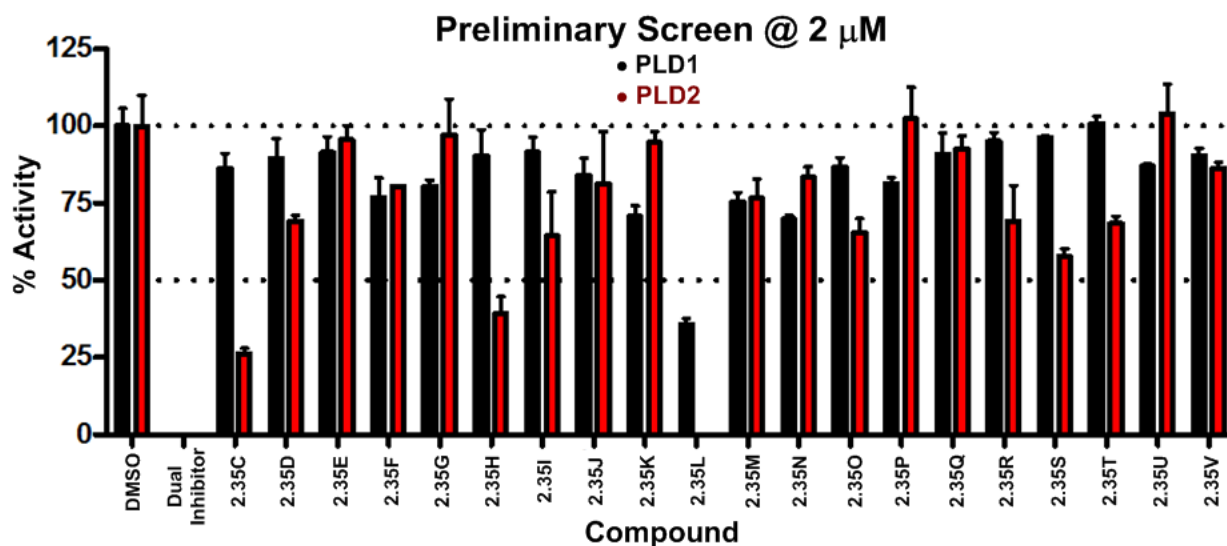
Figure 2.3.5.3 Single-point screnn of biaryl library

The single-point data propelled us to generate CRCs for **2.35C**, **2.35H**, and **2.35L**. Benzofuran **2.35C** and indole **2.35L** have the steric potential to adopt the same conformation, which explains why both were active as inhibitors. Indole **2.35L**, however, was much more

potent and selective than benzofuran **2.35C**, which only showed moderate potency at PLD2. Bromo-naphthyl compound **2.35H** was also a modest PLD2 selective inhibitor (**Figure 2.3.5.4**).
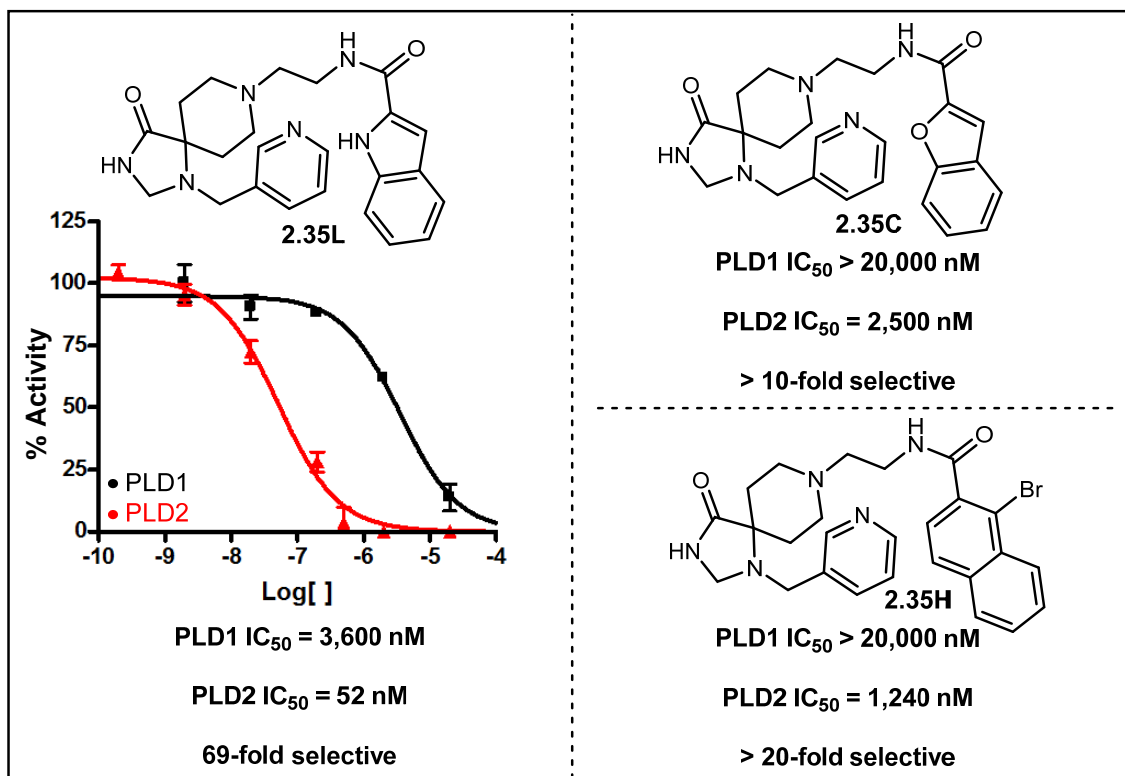
Figure 2.3.5.4 CRCs of indole and CRC data for benzofuran and naphthyl inhibitors

To summarize the chemistry efforts using iterative parallel synthesis to develop a more selective PLD2 inhibitor, we began looking at the underexplored region from previous inhibitors, which previously was a 3-fluoroaniline. By modifying that region with various groups, we found a methylene linked 3-pyridyl ring that conferred unprecedented selectivity and similar PLD2 potency to **ML298**. By holding the 3-pyridyl portion constant and performing a large amide scan, unfortunately, we did not discover any compounds with enhanced selectivity compared to the initial lead **2.30S**. Those modifications did allow us to understand the SAR of the aryl amide region on a deeper level, however, and it provided indole **2.35L** that had similar selectivity to naphthyl **2.30S** with a 7-fold boost in potency. All

things considered, we decided to move forward with biological characterization of **2.30S** as an antiviral agent and also examine its DMPK and physiochemical properties.

2.3.6 Physiochemical and DMPK properties

Inspecting **2.30S** as a probe, its atomic mass is less than 500 daltons (443 Da), it has less than 5 hydrogen bond donors (2), less than 10 hydrogen bond acceptors (3), and its cLogP is less than 5 (2.74). Therefore, **2.30S** conforms to all of Lipinski's rules making it "druglike," which means it is likely orally bioavailable. Solubility and stability in phosphate buffered saline (PBS) is an issue that has been problematic for previous generations of PLD inhibitors; however, **2.30S** was found to be both soluble (95 μM with pH = 7.4 @ 23 °C) and stable (~100% of parent compound remaining at 48 hours @ 23 °C) in PBS. Additionally, **2.30S** displayed a favorable cytochrome P450 (CYP) profile with modest inhibition of CYP 3A4 and CYP 2D6 (CYP3A4 IC_{50} = 3.9 μM; CYP2D6 IC_{50} = 16.4 μM; CYP1A2 IC_{50} > 30 μM; CYP2C9 IC_{50} > 30 μM). Another important property is plasma protein binding, and while previous PLD inhibitors generally were only 1-5% unbound (meaning only 1-5% of administered drug is available for binding of the biological target), **2.30S** is 26.3% unbound in rat and 8.8% unbound in human, which conveys a considerable advantage compared to previous compounds. Although all of these properties have been ideal, one apparent weakness of the compound is it clearance rate. In rat and human hepatic microsomes, **2.30S** exhibited moderate-to-high intrinsic clearance (rat CL_{int}: 82.1 mL/min/kg; human CL_{int}: 43 mL/min/kg) with predicted hepatic clearance rates near the respective rates of hepatic blood flow for each species (rat CL_{hep}: 64.3 mL/min/kg; human CL_{hep}: 17 mL/min/kg). Intravenous (IV) administration of **2.30S** in Sprague Dawley rats (*n* = 2) revealed a brain:plasma partition coefficient of 1.48, demonstrating **2.30S** to have excellent distribution to the CNS. Lastly,

2.30S has minimal ancillary pharmacology. **2.30S**, like all PLD inhibitors developed by our laboratory, was sent through a panel of common molecular targets including GPCRs, ion channels, and transporters. While the previously discussed PLD2 selective compounds (**2.8** and **ML298**) at 10 μM gave > 75% inhibition of 12 and 3 of the common molecular targets respectively, **2.30S** only inhibited 2 of those common molecular targets, demonstrating it to be a clean compound with minimal off target liabilities (**Figure 2.3.6.1**).
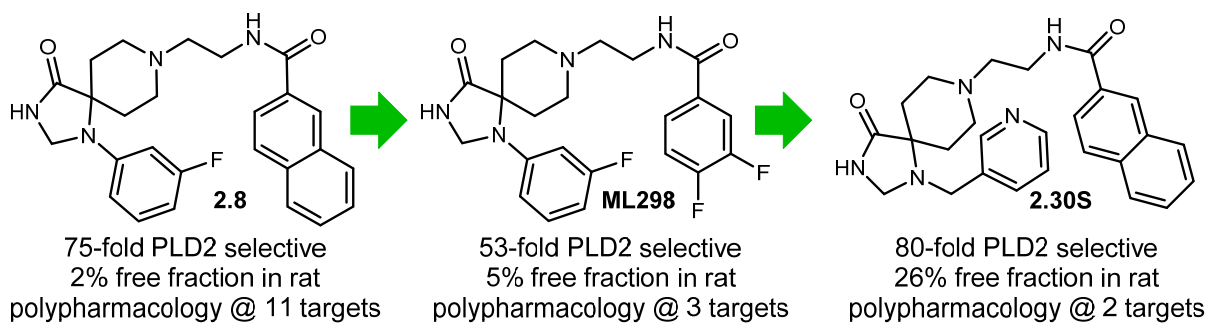
Figure 2.3.6.1 Comparison of PLD2 selective inhibitors

2.3.7 Antiviral activity of novel PLD inhibitors

Recently, the Brown, Lindsley, and Thomas Labs have implicated PLD2 in viral infection and proliferation. PLD2 selective inhibitor **2.8** and PLD2 RNA interference have delayed viral entry and reduced viral titers *in vitro*. Additionally, treatment of infected mice with **2.8** led to reduced viral titer, increased survival, and significant increases in transcription of innate antiviral effectors. Unfortunately, however, higher concentrations of **2.8** were cytotoxic to the cells *in vitro*, and concentrations far exceeding the PLD1 IC$_{50}$ of **2.8** were used in both the *in vitro* and *in vivo* studies. Since that was the case, the antiviral results from chemical inhibition cannot be conclusively tied to the sole inhibition of PLD2. With the novel 80-fold selective inhibitor **2.30S** in hand, we were anxious to evaluate its antiviral activity.

Initially, **2.30S** was evaluated alongside 75-fold selective inhibitor **2.8** to examine cytotoxicity with both inhibitors. In the assay, cells were treated with different concentrations of compound or vehicle ranging from 1 nM to 50 μM. The cells were allowed to grow for 24 hours, and then the number of dead cells was counted (**Figure 2.3.7.1**). Cells treated with **2.8** showed a slight increase in cytotoxicity at 10 μM, but that was followed by an enormous increase at 20 μM and an additionally large increase at 50 μM. Inhibitor **2.30S**, conversely, is indistinguishable from cells treated with DMSO or with growth media only. Using **2.30S** *in vitro* and *in vivo*, therefore, offers a considerable advantage when compared to the pronounced cytotoxicity of **2.8**.
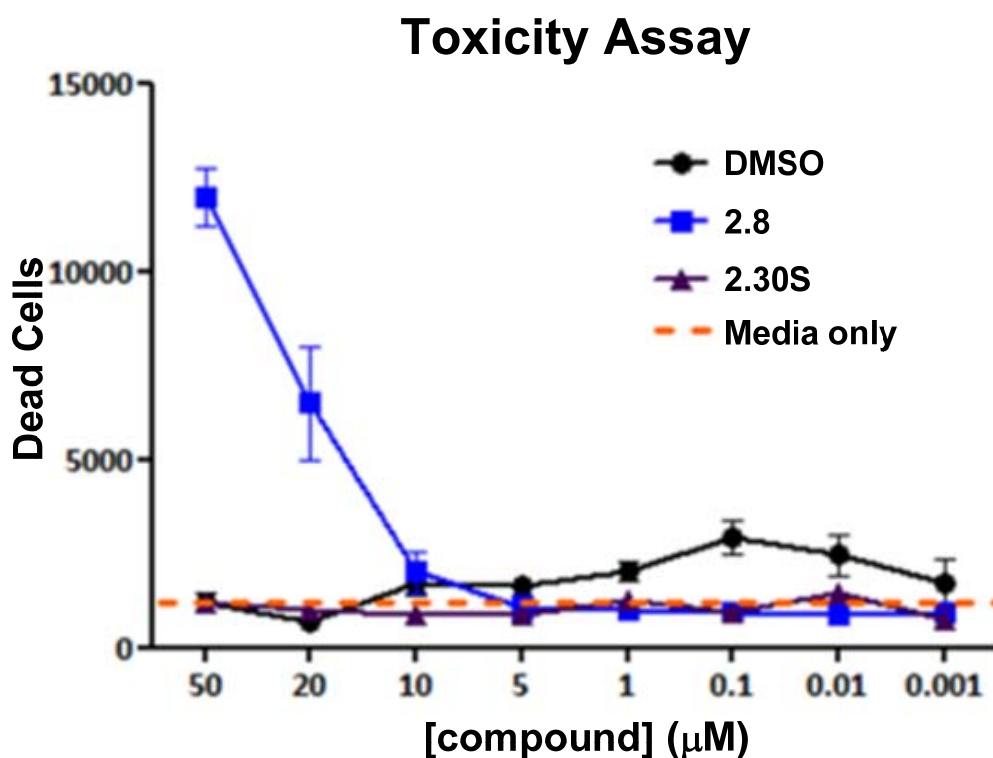
Figure 2.3.7.1 Cytotoxic effects of PLD inhibitors

To examine the antiviral effect of **2.8** versus **2.30S**, a standard $TCID_{50}$ assay was used to assess viral reproduction *in vitro*. A549 cells were treated with 10 μM concentrations of either DMSO, **2.8**, or **2.30S**, and the cells were infected with 0.01 multiplicity of infection

(MOI) with four distinct strains of influenza (A/California/04/2009 (H1N1), A/Brisbane/10/2007 (H3N2), rg-A/Vietnam/1203/2004 (H5N1), and A/Anhui/01/2013 (H7N9)). After 24 hours of treatment with the viruses, the viral supernatant is removed and titrated on MDCK cells to measure viral replication, and change in viral titer can be correlated to antiviral activity. Across all four viral strains, both **2.8** and **2.30S** significantly lowered viral replication (**Figure 2.3.7.2**).
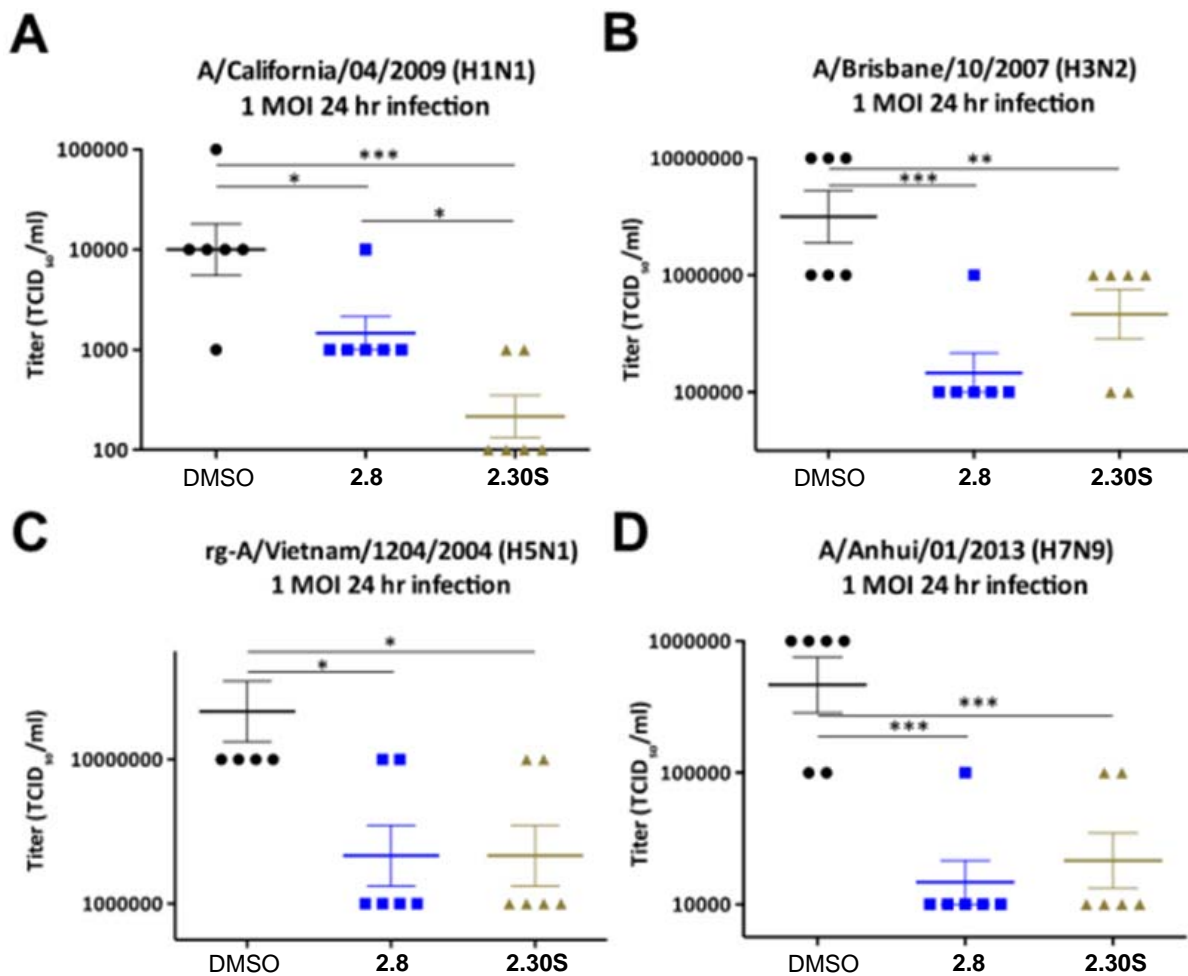
Figure 2.3.7.2 Effect of **2.8** (10 μM) and **2.30S** (10 μM) on viral replication and titer.

In these viral proliferation assays, the improved physiochemical properties of **2.30S** translated into comparable potency to **2.8**, despite a ~20-fold reduction in PLD2 potency. Notably, the antiviral activity of **2.30S** can be explicitly tied to PLD2 inhibition since 10 μM

concentrations were used and **2.30S** does not inhibit PLD1 until ~30 μM. Conversely, when **2.8** is used in this assay at 10 μM, it inhibits both PLD isoforms so the antiviral effect cannot be linked to either PLD isoform. Importantly, both PLD inhibitors displayed *pan*-anti-influenza activity across seasonal influenza (H1N1), low pathogenicity influenza (H3N2), highly pathogenic avian influenza (H5N1), and recently emergent influenza with pandemic potential (H7N9). Since Tamiflu has no efficacy against H7N9, PLD inhibition could represent an exciting new mechanism to combat pathogenic influenza.

In summary, we developed **2.30S**, a potent (PLD2 IC_{50} = 360 nM) and selective (80-fold selective, PLD1 IC_{50} > 30,000 nM) PLD2 inhibitor. Compared to previous generations of PLD inhibitors, compound **2.30S** has unprecedented selectivity, improved physiochemical properties, no cytotoxicity to cells, high CNS penetration, and a favorable DMPK profile that will be improved once the metabolic soft spots are addressed. In developing this molecule, we addressed portions of the triazaspirone scaffold that had never been altered, and in doing so we charted SAR that could be useful in future efforts. **2.30S** was used in cell-based antiviral assays and was found to inhibit infection and viral replication of not only H1N1 and H3N2, but also the highly virulent bacterial strains H5N1 and H7N9. Medicinal chemistry efforts to address the metabolic liabilities of this compound are underway to develop a compound that could be delivered orally, and results of those studies will be reported in due course.

2.4 PLD inhibitors: overview of our efforts and future directions

2.4.1 PLD inhibitors prior to my efforts

Prior to the Brown and Lindsley efforts toward the discovery of novel isoform selective PLD inhibitors, genetic knock outs, siRNA, and adding *n*-butanol as a competitive

substrate were the only means of modulating PLD activity and phosphatidic acid levels. Since genetic knock outs are extremely labor intensive, siRNA cannot be used effectively on an organismal level, and *n*-butanol is not a relevant *in vivo* strategy, small molecule inhibitors provide a considerable benefit to the field allowing more effective and facile modulation of these biological systems. After halopemide **2.1** was discovered to inhibit PLD1 and PLD2, efforts in our labs facilitated the discovery of potent and isoform selective inhibitors (**2.6** and **2.8**). These compounds provided the ability to modulate *in vitro* systems and methodically evaluate each isoenzyme in different cellular phenotypes. In many assay systems, however, the most selective inhibitors still required compound concentrations that should affect both PLD1 and PLD2. Any effect in these assays, therefore, could not be directly attributed to selective inhibition of either isoenzyme. The major goal of my research, as I began this project, was to develop inhibitors of PLD2 that could provide statistically significant effects in assays at concentrations below the PLD1 IC_{50}. Additionally, the known PLD inhibitors had other limitations. Specifically, (a) their *in vivo* DMPK profiles were suboptimal and (b) they had ancillary pharmacology profiles where significant off target activity was noted.

2.4.2 Novel PLD inhibitors and their advantages

In an attempt to increase selectivity of the PLD2 inhibitors, three major regions were modified iteratively to annotate the impact on biological activity. Initially, the amide region was varied with substituted aryl compounds, and this effort resulted in the discovery of **ML298**. This compound was less selective than **2.8** in the cellular reporter assay, but **ML298** had considerably decreased potency at PLD1 compared to **2.8**. Additionally, when **ML298** was used in a cancer cell invasive migration assay, it was shown to decrease that phenotype when used at 10 μM concentrations, which allows the invasive migration phenotype to be

directly linked to PLD2 inhibition. Compared to **2.8**, therefore, **ML298** can sometimes be advantageous when used *in vitro* if the effort is intended to probe the effect of single PLD isoform inhibition on a specific phenotype. Additionally, **ML298** complements **2.8**'s DMPK profile. Both compounds have very similar low free fraction and high clearance rates, but IV or IP dosing allow the compounds to circulate in therapeutically relevant concentrations. Considering CNS penetration, **2.8** and **ML298** are CNS penetrant and peripherally restricted, respectively, which provides complementary tools if *in vivo* dosing was required. Moreover, **ML298** has fewer off target effects when compared to **2.8**. In the ancillary pharmacology screen, **ML298** only bound three common molecular targets at 10 μM compared to **2.8** binding eleven of those same molecular targets.[51,52]

After varying the amide region of the triazaspirone scaffold, the linker region was modified with addition of an (*R*) or (*S*) methyl group. After surveying some of the most selective and potent PLD2 scaffolds with these methyl group modifications, we found that methylation of these scaffolds had an enormous impact on the biological activity. Essentially, an (*S*)-methyl increased PLD1 potency 200 to 590-fold depending on the substrate while an (*R*)-methyl also increased PLD1 potency, but to a lesser extent. These modifications provided **ML299**, our most potent PLD dual inhibitor. **ML299** has an attractive *in vivo* profile with IP dosing, which showed the compound to get into the lungs, plasma, and central nervous system in concentrations far exceeding its IC_{50}. Additionally, **ML299** was selective and only bound three of the common molecular targets that were screened for ancillary pharmacology. After fully evaluating **ML299**, it is our most potent PLD1/2 inhibitor with acceptable DMPK properties and decreased ancillary pharmacology when compared to previous dual PLD inhibitors.[52]

In an effort to discover more selective PLD2 inhibitors, the *N*-aryl region of the compound was next modified with an assortment of substituents. This led to the discovery of **2.30S**, which is the most selective PLD2 inhibitor known. The pyridyl group, which took the place of the 3-fluorophenyl group, adds extra polarity to the compound, and that change resulted in enhanced solubility. Upon analysis of the physiochemical and DMPK properties of **2.30S**, the added solubility seems to have had an effect on other compound characteristics. Namely, compared to previous PLD inhibitors, **2.30S** gained a sizeable increase in free fraction, had excellent CNS penetrance (B:P = 1.48), and had less ancillary pharmacology than any previous PLD inhibitor. Its only blemish was a high rate of hepatic clearance, which can likely be addressed by modification of the piperidine ring to halt the major metabolic pathway. Additionally, this compound provides a large concentration window before PLD1 is inhibited (PLD1 IC_{50} = 30 µM), and **2.30S** and **2.8** were used at 10 µM concentrations *in vitro* to determine their ability to decrease viral proliferation. Importantly, both compounds decreased viral proliferation, but **2.30S**'s effect could be directly linked to PLD2 inhibition while **2.8** would be inhibiting both PLD1 and PLD2 at 10 µM concentrations. **2.30S** offers a considerable advantage, therefore, while attempting to relate the activity of PLD1 and PLD2 to viral proliferation.[54]

2.4.3   Future studies to evaluate PLD

While the PLD inhibitors recently discovered provide the field with considerable advantages while studying PLD, large discoveries are required to provide the field with a better platform to evaluate PLD inhibitors and a better understanding of the mechanism of inhibition. Moving forward to study PLD and develop novel inhibitors with enhanced

potency and selectivity, various discoveries will facilitate more rapid discovery on an assortment of fronts.

In probe discovery—or drug discovery—organic synthesis can often be the slowest step to evaluate structure activity relationships of various compound classes. With PLD, however, the speed at which compounds can be biologically characterized limits the discovery efforts. One place that would enhance probe or drug discovery efforts, therefore, is development of an assay to decrease the labor necessary to evaluate compound libraries. While the current methods are effective,[39] I frequently wondered if we could be missing valuable SAR by not biologically evaluating enough of the compounds past a single-point screen. To make a high-throughput PLD screening paradigm, I have pondered methods to make the assay produce a reporter such as fluorescence or absorbance that can be measured using a plate reader. To do this, one potential option would be to link a PA signal cascade to the production of a reporter that could be quantified at the assay end-point. This will be difficult to develop since PA is a fleeting intermediate in the cell, but it may be possible if the cell line was extensively characterized. If completed, this assay could boost PLD medicinal chemistry efforts and allow vast SAR to be charted in record times.

An additional complication for those studying PLD is the inability to purify large quantities of the enzymes. Because a protocol is lacking for expression of large quantities of PLD1 or PLD2, this decreases our abilities for *in vitro* characterization of our compounds in a cell-free environment. Moreover, without large quantities of PLD, efforts to solve the structure of PLD—through crystallography—are deterred. To improve the understanding of the PLD structure, and how that structure relates to our inhibition efforts, protocols for purification of larger quantities of PLD are necessary. Once larger quantities of the PLD

isoforms can be purified, solving the structure of PLD can explain how our inhibitors exert their effects. This effort is paramount to developing more selective and potent PLD inhibitors. That structure could explain where our compounds are binding, which will improve efforts to design potent and selective probes in the future.

While the former two goals are long term and will enhance any effort to study PLD, short term goals to evaluate PLD and validate its importance in different disease states are also necessary. The most recent PLD2 selective probe compound (**2.30S**) looks like it could be effective as an *in vivo* probe after its metabolic hotspot is addressed. The recent data linking PLD2 to AD are provocative,[22] and the Brown and Lindsley labs are uniquely poised to evaluate this using chemical inhibition instead of genetic knock out studies. A congener of **2.30S** with decreased clearance may be orally bioavailable, and this compound—and the result of this study—could increase interest in PLD as a therapeutic target in CNS disorders.

An additional short term goal would be to evaluate the added methyl group's effect on potency.[52] As data is available for many congeners with the *des*-methyl, (*S*)-methyl, and (*R*)-methyl, *in silico* evaluation of each compound's low energy conformation coupled to the known potency data could provide insight into what is causing the conformational effect. After studying the modeling, there could likely be a way to modify the compounds into a more rigid conformation, which could bias them toward the conformation the modeling predicted. To rigidify the compounds, enantioselective cyclopropanation reactions could lock the linker region into a more defined conformational arrangement, and the methylene of the cyclopropane would serve to provide similar lipophilicity to that region as the initial methyl group. These experiments would be designed to provide a better explanation of the conformational effects that the methyl group is inducing.

References

(1)   Voelker, D. R. Organelle Biogenesis and Intracellular Lipid Transport in Eukaryotes. *Microbiol. Rev.* **1991**, *55*, 543–560.

(2)   Stace, C. L.; Ktistakis, N. T. Phosphatidic Acid- and Phosphatidylserine-Binding Proteins. *Biochim. Biophys. Acta* **2006**, *1761*, 913–926.

(3)   Selvy, P. E.; Lavieri, R. R.; Lindsley, C. W.; Brown, H. A. Phospholipase D: Enzymology, Functionality, and Chemical Modulation. *Chem. Rev.* **2011**, *111*, 6064–6119.

(4)   Strum, J. C. Raf-1 Kinase Possesses Distinct Binding Domains for Phosphatidylserine and Phosphatidic Acid. *J. Biol. Chem.* **1996**, *271*, 8472–8480.

(5)   Rizzo, M. a; Shome, K.; Watkins, S. C.; Romero, G. The Recruitment of Raf-1 to Membranes Is Mediated by Direct Interaction with Phosphatidic Acid and Is Independent of Association with Ras. *J. Biol. Chem.* **2000**, *275*, 23911–23918.

(6)   Fang, Y.; Vilella-Bach, M.; Bachmann, R.; Flanigan, a; Chen, J. Phosphatidic Acid-Mediated Mitogenic Activation of mTOR Signaling. *Science* **2001**, *294*, 1942–1945.

(7)   Foster, D. A.; Xu, L. Phospholipase D in Cell Proliferation and Cancer. *Mol. Cancer Res.* **2003**, *1*, 789–800.

(8)   Oliveira, T. G.; Di Paolo, G. Phospholipase D in Brain Function and Alzheimer's Disease. *Biochim. Biophys. Acta* **2010**, *1801*, 799–805.

(9)   Elvers, M.; Stegner, D.; Hagedorn, I.; Kleinschnitz, C.; Braun, A.; Kuijpers, M. E. J.; Boesl, M.; Chen, Q.; Heemskerk, J. W. M.; Stoll, G.; et al. Impaired alpha(IIb)beta(3) Integrin Activation and Shear-Dependent Thrombus Formation in Mice Lacking Phospholipase D1. *Sci. Signal.* **2010**, *3*, ra1.

(10)   Yang, Hongying; Roberts, M. F. Phosphohydrolase and Transphosphatidylation Reactions of Two Streptomyces Phospholipase D Enzymes : Covalent versus Noncovalent Catalysis. *Protein Sci.* **2003**, *12*, 2087–2098.

(11)   Ponting, C. P.; Kerr, I. D. A Novel Family of Phospholipase D Homologues That Includes Phospholipid Synthases and Putative Endonucleases: Identification of Duplicated Repeats and Potential Active Site Residues. *Protein Sci.* **1996**, *5*, 914–922.

(12)   Bader, M. F.; Vitale, N. . Phospholipase D in Calcium-Regulated Exocytosis: Lessons from Chromaffin Cells. *Biochim. Biophys. Acta* **2009**, *1791*, 936–941.

(13)   Freyberg, Z.; Bourgoin, S.; Shields, D. Phospholipase D2 Is Localized to the Rims of the Golgi Apparatus in Mammalian Cells. *Mol. Biol. Cell* **2002**, *13*, 3930–3942.

(14)   Freyberg, Z.; Siddhanta, A.; Shields, D. "Slip, Sliding Away": Phospholipase D and the Golgi Apparatus. *Trends Cell Biol.* **2003**, *13*, 540–546.

(15)   Freyberg, Z.; Sweeny, D.; Siddhanta, A.; Bourgoin, S.; Frohman, M.; Shields, D. Intracellular Localization of Phospholipase D1 in Mammalian Cells. *Mol. Biol. Cell* **2001**, *12*, 943–955.

(16)   Nozawa, Y. Roles of Phospholipase D in Apoptosis and pro-Survival. *Biochim. Biophys. Acta* **2002**, *1585*, 77–86.

(17)   Scott, S. a; Selvy, P. E.; Buck, J. R.; Cho, H. P.; Criswell, T. L.; Thomas, A. L.; Armstrong, M. D.; Arteaga, C. L.; Lindsley, C. W.; Brown, H. A. Design of Isoform-Selective Phospholipase D Inhibitors That Modulate Cancer Cell Invasiveness. *Nat. Chem. Biol.* **2009**, *5*, 108–117.

(18)   Kanaho, Y.; Funakoshi, Y.; Hasegawa, H. Phospholipase D Signaling and Its Involvement in Neurite Outgrowth. *Biochim. Biophys. Acta* **2009**, *1791*, 898–904.

(19)   Klein, J.; Chalifa, V.; Liscovitch, M.; Loffelholz, K. Role of Phospholipse D Activation in Nervous System Physiology and Pathophysiology. *J. Neurochem.* **1995**, *65*, 1445–1455.

(20)   Klein, J. Funtions and Pathophysiological Roles of Phospholipase D in the Brain. *J. Neurochem.* **2005**, *6*, 1473–1487.

(21)   Kanfer, J. N.; Singh, I. N.; Pettegrew, D. G.; McCartney, D. G.; Sorrentino, G. Phospho-Lipid Metabolism in Alzheimer's Disease and in Human Cholinergic Cells. *J. Lipid Mediat. Cell Signal.* **1996**, *14*, 361–363.

(22)   Oliveira, T. G.; Chan, R. B.; Tian, H.; Laredo, M.; Shui, G.; Staniszewski, A.; Zhang, H.; Wang, L.; Kim, T.-W.; Duff, K. E.; et al. Phospholipase d2 Ablation Ameliorates Alzheimer's Disease-Linked Synaptic Dysfunction and Cognitive Deficits. *J. Neurosci.* **2010**, *30*, 16419–16428.

(23)   Haass, C.; Selkoe, D. J. Soluble Protein Oligomers in Neurodegeneration: Lessons from the Alzheimer's Amyloid Beta-Peptide. *Nat. Rev. Mol. Cell Biol.* **2007**, *8*.

(24)   Lambert, M. P.; Barlow, A. K.; Chromy, B. A.; Edwards, C.; Freed, R.; Liosatos, M.; Morgan, T. E.; Rozovsky, I.; Trommer, B.; Viola, K. L.; Wals, P.; Zhang, C.; Finch, C. E.; Kraft, G. A.; Klein, W. L. Diffusable, Nonfibrillar Ligands Derived from Abetal-42 Are Potent Central Nervous System Neurotoxins. *Proc. Natl. Acad. Sci. U. S. A.* **1998**, *95*, 6448–6453.

(25) Vitolo, O. V.; Sant'Angelo, A.; Costanzo, V.; Battaglia, F.; Arancio, O.; Shelanski, M. Amyloid Beta-Peptide Inhibition of the PKA/CREB Pathway and Long-Term Potentiation: Reversibility by Drugs That Enhance cAMP Signaling. *Proc. Natl. Acad. Sci. U. S. A.* **2002**, *99*, 13217–13221.

(26) Foster, D. A.; Xu, L. Phospholipase D in Cell Proliferation and Cancer. *Mol. Cancer Res.* **2003**, *1*, 789–800.

(27) Snider, A. J.; Zhang, Z.; Xie, Y.; Meier, K. E. Epidermal Growth Factor Increases Lysophosphatidic Acid Production in Human Ovarian Cancer Cells: Roles for Phospholipase D2 and Receptor Transactivation. *Am. J. Physiol. Cell Physiol.* **2010**, *298*, C163–70.

(28) Park, M. H.; Ahn, B.-H.; Hong, Y.-K.; Min, D. S. Overexpression of Phospholipase D Enhances Matrix Metalloproteinase-2 Expression and Glioma Cell Invasion via Protein Kinase C and Protein Kinase A/NF-kappaB/Sp1-Mediated Signaling Pathways. *Carcinogenesis* **2009**, *30*, 356–365.

(29) Fibrosarcoma, E. H.; Exton, H.; Williger, B.; Ho, W.; Exton, J. H. Phospholipase D Mediates Matrix Metalloproteinase-9 Secretion in Phorbol Ester-Stimulated Human Fibrosarcoma Cells. *J. Biol. Chem.* **1999**, *274*, 735.

(30) Hui, L.; Abbas, T.; Pielak, R. M.; Joseph, T.; Bargonetti, J. .; Foster, D. A. Phospholipase D Elevates the Level of MDM2 and Suppresses DNA Damage-Induced Increases in p53. *Mol. Cell. Biol.* **2004**, *24*, 5677.

(31) Hui, L.; Zheng, Y.; Yan, Y.; Bargonetti, J.; Foster, D. A. Mutant p53 in MDA-MB-231 Breast Cancer Cells Is Stabilized by Elevated Phospholipase D Activity and Contributes to Survival Signals Generated by Phospholipase D. *Oncogene* **2006**, *25*, 7305.

(32) Chen, Y.; Rodrik, V.; Foster, D. A. Alternative Phospholipase D/mTOR Survival Signal in Human Breast Cancer Cells. *Oncogene* **2005**, *24*, 672–679.

(33) Zhao, C.; Du, G.; Skowronek, K.; Frohman, M. A.; Bar-Saqi, D. Phospholipase D2-Generated Phosphatidic Acid Couples EGFR Stimulation to Ras Activation by SOS. *Nat. Cell Biol.* **2007**, *9*, 706–712.

(34) Buchanan, F. G.; Mcreynolds, M.; Couvillon, A.; Kam, Y.; Holla, V. R.; Dubois, R. N.; Exton, J. H. Requirement of Phospholipase D1 Activity in H-Ras V12 -Induced Transformation. *Proc. Natl. Acad. Sci. U. S. A.* **2005**, *102*, 1638–1642.

(35) Goodsell, D. S. The Molecular Perspective: The Ras Oncogene. *Oncologist* **1999**, *4*, 263–264.

(36)   Downward, J. Targeting RAS Signalling Pathways in Cancer Therapy. *Nat. Rev. Cancer* **2003**, *3*, 11–22.

(37)   Rizzo, M. A.; Shome, K.; Vasudevan, C.; Stolz, D. B.; Sung, T.; Frohman, M. A.; Watkins, S. C.; Romero, G. Phospholipase D and Its Product , Phosphatidic Acid , Mediate Agonist-Dependent Raf-1 Translocation to the Plasma Membrane and the Activation of the Mitogen-Activated Protein Kinase Pathway. *J. Biol. Chem.* **1999**, *274*, 1131–1139.

(38)   Stanacev, N. Z.; Stuhne-Sekalec, L. On the Mechanism of Enzymatic Phosphatidylation. Biosynthesis of Cardiolipin Catalyzed by Phospholipase D. *Biochim. Biophys. Acta* **1970**, *210*, 350–352.

(39)   Brown, H. A.; Henage, L. G.; Preininger, A. M.; Xiang, Y.; Exton, J. H. Biochemical Analysis of Phospholipase D. *Methods Enzymol.* **2007**, *434*, 49–87.

(40)   Tou, J. S.; Urbizo, C. Diethylstilbestrol Inhibits Phospholipase D Activity and Degranulation by Stimulated Human Neutrophils. *Steroids* **2008**, *73*, 215–221.

(41)   Tou, J. S.; Urbizo, C. Resveratrol Inhibits the Formation of Phosphatidic Acid and Diglyceride in Chemotactic Piptide- or Phorbol Ester-Stimulated Human Neutrophils. *Cell. Signal.* **2001**, *13*, 191–197.

(42)   Garcia, A.; Zheng, Y.; Zhao, C.; Toschi, A.; Fan, J.; Shraibman, N.; Brown, H. A.; Bar-Sagi, D.; Foster, D. A.; Arbiser, J. L. Honokiol Suppresses Survival Signals Mediated by Ras-Dependent Phospholipase D Activity in Human Cancer Cells. *Clin. Cancer Res.* **2008**, *14*, 4267–4274.

(43)   Puar, M. S.; Barrabee, E.; Hallade, M.; Patel, M. SCH420789: A Novel Fungal Metabolite with Phospholipase D Inhibitory Activity. *J. Antibiot. (Tokyo).* **2000**, *53*, 837–838.

(44)   McDonald, L. A.; Barbieri, L. R.; Bernan, V. S.; Janso, J.; Lassota, P.; Carter, G. T. 07H239-A, A New Cytotoxic Eremophilane Sesquiterpene from the Marine-Derived Xylariaceous Fungus LL-07H239. *J. Nat. Prod.* **2004**, *67*, 1565–1567.

(45)   Levy, B. D.; Hickey, L.; Morris, A. J.; Larvie, M.; Keledjian, R.; Petasis, N. A.; Bannenberg, G.; Serhan, C. N. Novel Polyisoprenyl Phosphates Block Phospholipase D and Human Neutrolphil Activation in Vitro and Murine Peritoneal Inflammation in Vivo. *Br. J. Pharmacol.* **2005**, *146*, 344–351.

(46)   Eisen, S. F.; Brown, H. A. Selective Estrogen Receptor (ER) Modulators Differentially Regulate Phospholipase D Catalytic Activity in ER-Negative Breast Cancer Cells. *Mol. Pharmacol.* **2002**, *62*, 911–920.

(47) Monovich, L.; Mugrage, B.; Quadros, E.; Toscano, K.; Tommasi, R.; LaVoie, S.; Liu, E.; Du, Z.; LaSala, D.; Boyar, W.; et al. Optimization of Halopemide for Phospholipase D2 Inhibition. *Bioorg. Med. Chem. Lett.* **2007**, *17*, 2310–2311.

(48) Loonen, A. J.; Soudijn, W. Halopemide, a New Psychotropic Agent. Cerebral Distribution and Receptor Interactions. *Pharm. Weekbl. Sci.* **1985**, *7*, 1–9.

(49) Lewis, J. a; Scott, S. a; Lavieri, R.; Buck, J. R.; Selvy, P. E.; Stoops, S. L.; Armstrong, M. D.; Brown, H. A.; Lindsley, C. W. Design and Synthesis of Isoform-Selective Phospholipase D (PLD) Inhibitors. Part I: Impact of Alternative Halogenated Privileged Structures for PLD1 Specificity. *Bioorg. Med. Chem. Lett.* **2009**, *19*, 1916–1920.

(50) Lavieri, R.; Scott, S. a; Lewis, J. a; Selvy, P. E.; Armstrong, M. D.; Alex Brown, H.; Lindsley, C. W. Design and Synthesis of Isoform-Selective Phospholipase D (PLD) Inhibitors. Part II. Identification of the 1,3,8-triazaspiro[4,5]decan-4-One Privileged Structure That Engenders PLD2 Selectivity. *Bioorg. Med. Chem. Lett.* **2009**, *19*, 2240–2243.

(51) Lavieri, R. R.; Scott, S. a; Selvy, P. E.; Kim, K.; Jadhav, S.; Morrison, R. D.; Daniels, J. S.; Brown, H. A.; Lindsley, C. W. Design, Synthesis, and Biological Evaluation of Halogenated N-(2-(4-Oxo-1-Phenyl-1,3,8-triazaspiro[4.5]decan-8-Yl)ethyl)benzamides: Discovery of an Isoform-Selective Small Molecule Phospholipase D2 Inhibitor. *J. Med. Chem.* **2010**, *53*, 6706–6719.

(52) O'Reilly, M. C.; Scott, S. A.; Brown, K. A.; Oguin, T. H.; Thomas, P. G.; Daniels, J. S.; Morrison, R.; Brown, H. A.; Lindsley, C. W. Development of Dual PLD1/2 and PLD2 Selective Inhibitors from a Common 1,3,8-Triazaspiro[4.5]decane Core: Discovery of ML298 and ML299 That Decrease Invasive Migration in U87-MG Glioblastoma Cells. *J. Med. Chem.* **2013**, *56*, 2695–2699.

(53) Schönherr, H.; Cernak, T. Profound Methyl Effects in Drug Discovery and a Call for New C-H Methylation Reactions. *Angew. Chem. Int. Ed. Engl.* **2013**, *52*, 12256–12267.

(54) O'Reilly, M, C; Oguin III, T. H.; Scott, S, A; Thomas, P. G.; Locuson, C. W.; Morrison, R. D.; Daniels, J. S. Brown, H, A; Lindsley, C, W. Discovery of a Highly Selective PLD2 Inhibitor, VU0468809 (ML395): A New Probe with Improved Physiochemical Properties and Broad Spectrum Antiviral Activity against Influenza Strains. *Unpubl. Results* **2014**.

Experimental for the discovery of PLD2 selective and PLD1/2 dual inhibitors ML298 and ML299

All reagents were purchased from Sigma-Aldrich Corp., TCI America, Rieke Metals, Inc. and were used without purification. Analytical thin-layer chromatography (TLC) was performed on 250 µm silica plates from Sorbent Technologies. Visualization was accomplished via UV light, and/or the use of ninhydrin, iodine, and potassium permanganate solutions followed by application of heat. Chromatography was performed using Silica Gel 60 (230-400 mesh) from Sorbent Technologies or Silica RediSep Rf flash columns on a CombiFlash Rf automated flash chromatography system. All ^{1}H and ^{13}C NMR spectra were recorded on a Bruker AV-400 (400 MHz) instrument. Chemical shifts are reported in ppm relative to residual solvent peaks as an internal standard set to δ 7.26 and δ 77.16 (CDCl$_3$). Data are reported as follows: chemical shift, multiplicity (s = singlet, d = doublet, t = triplet, q = quartet, p = pentet, br = broad, dd = doublet of doublets, dq = doublet of quartets, td = triplet of doublets, pd = pentet of doublets, m = multiplet), coupling constat (Hz), integration. Low resolution mass spectra (LCMS) were recorded on an Agilent 1200 LCMS with electrospray ionization. High resolution mass spectra (HRMS) were recorded on a Waters Qtof-API-US plus Acuity system with ES as the ion source. Analytical high performance liquid chromatography (HPLC) was performed on an Agilent 1200 analytical LCMS with UV detection at 214 nm and 254 nm along with ELSD detection. Chiral separations were performed on a Thar Investigator II supercritical fluid chromatograph (SFC) utilizing Chiralcel® OD, OD-Cl, OJ, and Chiralpak® IA columns. Optical rotations were acquired on a Jasco P-2000 polarimeter at 23 ^{0}C and 589 nm. The specific rotations were calculated

according to the equation $[\alpha]23/D = 100\alpha/l \times c$ where l is the path length in decimeters and c is the concentration in g/100 mL.


1-(3-fluorophenyl)-1,3,8-triazaspiro[4.5]decan-4-one (2.13). To a solution of 1-benzylpiperidin-4-one **2.9** (13.25 g, 70 mmol) in glacial acetic acid (70 mL) and water (12 mL) cooled to 0 °C was added 3-fluoroaniline (8.55 g, 77 mmol) and potassium cyanide (4.55 g, 70 mmol). The reaction was allowed to warm to room temperature and agitated for approximately 12 hours. The reaction was then cooled to 0 °C and ammonium hydroxide (18 M) was added dropwise until the solution pH was 11 or greater. The mixture was then extracted into dichloromethane and dried under reduced pressure to yield the crude product as a tan oil (20.5 g). The crude product was then immediately cooled to 0 °C and concentrated sulfuric acid (18 M, 120 mL) was added dropwise with vigorous stirring. The reaction was allowed to warm to room temperature and agitated for approximately 12 hours. The reaction was then cooled to 0 °C and ammonium hydroxide (18 M) was added dropwise until the solution pH was 11 or greater. The mixture was then extracted into dichloromethane and dried under reduced pressure to afford a tan solid (15.78 g, 48.25 mmol, 68%). 1H NMR (400.1 MHz, CDCl3) δ (ppm): 7.51 - 7.37 (m, 7H), 6.67 - 6.47 (m, 4H), 4.27 (s, 1H), 3.64 (s, 2H), 2.95 - 2.87 (m, 2H), 2.53 - 2.44 (m, 2H), 2.29 - 2.21 (m, 2H), 2.07 (d, $J = 13$ Hz, 2H); 13C NMR (100.6 MHz, CDCl3) δ (ppm): 178.0, 162.6, 145.7, 138.3, 130.5, 129.1 (2C), 128.4 (2C), 127.2, 111.8, 106.1, 103.1, 63.1, 58.5, 48.7 (2C), 34.8, 31.5; HRMS (TOF, ESI)

C$_{19}$H$_{23}$N$_3$OF [M+H]+ calculated 328.1825, found 328.1827; LC-MS: rt (min) = 1.855; LRMS (ESI) m/z = 328.2. 1-Benzyl-4-((3-fluorophenyl)amino)piperidine-4-carboxamide (15.78 g, 48.25 mmol), trimethyl orthoformate (80 mL), and glacial acetic acid (40 mL) were combined and subjected to microwave irradiation at 150 °C for 15 minutes. The mixture was adjusted to pH 12 with ammonium hydroxide (18 M) and extracted into dichloromethane and dried under reduced pressure. This material was then added to a suspension of sodium borohydride (4.56 g, 120.6 mmol) in methanol (150 mL) and stirred for about 3 hours. The reaction was quenched with water, extracted into dichloromethane, and dried under reduced pressure. The material was then chromatographed on a 330 g flash column (Teledyne) as follows: (1) a gradient from 0-80% ethyl acetated in hexanes over 10 minutes was run, and on the same column (2) a gradient from 0-10 % methanol in dichloromethane was run. The purity of the isolated intermediate was established via LCMS, rt (min) 1.723; LRMS (ESI) m/z = 340.1. This intermediate (1.94 g) was immediately dissolved in methanol (40 mL) and glacial acetic acid (10 mL), and treated with palladium on carbon (cat., 80 mg) under an atmosphere of hydrogen. After about 36 hours the reaction mixture was filtered through celite, concentrated under reduced pressure, diluted with water, made alkaline with saturated sodium bicarbonate and extracted 8 times into dichloromethane to afford **2.13** as a white solid (1.37 g, 5.49 mmol, 11 %). 1H NMR (400.1 MHz, DMSO-*d6*) δ (ppm): 8.67 (s, 1H), 7.20 (q, *J* = 8 Hz, 1H), 6.73 (d, *J* = 8 Hz, 1H), 6.62 (d, *J* = 13 Hz, 1H), 6.52 - 6.46 (m, 1H), 4.57 (s, 2H), 3.20 - 3.09 (m, 3H), 2.91 - 2.82 (m, 2H), 2.46 - 2.36 (m, 2H), 1.48 (d, *J* = 14 Hz, 2H); 13C NMR (100.6 MHz, DMSO-*d6*) δ (ppm): 176.0, 164.3, 145.0, 130.1, 109.3, 103.1, 100.2, 58.8, 58.6, 42.1 (2C), 28.9 (2C); HRMS (TOF, ESI) C13H17N3OF [M+H]+ calculated 250.1356, found 250.1351; LC-MS: rt (min) = 1.394; LRMS (ESI) m/z = 250.1.
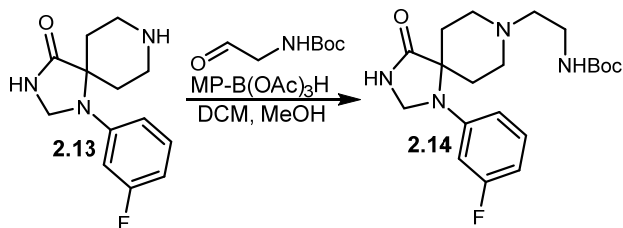
tert-Butyl-(2-3-fluorophenyl)-4-oxo-1,3,8-triazasprio[4.5]decan-8-yl)ethyl)carbamate

(2.14). 1-(3-fluorophenyl)-1,3,8-triazaspiro[4.5]decan-4-one **2.13** (1370 mg, 5.49 mmol) and *tert*-butyl (2-oxoethyl)carbamate (961 mg, 6.03 mmol) were combined and dissolved in dichloromethane (25 mL) and methanol (10 mL) and stirred for about 30 minutes at room temperature. After about 30 minutes macroporous triacetoxyborohydride (3 g, 7.26 mmol) was added to the reaction and after 14 hours an additional amount of *tert*-butyl (2-oxoethyl)carbamate (200 mg, 1.25 mmol) was added to drive the reaction to completion. After about 24 hours the reaction mixture was filtered through celite and concentrated under reduced pressure. The crude compound was chromatographed on an 80 g flash column eluting in a gradient of 0-10 % methanol in dichloromethane to afford **2.14** as a white solid (1.64 g, 4.18 mmol, 76 %). ^{1}H NMR (400.1 MHz, DMSO-d_6) δ (ppm): 8.69 (s, 1H), 7.22 (q, J = 8 Hz, 1H), 6.72 - 6.63 (m, 2H), 6.60 - 6.49 (m, 2H), 4.58 (s, 2H), 2.83 - 2.75 (m, 2H), 2.74 - 2.65 (m, 2H), 2.61 - 2.48 (m, 2H), 2.42 - 2.35 (m, 2H), 1.91 (s, 2H), 1.55 (d, J = 13 Hz, 2H), 1.39 (s, 9H); ^{13}C NMR (100.6 MHz, DMSO-d_6) δ (ppm): 175.8, 161.9, 155.6, 145.0, 130.4, 109.4, 103.2, 100.3, 77.5, 58.7, 58.1, 57.4, 49.3 (2C), 37.6, 28.3 (3C), 28.1 (2C); HRMS (TOF, ESI) $C_{20}H_{30}N_4O_3F$ [M+H]+ calculated 393.2302, found 393.2301; LC-MS: rt (min) = 1.966; LRMS (ESI) m/z = 393.2.
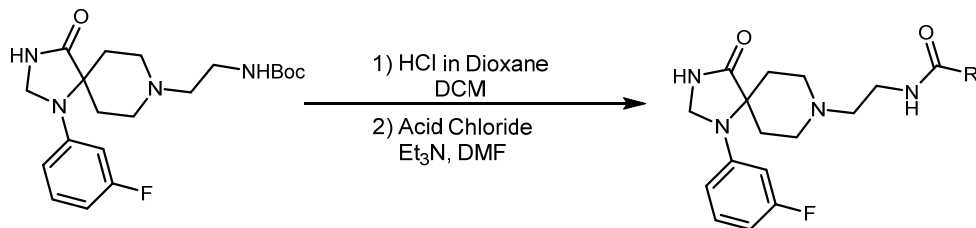
That starting material (1 eq.) was dissolved in DCM (0.1 M) and a solution of HCl in Dioxane (4 M, 30 eq.) was added to the mixture. It was allowed to stir until consumption of starting material was determined by LC-MS. The crude mixture was then concentrated *in vacuo,* and was then redissolved in DMF (0.1 M). Triethylamine (5 eq.) followed by acid chloride (1.5 eq.) were added to this stirred mixture and the reaction was quenched in less than ~10 minutes, determined by consumption of starting material seen via LC-MS. The reaction was quenched with water/brine and was extracted 3X with ethyl acetate. The organic extract was concentrated and the product was purified via reverse phase HPLC eluting with MeCN/H$_2$O/TFA to afford the product as a white solid trifluoroacetic acid salt (50-80%).

ML298
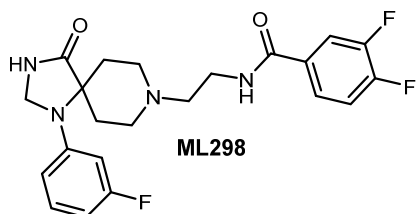
3,4-difluoro-*N*-(2-(1-(3-fluorophenyl)-4-oxo-1,3,8-triazaspiro[4.5]decan-8-yl)ethyl)benzamide

^{1}H NMR (400.1 MHz, MeOD (D$_4$)) δ (ppm): 7.86-7.79 (m, 1H); 7.77-7.72 (m, 1H); 7.43-7.35 (m, 1H); 7.25 (q, *J* = 7.5 Hz, 1H); 6.76 (dd, *J$_1$* = 11.4 Hz, *J$_2$* = 2.2 Hz, 1H); 6.67 (dt, *J$_1$* = 12.4 Hz, *J$_2$* = 2.3 Hz, 1H); 6.58 (td, *J$_1$* = 8.3 Hz, *J$_2$* = 1.5 Hz, 1H); 4.74 (s, 2H); 3.95-3.86 (m, 2H); 3.83-3.72 (m, 4H); 3.44 (t, *J* = 5.9 Hz, 2H); 2.97 (td, *J$_1$* = 13.6 Hz, *J$_2$* = 3.8 Hz, 2H); 2.05 (d, *J* = 15.2 Hz, 2H). ^{13}C NMR (100.6 MHz, MeOD (D$_4$)) δ (ppm): 176.9, 168.9, 165.3

(d, J = 243 Hz), 154.0 (dd, J_1 = 253 Hz, J_2 = 13 Hz), 151.4 (dd, J_1 = 248 Hz, J_2 = 13 Hz), 145.8 (d, J = 11 Hz), 132.1-131.9 (m), 131.8 (d, J = 10 Hz), 125.7 (dd, J_1 = 7 Hz, J_2 = 4 Hz), 118.6 (d, J = 18 Hz), 118.1 (d, J = 18 Hz), 111.8, 106.6 (d, J = 22 Hz), 103.0 (d, J = 28 Hz), 60.6, 58.5, 58.0, 51.0, 36.4, 28.1. HRMS (TOF, ES+) $C_{22}H_{24}N_4O_2F_3$ [M+H]$^+$ calc. mass 433.1851, found 433.1849.
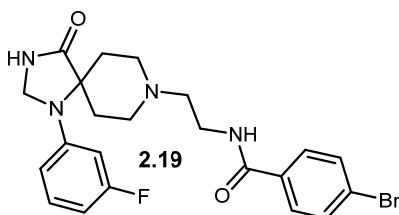
4-bromo-*N*-(2-(1-(3-fluorophenyl)-4-oxo-1,3,8-triazaspiro[4.5]decan-8-yl)ethyl)benzamide

^{1}H NMR (400.1 MHz, MeOD (D$_4$)) δ (ppm): 7.81 (d, J = 8.5 Hz, 2H); 7.67 (d, J = 8.6 Hz, 2H); 7.27 (q, J = 7.4 Hz, 1H); 6.76 (dd, J_1 = 8.4 Hz, J_2 = 2.1 Hz, 1H); 6.69 (dt, J_1 = 12.3 Hz, J_2 = 2.3 Hz, 1H); 6.59 (td, J_1 = 8.3 Hz, J_2 = 1.6 Hz, 1H); 4.47 (s, 2H); 3.96-3.86 (m, 2H); 3.84-3.72 (m, 4H); 3.44 (t, J = 5.8 Hz, 2H); 2.96 (td, J_1 = 14.9 Hz, J_2 = 3.8 Hz, 2H); 2.07 (d, 15.1 Hz, 2H). ^{13}C NMR (100.6 MHz, MeOD (D$_4$)) δ (ppm): 176.9, 170.4, 165.3 (d, J = 243 Hz), 145.8 (d, J = 10 Hz), 133.6, 132.9, 131.8 (d, J = 10 Hz), 130.4, 127.8, 111.9, 106.7 (d, J = 22 Hz), 102.1 (d, J = 27 Hz), 60.6, 58.5, 58.2, 51.1, 36.5, 28.2. HRMS (TOF, ES+) $C_{23}H_{27}N_4O_2BrF$ [M+H]$^+$ calc. mass 475.1145, found 474.1142.

2.22
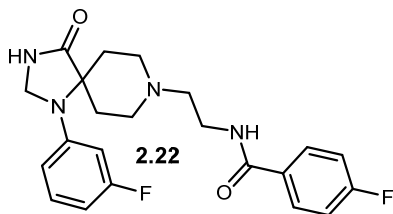
4-fluoro-*N*-(2-(1-(3-fluorophenyl)-4-oxo-1,3,8-triazaspiro[4.5]decan-8-yl)ethyl)benzamide

^{1}H NMR (400.1 MHz, MeOD (D$_4$)) δ (ppm): 7.99-7.93 (m, 2H); 7.30-7.18 (m, 3H); 6.77 (dd, J_1 = 8.3 Hz, J_2 = 2.3 Hz, 1H); 6.68 (dt, J_1 = 12.4 Hz, J_2 = 2.3 Hz, 1H); 6.58 (td, J_1 = 8.3 Hz, J_2 = 1.5 Hz, 1H); 4.74 (s, 2H); 3.95-3.85 (m, 2H); 3.84-3.72 (m, 4H); 3.44 (t, J = 5.8 Hz, 2H); 2.98 (td, J_1 = 14.8 Hz, J_2 = 3.7 Hz, 2H); 2.06, (d, J = 15.2 Hz, 2H). ^{13}C NMR (100.6 MHz, MeOD (D$_4$)) δ (ppm): 176.9, 170.2, 166.6 (d, J = 252 Hz), 165.3 (d, J = 243 Hz), 145.8 (d, J = 11 Hz), 131.8 (d, J = 10 Hz), 131.2 (d, J = 9 Hz), 130.9 (d, J = 3 Hz), 116.5 (d, J = 22 Hz), 111.8, 106.6 (d, J = 22 Hz), 103.0 (d, J = 27 Hz), 60.6, 58.5, 58.2, 51.0, 36.4, 28.1. HRMS (TOF, ES+) C$_{23}$H$_{27}$N$_4$O$_2$BrF [M+H]$^+$ calc. mass 415.1946, found 415.1943.
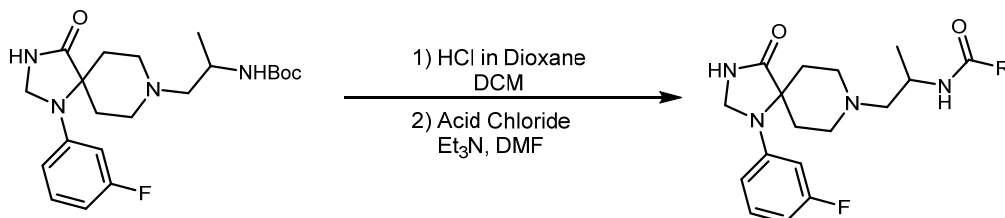
The starting material (1 eq.) was dissolved in DCM (0.1 M) and a solution of HCl in Dioxane (4 M, 30 eq.) was added to the mixture. It was allowed to stir until consumption of starting material was determined by LC-MS. The crude mixture was then concentrated *in vacuo*, and was then redissolved in DMF (0.1 M). Triethylamine (5 eq.) followed by acid chloride (1.5 eq.) were added to this stirred mixture and the reaction was quenched in less than 30 minutes, determined by consumption of starting material seen via LC-MS. The reaction was quenched with water/brine and was extracted 3X with ethyl acetate. The

organic extract was concentrated and the product was purified via reverse phase HPLC eluting with MeCN/H$_2$O/TFA to afford the product as a white solid trifluoroacetic acid salt (50-80%).

2.18
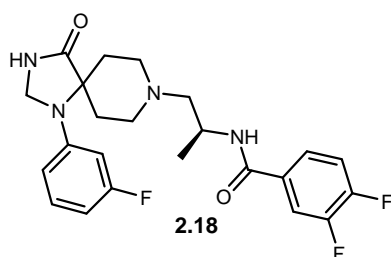
(*S*)-3,4-difluoro-*N*-(1-(1-(3-fluorophenyl)-4-oxo-1,3,8-triazaspiro[4.5]decan-8-yl)propan-2-yl)benzamide

^{1}H NMR (400.1 MHz, MeOD (D$_4$)) δ (ppm): 7.92-7.83 (m, 1H); 7.81-7.76 (m, 1H); 7.39 (q, *J* = 7.6 Hz, 1H); 7.25 (d, *J* = 7.2 Hz, 1H); 6.75 (d, *J$_1$* = 8.4 Hz, 1H); 6.68 (d, *J$_1$* = 12.3 Hz, 1H); 6.62-6.53 (m, 1H); 4.73 (s, 2H); 4.68-4.58 (m, 1H); 4.05-3.78 (m, 3H); 3.65-3.51 (m, 1H); 3.45-3.32 (m, 2H); 3.04-2.85 (m, 2H); 2.04 (dd, *J$_1$* = 24.6 Hz, *J$_2$* = 16.4 Hz, 2H); 1.38 (d, *J* = 6.8 Hz, 3H). ^{13}C NMR (125 MHz, MeOD (D$_4$)) δ (ppm): 176.9, 168.7, 165.3 (d, *J* = 242 Hz), 154.1 (dd, *J$_1$* = 253 Hz, *J$_2$* = 13 Hz), 151.4 (dd, *J$_1$* = 248 Hz, *J$_2$* = 13 Hz), 145.8 (d, *J* = 10 Hz), 132.1, 131.8 (d, *J* = 10 Hz), 125.9 (dd, *J$_1$* = 7 Hz, *J$_2$* = 3 Hz), 118.5 (d, *J* = 18 Hz), 118.3 (d, *J* = 21 Hz), 112.0, 106.8 (d, *J* = 22 Hz), 103.2 (d, *J* = 26 Hz), 63.8, 60.6, 58.6, 52.3, 50.4, 43.6, 28.2, 18.7. HRMS (TOF, ES+) C$_{23}$H$_{27}$N$_4$O$_2$BrF [M+H]$^+$ calc. mass 447.2008, found 447.2009. Specific rotation $[\alpha]_{D}^{23}$ = +26 (*c* = 0.5, MeOH).

2.20
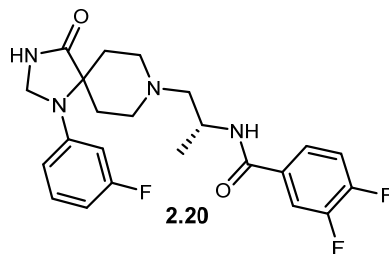
(*R*)-3,4-difluoro-*N*-(1-(1-(3-fluorophenyl)-4-oxo-1,3,8-triazaspiro[4.5]decan-8-yl)propan-2-yl)benzamide

^{1}H NMR (400.1 MHz, MeOD (D$_4$)) δ (ppm): 7.92-7.83 (m, 1H); 7.81-7.76 (m, 1H); 7.44-7.36 (m, 1H); 7.25 (q, *J* = 7.2 Hz, 1H); 6.75 (dd, *J$_1$* = 8.4 Hz, *J$_2$* = 2.3 Hz, 1H); 6.68 (dt, *J$_1$* = 12.3 Hz, *J$_2$* = 2.3 Hz, 1H); 6.59 (td, *J$_1$* = 8.2 Hz, *J$_2$* = 2.0 Hz, 1H); 4.73 (s, 2H); 4.68-4.58 (m, 1H); 3.99-3.78 (m, 3H); 3.58-3.50 (m, 1H); 3.41-3.32 (m, 2H); 2.98-2.85 (m, 2H); 2.04 (dd, *J$_1$* = 24.6 Hz, *J$_2$* = 16.4 Hz, 2H); 1.38 (d, *J* = 6.8 Hz, 3H). ^{13}C NMR (125 MHz, MeOD (D$_4$)) δ (ppm): 176.9, 168.7, 165.3 (d, *J* = 242 Hz), 163.1 (d, *J* = 34 Hz), 154.1 (dd, *J$_1$* = 253 Hz, *J$_2$* = 13 Hz), 151.4 (dd, *J$_1$* = 248 Hz, *J$_2$* = 13 Hz), 145.8 (d, *J* = 10 Hz), 132.1, 131.8 (d, *J* = 10 Hz), 125.9 (dd, *J$_1$* = 7 Hz, *J$_2$* = 3 Hz), 118.4 (t, *J* = 20 Hz), 112.0, 106.8 (d, *J* = 22 Hz), 103.2 (d, *J* = 26 Hz), 63.8, 60.6, 58.6, 52.3, 50.4, 43.6, 28.2, 18.7. HRMS (TOF, ES+) C$_{23}$H$_{27}$N$_4$O$_2$BrF [M+H]$^+$ calc. mass 447.2008, found 447.2009. Specific rotation [α]$\frac{23}{D}$ = -34 (*c* = 0.5, MeOH).

ML299
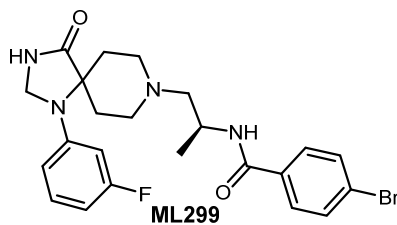
(*S*)-4-bromo-*N*-(1-(1-(3-fluorophenyl)-4-oxo-1,3,8-triazaspiro[4.5]decan-8-yl)propan-2-yl)benzamide

^{1}H NMR (400.1 MHz, MeOD (D$_4$)) δ (ppm): 7.84 (d, *J* = 8.6 Hz, 2H); 7.67 (d, *J* = 8.7 Hz, 2H); 7.25 (q, *J* = 7.1 Hz, 1H); 6.76 (dd, *J$_1$* = 8.4 Hz, *J$_2$* = 2.3 Hz, 1H); 6.68 (dt, *J$_1$* = 12.4 Hz, *J$_2$* = 2.3 Hz, 1H); 6.59 (td, *J$_1$* = 8.3 Hz, *J$_2$* = 2.0 Hz, 1H); 4.73 (s, 2H); 4.68-4.59 (m, 1H);

4.01-3.83 (m, 3H); 3.60-3.52 (m, 1H); 3.44-3.33 (m, 2H); 3.00-2.86 (m, 2H); 2.04 (dd, J_1 = 24.3 Hz, J_2 = 15.6 Hz, 2H); 1.38 (d, J = 6.9 Hz, 3H). ^{13}C NMR (125 MHz, MeOD (D$_4$)) δ (ppm): 176.9, 170.2, 165.25 (d, J = 242 Hz), 145.7 (d, J = 10 Hz), 133.8, 132.8, 131.8 (d, J = 10 Hz), 130.6, 127.7, 112.0, 106.8 (d, J = 22 Hz), 103.2 (d, J = 26 Hz), 63.9, 60.6, 58.5, 52.3, 50.5, 43.7, 28.2, 18.7. HRMS (TOF, ES+) $C_{23}H_{27}N_4O_2BrF$ [M+H]$^+$ calc. mass 489.1301, found 489.1299. Specific rotation $[\alpha]\frac{23}{D}$ = +36 (c = 0.5, MeOH).
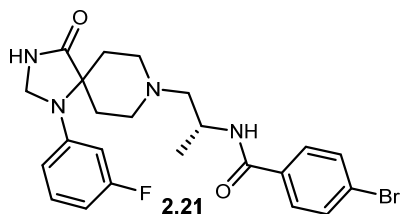
(*R*)-4-bromo-*N*-(1-(1-(3-fluorophenyl)-4-oxo-1,3,8-triazaspiro[4.5]decan-8-yl)propan-2-yl)benzamide

^{1}H NMR (400.1 MHz, MeOD (D$_4$)) δ (ppm): 7.84 (d, J = 8.6 Hz, 2H); 7.67 (d, J = 8.7 Hz, 2H); 7.25 (q, J = 7.1 Hz, 1H); 6.76 (dd, J_1 = 8.4 Hz, J_2 = 2.3 Hz, 1H); 6.68 (dt, J_1 = 12.4 Hz, J_2 = 2.3 Hz, 1H); 6.59 (td, J_1 = 8.3 Hz, J_2 = 2.0 Hz, 1H); 4.73 (s, 2H); 4.68-4.59 (m, 1H); 4.01-3.83 (m, 3H); 3.54 (dd, J_1 = 12.1 Hz, J_2 = 3.8 Hz, 1H); 3.44-3.33 (m, 2H); 3.00-2.86 (m, 2H); 2.04 (dd, J_1 = 24.3 Hz, J_2 = 15.6 Hz, 2H); 1.38 (d, J = 6.9 Hz, 3H). ^{13}C NMR (125 MHz, MeOD (D$_4$)) δ (ppm): 176.9, 170.2, 165.25 (d, J = 242 Hz), 145.7 (d, J = 10 Hz), 133.8, 132.8, 131.8 (d, J = 10 Hz), 130.6, 127.7, 112.0, 106.8 (d, J = 22 Hz), 103.2 (d, J = 26 Hz), 63.9, 60.6, 58.5, 52.3, 50.5, 43.7, 28.2, 18.7. HRMS (TOF, ES+) $C_{23}H_{27}N_4O_2BrF$ [M+H]$^+$ calc. mass 489.1301, found 489.1302. Specific rotation $[\alpha]\frac{23}{D}$ = -52 (c = 0.5, MeOH).

2.23
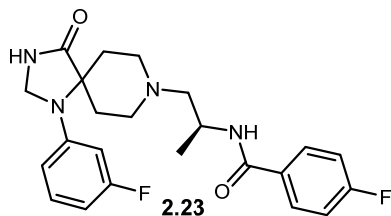
(*S*)-4-fluoro-*N*-(1-(1-(3-fluorophenyl)-4-oxo-1,3,8-triazaspiro[4.5]decan-8-yl)propan-2-yl)benzamide

^{1}H NMR (400.1 MHz, MeOD (D$_4$)) δ (ppm): 8.11-7.92 (m, 2H); 7.32-7.14 (m, 3H); 6.76 (d, 8.2 Hz, 1H); 6.69 (d, *J* = 12.3 Hz, 1H); 6.59 (t, *J* = 7.5 Hz, 1H); 4.73 (s, 2H); 4.69-4.57 (m, 1H); 4.04-3.81 (m, 3H); 3.56 (d, *J* = 9.9 Hz, 1H); 3.45-3.32 (m, 2H); 3.03-2.85 (m, 2H); 2.05 (dd, *J$_1$* = 26.3 Hz, *J$_2$* = 14.9 Hz, 2H); 1.38 (d, *J* = 6.6 Hz, 3H). ^{13}C NMR (125 MHz, MeOD (D$_4$)) δ (ppm): 176.9, 170.2, 166.6 (d, *J* = 251 Hz), 165.3 (d, *J* = 242 Hz), 145.8 (d, *J* = 10 Hz), 131.8 (d, *J* = 10 Hz), 131.4 (d, *J* = 9 Hz), 131.0, 116.4 (d, *J* = 23 Hz), 112.01, 106.7 (d, *J* = 22 Hz), 103.2 (d, *J* = 26 Hz), 64.0, 60.6, 58.5, 52.3, 50.5, 43.7, 28.2, 18.7. HRMS (TOF, ES+) C$_{23}$H$_{27}$N$_4$O$_2$BrF [M+H]$^+$ calc. mass 429.2102, found 429.2099. Specific rotation [α]$\frac{23}{D}$ = +37 (*c* = 0.5, MeOH).

2.24
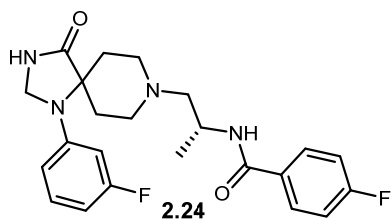
(*R*)-4-fluoro-*N*-(1-(1-(3-fluorophenyl)-4-oxo-1,3,8-triazaspiro[4.5]decan-8-yl)propan-2-yl)benzamide

^{1}H NMR (400.1 MHz, MeOD (D$_4$)) δ (ppm): 8.026-7.96 (m, 2H); 7.29-7.19 (m, 3H); 6.75 (dd, *J$_1$* = 8.4 Hz, *J$_2$* = 2.3 Hz, 1H); 6.69 (dt, *J$_1$* = 12.3 Hz, *J$_2$* = 2.4 Hz, 1H); 6.59 (td, *J$_1$* = 8.3 Hz, *J$_2$* = 2.2 Hz, 1H); 4.73 (s, 2H); 4.68-4.58 (m, 1H); 3.96-3.78 (m, 3H); 3.58-3.47 (m, 1H); 3.39-3.32 (m, 2H); 2.98-2.86 (m, 2H); 2.03 (dd, *J$_1$* = 24.7 Hz, *J$_2$* = 15.4 Hz, 2H); 1.38 (d, *J* = 6.8 Hz, 3H). ^{13}C NMR (125 MHz, MeOD (D$_4$)) δ (ppm): 176.9, 170.2, 166.6 (d, *J* = 251 Hz),

165.3 (d, J = 242 Hz), 145.8 (d, J = 10 Hz), 131.8 (d, J = 10 Hz), 131.4 (d, J = 9 Hz), 131.0,

116.4 (d, J = 23 Hz), 112.01, 106.7 (d, J = 22 Hz), 103.2 (d, J = 26 Hz), 64.0, 60.6, 58.5,

52.3, 50.5, 43.7, 28.2, 18.7. HRMS (TOF, ES+) $C_{23}H_{27}N_4O_2BrF$ $[M+H]^+$ calc. mass

429.2102, found 429.2103. Specific rotation $[\alpha]\frac{23}{D}$ = -47 (c = 0.5, MeOH).

Experimental for discovery of 80-fold selective phospholipase D2 inhibitor with enhanced physiochemical properties and antiviral activity

All reagents were purchased from Sigma-Aldrich Corp., TCI America, Rieke Metals, Inc. and were used without purification. Analytical thin-layer chromatography (TLC) was performed on 250 μm silica plates from Sorbent Technologies. Visualization was accomplished via UV light, and/or the use of ninhydrin, iodine, and potassium permanganate solutions followed by application of heat. Chromatography was performed using Silica Gel 60 (230-400 mesh) from Sorbent Technologies or Silica RediSep Rf flash columns on a CombiFlash Rf automated flash chromatography system. All ^{1}H and ^{13}C NMR spectra were recorded on a Bruker AV-400 (400 MHz) instrument. Chemical shifts are reported in ppm relative to residual solvent peaks as an internal standard set to δ 7.26 and δ 77.16 (CDCl$_3$). Data are reported as follows: chemical shift, multiplicity (s = singlet, d = doublet, t = triplet, q = quartet, p = pentet, br = broad, dd = doublet of doublets, dq = doublet of quartets, td = triplet of doublets, pd = pentet of doublets, m = multiplet), coupling constat (Hz), integration. Low resolution mass spectra (LCMS) were recorded on an Agilent 1200 LCMS with electrospray ionization. High resolution mass spectra (HRMS) were recorded on a Waters Qtof-API-US plus Acuity system with ES as the ion source. Analytical high performance liquid chromatography (HPLC) was performed on an Agilent 1200 analytical LCMS with UV detection at 214 nm and 254 nm along with ELSD detection. Chiral separations were performed on a Thar Investigator II supercritical fluid chromatograph (SFC) utilizing Chiralcel® OD, OD-Cl, OJ, and Chiralpak® IA columns. Optical rotations were acquired on a Jasco P-2000 polarimeter at 23 ^{0}C and 589 nm. The specific rotations were calculated

according to the equation $[\alpha]23/D = 100\alpha/l \times c$ where l is the path length in decimeters and c is the concentration in g/100 mL.

(a) To an oven dried round-bottomed flask equipped with a magnetic stir bar under argon was added triazaspirone **2.26** starting material (1.00 g, 4.08 mmol, 1.00 eq.), diisopropyl ethyl amine (2.63 g, 3.55 mL, 20.38 mmol, 5.00 eq.), 4-dimethylaminopyridine (0.25 g, 2.04 mmol, 0.50 eq.), and those contents were dissolved in THF (41 mL). Di-*tert*-butyl dicarbonate (0.98 g, 4.48 mmol, 1.10 eq) was added, as a liquid, to the mixture at room temperature, and the reaction was stirred for 1.5 hours at room temperature. The solvent was then removed under reduced pressure, and the residual material was dissolved in diethyl ether (150 mL). That organic layer was washed with saturated brine (2 X 100 mL), dried with magnesium sulfate, filtered, and concentrated under reduced pressure to provide 1.487 g of crude **2.36** that was used in the next reaction without further purification.
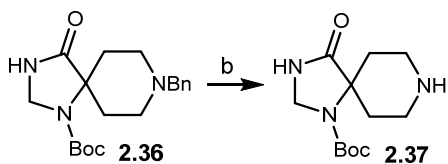
(b) Crude **2.36** (1.49 g), in a round-bottomed flask equipped with a magnetic stir bar, from the previous reaction was dissolved in methanol (82 mL), and 10% palladium on carbon (0.22 g, 0.20 mmol, 0.05 eq) was added to the solution under argon. The reaction was purged with hydrogen gas and was stirred under a hydrogen atmosphere for 15 hours. The reaction

was filtered through a celite pad to remove the palladium on carbon, and the filtrate was concentrated under reduced pressure to provide 1.10 g of crude **2.37**, which was used in the next reaction without further purification.
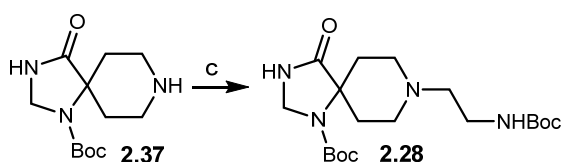
(c) Crude **2.37** (1.10 g), in a flame dried round-bottomed flask equipped with a magnetic stir bar, from the previous reaction was dissolved in DMF (8.2 mL). Potassium carbonate (2.82 g, 20.39 mmol, 5.00 eq) followed by *tert*-butyl (2-bromoethyl) carbamate (1.325 g, 4.91 mmol, 1.45 eq) were added to the reaction mixture at room temperature and it was stirred for 22 hours. The reaction was then partitioned between with ether (50 mL) and water (50 mL). The reaction mass was extracted with ether (3 X 50 mL), the combined organic was dried with magnesium sulfate, filtered, and concentrated under reduced pressure. The crude material was purified using flash column chromatography (0-20% methanol (w/ 10% NH$_4$OH) in ethyl acetate, stain with KMnO$_4$) to yield 1.01 g (62% over 3 steps) of the desired product **2.28**. ^{1}H NMR (400.1 MHz, MeOD) δ (ppm): 4.58 (s, 2H); 3.20 (t, J = 6.7 Hz, 2H); 2.83 (dt, J_1 = 11.8 Hz, J_2 = 3.6 Hz, 2H); 2.50 (t, J = 6.8 Hz, 2H); 2.39 (td, J_1 = 12.0 Hz, J_2 = 2.2 Hz, 2H); 1.91 (td, J_1 = 13.7 Hz, J_2 = 4.2 Hz, 2H); 1.65 (d, J = 13.1 Hz, 2H); 1.52 (s, 9H); 1.44 (s, 9H). ^{13}C NMR (100.6 MHz, MeOD) δ (ppm): 178.67, 158.39, 150.64, 84.45, 80.06, 62.41, 61.57, 58.73, 49.92, 38.44, 31.66, 28.75, 28.19. HRMS (TOF, ES+) C$_{19}$H$_{35}$N$_4$O$_5$ [M+H]$^+$ calc. mass 399.2607, found 399.2605.

2.28 → **2.38**
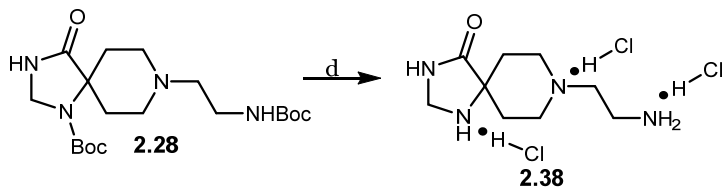
(d) To a solution of starting material **2.28** (0.94 g, 2.36 mmol, 1.00 eq) in dichloromethane (24 mL) was added 4 M HCl in dioxane (17.7 mL, 70.84 mmol, 30.00 eq), at room temperature all at once. The reaction was stirred for 18 hours at room temperature at which point the reaction was concentrated under reduced pressure to afford the *tris*-HCl salt **2.38** (0.726 g, quantitative yield). The product **2.38** was used in the next reaction without further purification.

2.38 → **2.34**
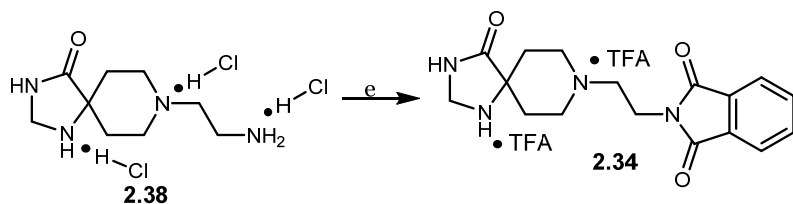
(e) The crude starting material **2.38** (0.726 g, 2.36 mmol, 1.00 eq) from the previous reaction, phthalic anhydride (0.524 g, 3.54 mmol, 1.50 eq), and diisopropyl ethyl amine (1.52 g, 2.06 mL, 11.80 mmol, 5.00 eq) were added to a microwave vial and dissolved in DMF (11.8 mL). The reaction was heated in a microwave reactor at 120 ˚C for 20 minutes. The crude mixture in DMF was injected onto a reverse phase HPLC (5-20% acetonitrile in water (0.1% trifluoroacetic acid)) for purification monitoring product elution at 221 nm to provide the *bis* trifluoroacetic acid salt **2.34** (956 mg, 73%). ^{1}H NMR (400.1 MHz, MeOD) δ (ppm): 7.93-7.88 (m, 2H); 7.87-7.81 (m, 2H); 4.57 (s, 2H); 4.13 (t, *J* = 5.89 Hz, 2H); 3.90-3.41 (m, 6H); 2.50-2.04 (m, 4H). ^{13}C NMR (100.6 MHz, MeOD) δ (ppm): 168.35, 160.26, 134.20, 131.88,

123.03, 57.17, 54.72, 48.38, 31.97, 27.70. HRMS (TOF, ES+) $C_{17}H_{21}N_4O_3$ [M+H]$^+$ calc. mass 329.1614, found 326.1617.
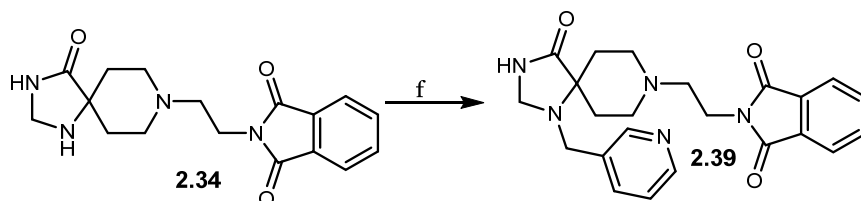
(f) A mixture of starting material **2.34** (0.37 g, 0.66 mmol, 1.00 eq) and 3-pyridine carboxaldehyde (0.36 g, 3.32 mmol, 5.00 eq) were stirred in glacial acetic acid (3.3 mL) for 20 minutes. Sodium triacetoxy borohydride (0.703 g, 3.32 mmol, 5.00 eq) was added to the mixture, and it was left to stir at room temperature for an additional 30 minutes. The acetic acid was then removed via vacuum distillation, and the dry reaction mass was resuspended in methanol (10 mL) and concentrated under reduced pressure to remove boron byproducts as trimethyl borate. The crude material was then purified via flash column chromatography (10-20% methanol in ethyl acetate) to afford the product **2.39** (0.254 g, 91%). ^{1}H NMR (400.1 MHz, MeOD) δ (ppm): 8.56-8.37 (m, 2H); 7.89-7.76 (m, 5H); 7.40 (dd, J_1 = 7.8 Hz, J_2 = 4.9 Hz, 1H); 3.98-3.91 (m, 4H); 3.79 (s, 2H); 3.30-3.23 (m, 2H); 3.17 (td, J_1 = 11.7 Hz, J_2 = 2.9 Hz, 2H); 3.02 (t, J = 6.2 Hz, 2H); 2.10- 2.00 (m, 2H); 1.95-1.87 (m, 2H). ^{13}C NMR (100.6 MHz, MeOD) δ (ppm): 179.37, 169.69, 150.06, 149.05, 138.41, 136.06, 135.27, 133.48, 125.23, 124.15, 62.24, 60.14, 56.20, 50.30, 48.72, 35.09, 28.90. HRMS (TOF, ES+) $C_{23}H_{26}N_5O_3$ [M+H]$^+$ calc. mass 420.2036, found 420.2034.
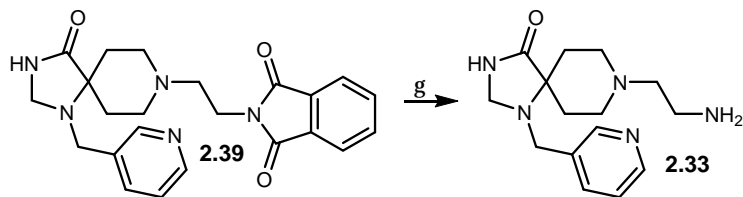
(g) To a mixture of starting material **2.39** (0.471 g, 1.12 mmol, 1.00 eq) in acetonitrile (9.4 mL) was added hydrazine (0.360 g, 11.23 mmol, 10.00 eq). The reaction was stirred for 15 hours before the acetonitrile was removed under reduced pressure. The solid material was redissolved in methanol and was passed through a cation exchange cartridge. The product **2.33** was eluted from the column with 2 M NH_4OH in methanol, and the filtrate was concentrated under reduced pressure to afford the product **2.33** as a crude solid (0.322 g, 99%) that was used without further purification.
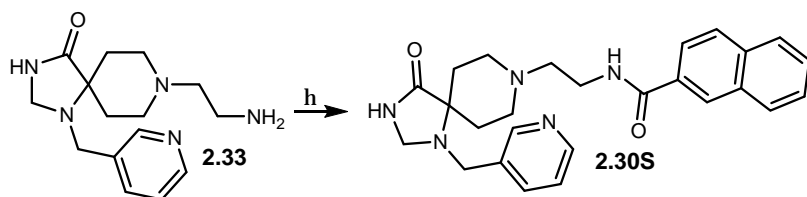
(h) Crude starting material **2.33** (0.12 g) and diisopropyl ethyl amine (0.266 g, 0.364 mL, 2.06 mmol, 5.00 eq), in a flame dried round-bottomed flask equipped with a magnetic stir bar, were dissolved in DMF (4.1 mL). To that flask was added naphthoyl chloride (0.10 g, 0.49 mmol, 1.20 eq), and the reaction was stirred for 30 minutes. The crude mixture was injected onto a reverse phase HPLC (5-80% acetonitrile in water (0.1% NH_4OH)) for purification monitoring product elution at 215 nm to provide the solid product **2.30S** (137 mg, 75%). ^1H NMR (400.1 MHz, MeOD) δ (ppm): 8.53-8.36 (m, 3H); 8.01-7.72 (m, 6H); 7.56-7.47 (m, 2H); 7.34 (dd, J_1 = 7.7 Hz, J_2 = 4.9 Hz, 1H); 3.88 (s, 2H); 3.72 (s, 2H); 3.61 (t, J = 6.8 Hz, 2H); 3.35 (s, 1H); 2.92-2.79 (m, 4H); 2.69 (t, J = 6.8 Hz, 2H); 1.89 (td, J_1 = 13.5

Hz, J_2 = 5.0 Hz, 2H); 1.82-1.73 (m, 2H). ^{13}C NMR (100.6 MHz, MeOD) δ (ppm): 179.96, 169.99, 150.08, 149.00, 138.37, 136.23, 136.14, 133.96, 132.81, 129.97, 129.29, 128.79, 128.77, 128.74, 127.81, 125.19, 124.87, 62.19, 60.88, 58.03, 50.48, 48.85, 38.34, 29.66. HRMS (TOF, ES+) $C_{26}H_{30}N_5O_2$ [M+H]$^+$ calc. mass 444.2400, found 444.2402.

APPENDIX

(1.70A)
Solvent: CDCl$_3$
400.13 MHz

11 10 9 8 7 6 5 4 3 2 1 0 -1 ppm

0.979 1.002 1.000   1.016 2.042 1.082 1.122 13.943 2.953

(1.70A)
Solvent: CDCl$_3$
100.61 MHz

220   200   180   160   140   120   100   80   60   40   20   0   ppm

208

(1.70B)
Solvent: CDCl₃
400.13 MHz

(1.70B)
Solvent: CDCl$_3$
100.61 MHz

210

(1.70C)
Solvent: CDCl$_3$
400.13 MHz

11 10 9 8 7 6 5 4 3 2 1 0 -1 ppm

1.940

0.992
1.012
1.000

0.992

4.259
2.022
1.030
3.002

2.890

211

(1.70C)
Solvent: CDCl₃
100.61 MHz

220 200 180 160 140 120 100 80 60 40 20 0 ppm

212

TBSO ⌒⌒⌒ OH
(1.70D) Cl
Solvent: CDCl₃
400.13 MHz

11 10 9 8 7 6 5 4 3 2 1 0 -1 ppm

1.000
1.013
3.088

0.967
1.028
2.068
1.236

9.371

6.150

213

(1.70D)
Solvent: CDCl$_3$
100.61 MHz

220 200 180 160 140 120 100 80 60 40 20 0 ppm

214

TBSO⌒⌒⌒OH

(1.70D) Cl

Elemental Composition Report

Page 1
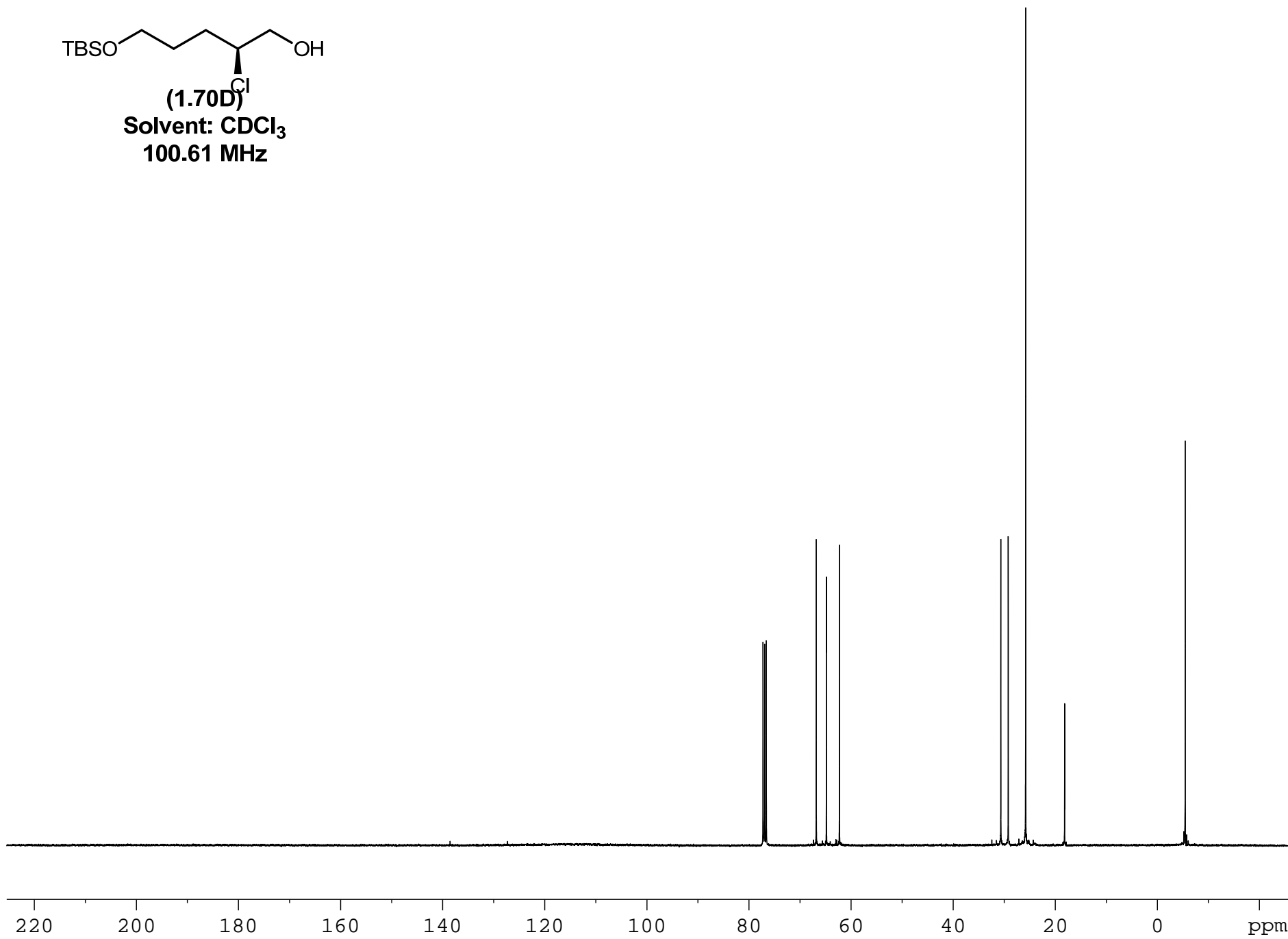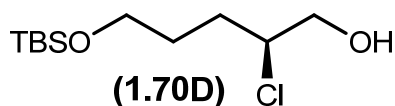
Single Mass Analysis

Tolerance = 5.0 PPM / DBE: min = -0.5, max = 25.0
Element prediction: Off
Number of isotope peaks used for i-FIT = 2

Monoisotopic Mass, Even Electron Ions
13 formula(e) evaluated with 1 results within limits (up to 50 closest results for each mass)
Elements Used:
C: 10-500   H: 10-1000   O: 1-200   Si: 1-1   Cl: 1-1

MCO-III-43

27-Oct-2011

S/N: UH193

13:27:08

MCO-III-43_102711_001 80 (1.491) AM (Cen,4, 80.00, Ar,8000.0,556.28,0.70); Sm (SG, 2x1.00); Cm (80:90)

TOF MS ES+
1.39e+003
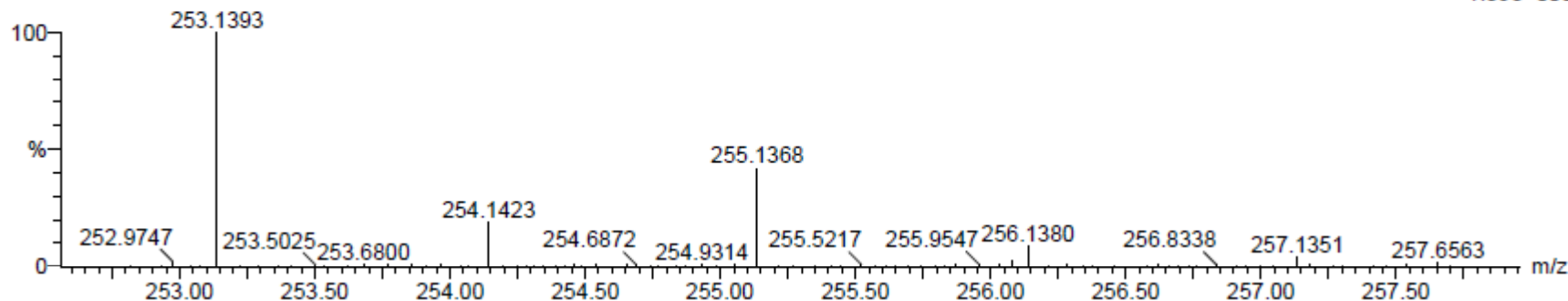
Minimum:				-0.5		
Maximum:		5.0	5.0	25.0		
Mass	Calc. Mass	mDa	PPM	DBE	i-FIT	Formula
253.1393	253.1391	0.2	0.8	-0.5	0.3	C11 H26 O2 Si Cl

(1.73A)
Solvent: CDCl$_3$
400.13 MHz

11 10 9 8 7 6 5 4 3 2 1 0 −1 ppm

4.897

1.035
4.000

4.832

1.030
2.090
15.650
3.028
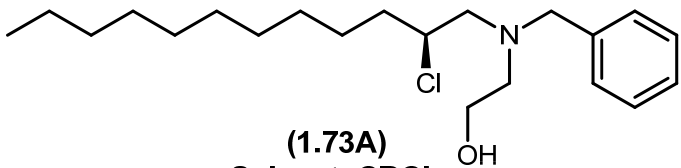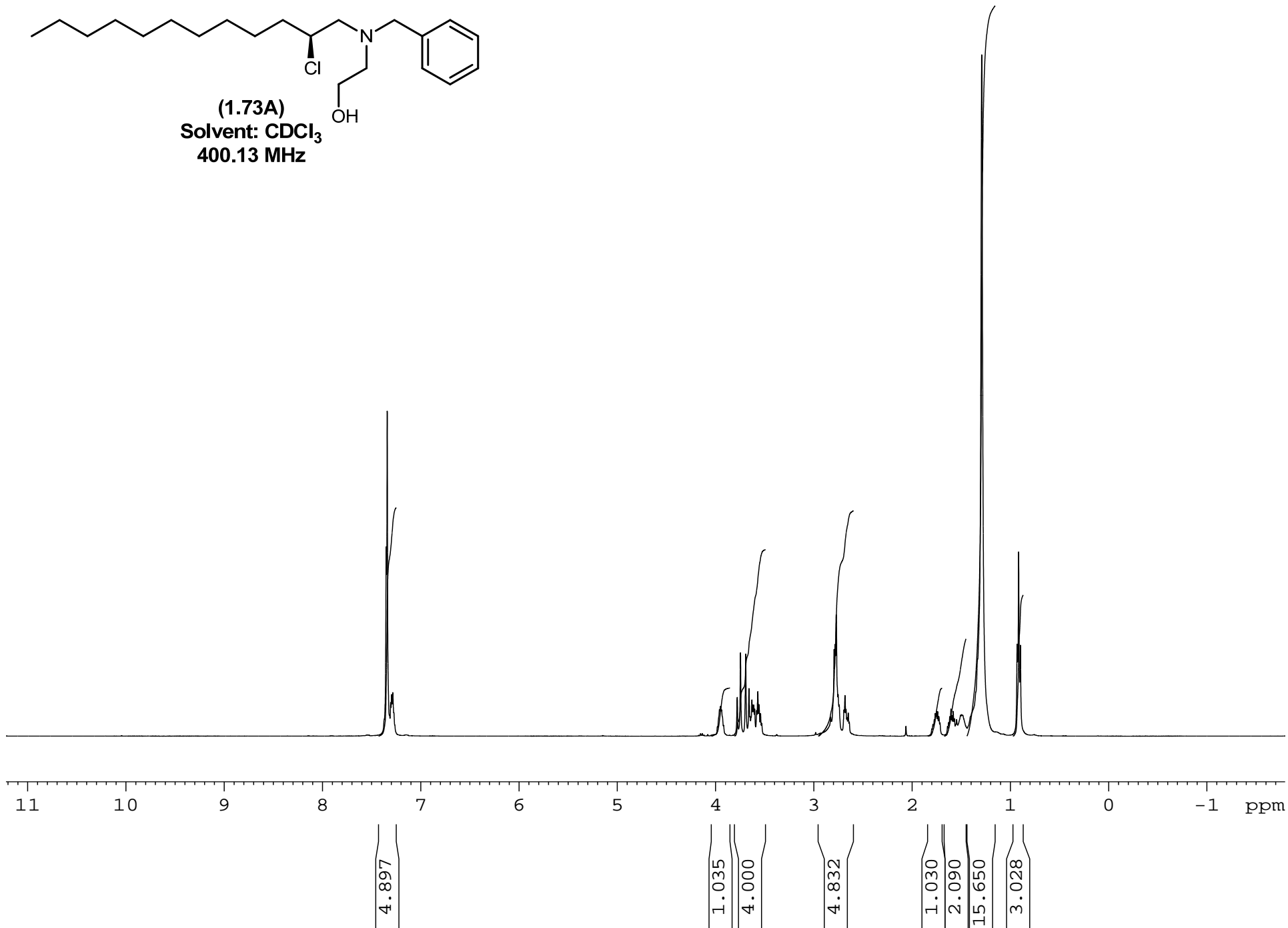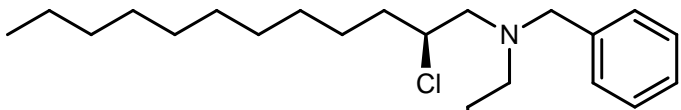
(1.73A)
Solvent: CDCl$_3$
100.61 MHz

(1.73A)

Elemental Composition Report

Page 1

Single Mass Analysis
Tolerance = 5.0 PPM   /   DBE: min = -0.5, max = 25.0
Element prediction: Off
Number of isotope peaks used for i-FIT = 2

Monoisotopic Mass, Even Electron Ions
209 formula(e) evaluated with 1 results within limits (up to 50 closest results for each mass)
Elements Used:
C: 20-500   H: 10-1000   N: 1-200   O: 1-200   Cl: 1-1

MCO-III-72

21-Nov-2011
14:09:01
S/N: UH193
MCO-III-72_112111_002 59 (1.117) AM (Cen,4, 80.00, Ar,8000.0,556.28,0.70); Sm (SG, 2x1.00); Cm (50:60)
TOF MS ES+
4.23e+003
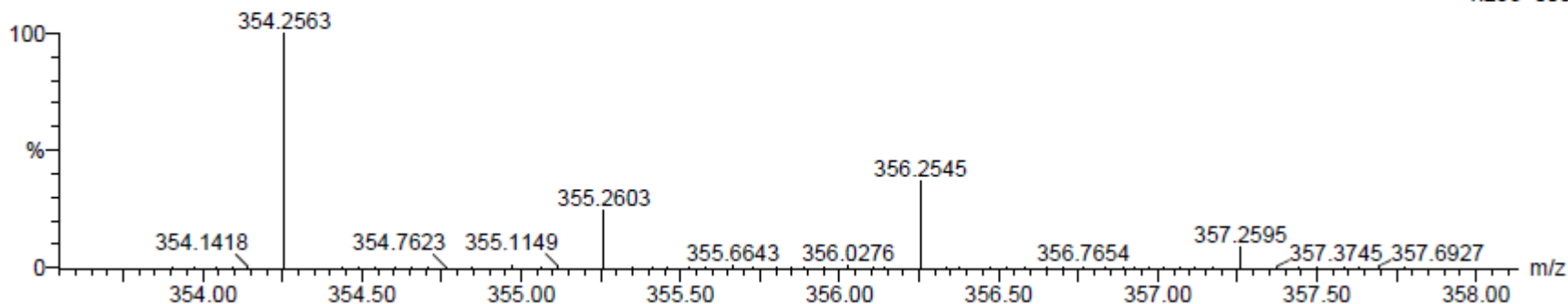
Minimum: -0.5
Maximum: 5.0   5.0   25.0

Mass	Calc. Mass	mDa	PPM	DBE	i-FIT	Formula
354.2563	354.2564	-0.1	-0.3	3.5	0.0	C21 H37 N O Cl

218
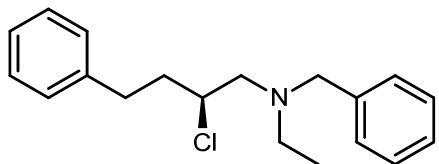
(1.73B)
Solvent: CDCl$_3$
400.13 MHz
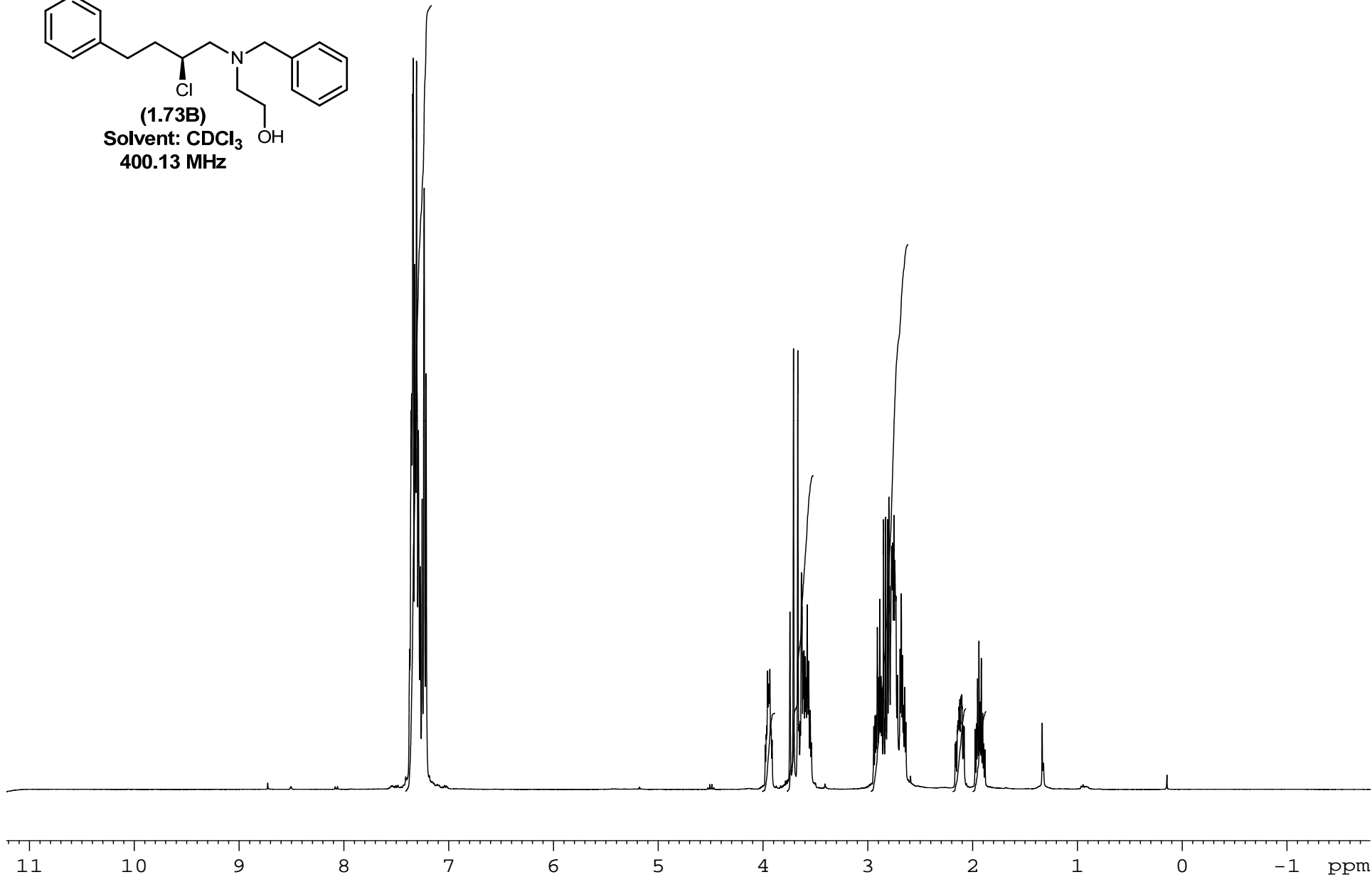
10.044

1.000
4.041

6.992

1.061
1.023
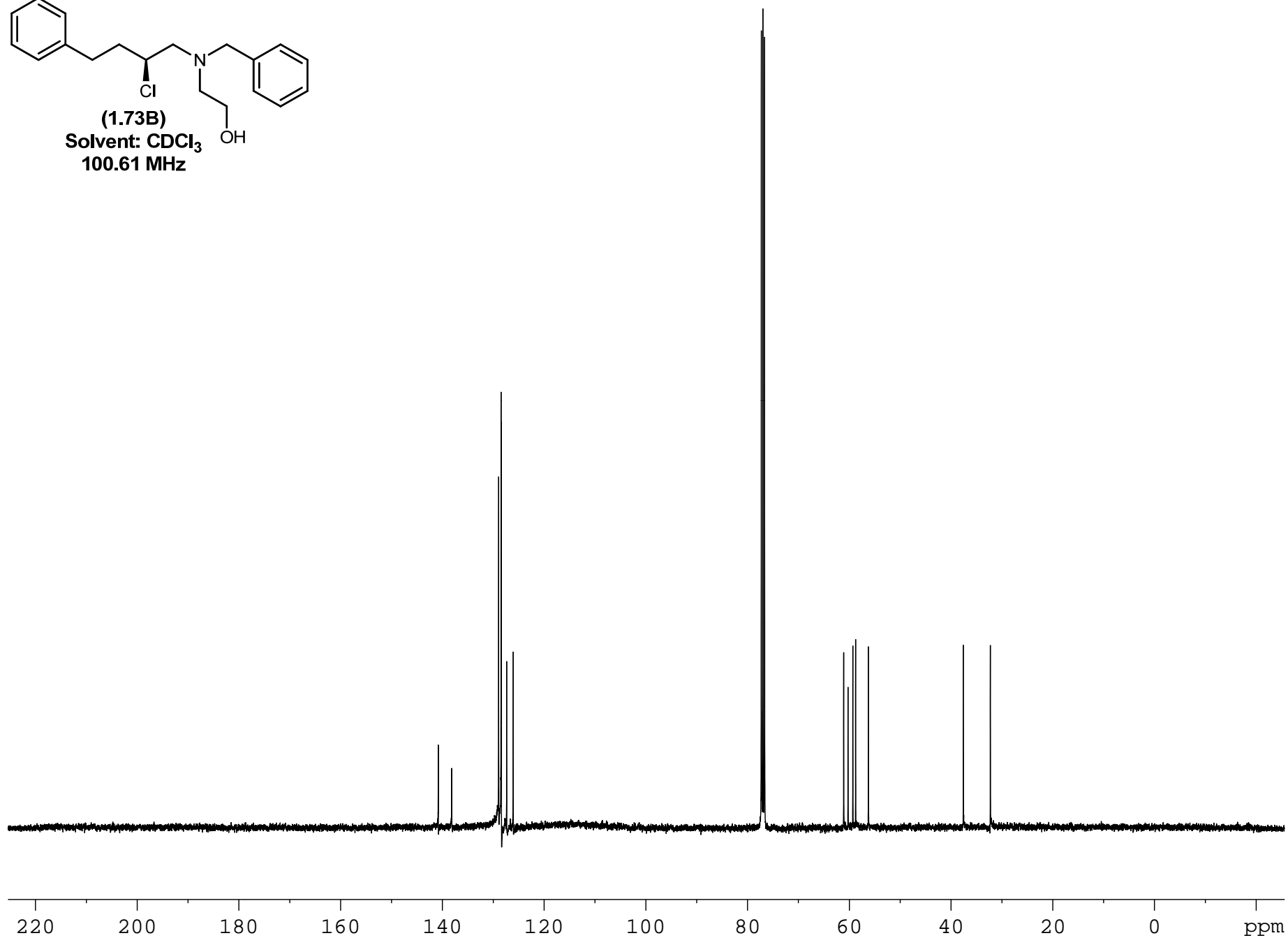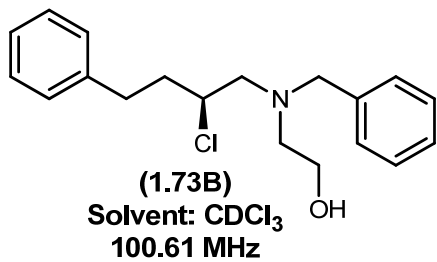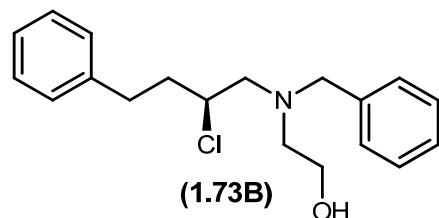
11 10 9 8 7 6 5 4 3 2 1 0 −1 ppm

219

(1.73B)
Solvent: CDCl$_3$
100.61 MHz

220 200 180 160 140 120 100 80 60 40 20 0 ppm

(1.73B)

Elemental Composition Report

Page 1

Single Mass Analysis
Tolerance = 5.0 PPM   /   DBE: min = -0.5, max = 25.0
Element prediction: Off
Number of isotope peaks used for i-FIT = 2

Monoisotopic Mass, Even Electron Ions
159 formula(e) evaluated with 1 results within limits (up to 50 best isotopic matches for each mass)
Elements Used:
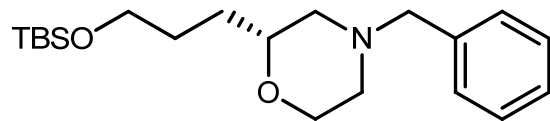C: 18-500   H: 10-1000   N: 1-200   O: 1-200   Cl: 1-1

MCO-III-94

01-Mar-2012
13:03:03

S/N: UH193

MCO-III-94_030112_001 80 (1.512) AM (Cen,4, 80.00, Ar,8000.0,556.28,0.70); Sm (SG, 2x1.00); Cm (80:90)

TOF MS ES+
7.39e+003
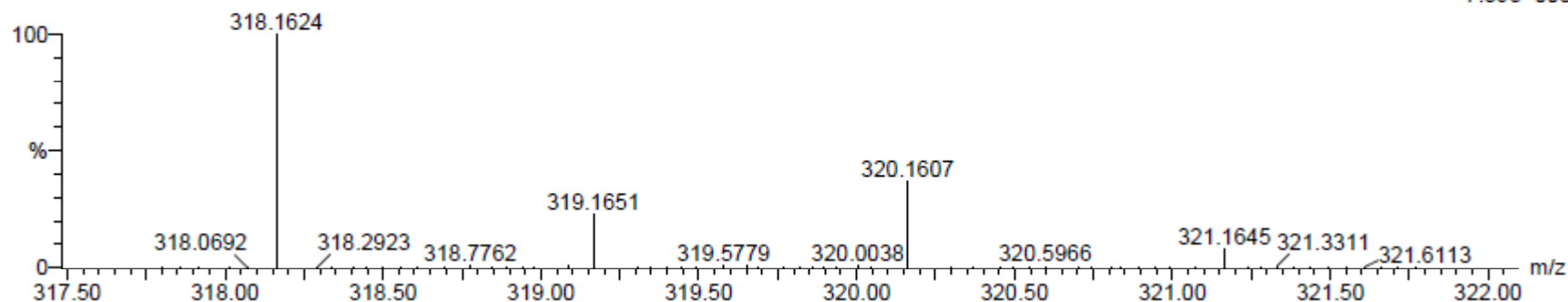
Minimum:				-0.5		
Maximum:		10.0	5.0	25.0		
Mass	Calc. Mass	mDa	PPM	DBE	i-FIT	Formula
318.1624	318.1625	-0.1	-0.3	7.5	0.6	C19 H25 N O Cl

221

(1.73C)
Solvent: CDCl₃
400.13 MHz

5.212   1.967   1.000 4.077   4.861   3.990 1.068 2.145 3.377   2.950

222
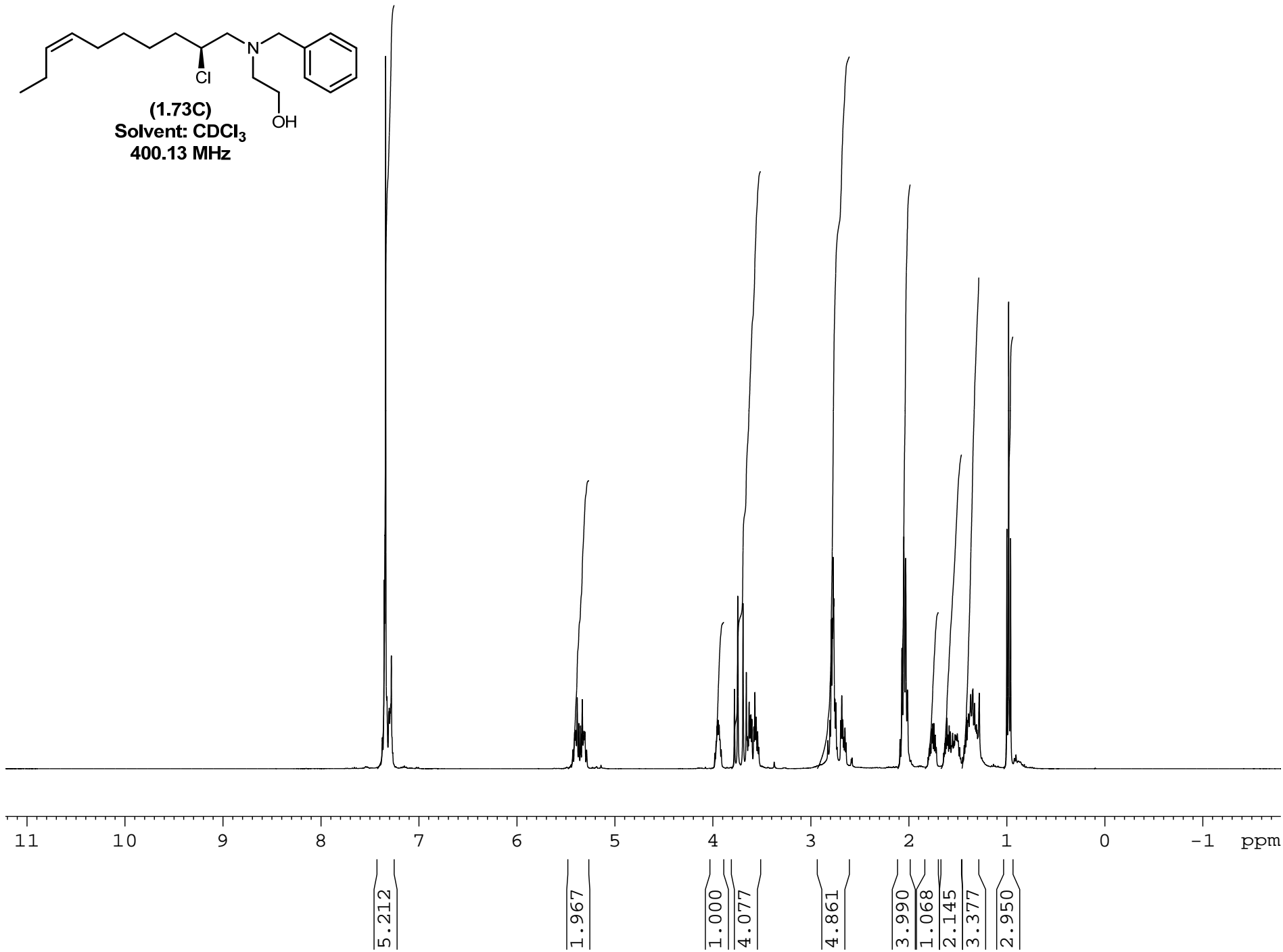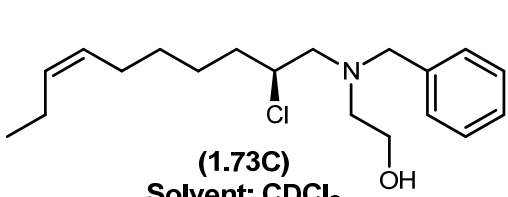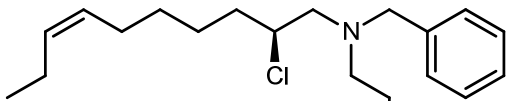
(1.73C)
Solvent: CDCl$_3$
100.61 MHz

220   200   180   160   140   120   100   80   60   40   20   0   ppm

(1.73C)

Elemental Composition Report

Page 1

Single Mass Analysis
Tolerance = 5.0 PPM / DBE: min = -0.5, max = 25.0
Element prediction: Off
Number of isotope peaks used for i-FIT = 2

Monoisotopic Mass, Even Electron Ions
168 formula(e) evaluated with 1 results within limits (up to 50 best isotopic matches for each mass)
Elements Used:
C: 18-500   H: 10-1000   N: 1-200   O: 1-200   Cl: 1-1
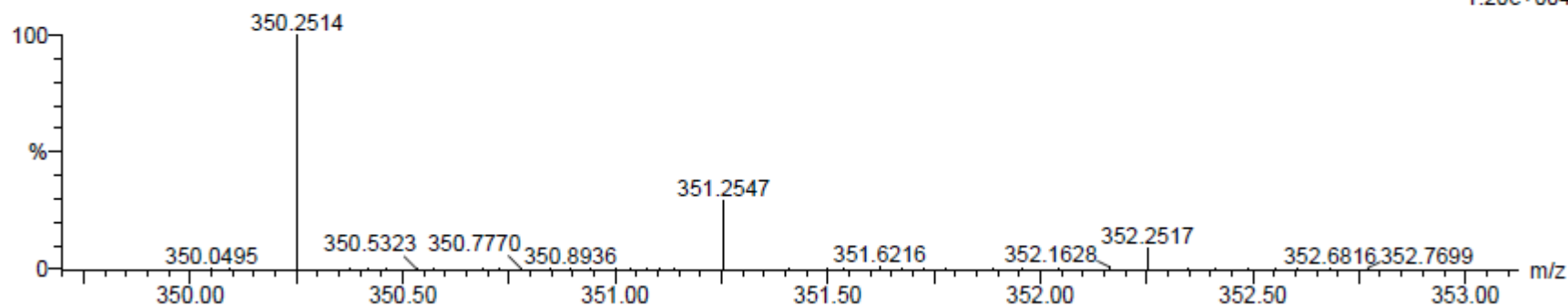
01-Mar-2012

S/N: UH193

14:04:54

MCO-III-174_030112_001 84 (1.587) AM (Cen,4, 80.00, Ar,8000.0,556.28,0.70); Sm (SG, 2x1.00); Cm (80:90)

TOF MS ES+
2.71e+003

Minimum:

Maximum:

			-0.5		
	10.0	5.0	25.0		
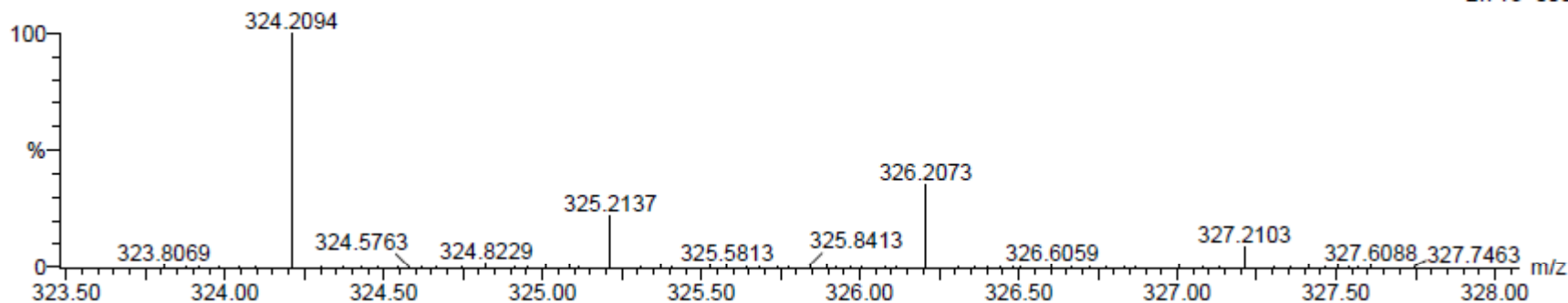
Mass	Calc. Mass	mDa	PPM	DBE	i-FIT	Formula
324.2094	324.2094	0.0	0.0	4.5	0.0	C19 H31 N O Cl
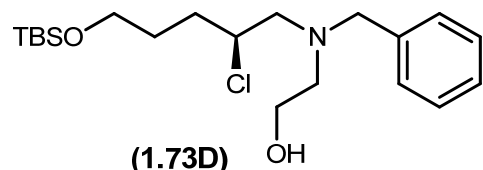
(1.73D)
Solvent: CDCl$_3$
400.13 MHz
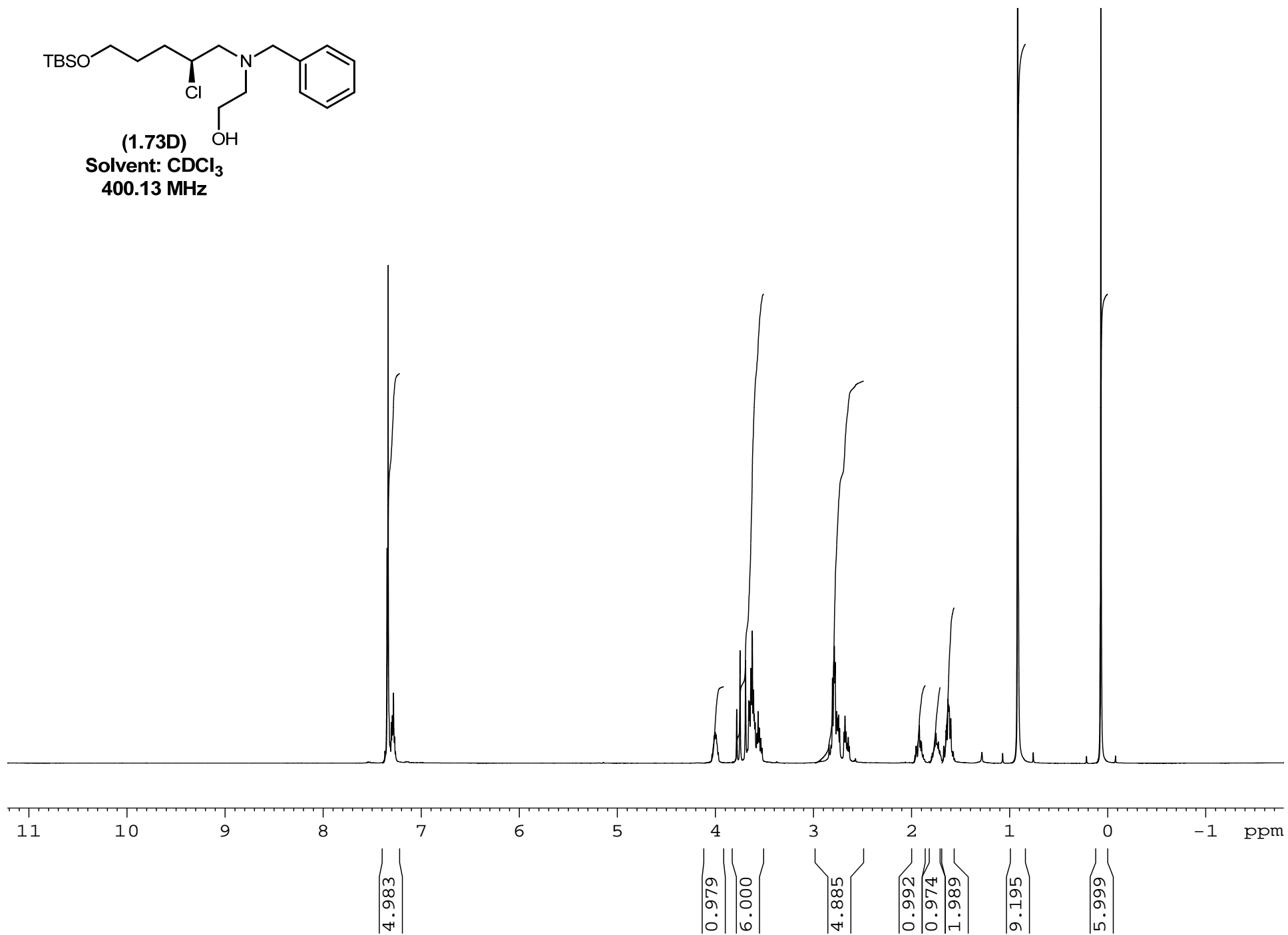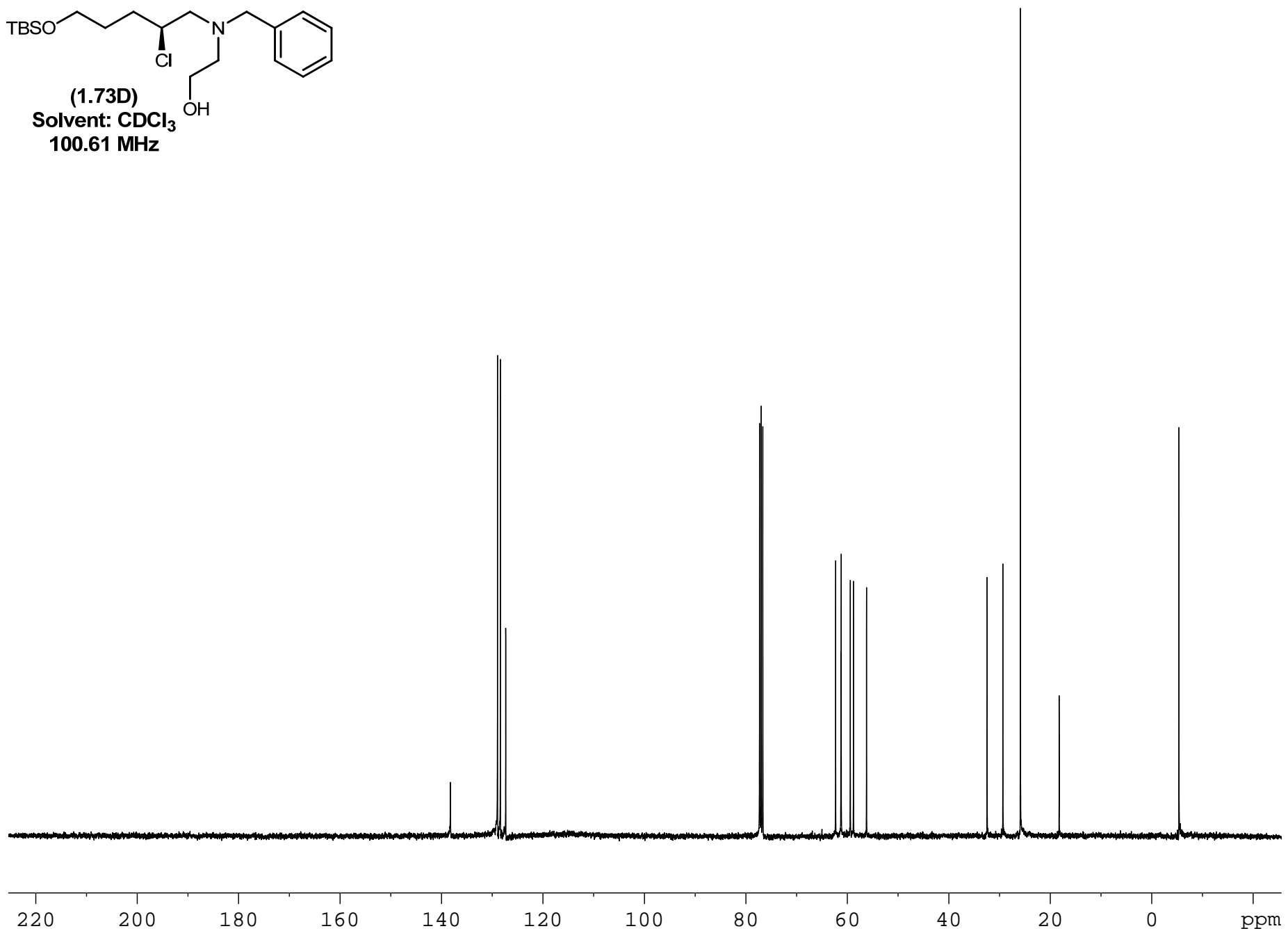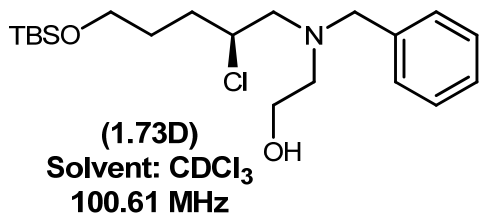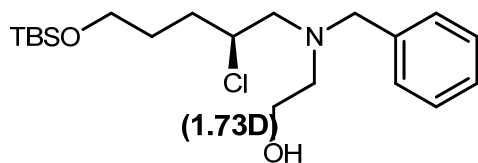
11   10   9   8   7   6   5   4   3   2   1   0   -1   ppm

4.983

0.979 6.000

4.885

0.992 0.974 1.989

9.195

5.999

(1.73D)
Solvent: CDCl$_3$
100.61 MHz

TBSO... (structure) Cl (1.73D) OH N benzyl

Elemental Composition Report

Page 1

Single Mass Analysis
Tolerance = 5.0 PPM   /   DBE: min = -0.5, max = 25.0
Element prediction: Off
Number of isotope peaks used for i-FIT = 2

Monoisotopic Mass, Even Electron Ions
215 formula(e) evaluated with 1 results within limits (up to 50 best isotopic matches for each mass)
Elements Used:
C: 20-500   H: 10-1000   N: 1-200   O: 1-200   Si: 1-1   Cl: 1-1

MCO-III-158A

01-Mar-2012
16:10:43
S/N: UH193
MCO-III-158A_030112_001 83 (1.568) AM (Cen,4, 80.00, Ar,8000.0,556.28,0.70); Sm (SG, 2x1.00); Cm (80:90)
TOF MS ES+
1.40e+004
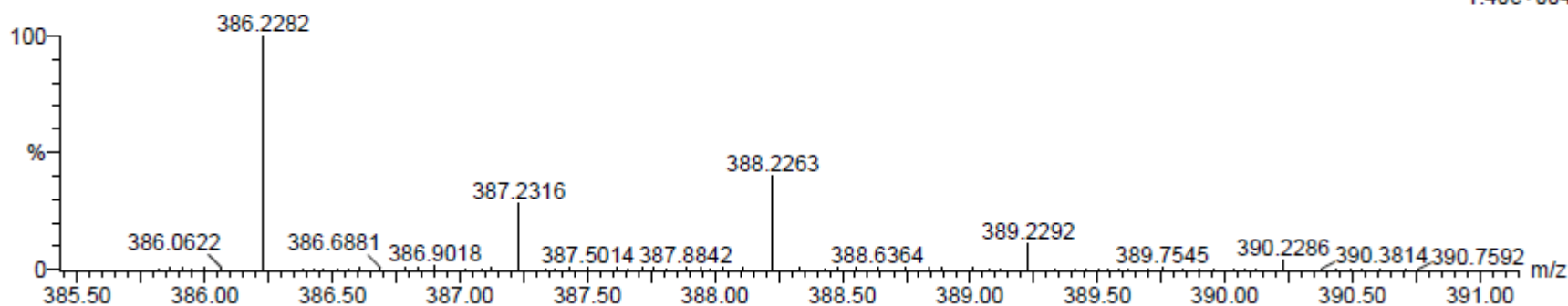
Minimum:				-0.5		
Maximum:		10.0	5.0	25.0		
Mass	Calc. Mass	mDa	PPM	DBE	i-FIT	Formula
386.2282	386.2282	0.0	0.0	3.5	0.0	C20 H37 N O2 Si Cl
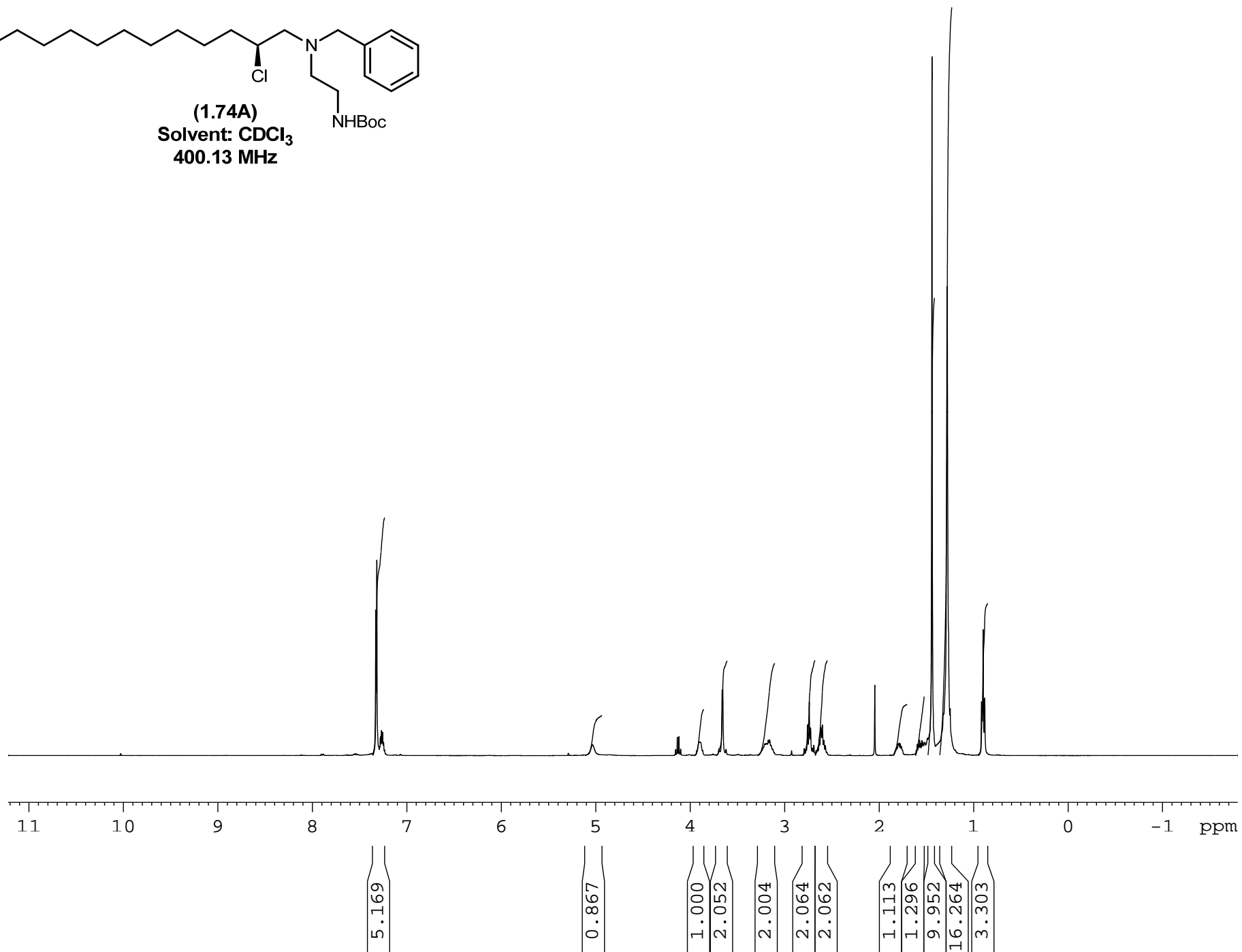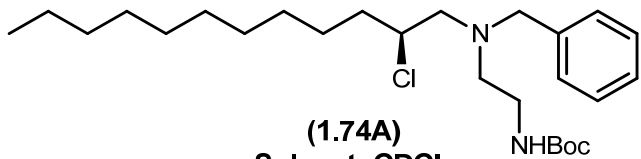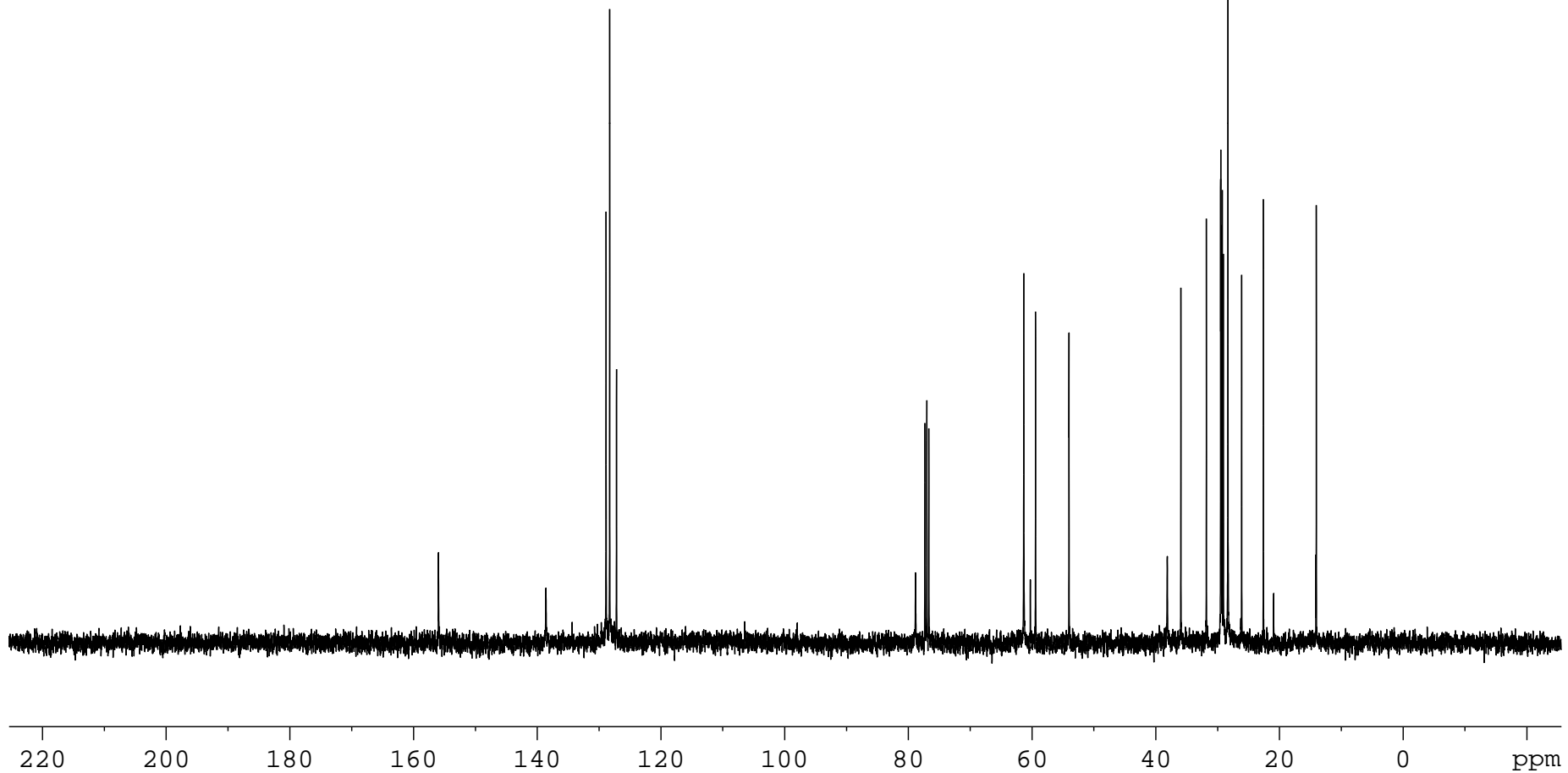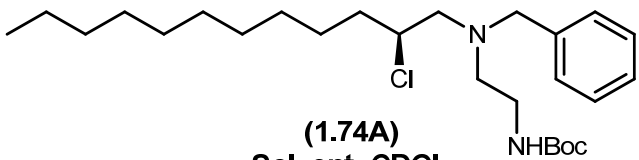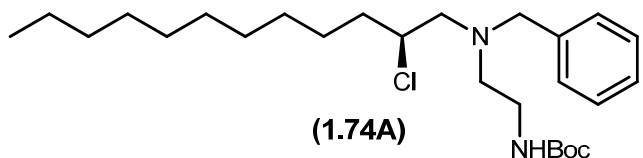
227

(1.74A)
Solvent: CDCl$_3$
400.13 MHz

5.169

0.867

1.000
2.052

2.004

2.064
2.062

1.113
1.296
9.952
16.264
3.303
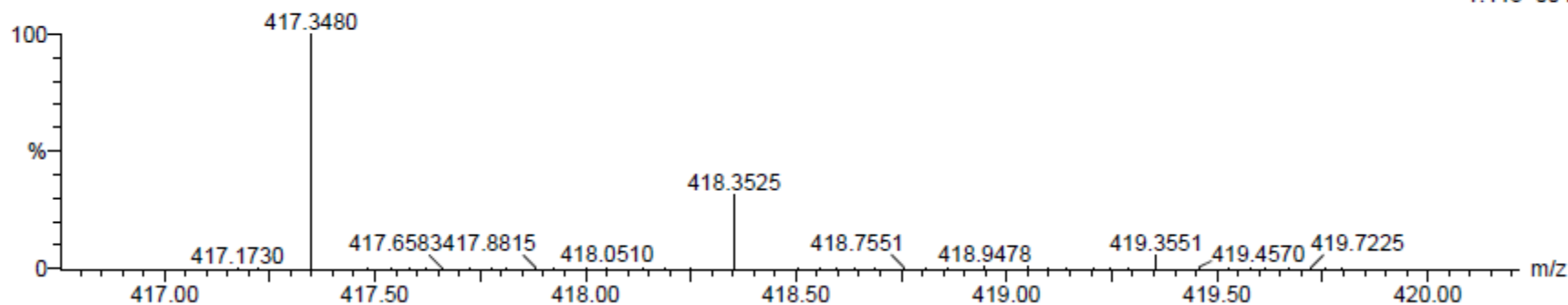
(1.74A)
Solvent: CDCl$_3$
100.61 MHz

(1.74A)

Elemental Composition Report

Page 1

Single Mass Analysis
Tolerance = 5.0 PPM / DBE: min = -0.5, max = 25.0
Element prediction: Off
Number of isotope peaks used for i-FIT = 2

Monoisotopic Mass, Even Electron Ions
394 formula(e) evaluated with 1 results within limits (up to 50 closest results for each mass)
Elements Used:
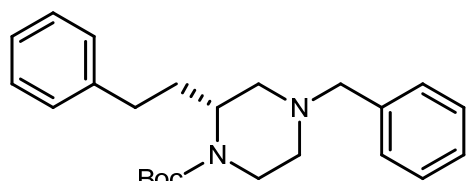C: 25-500   H: 10-1000   N: 1-200   O: 1-200   Cl: 1-1

MCO-III-30

S/N: UH193

20-Oct-2011
15:06:46

MCO-III-30_102011_001 50 (0.935) AM (Cen,4, 80.00, Ar,8000.0,556.28,0.70); Sm (SG, 2x1.00); Cm (50:60)

TOF MS ES+
6.52e+003
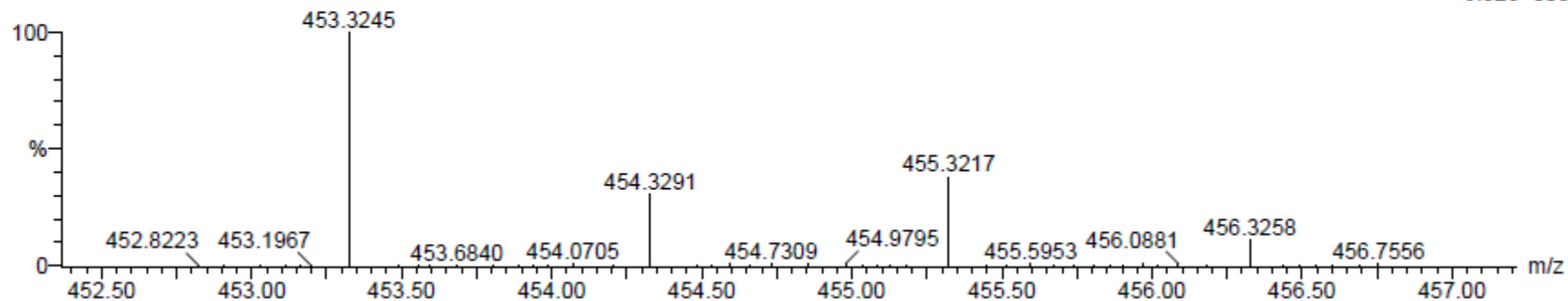
| Minimum: | | | | -0.5 | | |
| Maximum: | | 5.0 | 5.0 | 25.0 | | |

Mass	Calc. Mass	mDa	PPM	DBE	i-FIT	Formula
453.3245	453.3248	-0.3	-0.7	4.5	0.1	C26 H46 N2 O2 Cl
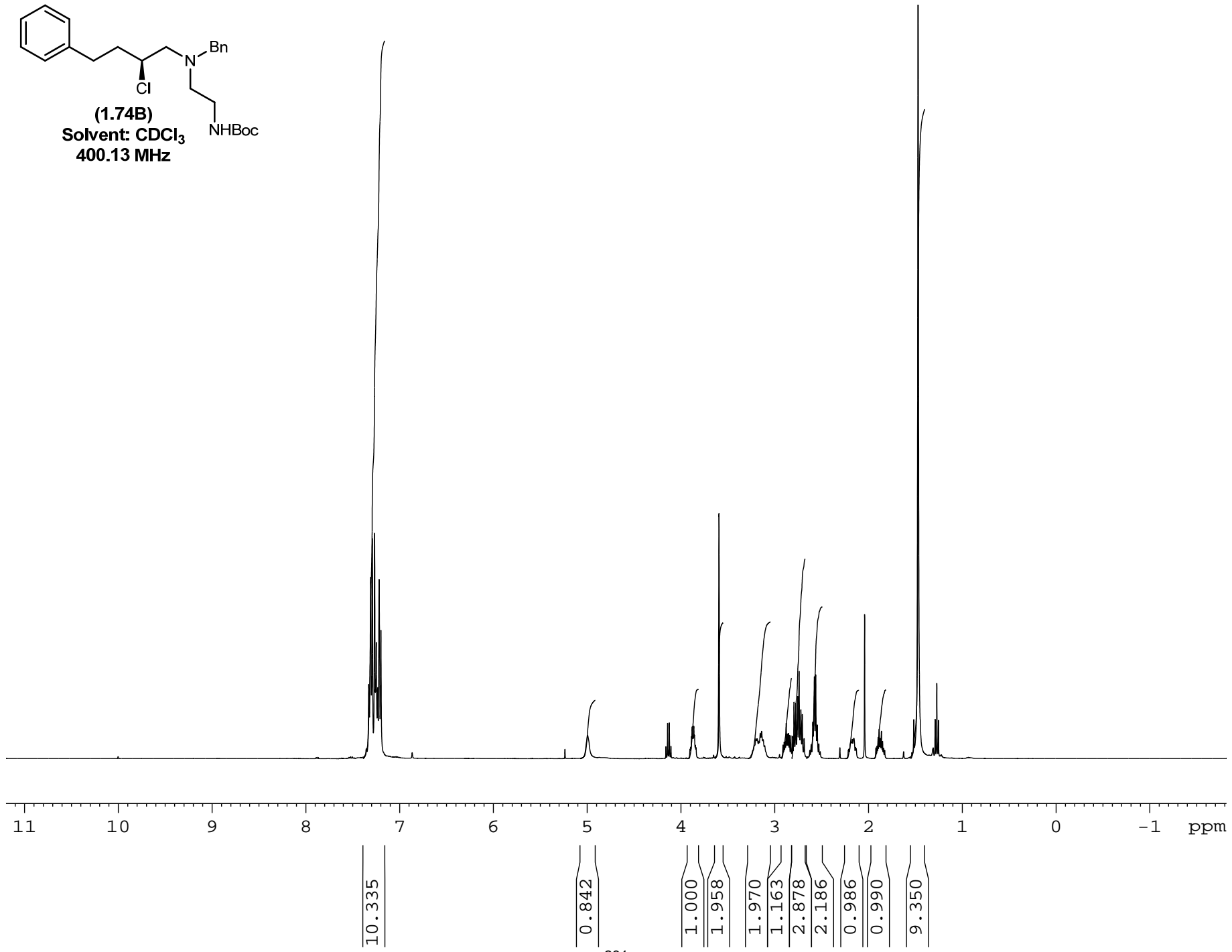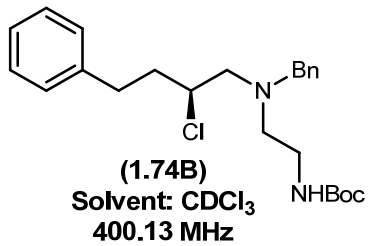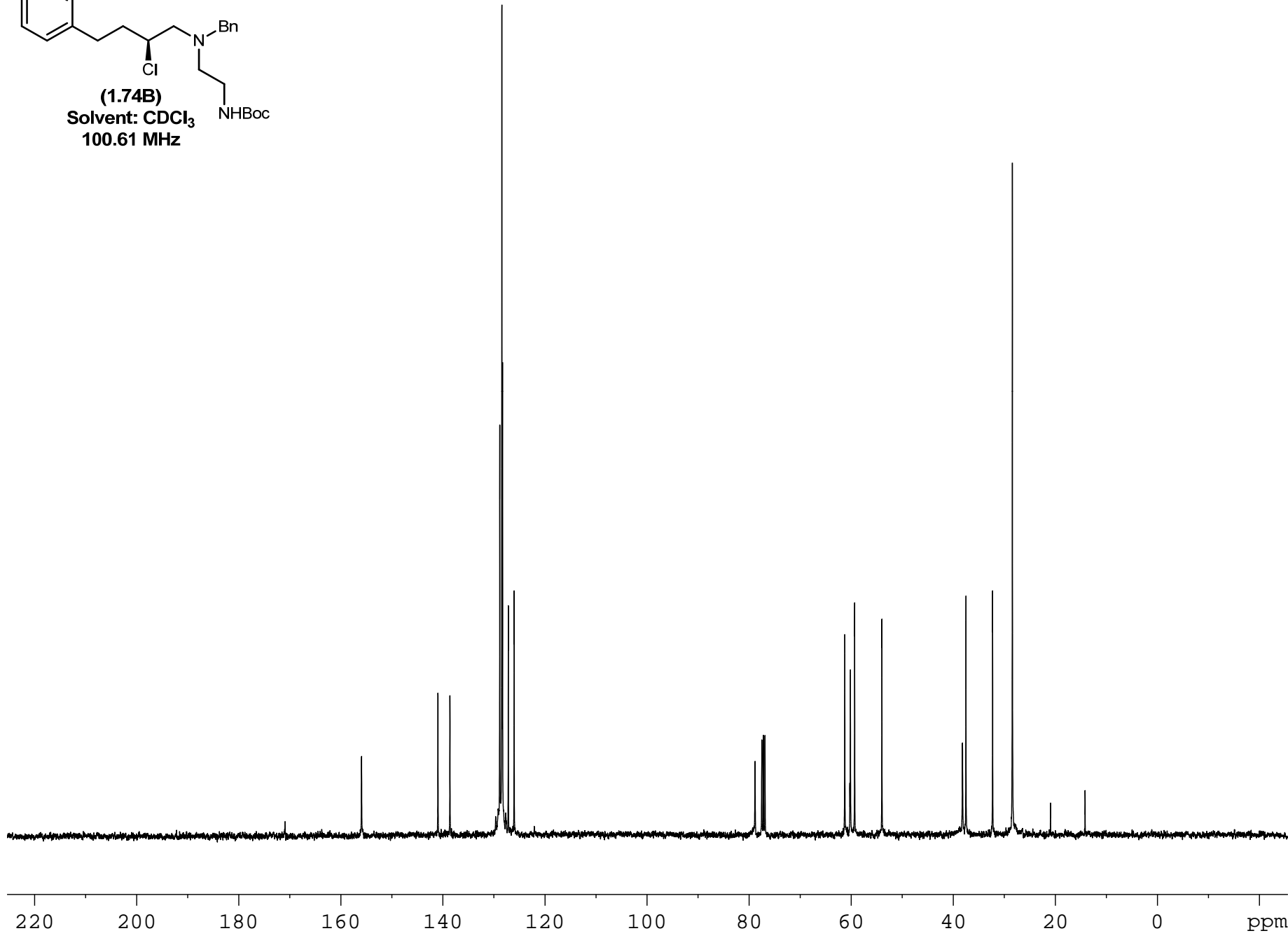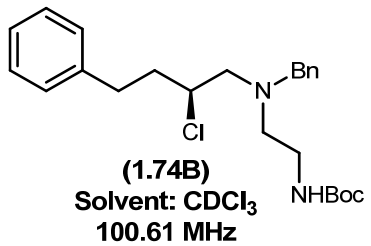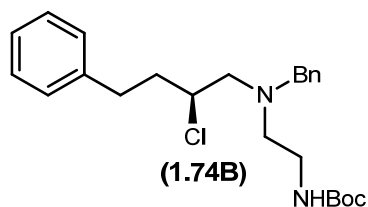
(1.74B)
Solvent: CDCl$_3$
400.13 MHz

10.335

0.842

231

1.000
1.958
1.970
1.163
2.878
2.186
0.986
0.990
9.350

11   10   9   8   7   6   5   4   3   2   1   0   -1   ppm

(1.74B)
Solvent: CDCl₃
100.61 MHz

232

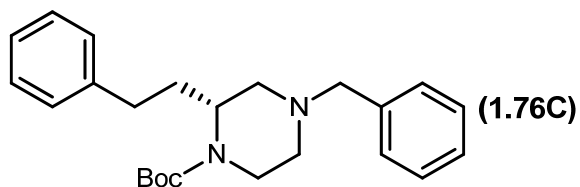**(1.74B)**

Elemental Composition Report

Page 1

Single Mass Analysis
Tolerance = 5.0 PPM   /   DBE: min = -0.5, max = 25.0
Element prediction: Off
Number of isotope peaks used for i-FIT = 2

Monoisotopic Mass, Even Electron Ions
360 formula(e) evaluated with 1 results within limits (up to 50 closest results for each mass)
Elements Used:
C: 20-500   H: 10-1000   N: 1-200   O: 1-200   Cl: 1-1

MCO-III-75   21-Nov-2011
                                                          S/N: UH193   15:16:08
MCO-III-75_112111_001 97 (1.832) AM (Cen,4, 80.00, Ar,8000.0,556.28,0.70); Sm (SG, 2x1.00); Cm (90:100)   TOF MS ES+
   1.15e+004
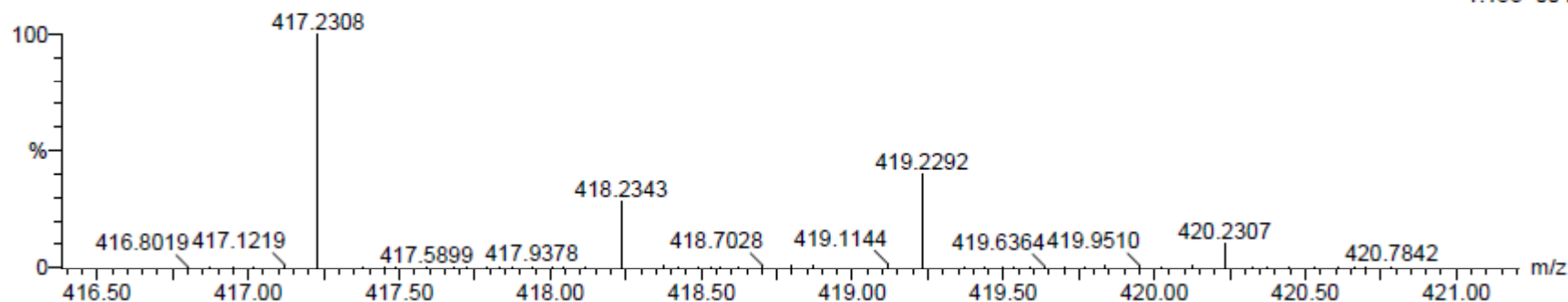

Minimum:				-0.5		
Maximum:		5.0	5.0	25.0		
Mass	Calc. Mass	mDa	PPM	DBE	i-FIT	Formula
417.2308	417.2309	-0.1	-0.2	8.5	0.1	C24 H34 N2 O2 Cl
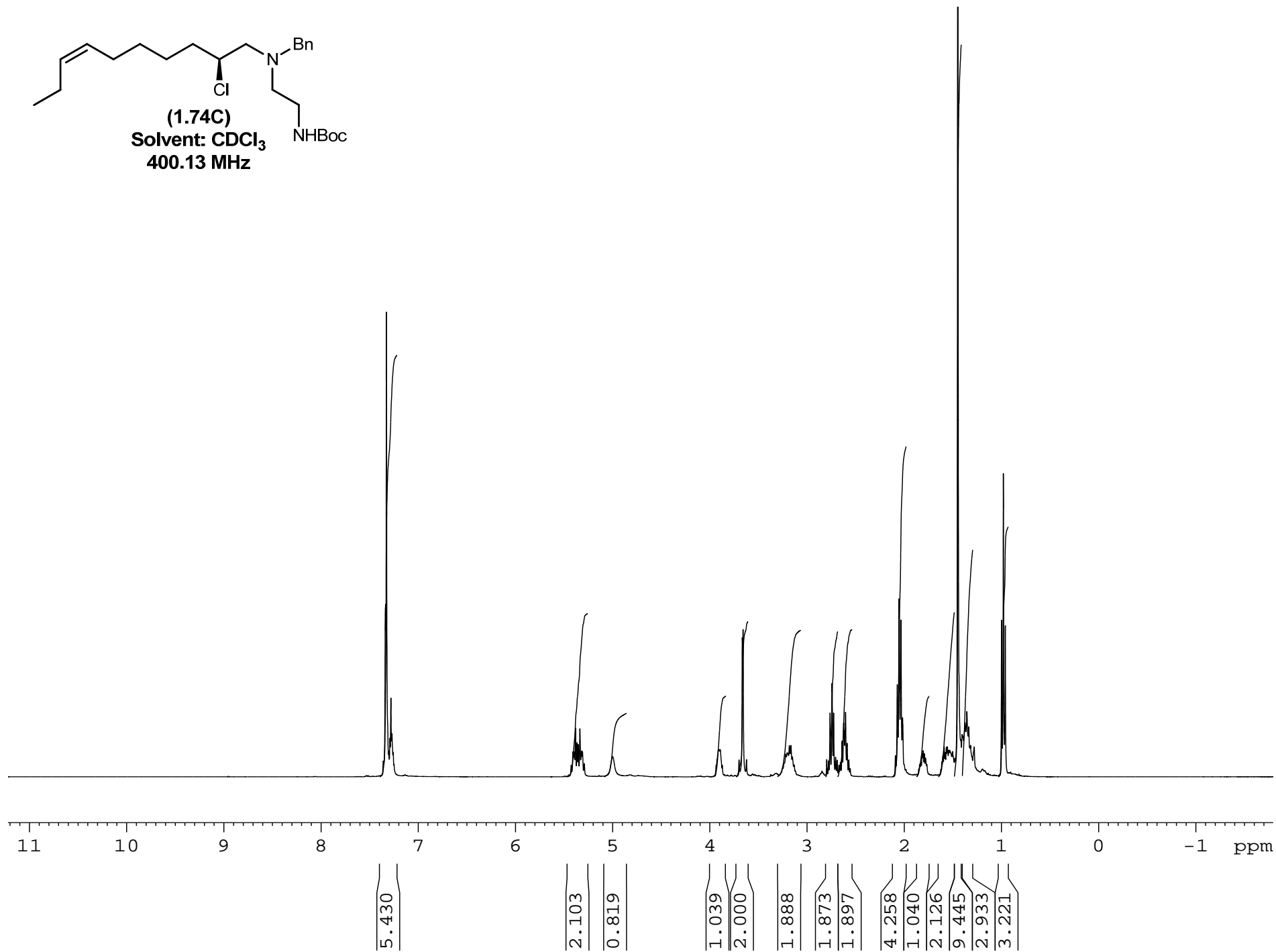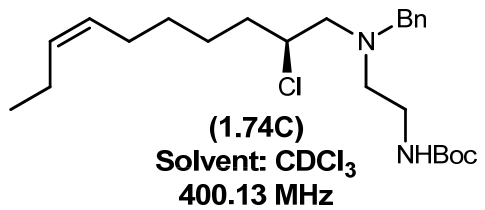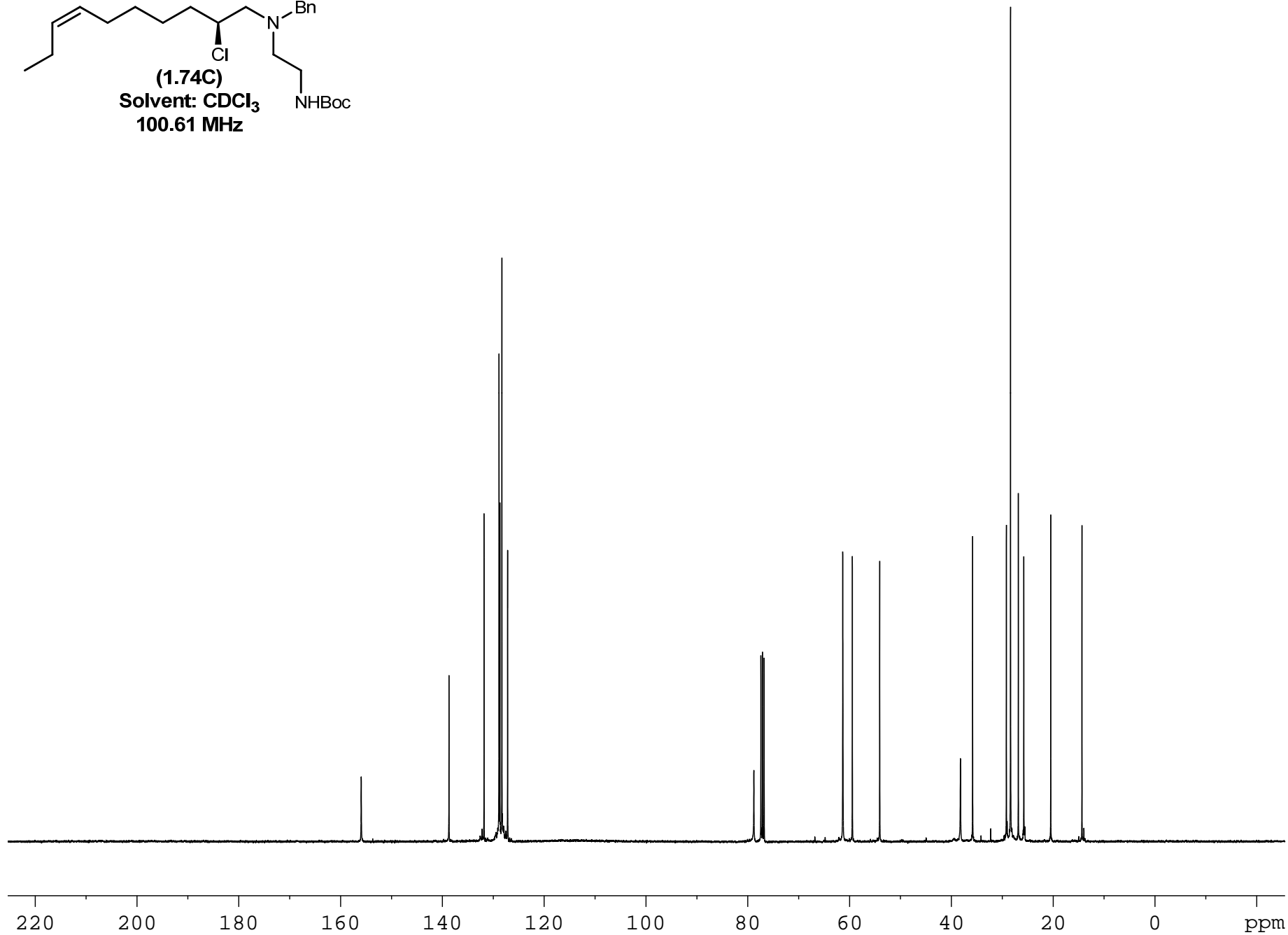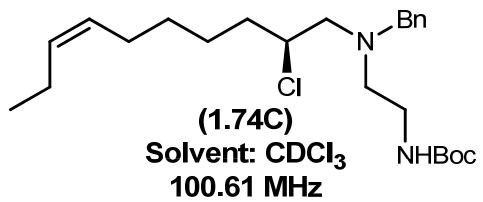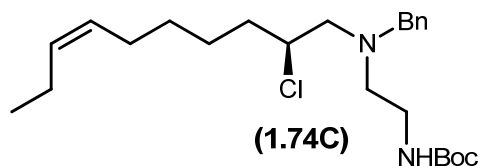
233

(1.74C)
Solvent: CDCl₃
400.13 MHz

5.430

2.103 0.819

1.039 2.000

1.888

1.873 1.897

4.258 1.040 2.126 9.445 2.933 3.221

(1.74C)
Solvent: CDCl₃
100.61 MHz

235

(1.74C)

Elemental Composition Report

Page 1

Single Mass Analysis
Tolerance = 5.0 PPM / DBE: min = -0.5, max = 25.0
Element prediction: Off
Number of isotope peaks used for i-FIT = 2

Monoisotopic Mass, Even Electron Ions
372 formula(e) evaluated with 1 results within limits (up to 50 closest results for each mass)
Elements Used:
C: 20-500   H: 10-1000   N: 1-200   O: 1-200   Cl: 1-1

MCO-III-41

S/N: UH193

MCO-III-41_102711_001 88 (1.640) AM (Cen,4, 80.00, Ar,8000.0,556.28,0.70); Sm (SG, 2x1.00); Cm (80:90)
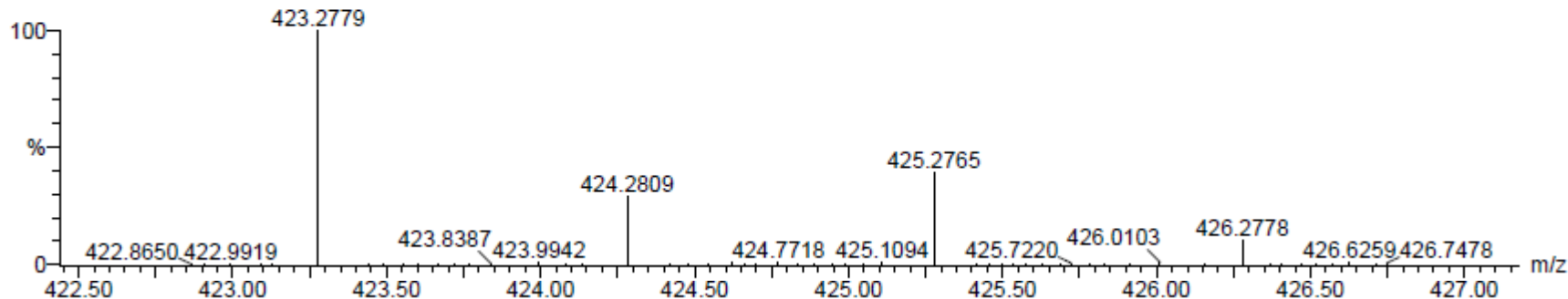
Minimum:				-0.5		
Maximum:		5.0	5.0	25.0		
Mass	Calc. Mass	mDa	PPM	DBE	i-FIT	Formula
423.2779	423.2778	0.1	0.2	5.5	0.8	C24 H40 N2 O2 Cl
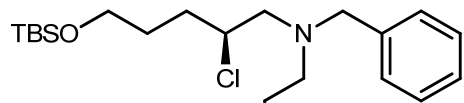
(1.74D)
Solvent: CDCl$_3$
400.13 MHz
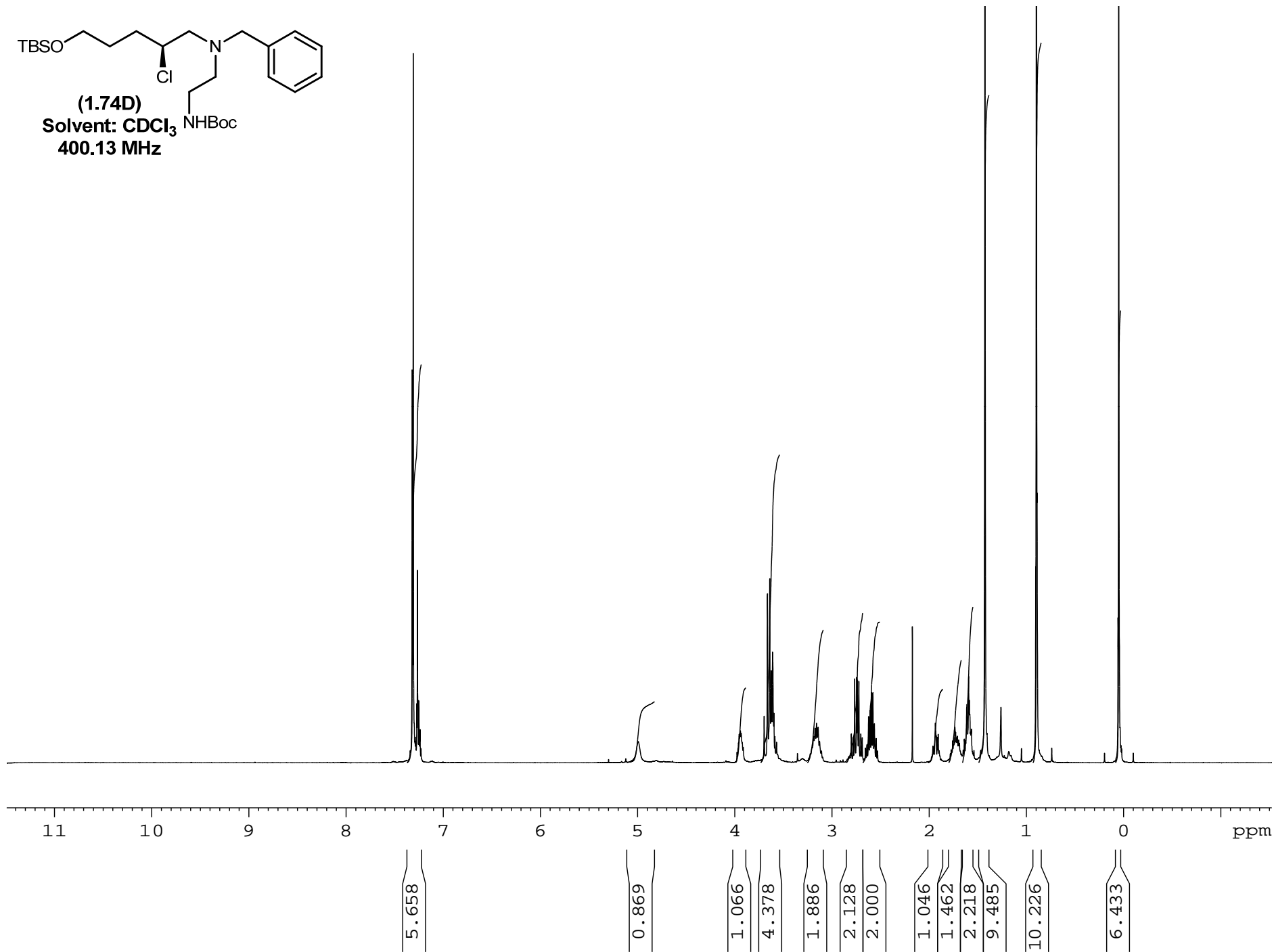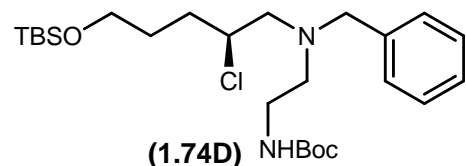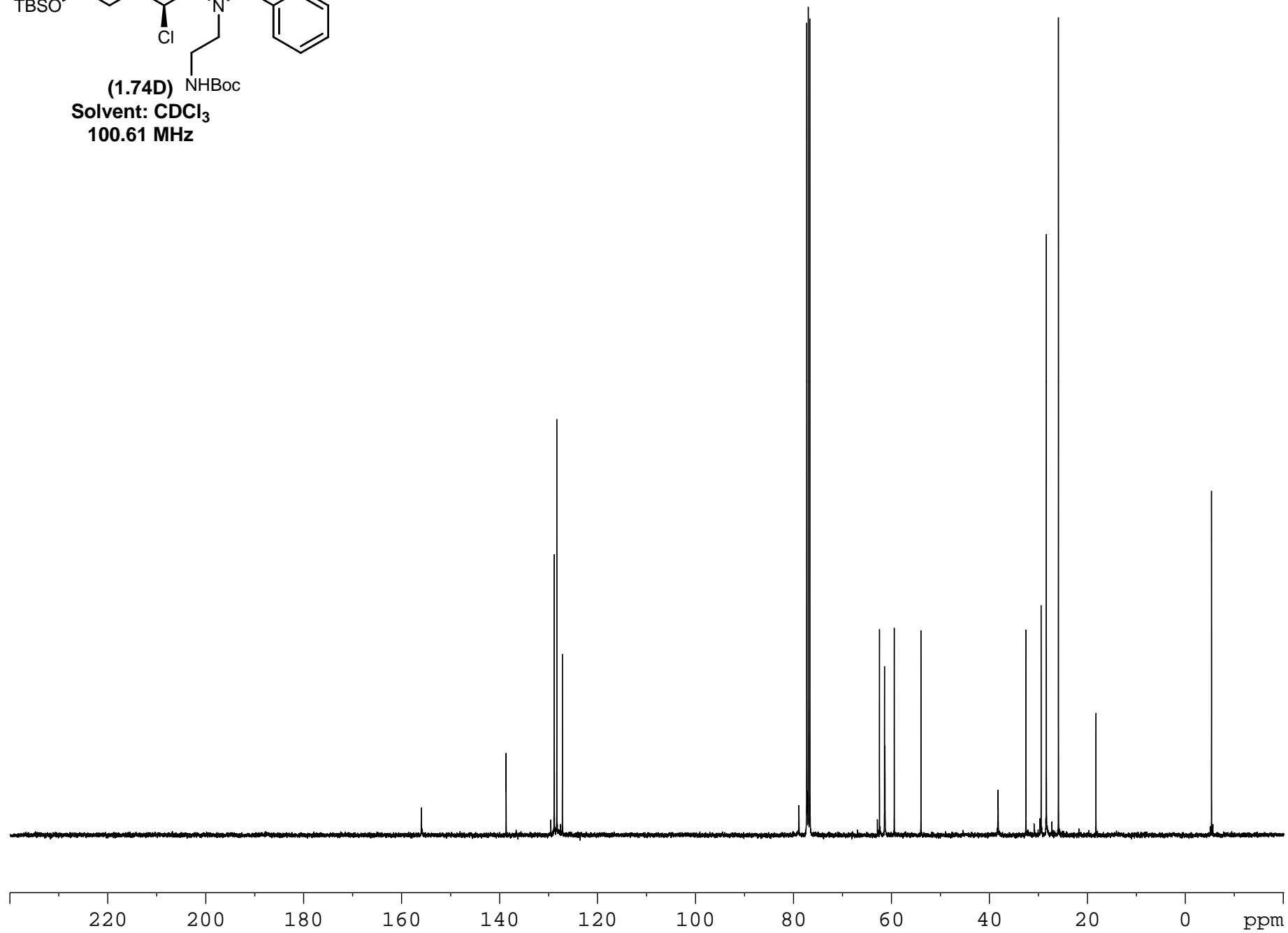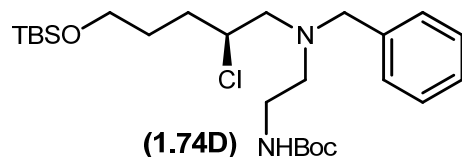
5.658   0.869   1.066 4.378   1.886 2.128 2.000   1.046 1.462 2.218 9.485   10.226   6.433

11   10   9   8   7   6   5   4   3   2   1   0   ppm

237

(1.74D) NHBoc
Solvent: CDCl₃
100.61 MHz

238

(1.74D)

Elemental Composition Report

Single Mass Analysis
Tolerance = 5.0 PPM / DBE: min = -0.5, max = 25.0
Element prediction: Off
Number of isotope peaks used for i-FIT = 2

Monoisotopic Mass, Even Electron Ions
406 formula(e) evaluated with 1 results within limits (up to 50 closest results for each mass)
Elements Used:
C: 25-500   H: 10-1000   N: 1-200   O: 1-200   Cl: 1-1   Si: 1-1

MCO-III-50

17-Nov-2011
14:50:49

S/N: UH193

MCO-III-50_111711_001 59 (1.117) AM (Cen,4, 80.00, Ar,8000.0,556.28,0.70); Sm (SG, 2x1.00); Cm (50:60)

TOF MS ES+
4.76e+003
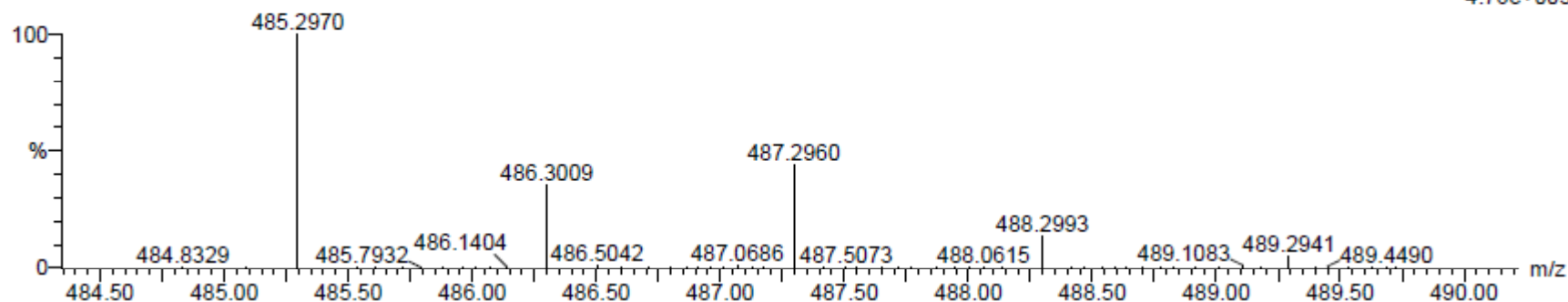
Minimum:				-0.5		
Maximum:		5.0	5.0	25.0		
Mass	Calc. Mass	mDa	PPM	DBE	i-FIT	Formula
485.2970	485.2966	0.4	0.8	4.5	0.2	C25 H46 N2 O3 Cl Si
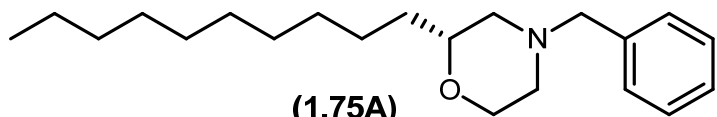
(1.75A)
Solvent: CDCl$_3$
400.13 MHz
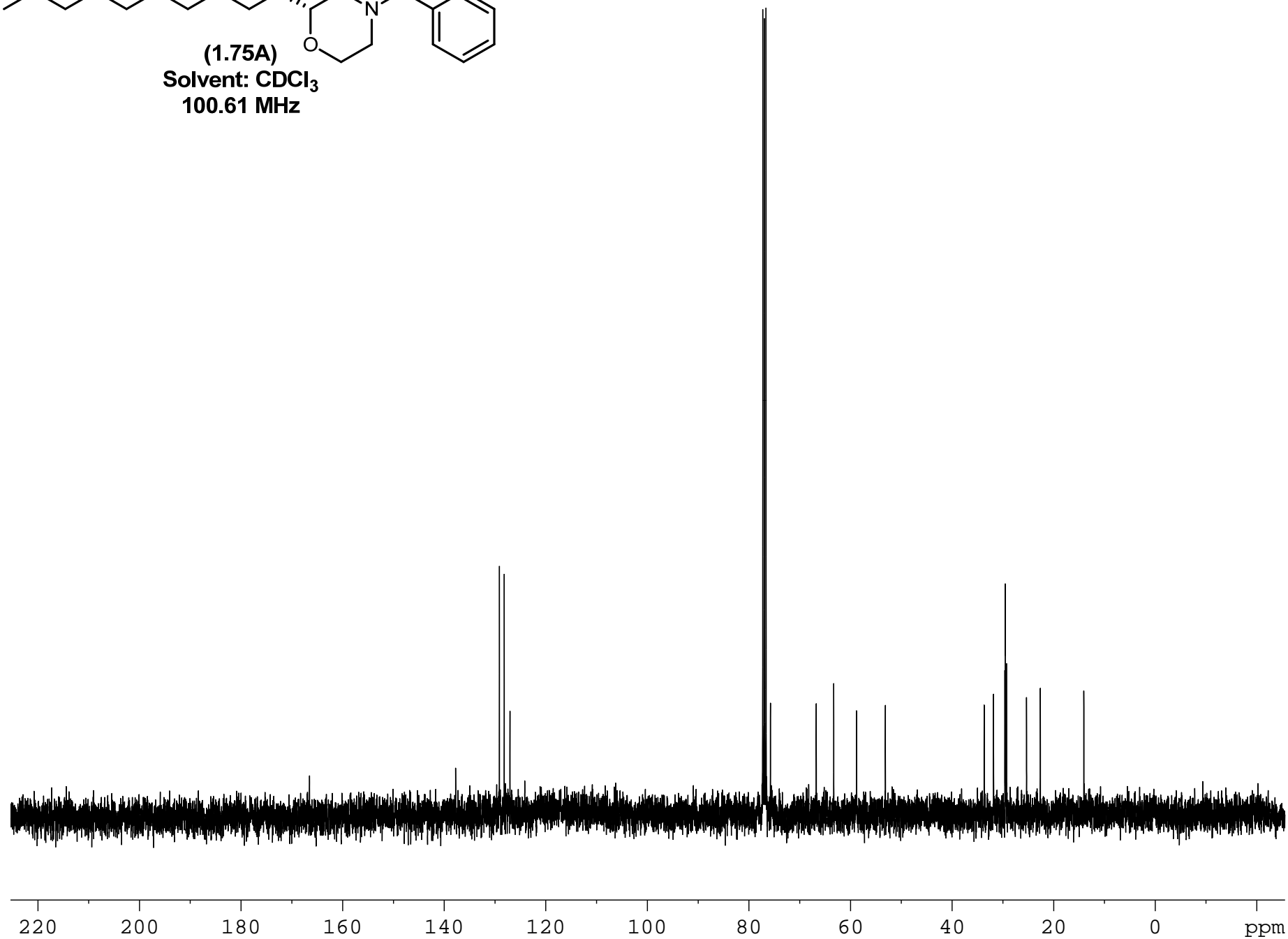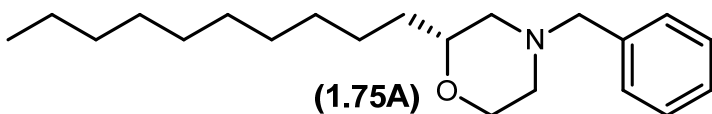
5.789

1.000
1.081
3.045

2.013

1.009
1.076

18.480

3.241

11   10   9   8   7   6   5   4   3   2   1   0   -1   ppm

240

(1.75A)
Solvent: CDCl$_3$
100.61 MHz

(1.75A)

Elemental Composition Report

Page 1

Single Mass Analysis

Tolerance = 5.0 PPM   /   DBE: min = -0.5, max = 25.0
Element prediction: Off
Number of isotope peaks used for i-FIT = 2

Monoisotopic Mass, Even Electron Ions
294 formula(e) evaluated with 1 results within limits (up to 50 closest results for each mass)
Elements Used:
C: 10-500   H: 10-1000   N: 1-200   O: 1-200

MCO-III-46

S/N: UH193

27-Oct-2011
14:31:35
TOF MS ES+
1.08e+004

MCO-III-46_102711_001 60 (1.120) AM (Cen,4, 80.00, Ar,8000.0,556.28,0.70); Sm (SG, 2x1.00); Cm (60:70)
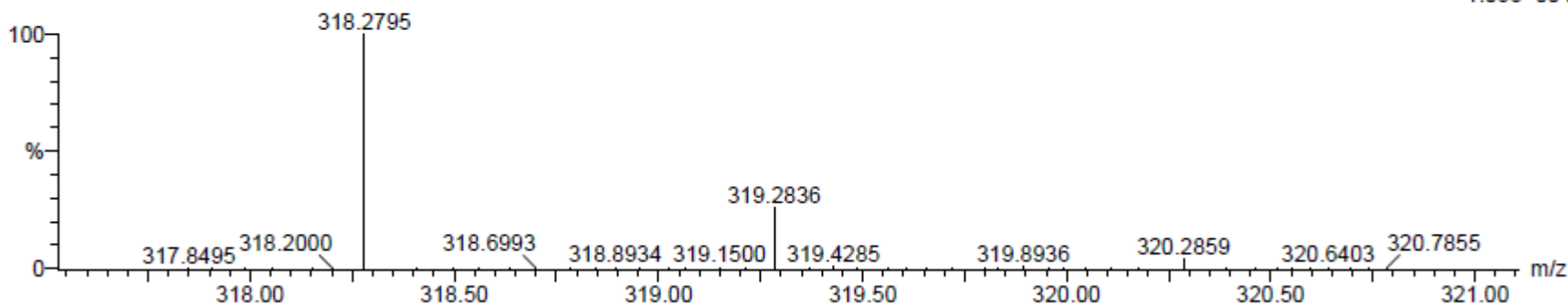

```
Minimum:                              -0.5
Maximum:             5.0      5.0     25.0

Mass        Calc. Mass      mDa      PPM      DBE      i-FIT      Formula

318.2795    318.2797        -0.2     -0.6     4.5      1.9        C21  H36  N  O
```

(1.75C)
Solvent: CDCl$_3$
400.13 MHz

10.405

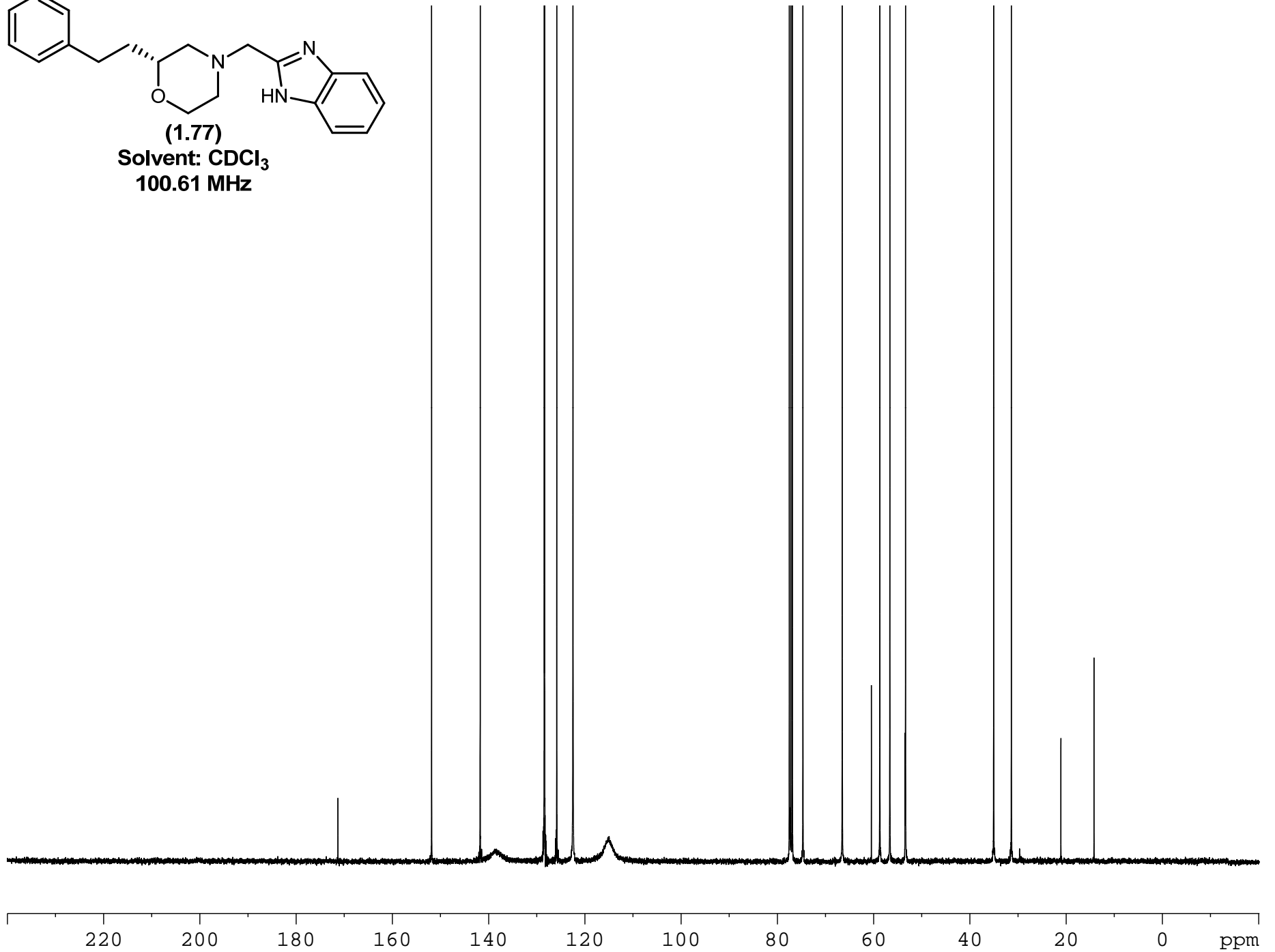1.000 1.057 2.943 4.032 1.002 1.138 1.175 1.053
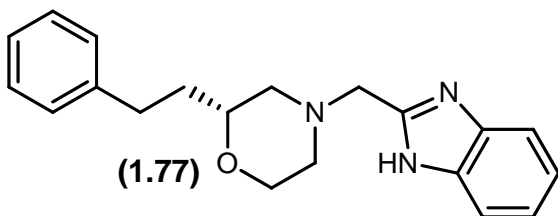
243
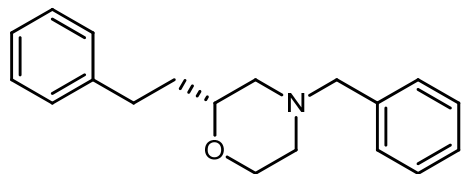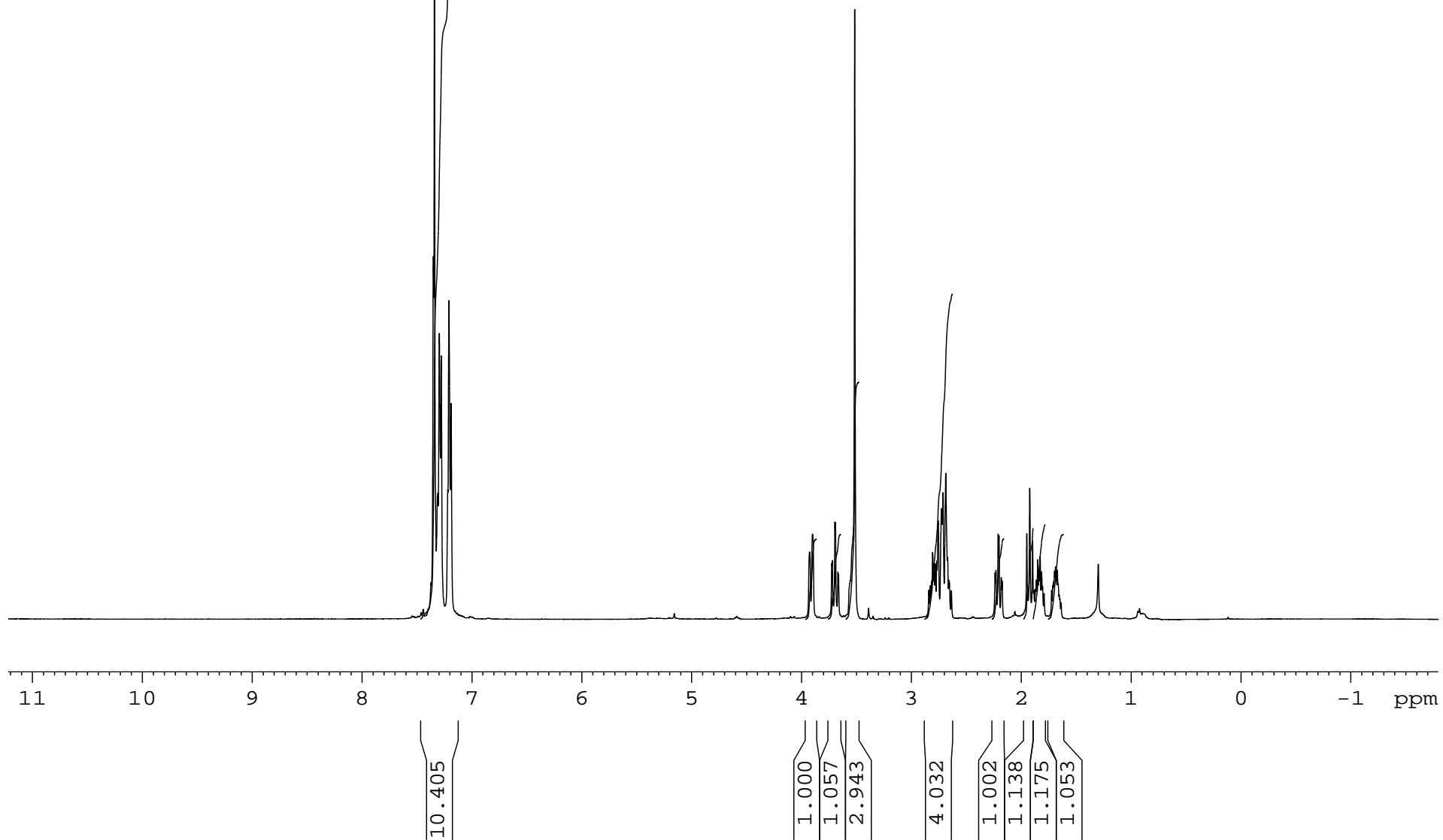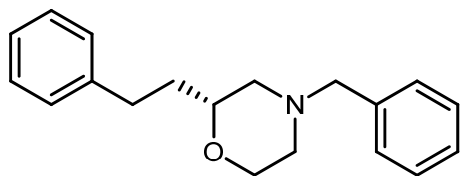
(1.75C)
Solvent: CDCl$_3$
100.61 MHz
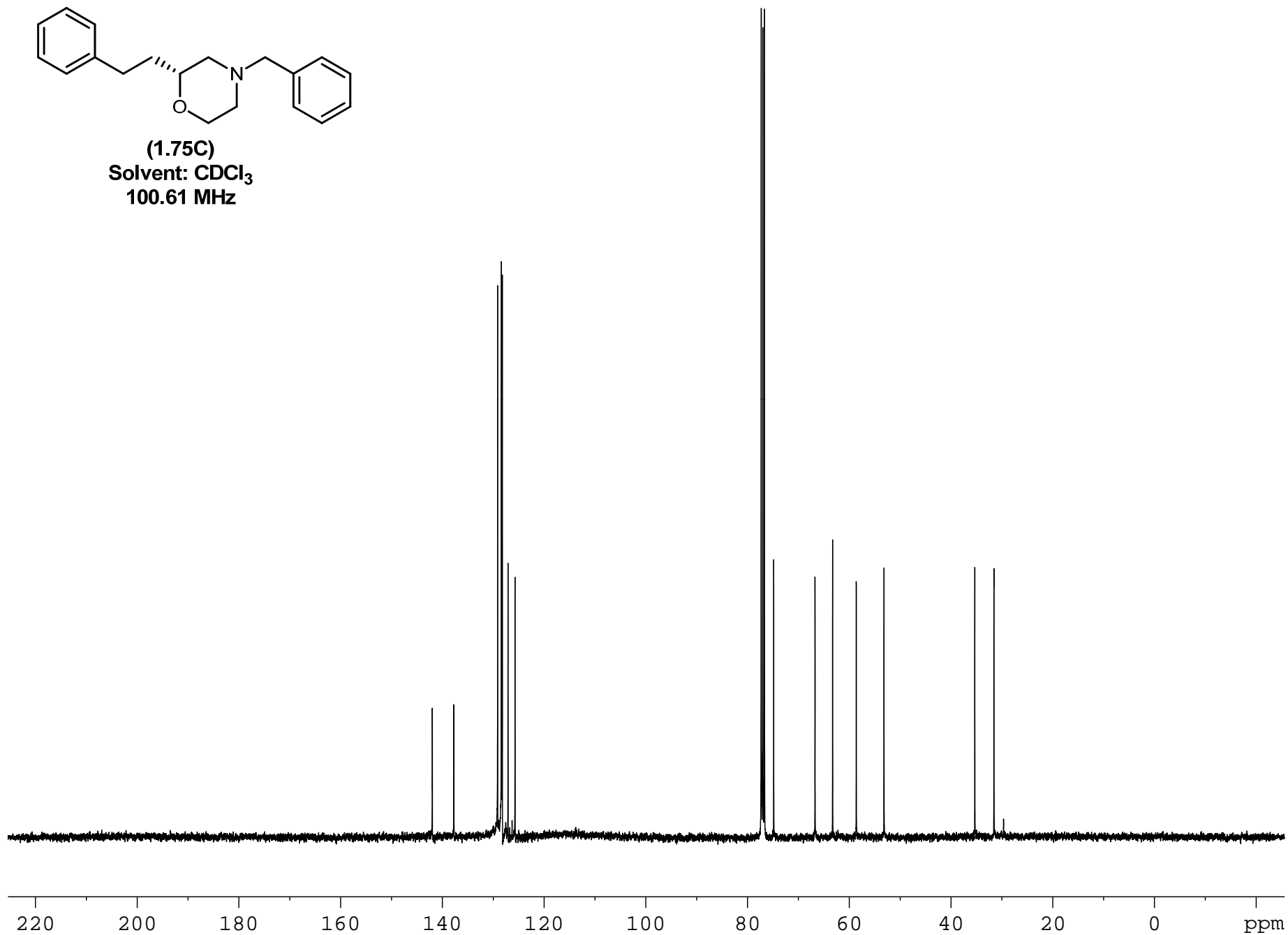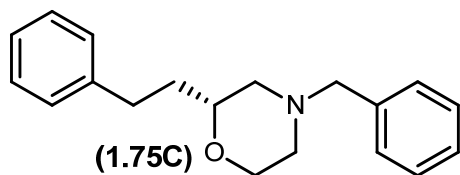
(1.75C)

Elemental Composition Report

Page 1

Single Mass Analysis
Tolerance = 5.0 PPM / DBE: min = -0.5, max = 25.0
Element prediction: Off
Number of isotope peaks used for i-FIT = 2

Monoisotopic Mass, Even Electron Ions
159 formula(e) evaluated with 1 results within limits (up to 50 best isotopic matches for each mass)
Elements Used:
C: 18-500   H: 10-1000   N: 1-200   O: 1-200

MCO-III-97

01-Mar-2012

S/N: UH193

13:24:57

MCO-III-97_030112_001 90 (1.700) AM (Cen,4, 80.00, Ar,8000.0,556.28,0.70); Sm (SG, 2x1.00); Cm (90:100)

TOF MS ES+
1.08e+004
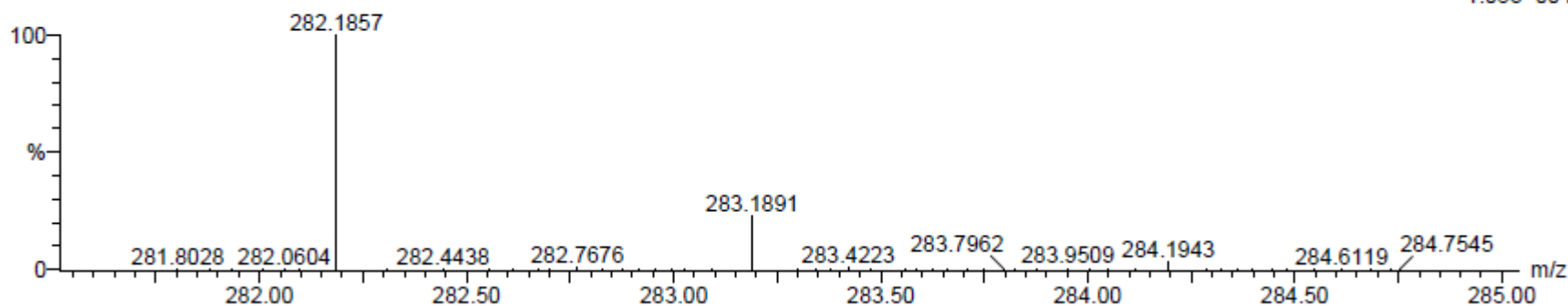
| | | Minimum: | | | -0.5 | | |
| | | Maximum: | 10.0 | 5.0 | 25.0 | | |

Mass	Calc. Mass	mDa	PPM	DBE	i-FIT	Formula
282.1857	282.1858	-0.1	-0.4	8.5	1.0	C19 H24 N O

(1.75B)
Solvent: CDCl$_3$
400.13 MHz

5.440

2.081

1.000
1.037
2.944

2.006

0.987
4.125
1.090

6.110

3.140

11   10   9   8   7   6   5   4   3   2   1   0   -1   ppm
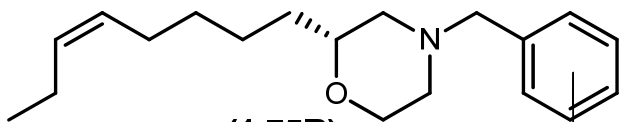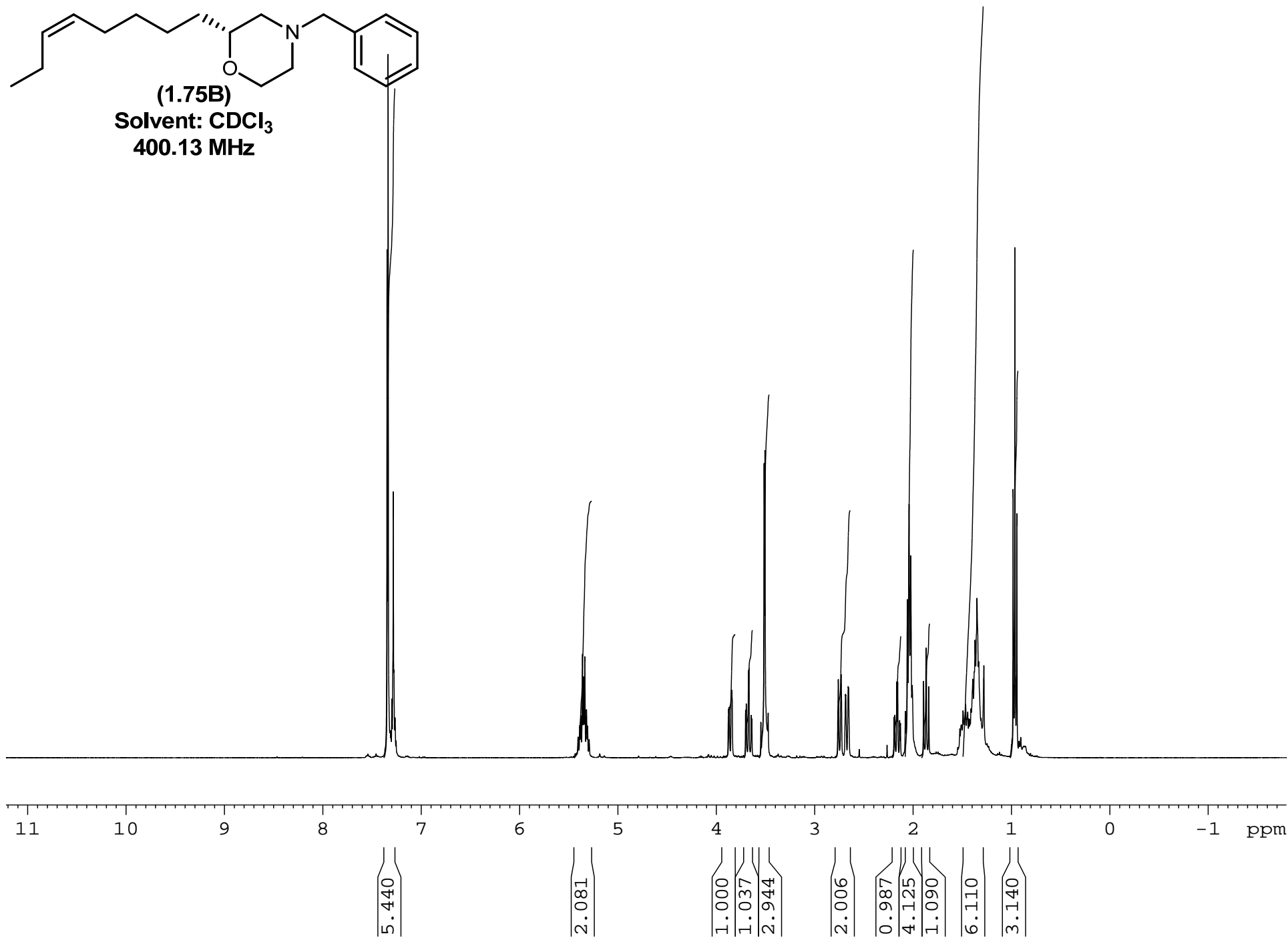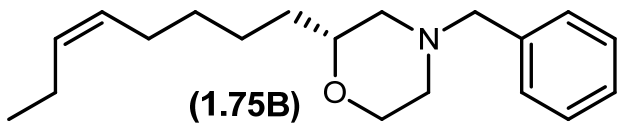
(1.75B)
Solvent: CDCl$_3$
100.61 MHz

(1.75B)

Elemental Composition Report

Page 1

Single Mass Analysis
Tolerance = 5.0 PPM / DBE: min = -0.5, max = 25.0
Element prediction: Off
Number of isotope peaks used for i-FIT = 2

Monoisotopic Mass, Even Electron Ions
168 formula(e) evaluated with 1 results within limits (up to 50 best isotopic matches for each mass)
Elements Used:
C: 18-500   H: 10-1000   N: 1-200   O: 1-200

MCO-III-175

01-Mar-2012

S/N: UH193

14:31:08

MCO-III-175_030112_001 55 (1.041) AM (Cen,4, 80.00, Ar,8000.0,556.28,0.70); Sm (SG, 2x1.00); Cm (50:60)

TOF MS ES+
8.68e+003
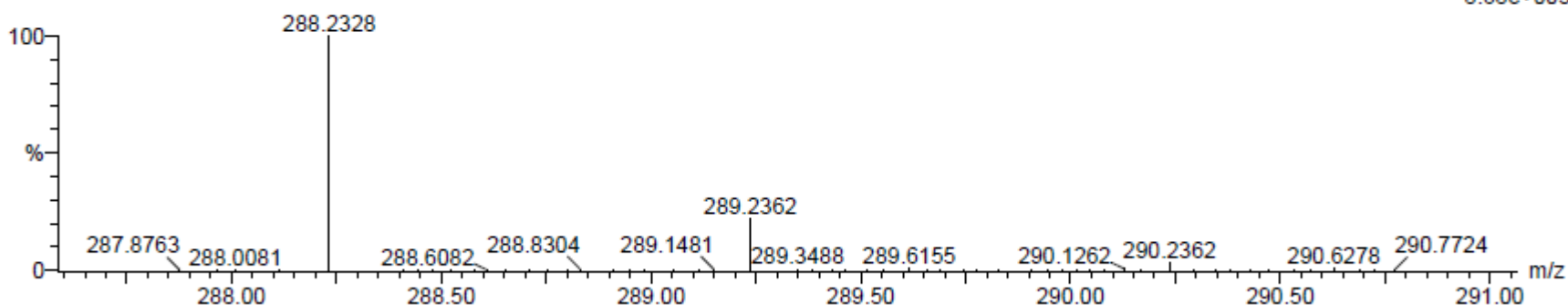
| Minimum: | | | | -0.5 | | |
| Maximum: | | 10.0 | 5.0 | 25.0 | | |

Mass	Calc. Mass	mDa	PPM	DBE	i-FIT	Formula
288.2328	288.2327	0.1	0.3	5.5	0.1	C19 H30 N O

248

(1.75D)
Solvent: CDCl$_3$
400.13 MHz
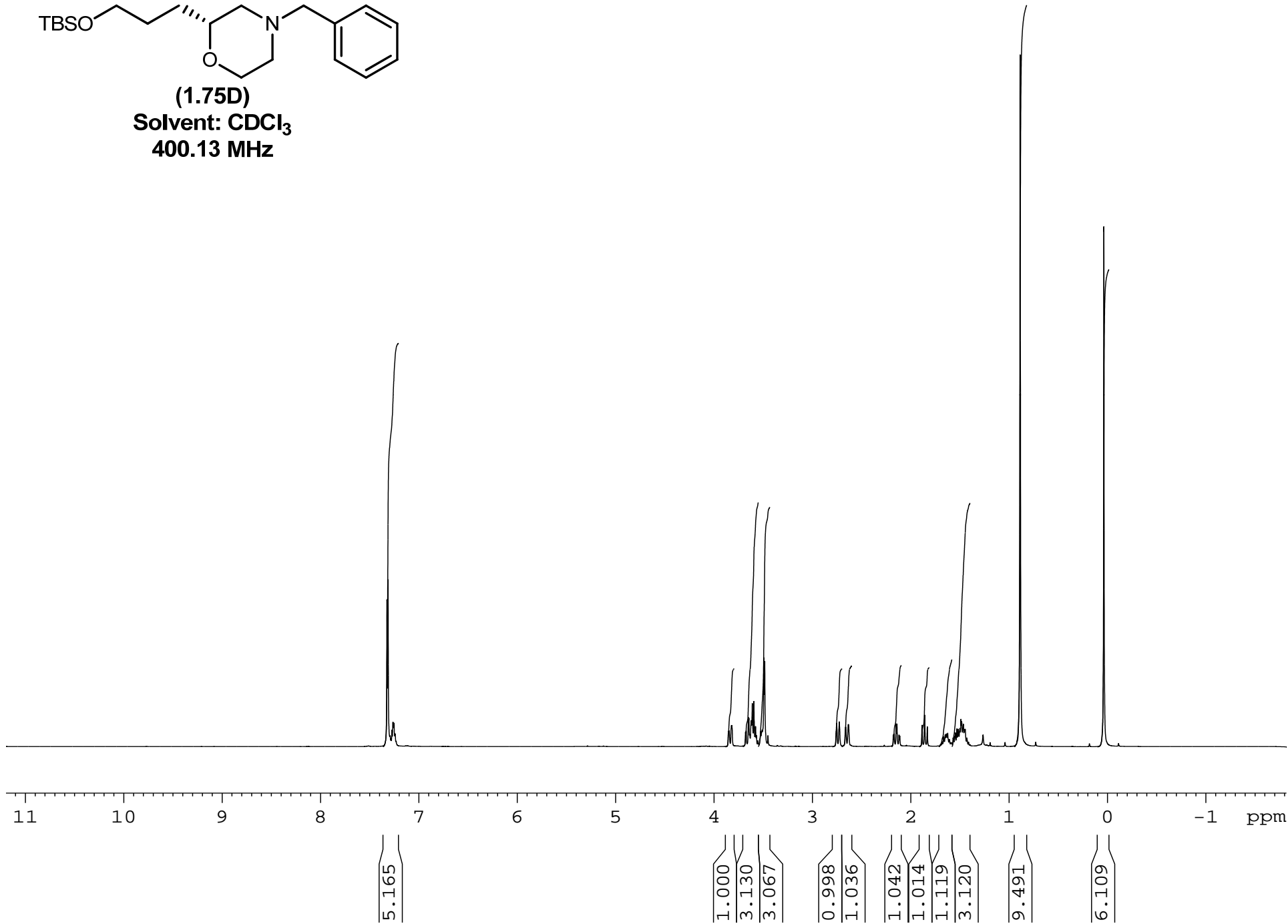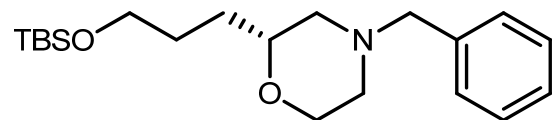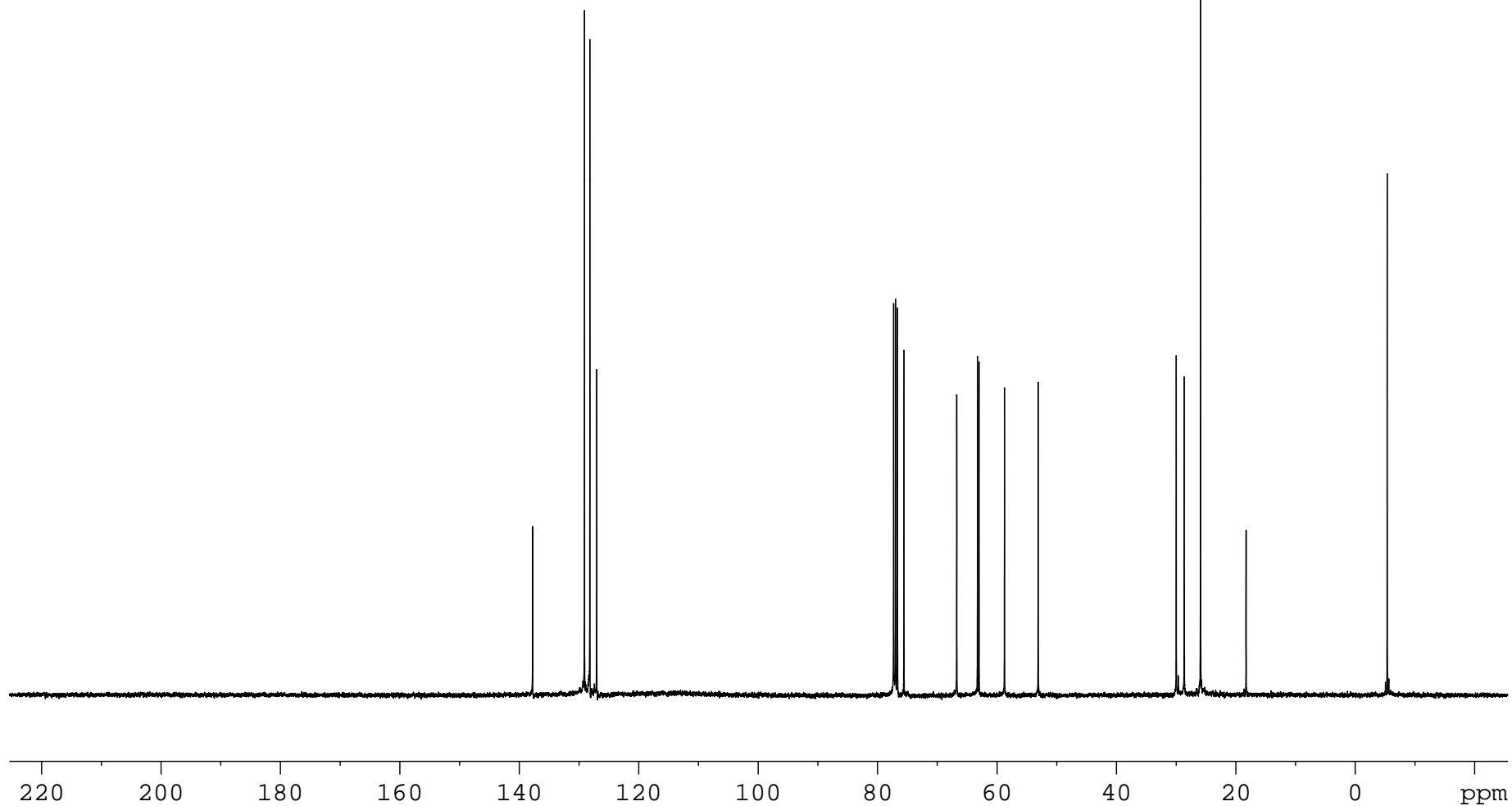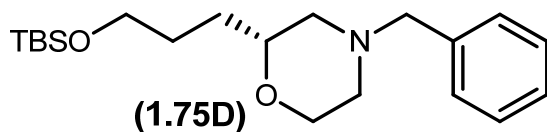
11 10 9 8 7 6 5 4 3 2 1 0 -1 ppm

5.165

1.000
3.130
3.067

0.998
1.036

1.042
1.014
1.119
3.120

9.491

6.109

(1.75D)
Solvent: CDCl$_3$
100.61 MHz

250

TBSO ... **(1.75D)** [structure: morpholine with N-benzyl, 2-substituent (CH2CH2CH2-OTBS)]

Single Mass Analysis
Tolerance = 5.0 PPM   /   DBE: min = -0.5, max = 25.0
Element prediction: Off
Number of isotope peaks used for i-FIT = 2

Monoisotopic Mass, Even Electron Ions
227 formula(e) evaluated with 1 results within limits (up to 50 best isotopic matches for each mass)
Elements Used:
C: 18-500   H: 10-1000   N: 1-200   O: 1-200   Si: 1-1

MCO-III-160   01-Mar-2012
                                                          S/N: UH193   13:53:12
MCO-III-160_030112_001 99 (1.869) AM (Cen,4, 80.00, Ar,8000.0,556.28,0.70); Sm (SG, 2x1.00); Cm (90:100)   TOF MS ES+
                                                                                                           1.20e+004

[mass spectrum: base peak 350.2514 at 100%; 351.2547; 352.2517; other labeled peaks: 350.0495, 350.5323, 350.7770, 350.8936, 351.6216, 352.1628, 352.6816, 352.7699]

Minimum: -0.5
Maximum: 10.0   5.0   25.0

Mass   Calc. Mass   mDa   PPM   DBE   i-FIT   Formula

350.2514   350.2515   -0.1   -0.3   4.5   0.3   C20 H36 N O2 Si

(1.76A)
Solvent: CDCl$_3$
400.13 MHz

5.469

1.056 1.000 1.054 1.080 0.999 2.069 2.137 2.285 9.625 16.244 3.267
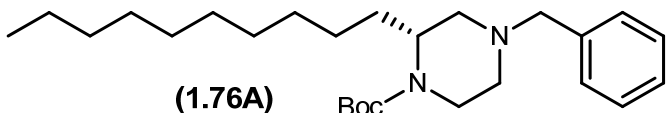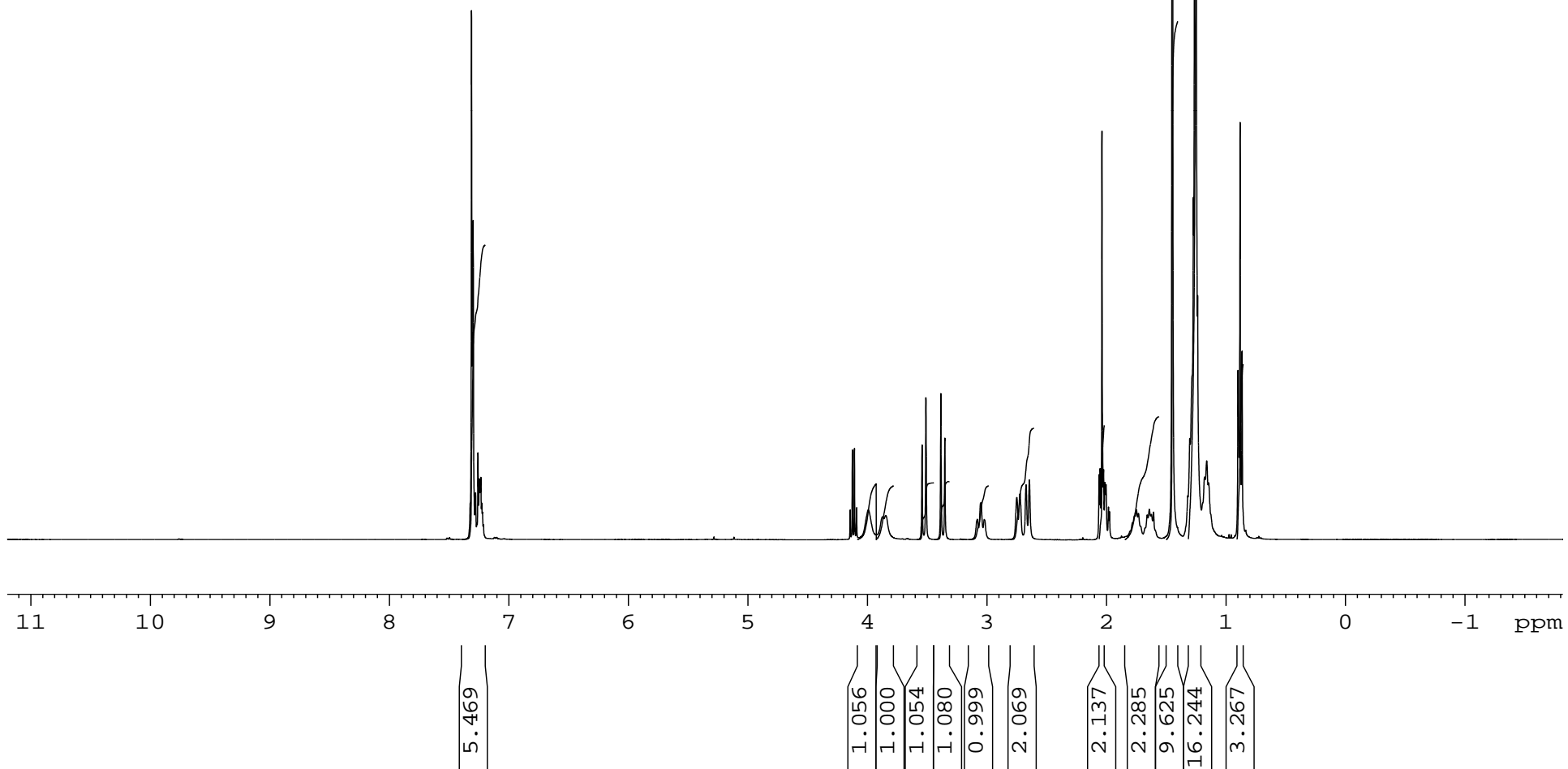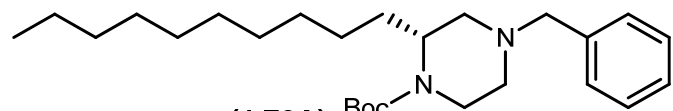
(1.76A)
Solvent: CDCl$_3$
100.61 MHz

(1.76A)   Boc

Elemental Composition Report

Single Mass Analysis
Tolerance = 5.0 PPM   /   DBE: min = -0.5, max = 25.0
Element prediction: Off
Number of isotope peaks used for i-FIT = 2

Monoisotopic Mass, Even Electron Ions
507 formula(e) evaluated with 1 results within limits (up to 50 best isotopic matches for each mass)
Elements Used:
C: 18-500   H: 10-1000   N: 1-200   O: 1-200

MCO-III-109

01-Mar-2012
13:36:44

S/N: UH193

MCO-III-109_030112_001 94 (1.775) AM (Cen,4, 80.00, Ar,8000.0,556.28,0.70); Sm (SG, 2x1.00); Cm (90:100)

TOF MS ES+
1.44e+004

417.3480

100

%

417.1730   417.6583 417.8815   418.0510   418.3525   418.7551   418.9478   419.3551 419.4570 419.7225

0

417.00   417.50   418.00   418.50   419.00   419.50   420.00   m/z

Minimum:				-0.5		
Maximum:		10.0	5.0	25.0		
Mass	Calc. Mass	mDa	PPM	DBE	i-FIT	Formula
417.3480	417.3481	-0.1	-0.2	5.5	1.5	C26 H45 N2 O2

(1.76C)
Solvent: CDCl₃
400.13 MHz

10.196

1.073
0.923
1.000
1.016
0.974
1.963
1.994
4.237
8.953

11   10   9   8   7   6   5   4   3   2   1   0   -1   ppm

255
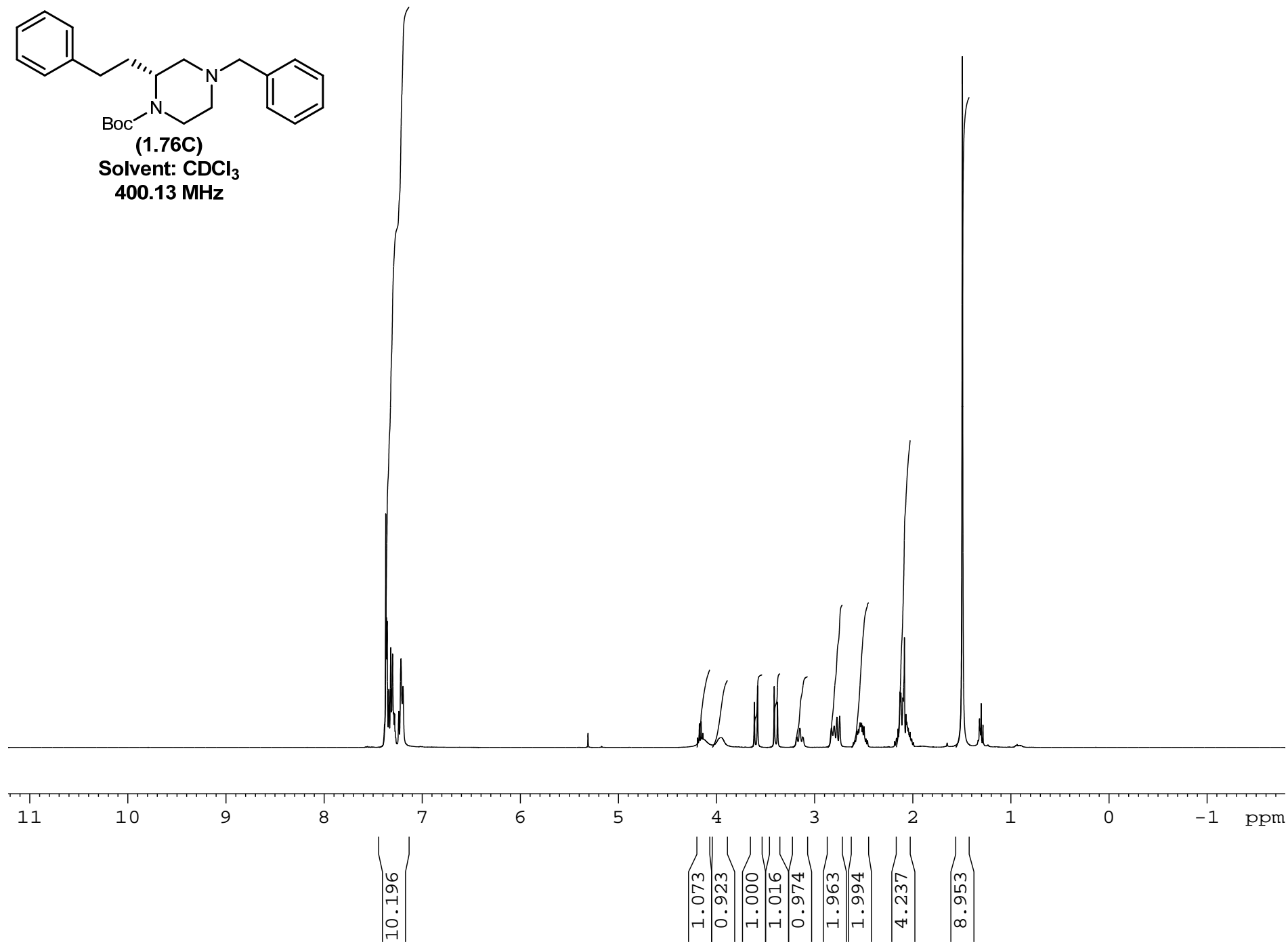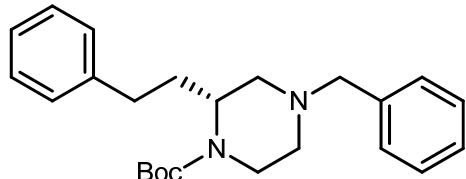
(1.76C)
Solvent: CDCl₃
100.61 MHz

(1.76C)

Elemental Composition Report

Page 1

Single Mass Analysis
Tolerance = 5.0 PPM / DBE: min = -0.5, max = 25.0
Element prediction: Off
Number of isotope peaks used for i-FIT = 2

Monoisotopic Mass, Even Electron Ions
352 formula(e) evaluated with 1 results within limits (up to 50 closest results for each mass)
Elements Used:
C: 20-500   H: 10-1000   N: 1-200   O: 1-200

MCO-III-40

20-Oct-2011
15:34:02

S/N: UH193

MCO-III-40_102011_002 90 (1.677) AM (Cen,4, 80.00, Ar,8000.0,556.28,0.70); Sm (SG, 2x1.00); Cm (80:90)

TOF MS ES+
9.41e+003
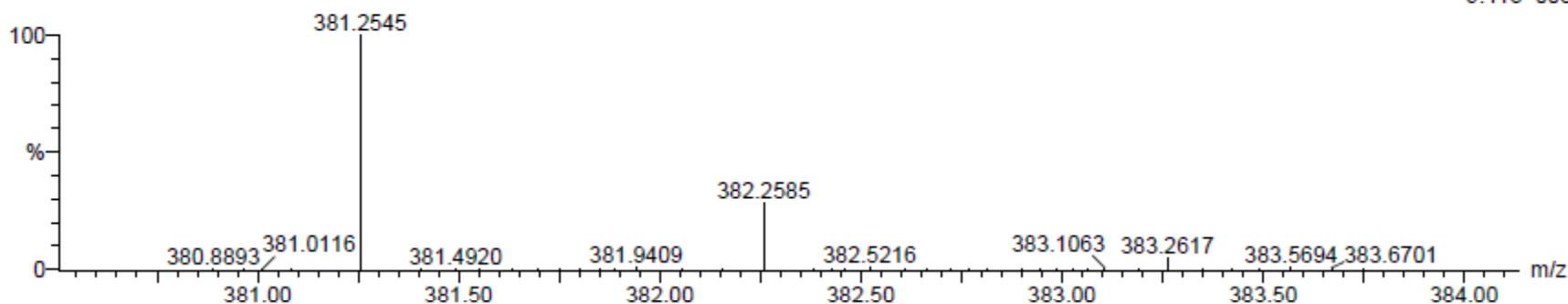
Minimum:				-0.5	
Maximum:		5.0	5.0	25.0	
Mass	Calc. Mass	mDa	PPM	DBE	i-FIT	Formula
381.2545	381.2542	0.3	0.8	9.5	0.3	C24 H33 N2 O2

257
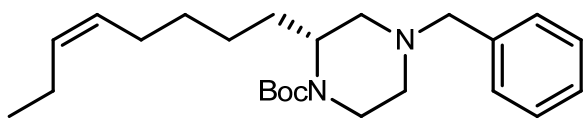
(1.76B)
Solvent: CDCl$_3$
400.13 MHz

258
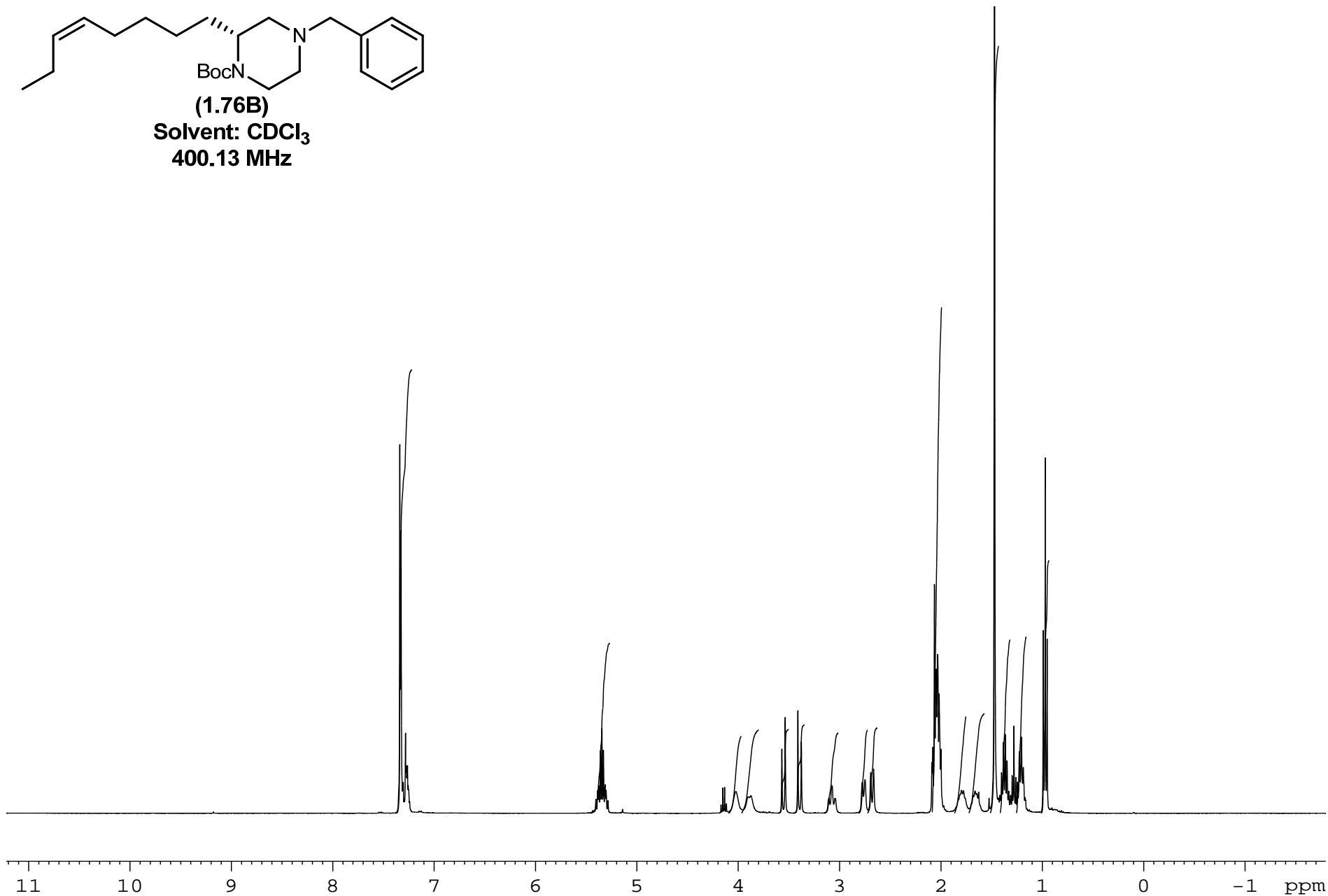
5.285

2.025

0.921
0.993
1.000
1.054
0.958
0.994
1.019

6.038
1.160
1.188
9.148
2.074
2.106
3.016

11 10 9 8 7 6 5 4 3 2 1 0 −1 ppm
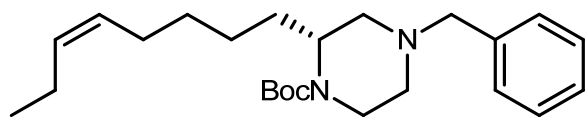
(1.76B)
Solvent: CDCl$_3$
100.61 MHz
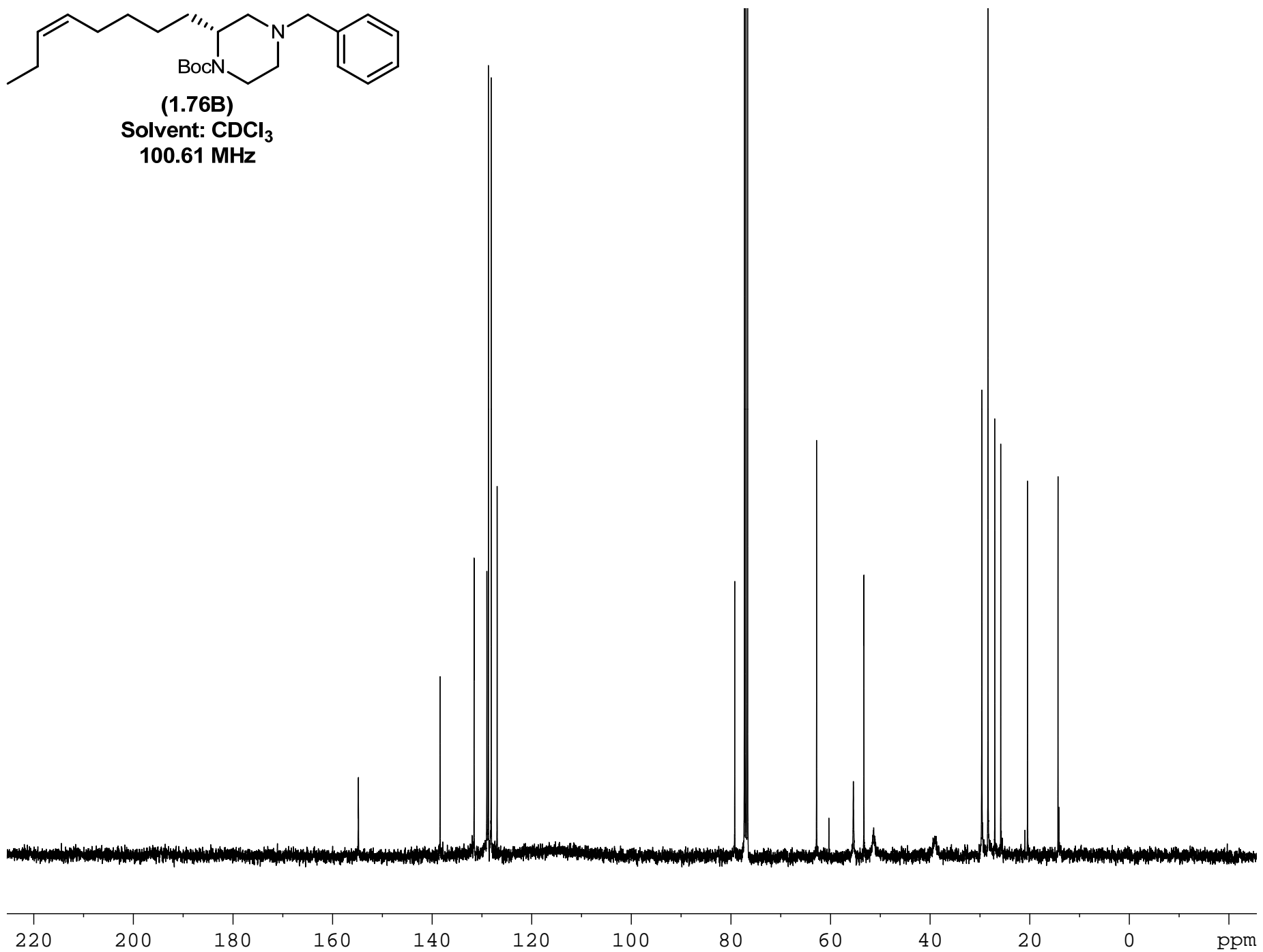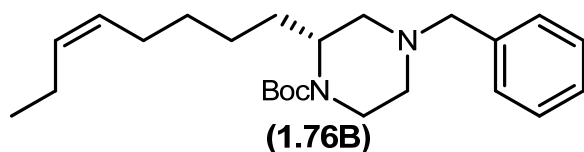
(1.76B)

Elemental Composition Report

Single Mass Analysis
Tolerance = 5.0 PPM / DBE: min = -0.5, max = 25.0
Element prediction: Off
Number of isotope peaks used for i-FIT = 2

Monoisotopic Mass, Even Electron Ions
366 formula(e) evaluated with 1 results within limits (up to 50 closest results for each mass)
Elements Used:
C: 20-500   H: 10-1000   N: 1-200   O: 1-200

MCO-III-55

MCO-III-55_111711_001 94 (1.775) AM (Cen,4, 80.00, Ar,8000.0,556.28,0.70); Sm (SG, 2x1.00); Cm (90:100)

S/N: UH193

17-Nov-2011
15:19:26
TOF MS ES+
3.04e+003
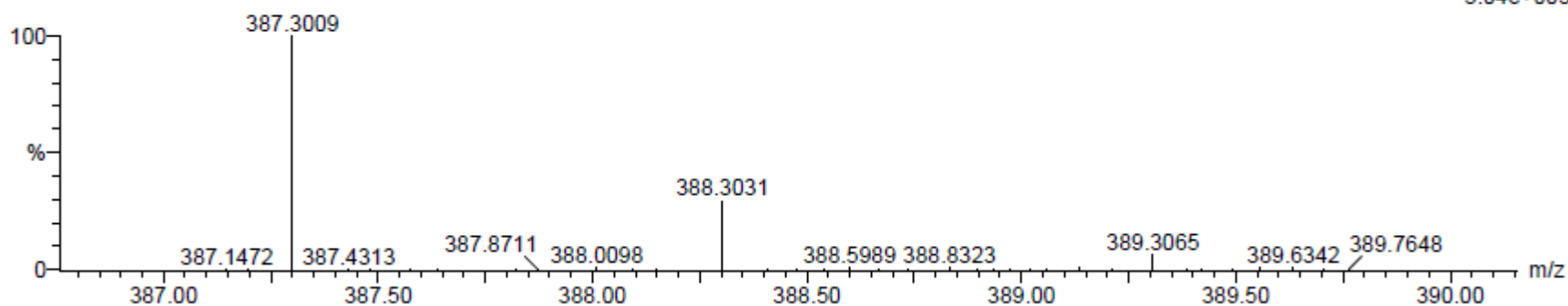
Minimum:				-0.5		
Maximum:		5.0	5.0	25.0		

Mass	Calc. Mass	mDa	PPM	DBE	i-FIT	Formula
387.3009	387.3012	-0.3	-0.8	6.5	0.6	C24 H39 N2 O2
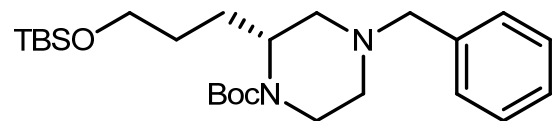
(1.76D)
Solvent: CDCl₃
400.13 MHz

261
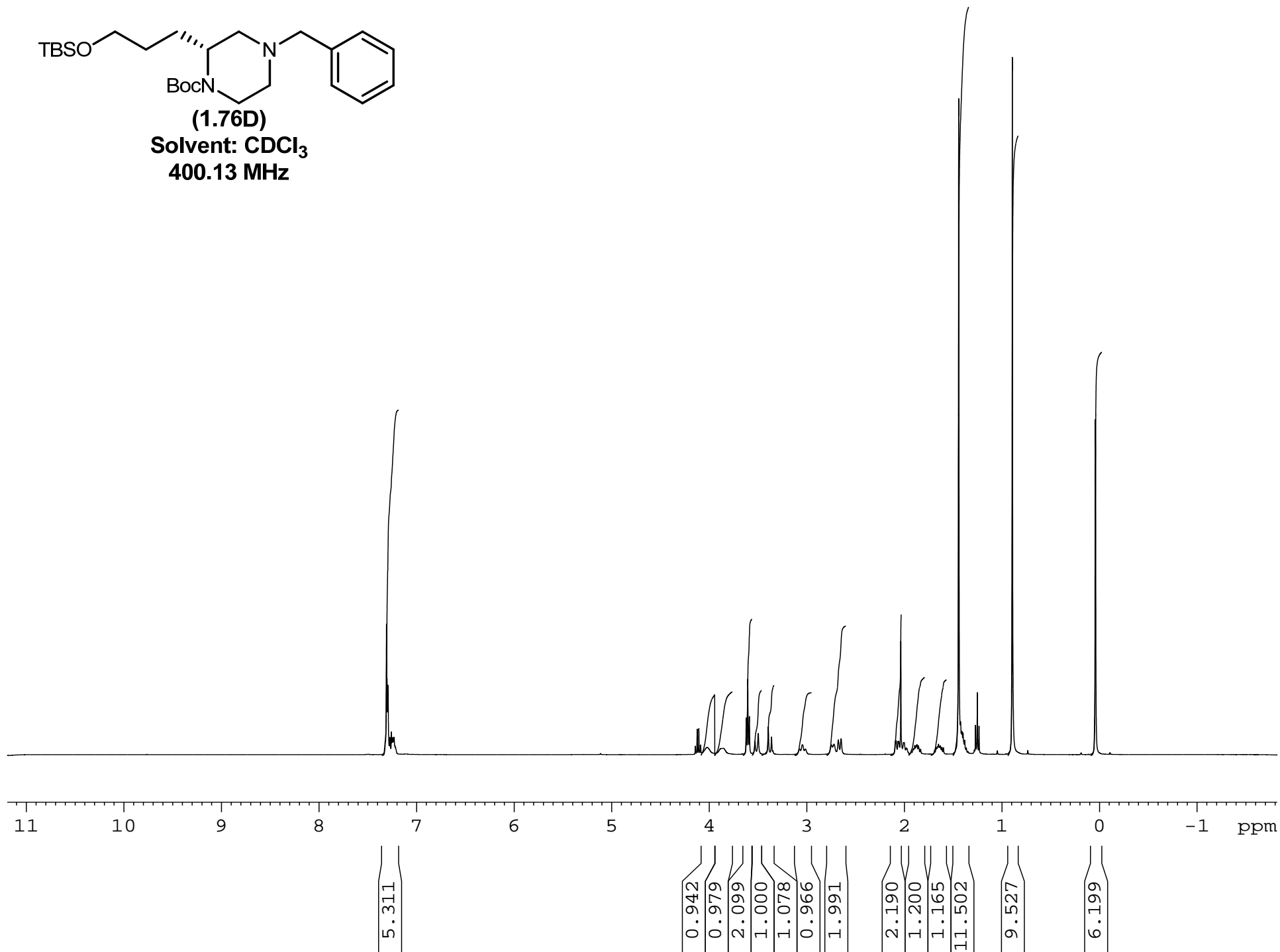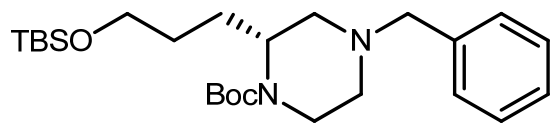
(1.76D)
Solvent: CDCl₃
100.61 MHz
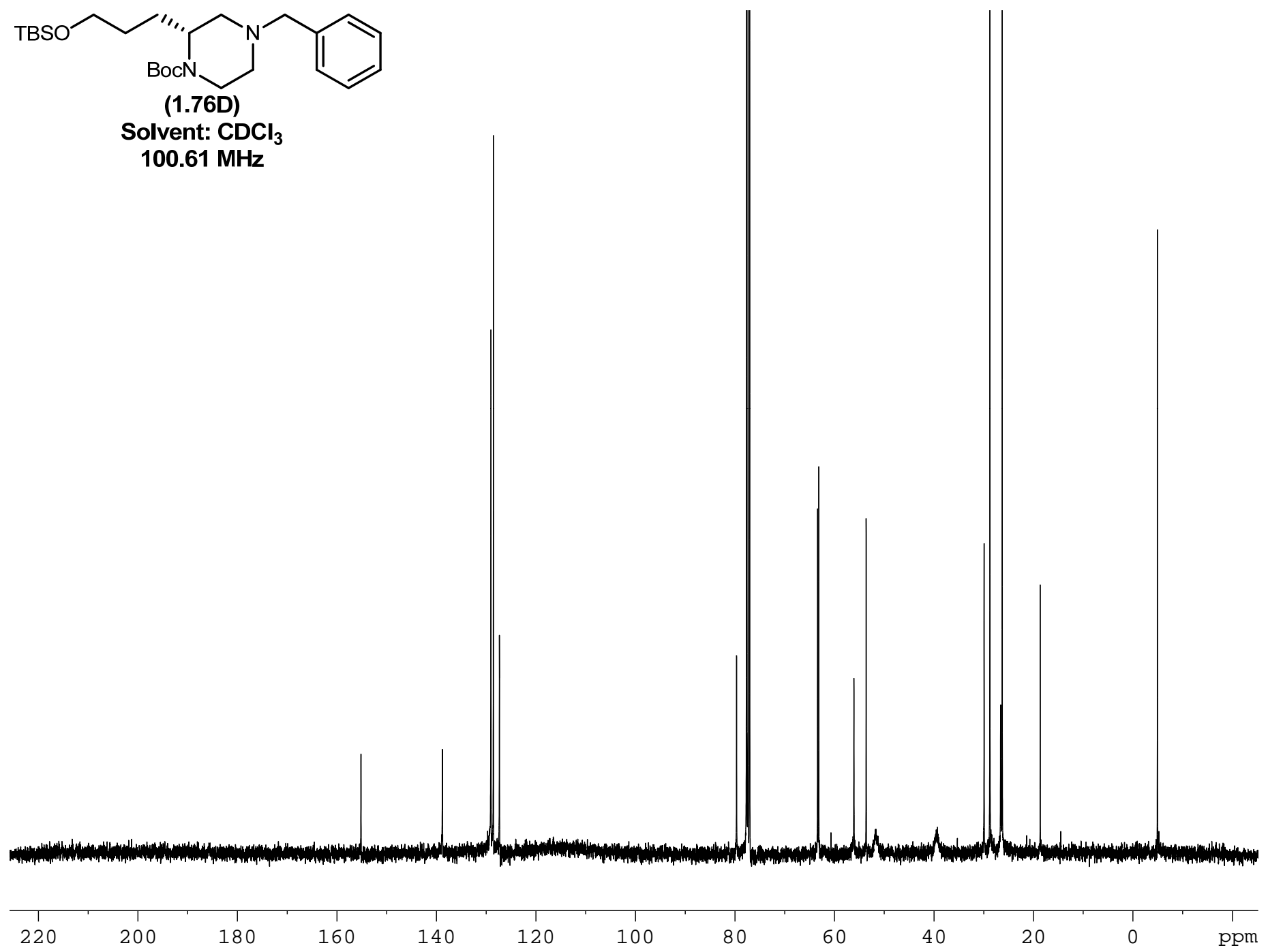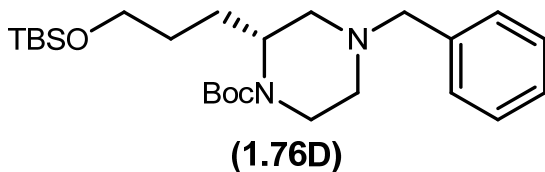
(1.76D)

Elemental Composition Report

Page 1

Single Mass Analysis
Tolerance = 5.0 PPM   /   DBE: min = -0.5, max = 25.0
Element prediction: Off
Number of isotope peaks used for i-FIT = 2

Monoisotopic Mass, Even Electron Ions
400 formula(e) evaluated with 1 results within limits (up to 50 closest results for each mass)
Elements Used:
C: 25-500   H: 10-1000   N: 1-200   O: 1-200   Si: 1-1

MCO-III-53

17-Nov-2011

S/N: UH193

15:07:33

MCO-III-53_111711_002 99 (1.869) AM (Cen,4, 80.00, Ar,8000.0,556.28,0.70); Sm (SG, 2x1.00); Cm (90:100)

TOF MS ES+
2.46e+004
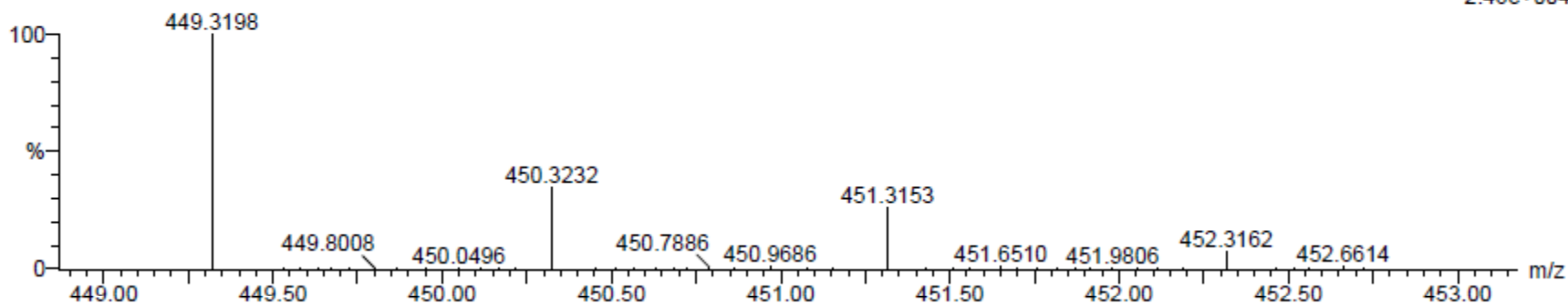
Minimum:				-0.5		
Maximum:		5.0	5.0	25.0		
Mass	Calc. Mass	mDa	PPM	DBE	i-FIT	Formula
449.3198	449.3199	-0.1	-0.2	5.5	0.0	C25 H45 N2 O3 Si
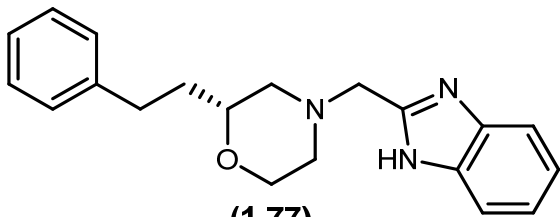
(1.77)
Solvent: CDCl$_3$
400.13 MHz
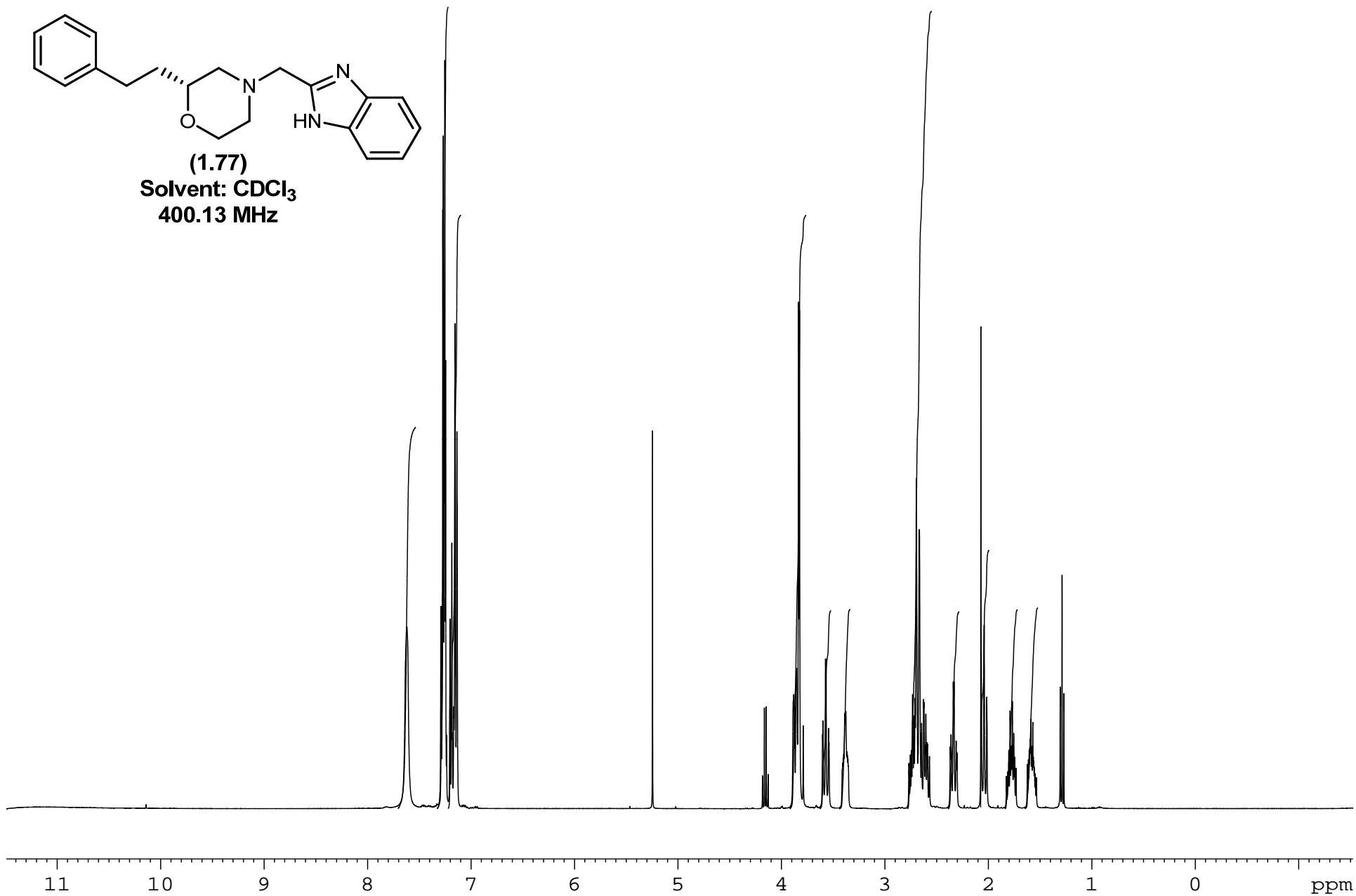
1.912 4.017 2.973

2.973 0.993 1.000

3.994 0.987 1.295 0.998 1.007
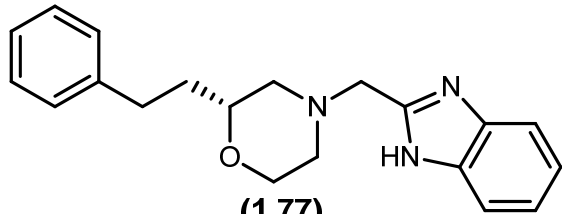
11   10   9   8   7   6   5   4   3   2   1   0   ppm

(1.77)
Solvent: CDCl$_3$
100.61 MHz

(1.77)

Single Mass Analysis
Tolerance = 5.0 PPM / DBE: min = -0.5, max = 25.0
Element prediction: Off
Number of isotope peaks used for i-FIT = 2

Monoisotopic Mass, Even Electron Ions
215 formula(e) evaluated with 1 results within limits (up to 50 best isotopic matches for each mass)
Elements Used:
C: 20-500   H: 10-1000   N: 1-200   O: 1-200

MCO-III-157   05-Mar-2012
                                                                S/N: UH193   11:03:16
MCO-III-157_030512_001 70 (1.324) AM (Cen,4, 80.00, Ar,8000.0,556.28,0.70); Sm (SG, 2x1.00); Cm (60:70)   TOF MS ES+
                                                                                                           8.64e+003
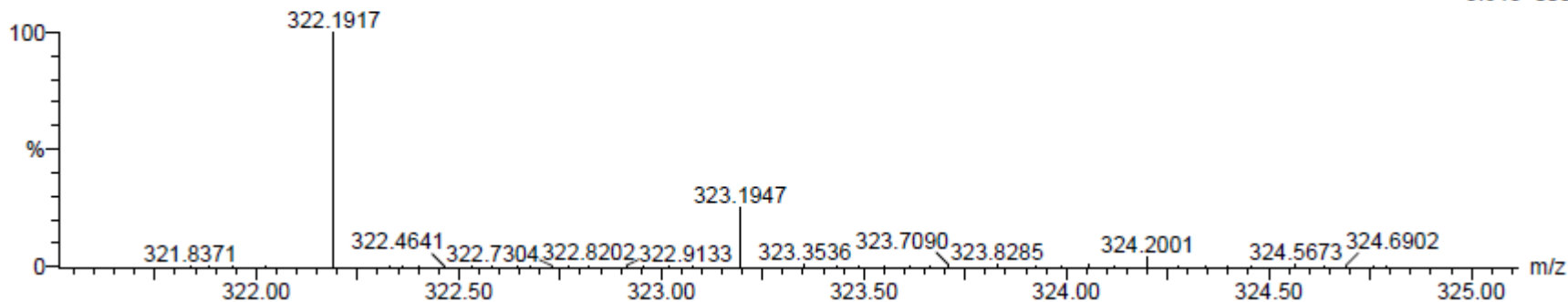
Minimum:			-0.5		
Maximum:	10.0	5.0	25.0		

Mass	Calc. Mass	mDa	PPM	DBE	i-FIT	Formula
322.1917	322.1919	-0.2	-0.6	10.5	2.1	C20 H24 N3 O

(1.75A)

TharSFC

Single Absorbance

RT: Ret Time | A: Area
A%: Area Perc | PN: Peak Name

Absorbance at 210 nm

Injection Info			Temp	40.1
Inj Vol	5		Flow	3.5
Solvent	MeOH (0.1% DEA)		% Modifier	5
Column	CHIRALPAK IA		Pressure	100
Sample	MCO-III-46			
Well location	P1: 4D			

Peak Info

Peak No	% Area	Area	RT (min)	Height (mV)	K'
1	53.2329	5528.3527	2.11	760.0137	0.0021
2	46.7671	4856.8689	2.77	948.8215	0.0028
Total:	100	10385.2216			

(1.75A)

Single Absorbance

RT: Ret Time	A: Area
AR: Area Pers	PN: Peak Name

RT:2.76 A:9000.2874 A:95.9% PN:Peak2

RT:2.12 A:381.6471 A:4.0679 PN:Peak1

Absorbance at 218 nm
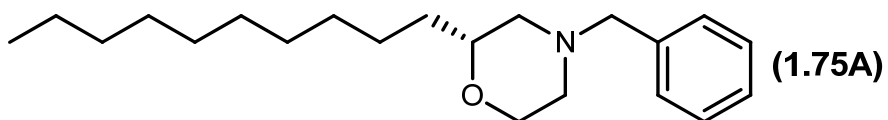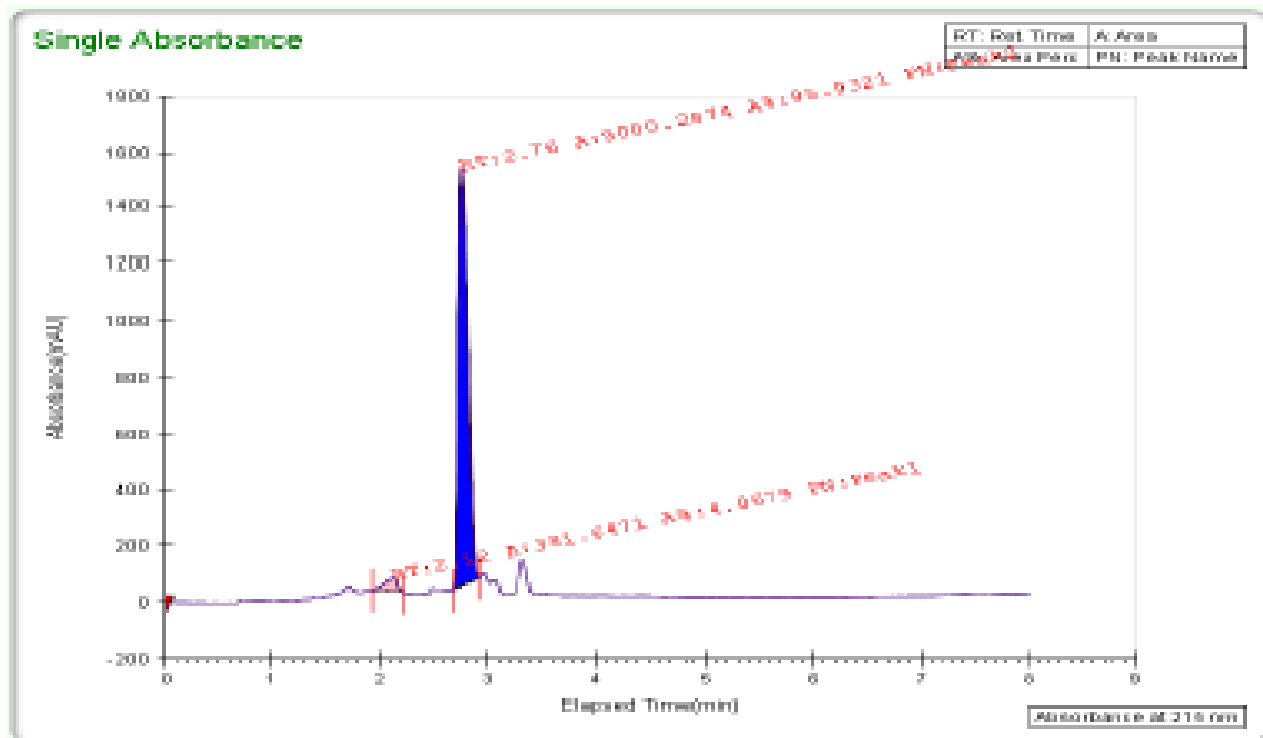
General Info

Log Author

Log Date	11/22/2011 4:33:15 PM
Report By	current_User
Report Date	11/22/2011
Method Name	5_50_gradient.met

Notes

Injection Info		Temp	39.9
Inj Vol	5	Flow	3.5
Solvent	MeOH (0.1% DEA)	% Modifier	5
Column	CHIRALPAK IA	Pressure	100
Sample	MCO-III-79		
Well location	P1: 4B		

Peak Info

Peak No	% Area	Area	RT (min)	Height (mV)	K'
1	4.0679	381.6471	2.12	49.4921	0.0021
2	95.9321	9000.2874	2.76	1486.41	0.0028
Total:	100	9381.9345			

TharSFC

C:\SFC\Data\General\MCO-III-79_11-22-2011_4_33_15_PM.tta
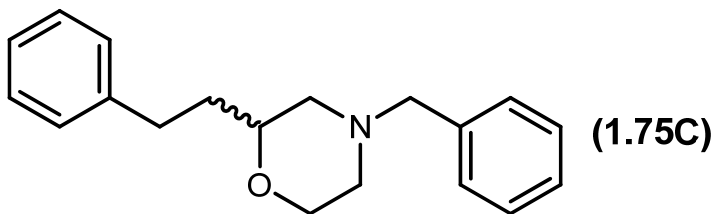
(1.75C)

TharSFC

Single Absorbance

RT: Ret. Time	A: Area
A%: Area Perc	Pk: Peak Name

RT:2.53 A:7923.1949 A%:49...
RT:3.39 A:9339.7349 A%:51.85

Absorbance at 220 nm
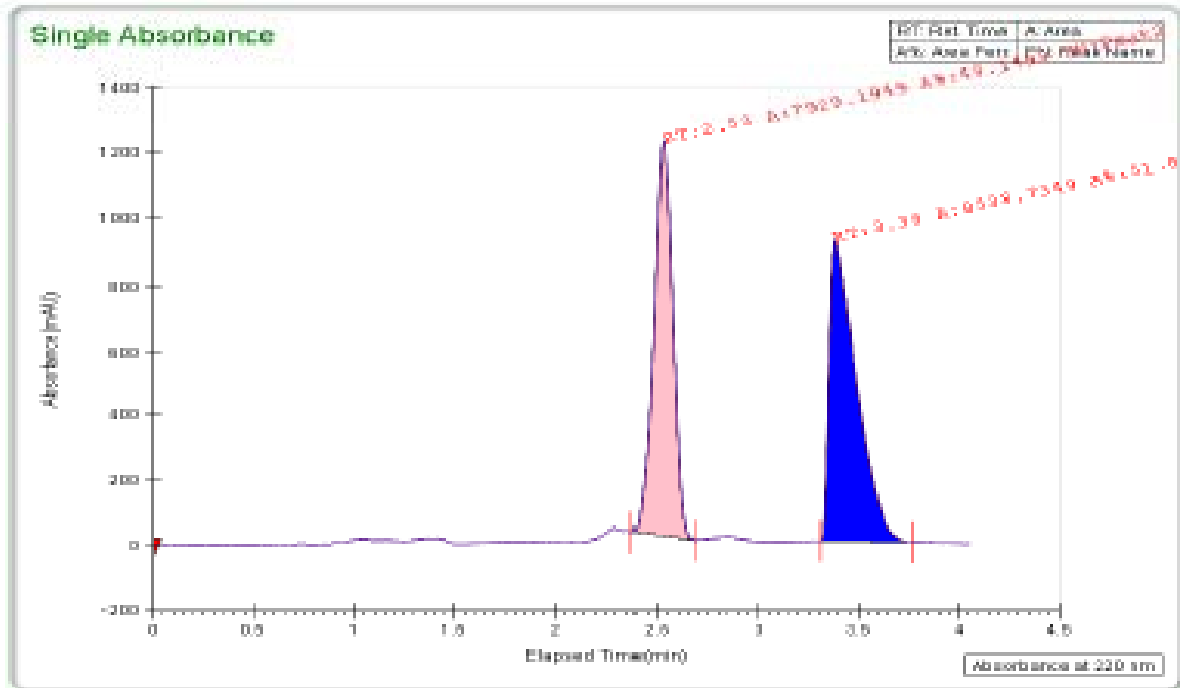
General Info
Log Author
Log Date   12/14/2011 9:58:49 AM
Report By   current_User

Report Date   12/14/2011
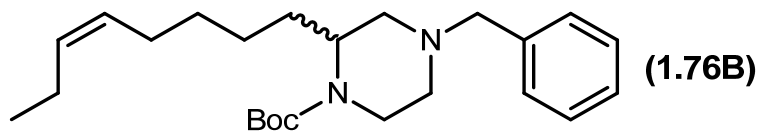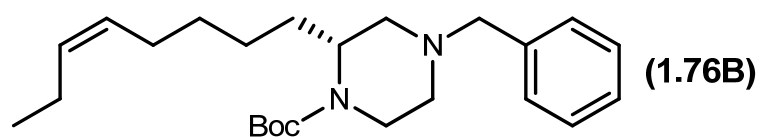Method Name   ISOCRATIC.met
Notes

Injection Info
Inj Vol   10
Solvent   MeOH (0.1% DEA)
Column   CHIRALPAK IB
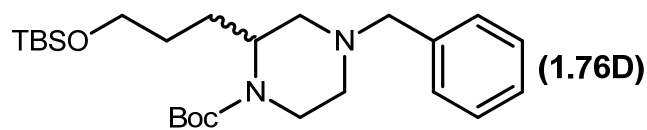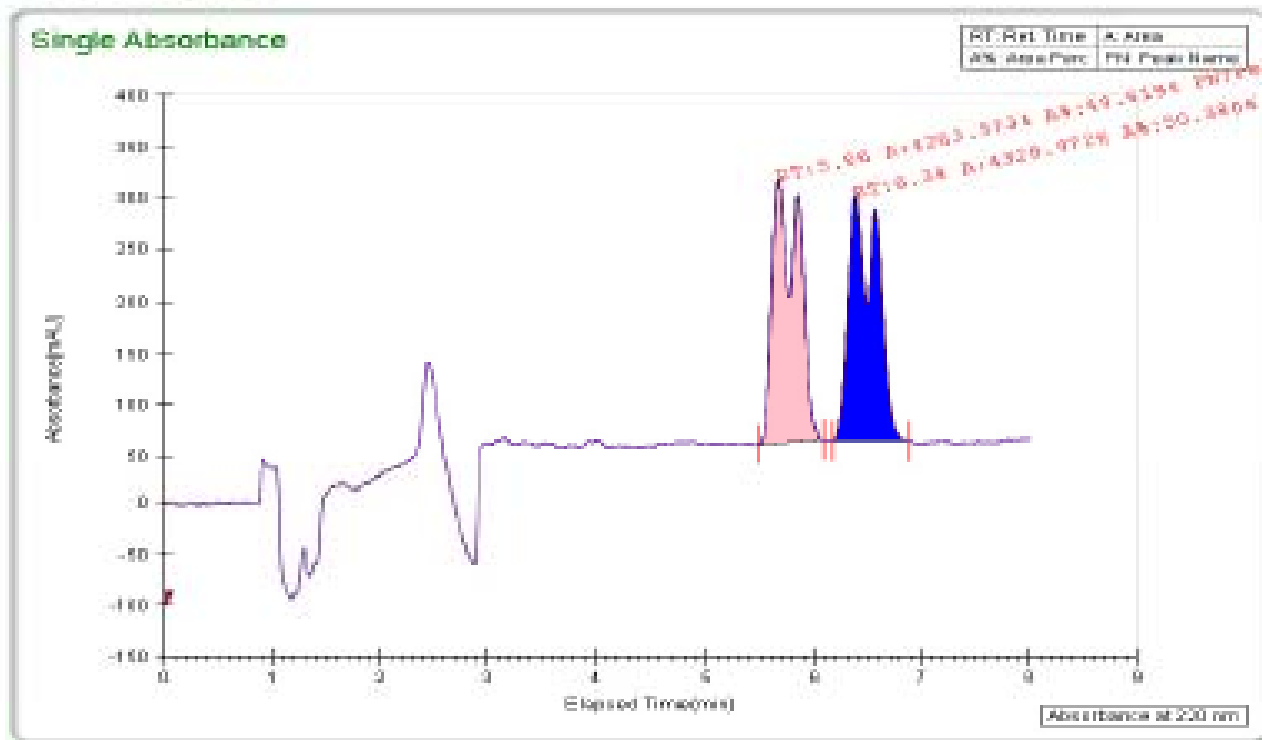Sample   MCO-III-97
Well location   P1: 4B

Temp   41.4
Flow   5
% Modifier   10
Pressure   100

Peak Info

Peak No	% Area	Area	RT (min)	Height (mV)	K'
1	48.1493	7929.1949	2.53	1203.0953	0.0042
2	51.8507	8538.7349	3.39	948.4999	0.0000
Total:	100	16467.9298			

TharSFC

C:\SFC\Data\General\MCO-III-97_12-14-2011_9_58_49 AM.tta.
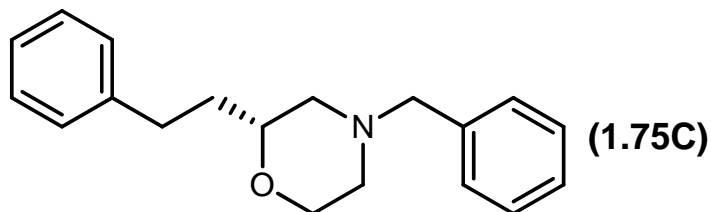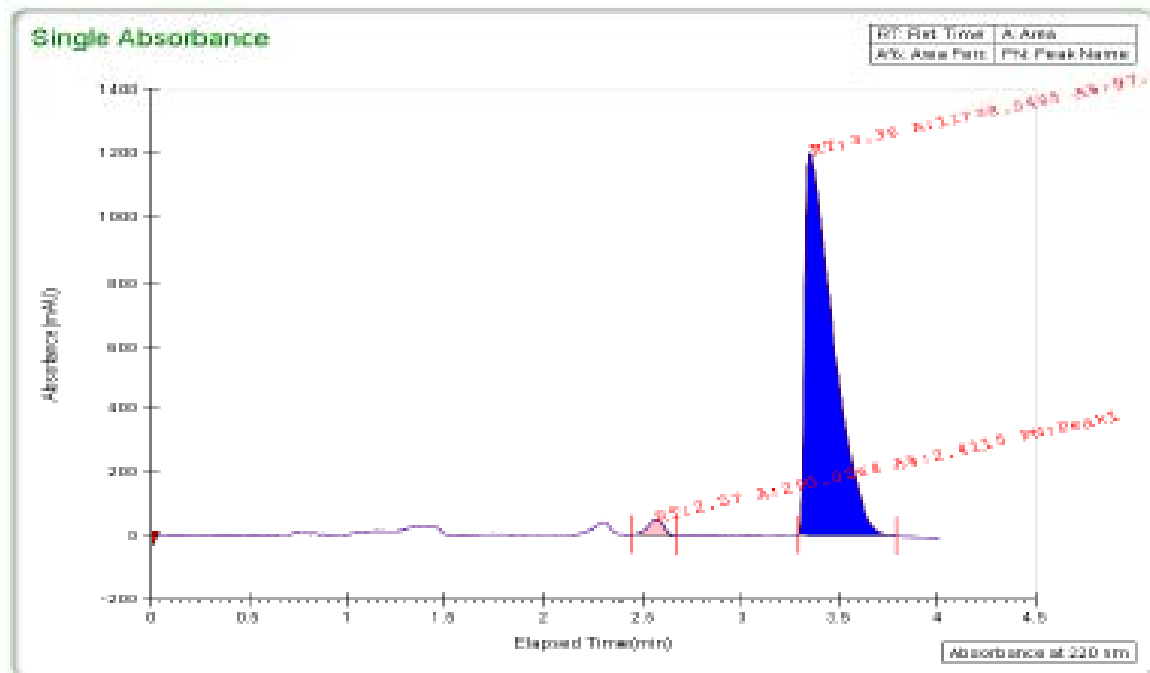
(1.75C)

Single Absorbance

RT: Ret Time | A: Area
A%: Area Perc | PN: Peak Name

Absorbance at 220 nm

General Info		Report Date	12/14/2011
Log Author		Method Name	ISOCRATIC.met
Log Date	12/14/2011 10:04:37 AM	Notes	
Report By	current_User		

Injection Info		Temp	42.3
Inj Vol	10	Flow	5
Solvent	MeOH (0.1% DEA)	% Modifier	10
Column	CHIRALPAK IB	Pressure	100
Sample	MCO-III-91		
Well Location	P1: 5A		

Peak Info

Peak No	% Area	Area	RT (min)	Height (mV)	K'
1	2.4115	290.0564	2.57	50.6099	0.0042
2	97.5885	11738.0485	3.36	1195.4413	0.0055
Total:	100	12028.1049			
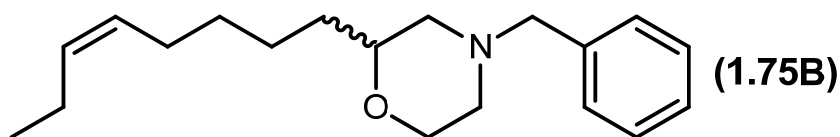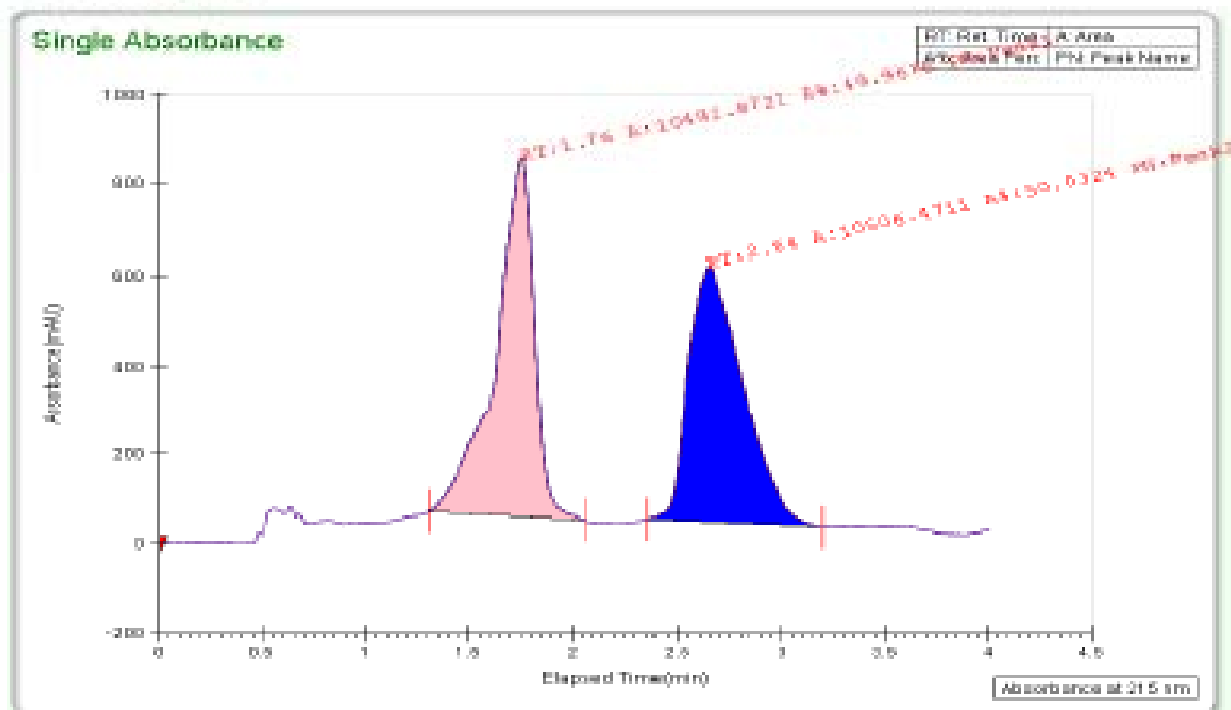
(1.75B)

Single Absorbance

Absorbance at 215 nm

General Info			Report Date	12/14/2011
Log Author			Method Name	ISOCRATIC.met
Log Date	12/14/2011 12:26:24 PM		Notes	
Report By	current_User			

Injection Info

Inj Vol	10
Solvent	MeOH (0.1% DEA)
Column	CHIRALPAK IA (4.6 x 150 mm)
Sample	MCO-II-70
Well location	P1: 1A
Temp	39.8
Flow	5
% Modifier	5
Pressure	100

Peak Info

Peak No	% Area	Area	RT (min)	Height (mV)	K'
1	49.9676	10492.8721	1.76	801.4662	0.0024
2	50.0324	10506.4711	2.64	575.1337	0.0035
Total:	100	20999.3432			
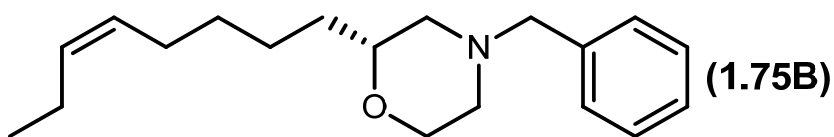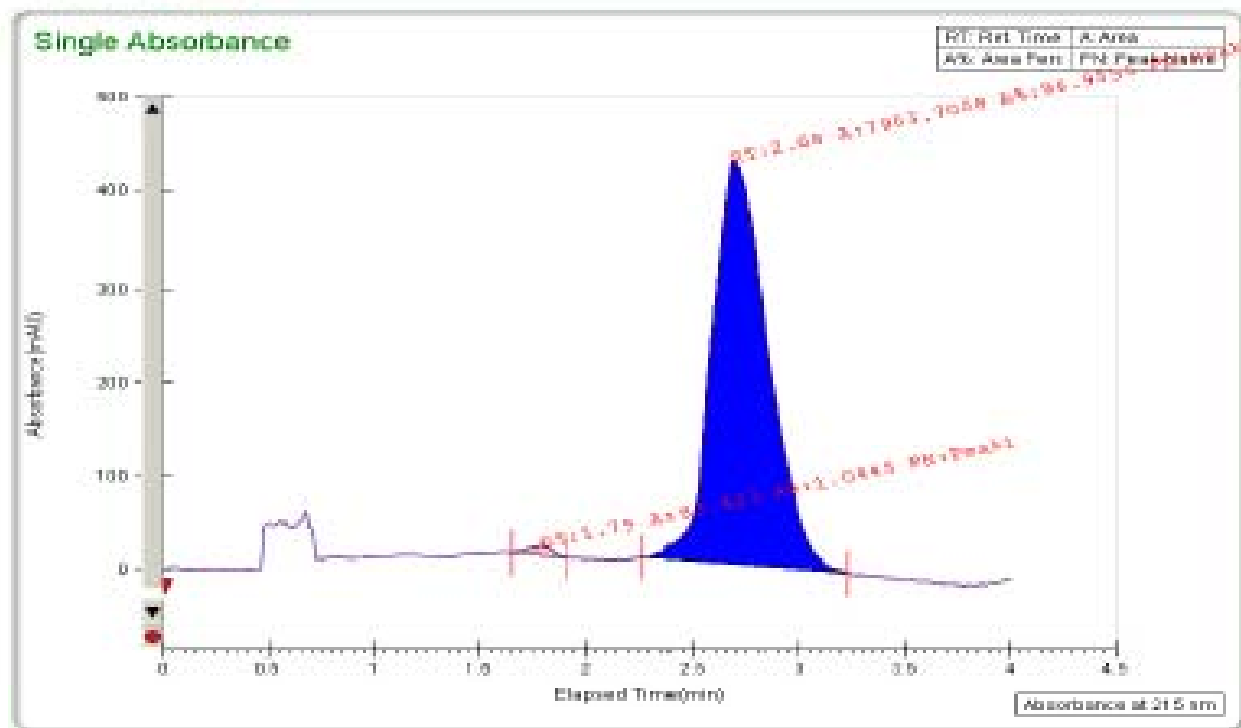
(1.75B)

Single Absorbance

RT: Ret Time	A: Area
A%: Area Perc	PN: Peak-halfWt

Absorbance at 215 nm

Injection Info
Inj Vol   15
Solvent   MeOH (0.1% DEA)
Column   CHIRALPAK IA (4.6 x 150 mm)
Sample   NCO-III-104
Well location   P1: 1B
Temp   40
Flow   5
% Modifier   5
Pressure   101

Peak Info

Peak No	% Area	Area	RT (min)	Height (mV)	K'
1	1.0445	83.423	1.79	10.9276	0.0024
2	98.9555	7903.7000	2.68	425.9888	0.0036
Total:	100	7987.1230			

(1.75D)

Th*SFC

Single Absorbance

RT: Ret Time	A: Area
A%: Area Pec	PN: Peak Name

Absorbance at 220 nm

General Info
Log Author
Log Date   2/9/2012 11:46:30 AM
Report By   current_User

Report Date   2/10/2012
Method Name   5_50_gradient.met
Notes

Injection Info

Inj Vol	10
Solvent	MeOH (0.1% DEA)
Column	CHIRALPAK IA (4.6 x 150 mm)
Sample	MCO-III-111
Well location	P1: 1A
Temp	40.1
Flow	3.5
% Modifier	5
Pressure	100

Peak Info

Peak No	% Area	Area	RT (min)	Height (mV)	K'
1	49.7612	2931.7282	2.68	467.3516	0.0038
2	50.2388	2959.8695	3.13	465.0256	0.0044
Total:	100	5891.5977			

ThlrSFC

C:\SFC\Data\General\MCO-III-111_2-9-2012_11_46_30 AM.tta
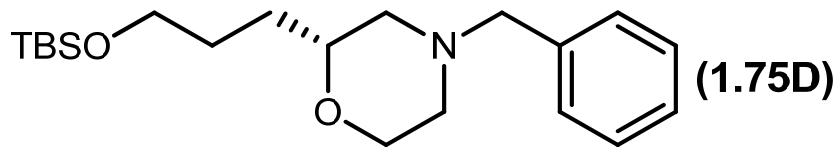
TBSO ... **(1.75D)**
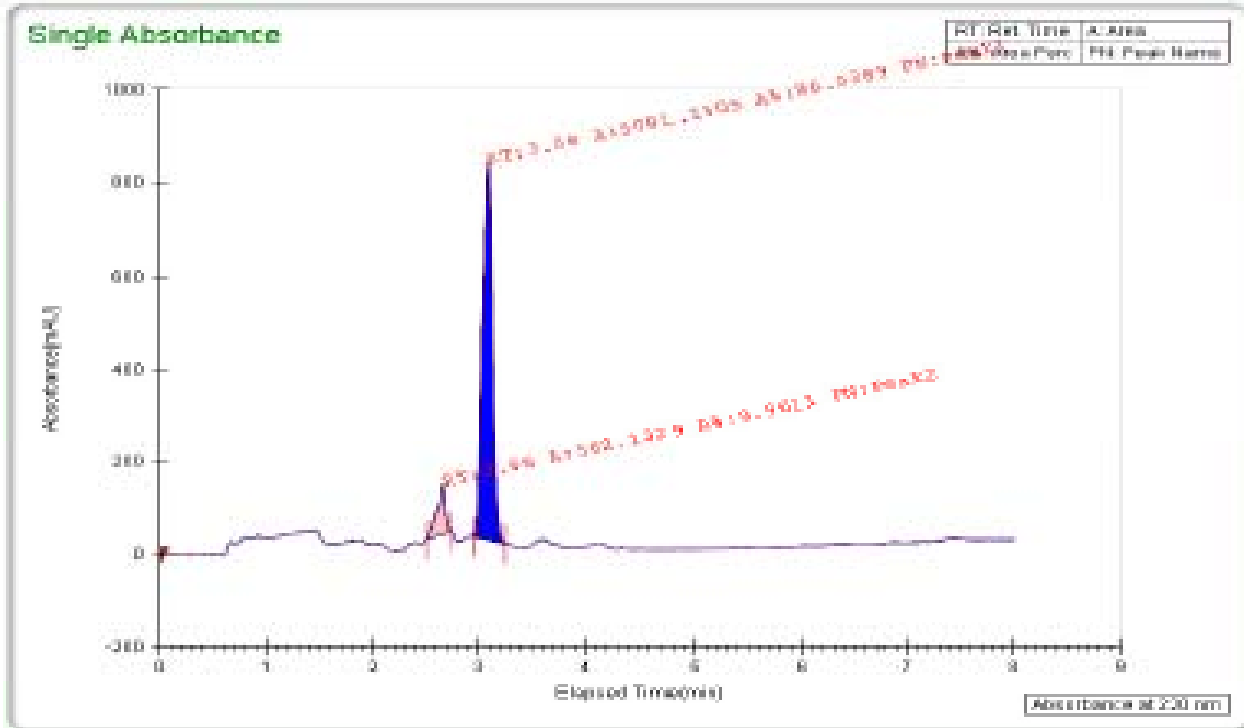
ThatSFC

Single Absorbance

Absorbance at 230 nm

Injection Info

Inj Vol	10
Solvent	MeOH (0.1% DEA)
Column	CHIRALPAK IA (4.6 x 150 mm)
Sample	MCO-III-161
Well location	P1: 1B
Temp	39.9
Flow	3.5
% Modifier	5
Pressure	100

Peak Info

Peak No	% Area	Area	RT (min)	Height (mV)	K'
1	9.9611	562.1329	2.66	109.9528	0.0037
2	90.0389	5081.1505	3.08	814.7592	0.0043
Total:	100	5643.2834			

(1.76A)
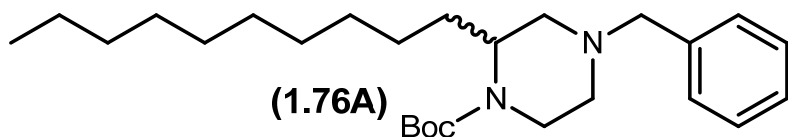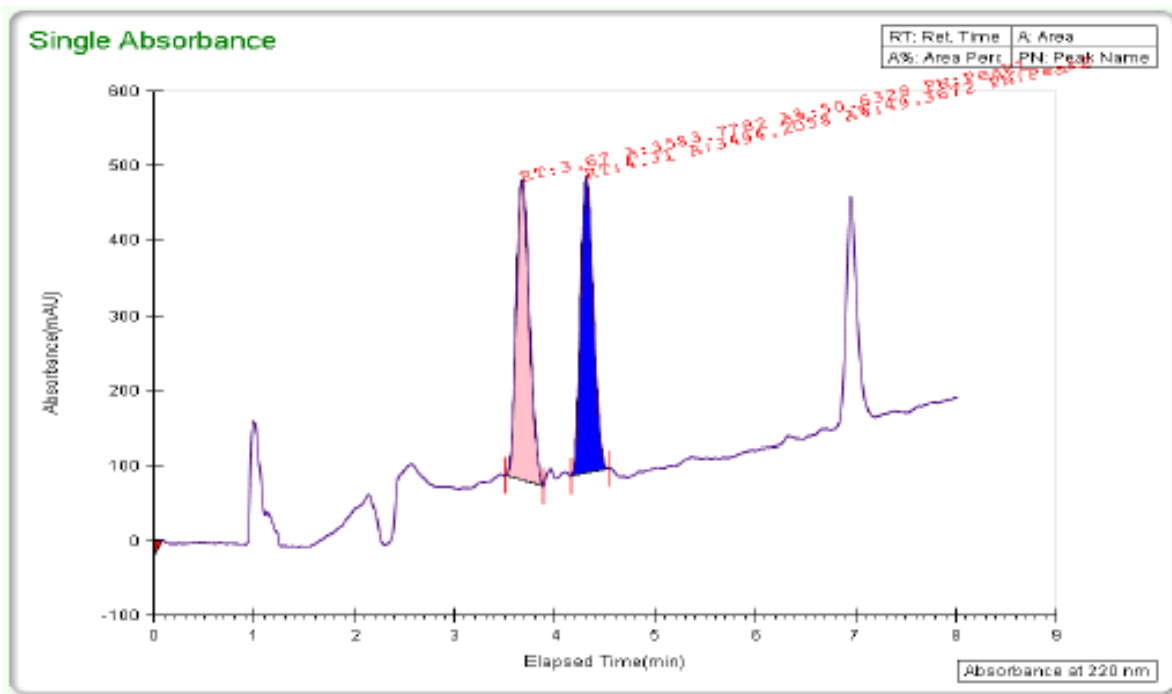
General Info
Log Author
Log Date   7/28/2011 10:01:41 AM
Report By   current_User
Report Date   7/28/2011
Method Name   5_50_gradient.met
Notes

Injection Info		Temp	40.2
Inj Vol	10	Flow	3.5
Solvent	MeOH 0.1% DEA	% Modifier	5
Column	Lux Cellulose-4	Pressure	101
Sample	MCO-II-141 racemic		
Well location	P1: 1A		

Peak Info

Peak No	% Area	Area	RT (min)	Height (mV)	K'
1	50.6328	3583.7782	3.67	400.0073	0.0061
2	49.3672	3494.2058	4.31	395.3763	0.0072
Total:	100	7077.984			

TharSFC

C:\SFC\Data\General\MCO-II-141 racemic_7-28-2011_10_01_41 AM.tta

(1.76A)

Single Absorbance

RT: Ret. Time | A: Area
A%: Area Perc | PN: Peak Name

RT:4.49 A:12345.2106 A%:94.2758 PN:Peak

RT:3.78 A:749.5692 A%:5.7242 PN:Peak1

Absorbance at 215 nm
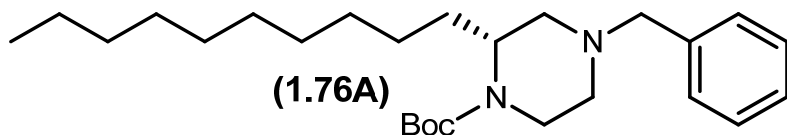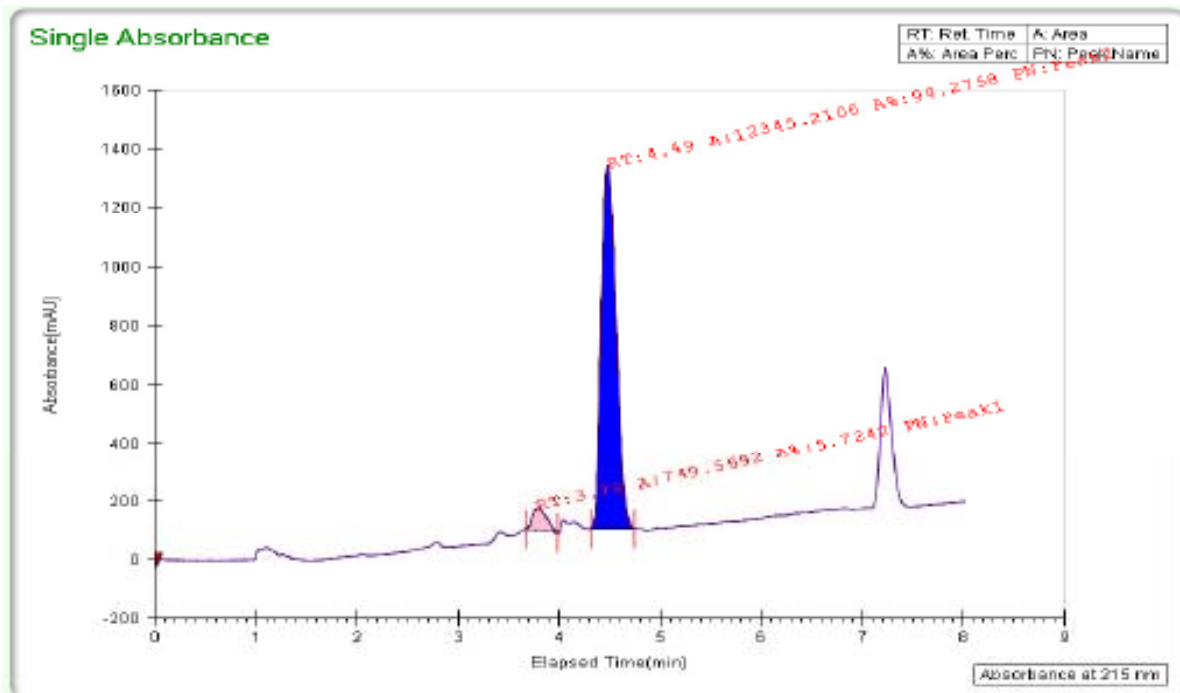
General Info		Report Date	11/2/2011
Log Author		Method Name	5_50_gradient.met
Log Date	11/2/2011 2:53:38 PM	Notes	
Report By	current_User		

Injection Info		Temp	39.2
Inj Vol	10	Flow	3.5
Solvent	MeOH (0.1% DEA)	% Modifier	5
Column	Lux Cellulose-4	Pressure	99
Sample	MCO-III-67		
Well location	P1: 1B		

Peak Info

Peak No	% Area	Area	RT (min)	Height (mV)	K'
1	5.7242	749.5692	3.78	76.6515	0.0042
2	94.2758	12345.2106	4.49	1239.2579	0.005
Total:	100	13094.7798			

(1.76C)

Single Absorbance

Absorbance at 215 nm

| RT: Ret Time | A: Area |
| A%: Area Pes | PN: Peak Name |
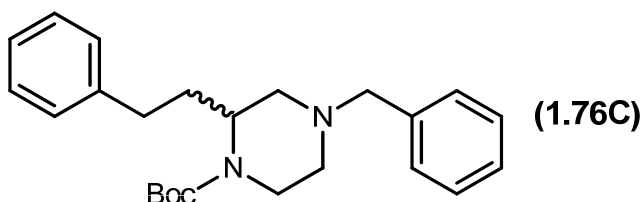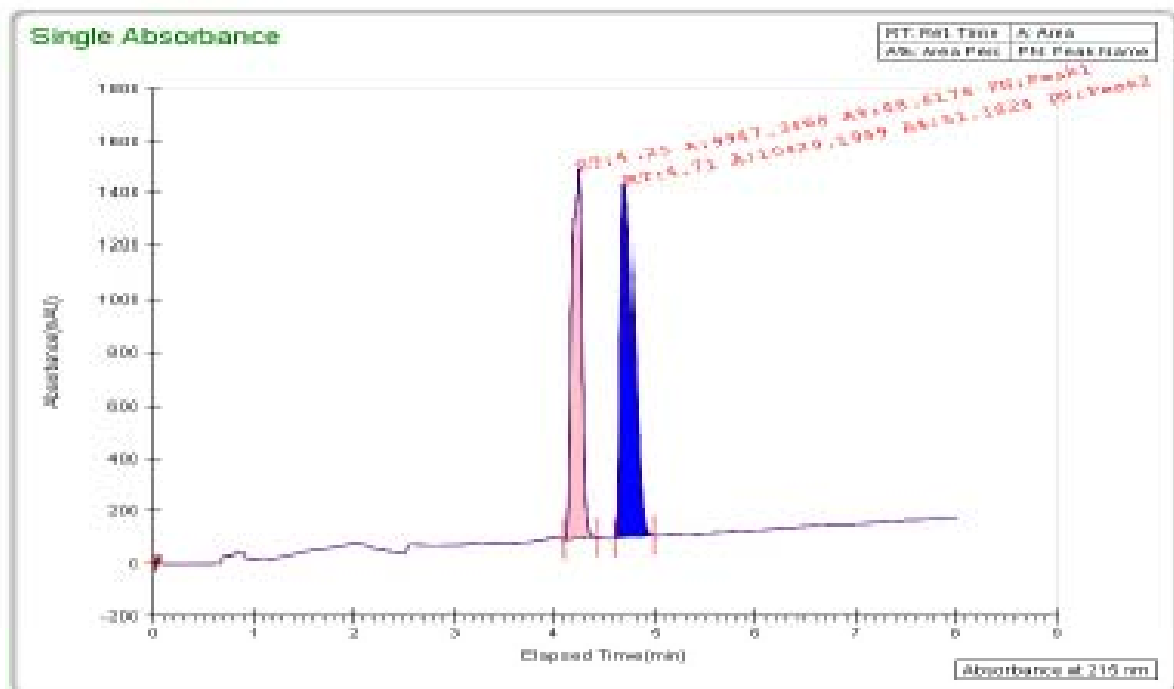
General Info

Log Author
Log Date   11/16/2011 8:48:54 AM
Report By   current_User
Report Date   11/16/2011
Method Name   5_50_gradient.met
Notes

Injection Info		Temp	40.2
Inj Vol	5	Flow	3.5
Solvent	MeOH (0.1% DEA)	% Modifier	5
Column	CHIRALPAK IA	Pressure	100
Sample	MCO-III-44		
Well Location	P1: 4A		

Peak Info

Peak No	% Area	Area	RT (min)	Height (mV)	K"
1	48.8176	9947.3468	4.25	1392.1597	0.008
2	51.1824	10429.1959	4.71	1333.5602	0.0089
Total:	100	20376.5427			
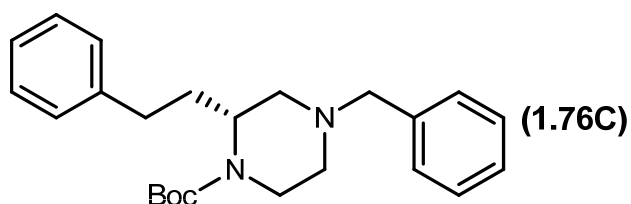
(1.76C)
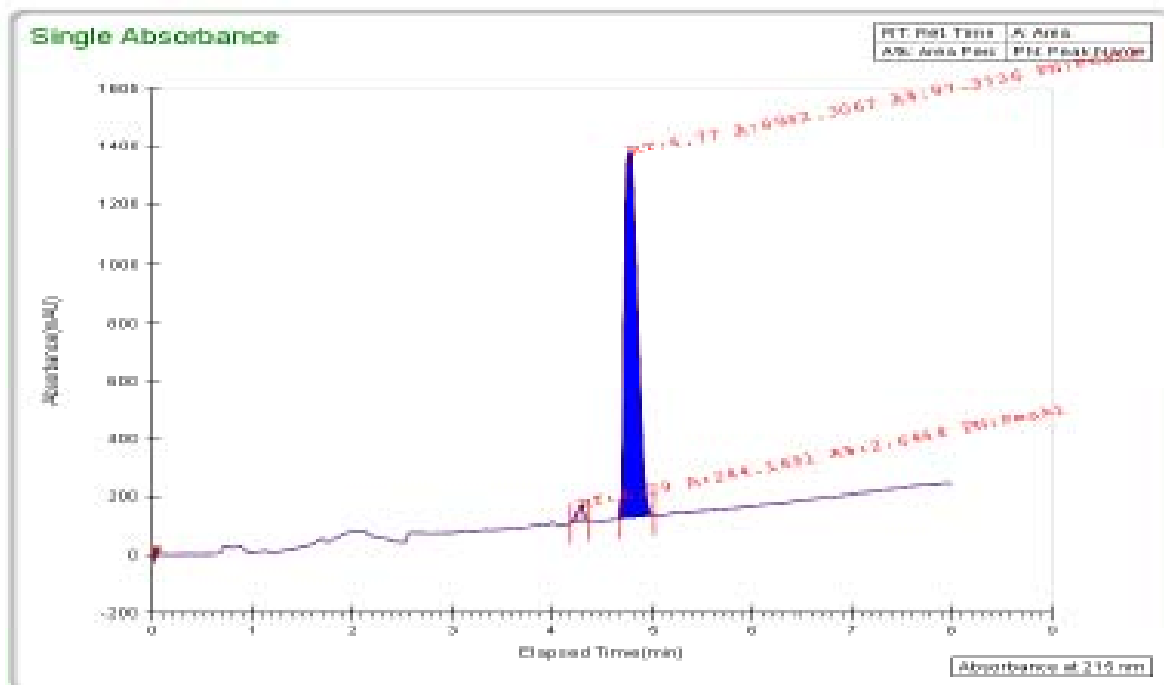
General Info

Log Author

Log Date	11/16/2011 8:59:14 AM
Report By	current_User
Report Date	11/16/2011
Method Name	5_50_gradient.met

Notes

Injection Info			Temp	39.8
Inj Vol	5		Flow	3.5
Solvent	MeOH (0.1% DEA)		% Modifier	5
Column	CHIRALPAK IA		Pressure	100
Sample	MCO-III-82			
Well location	P1: 4B			

Peak Info

Peak No	% Area	Area	RT (min)	Height (mV)	K'
1	2.6464	244.1691	4.29	56.7093	0.008
2	97.3536	8982.3067	4.77	1251.4887	0.0089
Total:	100	9226.4758			

ThaiSFC

C:\SFC\Data\General\MCO-III-82_11-16-2011_8_59_14 AM.tta

(1.76B)

Single Absorbance

RT: Ret. Time; AA: Area
AR: Area Pen; PN: Peak Name

Absorbance at 220 nm
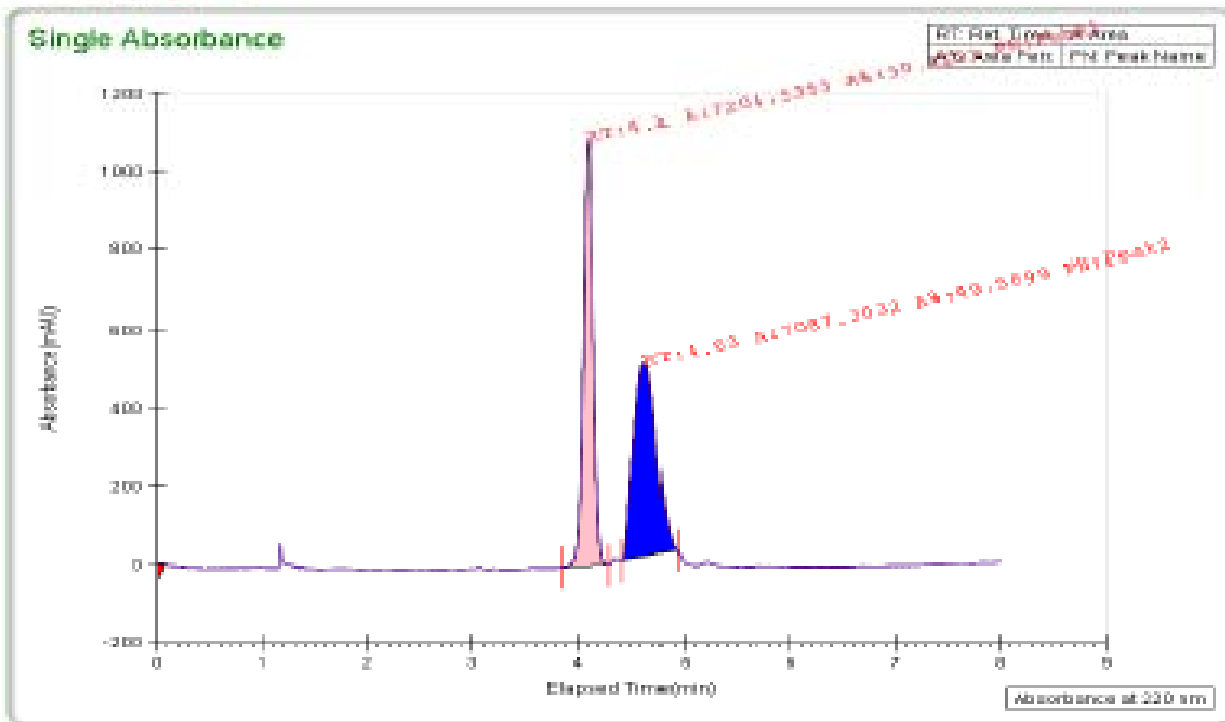
General Info

Log Author

Log Date	12/14/2011 2:44:59 PM
Report By	current_User
Report Date	12/14/2011
Method Name	5_50_gradient.met

Notes

Injection Info

Inj Vol	10	Temp	39.9	
Solvent	MeOH (0.1% DEA)	Flow	3.5	
Column	CHIRALPAK IC	% Modifier	5	
Sample	MCO-II-139	Pressure	100	
Well location	P1: 2A			

Peak Info

Peak No	% Area	Area	RT (min)	Height (mV)	K'
1	50.4101	7204.5355	4.1	1085.3106	0.0046
2	49.5899	7087.3032	4.63	495.944	0.0052
Total:	100	14291.8387			

(1.76B)

Single Absorbance

RT: Ret. Time	A: Area
A%: Area Perc	PN: Peak Name

RT:4.62 A:14625.3076 A%:97.4679 PN:Peak2

RT:4.1 A:379.9406 A%:2.5321 PN:Peak1

Absorbance at 220 nm

Absorbance(mAU)

Elapsed Time(min)
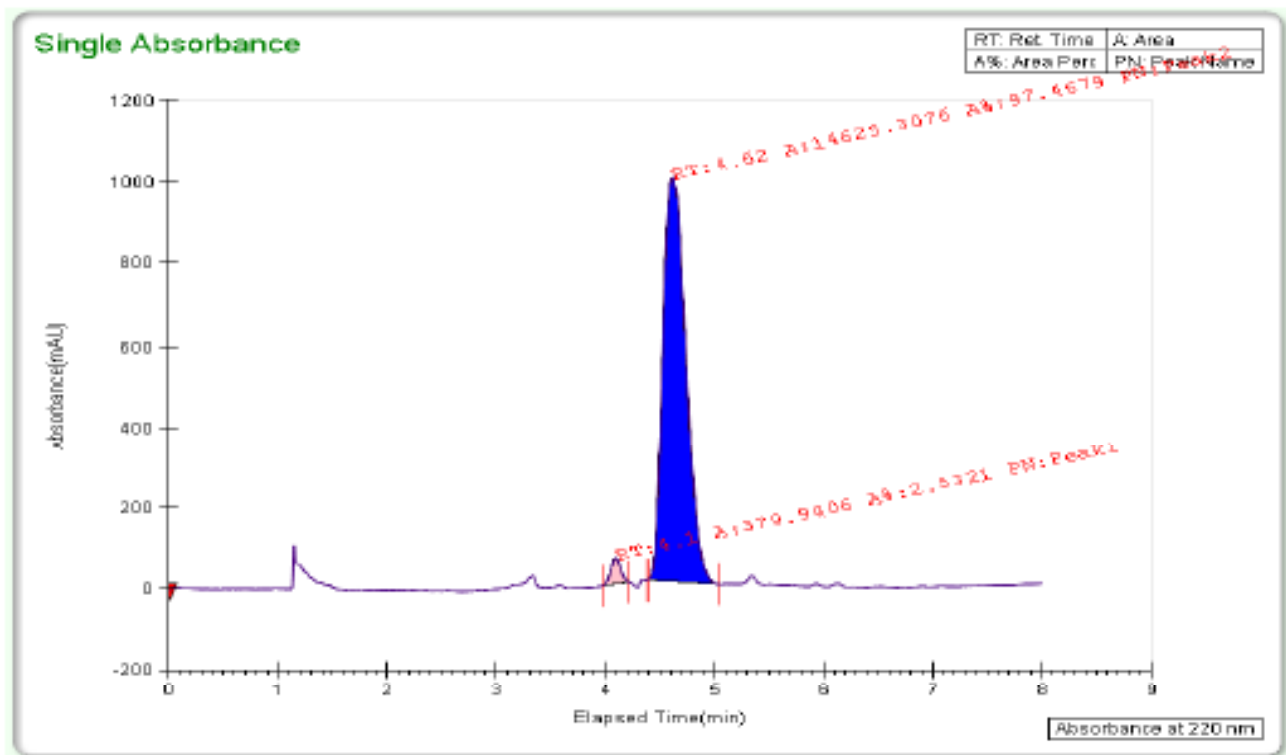
General Info
Log Author
Log Date   12/14/2011 2:55:19 PM
Report By   current_User
Report Date   12/14/2011
Method Name   5_50_gradient.met
Notes

Injection Info

Inj Vol	10	Temp	40.1
Solvent	MeOH (0.1% DEA)	Flow	3.5
Column	CHIRALPAK IC	% Modifier	5
Sample	MCO-III-107	Pressure	100
Well location	P1: 2B		

Peak Info

Peak No	% Area	Area	RT (min)	Height (mV)	K'
1	2.5321	379.9406	4.1	65.0481	0.0046
2	97.4679	14625.3076	4.62	994.909	0.0052
Total:	100	15005.2482			

TharSFC

280

(1.76D)

TBSO...N(Boc)...N-benzyl piperazine structure

ThusSFC

Single Absorbance

	RT: Ret Time	A: Area
	A%: Area Perc	PN: Peak Name

Absorbance at 220 nm

General Info

Log Author

Log Date	2/9/2012 11:09:02 AM
Report By	current_User
Report Date	2/9/2012
Method Name	15_60_gradient.met
Notes	

Injection Info

Inj Vol	15		Temp	39.9
Solvent	IPA 0.1% DEA		Flow	3.5
Column	Lux Cellulose-2 (OI)		% Modifier	15
Sample	MCO-III-128		Pressure	100
Well location	P1: 4A			

Peak Info

Peak No	% Area	Area	RT (min)	Height (mV)	K'
1	49.6194	4263.5734	5.66	256.0257	0.0085
2	50.3806	4328.9726	6.38	237.3683	0.0095
Total:	100	8592.546			

(1.76D)

Single Absorbance

RT:Ret Time	A:Area
A%:Area Perc	PN:Peak Name

Absorbance at 220 nm

Injection Info			Temp	40.1
Inj Vol	10		Flow	3.5
Solvent	IPA 0.1% DEA		% Modifier	15
Column	Lux Cellulose-2 (OI)		Pressure	100
Sample	MCO-III-162			
Well location	P1: 4B			

Peak Info

Peak No	% Area	Area	RT (min)	Height (mV)	K'
1	12.3818	908.675	5.73	62.1378	0.0084
2	87.6182	6430.0997	6.54	384.3059	0.0096
Total:	100	7338.7747			
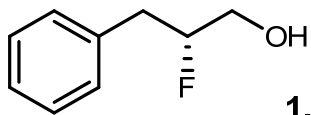
1.94A

(*R*)-2-fluoro-3-phenylpropan-1-ol
Solvent: CDCl$_3$
400.13 MHz
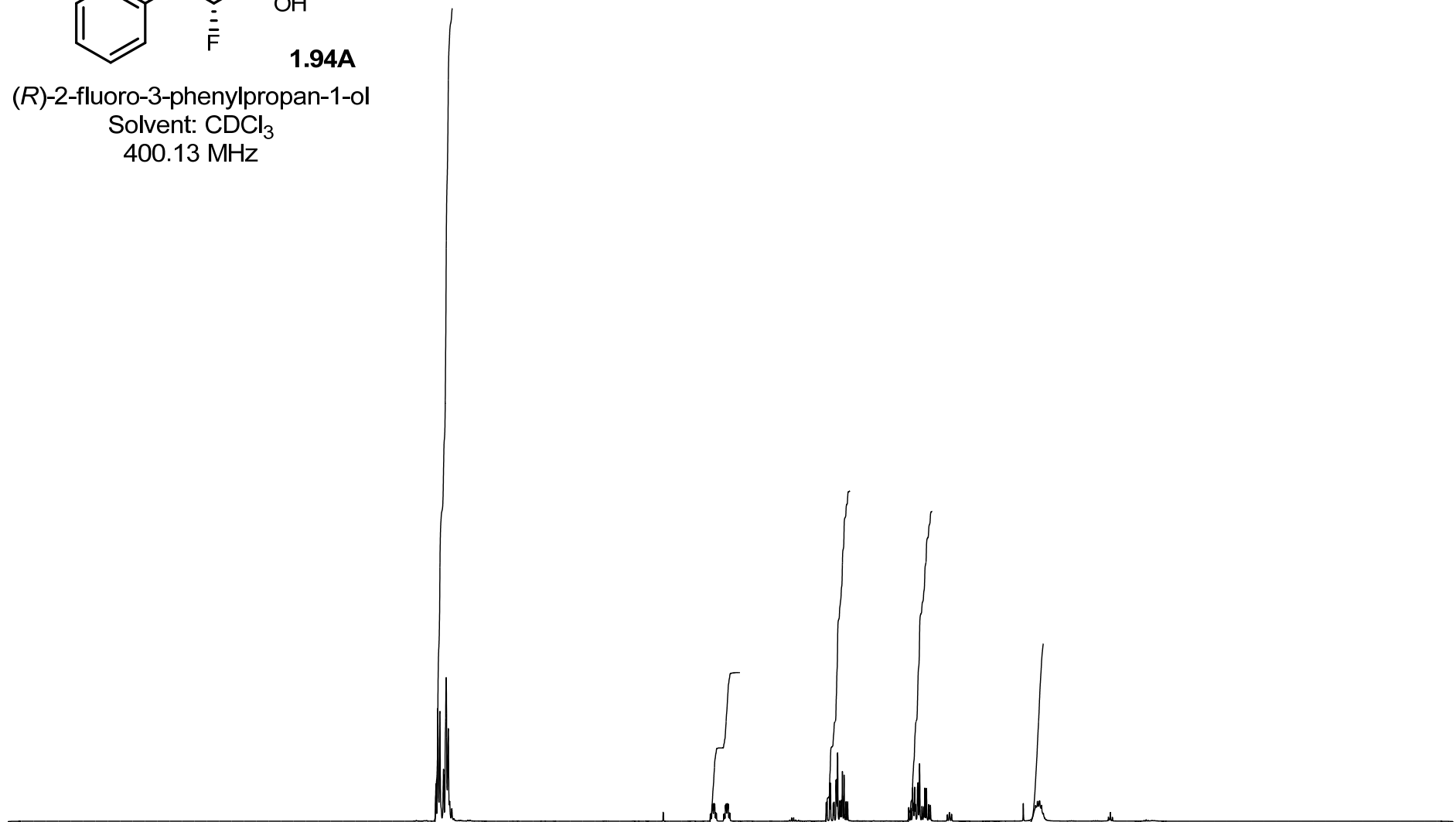
5.424

1.000

283

2.208

2.073

1.198

11 10 9 8 7 6 5 4 3 2 1 0 −1 ppm
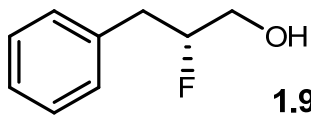
(R)-2-fluoro-3-phenylpropan-1-ol
Solvent: CDCl$_3$
100.6 MHz

1.94A

136.548
136.493
129.333
128.576
126.751

95.548
93.839

64.120
63.905

37.551
37.340
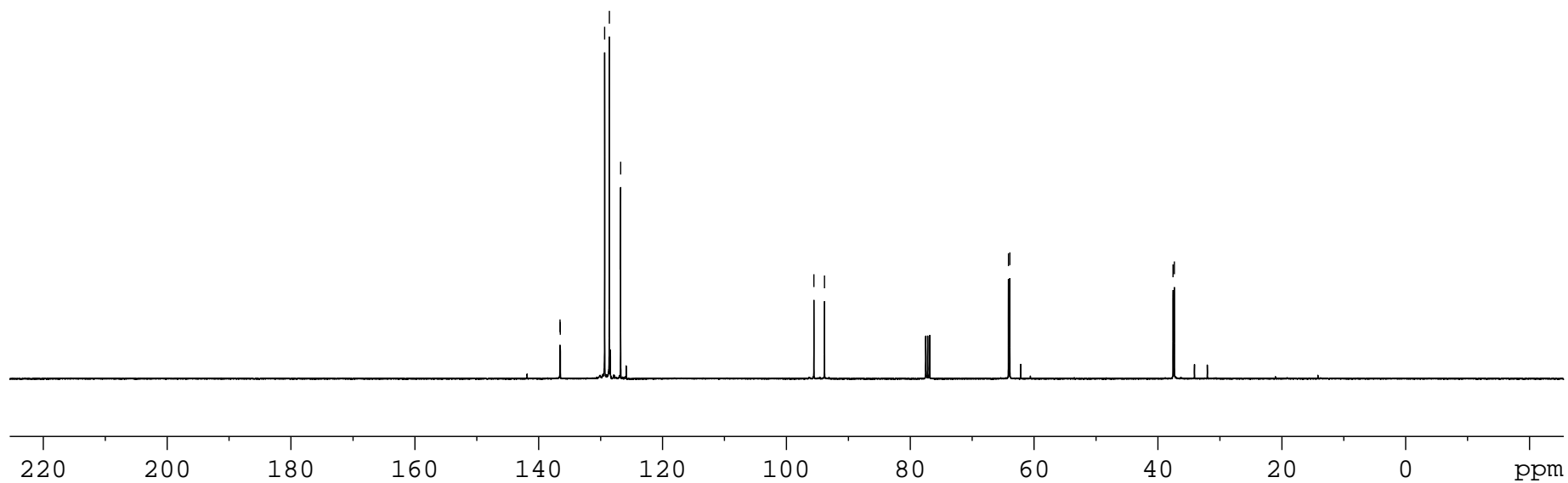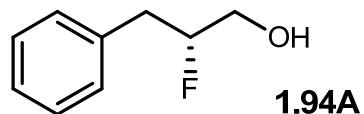
220   200   180   160   140   120   100   80   60   40   20   0   ppm

1.94A

Elemental Composition Report

Single Mass Analysis
Tolerance = 5.0 PPM   /   DBE: min = -0.5, max = 25.0
Element prediction: Off
Number of isotope peaks used for i-FIT = 2

Monoisotopic Mass, Even Electron Ions
8 formula(e) evaluated with 1 results within limits (up to 50 best isotopic matches for each mass)
Elements Used:
C: 8-500   H: 10-1000   O: 1-200   F: 1-1   Na: 1-1

MCO-IV-151

07-Dec-2012
13:11:55
TOF MS ES+
3.35e+003

S/N: UH193
MCO-IV-151_120712_001 45 (0.842) AM (Cen,4, 80.00, Ar,8000.0,556.28,0.70); Sm (SG, 2x1.00); Cm (40:50)
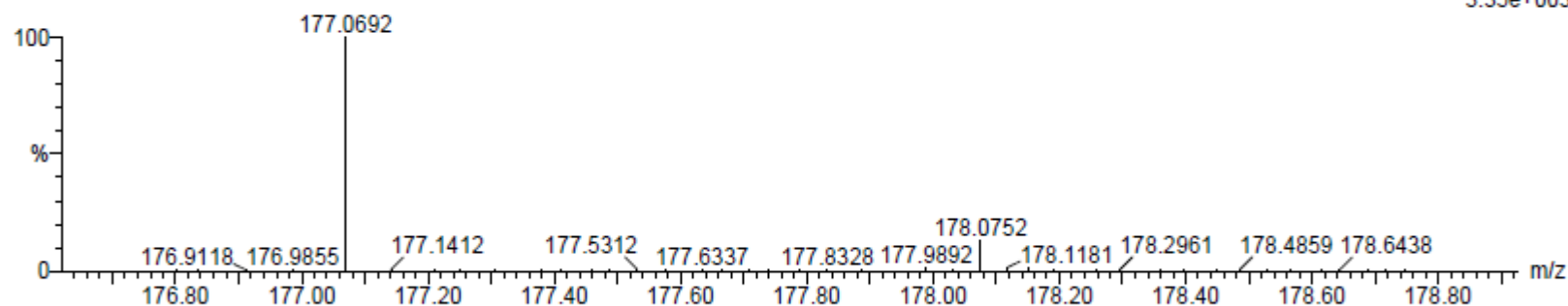
| Minimum: | | | -0.5 | | |
| Maximum: | 5.0 | 5.0 | 25.0 | | |

Mass	Calc. Mass	mDa	PPM	DBE	i-FIT	Formula
177.0692	177.0692	0.0	0.0	3.5	7.5	C9 H11 O F Na
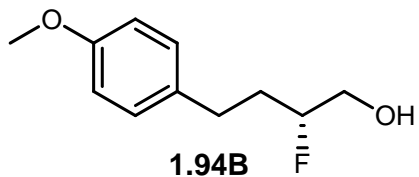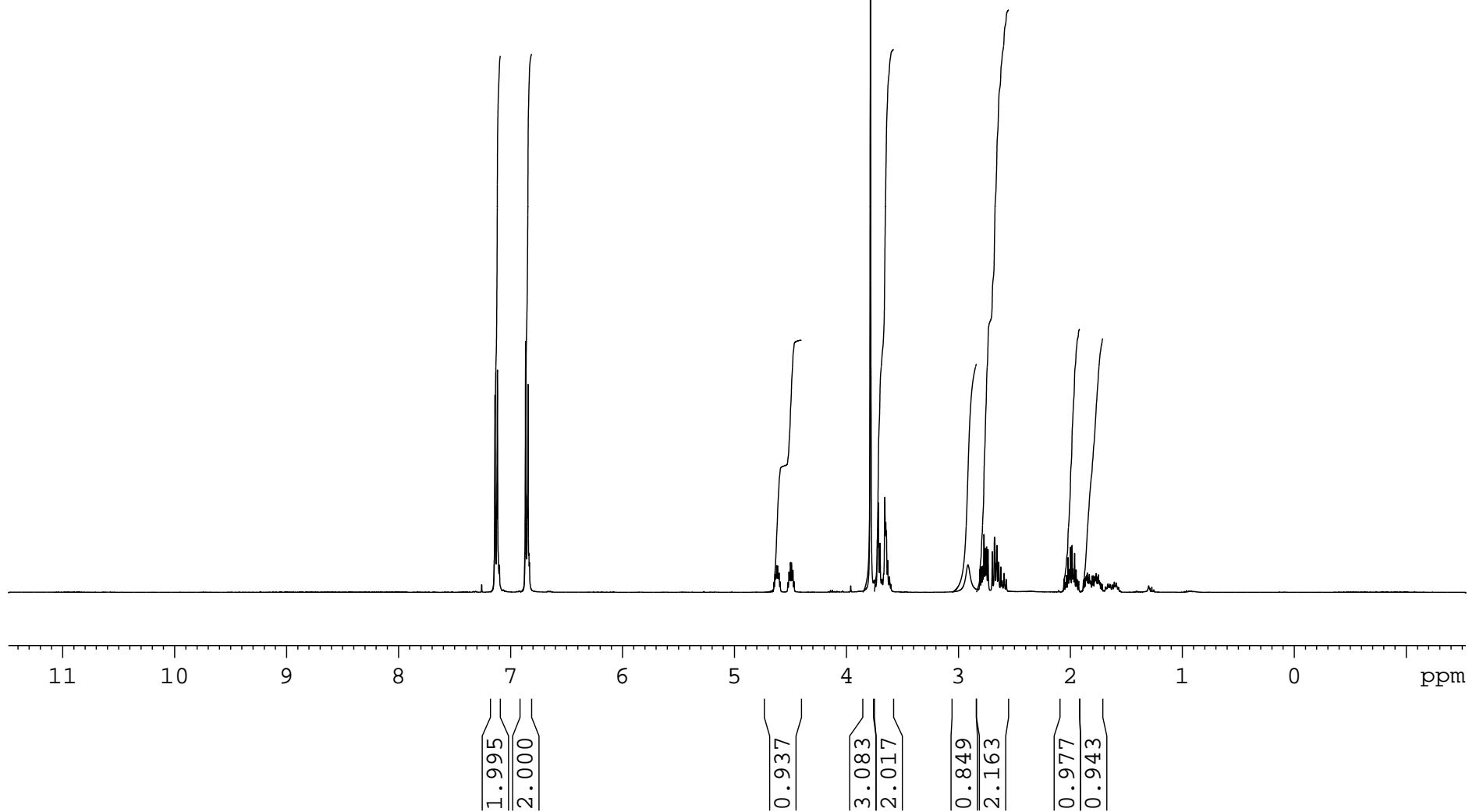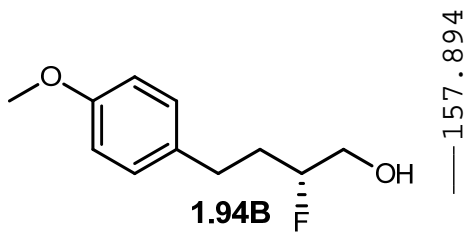
1.94B

(*R*)-2-fluoro-4-(4-methoxyphenyl)butan-1-ol
Solvent: CDCl$_3$
400.13 MHz

1.995 2.000   0.937   3.083 2.017   0.849 2.163   0.977 0.943

286

(R)-2-fluoro-4-(4-methoxyphenyl)butan-1-ol
Solvent: CDCl₃
100.6 MHz

1.94B

157.894
133.116
129.328
113.889
94.557
92.880
64.854
64.638
55.198
32.937
32.732
30.132
30.085

220 200 180 160 140 120 100 80 60 40 20 0 ppm

287

Elemental Composition Report

1.94B

Page 1
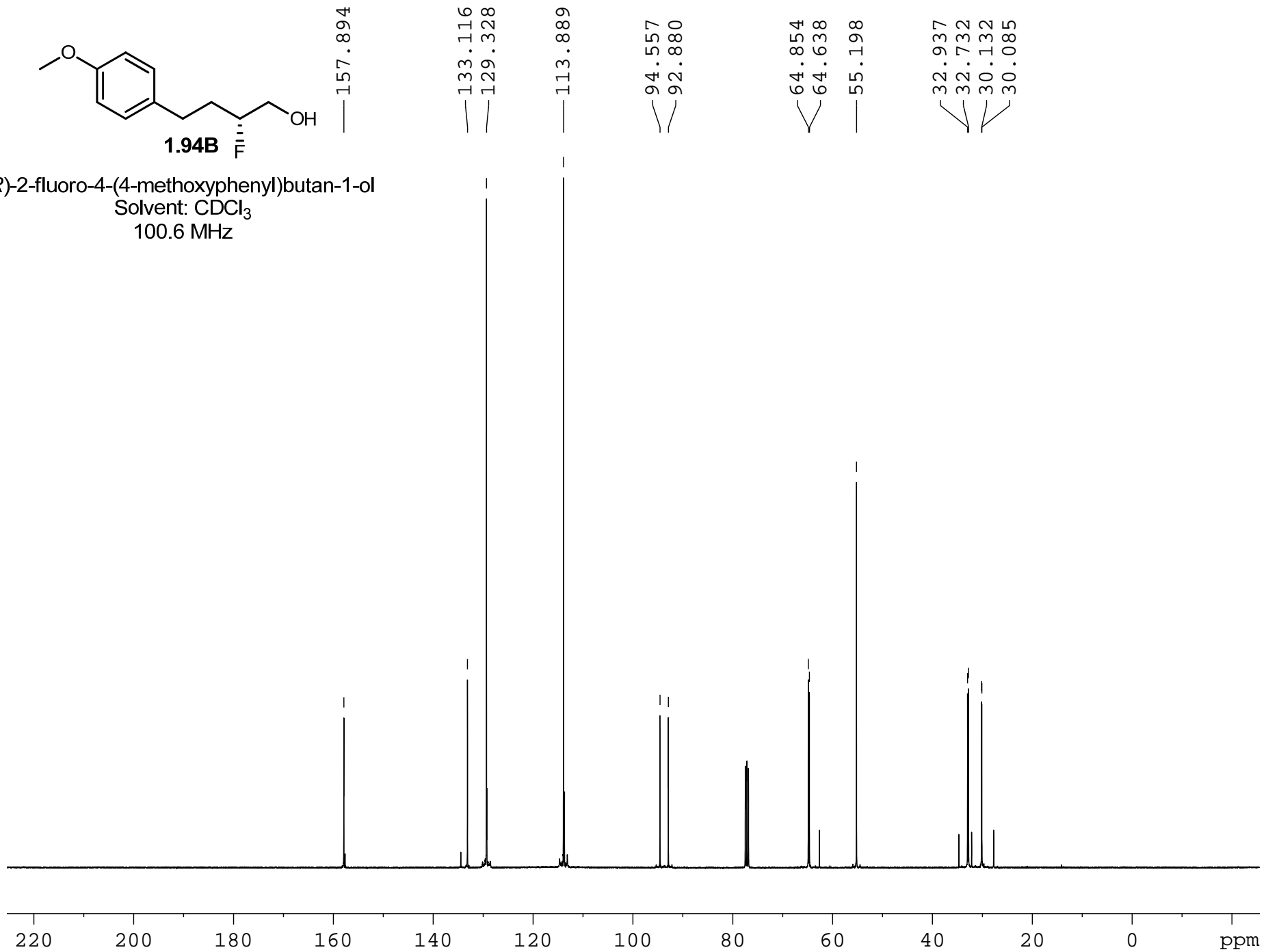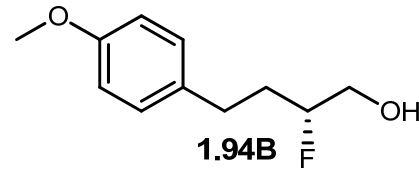
Single Mass Analysis
Tolerance = 5.0 PPM / DBE: min = -0.5, max = 25.0
Element prediction: Off
Number of isotope peaks used for i-FIT = 2

Monoisotopic Mass, Even Electron Ions
12 formula(e) evaluated with 1 results within limits (up to 50 best isotopic matches for each mass)
Elements Used:
C: 10-500   H: 10-1000   O: 1-200   F: 1-1   Na: 1-1

06-Dec-2012
13:37:14
TOF MS ES+
3.78e+003

S/N: UH193
MCO-IV-148_120612_001 79 (1.473) AM (Cen,4, 80.00, Ar,8000.0,556.28,0.70); Sm (SG, 2x1.00); Cm (70:80)
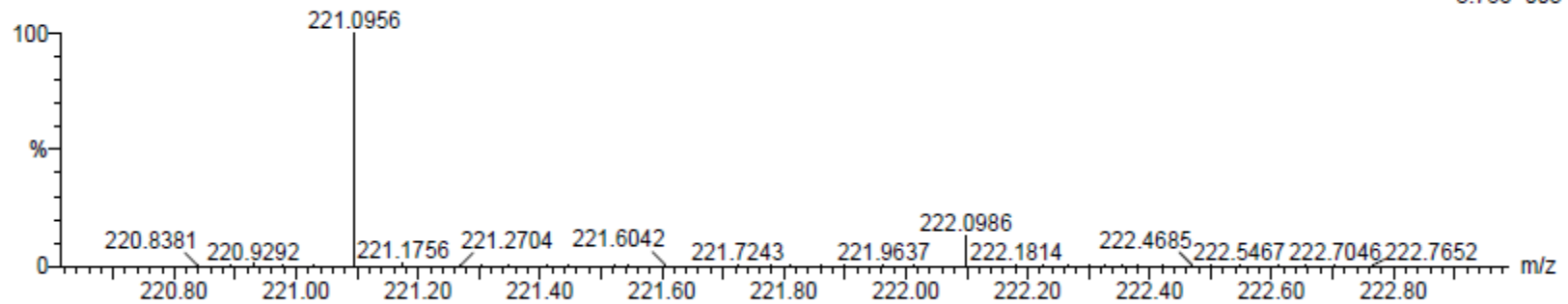
Minimum:				-0.5		
Maximum:		5.0	5.0	25.0		
Mass	Calc. Mass	mDa	PPM	DBE	i-FIT	Formula
221.0956	221.0954	0.2	0.9	3.5	0.3	C11 H15 O2 F Na
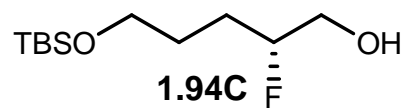
288

(R)-5-((*tert*-butyldimethylsilyl)oxy)-2-fluoropentan-1-ol
Solvent: CDCl₃
400.13 MHz

1.94C

TBSO, OH, F

0.951 4.000 0.867 4.016 9.202 6.090

1.94C

(R)-5-((*tert*-butyldimethylsilyl)oxy)-2-fluoropentan-1-ol
Solvent: CDCl₃
100.6 MHz

94.961
93.279

64.391
64.170
62.467

27.988
27.946
27.470
27.263
25.719
18.044

-5.604

220   200   180   160   140   120   100   80   60   40   20   0   ppm

Elemental Composition Report

Page 1
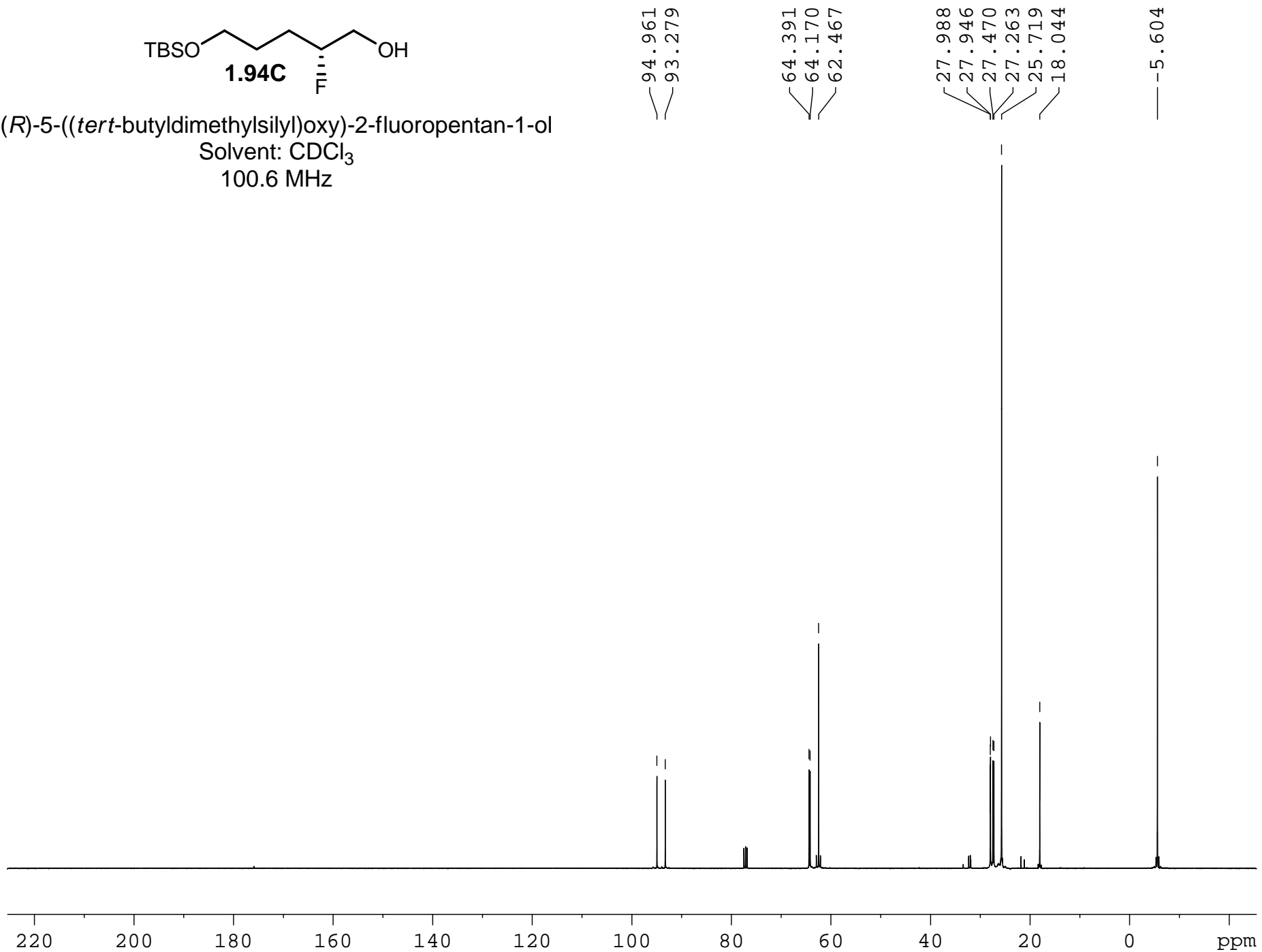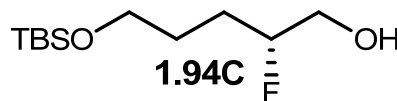
Single Mass Analysis
Tolerance = 5.0 PPM   /   DBE: min = -0.5, max = 25.0
Element prediction: Off
Number of isotope peaks used for i-FIT = 2

Monoisotopic Mass, Even Electron Ions
13 formula(e) evaluated with 1 results within limits (up to 50 best isotopic matches for each mass)
Elements Used:
C: 10-500   H: 10-1000   O: 1-200   F: 1-1   Si: 1-1

MCO-IV-166

07-Dec-2012
10:27:41
TOF MS ES+
7.10e+003

S/N: UH193
MCO-IV-166_120712_001 51 (0.954) AM (Cen,4, 80.00, Ar,8000.0,556.28,0.70); Sm (SG, 2x1.00); Cm (50:60)

TBSO ~~~~~ OH
1.94C F
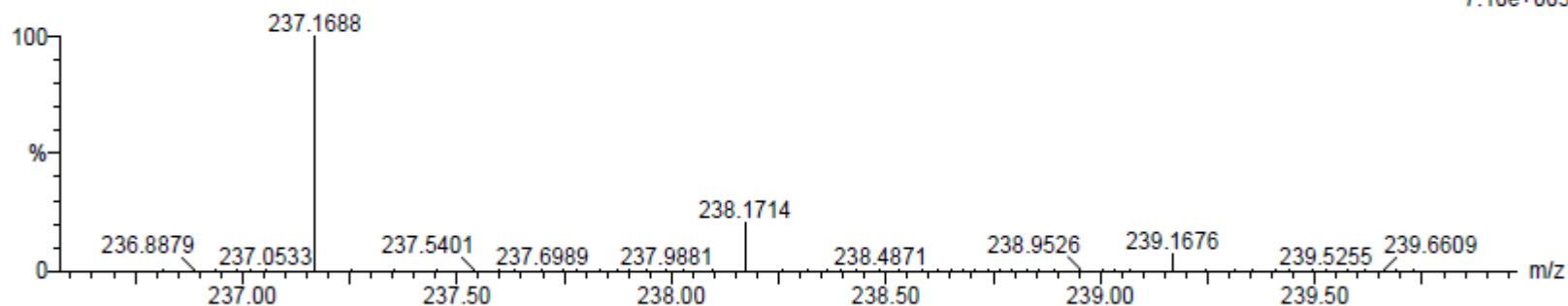
Mass	Calc. Mass	mDa	PPM	DBE	i-FIT	Formula
237.1688	237.1686	0.2	0.8	-0.5	7.8	C11 H26 O2 F Si
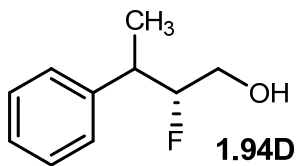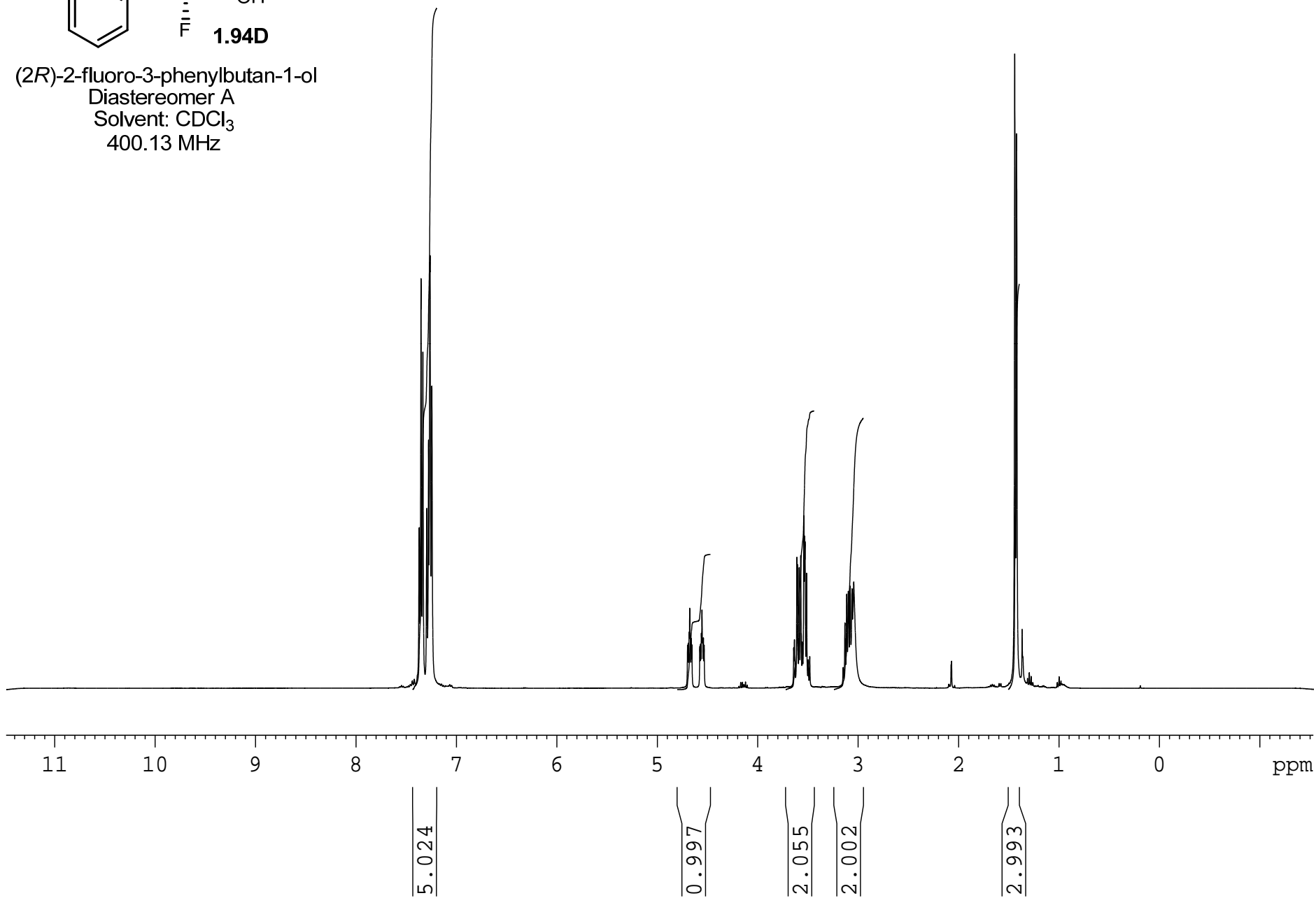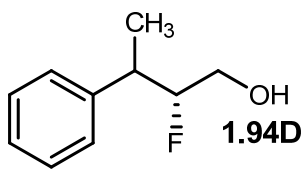
Minimum: -0.5
Maximum: 5.0   5.0   25.0

291

(2*R*)-2-fluoro-3-phenylbutan-1-ol
Diastereomer A
Solvent: CDCl₃
400.13 MHz

1.94D

5.024   0.997   2.055   2.002   2.993

(2*R*)-2-fluoro-3-phenylbutan-1-ol
Diastereomer A
Solvent: CDCl₃
100.6 MHz

CH₃

OH

F   **1.94D**

142.360
142.285
128.657
127.592
126.894
98.888
97.144
63.125
62.910
41.035
40.832
17.215
17.165

220   200   180   160   140   120   100   80   60   40   20   0   ppm

Elemental Composition Report

Page 1

Single Mass Analysis

Tolerance = 5.0 PPM   /   DBE: min = -0.5, max = 25.0
Element prediction: Off
Number of isotope peaks used for i-FIT = 2

Monoisotopic Mass, Even Electron Ions
8 formula(e) evaluated with 1 results within limits (up to 50 best isotopic matches for each mass)
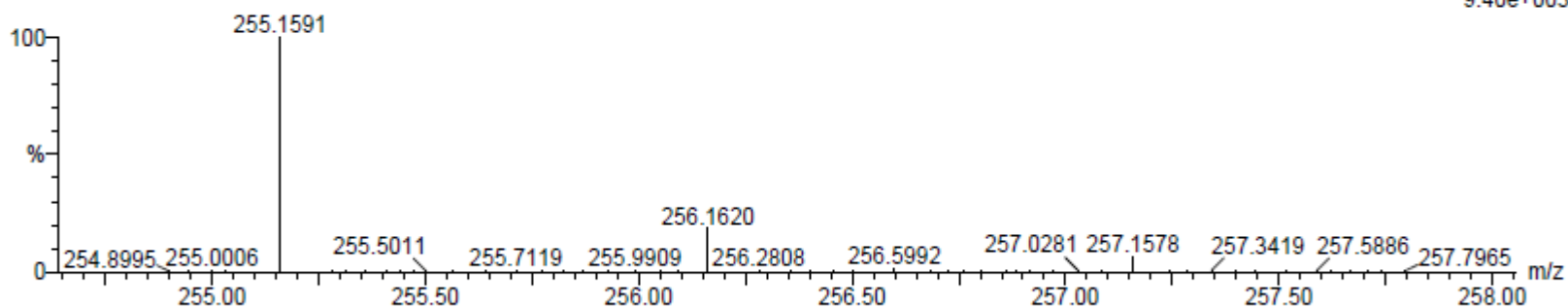Elements Used:
C: 10-500   H: 10-1000   O: 1-200   F: 1-1   Na: 1-1

06-Dec-2012

S/N: UH193

15:53:48
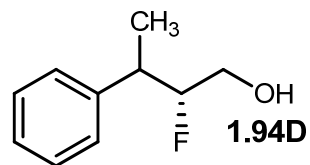
MCO-IV-153-NP_120612_001 60 (1.121) AM (Cen,4, 80.00, Ar,8000.0,556.28,0.70); Sm (SG, 2x1.00); Cm (50:60)

TOF MS ES+
2.48e+003

Diastereomer A

1.94D
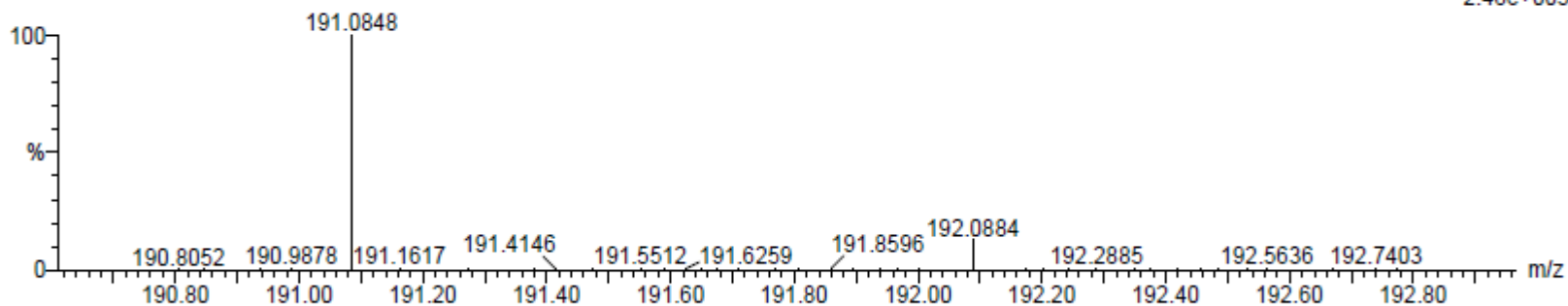
| Minimum: | | | | -0.5 | | | |
| Maximum: | | 5.0 | 5.0 | 25.0 | | | |

Mass	Calc. Mass	mDa	PPM	DBE	i-FIT	Formula				
191.0848	191.0848	0.0	0.0	3.5	1.1	C10	H13	O	F	Na
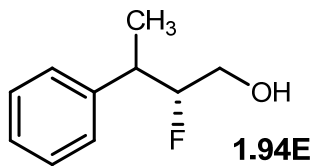
294
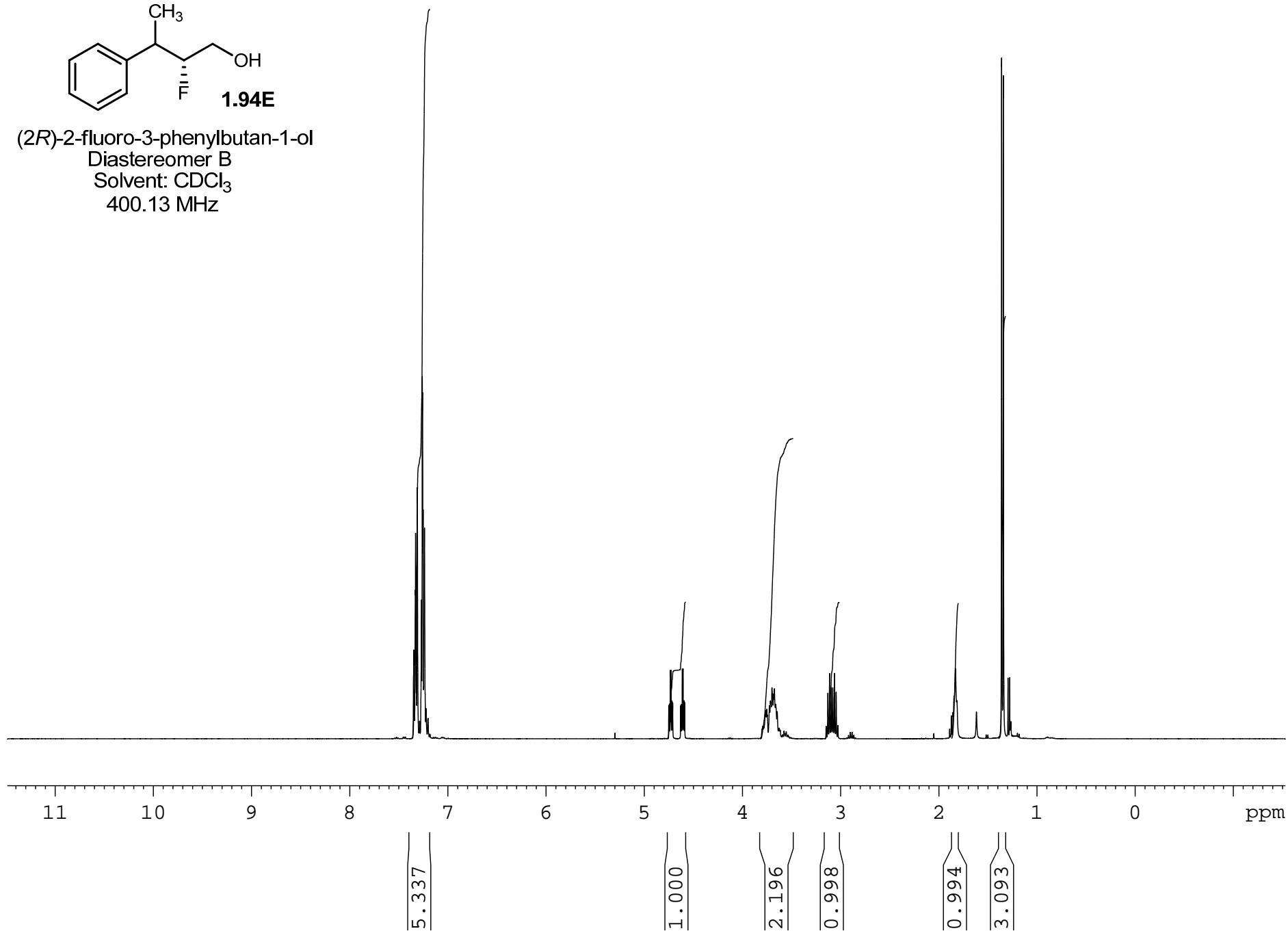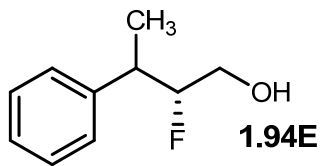
(2R)-2-fluoro-3-phenylbutan-1-ol
Diastereomer B
Solvent: CDCl₃
400.13 MHz

1.94E

(2*R*)-2-fluoro-3-phenylbutan-1-ol
Diastereomer B
Solvent: CDCl$_3$
125 MHz
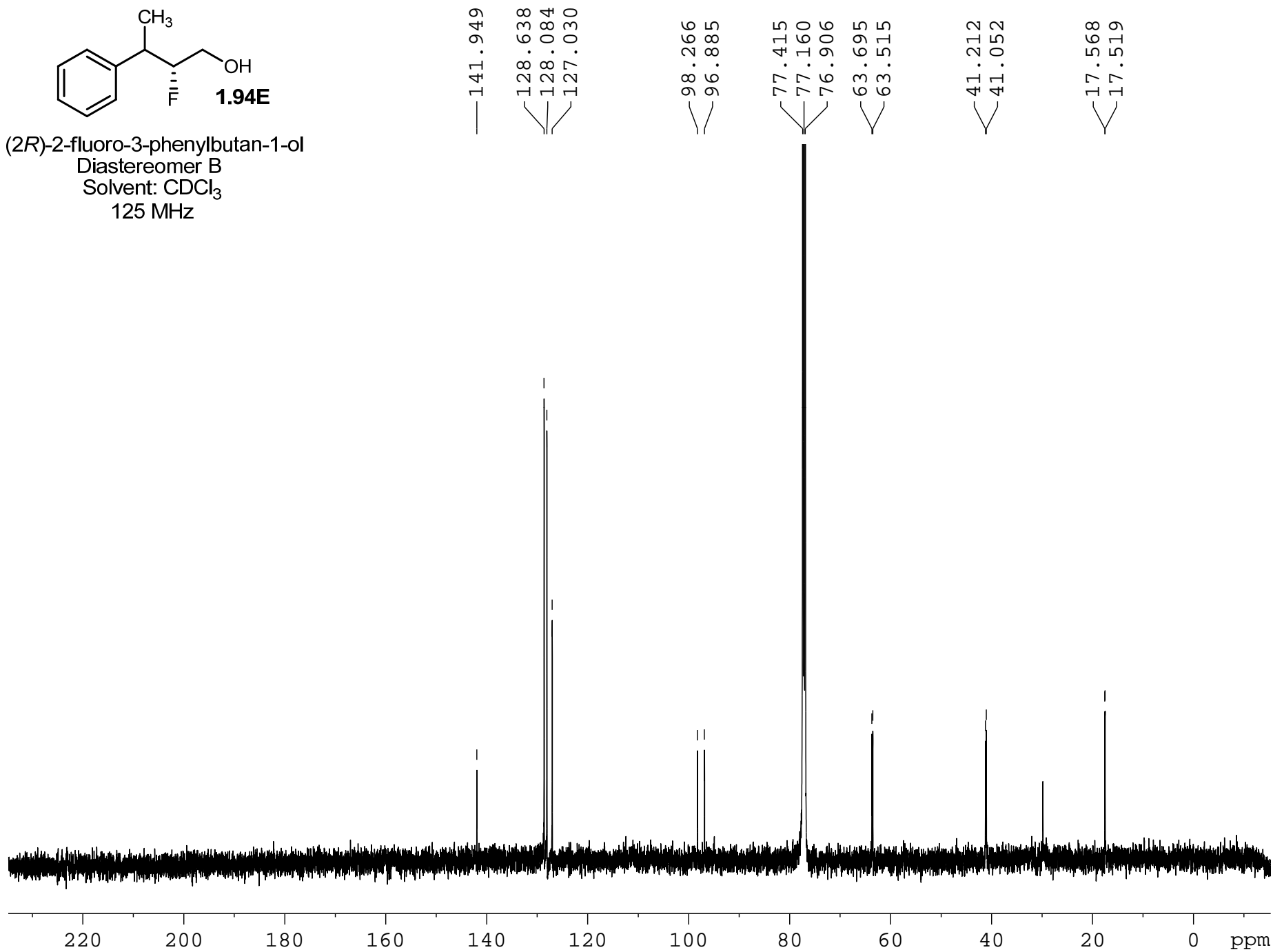
141.949
128.638
128.084
127.030
98.266
96.885
77.415
77.160
76.906
63.695
63.515
41.212
41.052
17.568
17.519

220 200 180 160 140 120 100 80 60 40 20 0 ppm

296

Elemental Composition Report

Page 1

1.94E

Diastereomer B

Single Mass Analysis
Tolerance = 5.0 PPM   /   DBE: min = -0.5, max = 25.0
Element prediction: Off
Number of isotope peaks used for i-FIT = 2

Monoisotopic Mass, Even Electron Ions
8 formula(e) evaluated with 1 results within limits (up to 50 best isotopic matches for each mass)
Elements Used:
C: 10-500   H: 10-1000   O: 1-200   F: 1-1   Na: 1-1

MCO-IV-153 Polar

06-Dec-201
16:00:2
S/N: UH193
TOF MS ES+
MCO-IV-153-P_120612_001 98 (1.825) AM (Cen,4, 80.00, Ar,8000.0,556.28,0.70); Sm (SG, 2x1.00); Cm (90:100)
1.38e+00
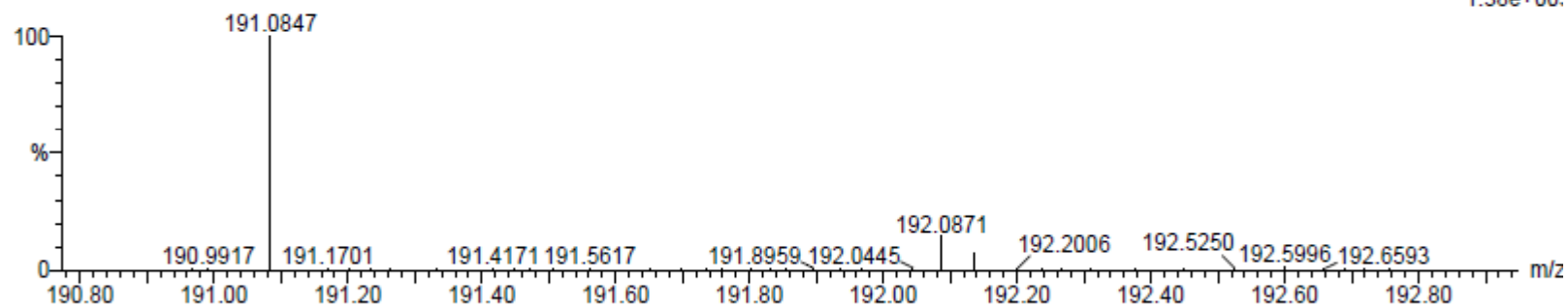
| | | | Minimum: | | | -0.5 | | |
| | | | Maximum: | 5.0 | 5.0 | 25.0 | | |

Mass	Calc. Mass	mDa	PPM	DBE	i-FIT	Formula
191.0847	191.0848	-0.1	-0.5	3.5	3.6	C10 H13 O F Na

297
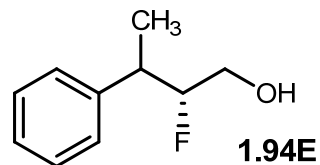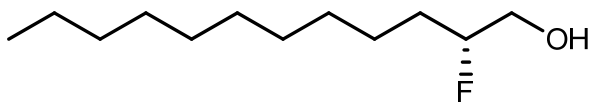
(*R*)-2-fluorododecan-1-ol
Solvent: CDCl$_3$
400.13 MHz

1.94F

0.833

2.740

18.464

3.000

298
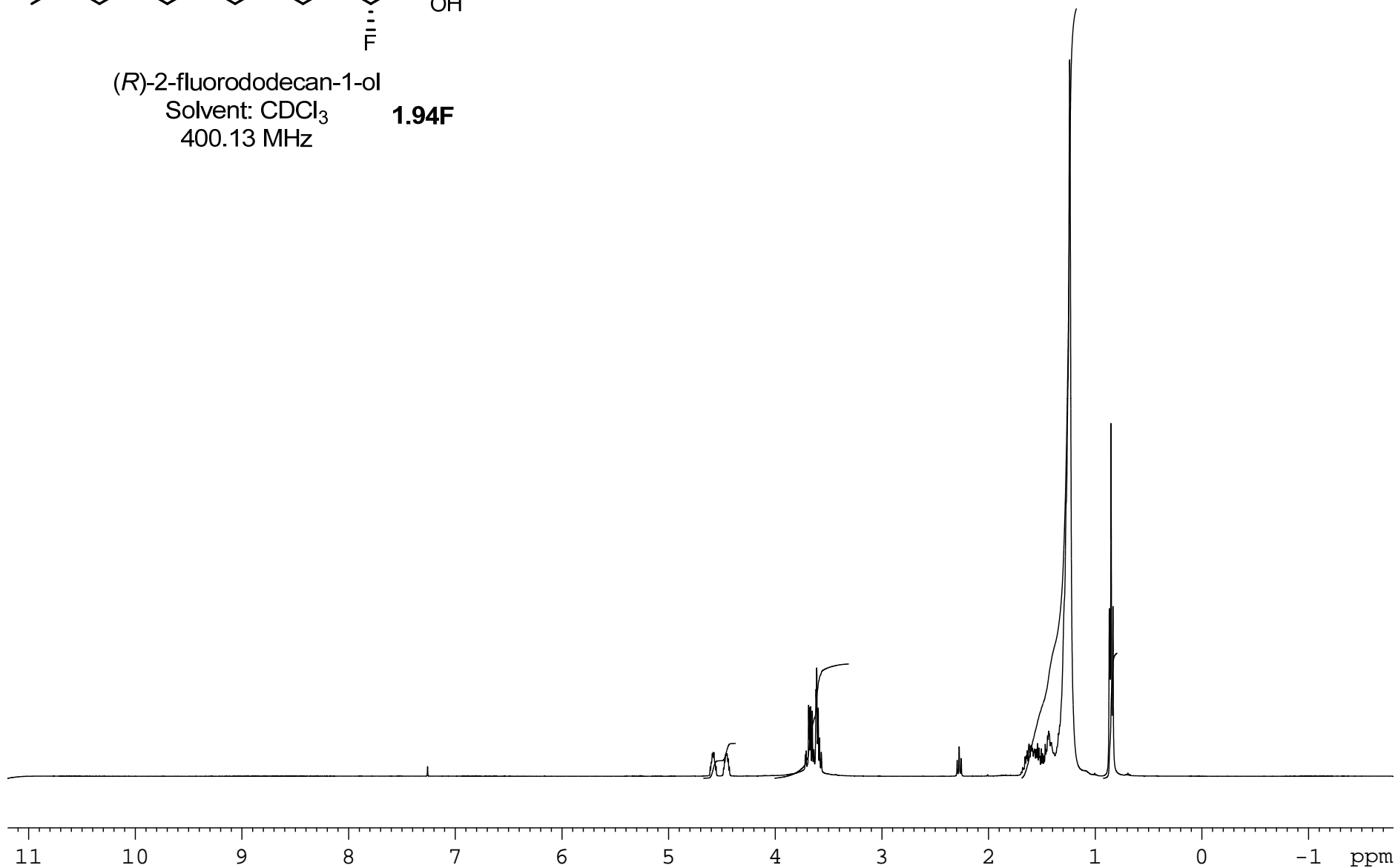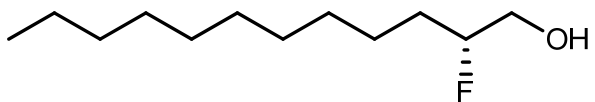
(*R*)-2-fluorododecan-1-ol
Solvent: CDCl$_3$
100.6 MHz

1.94F

95.662
93.992

65.063
64.846

31.993
31.171
30.968
29.688
29.650
29.566
29.541
29.418
25.044
24.997
22.757
14.139
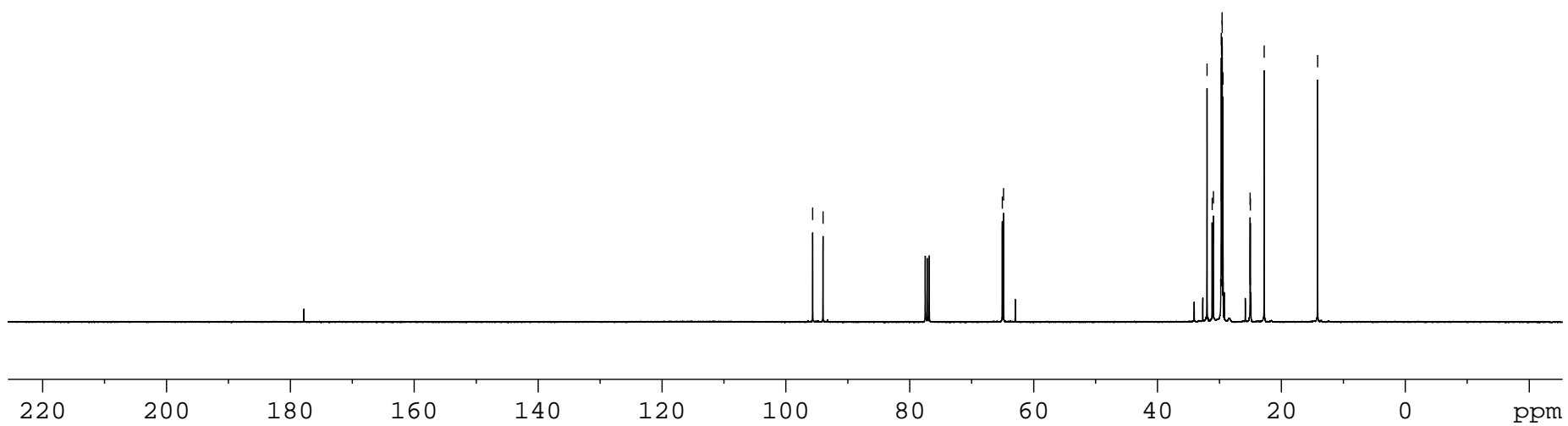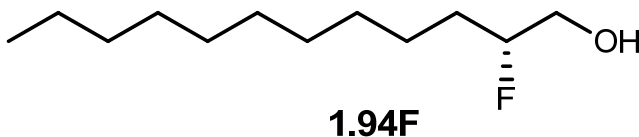
220   200   180   160   140   120   100   80   60   40   20   0   ppm

299

1.94F

Single Mass Analysis
Tolerance = 5.0 PPM   /   DBE: min = -0.5, max = 25.0
Element prediction: Off
Number of isotope peaks used for i-FIT = 2

Monoisotopic Mass, Even Electron Ions
13 formula(e) evaluated with 1 results within limits (up to 50 best isotopic matches for each mass)
Elements Used:
C: 10-500   H: 10-1000   O: 1-200   F: 1-1   Na: 1-1

MCO-IV-147   06-Dec-2012
                                                   S/N: UH193   13:14:46
MCO-IV-147_120612_001 70 (1.306) AM (Cen,4, 80.00, Ar,8000.0,556.28,0.70); Sm (SG, 2x1.00); Cm (60:70)   TOF MS ES+
                                                                                                       4.68e+003
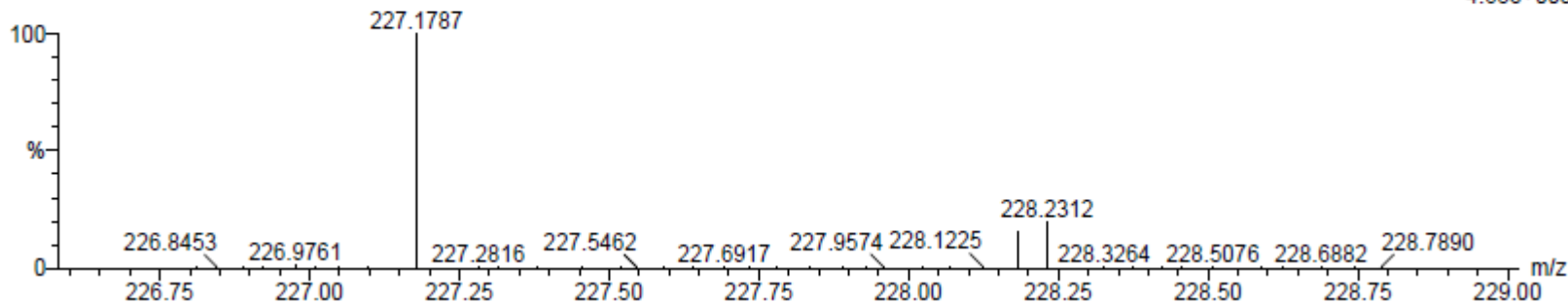
Mass	Calc. Mass	mDa	PPM	DBE	i-FIT	Formula
Minimum:				-0.5		
Maximum:		5.0	5.0	25.0		
227.1787	227.1787	0.0	0.0	-0.5	4.0	C12 H25 O F Na
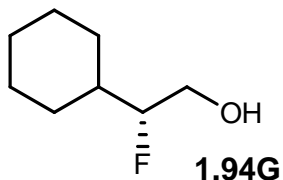
300

1.94G

(*R*)-2-cyclohexyl-2-fluoroethanol
Solvent: CDCl$_3$
400.13 MHz
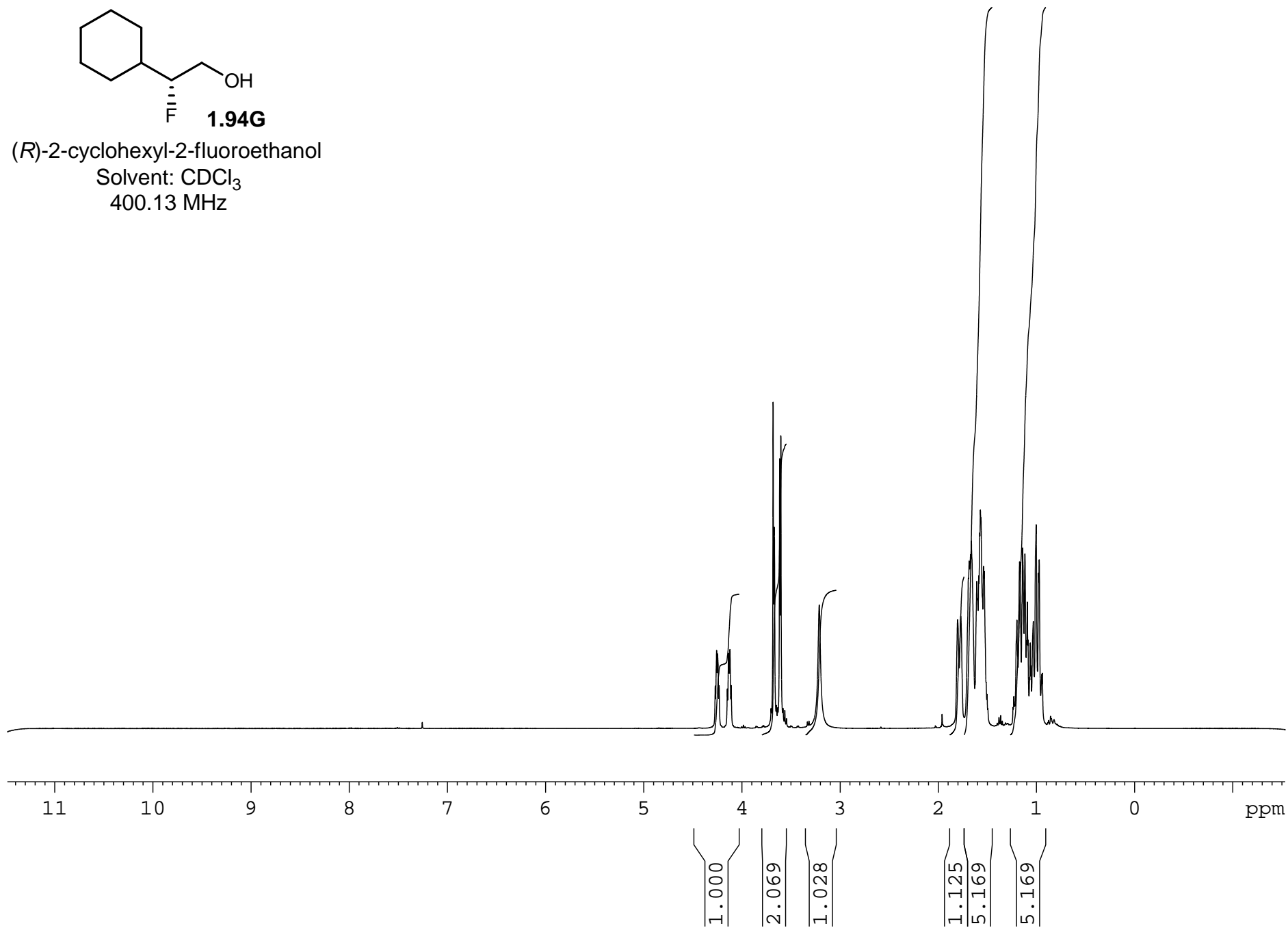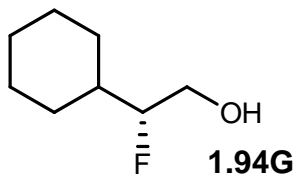
1.000 2.069 1.028 1.125 5.169 5.169

(*R*)-2-cyclohexyl-2-fluoroethanol
Solvent: CDCl$_3$
100.6 MHz
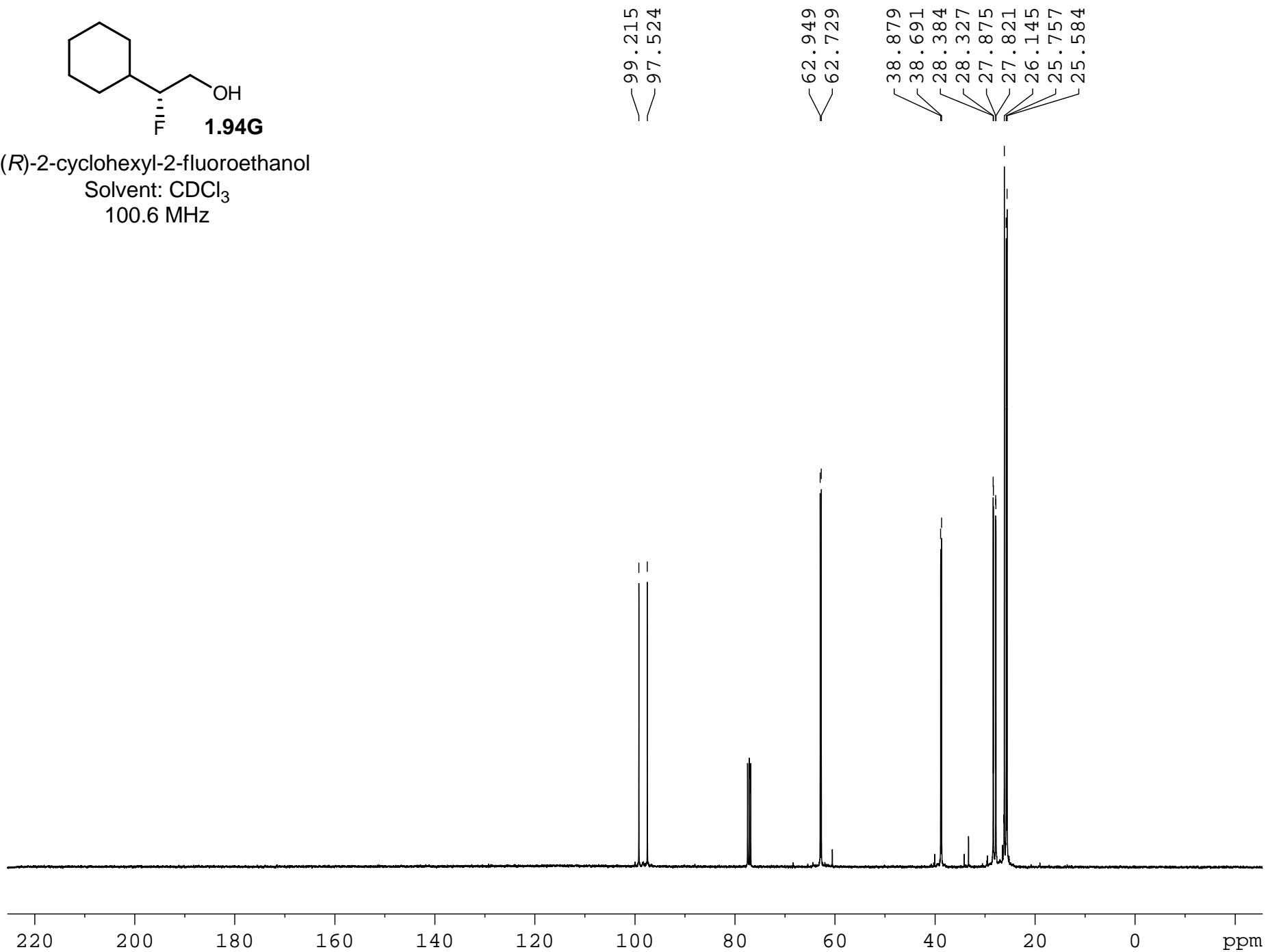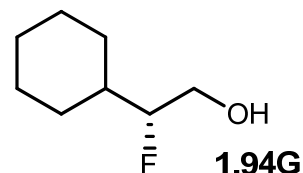
99.215
97.524

62.949
62.729

38.879
38.691
28.384
28.327
27.875
27.821
26.145
25.757
25.584

220   200   180   160   140   120   100   80   60   40   20   0   ppm

302

Elemental Composition Report

Single Mass Analysis
Tolerance = 5.0 PPM   /   DBE: min = -0.5, max = 25.0
Element prediction: Off
Number of isotope peaks used for i-FIT = 2

Monoisotopic Mass, Even Electron Ions
8 formula(e) evaluated with 1 results within limits (up to 50 best isotopic matches for each mass)
Elements Used:
C: 5-500   H: 10-1000   O: 1-200   F: 1-1   Na: 1-1

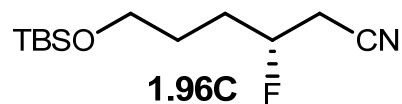MCO-IV-154

Page 1

S/N: UH193
MCO-IV-154_120612_001 69 (1.287) AM (Cen,4, 80.00, Ar,8000.0,556.28,0.70); Sm (SG, 2x1.00); Cm (60:70)

1.94G
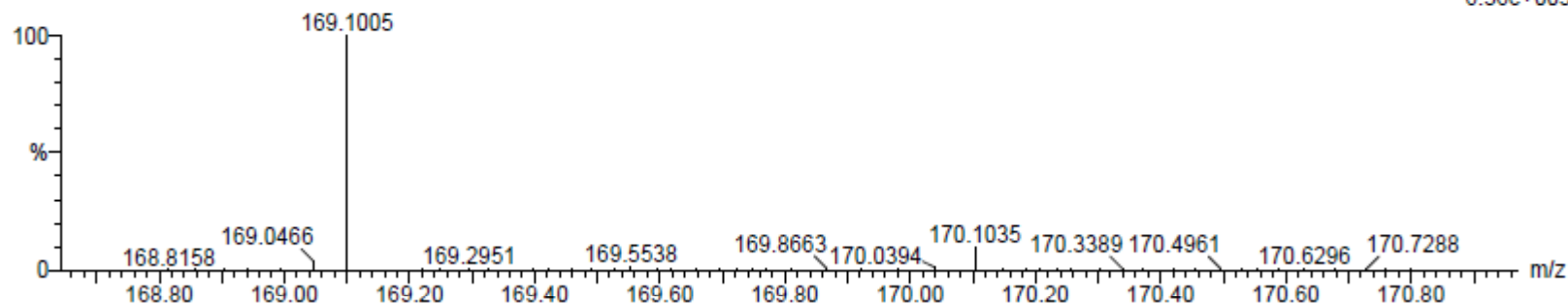
Mass	Calc. Mass	mDa	PPM	DBE	i-FIT	Formula
Minimum:				-0.5		
Maximum:		5.0	5.0	25.0		
169.1005	169.1005	0.0	0.0	0.5	1.1	C8 H15 O F Na

303

5-((*tert*-butyldimethylsilyl)oxy)-2,2-difluoropentan-1-ol
Solvent: CDCl$_3$
400.13 MHz
1.104
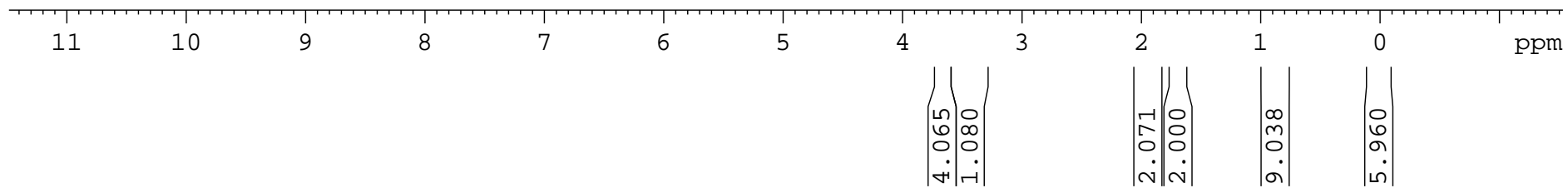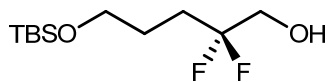
4.065 1.080   2.071 2.000   9.038   5.960

5-((*tert*-butyldimethylsilyl)oxy)-2,2-difluoropentan-1-ol
Solvent: CDCl₃
100.6 MHz
1.104
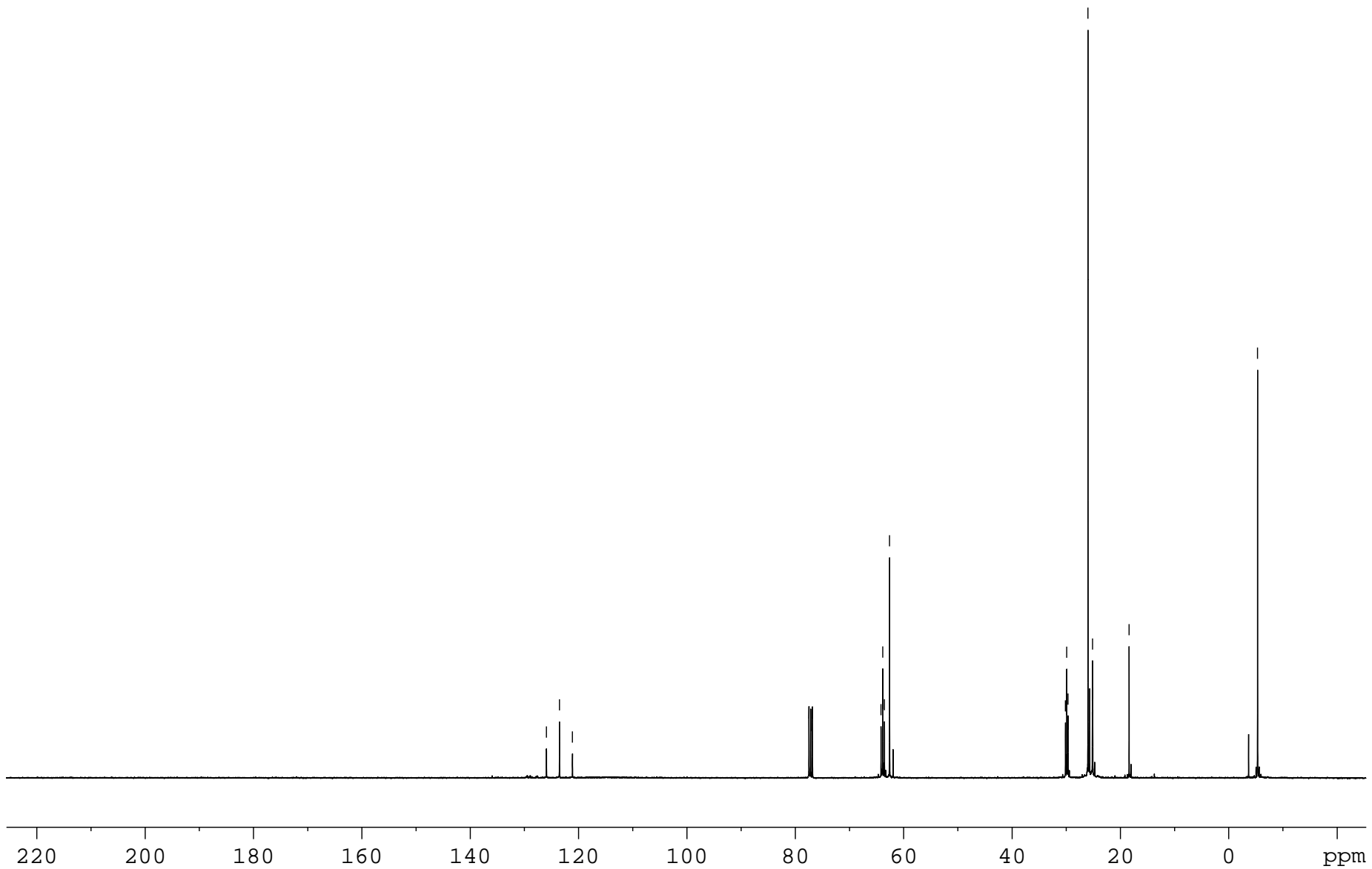
Elemental Composition Report

Page 1

Single Mass Analysis
Tolerance = 5.0 PPM / DBE: min = -0.5, max = 25.0
Element prediction: Off
Number of isotope peaks used for i-FIT = 2
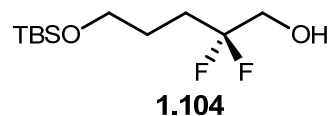
Monoisotopic Mass, Even Electron Ions
13 formula(e) evaluated with 1 results within limits (up to 50 best isotopic matches for each mass)
Elements Used:
C: 10-500   H: 10-1000   O: 1-200   F: 2-2   Si: 1-1

MCO-V-15

07-Dec-2012
11:50:46
TOF MS ES+
9.40e+003

S/N: UH193
MCO-V-15_120712_001 97 (1.807) AM (Cen,4, 80.00, Ar,8000.0,556.28,0.70); Sm (SG, 2x1.00); Cm (90:100)

1.104

255.1591

256.1620

254.8995 255.0006 255.5011 255.7119 255.9909 256.2808 256.5992 257.0281 257.1578 257.3419 257.5886 257.7965

255.00   255.50   256.00   256.50   257.00   257.50   258.00   m/z

Minimum:			-0.5	
Maximum:	5.0	5.0	25.0	

Mass	Calc. Mass	mDa	PPM	DBE	i-FIT	Formula
255.1591	255.1592	-0.1	-0.4	-0.5	0.8	C11 H25 O2 F2 Si
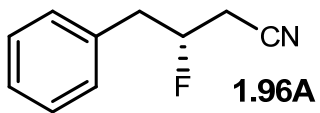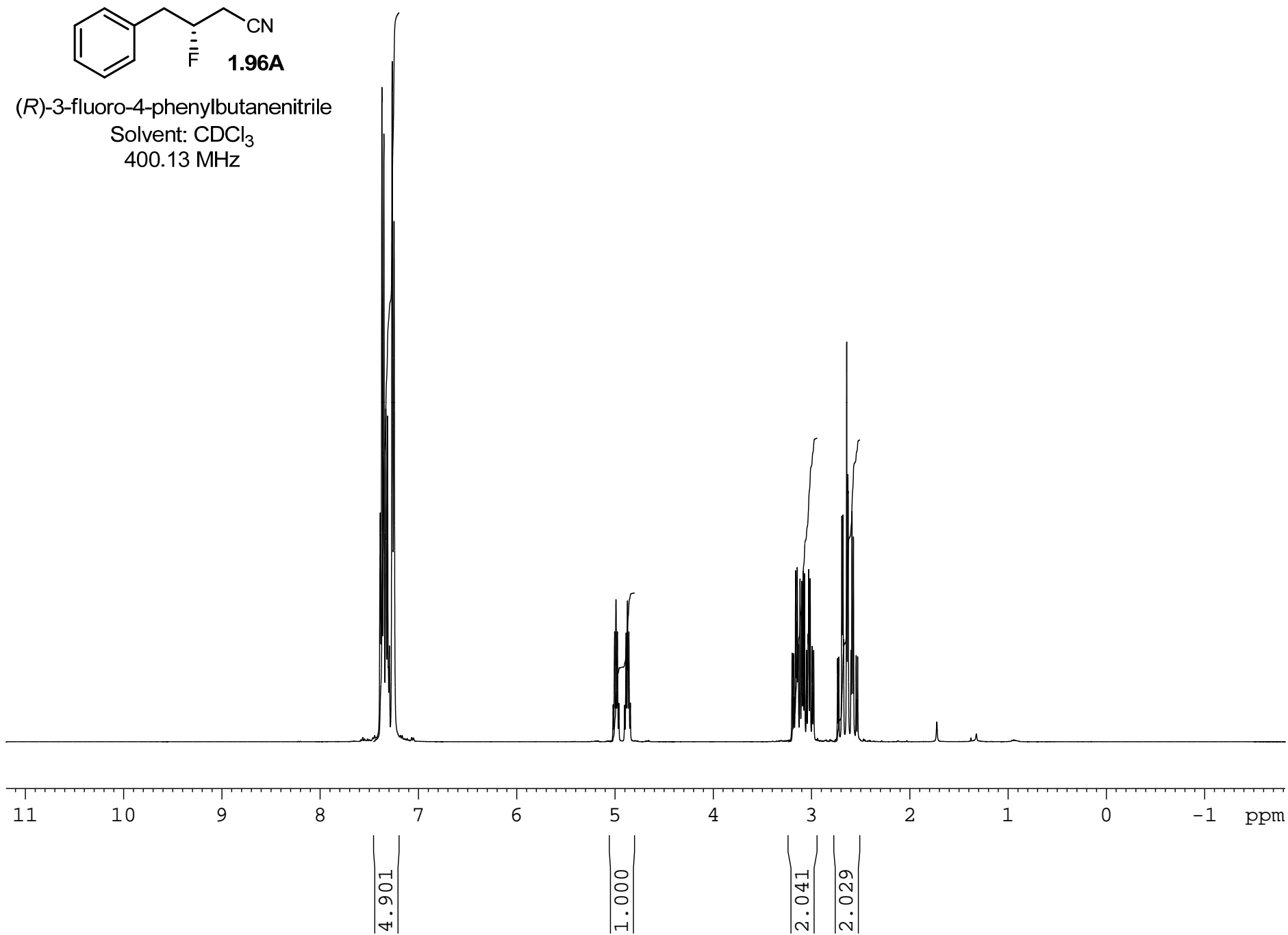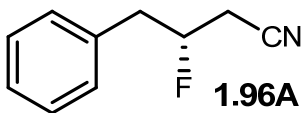
306

(*R*)-3-fluoro-4-phenylbutanenitrile
Solvent: CDCl$_3$
400.13 MHz

1.96A

4.901 1.000 2.041 2.029

11 10 9 8 7 6 5 4 3 2 1 0 -1 ppm

(R)-3-fluoro-4-phenylbutanenitrile
Solvent: CDCl₃
100.6 MHz

1.96A

134.800
134.744
129.385
128.856
127.374
116.091
116.037
89.599
87.802
40.267
40.060
23.230
22.984

220   200   180   160   140   120   100   80   60   40   20   0   ppm
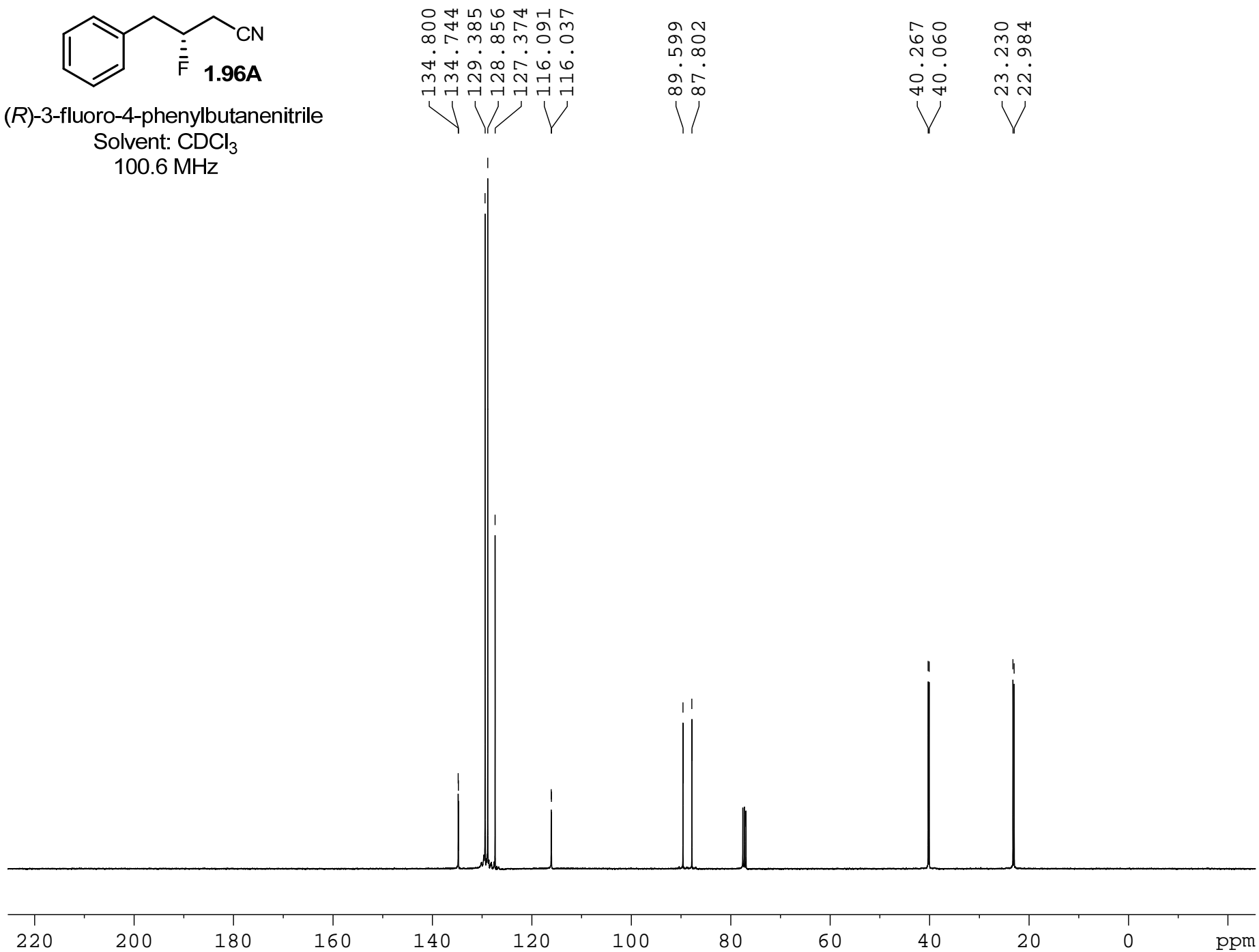
Elemental Composition Report
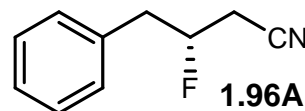
Page 1

Single Mass Analysis
Tolerance = 5.0 PPM / DBE: min = -0.5, max = 25.0
Element prediction: Off
Number of isotope peaks used for i-FIT = 2

Monoisotopic Mass, Even Electron Ions
9 formula(e) evaluated with 1 results within limits (up to 50 best isotopic matches for each mass)
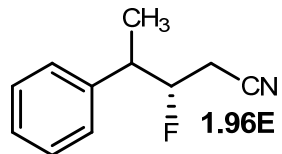Elements Used:
C: 10-500   H: 10-1000   N: 1-200   F: 1-1   Na: 1-1
MCO-IV-155

06-Dec-2012
17:11:33

S/N: UH193

MCO-IV-155_120612_001 87 (1.621) AM (Cen,4, 80.00, Ar,8000.0,556.28,0.70); Sm (SG, 2x1.00); Cm (80:90)

TOF MS ES+
2.11e+003
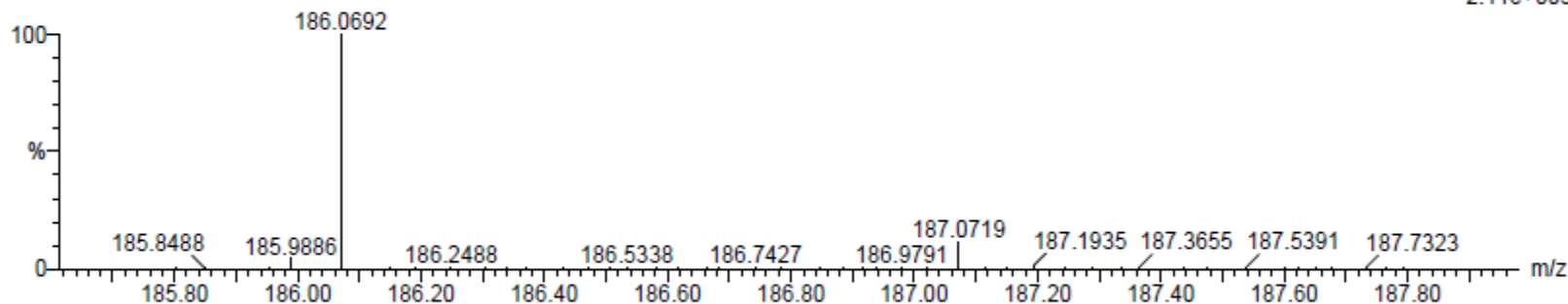
| Minimum: | | | -0.5 | | |
| Maximum: | 5.0 | 5.0 | 25.0 | | |

Mass	Calc. Mass	mDa	PPM	DBE	i-FIT	Formula
186.0692	186.0695	-0.3	-1.6	5.5	0.0	C10 H10 N F Na
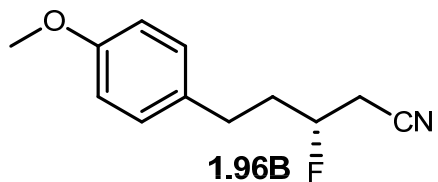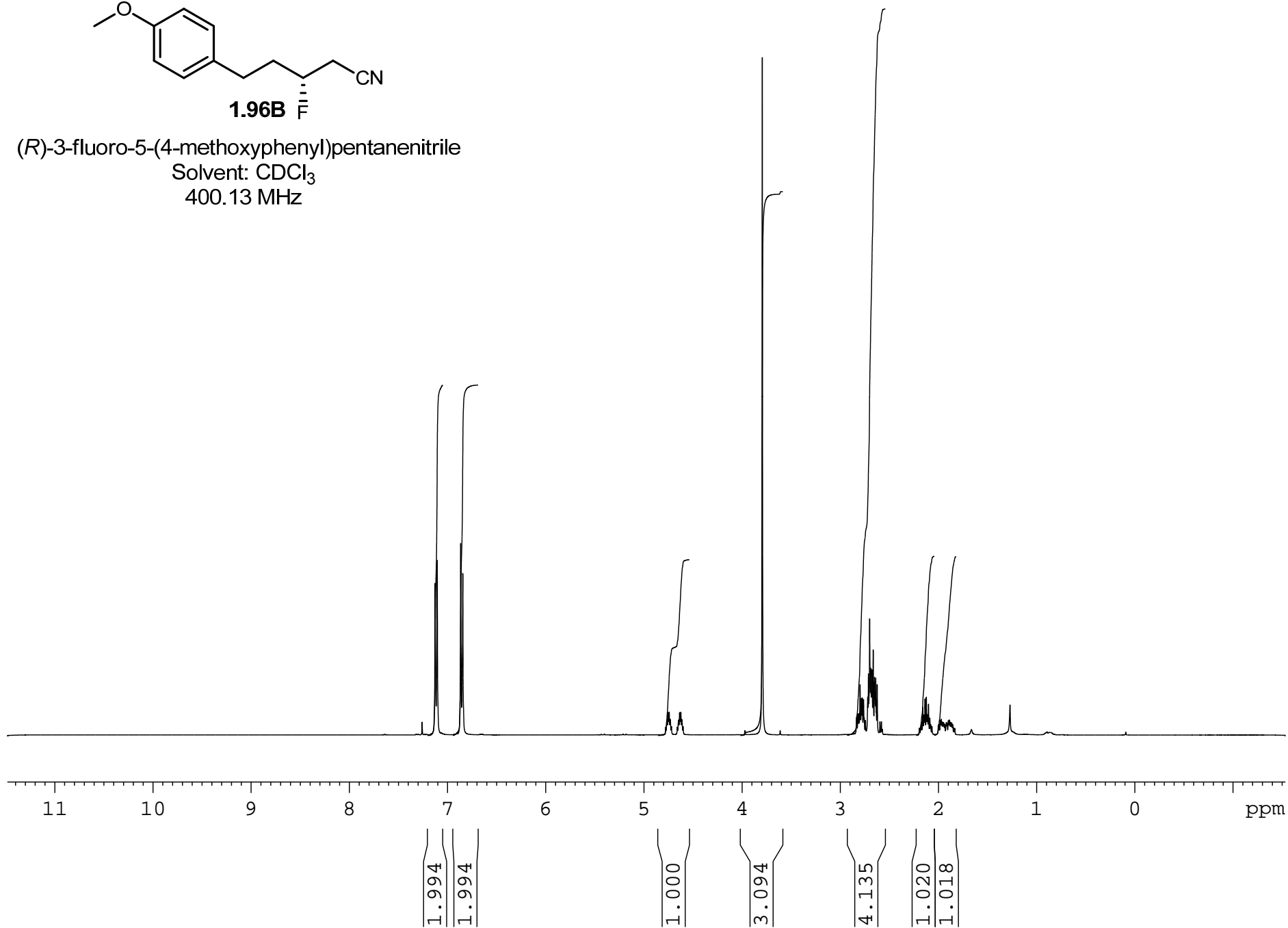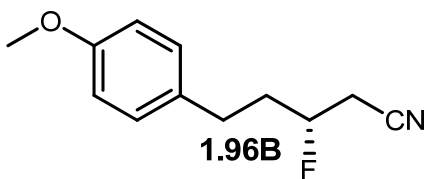
309

1.96B

(*R*)-3-fluoro-5-(4-methoxyphenyl)pentanenitrile
Solvent: CDCl$_3$
400.13 MHz

1.994 1.994 1.000 3.094 4.135 1.020 1.018

(R)-3-fluoro-5-(4-methoxyphenyl)pentanenitrile

Solvent: CDCl$_3$
100.6 MHz

158.253
132.050
129.444
115.996
115.934
114.134
88.369
86.601
55.330
36.259
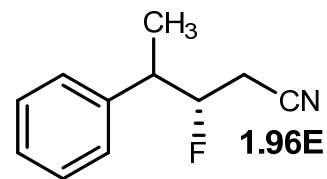36.057
29.921
29.880
24.227
23.974

Elemental Composition Report

1.96B
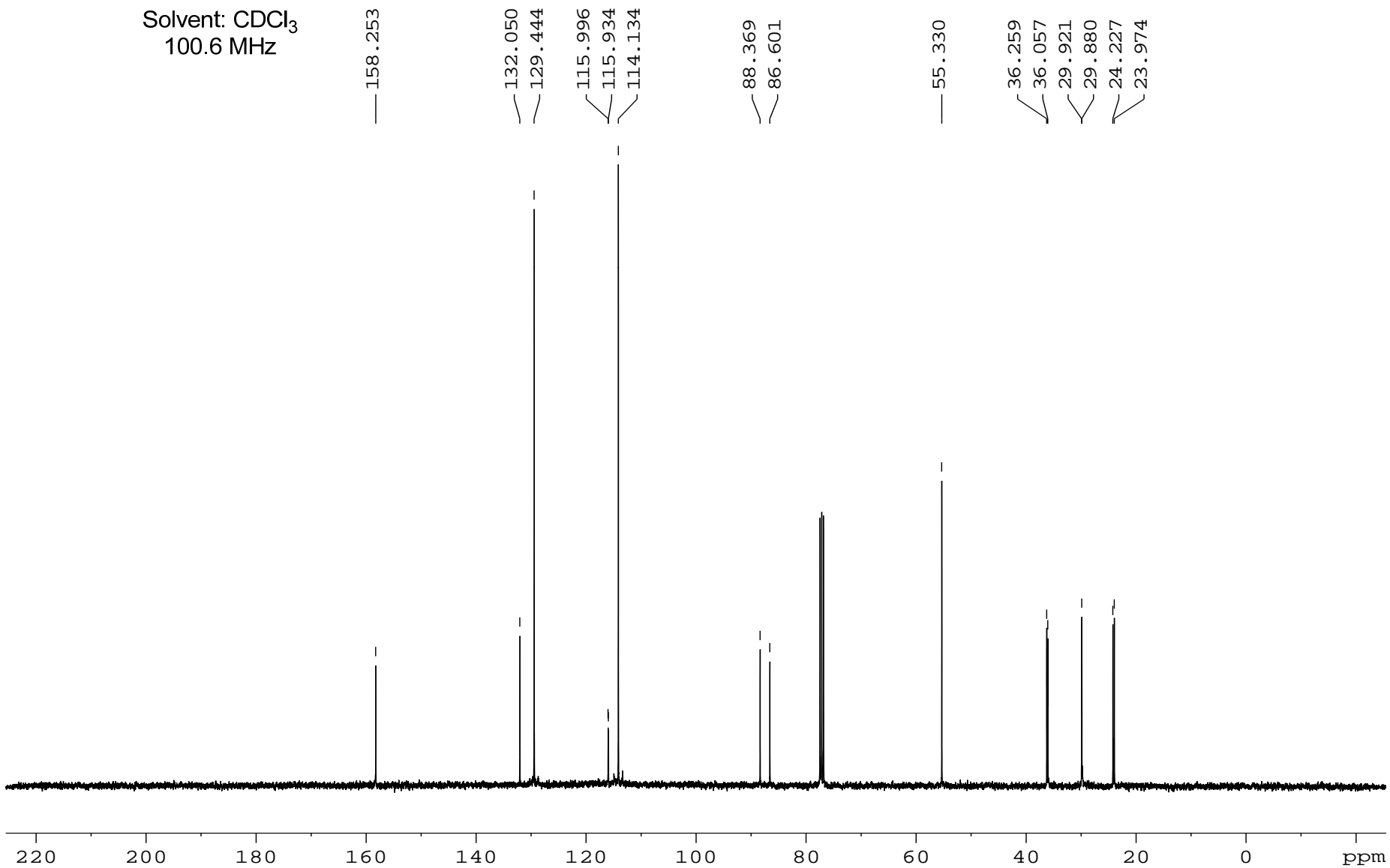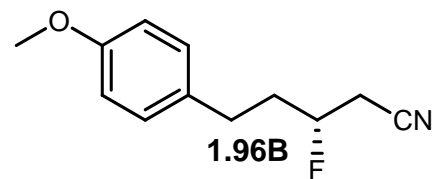
Single Mass Analysis
Tolerance = 5.0 PPM / DBE: min = -0.5, max = 25.0
Element prediction: Off
Number of isotope peaks used for i-FIT = 2

Monoisotopic Mass, Even Electron Ions
155 formula(e) evaluated with 1 results within limits (up to 50 best isotopic matches for each mass)
Elements Used:
C: 10-500   H: 10-1000   N: 1-200   O: 1-200   F: 1-1   Na: 0-1

MCO-IV-150

06-Dec-2012
14:26:21

S/N: UH193

MCO-IV-150_120612_001 60 (1.121) AM (Cen,4, 80.00, Ar,8000.0,556.28,0.70); Sm (SG, 2x1.00); Cm (50:60)

TOF MS ES+
3.20e+003
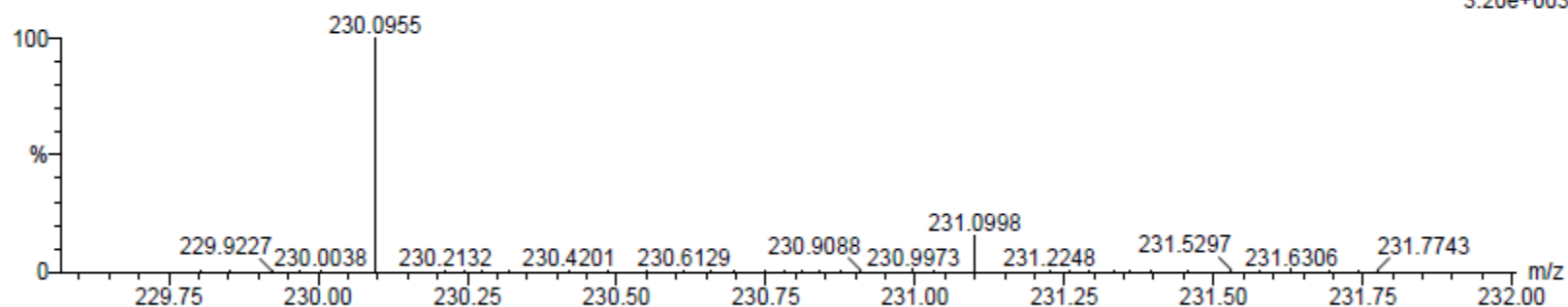
Minimum:			-0.5		
Maximum:	5.0	5.0	25.0		

Mass	Calc. Mass	mDa	PPM	DBE	i-FIT	Formula
230.0955	230.0957	-0.2	-0.9	5.5	2.9	C12 H14 N O F Na
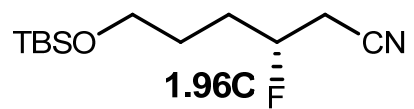
(R)-6-((*tert*-butyldimethylsilyl)oxy)-3-fluorohexanenitrile

Solvent: CDCl$_3$

400.13 MHz

1.96C

1.000   2.037   2.001   4.129   9.280   6.088

313

1.96C
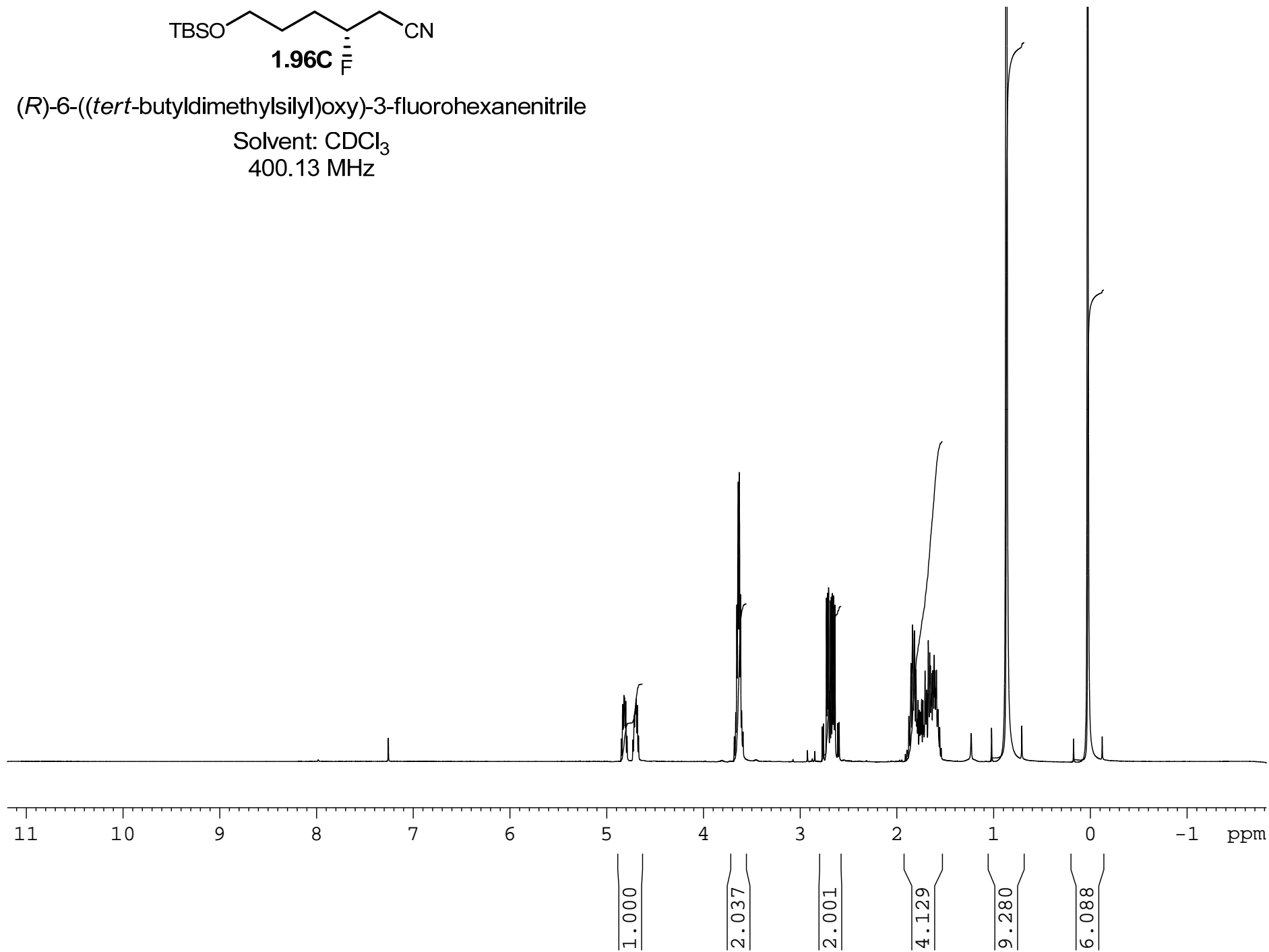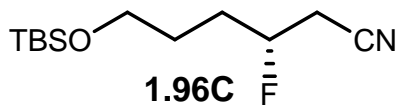
(*R*)-6-((*tert*-butyldimethylsilyl)oxy)-3-fluorohexanenitrile
Solvent: CDCl₃
100.6 MHz

116.061
116.003

89.396
87.633

62.240

31.206
31.003
27.867
27.824
25.941
24.210
23.958
18.300

−5.350
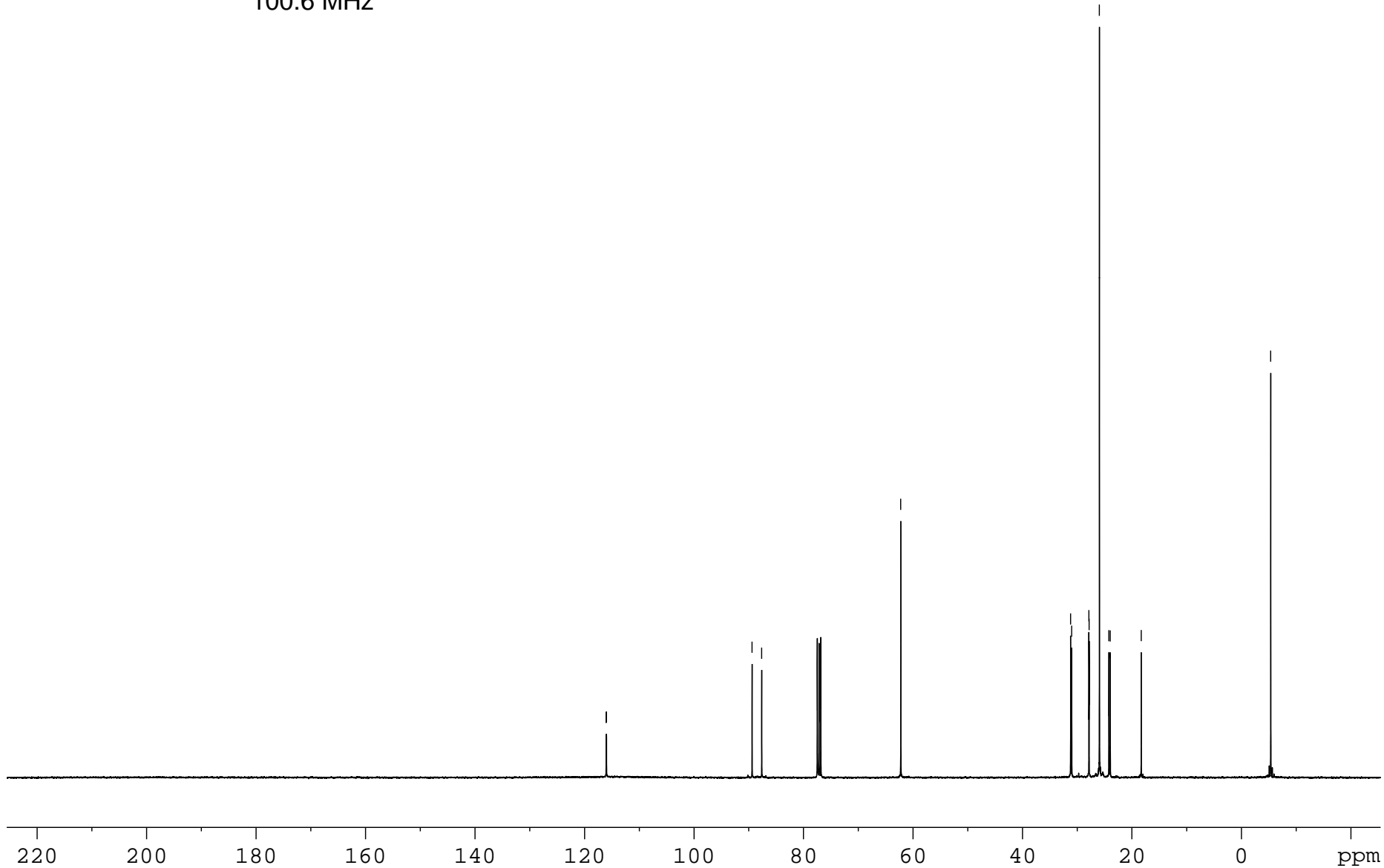
220   200   180   160   140   120   100   80   60   40   20   0   ppm

314

Elemental Composition Report

Page 1

Single Mass Analysis

Tolerance = 5.0 PPM   /   DBE: min = -0.5, max = 25.0
Element prediction: Off
Number of isotope peaks used for i-FIT = 2

Monoisotopic Mass, Even Electron Ions
76 formula(e) evaluated with 1 results within limits (up to 50 best isotopic matches for each mass)
Elements Used:
C: 10-500   H: 10-1000   N: 1-200   O: 1-200   F: 1-1   Si: 1-1

MCO-IV-171

07-Dec-2012
10:58:05

S/N: UH193

MCO-IV-171_120712_001 60 (1.120) AM (Cen,4, 80.00, Ar,8000.0,556.28,0.70); Sm (SG, 2x1.00); Cm (60:70)

TOF MS ES+
6.09e+003
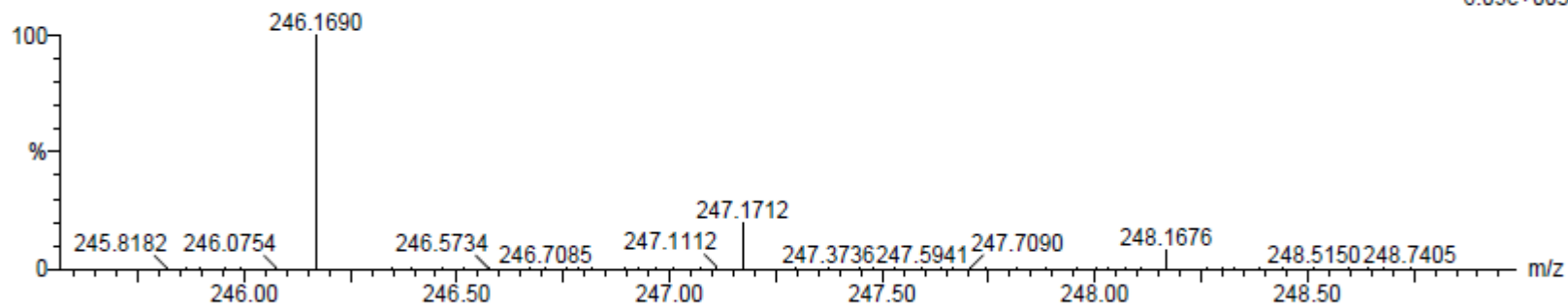
Minimum:				-0.5						
Maximum:		5.0	5.0	25.0						
Mass	Calc. Mass	mDa	PPM	DBE	i-FIT	Formula				
246.1690	246.1689	0.1	0.4	1.5	0.5	C12	H25	N	O	F	Si
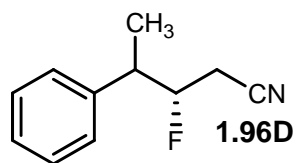
315

(3*S*)-3-fluoro-4-phenylpentanenitrile
Diastereomer A
Solvent: CDCl$_3$
400.13 MHz

4.996
1.000
0.992
2.051
3.082

11 10 9 8 7 6 5 4 3 2 1 0 ppm

316

(3*S*)-3-fluoro-4-phenylpentanenitrile
Diastereomer A
Solvent: CDCl$_3$
100.6 MHz

140.766
140.684
129.226
127.762
127.588
116.162
116.129
93.119
91.285
77.478
77.160
76.842
44.171
43.973
22.673
22.439
17.340
17.299

220   200   180   160   140   120   100   80   60   40   20   0   ppm

317
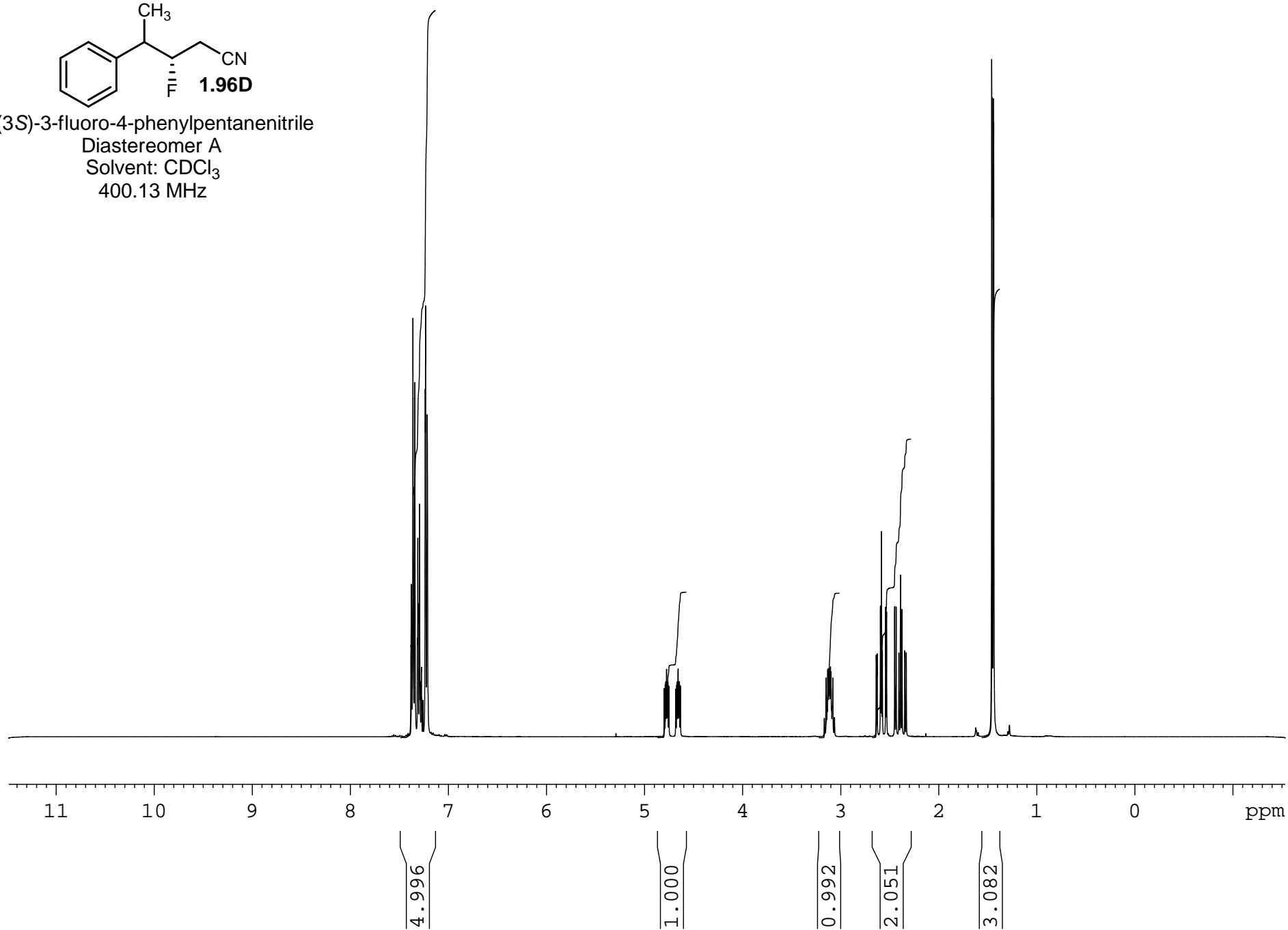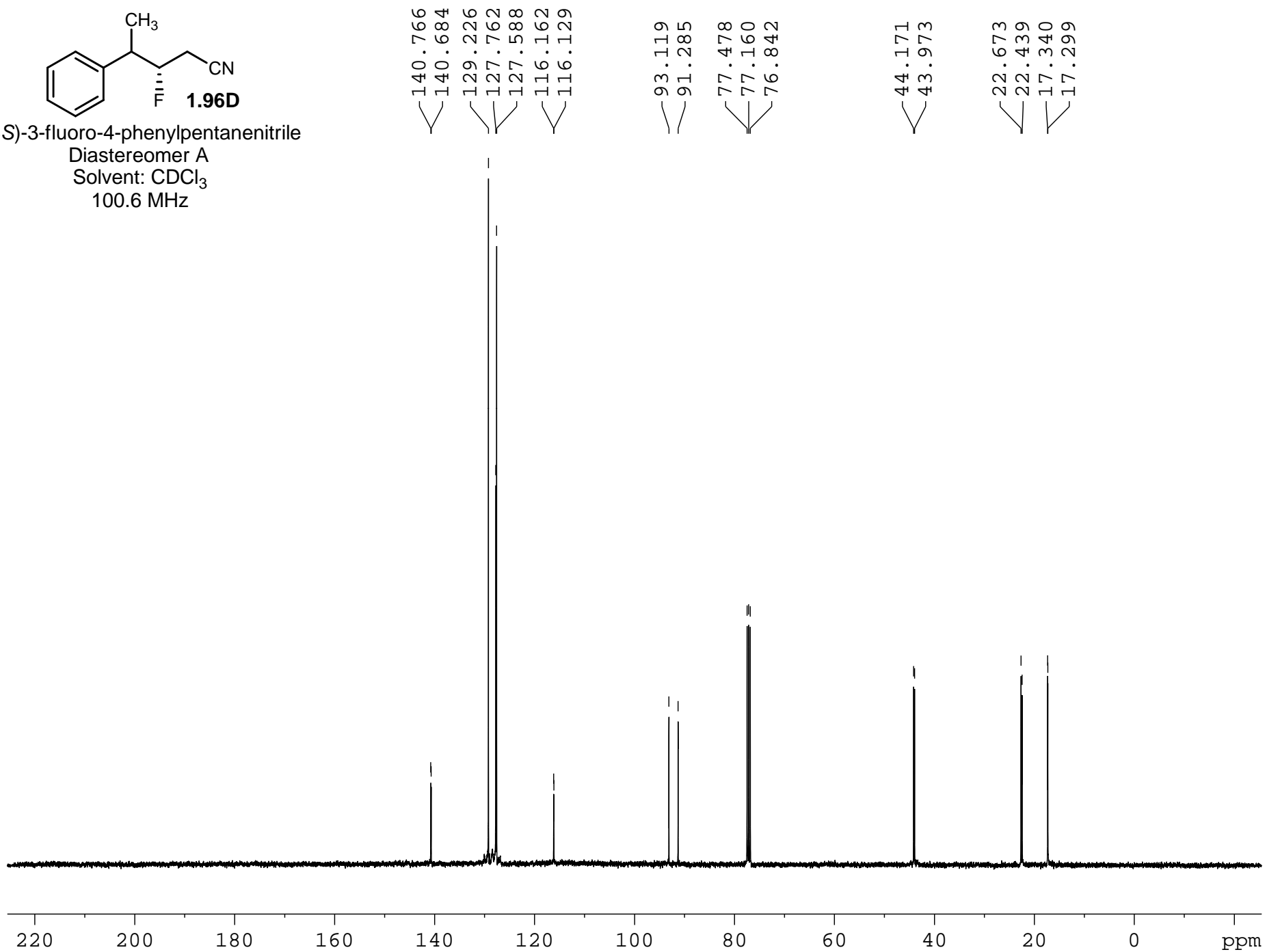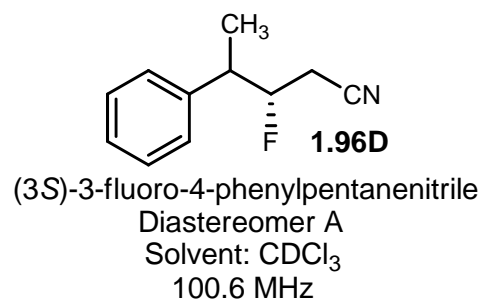
Elemental Composition Report

Page 1

Single Mass Analysis
Tolerance = 5.0 PPM   /   DBE: min = -0.5, max = 25.0
Element prediction: Off
Number of isotope peaks used for i-FIT = 2
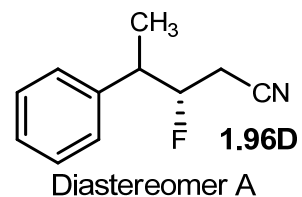
Monoisotopic Mass, Even Electron Ions
11 formula(e) evaluated with 1 results within limits (up to 50 best isotopic matches for each mass)
Elements Used:
C: 10-500   H: 10-1000   N: 1-200   F: 1-1

MCO-IV-160

S/N: UH193

07-Dec-2012
09:28:39
TOF MS ES+
2.40e+003

MCO-IV-160_120712_001 52 (0.972) AM (Cen,4, 80.00, Ar,8000.0,556.28,0.70); Sm (SG, 2x1.00); Cm (50:60)

Diastereomer A

1.96D
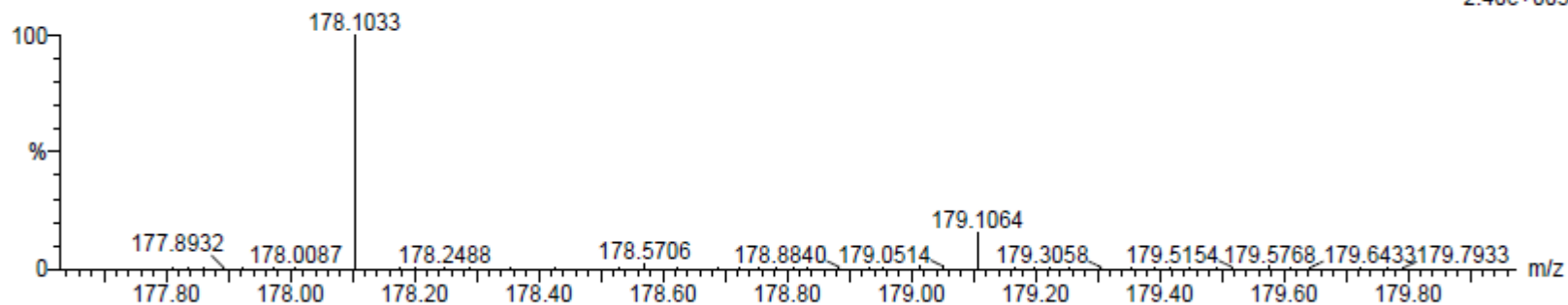
Minimum:				-0.5		
Maximum:		5.0	5.0	25.0		
Mass	Calc. Mass	mDa	PPM	DBE	i-FIT	Formula
178.1033	178.1032	0.1	0.6	5.5	3.9	C11 H13 N F

318

(3S)-3-fluoro-4-phenylpentanenitrile
Diastereomer B
Solvent: CDCl$_3$
400.13 MHz

1.96E

CH$_3$

CN

F

4.936
1.000
0.991
2.050
3.052

11 10 9 8 7 6 5 4 3 2 1 0 -1 ppm

(3S)-3-fluoro-4-phenylpentanenitrile
Diastereomer B
Solvent: CDCl$_3$
100.6 MHz

139.658
139.647
128.776
128.298
127.531
116.266
116.188

92.490
90.663

77.479
77.160
76.842

43.349
43.160

22.172
21.904
17.093
17.038

220 200 180 160 140 120 100 80 60 40 20 0 ppm

320

Elemental Composition Report

Single Mass Analysis
Tolerance = 5.0 PPM / DBE: min = -0.5, max = 25.0
Element prediction: Off
Number of isotope peaks used for i-FIT = 2

Monoisotopic Mass, Even Electron Ions
11 formula(e) evaluated with 1 results within limits (up to 50 best isotopic matches for each mass)
Elements Used:
C: 10-500   H: 10-1000   N: 1-200   F: 1-1

MCO-IV-161

Page 1
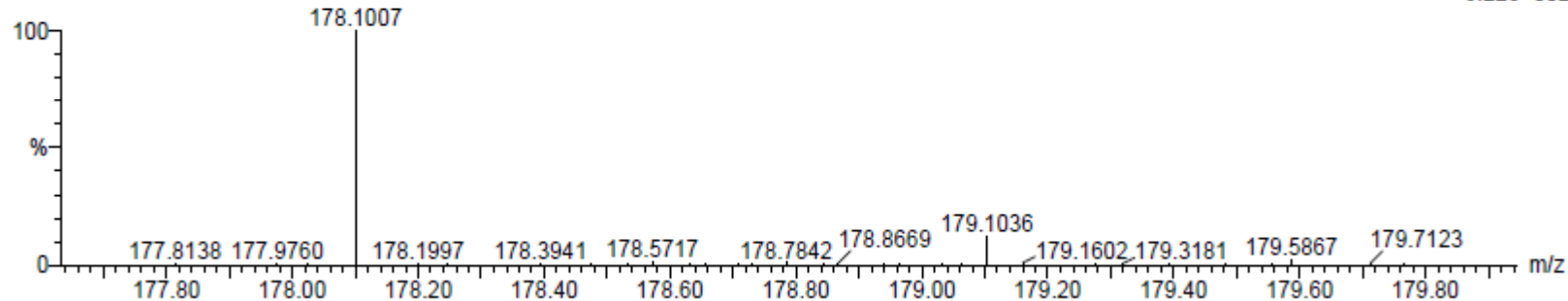
07-Dec-2012
09:40:43
TOF MS ES+
8.15e+002

CH₃ ... CN 1.96E
F
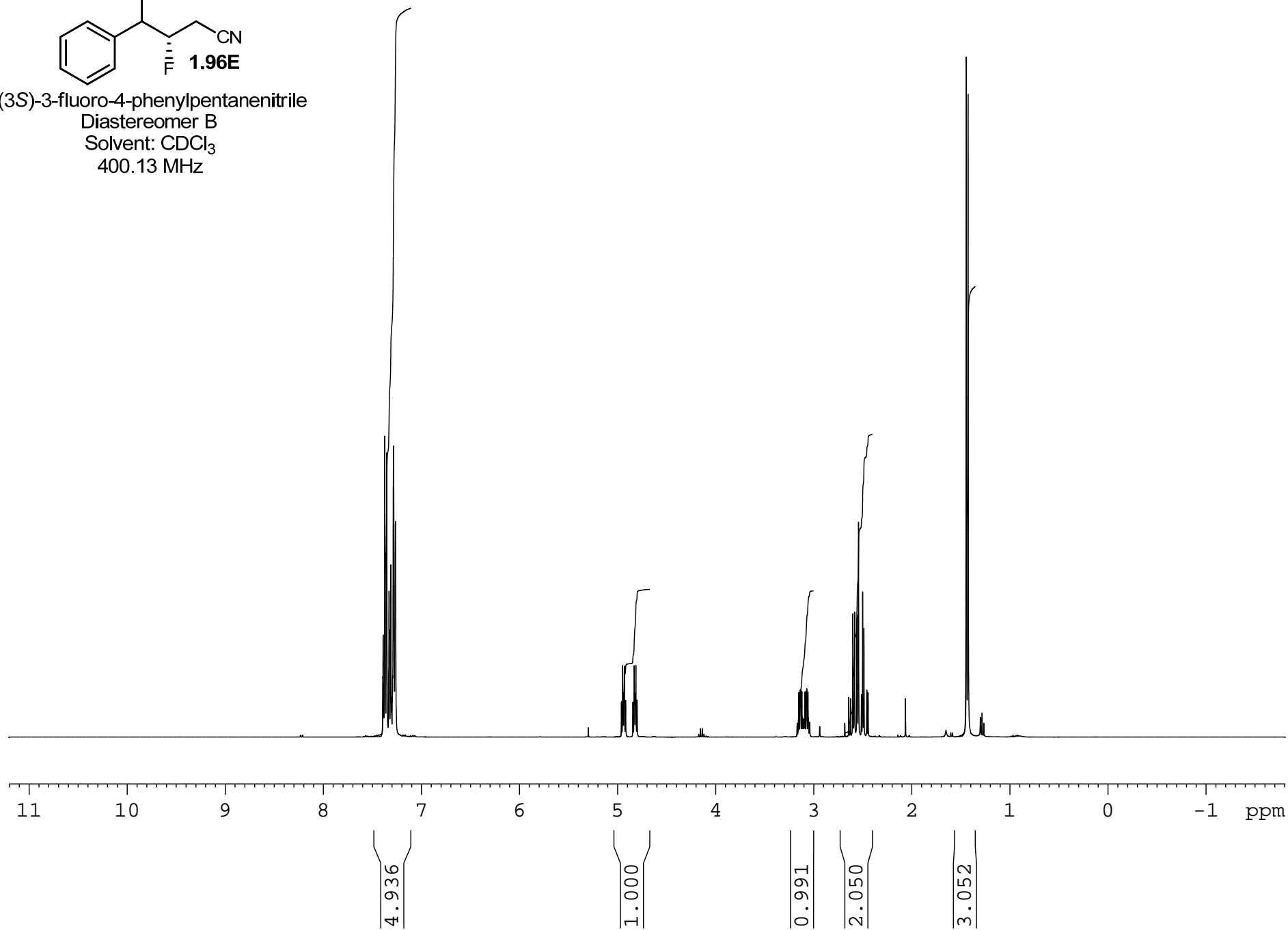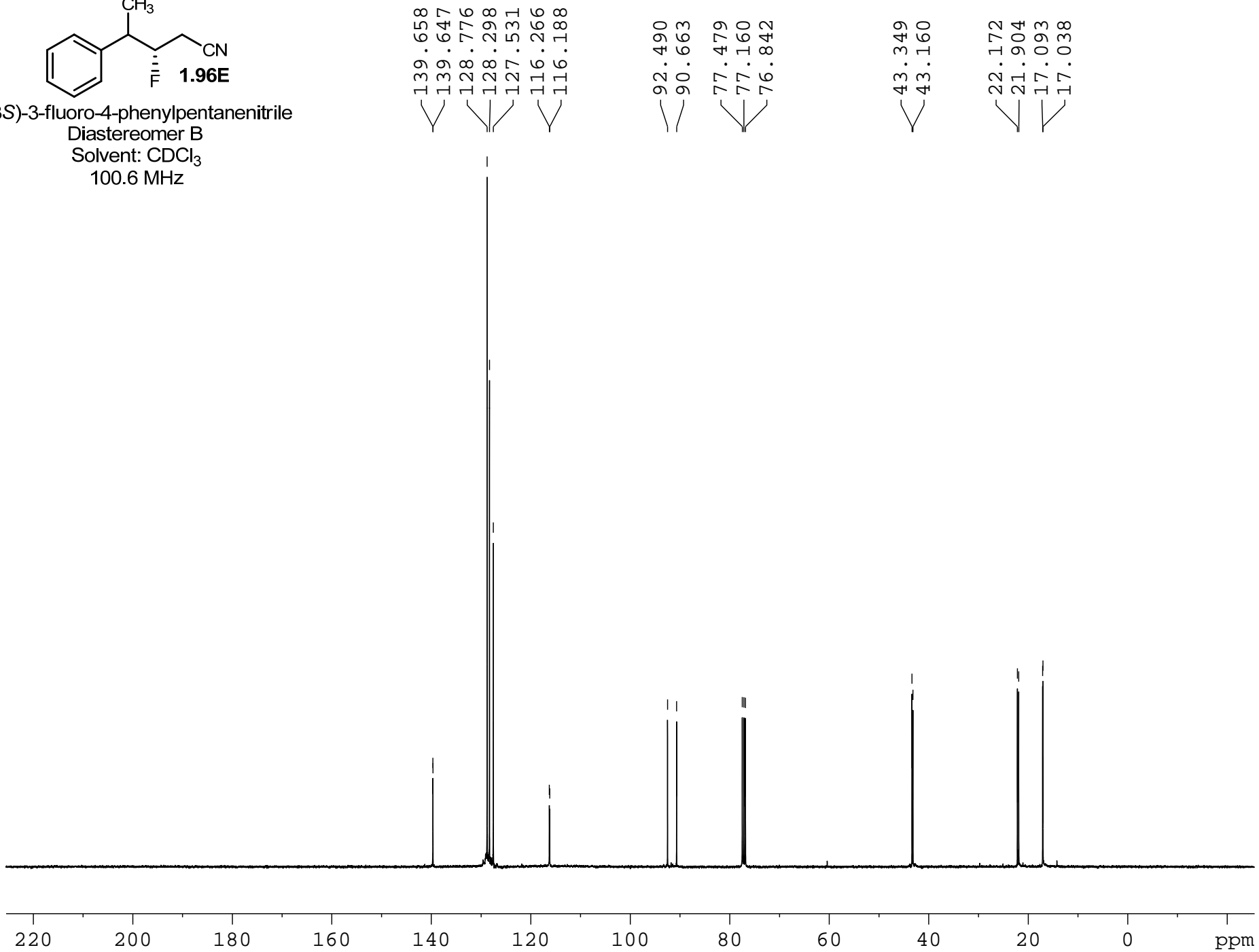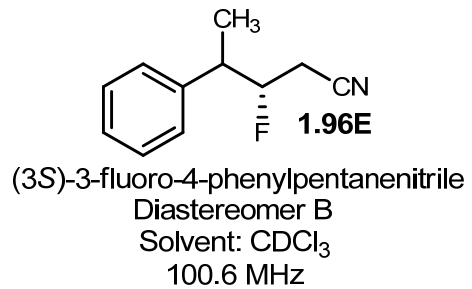
Diastereomer B

S/N: UH193
MCO-IV-161_120712_001 80 (1.492) AM (Cen,4, 80.00, Ar,8000.0,556.28,0.70); Sm (SG, 2x1.00); Cm (80:90)
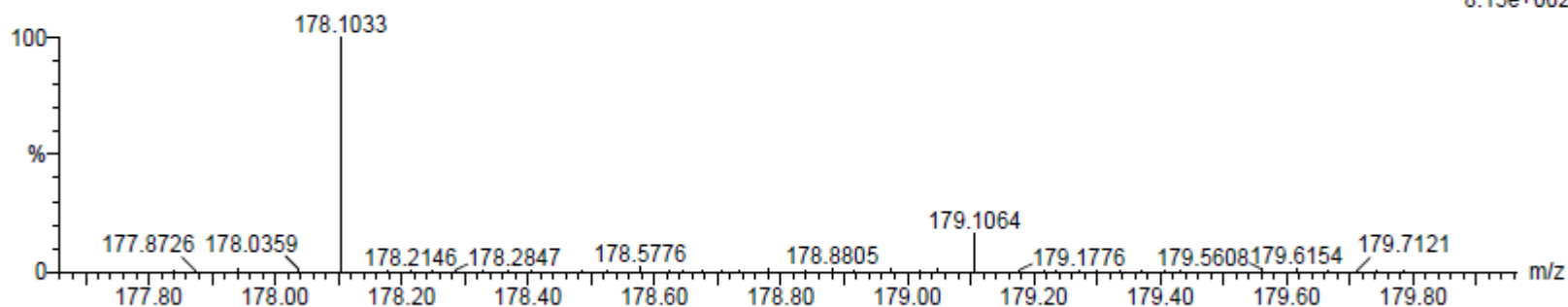
Minimum:				-0.5		
Maximum:		5.0	5.0	25.0		
Mass	Calc. Mass	mDa	PPM	DBE	i-FIT	Formula
178.1033	178.1032	0.1	0.6	5.5	2.5	C11 H13 N F
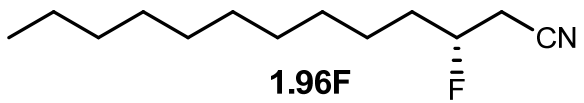
321

1.96F

(*R*)-3-fluorotridecanenitrile
Solvent: CDCl$_3$
400.13 MHz

1.000

2.003

2.177

16.042

3.130
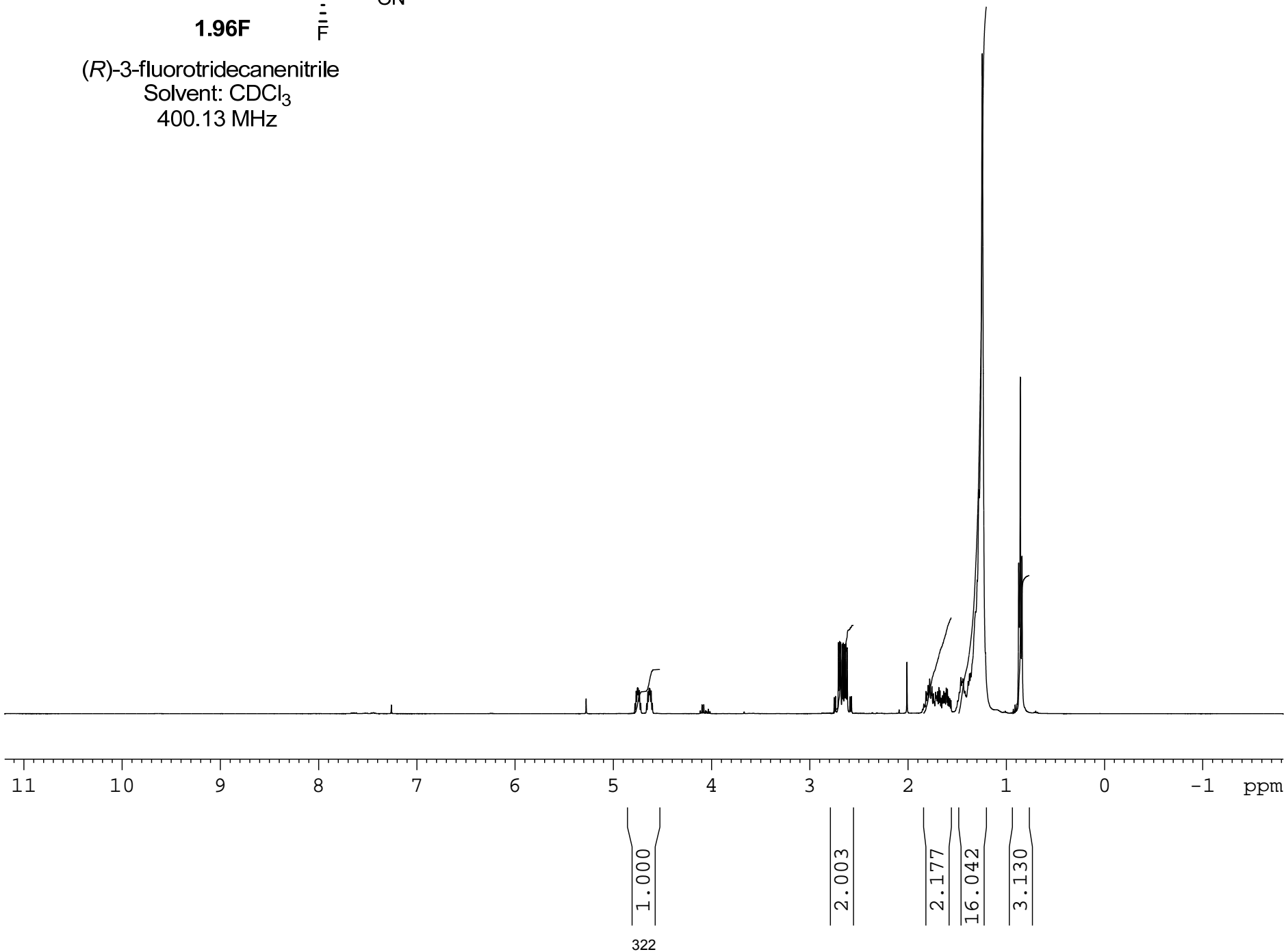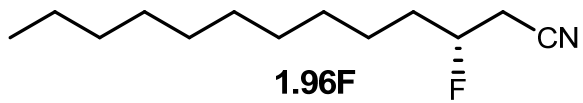
1.96F

(*R*)-3-fluorotridecanenitrile
Solvent: CDCl$_3$
100.6 MHz

116.139
116.078

89.424
87.661

34.374
34.174
31.916
29.583
29.516
29.406
29.335
29.171
24.684
24.641
24.144
23.889
22.700
14.114
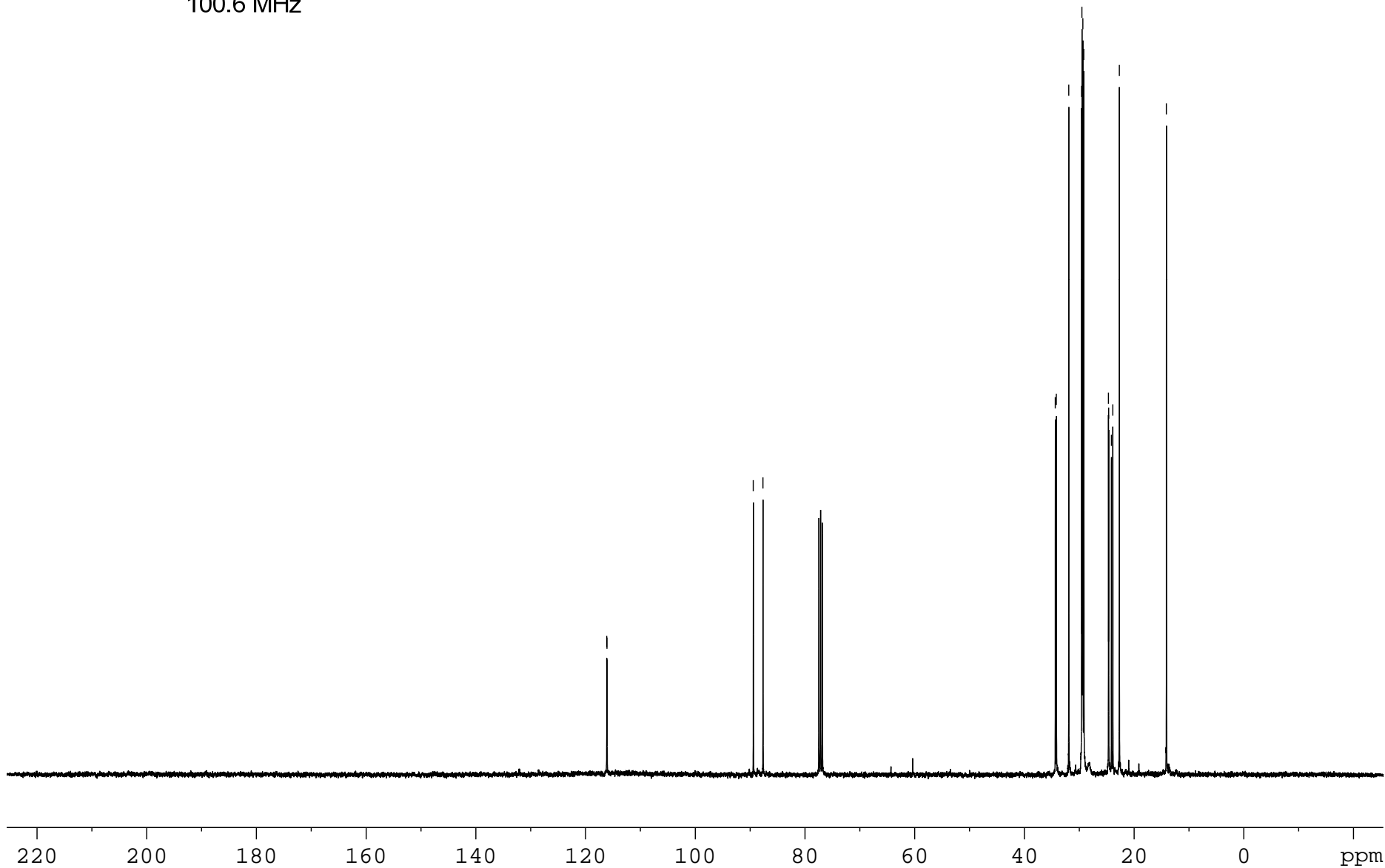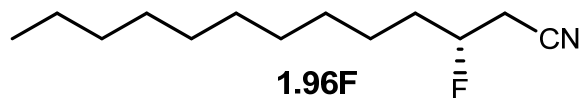
220 200 180 160 140 120 100 80 60 40 20 0 ppm

1.96F

**Single Mass Analysis**
Tolerance = 5.0 PPM / DBE: min = -0.5, max = 25.0
Element prediction: Off
Number of isotope peaks used for i-FIT = 2

Monoisotopic Mass, Even Electron Ions
37 formula(e) evaluated with 1 results within limits (up to 50 best isotopic matches for each mass)
Elements Used:
C: 10-500   H: 10-1000   N: 1-200   F: 1-1   Na: 0-1

MCO-IV-149   06-Dec-2012
                             S/N: UH193   14:14:20
MCO-IV-149_120612_001 72 (1.343) AM (Cen,4, 80.00, Ar,8000.0,556.28,0.70); Sm (SG, 2x1.00); Cm (70:80)   TOF MS ES+
                                                                      2.40e+003
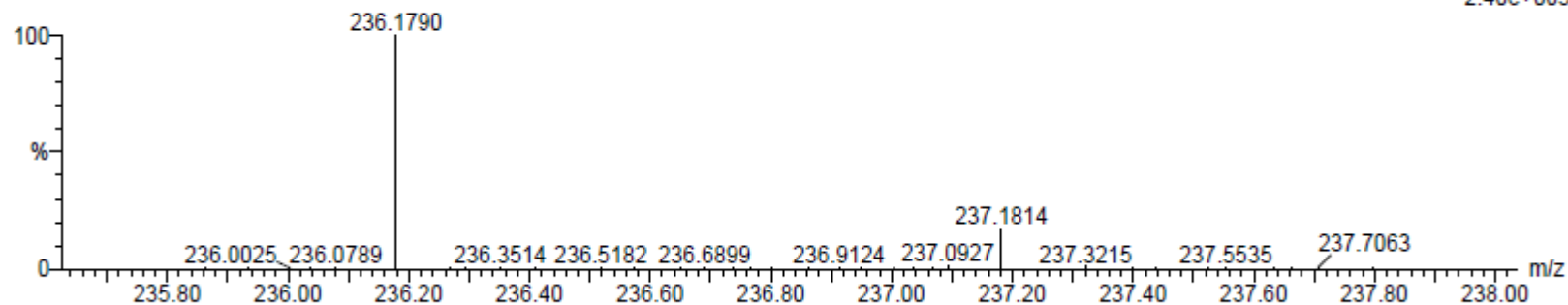

```
Minimum:                        -0.5
Maximum:          5.0     5.0    25.0

Mass        Calc. Mass    mDa    PPM    DBE    i-FIT      Formula

236.1790    236.1790      0.0    0.0    1.5    2.1        C13  H24  N  F  Na
```
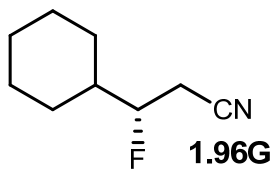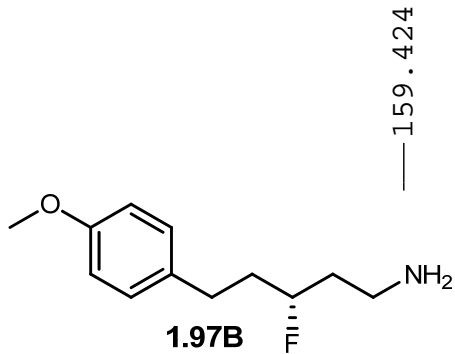
(S)-3-cyclohexyl-3-fluoropropanenitrile
Solvent: CDCl$_3$
400.13 MHz

1.96G

1.000   2.012   1.023   5.144   5.163
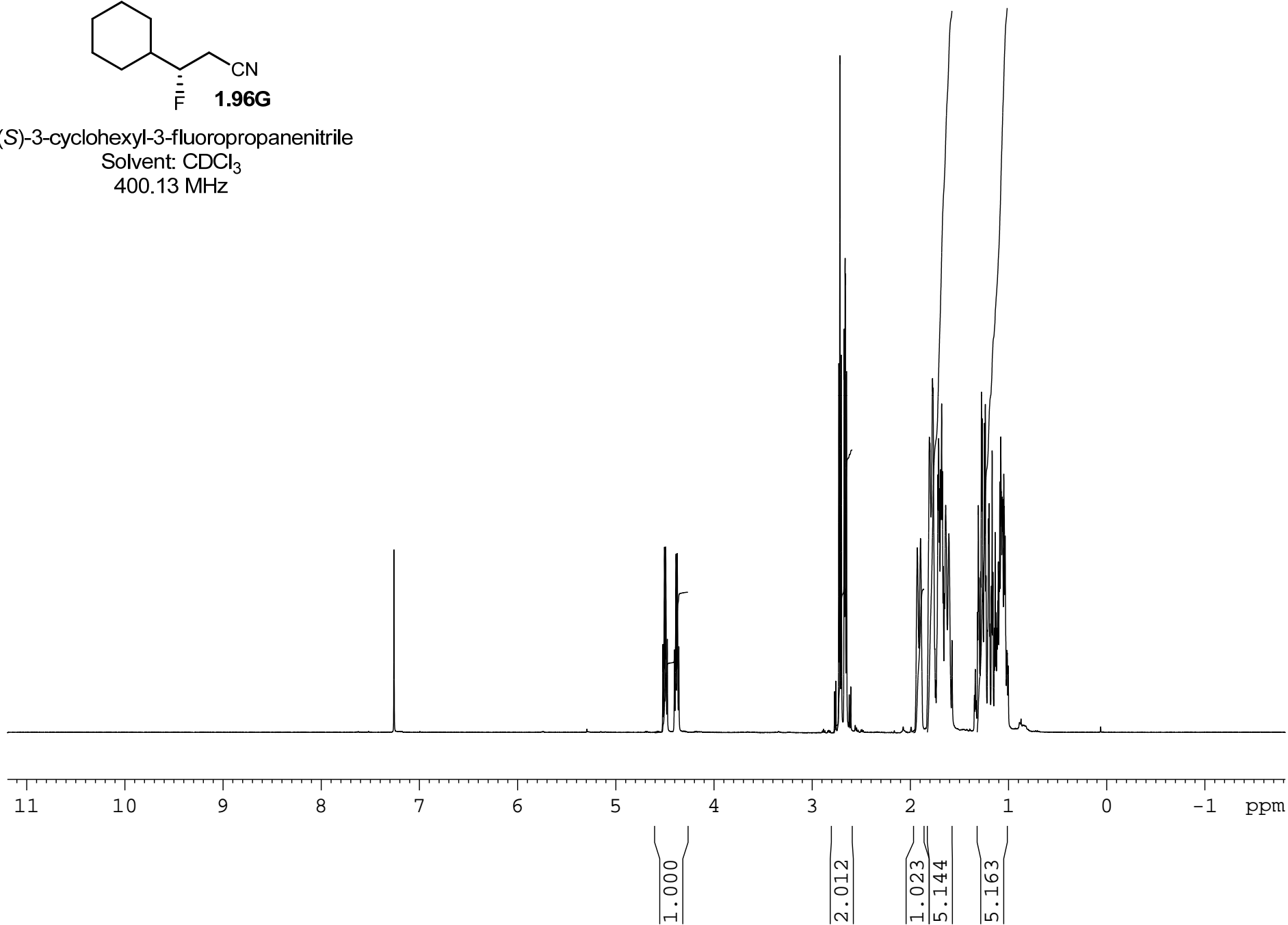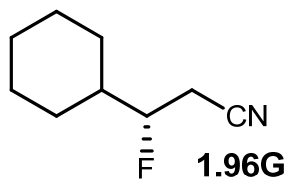
(S)-3-cyclohexyl-3-fluoropropanenitrile
Solvent: CDCl$_3$
100.6 MHz

116.473
116.419

93.068
91.282

41.402
41.215
28.257
28.201
27.478
27.429
26.050
25.676
25.414
21.916
21.659
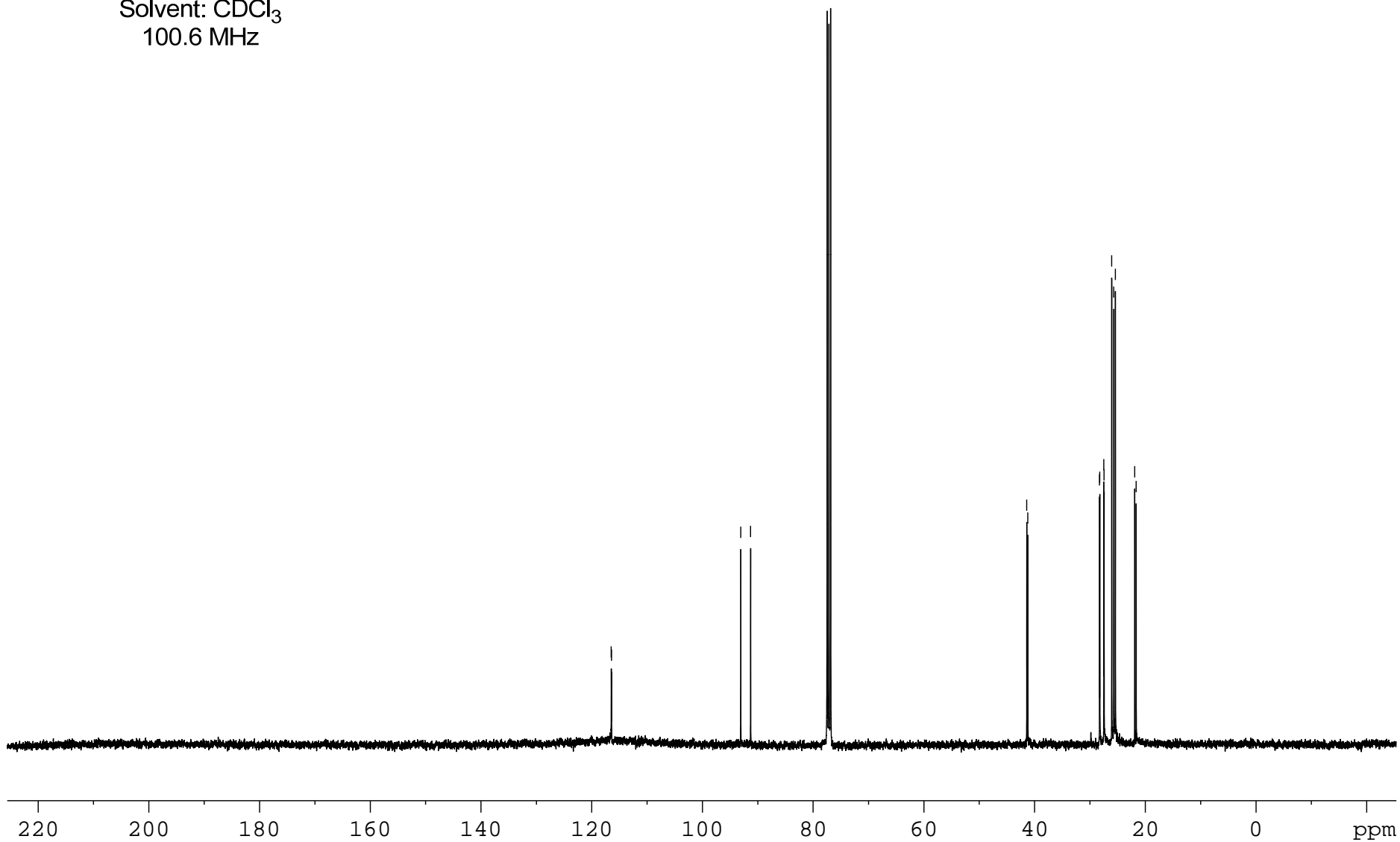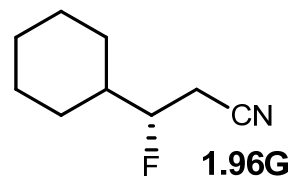
1.96G

220   200   180   160   140   120   100   80   60   40   20   0   ppm
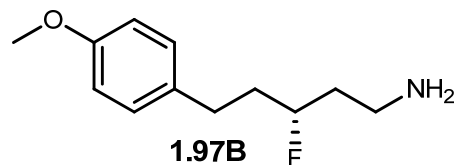
Elemental Composition Report

Page 1

Single Mass Analysis
Tolerance = 5.0 PPM / DBE: min = -0.5, max = 25.0
Element prediction: Off
Number of isotope peaks used for i-FIT = 2

Monoisotopic Mass, Even Electron Ions
11 formula(e) evaluated with 1 results within limits (up to 50 best isotopic matches for each mass)
Elements Used:
C: 5-500   H: 10-1000   N: 1-200   F: 1-1   Na: 1-1

MCO-IV-157

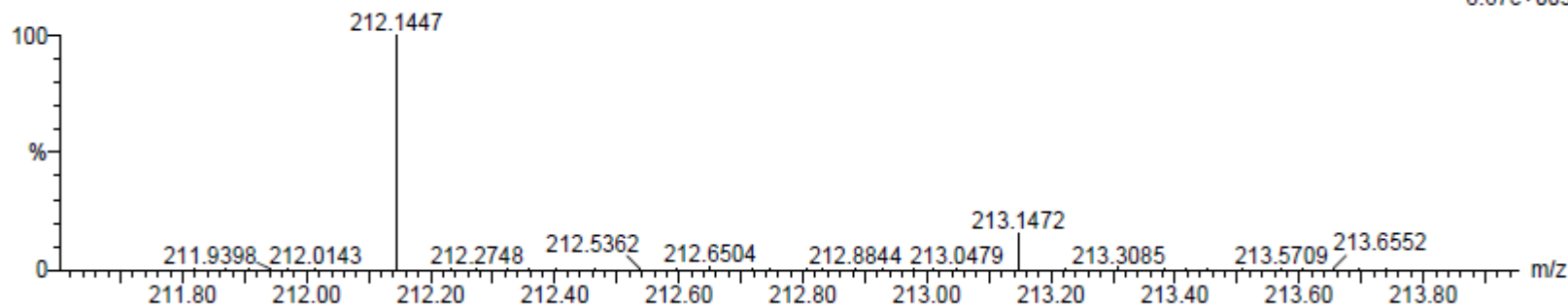06-Dec-2012
17:26:07
TOF MS ES+
6.22e+002

S/N: UH193
MCO-IV-157_120612_001 50 (0.935) AM (Cen,4, 80.00, Ar,8000.0,556.28,0.70); Sm (SG, 2x1.00); Cm (40:50)

178.1007

177.8138 177.9760 178.1997 178.3941 178.5717 178.7842 178.8669 179.1036 179.1602 179.3181 179.5867 179.7123

Minimum:			-0.5
Maximum:	5.0	5.0	25.0

Mass	Calc. Mass	mDa	PPM	DBE	i-FIT	Formula
178.1007	178.1008	-0.1	-0.6	2.5	0.4	C9 H14 N F Na
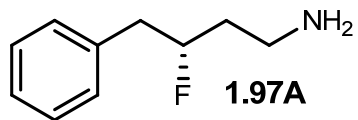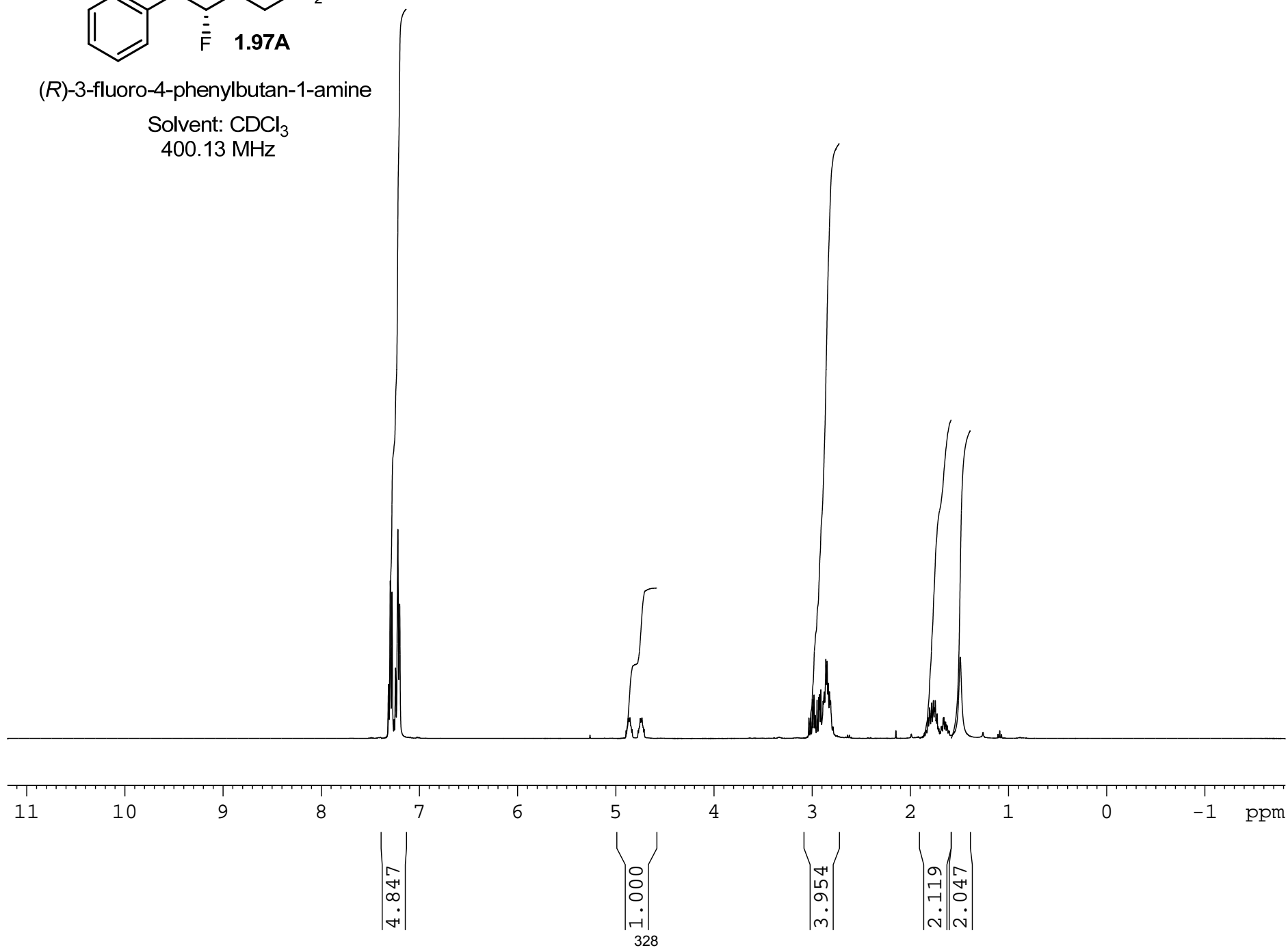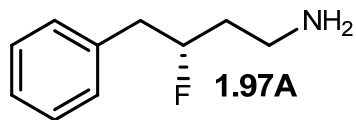
327

(R)-3-fluoro-4-phenylbutan-1-amine

Solvent: CDCl$_3$

400.13 MHz

4.847

1.000

328

3.954

2.119

2.047

(*R*)-3-fluoro-4-phenylbutan-1-amine

Solvent: CDCl₃
100.6 MHz

137.134
137.085
129.424
128.487
126.648

93.817
92.122

41.959
41.746
38.404
38.364
38.220

220   200   180   160   140   120   100   80   60   40   20   0   ppm

Elemental Composition Report

Page 1

Single Mass Analysis

Tolerance = 5.0 PPM / DBE: min = -0.5, max = 25.0
Element prediction: Off
Number of isotope peaks used for i-FIT = 2
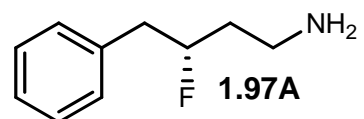
Monoisotopic Mass, Even Electron Ions
9 formula(e) evaluated with 1 results within limits (up to 50 best isotopic matches for each mass)
Elements Used:
C: 10-500   H: 10-1000   N: 1-200   F: 1-1

MCO-IV-169

07-Dec-2012
10:37:01
TOF MS ES+
8.83e+003

S/N: UH193

MCO-IV-169_120712_001 93 (1.733) AM (Cen,4, 80.00, Ar,8000.0,556.28,0.70); Sm (SG, 2x1.00); Cm (90:100)
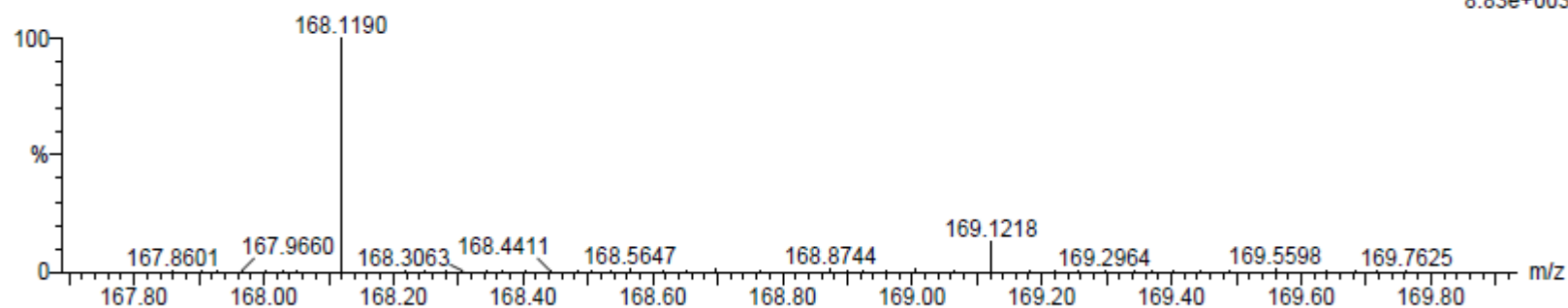
| Minimum: | | | -0.5 | | |
| Maximum: | 5.0 | 5.0 | 25.0 | | |

Mass	Calc. Mass	mDa	PPM	DBE	i-FIT	Formula
168.1190	168.1189	0.1	0.6	3.5	6.2	C10 H15 N F
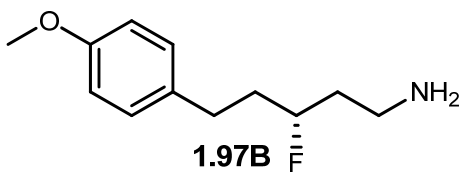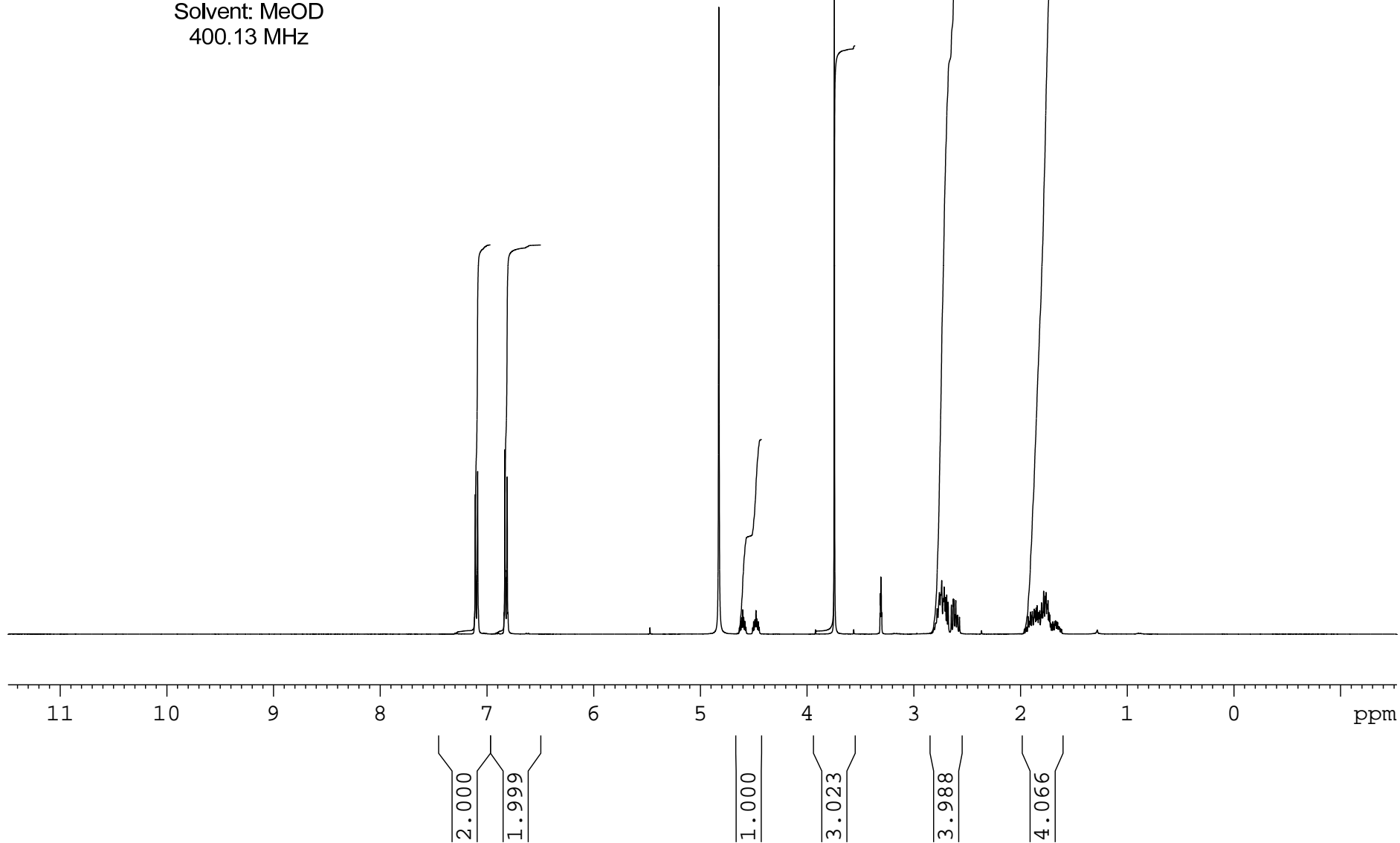
330

1.97B

(*R*)-3-fluoro-5-(4-methoxyphenyl)pentan-1-amine
Solvent: MeOD
400.13 MHz

2.000 1.999 1.000 3.023 3.988 4.066

11 10 9 8 7 6 5 4 3 2 1 0 ppm

1.97B

(*R*)-3-fluoro-5-(4-methoxyphenyl)pentan-1-amine
Solvent: MeOD
100.6 MHz

159.424
134.762
130.335
114.873
93.837
92.180
55.635
39.223
39.021
38.928
38.886
38.709
38.502
31.418
31.372

220   200   180   160   140   120   100   80   60   40   20   0   ppm

Elemental Composition Report

Page 1

Single Mass Analysis

Tolerance = 5.0 PPM   /   DBE: min = -0.5, max = 25.0
Element prediction: Off
Number of isotope peaks used for i-FIT = 2

Monoisotopic Mass, Even Electron Ions
70 formula(e) evaluated with 1 results within limits (up to 50 best isotopic matches for each mass)
Elements Used:
C: 10-500   H: 10-1000   N: 1-200   O: 1-200   F: 1-1

MCO-IV-159

07-Dec-2012
09:08:00
TOF MS ES+
8.67e+003
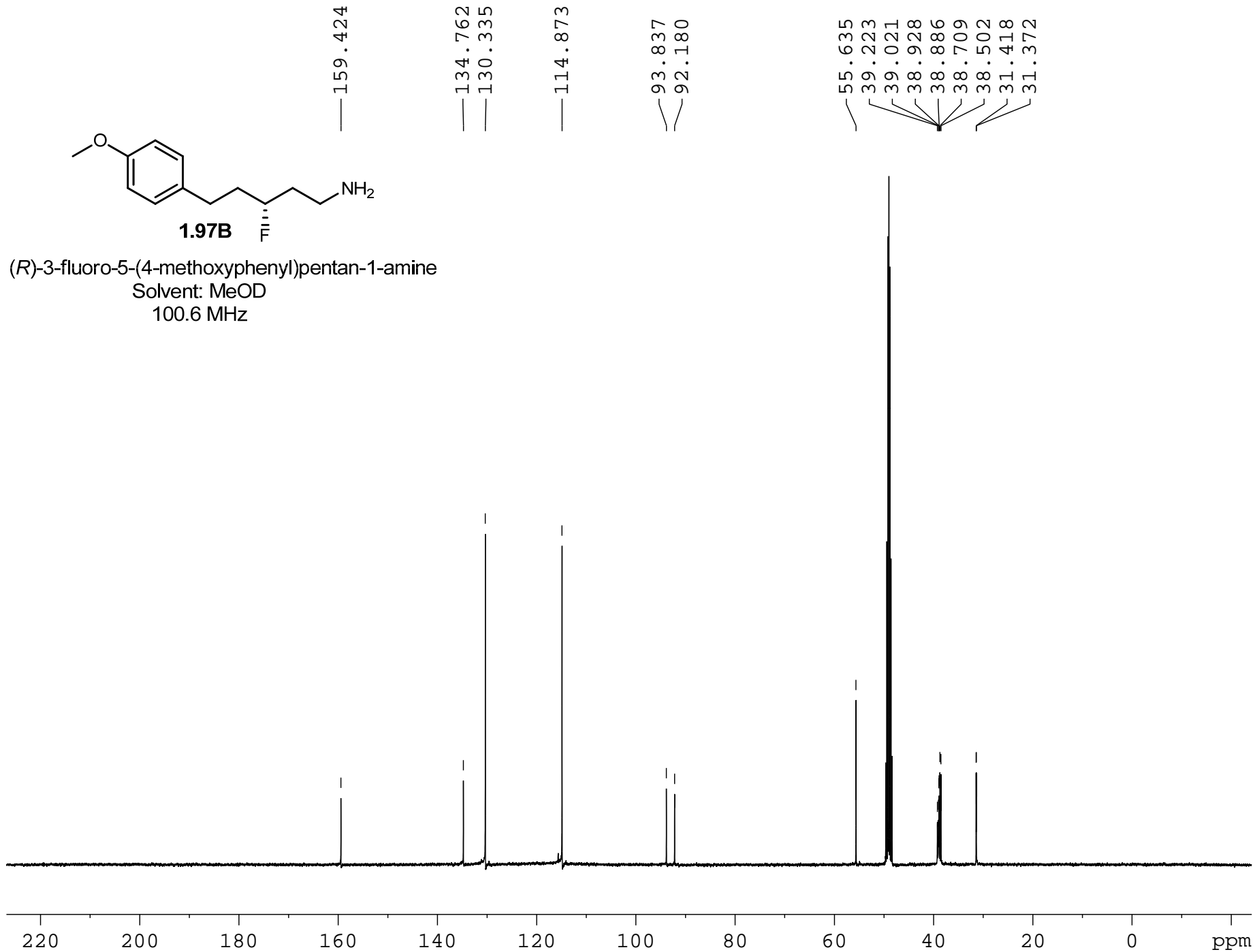
S/N: UH193
MCO-IV-159_120712_001 58 (1.083) AM (Cen,4, 80.00, Ar,8000.0,556.28,0.70); Sm (SG, 2x1.00); Cm (50:60)

1.97B

212.1447

213.1472

211.9398 212.0143   212.2748   212.5362   212.6504   212.8844 213.0479   213.3085   213.5709 213.6552

211.80   212.00   212.20   212.40   212.60   212.80   213.00   213.20   213.40   213.60   213.80

Minimum:				-0.5		
Maximum:		5.0	5.0	25.0		

Mass	Calc. Mass	mDa	PPM	DBE	i-FIT	Formula
212.1447	212.1451	-0.4	-1.9	3.5	5.5	C12 H19 N O F
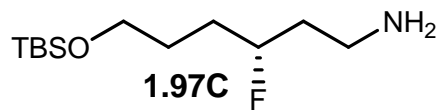
333

(*R*)-6-((*tert*-butyldimethylsilyl)oxy)-3-fluorohexan-1-amine

Solvent: MeOD

400.13 MHz

1.026 2.127 2.000 6.401 8.149 5.267

334

(R)-6-((tert-butyldimethylsilyl)oxy)-3-fluorohexan-1-amine
Solvent: MeOD
100.6 MHz

1.97C
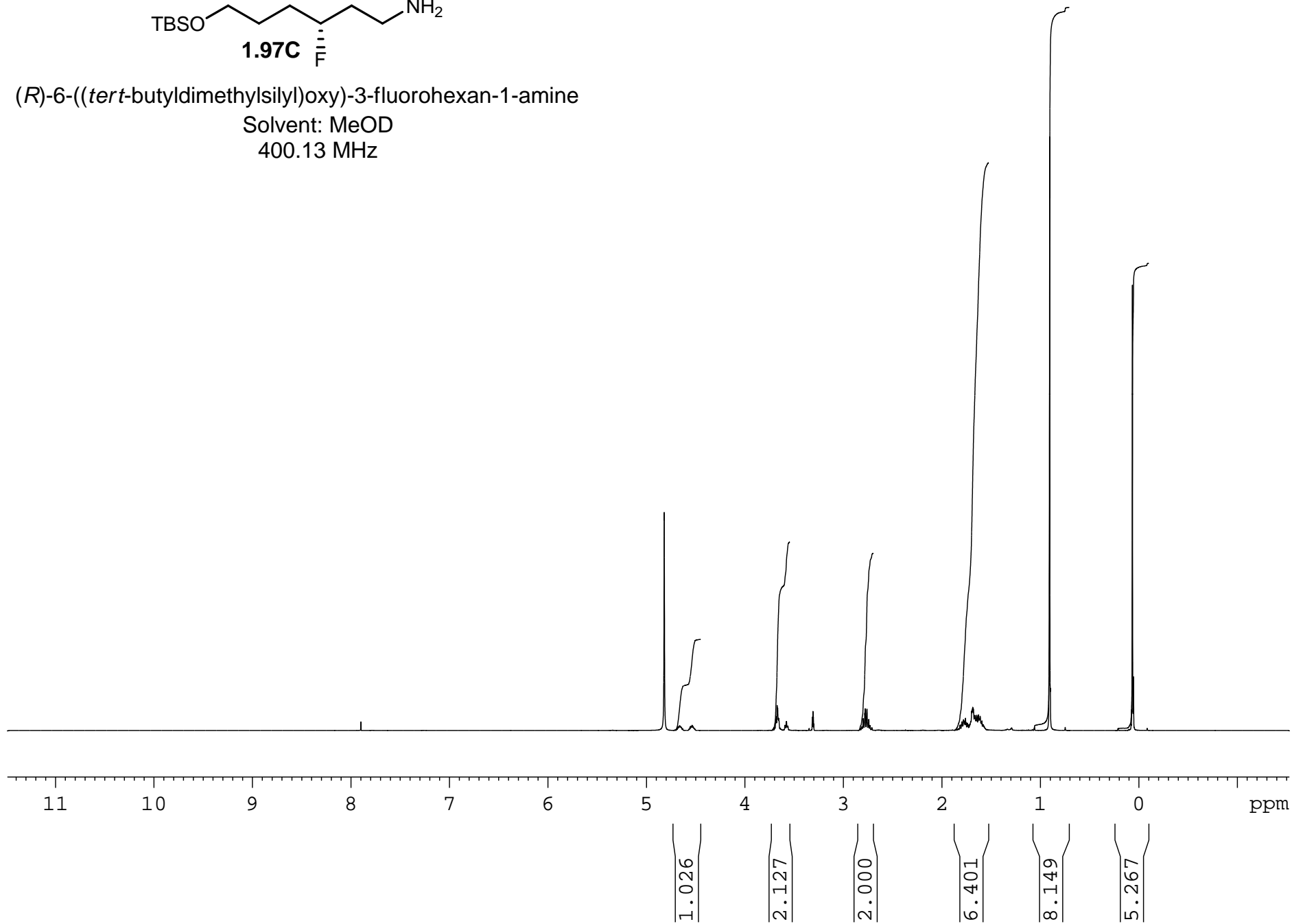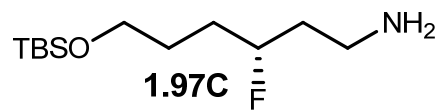
Peaks: 94.555, 92.901, 63.880, 39.369, 39.164, 38.972, 38.928, 33.071, 32.861, 29.509, 29.468, 26.413, 19.132, −5.184
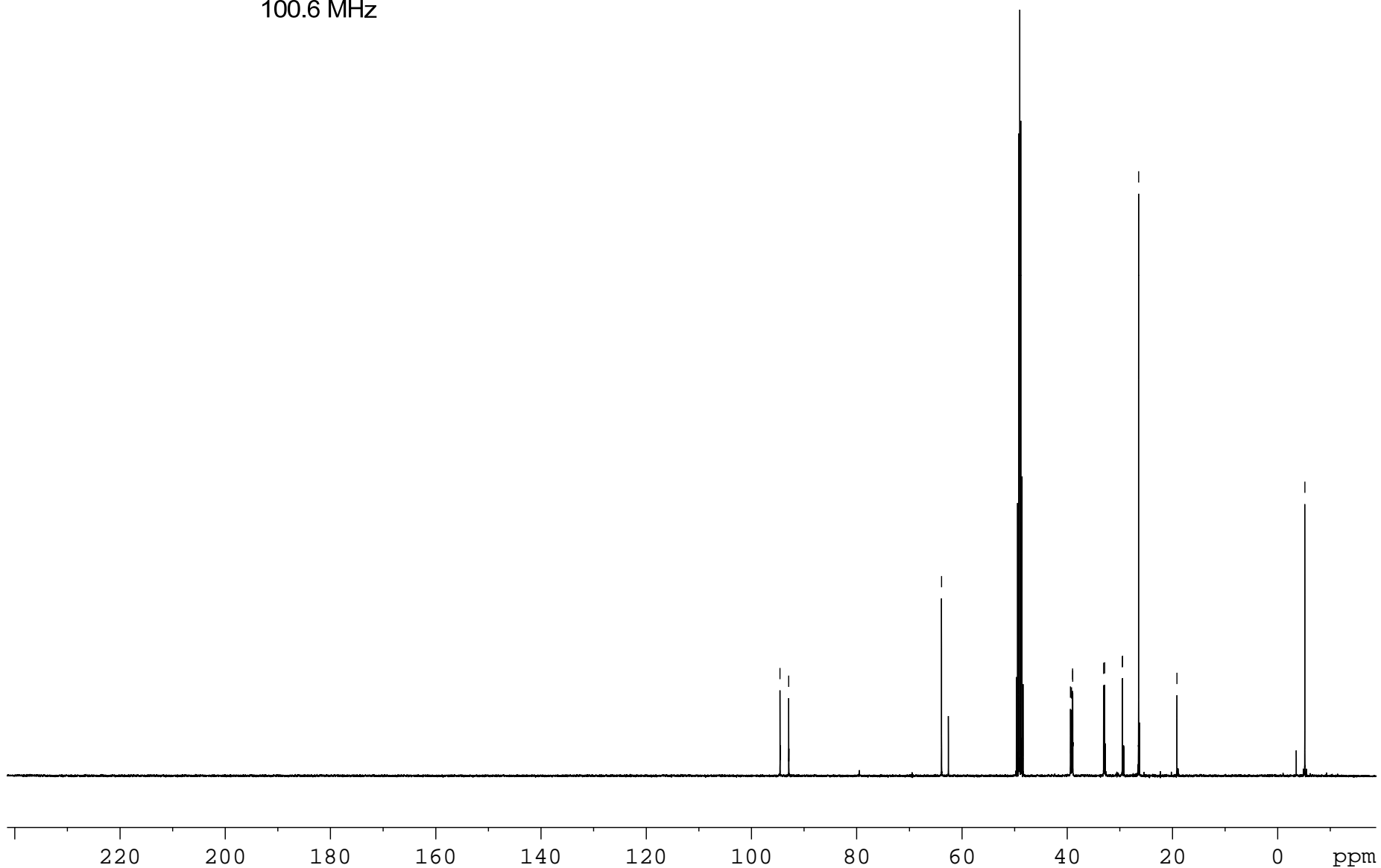
Elemental Composition Report
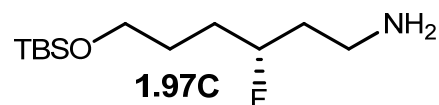
TBSO ⌁⌁⌁ NH₂

1.97C F

Page 1

Single Mass Analysis

Tolerance = 5.0 PPM / DBE: min = -0.5, max = 25.0
Element prediction: Off
Number of isotope peaks used for i-FIT = 2

Monoisotopic Mass, Even Electron Ions
80 formula(e) evaluated with 1 results within limits (up to 50 best isotopic matches for each mass)
Elements Used:
C: 10-500 H: 10-1000 N: 1-200 O: 1-200 F: 1-1 Si: 1-1

MCO-IV-172

07-Dec-2012
11:26:36

S/N: UH193
MCO-IV-172_120712_001 98 (1.825) AM (Cen,4, 80.00, Ar,8000.0,556.28,0.70); Sm (SG, 2x1.00); Cm (90:100)

TOF MS ES+
8.71e+003
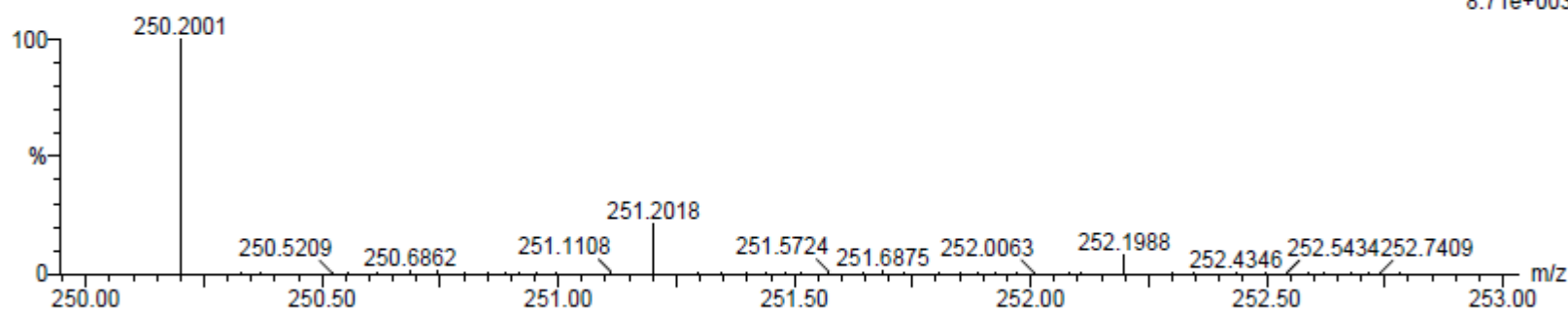
Mass	Calc. Mass	mDa	PPM	DBE	i-FIT	Formula
250.2001	250.2002	-0.1	-0.4	-0.5	7.0	C12 H29 N O F Si
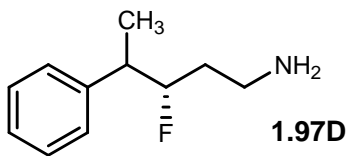
336

(3*S*)-3-fluoro-4-phenylpentan-1-amine
Diastereomer A
Solvent: MeOD
400.13 MHz

1.97D

2.118
3.136

1.134

1.097
1.920

2.163
3.221

11 10 9 8 7 6 5 4 3 2 1 0 ppm

337
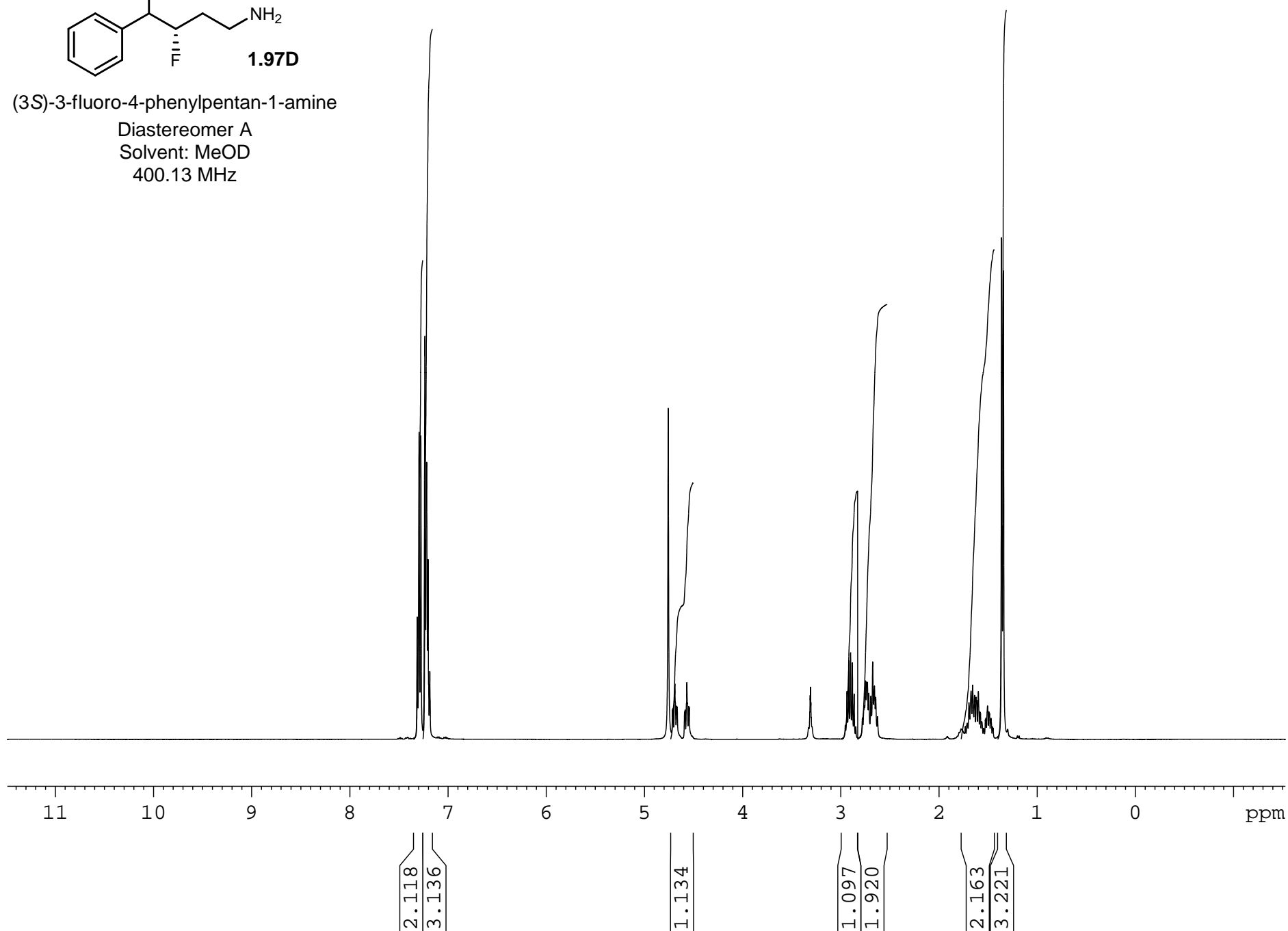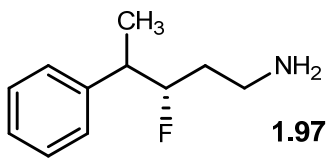
(3S)-3-fluoro-4-phenylpentan-1-amine

Diastereomer A
Solvent: MeOD
100.6 MHz

1.97D

144.515
144.447
129.635
128.888
127.796
98.198
96.477
46.288
46.085
39.113
39.079
37.415
37.209
17.699
17.645
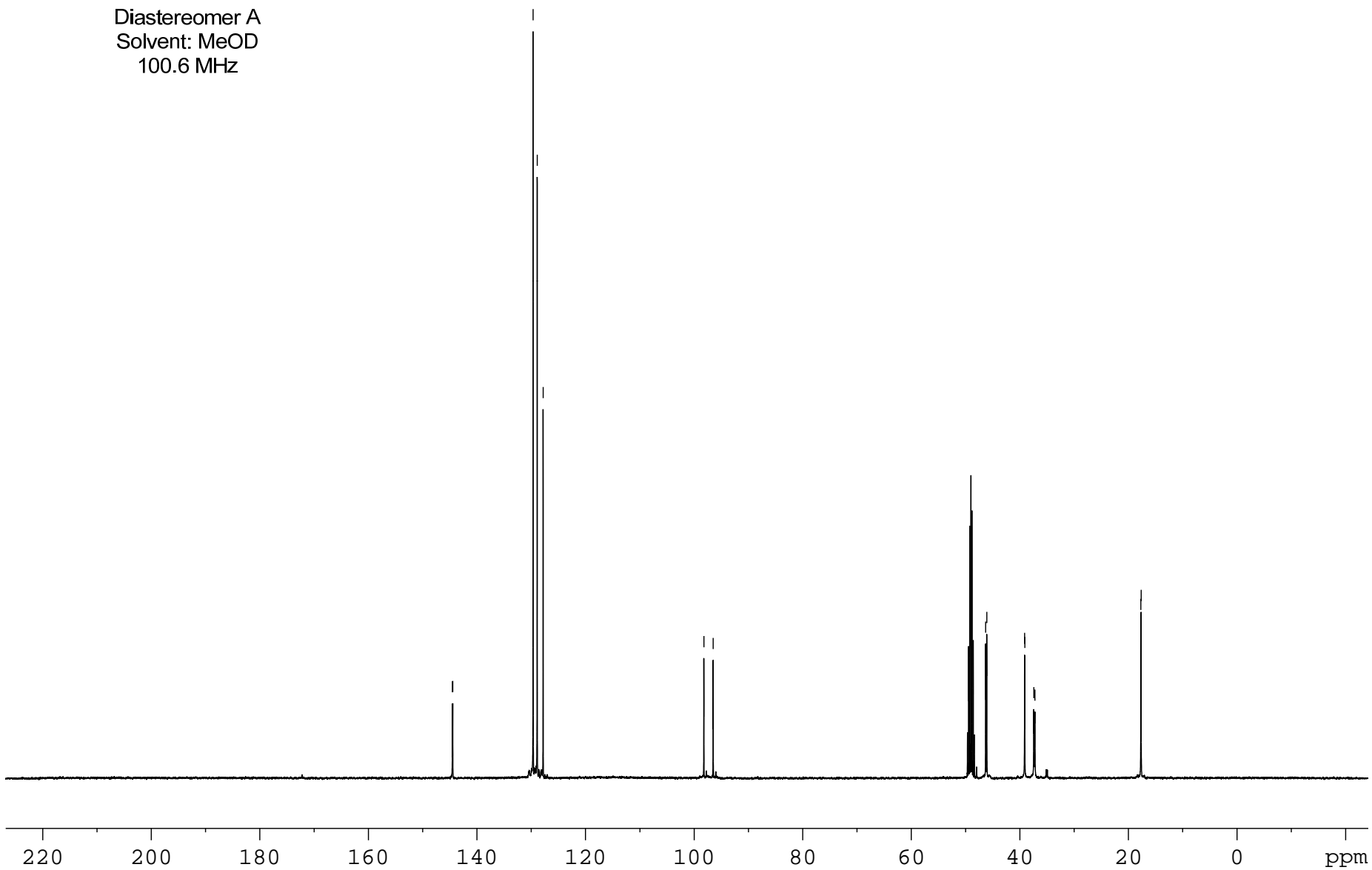
220   200   180   160   140   120   100   80   60   40   20   0   ppm

Elemental Composition Report

Page 1

Single Mass Analysis

Tolerance = 5.0 PPM / DBE: min = -0.5, max = 25.0
Element prediction: Off
Number of isotope peaks used for i-FIT = 2
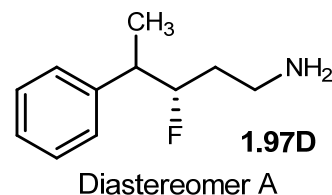
Monoisotopic Mass, Even Electron Ions
11 formula(e) evaluated with 1 results within limits (up to 50 best isotopic matches for each mass)
Elements Used:
C: 10-500   H: 10-1000   N: 1-200   F: 1-1

MCO-IV-163

07-Dec-2012
10:01:45
TOF MS ES+
9.07e+003

S/N: UH193
MCO-IV-163_120712_001 59 (1.102) AM (Cen,4, 80.00, Ar,8000.0,556.28,0.70); Sm (SG, 2x1.00); Cm (50:60)

1.97D
Diastereomer A
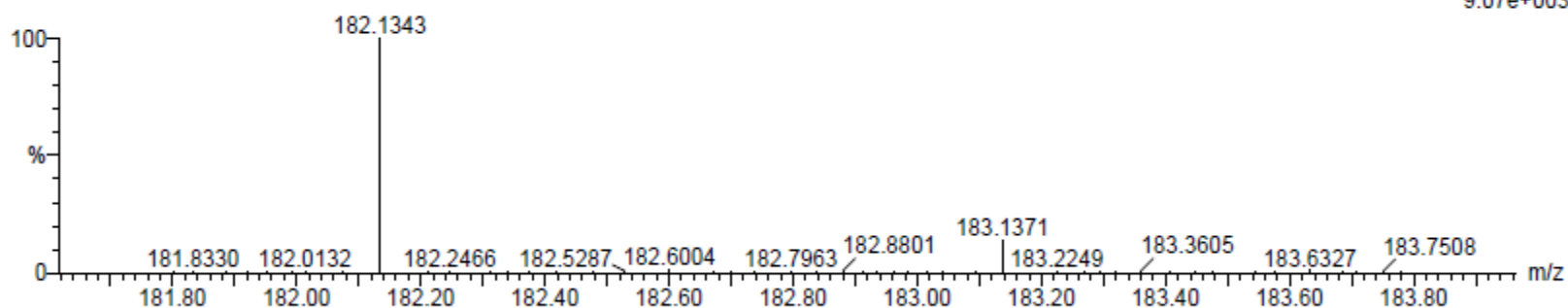
Minimum:			-0.5		
Maximum:	5.0	5.0	25.0		

Mass	Calc. Mass	mDa	PPM	DBE	i-FIT	Formula
182.1343	182.1345	-0.2	-1.1	3.5	1.5	C11 H17 N F
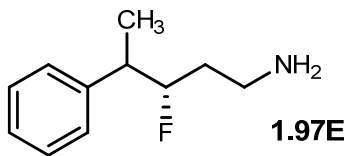
339

(3*S*)-3-fluoro-4-phenylpentan-1-amine

Diastereomer B
Solvent: MeOD
400.13 MHz

1.97E

CH₃

NH₂

F

11   10   9   8   7   6   5   4   3   2   1   0   ppm

5.207   1.073   1.068   1.950   2.051   3.128
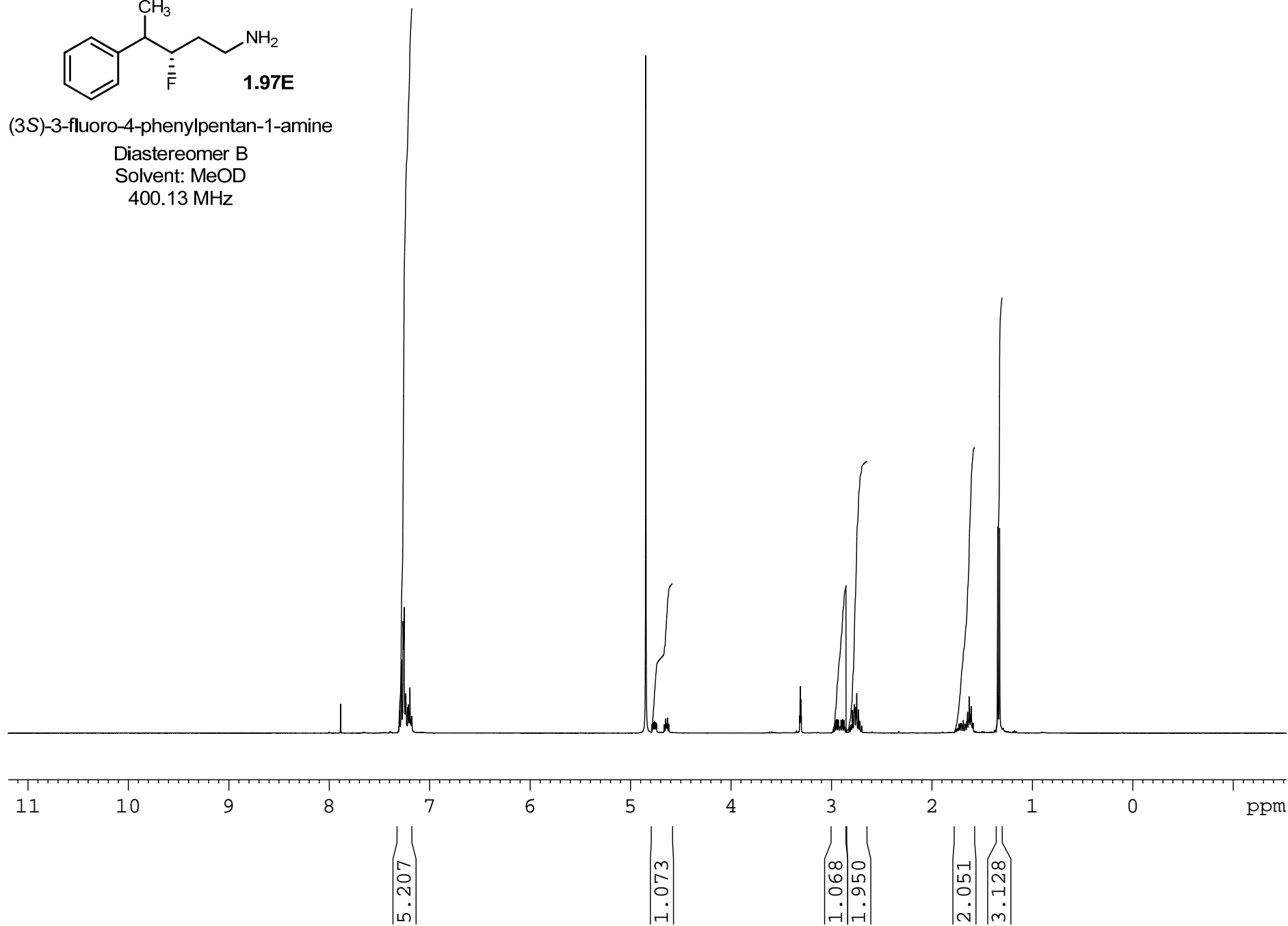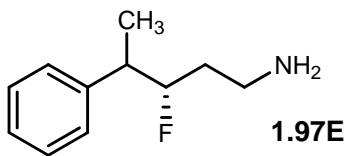
(3*S*)-3-fluoro-4-phenylpentan-1-amine

Diastereomer B
Solvent: MeOD
100.6 MHz

143.633
143.611
129.375
129.278
127.618
97.667
95.949
45.703
45.506
39.001
38.961
36.555
36.348
17.987
17.930
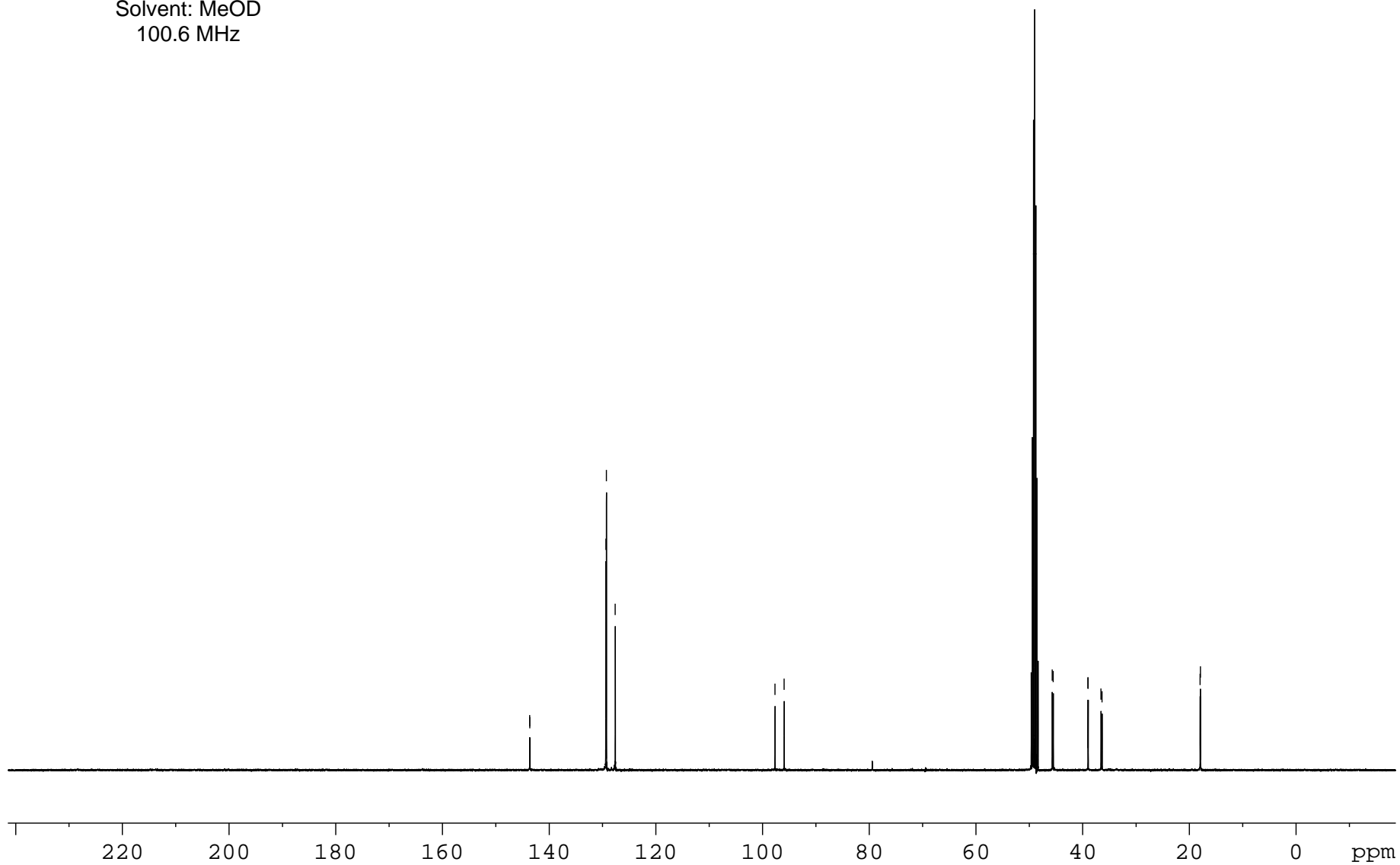
1.97E

CH₃

NH₂

F

220   200   180   160   140   120   100   80   60   40   20   0   ppm

341

Elemental Composition Report

Page 1

Single Mass Analysis
Tolerance = 5.0 PPM   /   DBE: min = -0.5, max = 25.0
Element prediction: Off
Number of isotope peaks used for i-FIT = 2
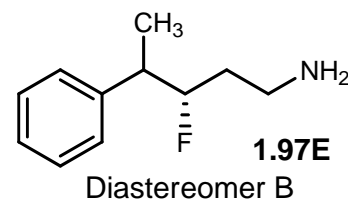
Monoisotopic Mass, Even Electron Ions
11 formula(e) evaluated with 1 results within limits (up to 50 best isotopic matches for each mass)
Elements Used:
C: 10-500   H: 10-1000   N: 1-200   F: 1-1

07-Dec-2012
10:45:32
S/N: UH193
MCO-IV-170_120712_001 60 (1.120) AM (Cen,4, 80.00, Ar,8000.0,556.28,0.70); Sm (SG, 2x1.00); Cm (60:70)
TOF MS ES+
9.08e+003

Structure label: **1.97E** Diastereomer B
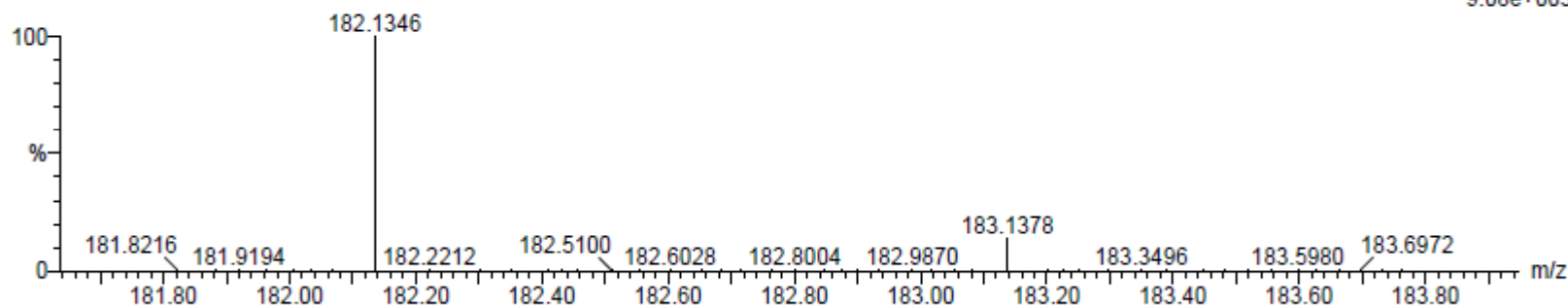
Minimum:				-0.5		
Maximum:		5.0	5.0	25.0		

Mass	Calc. Mass	mDa	PPM	DBE	i-FIT	Formula
182.1346	182.1345	0.1	0.5	3.5	3.1	C11 H17 N F
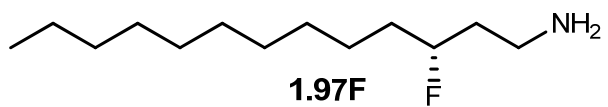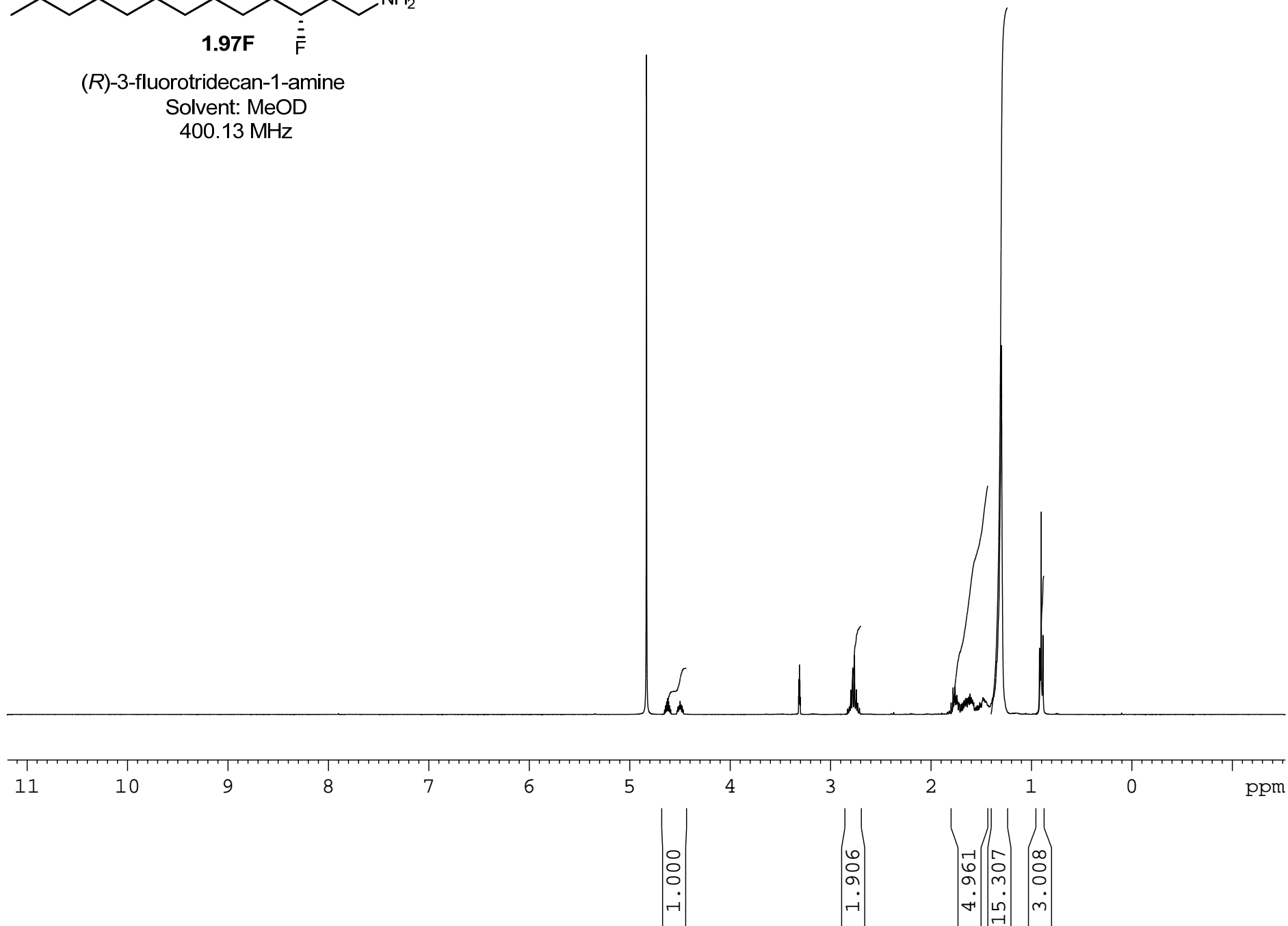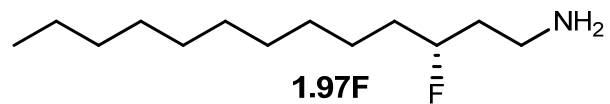
342

1.97F

(*R*)-3-fluorotridecan-1-amine
Solvent: MeOD
400.13 MHz

1.000   1.906   4.961   15.307   3.008

1.97F

F

(*R*)-3-fluorotridecan-1-amine
Solvent: MeOD
100.6 MHz

94.630
92.976

39.248
39.043
38.968
38.924
36.627
36.421
33.085
30.752
30.727
30.704
30.618
30.486
26.241
26.195
23.749
14.469

220   200   180   160   140   120   100   80   60   40   20   0   ppm

344

Elemental Composition Report

Page 1
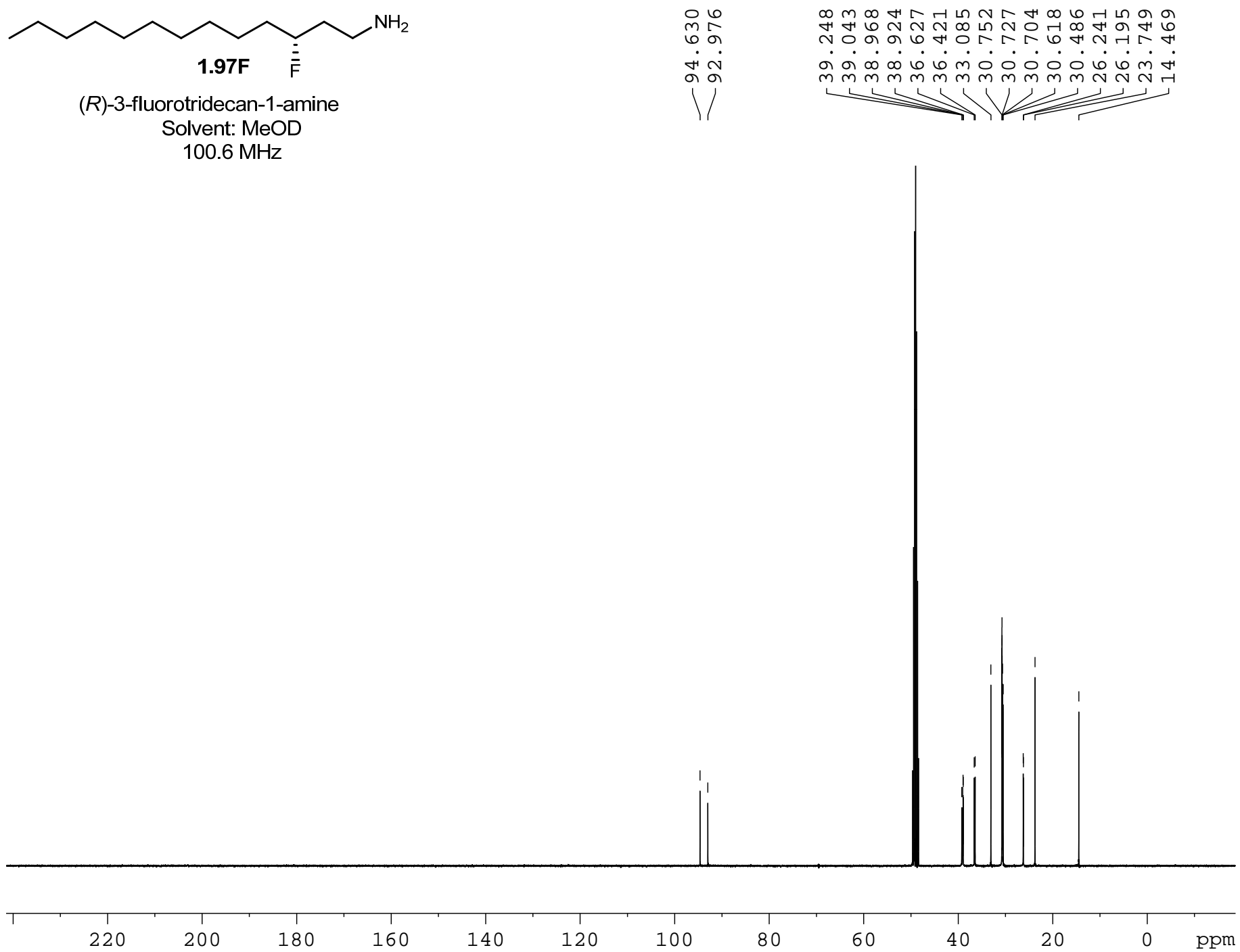
Single Mass Analysis

Tolerance = 5.0 PPM / DBE: min = -0.5, max = 25.0
Element prediction: Off
Number of isotope peaks used for i-FIT = 2

Monoisotopic Mass, Even Electron Ions
19 formula(e) evaluated with 1 results within limits (up to 50 best isotopic matches for each mass)
Elements Used:
C: 10-500   H: 10-1000   N: 1-200   F: 1-1

MCO-IV-158

1.97F
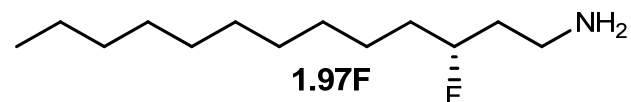
S/N: UH193

06-Dec-2012
17:50:51
MCO-IV-158_120612_001 74 (1.380) AM (Cen,4, 80.00, Ar,8000.0,556.28,0.70); Sm (SG, 2x1.00); Cm (70:80)
TOF MS ES+
8.10e+003
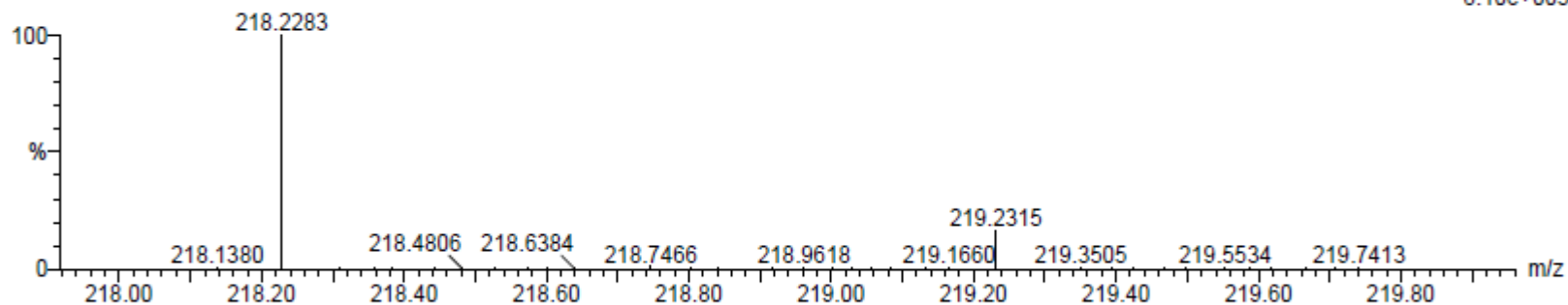
Minimum:				-0.5		
Maximum:		5.0	5.0	25.0		
Mass	Calc. Mass	mDa	PPM	DBE	i-FIT	Formula
218.2283	218.2284	-0.1	-0.5	-0.5	2.1	C13 H29 N F
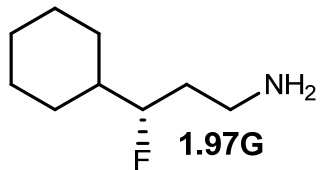
345

(*S*)-3-cyclohexyl-3-fluoropropan-1-amine
Solvent: MeOD
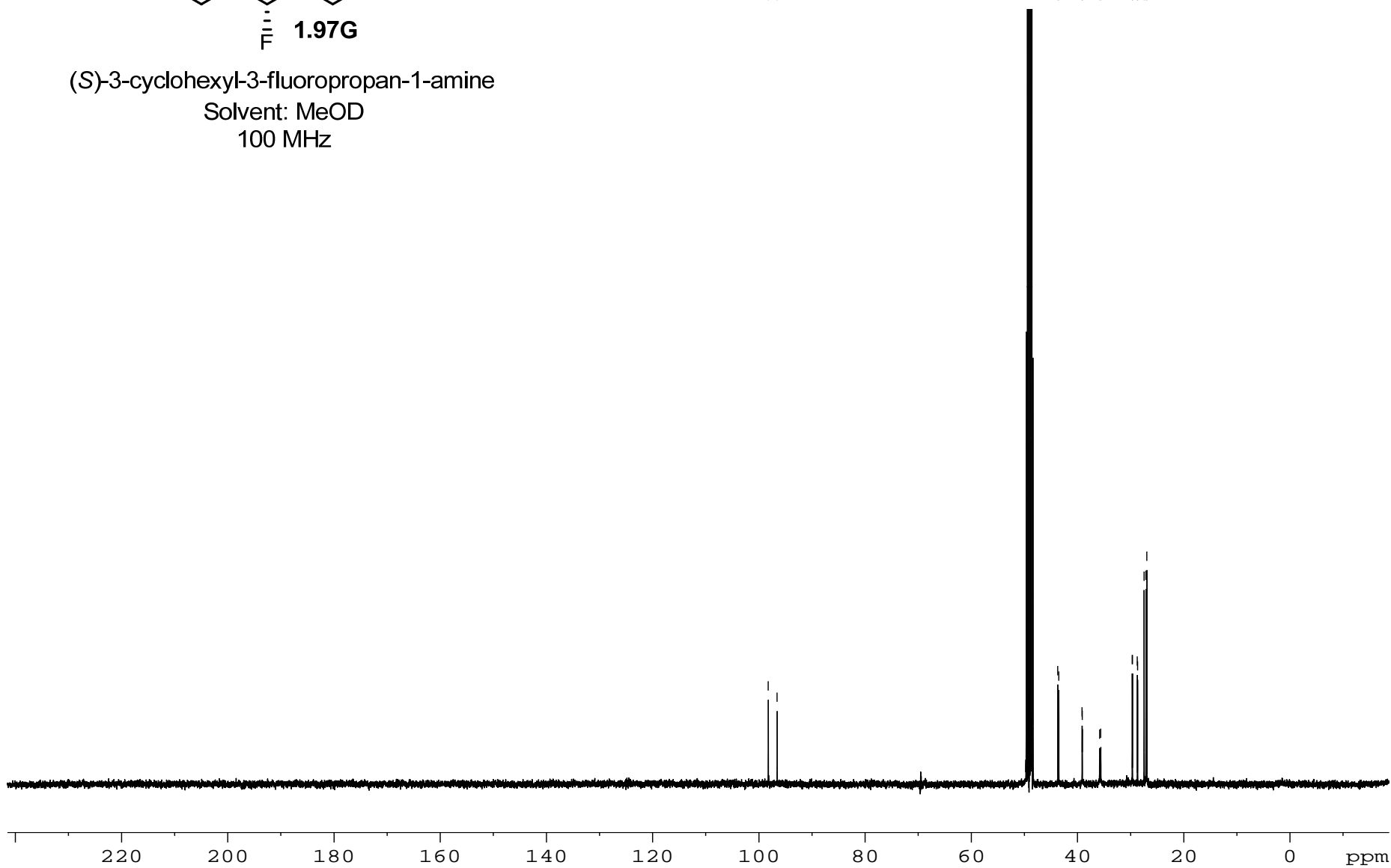400.13 MHz

0.883   1.729   0.955   5.486   1.000   5.344
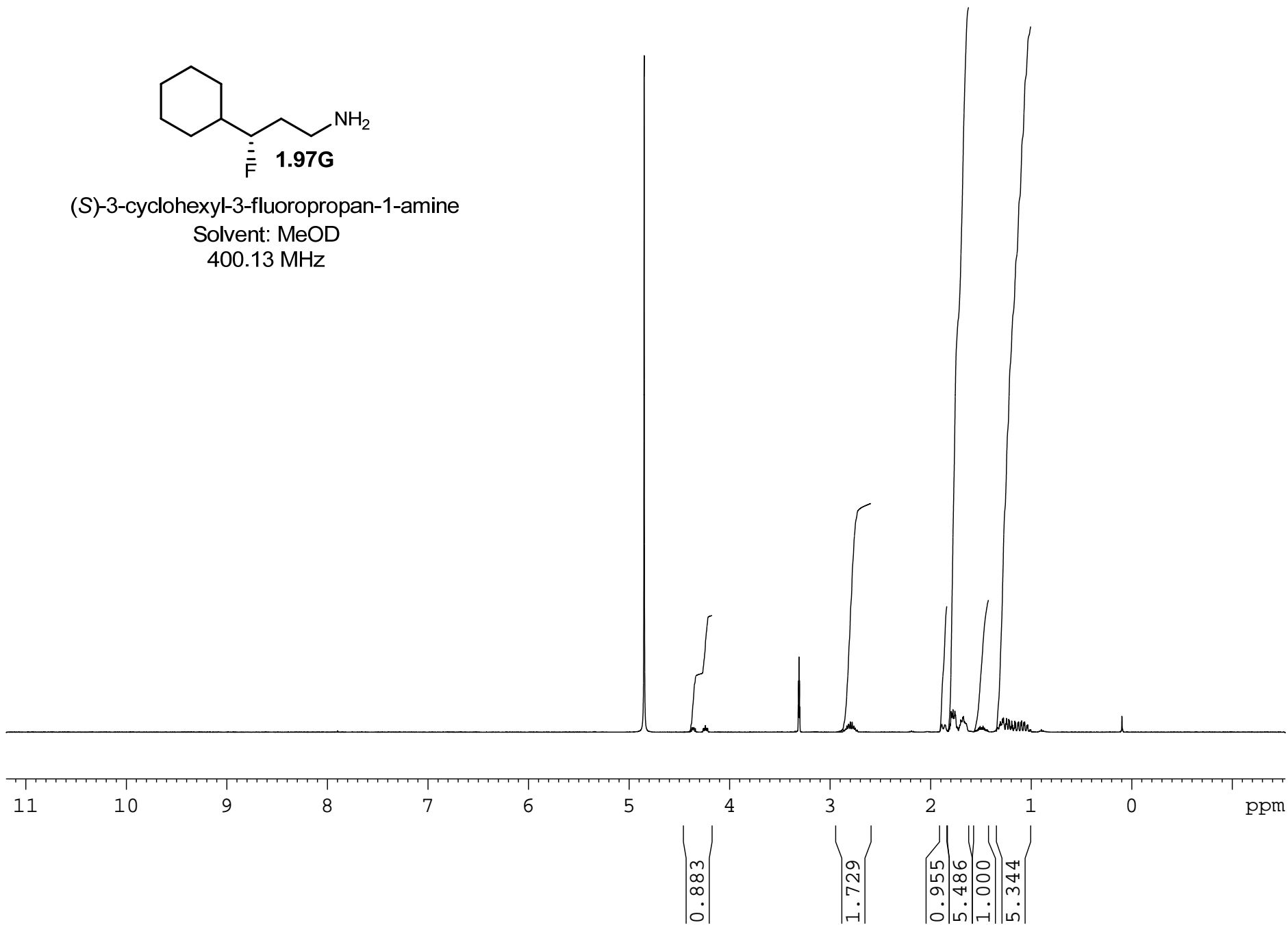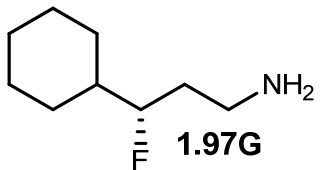
(S)-3-cyclohexyl-3-fluoropropan-1-amine
Solvent: MeOD
100 MHz

98.230
96.553

43.704
43.513
39.118
39.079
35.838
35.627
29.704
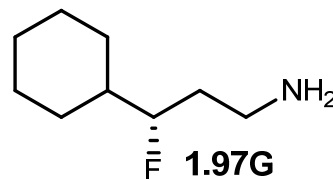29.652
28.745
28.688
27.470
27.116
26.935

1.97G

347

Elemental Composition Report

Single Mass Analysis
Tolerance = 5.0 PPM / DBE: min = -0.5, max = 25.0
Element prediction: Off
Number of isotope peaks used for i-FIT = 2

Monoisotopic Mass, Even Electron Ions
10 formula(e) evaluated with 1 results within limits (up to 50 best isotopic matches for each mass)
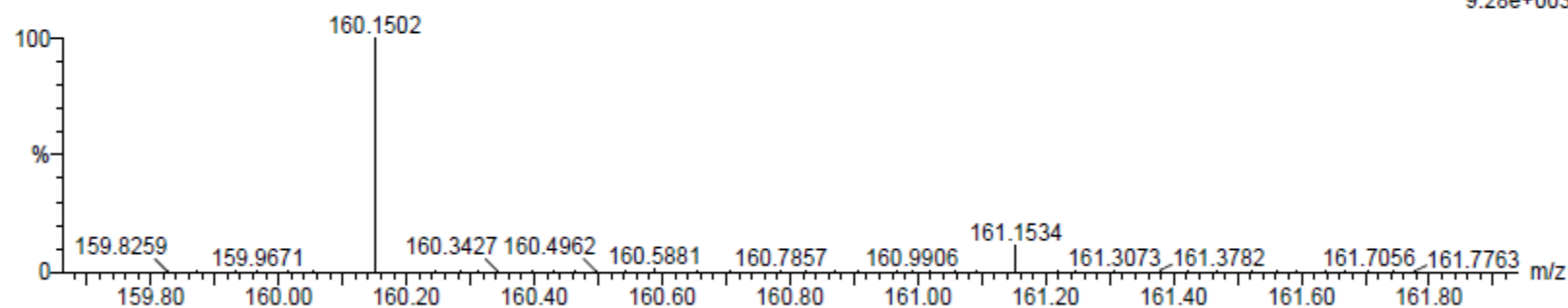Elements Used:
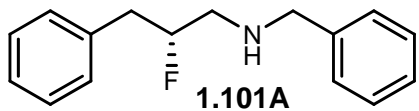C: 8-500   H: 10-1000   N: 1-200   F: 1-1

MCO-IV-162

07-Dec-2012
09:51:53
TOF MS ES+
9.28e+003

S/N: UH193

MCO-IV-162_120712_001 70 (1.306) AM (Cen,4, 80.00, Ar,8000.0,556.28,0.70); Sm (SG, 2x1.00); Cm (60:70)

Minimum:				-0.5		
Maximum:		5.0	5.0	25.0		

Mass	Calc. Mass	mDa	PPM	DBE	i-FIT	Formula
160.1502	160.1502	0.0	0.0	0.5	3.2	C9 H19 N F
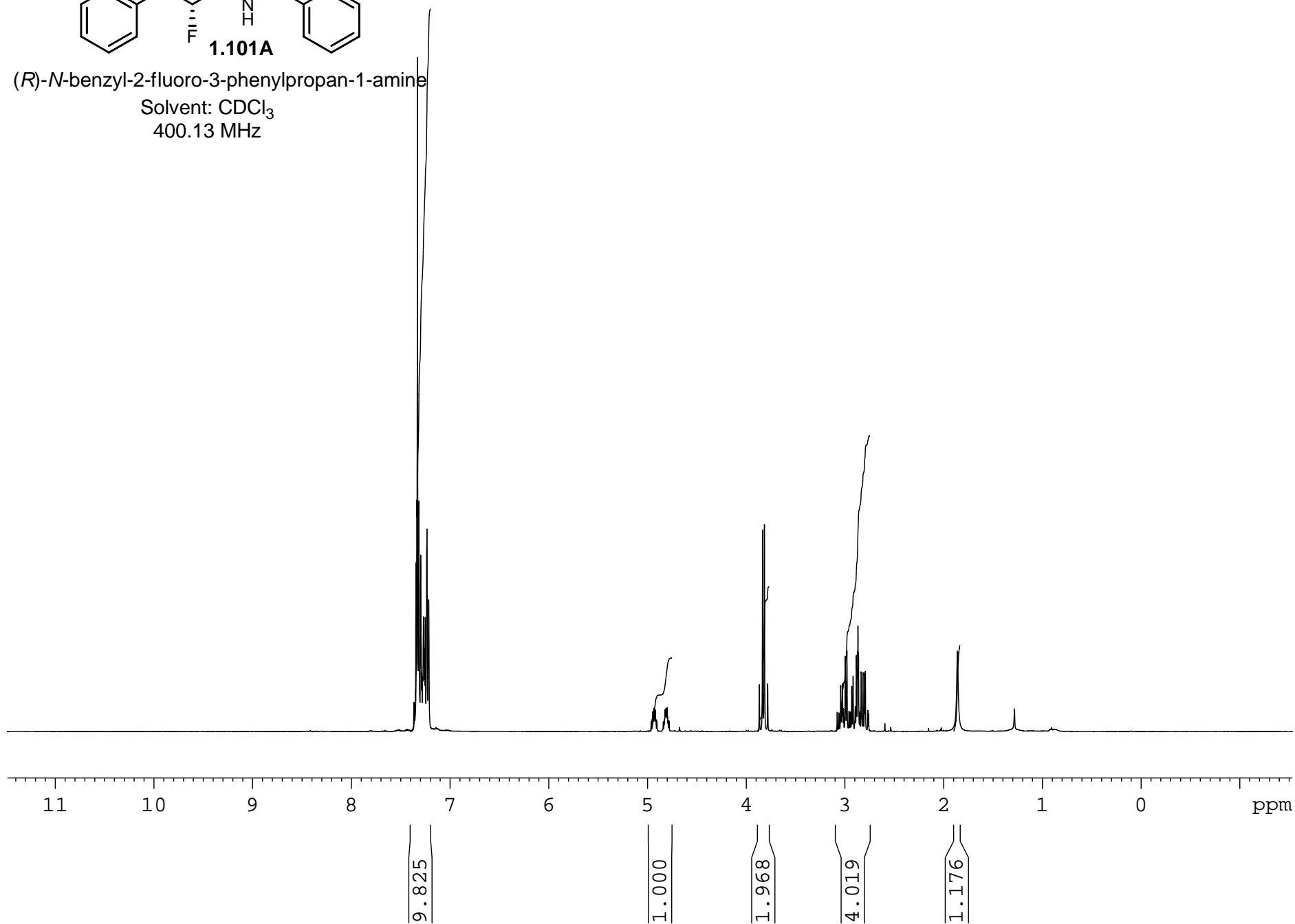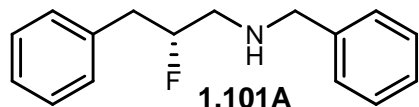
348

(*R*)-*N*-benzyl-2-fluoro-3-phenylpropan-1-amine
Solvent: CDCl$_3$
400.13 MHz

1.101A

9.825   1.000   1.968   4.019   1.176

11   10   9   8   7   6   5   4   3   2   1   0   ppm

1.101A

(*R*)-*N*-benzyl-2-fluoro-3-phenylpropan-1-amine
Solvent: CDCl$_3$
100.6 MHz

140.085
136.987
136.933
129.396
128.552
128.498
128.177
127.102
126.695

94.918
93.216

53.831
52.484
52.276
39.554
39.343

220 200 180 160 140 120 100 80 60 40 20 0 ppm

350
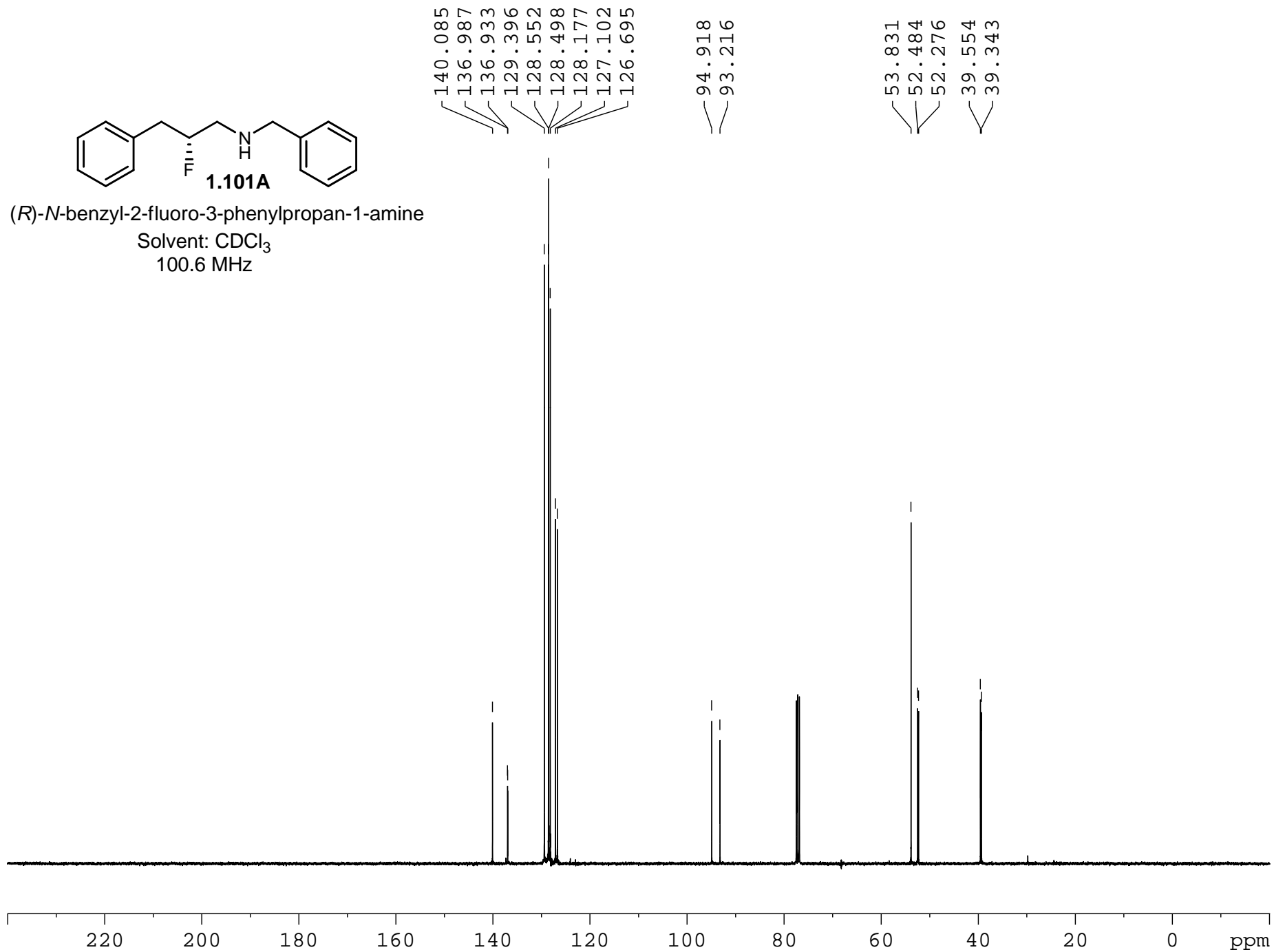
Elemental Composition Report

Page 1

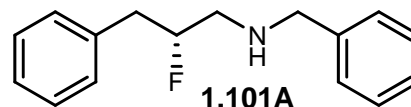## Single Mass Analysis
Tolerance = 5.0 PPM   /   DBE: min = -0.5, max = 25.0
Element prediction: Off
Number of isotope peaks used for i-FIT = 2

Monoisotopic Mass, Even Electron Ions
25 formula(e) evaluated with 1 results within limits (up to 50 best isotopic matches for each mass)
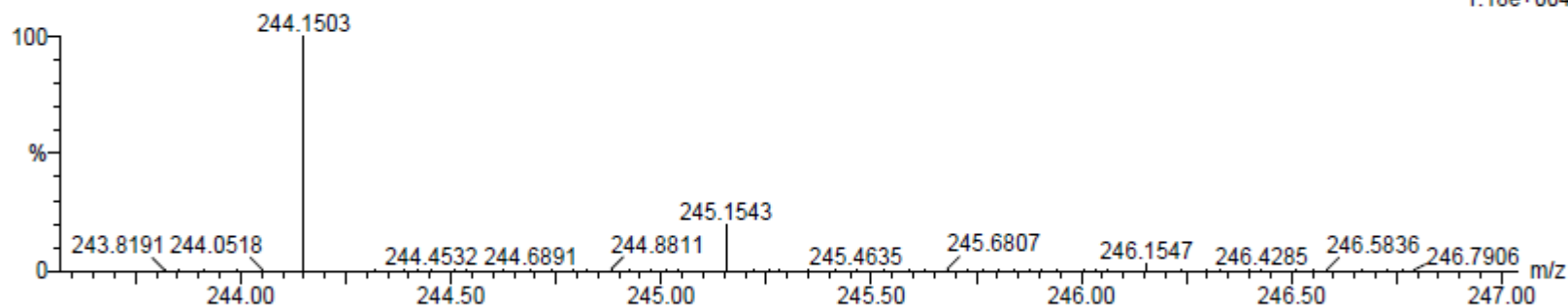Elements Used:
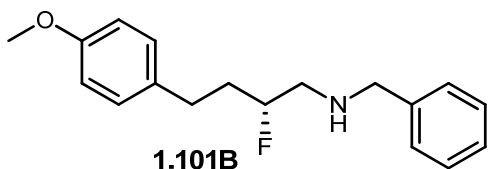C: 10-500   H: 10-1000   N: 1-200   F: 1-1

MCO-V-20

1.101A

07-Dec-2012
12:03:38

S/N: UH193

MCO-V-20_120712_001 50 (0.935) AM (Cen,4, 80.00, Ar,8000.0,556.28,0.70); Sm (SG, 2x1.00); Cm (50:60)

TOF MS ES+
1.18e+004

Minimum:				-0.5		
Maximum:		5.0	5.0	25.0		

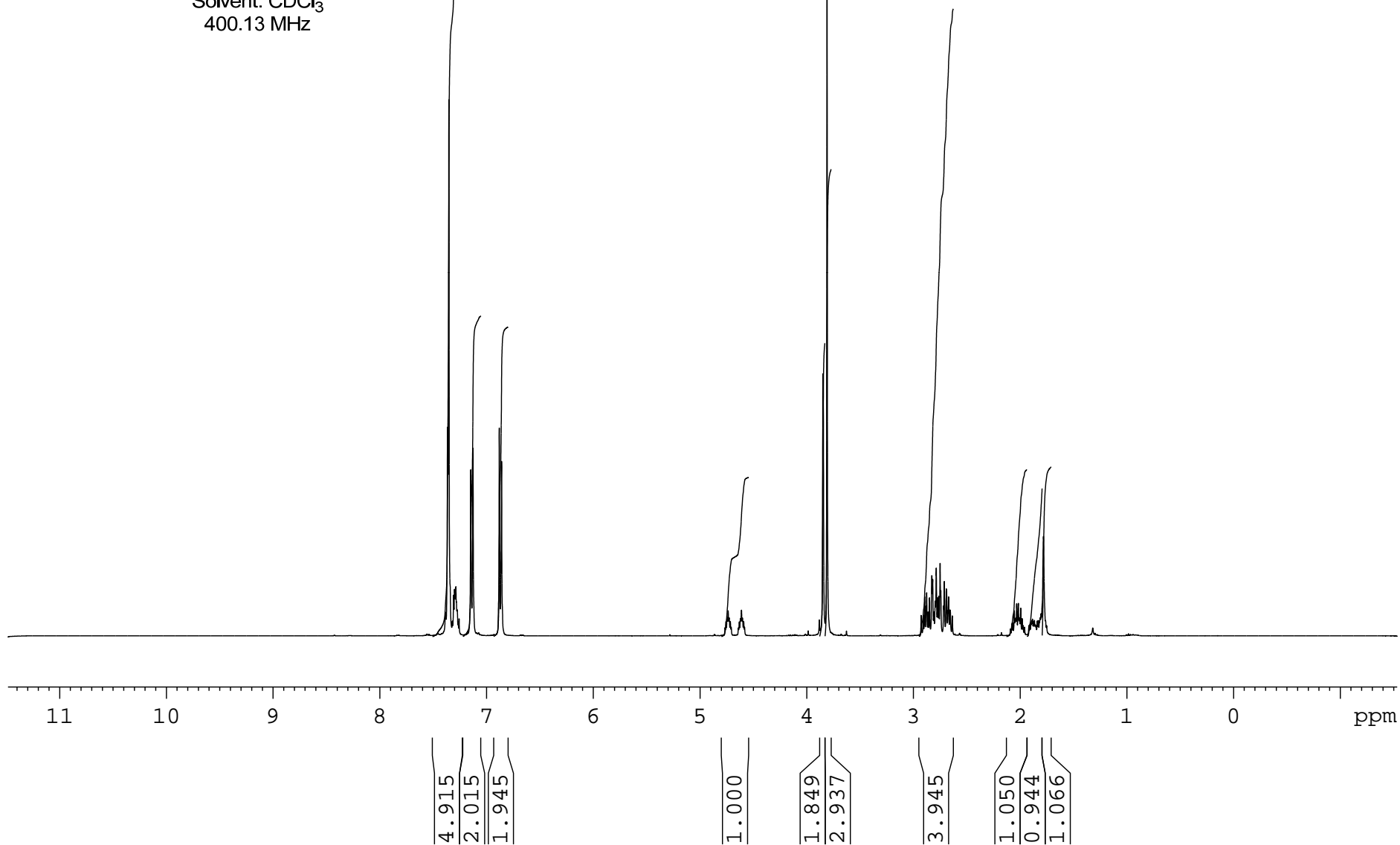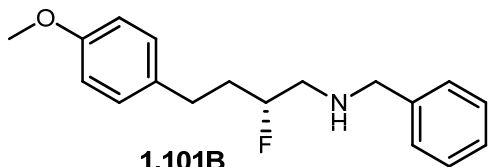| Mass	Calc. Mass	mDa	PPM	DBE	i-FIT	Formula
244.1503	244.1502	0.1	0.4	7.5	1.9	C16 H19 N F

351

1.101B

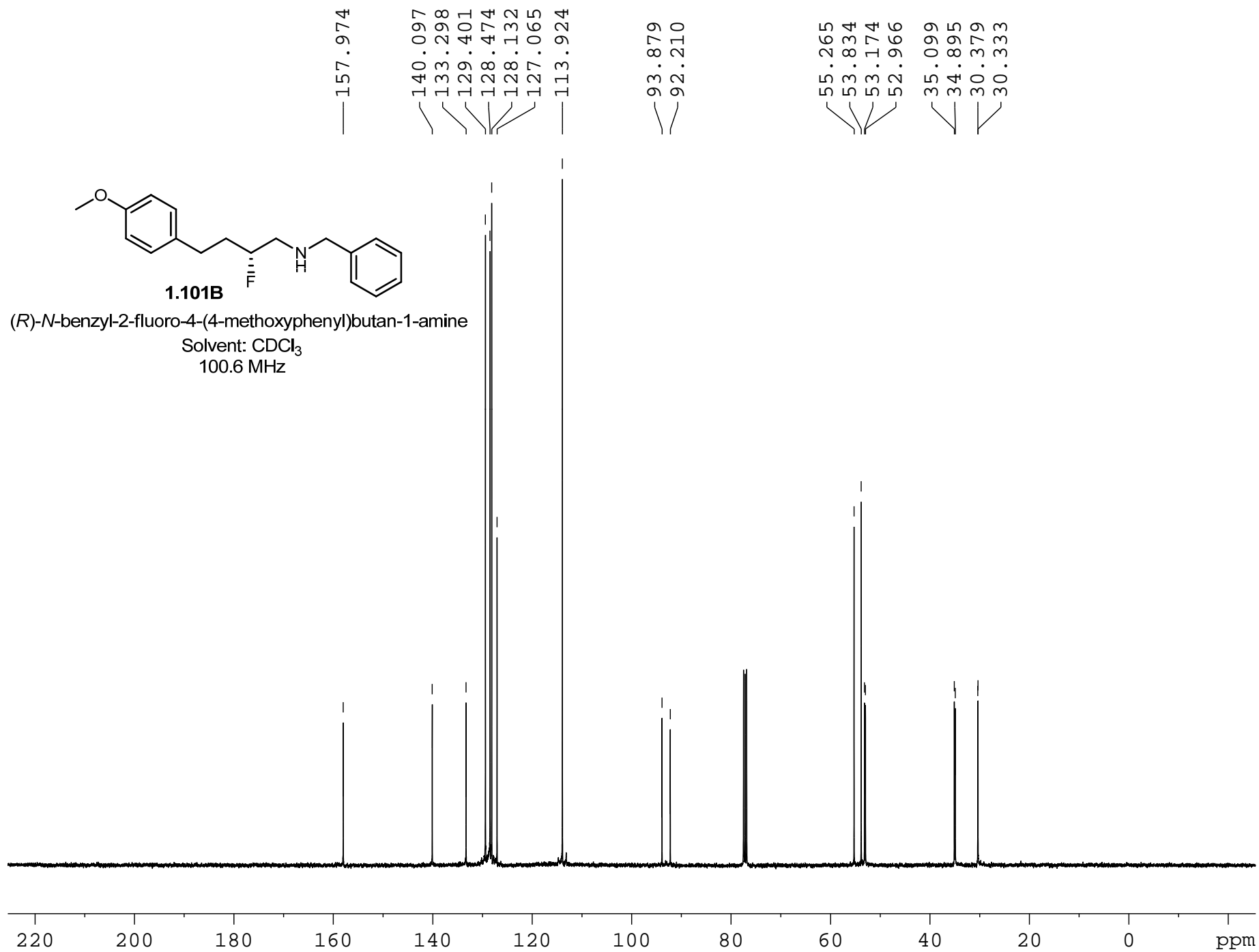(*R*)-*N*-benzyl-2-fluoro-4-(4-methoxyphenyl)butan-1-amine

Solvent: CDCl₃

400.13 MHz

1.101B

(*R*)-*N*-benzyl-2-fluoro-4-(4-methoxyphenyl)butan-1-amine
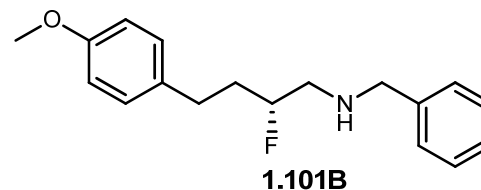Solvent: CDCl$_3$
100.6 MHz

157.974
140.097
133.298
129.401
128.474
128.132
127.065
113.924
93.879
92.210
55.265
53.834
53.174
52.966
35.099
34.895
30.379
30.333

220 200 180 160 140 120 100 80 60 40 20 0 ppm

Elemental Composition Report

Page 1

Single Mass Analysis
Tolerance = 5.0 PPM / DBE: min = -0.5, max = 25.0
Element prediction: Off
Number of isotope peaks used for i-FIT = 2

Monoisotopic Mass, Even Electron Ions
149 formula(e) evaluated with 1 results within limits (up to 50 best isotopic matches for each mass)
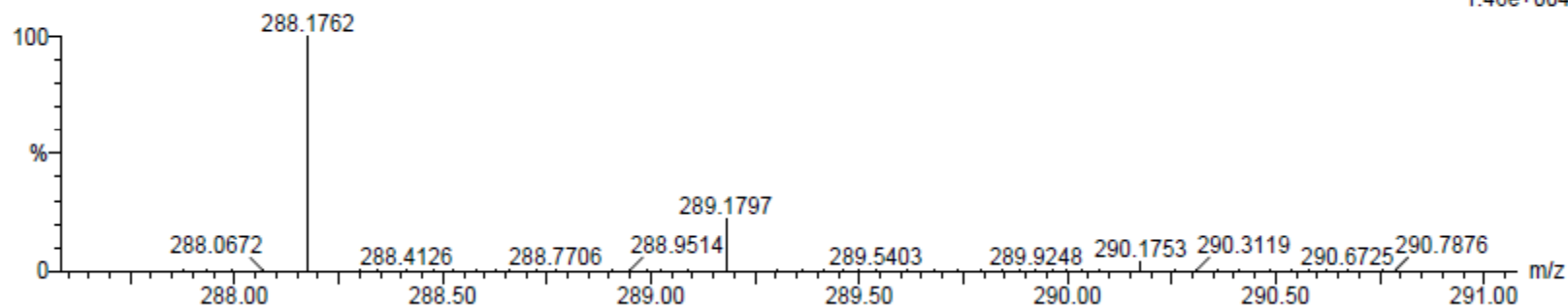Elements Used:
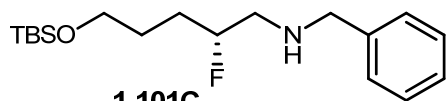C: 15-500   H: 10-1000   N: 1-200   O: 1-200   F: 1-1

MCO-V-25

1.101B

S/N: UH193

07-Dec-2012
12:48:33
TOF MS ES+
1.46e+004

MCO-V-25_120712_001 98 (1.825) AM (Cen,4, 80.00, Ar,8000.0,556.28,0.70); Sm (SG, 2x1.00); Cm (90:100)

		mDa	PPM	DBE	i-FIT	
Minimum:				-0.5		
Maximum:		5.0	5.0	25.0		

Mass	Calc. Mass	mDa	PPM	DBE	i-FIT	Formula
288.1762	288.1764	-0.2	-0.7	7.5	4.2	C18 H23 N O F

1.101C

(*R*)-*N*-benzyl-5-(((*tert*-butyldimethylsilyl)oxy)-2-fluoropentan-1-amine

Solvent: CDCl$_3$

400.13 MHz

4.869

1.000

1.976

2.018

1.981

5.145

9.229

5.972

140.183
128.541
128.191
127.122
94.813
93.149
62.762
53.901
53.335
53.127
29.715
29.510
28.452
28.410
26.060
18.433
-5.203

1.101C

(*R*)-*N*-benzyl-5-((*tert*-butyldimethylsilyl)oxy)-2-fluoropentan-1-amine

Solvent: CDCl$_3$

100.6 MHz

220   200   180   160   140   120   100   80   60   40   20   0   ppm
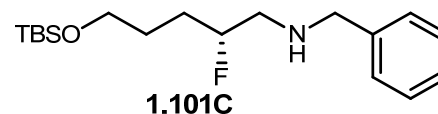
Elemental Composition Report

Page 1

Single Mass Analysis

Tolerance = 5.0 PPM / DBE: min = -0.5, max = 25.0
Element prediction: Off
Number of isotope peaks used for i-FIT = 2

1.101C

Monoisotopic Mass, Even Electron Ions
164 formula(e) evaluated with 1 results within limits (up to 50 best isotopic matches for each mass)
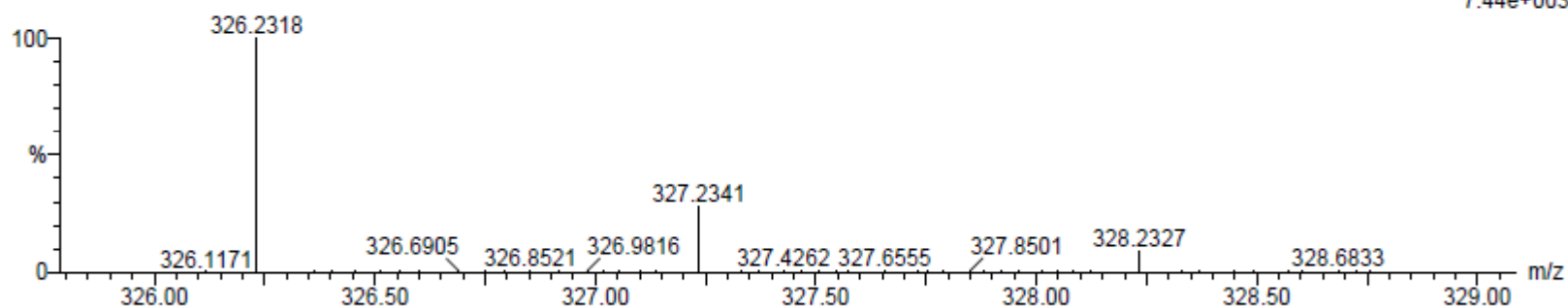Elements Used:
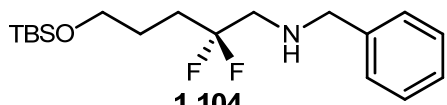C: 15-500   H: 10-1000   N: 1-200   O: 1-200   F: 1-1   Si: 1-1

07-Dec-2012
12:34:55
TOF MS ES+
7.44e+003
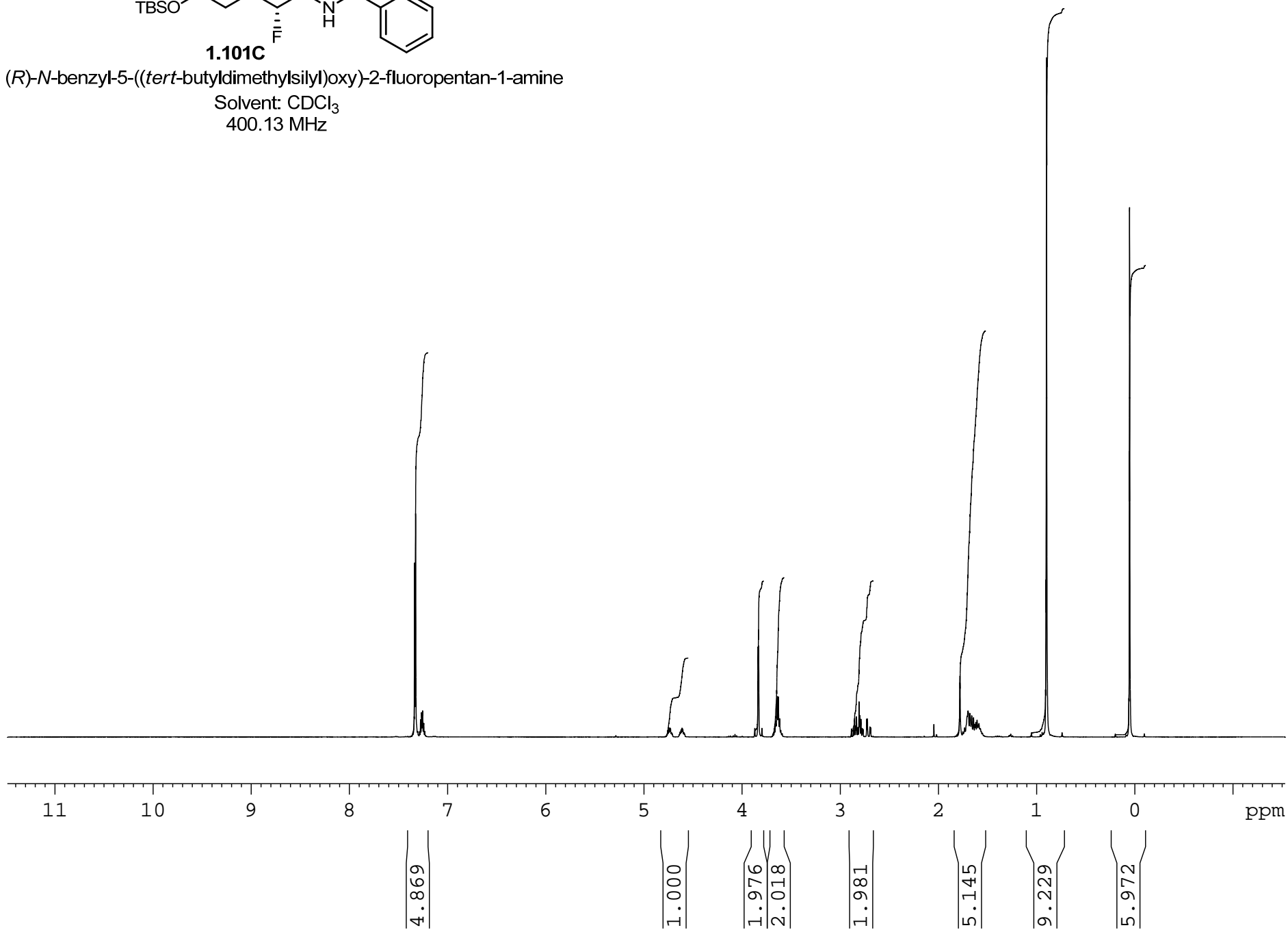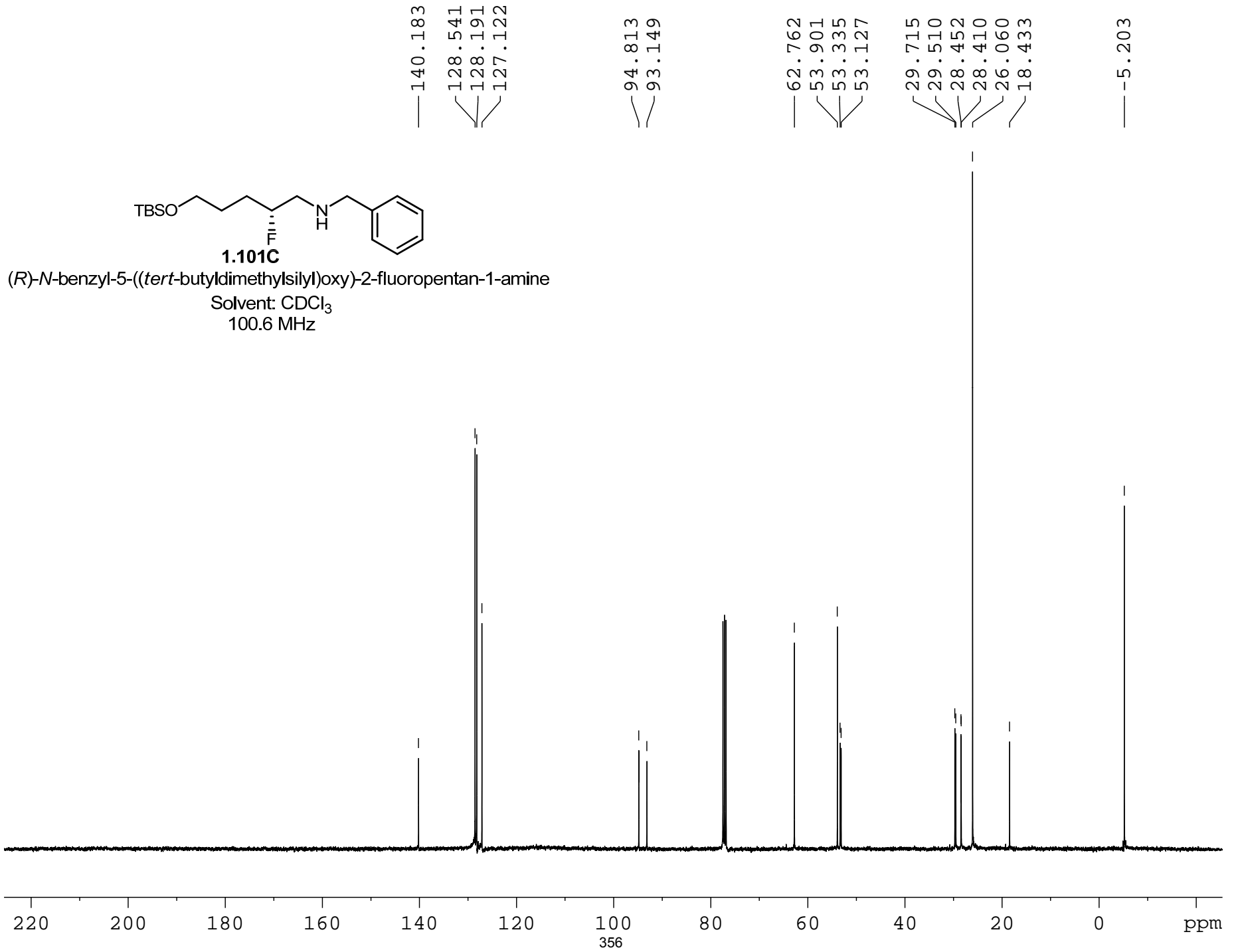
S/N: UH193
MCO-V-24_120712_001 97 (1.807) AM (Cen,4, 80.00, Ar,8000.0,556.28,0.70); Sm (SG, 2x1.00); Cm (90:100)

Minimum:		-0.5
Maximum:	5.0	5.0	25.0

Mass	Calc. Mass	mDa	PPM	DBE	i-FIT	Formula
326.2318	326.2315	0.3	0.9	3.5	3.4	C18 H33 N O F Si

357

1.104

N-benzyl-5-((*tert*-butyldimethylsilyl)oxy)-2,2-difluoropentan-1-amine

Solvent: CDCl$_3$

400.13 MHz

4.971

2.013 1.995

2.000

2.143 2.065 1.028

9.300

6.059

11 10 9 8 7 6 5 4 3 2 1 0 ppm

1.104

N-benzyl-5-((*tert*-butyldimethylsilyl)oxy)-2,2-difluoropentan-1-amine

Solvent: CDCl$_3$

100.6 MHz

139.959
128.546
128.168
127.234
124.875
122.479

62.525
53.782
52.979
52.699
52.417
31.510
31.265
31.021
26.037
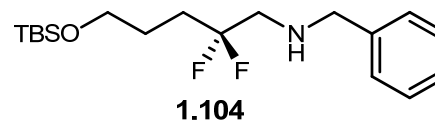25.613
25.570
25.528
18.408

−5.228

Elemental Composition Report

Page 1

Single Mass Analysis

Tolerance = 5.0 PPM   /   DBE: min = -0.5, max = 25.0
Element prediction: Off
Number of isotope peaks used for i-FIT = 2

1.104
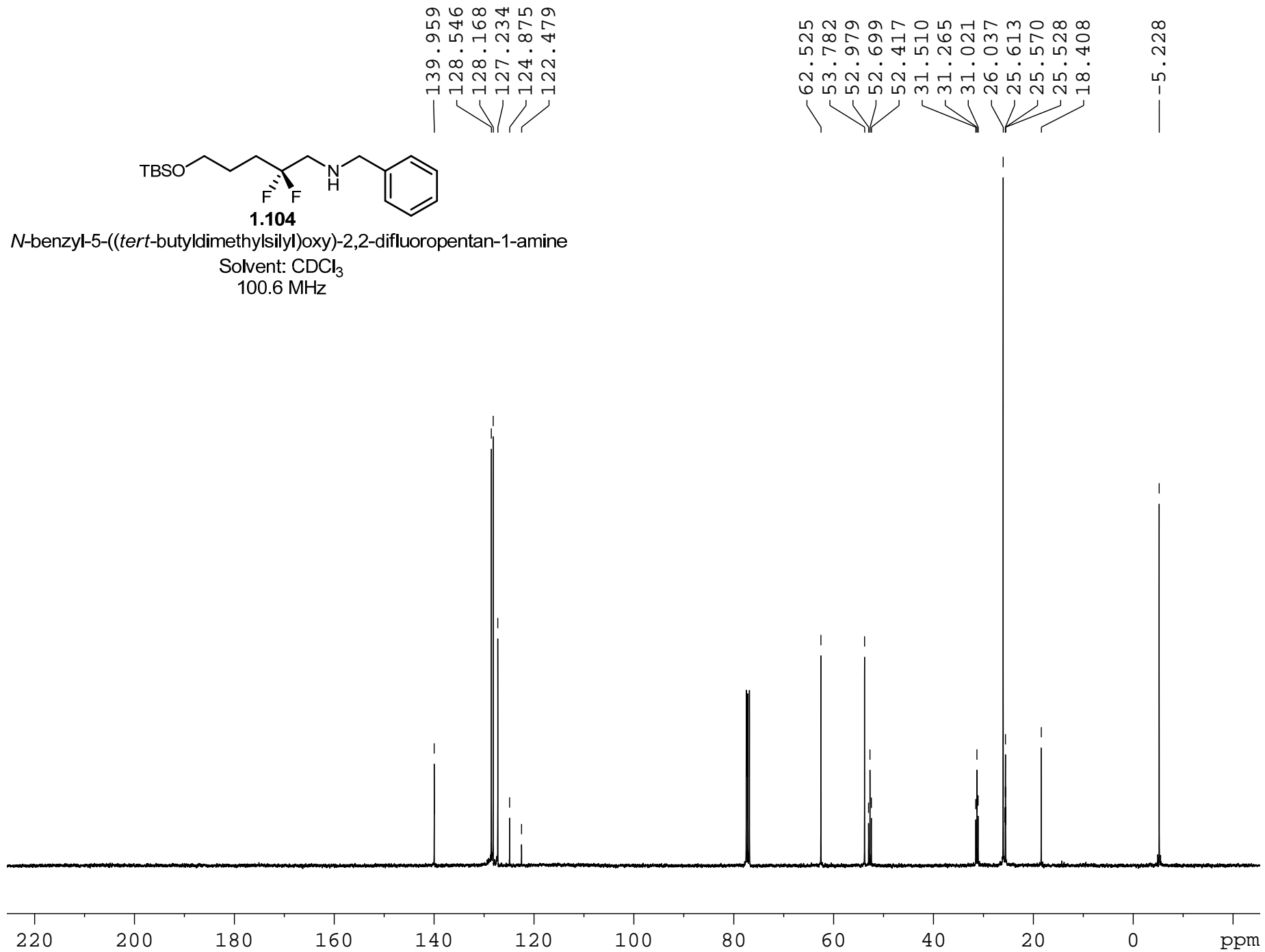
Monoisotopic Mass, Even Electron Ions
164 formula(e) evaluated with 1 results within limits (up to 50 best isotopic matches for each mass)
Elements Used:
C: 15-500   H: 10-1000   N: 1-200   O: 1-200   F: 2-2   Si: 1-1

MCO-V-45

S/N: UH193

MCO-V-45_120712_001 49 (0.916) AM (Cen,4, 80.00, Ar,8000.0,556.28,0.70); Sm (SG, 2x1.00); Cm (40:50)
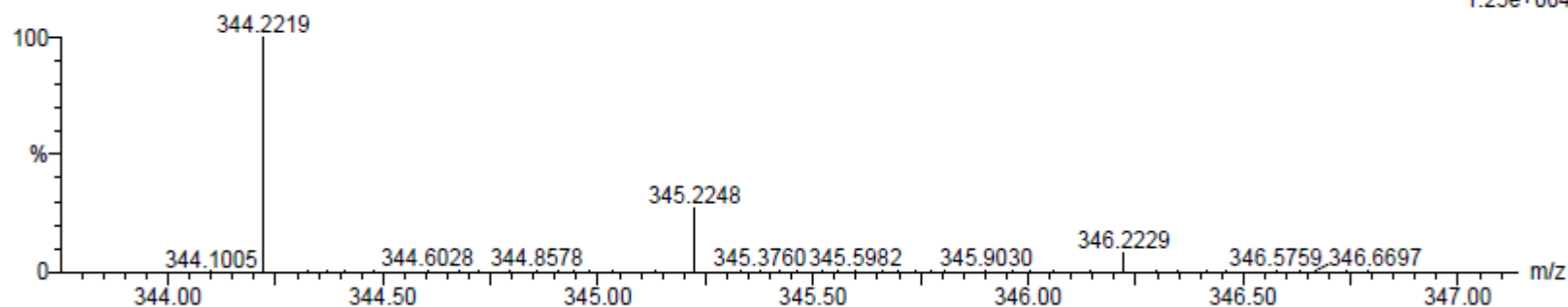
	Minimum:			-0.5		
	Maximum:	5.0	5.0	25.0		
Mass	Calc. Mass	mDa	PPM	DBE	i-FIT	Formula
344.2219	344.2221	-0.2	-0.6	3.5	2.6	C18 H32 N O F2 Si
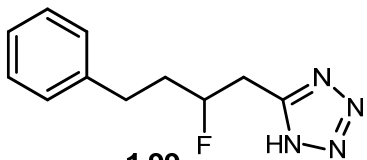
360

1.99
5-(2-fluoro-4-phenylbutyl)-1*H*-tetrazole
Solvent: MeOD
400.13 MHz

2.004
3.000
1.047
2.273
2.062
2.022

11 10 9 8 7 6 5 4 3 2 1 0 ppm

361

1.99
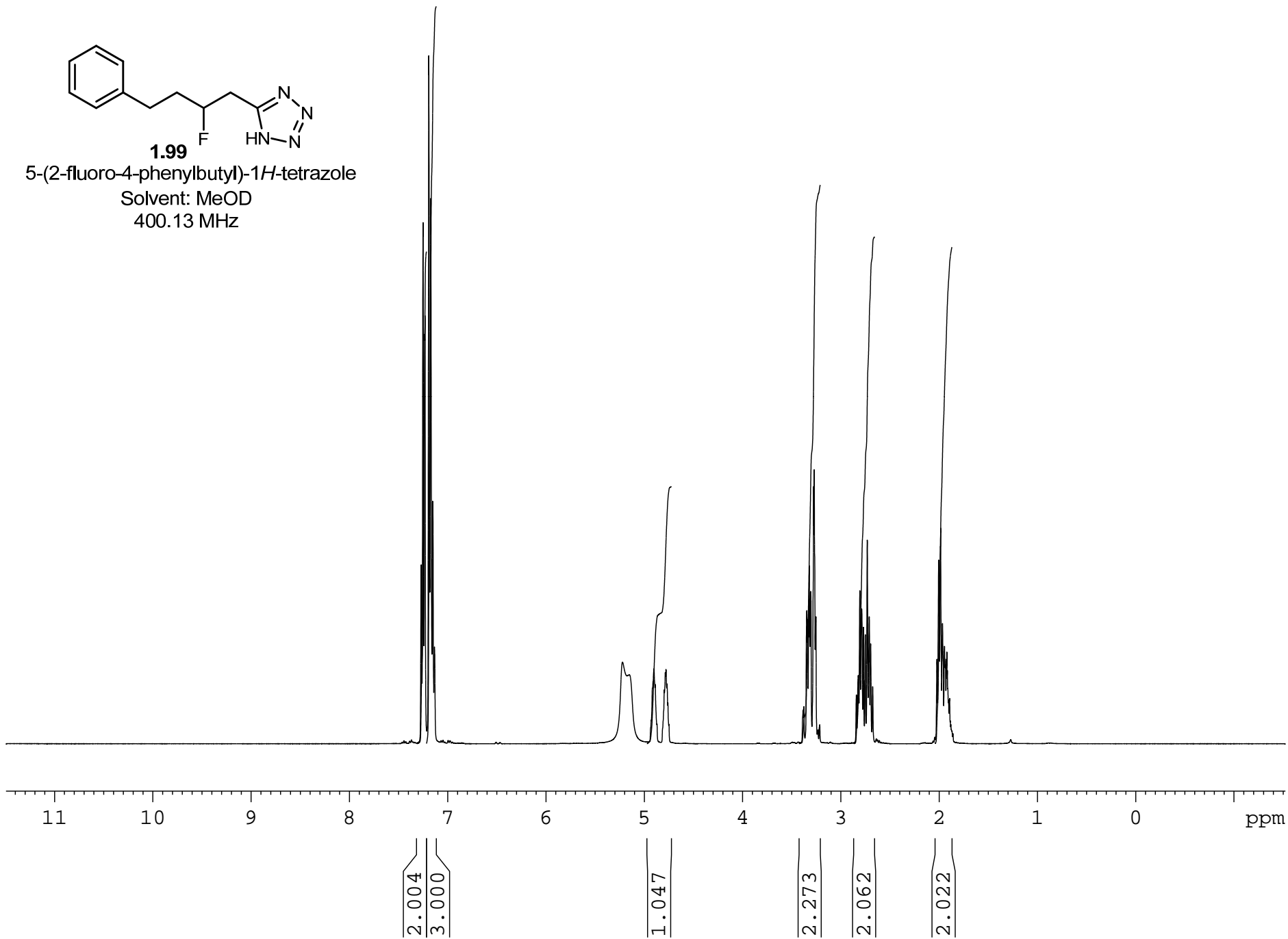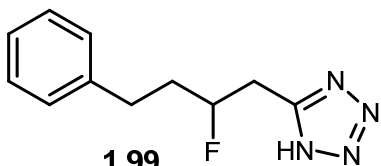
5-(2-fluoro-4-phenylbutyl)-1*H*-tetrazole
Solvent: MeOD
100.6 MHz

154.377

142.108

129.495
129.405
127.109

92.469
90.759

37.534
37.332
31.942
31.898
30.412
30.190
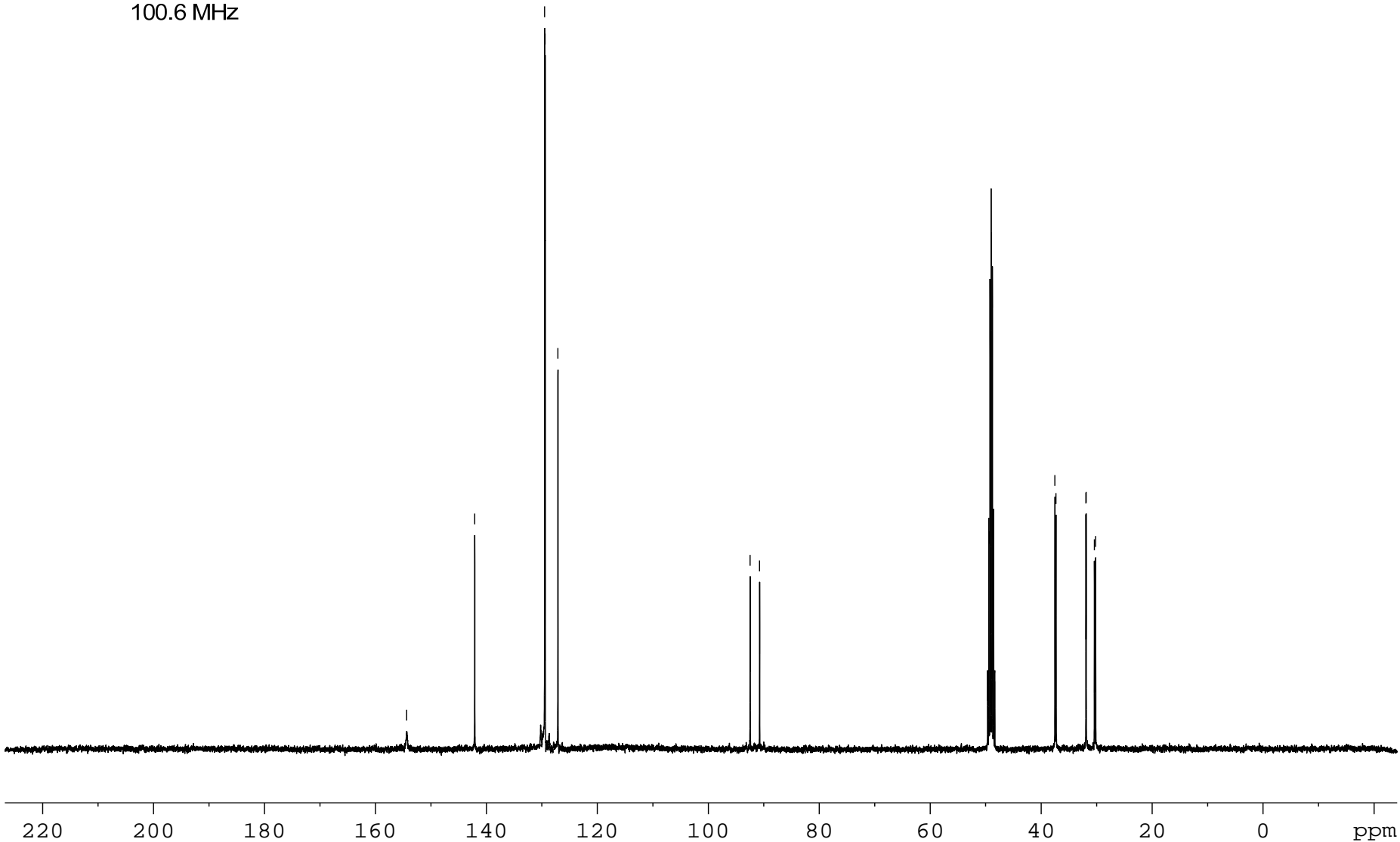
220   200   180   160   140   120   100   80   60   40   20   0   ppm

Single Mass Analysis
Tolerance = 5.0 PPM / DBE: min = -0.5, max = 25.0
Element prediction: Off
Number of isotope peaks used for i-FIT = 2

1.99
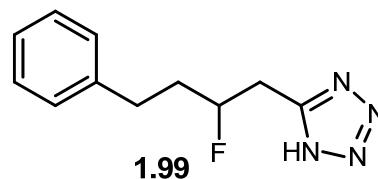
5-(2-fluoro-4-phenylbutyl)-1*H*-tetrazole

Monoisotopic Mass, Even Electron Ions
17 formula(e) evaluated with 1 results within limits (up to 50 best isotopic matches for each mass)
Elements Used:
C: 10-500   H: 10-1000   N: 1-200   F: 1-1

MCO-V-184

10-Apr-2013
10:56:47

S/N: UH193

MCO-V-184_041013_001 95 (1.770) AM (Cen,5, 80.00, Ar,8000.0,556.28,0.70); Sm (SG, 2x1.00); Cm (90:100)

1: TOF MS ES+
1.09e+004
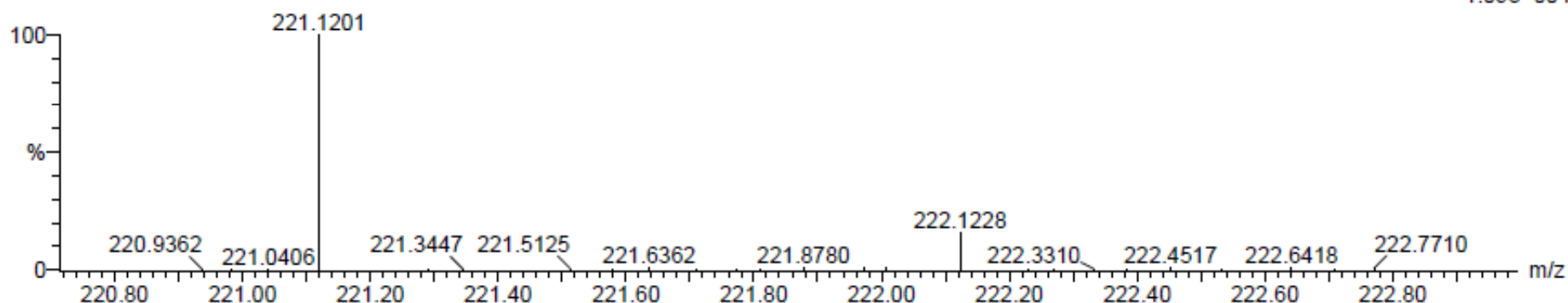

```
Minimum:                          -0.5
Maximum:              5.0    5.0   25.0

Mass        Calc. Mass   mDa    PPM    DBE    i-FIT    Formula

221.1201    221.1202    -0.1   -0.5   6.5    5.7      C11  H14  N4  F
```

1.98

(*E*)-3-fluoro-*N'*-hydroxy-5-phenylpentanimidamide
Solvent: MeOD
400.13 MHz

2.000
3.017
1.338
4.119
1.995

11   10   9   8   7   6   5   4   3   2   1   0   ppm

161.665

141.941
129.574
129.458
127.229

91.754
90.020

37.758
37.558
36.043
35.823
31.846
31.807
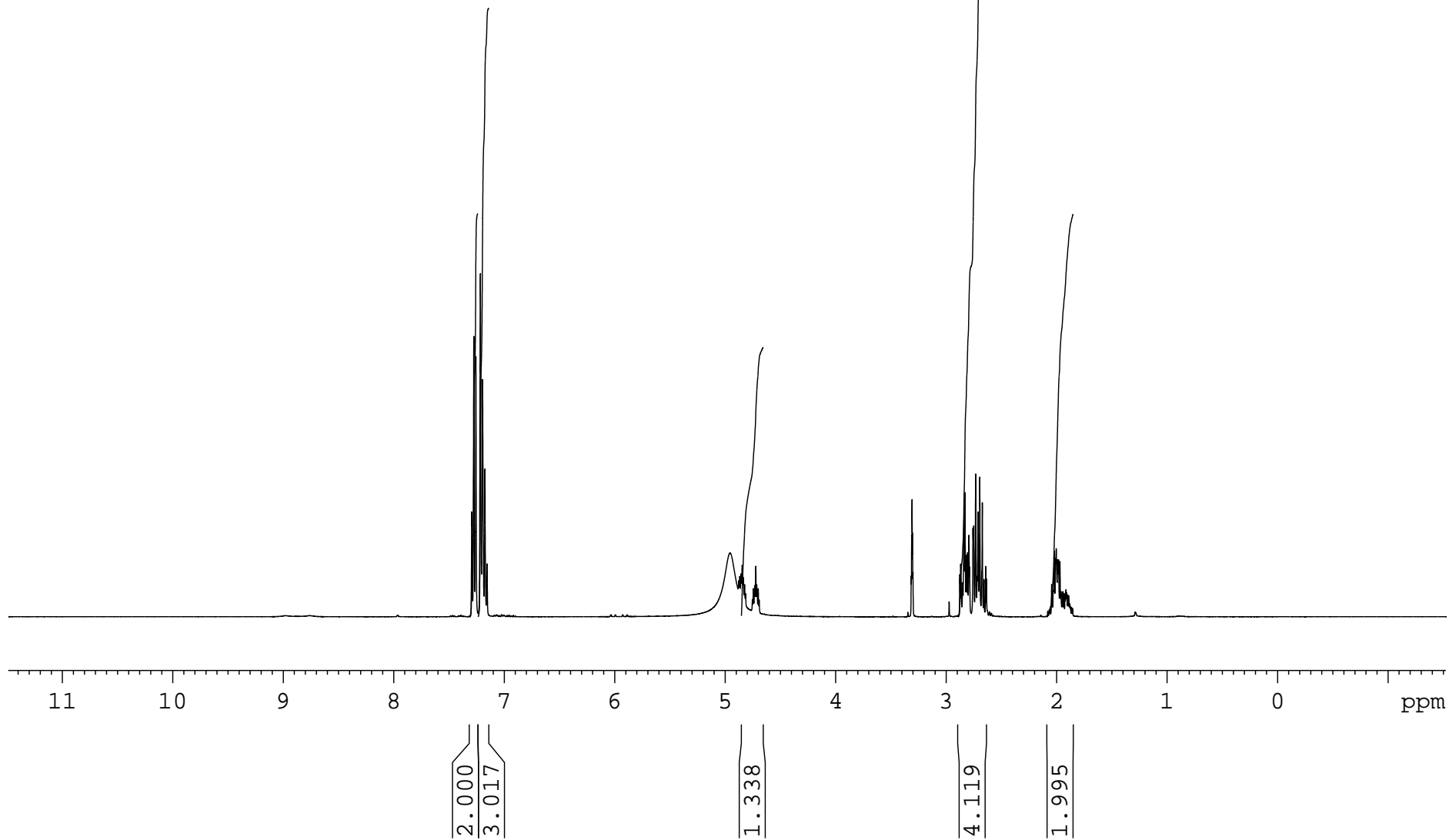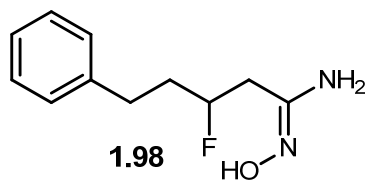
1.98
(*E*)-3-fluoro-*N'*-hydroxy-5-phenylpentanimidamide
Solvent: MeOD
100.6 MHz

220   200   180   160   140   120   100   80   60   40   20   0   ppm

Single Mass Analysis
Tolerance = 5.0 PPM / DBE: min = -0.5, max = 25.0
Element prediction: Off
Number of isotope peaks used for i-FIT = 2

1.98
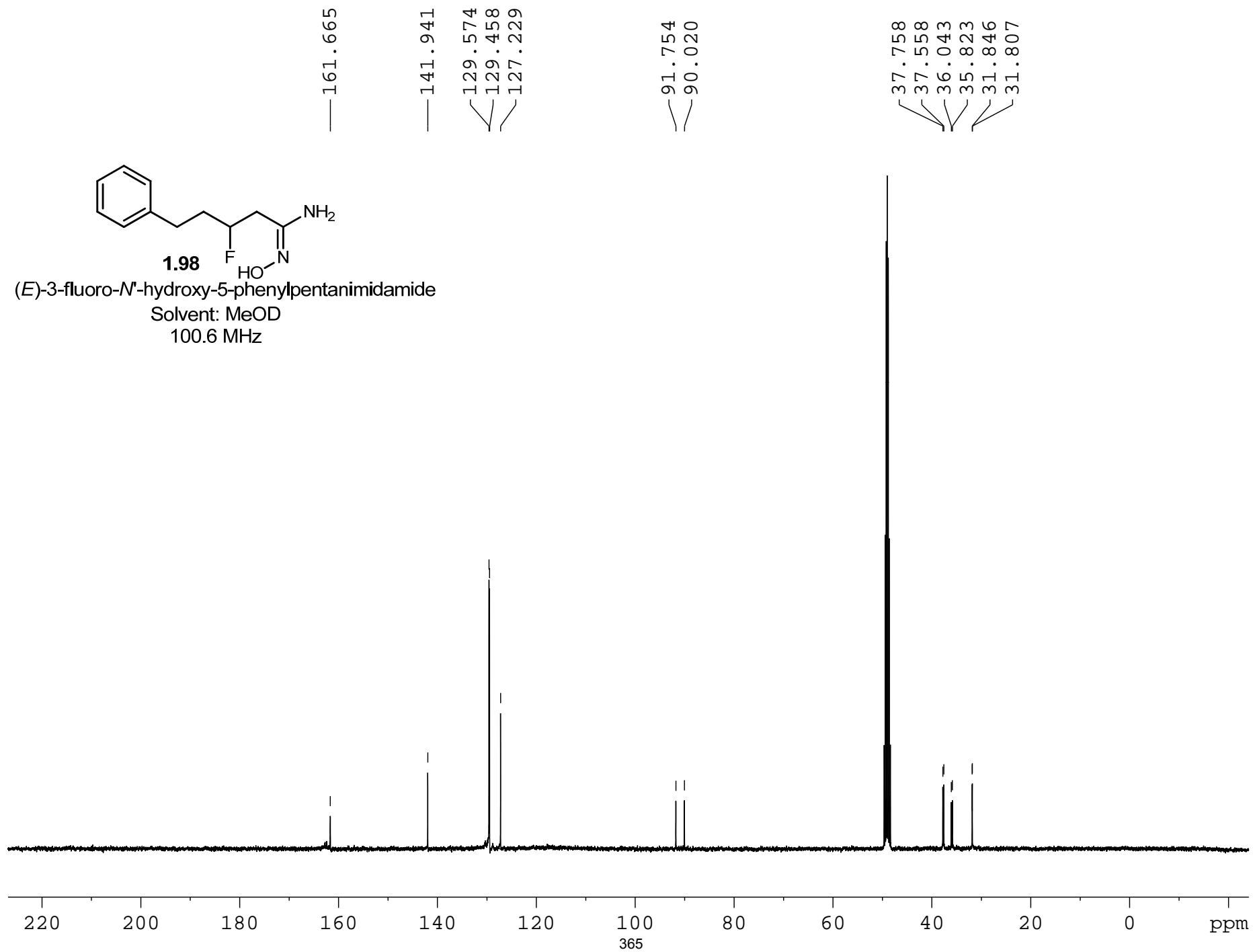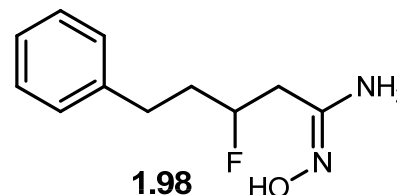
Monoisotopic Mass, Even Electron Ions
70 formula(e) evaluated with 1 results within limits (up to 50 best isotopic matches for each mass)
Elements Used:
C: 10-500   H: 10-1000   N: 1-200   O: 1-200   F: 1-1
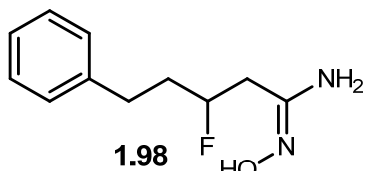
MCO-V-183   10-Apr-2013
S/N: UH193   10:29:04
MCO-V-183_041013_001 80 (1.491) AM (Cen,5, 80.00, Ar,8000.0,556.28,0.70); Sm (SG, 2x1.00); Cm (80:90)   1: TOF MS ES+
9.14e+003
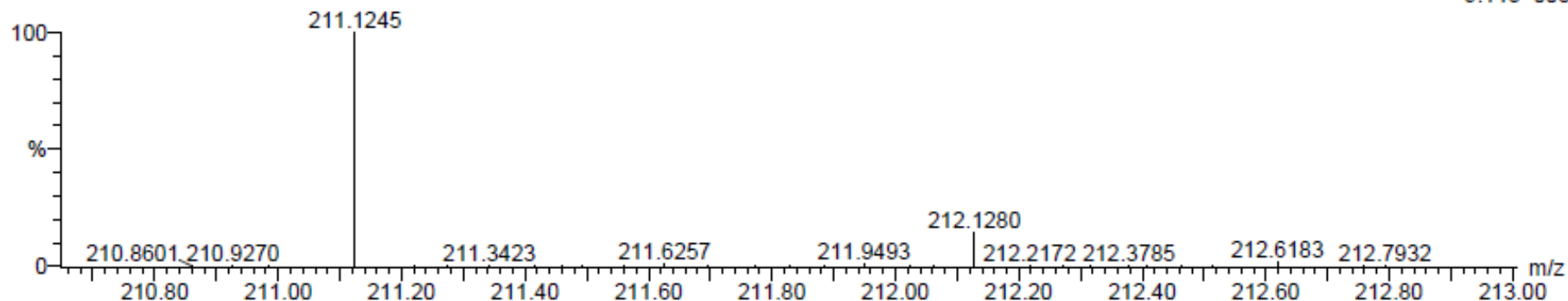
| Minimum: | | | -0.5 | | |
| Maximum: | 5.0 | 5.0 | 25.0 | | |

Mass	Calc. Mass	mDa	PPM	DBE	i-FIT	Formula
211.1245	211.1247	-0.2	-0.9	4.5	2.4	C11 H16 N2 O F
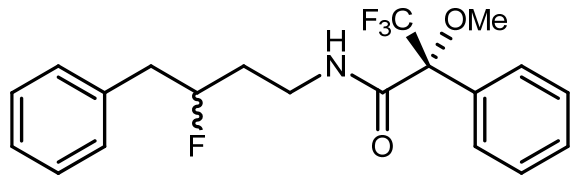
(2*R*)-3,3,3-trifluoro-*N*-(3-fluoro-4-phenylbutyl)-2-methoxy-2-phenylpropanamide
Fluorine NMR for ee determination of Mosher Amide
Racemic **1.97A**

−180.701
−180.941

−180.6   −180.7   −180.8   −180.9   −181.0   ppm

1.000   0.929

20   0   −20   −40   −60   −80   −100   −120   −140   −160   −180   −200   ppm

1.000   0.929
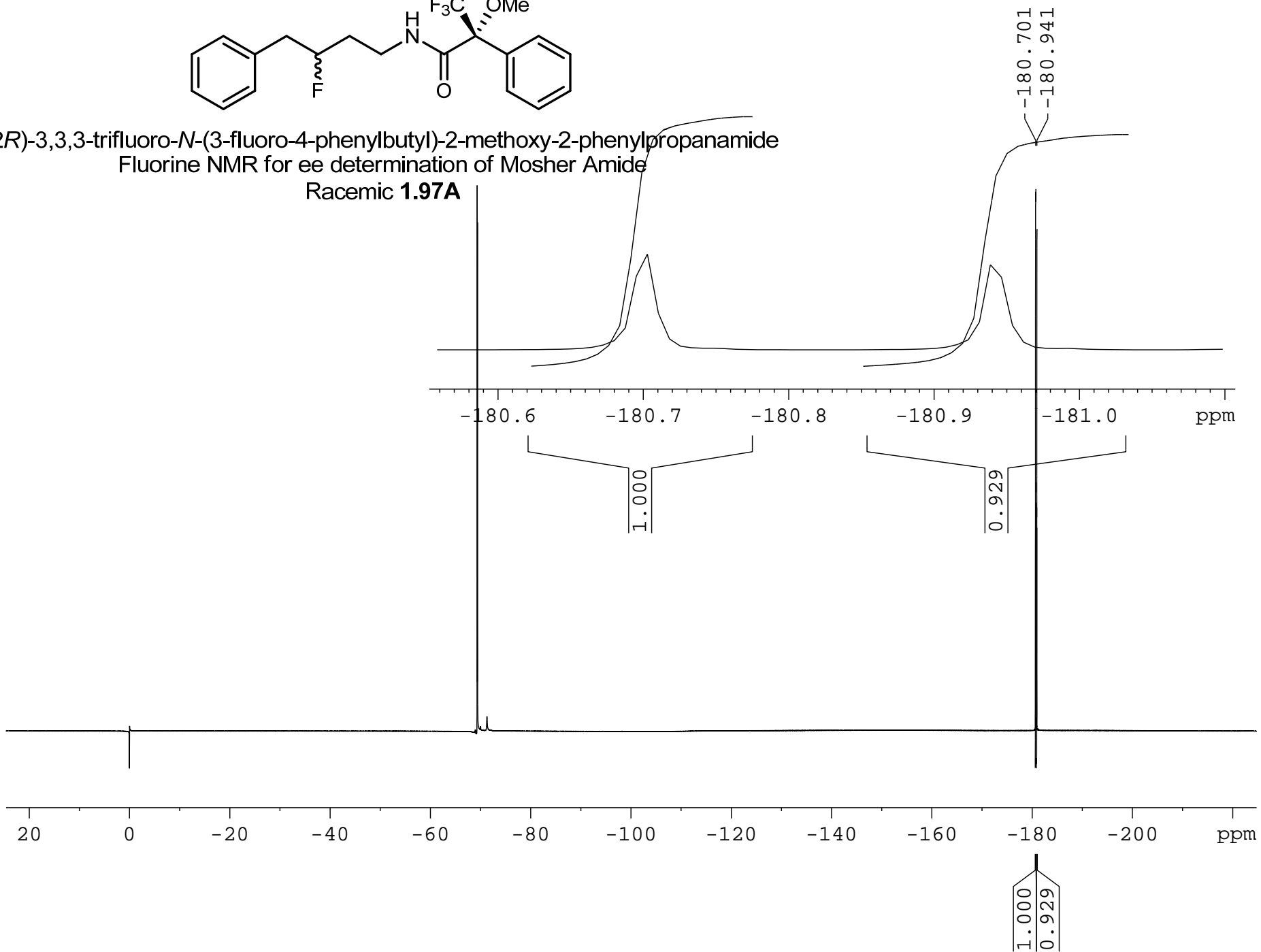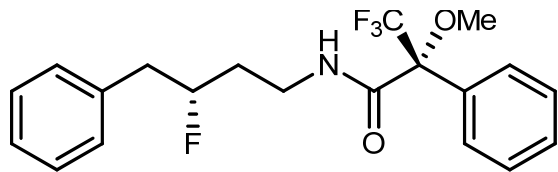
(R)-3,3,3-trifluoro-N-((R)-3-fluoro-4-phenylbutyl)-2-methoxy-2-phenylpropanamide
Fluorine NMR for ee determination of Mosher Amide
Chiral **1.97A**

−180.699
−180.956

0.031

1.000

−180.6   −180.8   −181.0   −181.2   ppm

20   0   −20   −40   −60   −80   −100   −120   −140   −160   −180   −200   ppm

0.031
1.000

(2*R*)-3,3,3-trifluoro-*N*-(3-fluoro-5-(4-methoxyphenyl)pentyl)-2-methoxy-2-phenylpropanamide
Fluorine NMR for ee determination of Mosher Amide
Racemic **1.97B**

-184.116
-184.154
-184.274
-184.313

-184.0   -184.2   ppm

1.000   0.991

20   0   -20   -40   -60   -80   -100   -120   -140   -160   -180   -200   ppm

1.000   0.991

(*R*)-3,3,3-trifluoro-*N*-((*R*)-3-fluoro-5-(4-methoxyphenyl)pentyl)-2-methoxy-2-phenylpropanamide
Fluorine NMR for ee determination of Mosher Amide
Chiral **1.97B**

-184.150
-184.321

-184.1   -184.2   -184.3   ppm

0.067   1.000

20   0   -20   -40   -60   -80   -100   -120   -140   -160   -180   -200   ppm

0.067   1.000

(2R)-N-(6-((tert-butyldimethylsilyl)oxy)-3-fluorohexyl)-3,3,3-trifluoro-2-methoxy-2-phenylpropanamide
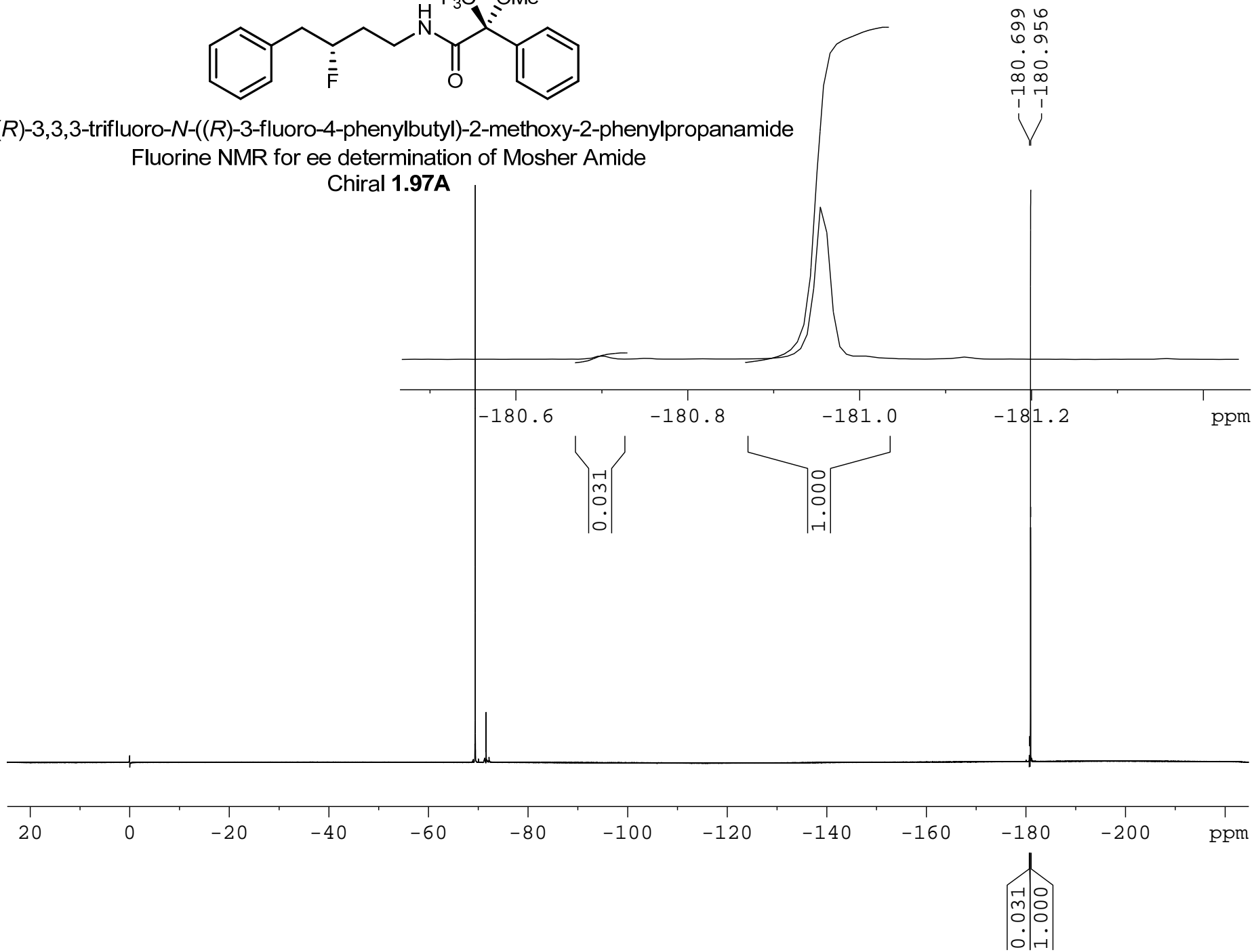Fluorine NMR for ee determination of Mosher Amide
Racemic **1.97C**

−182.198
−182.428

1.000

1.001

−182.2   −182.3   −182.4   ppm

1.000
1.001

20   0   −20   −40   −60   −80   −100   −120   −140   −160   −180   −200   ppm

(R)-N-((R)-6-((tert-butyldimethylsilyl)oxy)-3-fluorohexyl)-3,3,3-trifluoro-2-methoxy-2-phenylpropanamide

Fluorine NMR for ee determination of Mosher Amide

Chiral **1.97C**

−182.196
−182.430

−182.2   −182.4   ppm

0.042

1.000

20   0   −20   −40   −60   −80   −100   −120   −140   −160   −180   −200   ppm
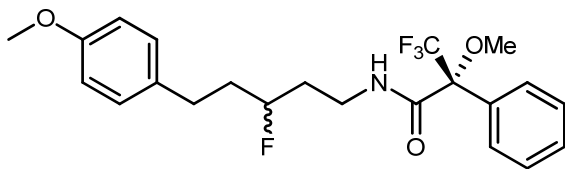
0.042 | 1.000

From **3d**

(2*R*)-3,3,3-trifluoro-*N*-(3-fluoro-4-phenylpentyl)-2-methoxy-2-phenylpropanamide
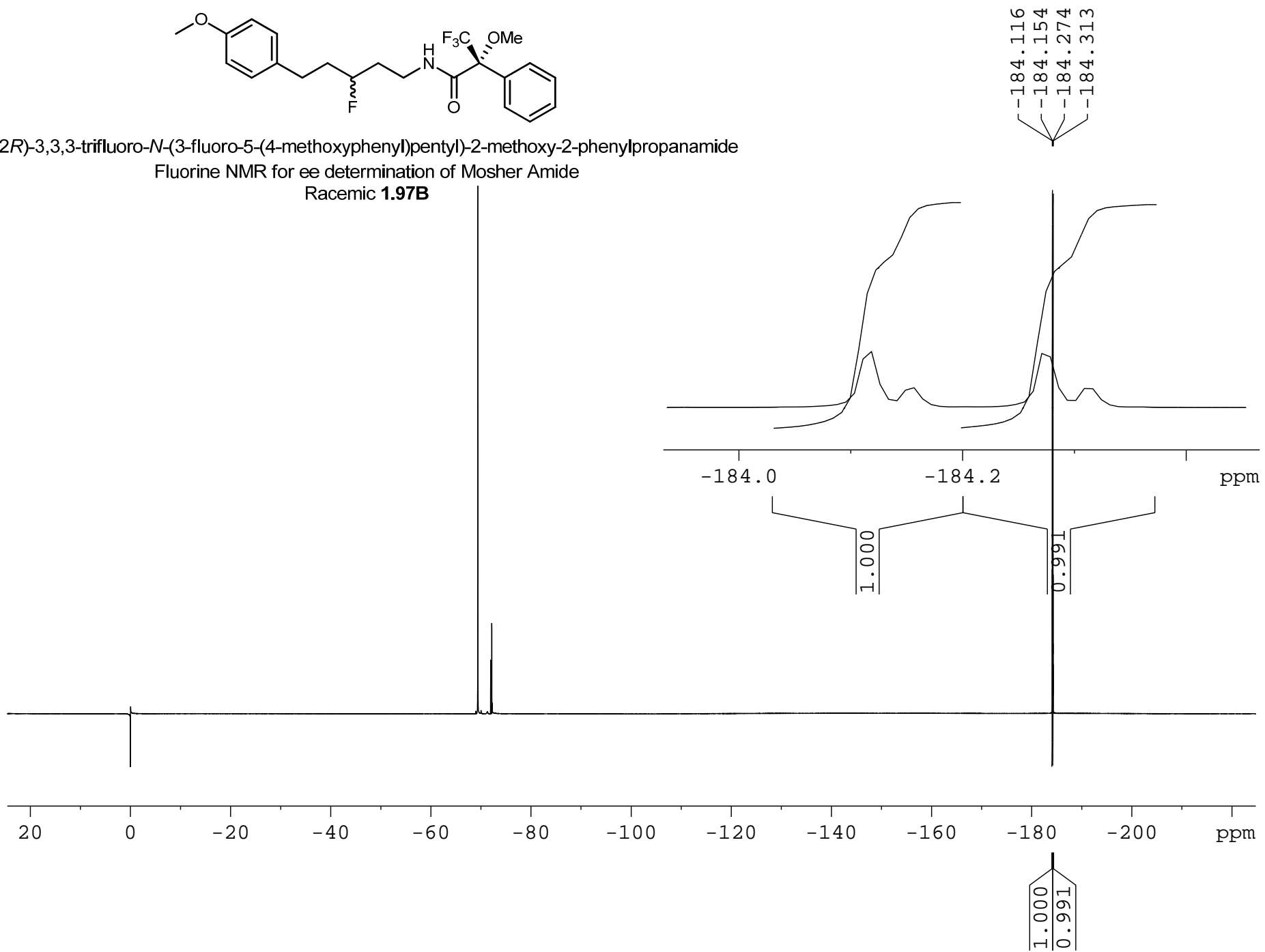Fluorine NMR for ee determination of Mosher Amide
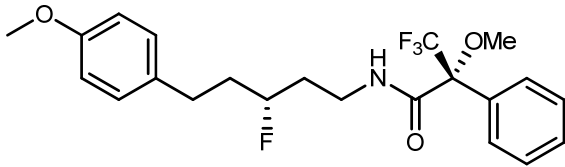Racemic **1.97D**

From **3d**

(2*R*)-3,3,3-trifluoro-*N*-((3*S*)-3-fluoro-4-phenylpentyl)-2-methoxy-2-phenylpropanamide
Fluorine NMR for ee determination of Mosher Amide
Chiral **1.97D**

-186.340
-186.388

-186.3   -186.4   ppm

1.000   0.022

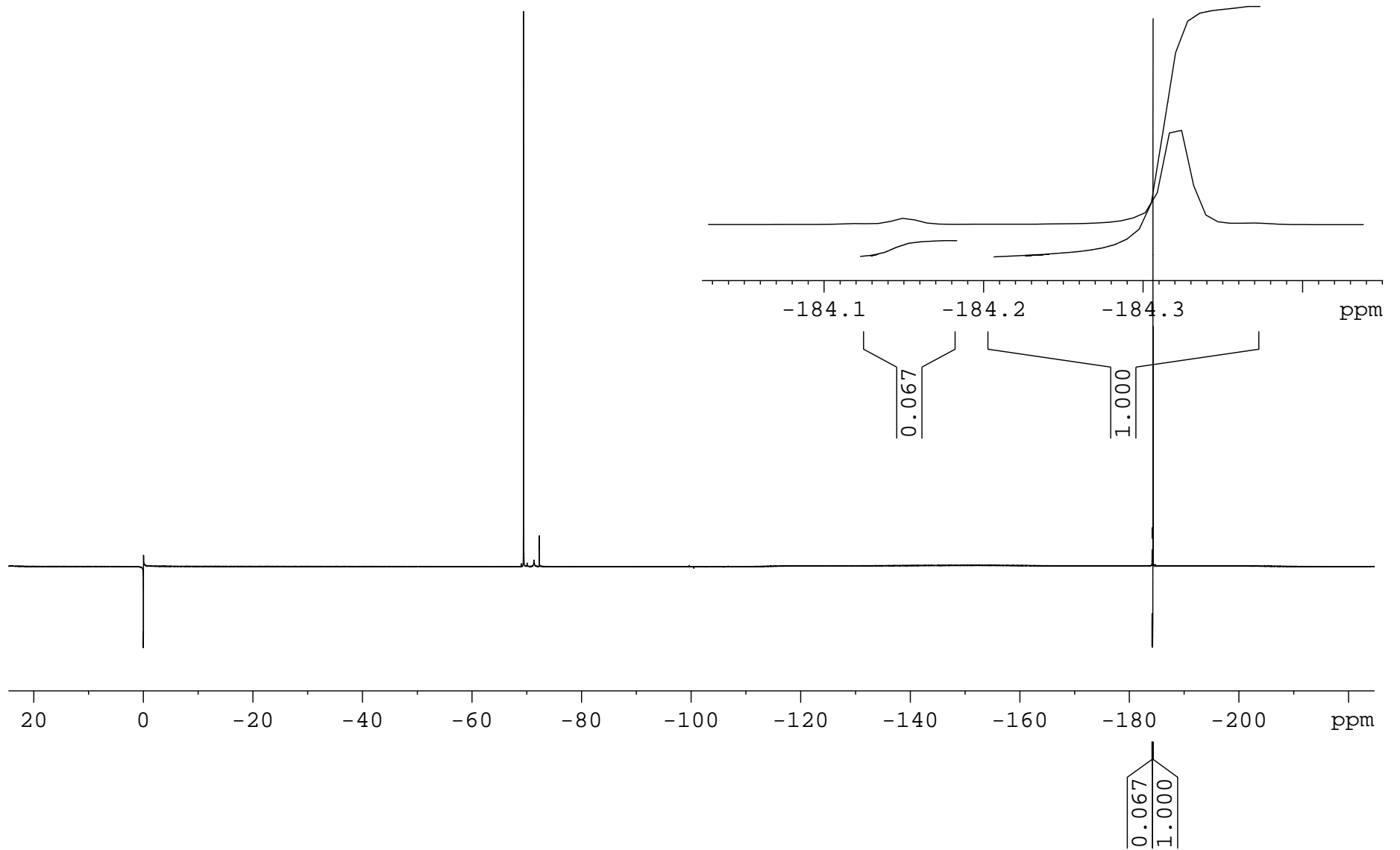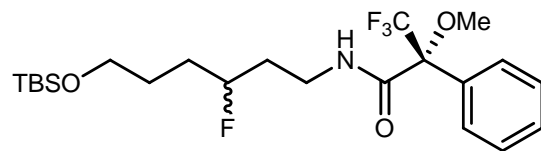0   -20   -40   -60   -80   -100   -120   -140   -160   -180   -200   ppm

1.000 0.022

(2*R*)-3,3,3-trifluoro-*N*-(3-fluoro-4-phenylpentyl)-2-methoxy-2-phenylpropanamide
Fluorine NMR for ee determination of Mosher Amide
Racemic **1.97E**

from **3e**
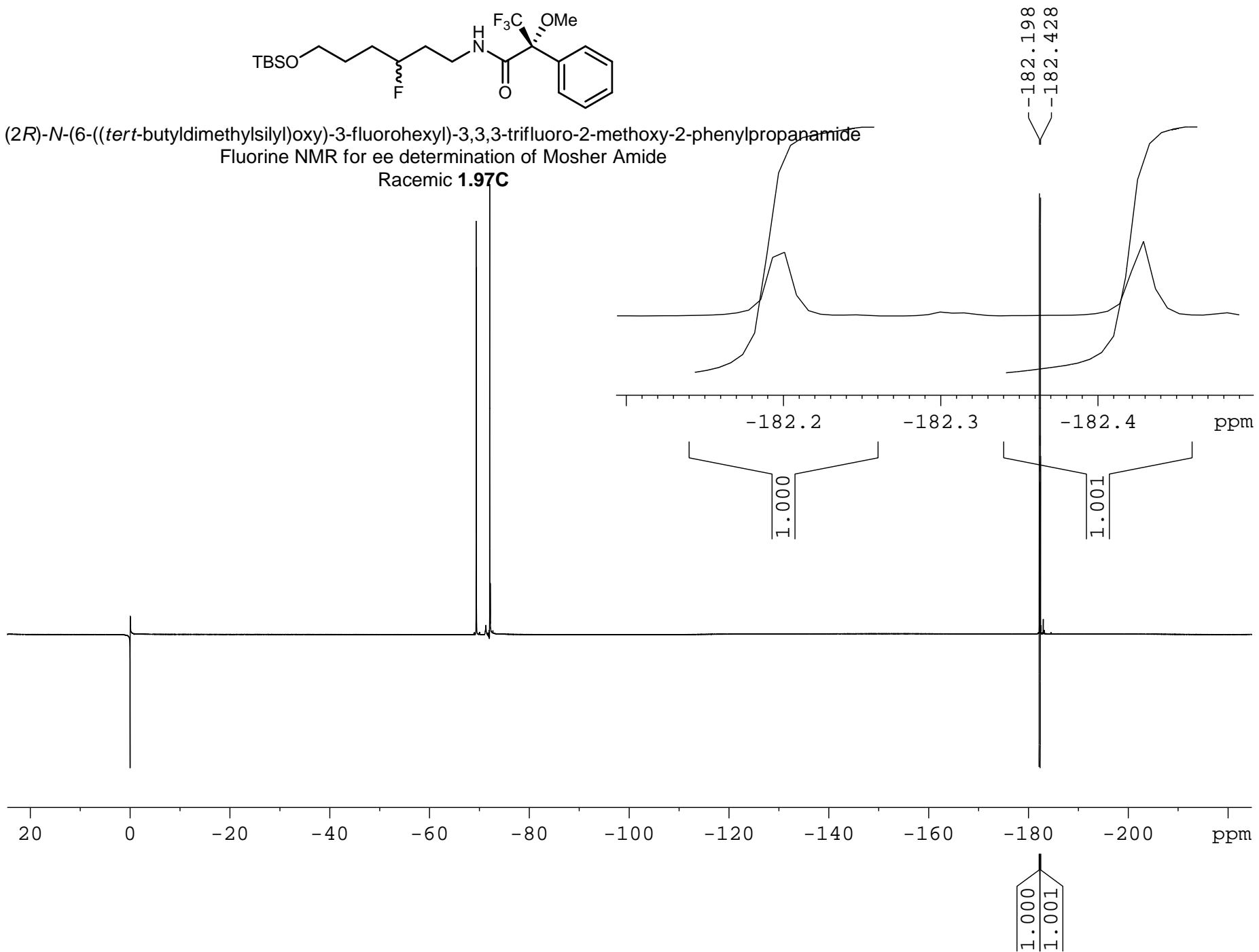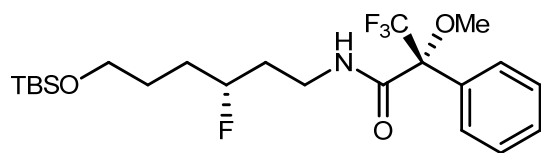
−187.253
−187.432

1.031
1.000

(2*R*)-3,3,3-trifluoro-*N*-((3*S*)-3-fluoro-4-phenylpentyl)-2-methoxy-2-phenylpropanamide
Fluorine NMR for ee determination of Mosher Amide
Chiral **1.97E**

from **3e**

−187.226
−187.429

0.019   1.000

(2*R*)-3,3,3-trifluoro-*N*-(3-fluorotridecyl)-2-methoxy-2-phenylpropanamide
Fluorine NMR for ee determination of Mosher Amide
Racemic **1.97F**

−181.974
−182.190

−181.8   −182.0   −182.2   ppm

1.029

1.000

20   0   −20   −40   −60   −80   −100   −120   −140   −160   −180   −200   ppm

1.029
1.000
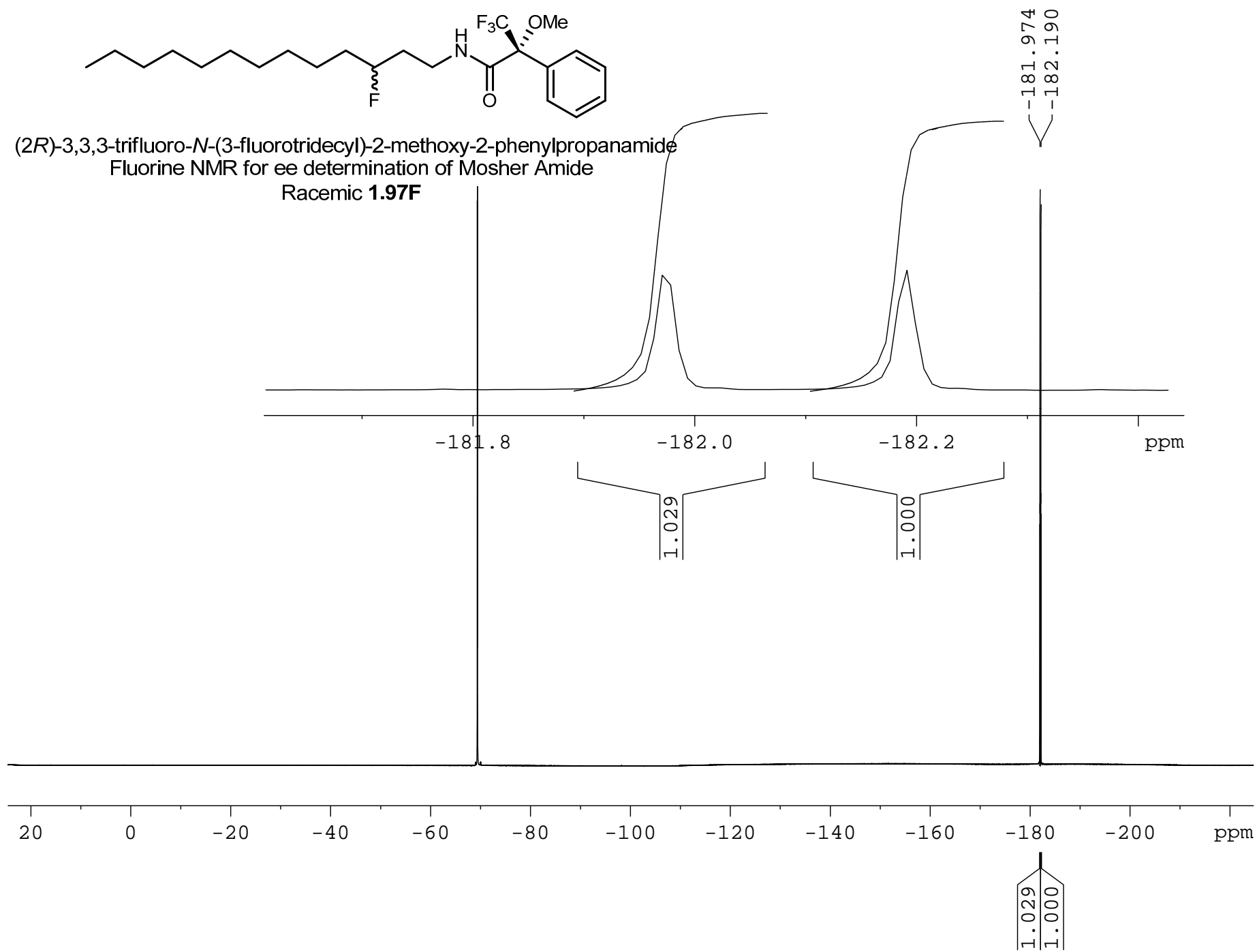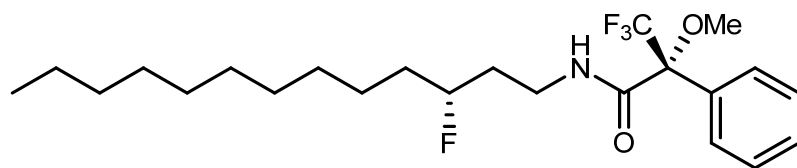
(R)-3,3,3-trifluoro-N-((R)-3-fluorotridecyl)-2-methoxy-2-phenylpropanamide
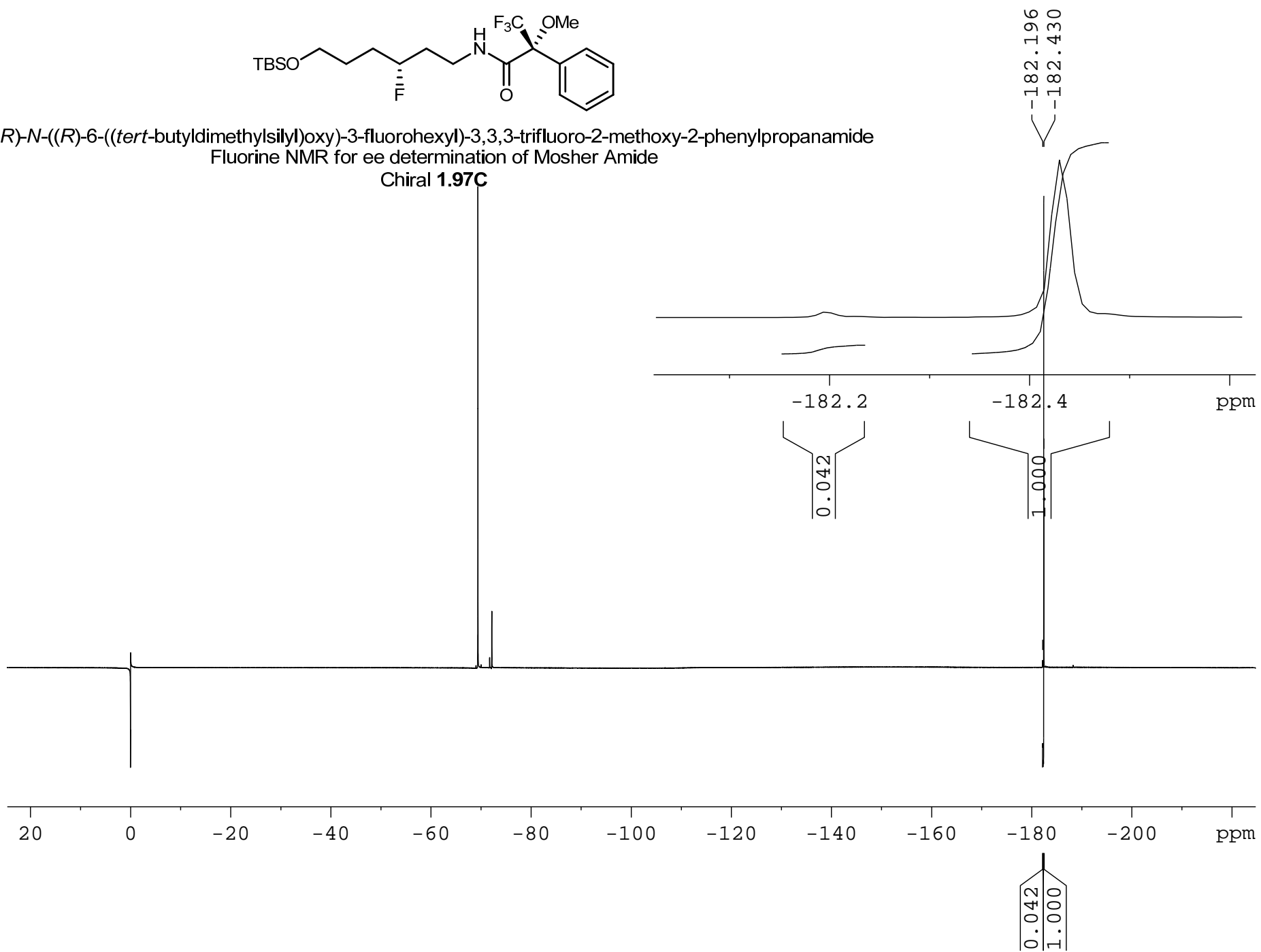Fluorine NMR for ee determination of Mosher Amide
chiral **1.97F**
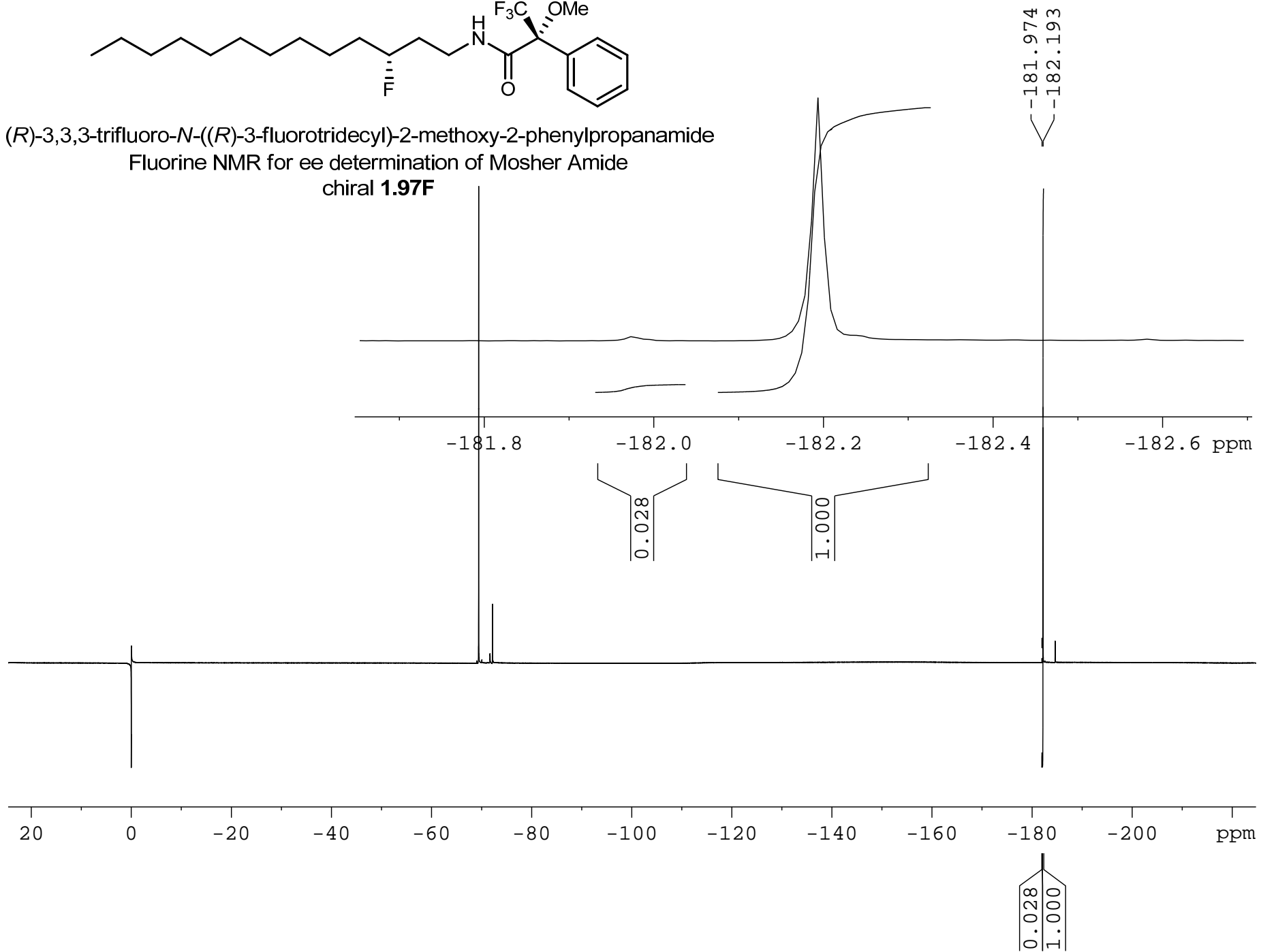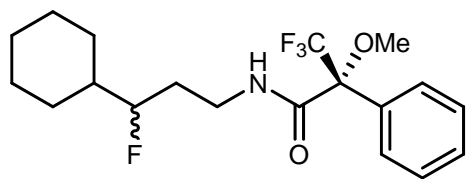
(2*R*)-*N*-(3-cyclohexyl-3-fluoropropyl)-3,3,3-trifluoro-2-methoxy-2-phenylpropanamide
Fluorine NMR for ee determination of Mosher Amide
Racemic **1.97G**

379
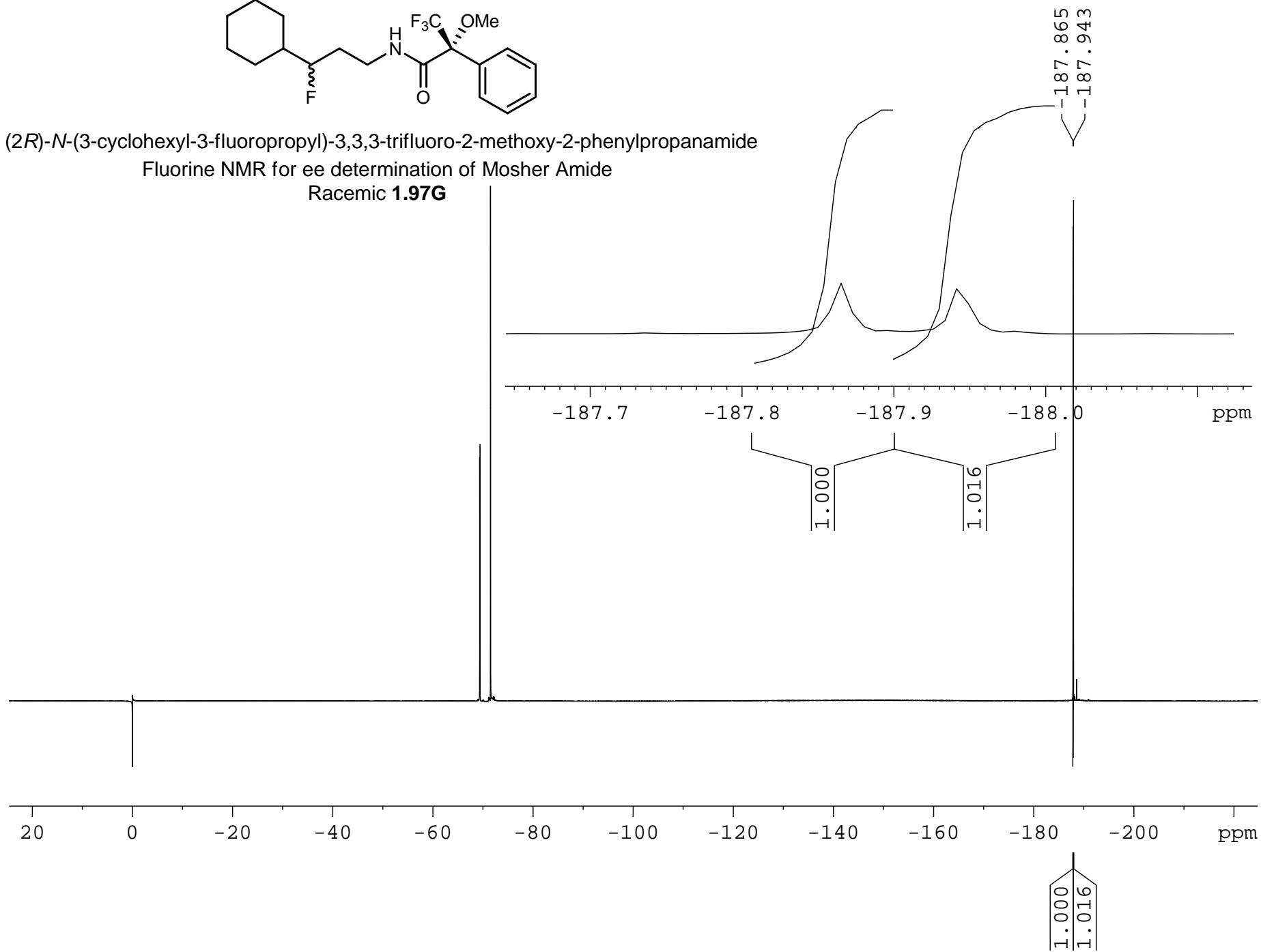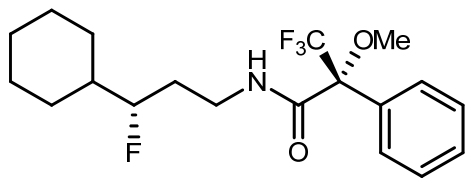
(R)-N-((S)-3-cyclohexyl-3-fluoropropyl)-3,3,3-trifluoro-2-methoxy-2-phenylpropanamide
Fluorine NMR for ee determination of Mosher Amide
chiral **1.97G**

Racemic **1.101A**
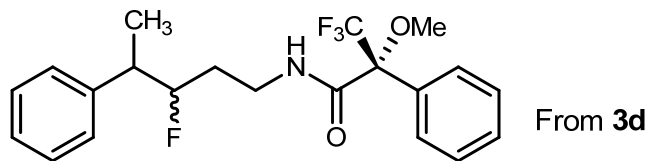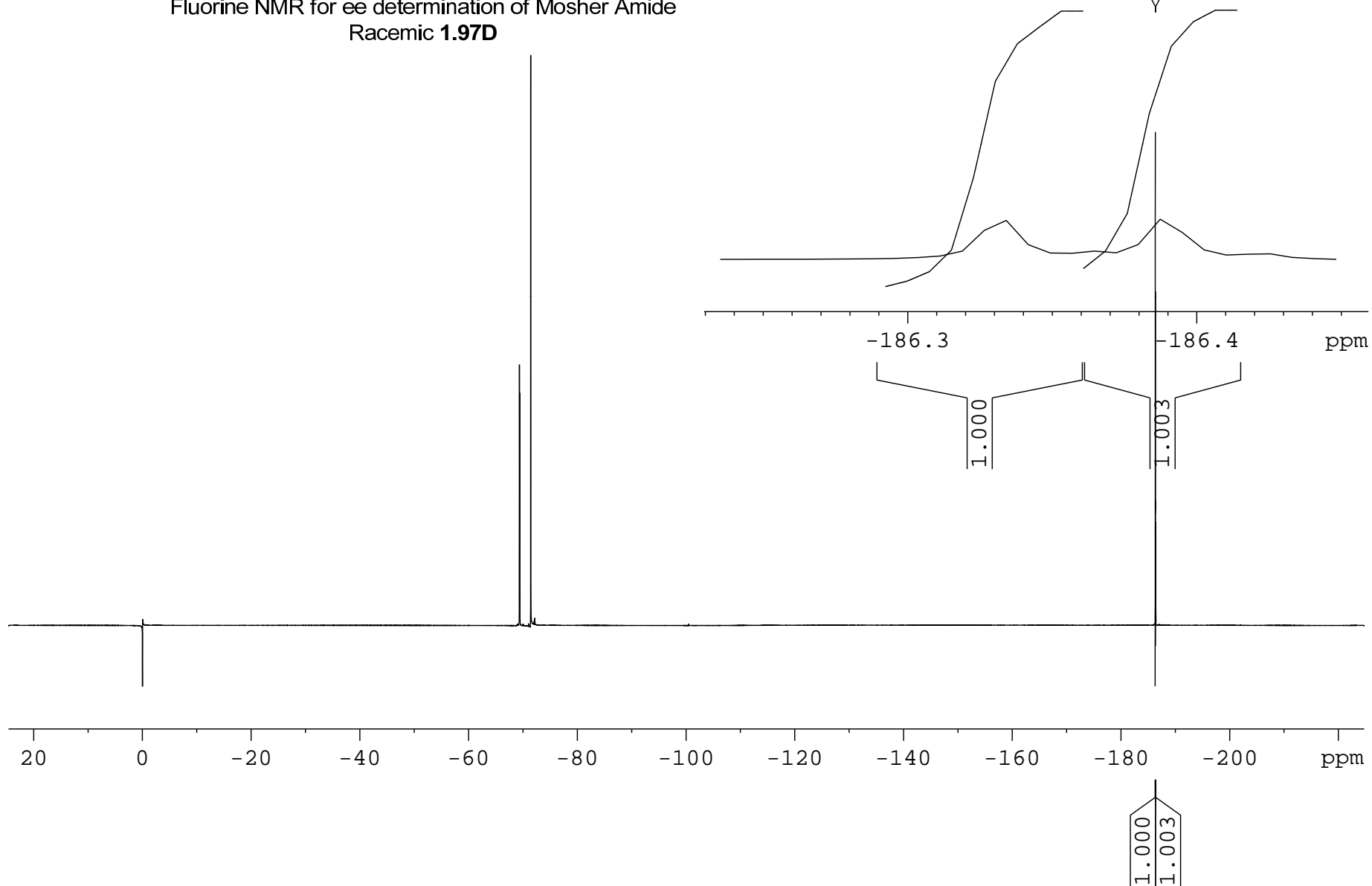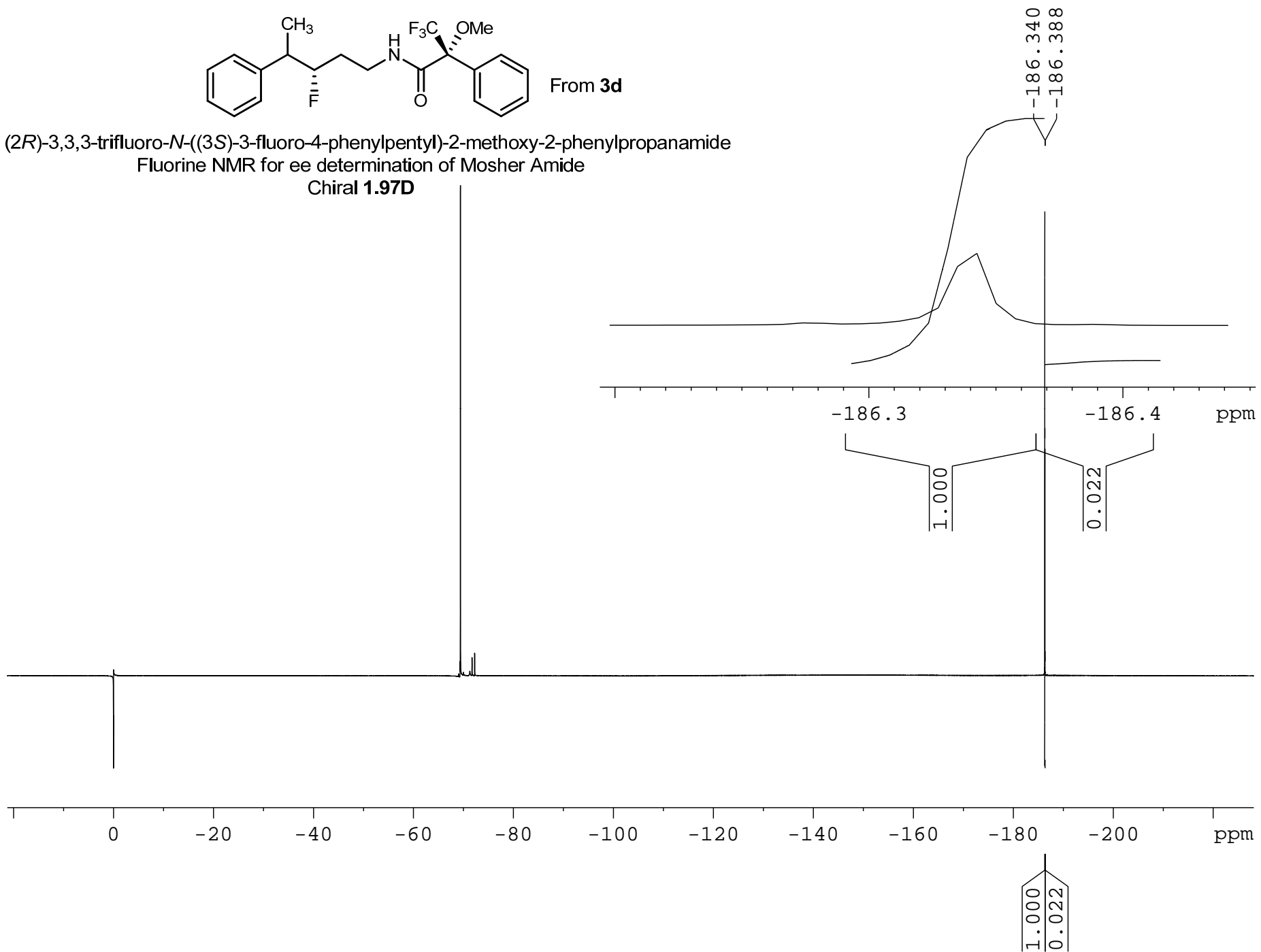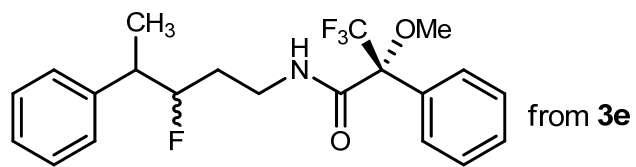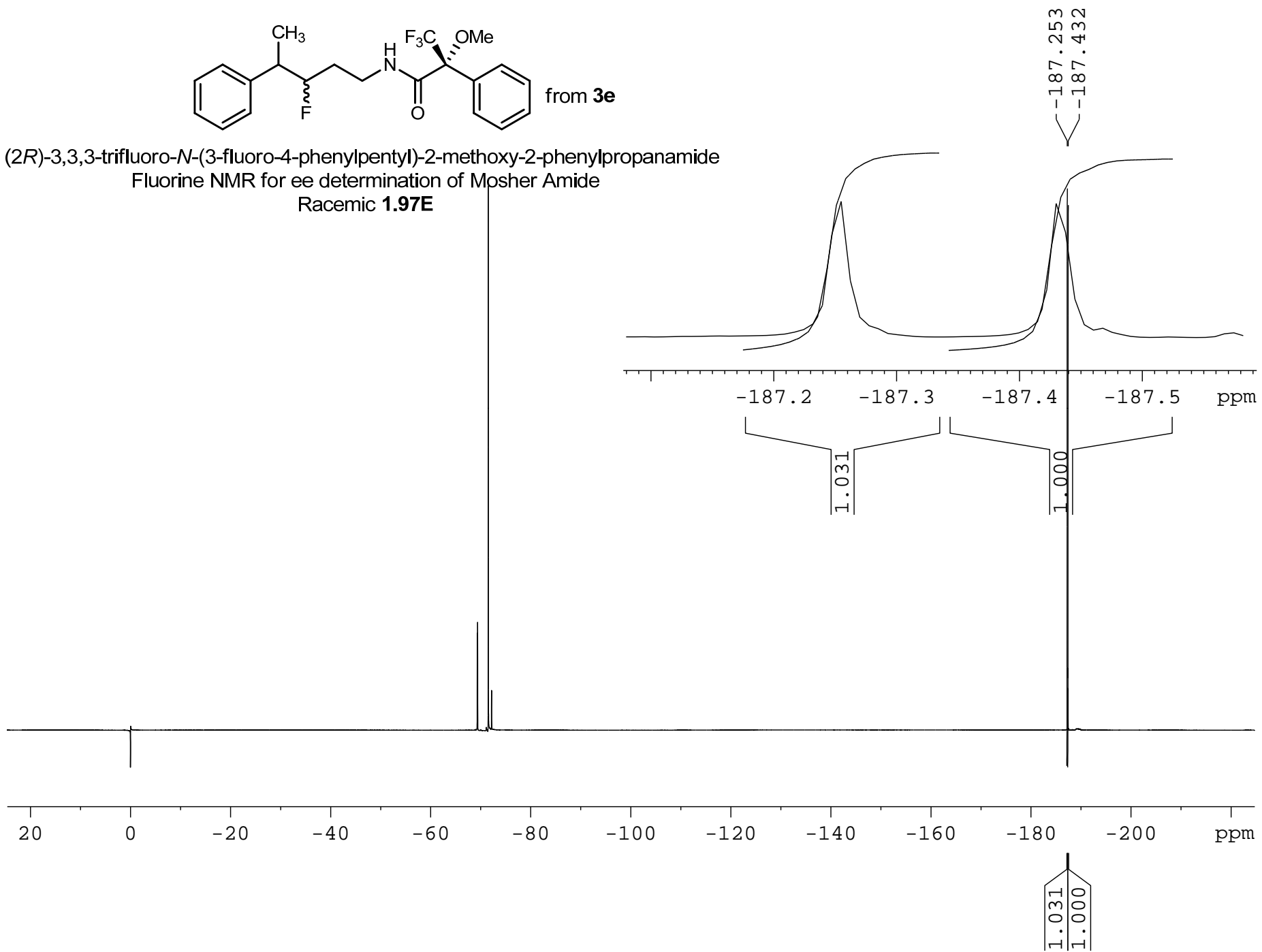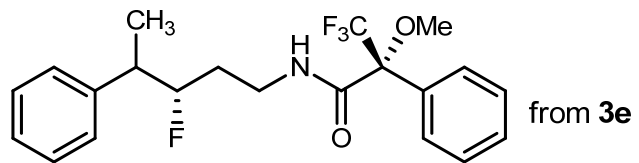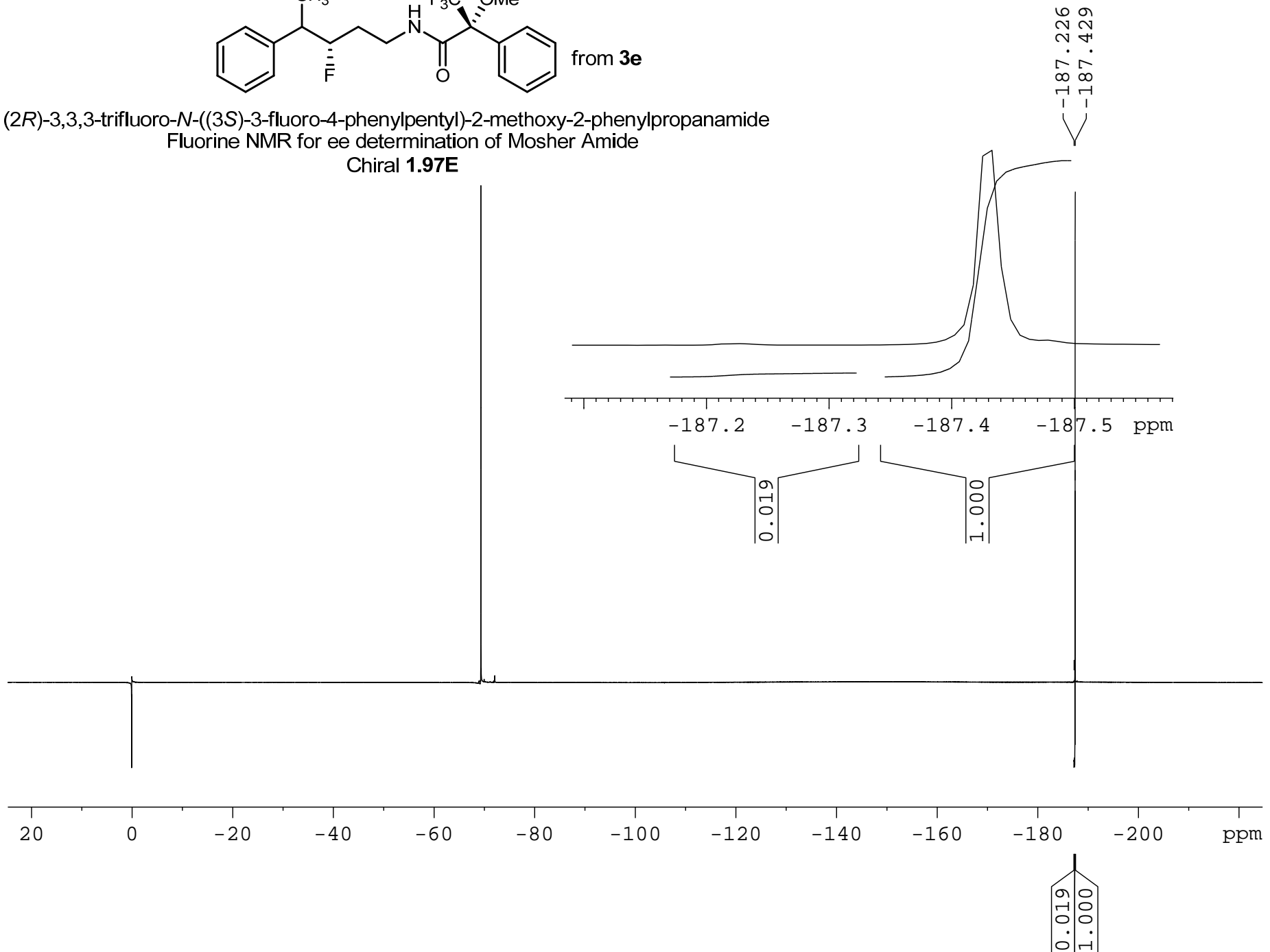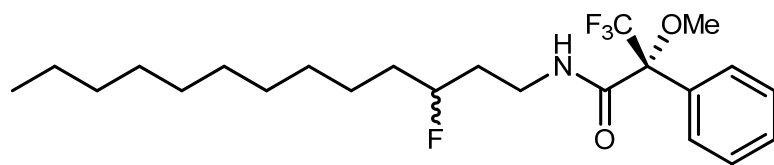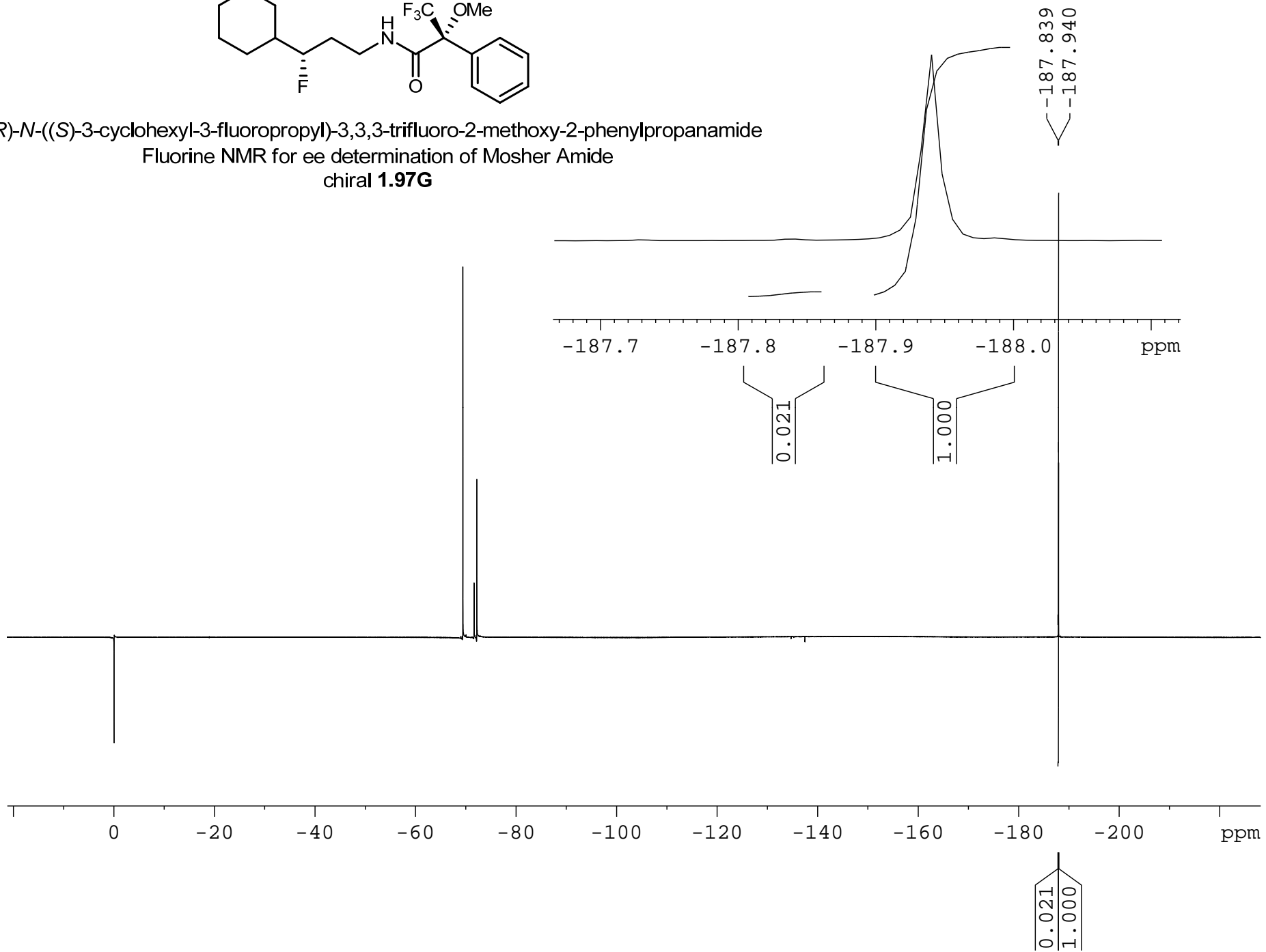
Data File C:\CHEM32\2\DATA\SINGLE 2012-11-13 12-08-33\1ED-0101.D
Sample Name: MCO-IV-184

==
Acq. Operator   :   Seq. Line :   1
Acq. Instrument : 12475 LC on SFC   Location : P1-E-04
Injection Date : 11/13/2012 12:09:10 PM   Inj :   1
                                       Inj Volume : 5.000 µl
Different Inj Volume from Sequence !   Actual Inj Volume : 1.000 µl
Acq. Method   : C:\CHEM32\2\DATA\SINGLE 2012-11-13 12-08-33\CHIRALPAK_IA_5_MEOH.M
Last changed   : 11/13/2012 12:08:57 PM
                  (modified after loading)
Analysis Method : C:\CHEM32\2\METHODS\CHIRALPAK_IC_5_MEOH.M
Last changed   : 11/13/2012 11:19:48 AM
                  (modified after loading)
Additional Info : Peak(s) manually integrated

==
                    Area Percent Report
==
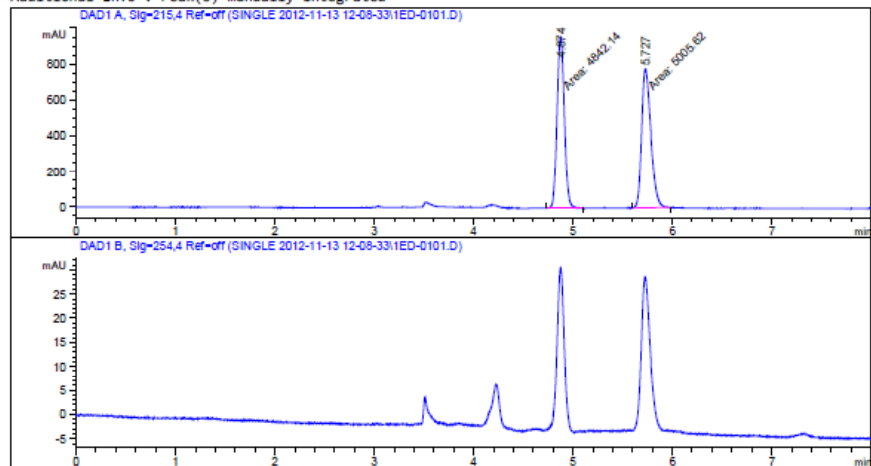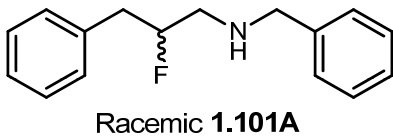
Sorted By   :   Signal
Multiplier: :   1.0000
Dilution: :   1.0000
Use Multiplier & Dilution Factor with ISTDs

Signal 1: DAD1 A, Sig=215,4 Ref=off

Peak RetTime Type Width   Area   Height   Area
 #   [min]   [min]   [mAU*s]   [mAU]   %
----|-------|----|-------|----------|----------|--------|
 1   4.874 MM   0.0841 4842.13574 959.32269 49.1699
 2   5.727 MM   0.1071 5005.61963 778.75336 50.8301

Totals :   9847.75537 1738.07605

381

94% ee
Chiral 1.101A

Data File C:\CHEM32\2\DATA\SINGLE 2012-11-13 12-28-47\1EE-0401.D
Sample Name: MCO-V-20

==
Acq. Operator   :   Seq. Line :   4
Acq. Instrument : 12475 LC on SFC   Location : P1-E-05
Injection Date : 11/13/2012 12:53:32 PM   Inj :   1
                                         Inj Volume : 5.000 µl
Different Inj Volume from Sequence !   Actual Inj Volume : 1.000 µl
Acq. Method   : C:\CHEM32\2\DATA\SINGLE 2012-11-13 12-28-47\CHIRALPAK_IA_5_MEOH.M
Last changed   : 11/13/2012 12:35:48 PM
                  (modified after loading)
Analysis Method : C:\CHEM32\2\METHODS\CHIRALPAK_IC_5_MEOH.M
Last changed   : 11/13/2012 11:19:48 AM
                  (modified after loading)
Additional Info : Peak(s) manually integrated

DAD1 A, Sig=215,4 Ref=off (SINGLE 2012-11-13 12-28-47\1EE-0401.D)

DAD1 B, Sig=254,4 Ref=off (SINGLE 2012-11-13 12-28-47\1EE-0401.D)

==
                    Area Percent Report
==
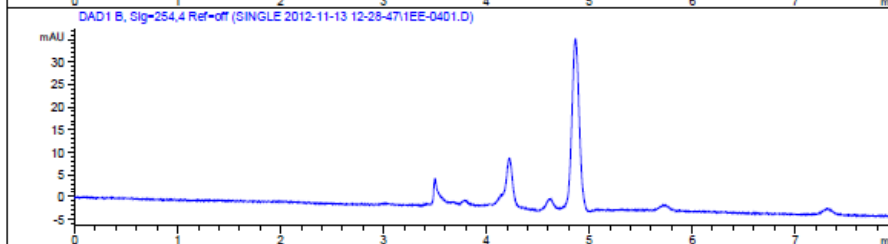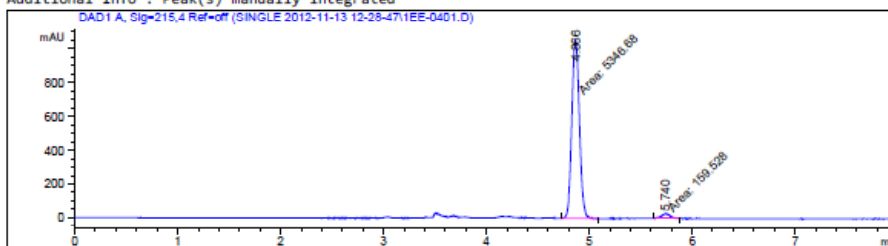
Sorted By   :   Signal
Multiplier: :   1.0000
Dilution: :   1.0000
Use Multiplier & Dilution Factor with ISTDs

Signal 1: DAD1 A, Sig=215,4 Ref=off

Peak RetTime Type Width   Area   Height   Area
 #   [min]   [min]   [mAU*s]   [mAU]   %
----|-------|----|-------|----------|----------|--------|
  1   4.866 MM   0.0839 5346.67529 1062.06238 97.1028
  2   5.740 MM   0.0988 159.52835   26.91542   2.8972

Totals :   5506.20364 1088.97780

Racemic **1.101B**

Data File C:\CHEM32\2\DATA\SINGLE 2012-11-13 10-55-36\1EC-0101.D
Sample Name: MCO-IV-185

```
==========================================================================
Acq. Operator   :                          Seq. Line :   1
Acq. Instrument : 12475 LC on SFC              Location : P1-E-03
Injection Date  : 11/13/2012 11:01:13 AM           Inj :   1
                                         Inj Volume : 5.000 µl
Different Inj Volume from Sequence !     Actual Inj Volume : 2.000 µl
Acq. Method     : C:\CHEM32\2\DATA\SINGLE 2012-11-13 10-55-36\CHIRALPAK_IB_3_MEOH.M
Last changed    : 11/13/2012 11:08:26 AM
                  (modified after loading)
Analysis Method : C:\CHEM32\2\METHODS\CHIRALPAK_IC_5_MEOH.M
Last changed    : 11/13/2012 11:19:48 AM
                  (modified after loading)
Additional Info : Peak(s) manually integrated
```

DAD1 A, Sig=215,4 Ref=off (SINGLE 2012-11-13 10-55-36\1EC-0101.D)

DAD1 B, Sig=254,4 Ref=off (SINGLE 2012-11-13 10-55-36\1EC-0101.D)

```
==========================================================================
                        Area Percent Report
==========================================================================

Sorted By            :       Signal
Multiplier:                  :      1.0000
Dilution:                    :      1.0000
Use Multiplier & Dilution Factor with ISTDs


Signal 1: DAD1 A, Sig=215,4 Ref=off

Peak RetTime Type  Width     Area       Height     Area
 #   [min]        [min]   [mAU*s]      [mAU]       %
----|-------|----|-------|----------|----------|--------|
  1   5.865 MM   0.1166 7582.83887 1083.60217  50.2709
  2   6.483 MM   0.1255 7501.11475  996.49432  49.7291

Totals :               1.50840e4  2080.09650
```
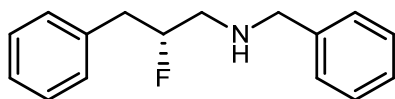
90% ee
Chiral **1.101B**

Data File C:\CHEM32\2\DATA\SINGLE 2012-11-15 11-06-30\001-0201.D
Sample Name: MCO-V-25

===
Acq. Operator   :   Seq. Line :   2
Acq. Instrument : 12475 LC on SFC   Location : Vial 1
Injection Date : 11/15/2012 11:16:55 AM   Inj :   1
                                          Inj Volume : 5.000 µl
Different Inj Volume from Sequence !   Actual Inj Volume : 2.500 µl
Acq. Method   : C:\CHEM32\2\DATA\SINGLE 2012-11-15 11-06-30\CHIRALPAK_IB_3_MEOH.M
Last changed   : 11/15/2012 10:55:44 AM
Analysis Method : C:\CHEM32\2\DATA\SINGLE 2012-11-15 11-06-30\001-0201.D\DA.M (CHIRALPAK_IB_
                  3_MEOH.M, From Data File)
Last changed   : 11/15/2012 11:26:56 AM
                  (modified after loading)
Additional Info : Peak(s) manually integrated
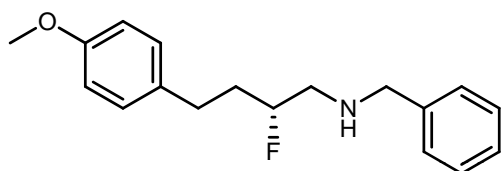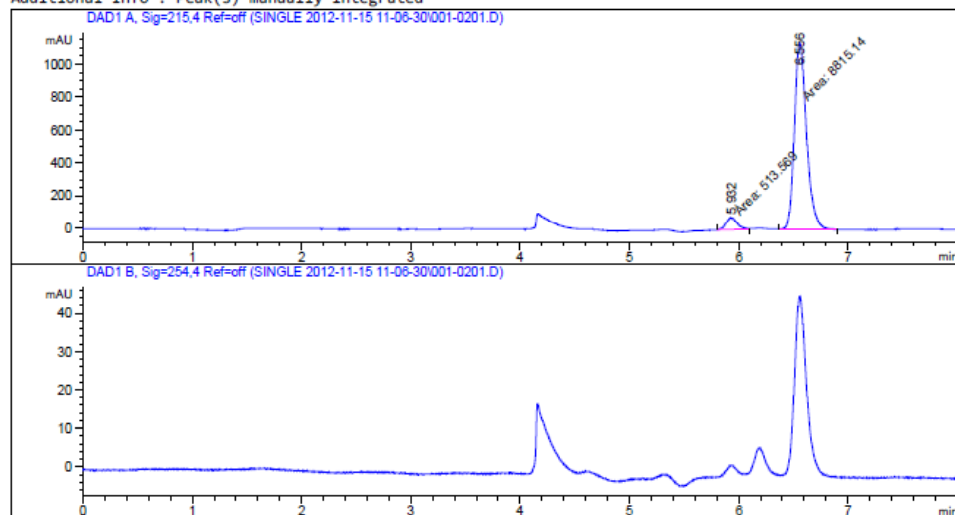
===
                        Area Percent Report
===

Sorted By   :   Signal
Multiplier: :   1.0000
Dilution: :   1.0000
Use Multiplier & Dilution Factor with ISTDs

Signal 1: DAD1 A, Sig=215,4 Ref=off

Peak RetTime Type Width   Area   Height   Area
  #   [min]   [min]   [mAU*s]   [mAU]   %
----|-------|----|-------|----------|-----------|--------|
  1   5.932 MM   0.1156 513.56860   74.04364   5.5052
  2   6.556 MM   0.1293 8815.13965 1136.69775   94.4948

Totals :   9328.70825 1210.74139

Racemic **1.101C** (silyl cleavage)
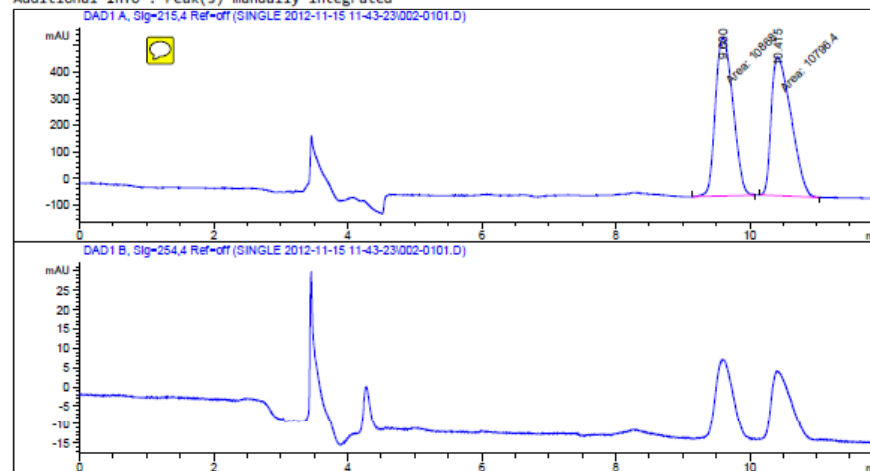
Data File C:\CHEM32\2\DATA\SINGLE 2012-11-15 11-43-23\002-0101.D
Sample Name: MCO-V-14

==
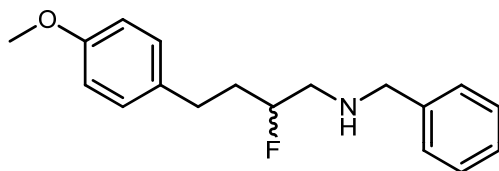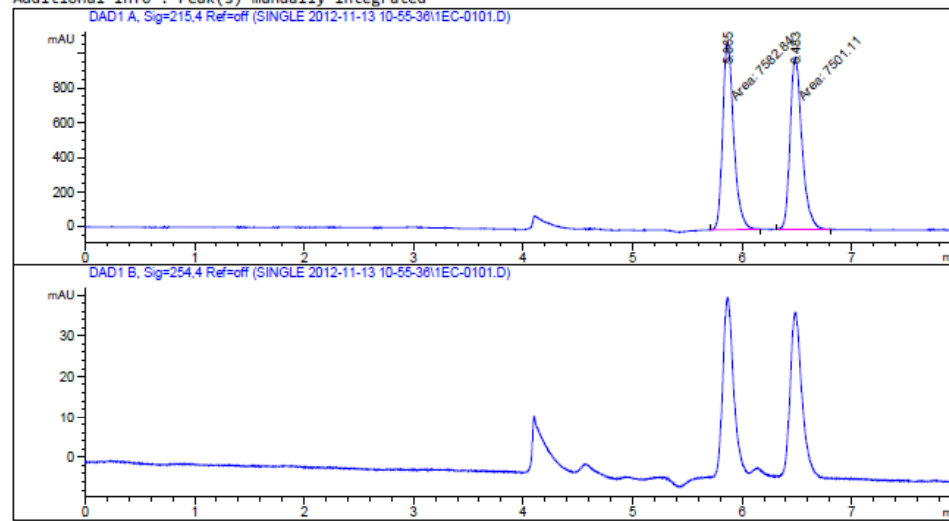Acq. Operator   :   Seq. Line :   1
Acq. Instrument : 12475 LC on SFC   Location : Vial 2
Injection Date : 11/15/2012 11:44:39 AM   Inj :   1
                                            Inj Volume : 5.000 µl
Different Inj Volume from Sequence !   Actual Inj Volume : 15.000 µl
Acq. Method   : C:\CHEM32\2\DATA\SINGLE 2012-11-15 11-43-23\CHIRALPAK_ID_7_MEOH.M
Last changed   : 11/15/2012 11:36:24 AM
Analysis Method : C:\CHEM32\2\DATA\SINGLE 2012-11-15 11-43-23\002-0101.D\DA.M (CHIRALPAK_ID_
                  7_MEOH.M, From Data File)
Last changed   : 11/15/2012 2:24:41 PM
                  (modified after loading)
Additional Info : Peak(s) manually integrated

==
                        Area Percent Report
==

Sorted By   :   Signal
Multiplier: :   1.0000
Dilution: :   1.0000
Use Multiplier & Dilution Factor with ISTDs

Signal 1: DAD1 A, Sig=215,4 Ref=off

Peak RetTime Type Width   Area   Height   Area
  #   [min]   [min]   [mAU*s]   [mAU]   %
----|-------|----|-------|----------|----------|--------|
  1   9.600 MM   0.3032 1.08680e4   597.32648 50.1652
  2 10.415 MM   0.3431 1.07964e4   524.43738 49.8348

Totals :   2.16643e4 1121.76385

94% ee
Chiral **1.101C** (silyl cleavage)

Data File C:\CHEM32\2\DATA\SINGLE 2012-11-15 12-27-32\003-0101.D
Sample Name: MCO-V-26

===
Acq. Operator   :   Seq. Line :   1
Acq. Instrument : 12475 LC on SFC   Location : Vial 3
Injection Date : 11/15/2012 12:28:55 PM   Inj :   1
                                        Inj Volume : 5.000 µl
Different Inj Volume from Sequence !   Actual Inj Volume : 10.000 µl
Acq. Method   : C:\CHEM32\2\DATA\SINGLE 2012-11-15 12-27-32\CHIRALPAK_ID_7_MEOH.M
Last changed   : 11/15/2012 12:40:48 PM
                  (modified after loading)
Analysis Method : C:\CHEM32\2\DATA\SINGLE 2012-11-15 12-27-32\003-0101.D\DA.M (CHIRALPAK_ID_
                  7_MEOH.M, From Data File)
Last changed   : 11/15/2012 12:41:31 PM
                  (modified after loading)
Additional Info : Peak(s) manually integrated

===
                        Area Percent Report
===

Sorted By   :   Signal
Multiplier: :   1.0000
Dilution: :   1.0000
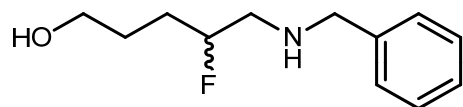Use Multiplier & Dilution Factor with ISTDs

Signal 1: DAD1 A, Sig=215,4 Ref=off

Peak RetTime Type Width   Area   Height   Area
 #   [min]   [min]   [mAU*s]   [mAU]   %
----|-------|----|-------|----------|----------|--------|
  1   9.743 MM   0.2379 6149.81494 430.90405 96.8046
  2 10.651 MM   0.2380   202.99626   14.21245   3.1954

Totals :   6352.81120 445.11650